Towards understanding EC coupling protein expression with age

by

Hermia Willemse
MSc (Human Physiology)

A thesis submitted for the degree of Doctor of Philosophy of The Australian National University

December 2013

The John Curtin School of Medical Research
The Australian National University
Canberra
Australia

Australian National University

Statement

This thesis describes research conducted with the Muscle Research Group, Department of Molecular Bioscience, The John Curtin School of Medical Research, The Australian National University, Canberra, Australia between August 2009 and August 2013. The research conducted in this PhD was supported by grants from the National Health Research Council (#1020589 and #1002589), an Australian Postgraduate Award and a John Curtin School of Medical Research supplementary scholarship.

The results and analyses presented in this thesis are my own original work, conducted under the supervision of Professor Angela Dulhunty, Associate Professor Marco Casarotto and Professor Philip Board, except where otherwise acknowledged.

Hermia Willemse

Muscle Research Group

Department of Molecular Bioscience

John Curtin School of Medical Research

The Australian National University

Acknowledgements

I would like to sincerely thank the members of my supervisory panel, Prof Angela Dulhunty, Assoc Prof Marco Casarotto and Prof Phil Board, for their support and guidance throughout this project. In particular I would like to thank Angela as chair of my supervisory panel. To Asst Prof Nicole Beard and Dr Angelo Theodoratos for their technical advice, I am truly very thankful.

I would also like to thank all the members of the Muscle Research Group, Skeletal and Cardiac Muscle Proteomics Group, Molecular Genetics Group and Biomolecular Interactions Group. In particular I would like to thank Ms Suzy Pace and Joan Stivala for the preparation of microsomal vesicles as well as their assistance in the muscle collection process.

To Prof Paul Smith and the staff at the John James Calvary Hospital I would also like to extend many thanks for their collaboration in the collection of the human muscle tissue.

To my husband Adan, I would not be able to ever thank you enough for all your love and support during the past four years. I would not have been able to finish this without you. Thank you from the bottom of my heart.

To my friends and family a very big thank you for being patient with me and your support from afar.

Abstract

Sarcopenia is characterised by a decrease in muscle specific force that can only partially be attributed to muscle atrophy. Changes in fiber type composition of muscle have also been observed in humans with age. Additionally, it is suggested that excitation contraction coupling (EC coupling) is impaired in aging by uncoupling of the two Ca^{2+} channels facilitating EC coupling, the dihydropyridine receptor (DHPR) and the ryanodine receptor (RyR1), perhaps due to a decrease in expression of the DHPR α_{1s} subunit which has been demonstrated in rodents. Changes in DHPR β_{1a} subunit expression have also been reported in aging mice but not investigated in humans. The 12kDa FK506 binding protein (FKBP12) stabilizes RyR1 in the closed state. Its dissociation from RyR1 causes a "leaky" channel and decreased EC coupling. Furthermore, RyR1 has two variably spliced regions, ASI and ASII, thought to be developmentally regulated. The ASI region, which lies close to a DHPR β_{1a} binding site, affects EC coupling. The juvenile isoform (ASI(-)RyR1) shows enhanced Ca^{2+} release during EC coupling and its overexpression is linked to myopathy in myotonic dystrophy. Regeneration in aging muscle due to increased denervation and reinnervation can give rise to immature muscle fibers with higher levels of the juvenile isoforms of some proteins.

Therefore the aim of this study was to investigate the fiber type distribution as well as levels of RyR1, DHPR α_{1s}, β_{1a}, and FKBP12 in aged human muscle from 42 donors (aged 40-90yr) undergoing knee (vastus medialis) and hip replacements (gluteus minimus and gluteus medius). The levels of ASI splice variant transcripts in the muscle were investigated using RT-PCR. Furthermore, the effect of the addition of β_{1a} to recombinant ASI splice variant channels in lipid bilayers was investigated.

Vastus medialis was predominantly fast twitch, whereas gluteus minimus and gluteus medius were predominantly slow twitch fibers. Contrary to expectation, age affected fiber type composition differently in the three human muscles. Also, contrary to rodent studies, no significant difference in the human expression levels of the RyR1, DHPR α_{1s} and β_{1a} or FKBP12 with age was found. The ASI(+)RyR1:ASI(-)RyR1 ratio showed no significant change with age, however, an unexpected strong correlation between the fiber type and splice variant was found. In muscle with a high fraction of slow-twitch fibers, ASI(-)RyR1 predominates and vice versa. This novel finding suggests the ASI splice variants are fiber type specific rather than developmentally regulated. Finally, novel lipid bilayer results showed that ASI(+)RyR1 was activated more by 10nM β_{1a} than ASI(-)RyR1, but was similarly activated by 50nM β_{1a}, indicating a higher affinity of ASI(+)RyR1 for β_{1a}.

Although no significant difference in expression levels of EC coupling proteins with age in humans was found, the discovery of fiber type specificity in RyR1 splice variants is important.

This has not been shown before and provides a paradigm shift in understanding skeletal muscle changes in myotonic dystrophy. The discovery of different isoform affinities for β_{1a} may explain differences between EC coupling in fast and slow twitch fibers and changes in EC coupling in myotonic dystrophy.

Publications

Tae, H., L. Wei, **H. Willemse**, S. Mirza, E. M. Gallant, P. G. Board, R. T. Dirksen, M. G. Casarotto and A. Dulhunty (2011). "The elusive role of the SPRY2 domain in RyR1." Channels (Austin) 5(2): 148-160.

Conference Abstracts

Gage Ion Channels & Transporters Conference
H. Willemse, P.N. Smith, P.G. Board, M.G. Casarotto, A.F. Dulhunty
Human aging and expression of proteins interacting with the ryanodine receptor in skeletal muscle.
Canberra, Australia, 04/2013, Poster presentation

57th Annual Meeting of the Biophysical Society
H. Willemse, P.N. Smith, P.G. Board, M.G. Casarotto, A.F. Dulhunty
Human aging and expression of proteins interacting with the ryanodine receptor in skeletal muscle.
Philadelphia, USA, 02/2013, Poster presentation

AuPS/ASB/PSNZ Joint meeting
H. Willemse, P.N. Smith, P.G. Board, M.G. Casarotto, A.F. Dulhunty
Human aging and expression of proteins interacting with the ryanodine receptor in skeletal muscle.
Sydney, Australia, 12/2012, Poster presentation

Annual Scientific Meeting of the Australian Orthopaedic Association ACT Branch
H. Willemse, P.N. Smith, P.G. Board, M.G. Casarotto, A.F. Dulhunty
Human aging and expression of proteins interacting with the ryanodine receptor in skeletal muscle
Canberra, Australia, 11/2012, Poster presentation

Gage Muscle Conference
H. Willemse; M.G. Casarotto; P.G. Board; P.N. Smith; A.F. Dulhunty
Possible effects of aging on interactions between the DHPR and RyR1 in human skeletal muscle
Canberra, Australia, 4/2012, Poster presentation

AuPS/ASB Joint meeting
H. Willemse, S. Mirza, E.M. Gallant, H.S. Tae, L. Wei, M.G. Casarotto, R.T. Dirksen and A.F. Dulhunty
Possible contribution of SPRY2 and ASI regions of RyR1 to interdomain interaction
Adelaide, Australia, 11/2010, Poster presentation

Gage Muscle Conference
H. Willemse, Y. Karunasekara, N. A. Beard, M.C. Casarotto and A. F. Dulhunty
Interactions between a variably spliced region of RyR1 and regions of the DHPR involved in skeletal excitation contraction coupling
Canberra, Australia, 4/2010, Poster presentation

Commonly Used Abbreviations

4-cmc	4-chloro-m-cresol
ACh	Acetylcholine
AChR	Acetylcholine receptor
AID	Alpha interaction domain
APS	Ammonium persulphate
ASI	Alternative splicing region I
ATP	Adenosine-5'-triphosphate
BSA	Bovine serum albumin
CaM	Calmodulin
CCD	Central core disease
CICR	Calcium induced calcium release
CRU	Calcium release unit
CSQ	Calsequestrin
DHPR	Dihydropyridine receptor
DTT	Dithiothreitol
EC coupling	Excitation-contraction coupling
EDL	Extensor digitorum longus
EDTA	Ethylene diamine tetraacetic acid
EGTA	Ethylene glycol tetraacetic acid
EM	Electron microscopy
FCS	Foetal calf serum
FDB	Flexor digitorum brevis
FKBP	F506 binding protein
GK domain	Guanylate kinase-like domain
GSH	Glutathione
GSSG	Glutathione disulphide
GST	Glutathione S-transferase
HEK	Human embryonic kidney
I'	Mean current
I'f	Fractional mean current
I_{max}	Maximum current
IPTG	Isopropyl thiogalactopyranoside
LB	Luria Broth
MEM	Minimum essential medium
MH	Malignant Hyperthermia
MmD	Multi-minicore disease
mRNA	messenger RNA

MyHC	Myosin heavy chain
n	Number of observations
NMJ	Neuromuscular junction
NO	Nitric oxide
PAS staining	Periodic acid-Schiff staining
PBS	Phosphate buffered saline
pCa	$\log[Ca^{2+}]$
PCR	Polymerase chain reaction
PMSF	Phenylmethylsulfonylfluoride
P_o	Open probability
R	Pearson's correlation coefficient
ROS	Reactive oxygen species
RyR	Ryanodine receptor
SDH	Succinate dehydrogenase
SDS-PAGE	Sodium dodecyl sulphate polyacrylamide gel electrophoresis
sem	Standard error of the mean
SERCA	Sarcoplasmic/endoplasmic reticulum Ca^{2+}-ATPase
SH3 domain	Src homology domain
siRNA	Small interfering RNA
SR	Sarcoplasmic reticulum
TA	Tibialis Anterior
T_c	Mean closed time
TEMED	Tetramethylethylenediamine
TES	Tetraethylsulfamide
TnC	Troponin C
T_o	Mean open time

Table of Contents

Chapter 1: Introduction

Muscle is a dynamic and versatile tissue that plays an important part in the physiology of mammals. The main function of muscle is to facilitate movement, but it also plays a role in metabolism and temperature homeostasis.

The content of this chapter is mainly sourced from the following references unless otherwise referenced (Ganong 1997; Silverthorn 1998; Hille 2001; Sambrook 2001; Johnson and Byrne 2003; Solomon 2009; Marieb and Hoehn 2010; Hall and Guyton 2011; Kandel 2012).

1.1 Overview of muscle tissue

Mammalians have three types of muscle tissue: smooth muscle, skeletal muscle and cardiac muscle.

Smooth muscle is the primary muscle of internal organs and vessels. It has no striations due to the fact that it has a less organized arrangement of its contractile filaments. Muscle cells are elongated and are therefore referred to as muscle fibers. Smooth muscle fibers are variable in size (5-10μm in diameter; 30-200μm in length) and they have one central nucleus per muscle fiber. Smooth muscle is not under voluntary control. It is controlled by autonomic innervations, but it can also contract spontaneously and is subject to endocrine modulation. Its contractions are slow and sustained and smooth muscle is resistant to fatigue.

Cardiac muscle is found in the heart and makes up most of the heart walls. Its contractile filaments are arranged in a very organized way which gives it a banded appearance. Cardiac muscle is therefore referred to as striated muscle. Cardiac muscle fibers mostly have one central nucleus, but sometimes there can be two. The fibers branch and fit together with tight junctions referred to as intercalated discs. Cardiac muscle is also not under voluntary control and it is innervated by the autonomic nervous system, however, it can contract spontaneously and respond to endocrine input. It contracts at a steady rate determined by the heart's pacemaker, but is responsive to neural and endocrine modulation

Skeletal muscle is attached the skeleton and facilitates movement, maintains posture and stabilizes joints. It is striated, but unlike cardiac muscle, it is under voluntary control. It can, however, be activated by reflexes as well. Skeletal muscle fibers are long cylindrical cells with multiple oval nuclei located just beneath the plasma membrane or sarcolemma. The fiber

diameter ranges from 10-100μm and fibers can be up to 30cm long. Healthy skeletal muscle doesn't contract spontaneously. It contracts in response to somatic motor neuron stimulus and is not directly modulated by the endocrine system. Skeletal muscle contraction can occur rapidly but it fatigues and cannot sustain continuous rapid contraction for an extended time. The range of pressure and force that skeletal muscle can produce is quite large and is therefore very adaptable in this regard.

This study involves exclusively skeletal muscle and the introduction will therefore focus on this type of muscle.

1.2 Gross anatomy of skeletal muscle

Each muscle is a discrete organ made up of a several kinds of tissues. The most predominant tissue is skeletal muscle, but there are also blood vessels, nerve fibers and substantial amounts of connective tissue present.

1.2.1 Nerve and blood supply

Generally each muscle is served by one nerve, an artery and one or more veins. These structures enter or exit near the middle of the muscle and then branch liberally throughout the connective tissue sheaths. A nerve ending connects to each muscle fiber and controls its activity. Contracting muscle expends large amounts of energy and need an almost continuous delivery of oxygen and nutrients and the removal of metabolic waste that are produced in large quantities. It therefore has a rich blood supply

1.2.2 Connective tissue sheaths

Each individual muscle fiber is surrounded by a sheath of connective tissue referred to as the endomysium. It consists of fine areolar connective tissue. Within the muscle, the muscle fibers are grouped together in "bundles of sticks" called fascicles and each fascicle is surrounded by a fibrous connective tissue sheath referred to as the perimysium. Surrounding the whole muscle is another connective tissue sheath, the epimysium, consisting of dense irregular connective tissue (see **Figure 1.1**). Together, the connective tissue sheaths serve to support each cell and to reinforce the muscle as a whole, preventing damage during strong contractions. They are continuous with each other as well as the tendons that connect the muscle to the bone of the skeleton. As the muscle contracts and shortens the connective tissue sheaths and tendons transmit the pulling force to the bone thus facilitating movement of the skeleton. Not only do

the sheaths contribute to the natural elasticity of muscle, they also serve as a corridor for blood vessels and nerve fibers entering and exiting the muscle.

1.3 Microscopic anatomy of skeletal muscle

Skeletal muscle fibers are long cylindrical cells with multiple oval nuclei just beneath the plasma membrane or sarcolemma. The cytoplasm of the skeletal muscle fiber is referred to as the sarcoplasm. It contains large amounts of glycosomes, which are granules of stored glycogen that provides glucose when needed. The sarcoplasm also contains myoglobin, which is a red pigment that can store oxygen. The usual organelles are present in skeletal muscle fibers, along with some organelles that are specialized for muscle's function e.g. myofibrils, sarcoplasmic reticulum and t-tubule network.

1.3.1 Myofibrils

Myofibrils are bundles of contractile and elastic proteins that carry out the work of contraction. They are rod like and run parallel to the fiber's length. Each myofibril is 1-2μm in diameter and the bundles occupy most of the intracellular space, leaving little space for mitochondria and other organelles. In fact, myofibrils make up about 80% of the cellular volume. They contain the contractile elements of skeletal muscle cells, the sarcomere, which is formed by even smaller rod-like structures called myofiliments.

When skeletal muscle is observed under a light microscope, a repeating series of light and dark bands is visible along the length of the myofibril. As mentioned previously, these repeating bands are referred to as striations and skeletal muscle as striated. The dark bands are called A bands (A stands for anisotropic because the proteins in this area scatter light unevenly under a polarizing microscope). The light bands are called I bands (I stand for isotropic because the proteins in this area reflects light uniformly under a polarizing microscope. Each dark A band has a lighter region in its mid-section called the H zone (H for "helle"; bright), which it turn is bisected by a dark line called the M line (M for "mittle"; middle) that is formed by the protein myomesin. The light bands also have a midline interruption, a darker area called the Z disc or Z line (Z stands for "zwischen"; between) (See **Figure 1.2**).

The sarcomere is the region stretching from one Z disc to the next and encompasses an A band flanked by half an I band at each end. Within the myofibril, the sarcomeres are arranged end-to-end and form the functional unit of muscle.

The orderly arrangement of the contractile myofilaments, which are myosin and actin, give rise to the banding pattern. The myofilaments are organized by a subset of cytoskeleton proteins, which include α-actinin, myomesin, titin, obscurin, desmin and nebulin.

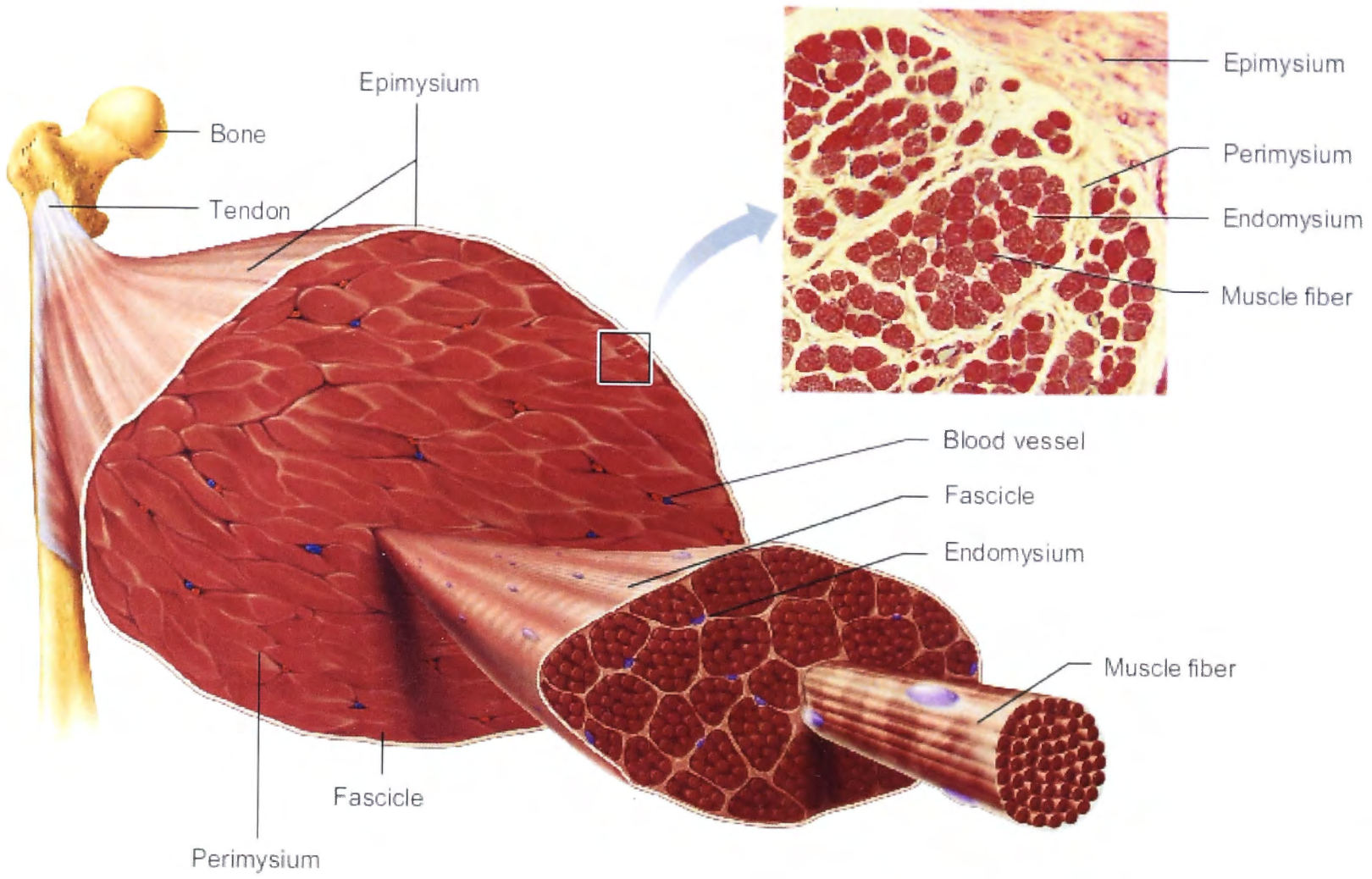

Figure 1.1: Connective tissue sheaths of skeletal muscle (Marieb and Hoehn 2010).

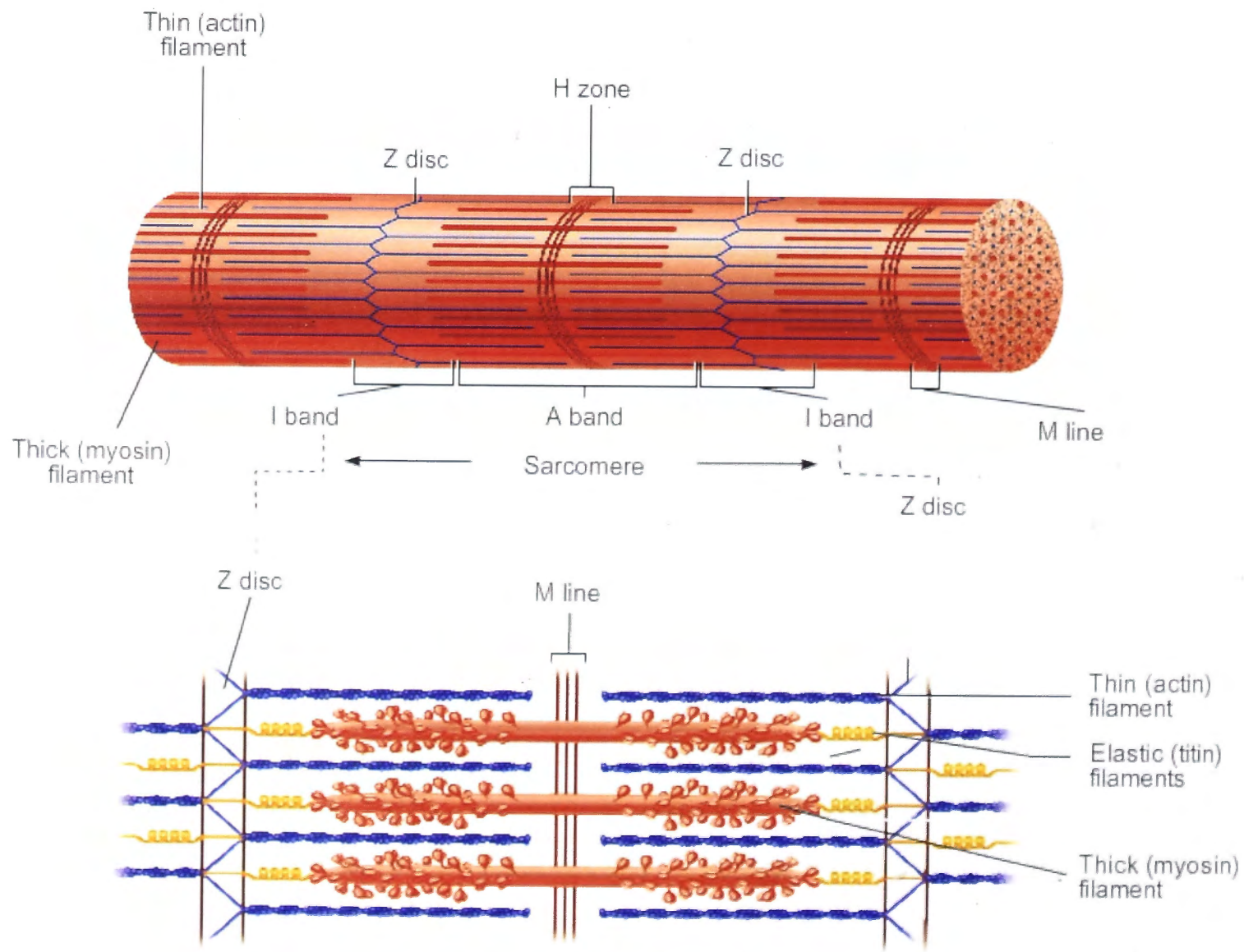

Figure 1.2: Microscopic anatomy of skeletal muscle (Marieb and Hoehn 2010).

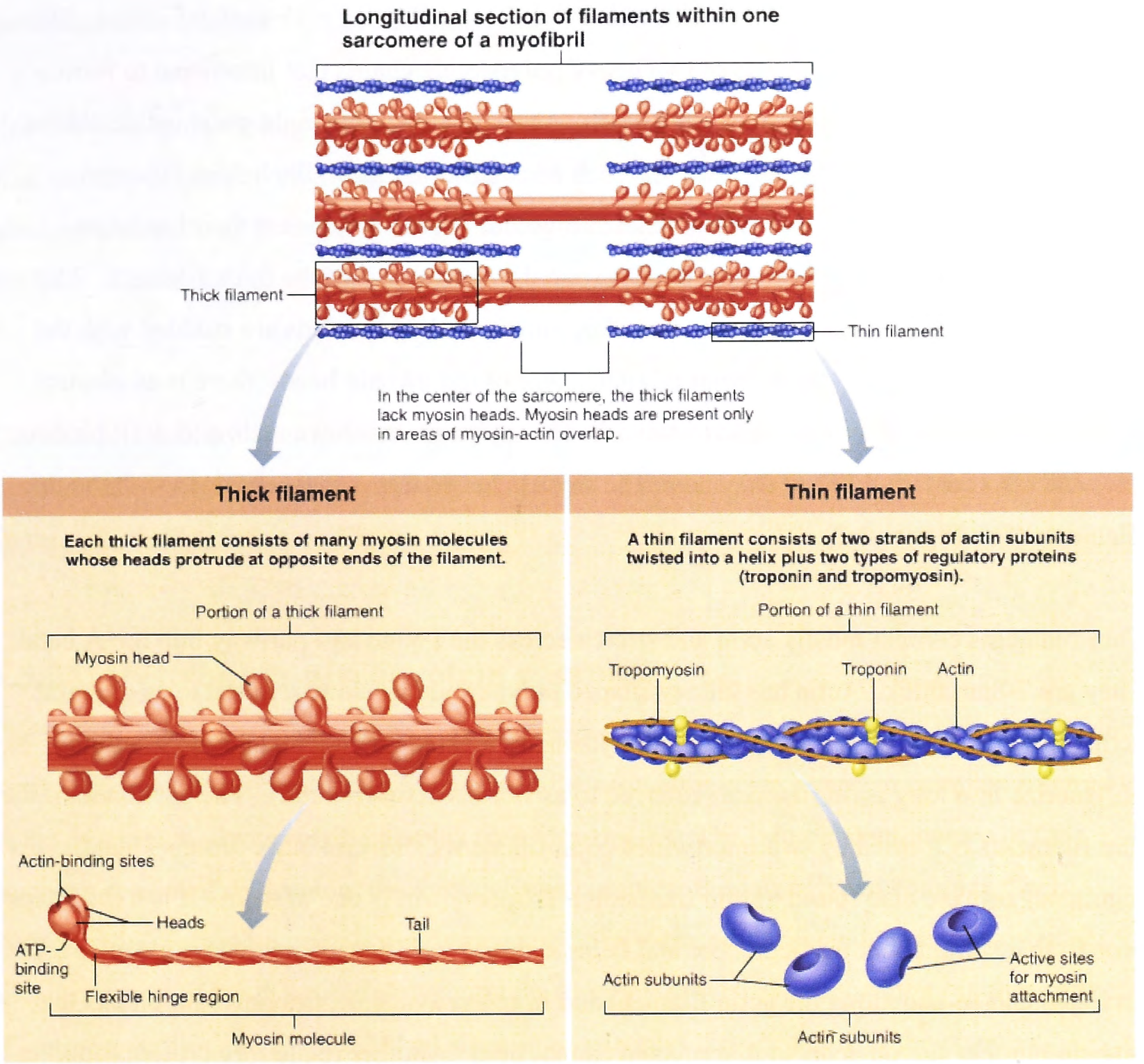

Figure 1.3: Composition of thick and thin filaments (Marieb and Hoehn 2010)

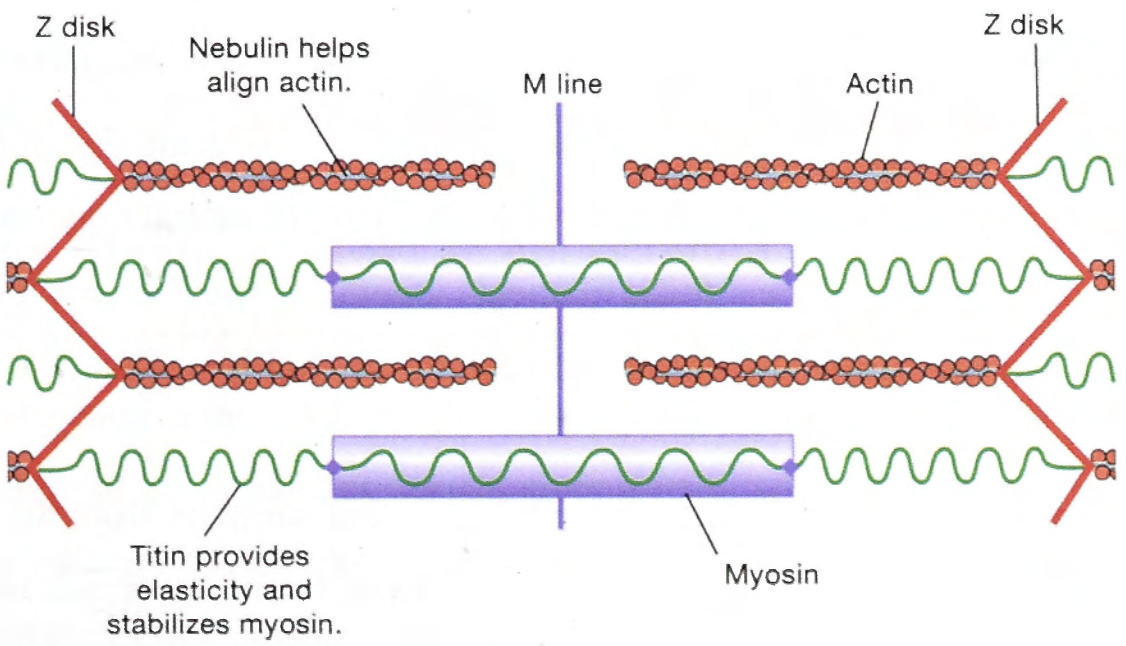

Figure 1.4: Titin and Nebulin (Silverthorn 2004).

Thick filaments extend the entire length of the A band. The thick filaments are about 16nm in diameter and are composed primarily of myosin. Various isoforms occur in different types of skeletal muscle fiber which will be discussed in the section dealing with skeletal muscle fiber types. Each myosin head consists of two heavy polypeptide chains that intertwine to form a long coiled tail and a pair of tadpole like heads as well as two lightweight polypeptide chains that are associated with the heavy chain of each head (four in total). Each thick filament contains about 300 myosin molecules bundled together in such a way that their heads are clustered together at the ends and their tails are in the central part of the thick filament. The middle portion of the thick filament is therefore smooth, while the ends are studded with the staggered myosin heads. At the point of attachment of the myosin heads, there is an elastic hinge region which allows the head to swivel. The myosin heads have actin and ATP binding sites and also contain ATPase enzymes. The myosin heads form cross—bridges with the thin filaments (See **Figure 1.3**).

Thin filaments contain mostly actin and stretch across the I band and partway into the A band. They are 7-8nm thick. Actin has kidney shaped polypeptide subunits referred to as globular actin (G-actin). The active sites that bind myosin are located on G-actin and the subunits polymerize into long actin filaments referred to as fibrous actin (F-actin). The backbone of the thin filaments is formed by two intertwined actin filaments. Several other proteins that have a regulatory role are also found in thin filaments. Tropomyosin is one of them. It is a rod shaped protein that spiral about the actin core and helps stabilize it. The tropomyosin molecules are arranged end-to-end along the actin filament and in relaxed muscle, tropomyosin blocks the myosin binding site on actin so that myosin cannot bind. Another regulatory protein found in thin filaments is troponin. Troponin is a globular three-polypeptide complex consisting of troponin I (TnI), troponin T (TnT), and troponin C (TnC). TnI is an inhibitory subunit that binds to actin. TnT binds to tropomyosin and helps position it on actin and TnC binds calcium ions (see **Figure 1.3**).

The H zone of the A band appears less dense because the thin filaments do not extend into this region (see **Figure 1.2**). The M line in the center of the H zone is darker due to the presence of fine protein strands that hold adjacent thick filaments together. The Z disc is a coin shaped disc that consists mainly of the protein α-actinin and anchors the thin filaments.

Elastic filaments consist of titin, a large elastic molecule that stretches from the Z disc to the thick filament and then runs parallel with the thick filament (forming its core) to attach to the M line. It holds the thick filament in place, therefore maintaining the organization of the A band. It also helps the muscle to spring back into shape after being stretched. The I band spanning part of titin is extensible. It unfolds when the muscle is stretched and recoils when the

tension is released. In the normal range of extension, titin does not resist stretching, but as it uncoils it stiffens. This helps the muscle to resist excessive stretching that would have pulled the sarcomeres apart (see **Figure 1.2**).

Nebulin is an inelastic large protein that lies alongside the thin filaments and attaches to the Z disc, thereby helping to align the actin filaments (see **Figure 1.4**). The intermediate filament (desmin) that extends from the Z disc connects each myofibril to the next through the width of the fiber. The myofilaments are connected to the sarcomere and held in place at the Z discs and the M lines.

Electron-microscopy of cross sections of the sarcomere show each thick filament is actually surrounded by a hexagonal arrangement of six thin filaments and each thin filament is enclosed by three thick filaments (see **Figure 1.5**).

1.3.2 Dystrophin-glycoprotein complex

The thin filaments are connected to the sarcolemma via a large protein, called dystrophin, which forms a rod that connects the thin filaments to the sarcolemma via a protein complex referred to as the dystrophin-glycoprotein complex (see **Figure 1.6**). The integral components of the complex consist of dystrophin, the dystroglycan complex, the sarcoglycan complex, the dystrobrevin/syntrophin complex and sarcospan. An extracellular ligand, namely laminin-2, also forms part of the dystrophin-glycoprotein complex as well as intracellular binding partners (F-actin, syncoilin and filamin 2) and signaling molecules associated with the complex (calmodulin, Grb2 and neuronal nitric oxide synthase - nNOS) (Ganong 1997; Rando 2001; Sciandra et al. 2003; Lapidos et al. 2004; Ervasti and Sonnemann 2008).

The primary role for the dystrophin-glycogen protein complex is the stabilization of the sarcolemma but it also plays a role in organizing molecules involved in cellular signaling (Rando 2001; Ervasti and Sonnemann 2008).

1.3.3 Sliding filament theory of contraction

The force created by contracting muscle is referred to as muscle tension and the weight or force opposing the contraction is the load. Sir Andrew Huxley and Rolf Niedergerke discovered in 1954, that the length of the A band of the sarcomeres in a myofibril remains constant during contraction (Huxley and Niedergerke 1954). They proposed the sliding filament theory of contraction which states that during contraction, the thin filaments slide past the thick filaments so that they overlap to a greater degree and in an energy requiring process (Huxley and Niedergerke 1954).

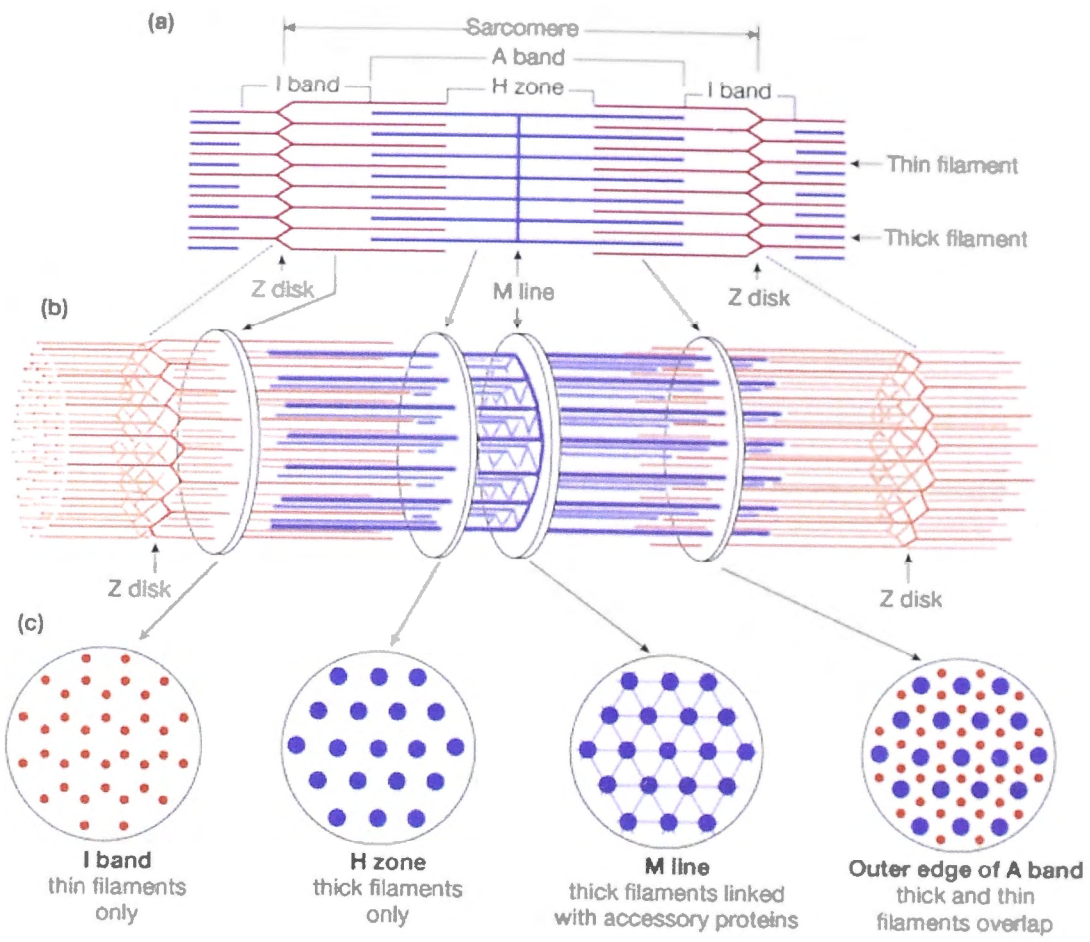

Figure 1.5: The 2D and 3D organization of the sarcomere (Silverthorn 2004).

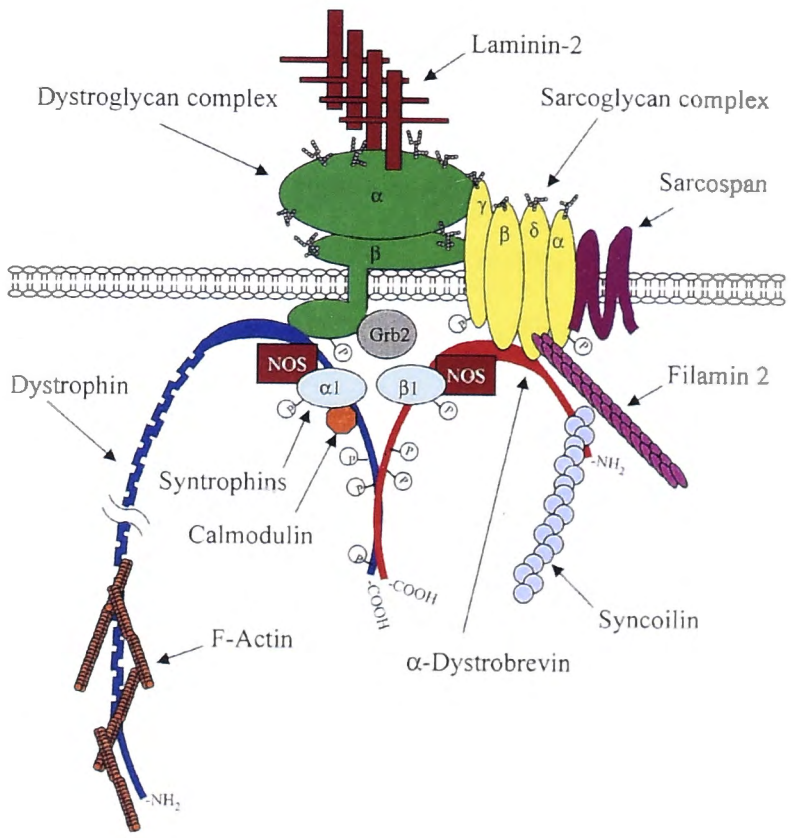

Figure 1.6: The dystrophin-glycoprotein complex (Rando 2001).

The sliding filament theory of contraction takes into account the fact that muscle does not always shorten during contraction. Muscle contraction can occur without creating movement, for example when we push against a wall. The tension generated in the muscle is directly proportional to the interaction between the thick and thin filaments (Huxley and Niedergerke 1954).

A myofibril at resting length has sarcomeres that have the ends of the thick and thin filaments overlapping slightly. As the muscle contracts, the thick and thin filaments slide past each other,

moving the Z discs of each sarcomere closer together. In the relaxed state, a sarcomere has a larger I band (thin filaments only) and an A band the length of the thick filament. As contraction proceeds, the sarcomere shortens. The Z discs move closer together, while the I band and H zone almost disappear. The changes occurring in the sarcomere are consistent with the sliding of the thin actin filaments along the thick myosin filaments as they move toward the M line in the middle of the sarcomere (Huxley and Niedergerke 1954) (see **Figure 1.7**).

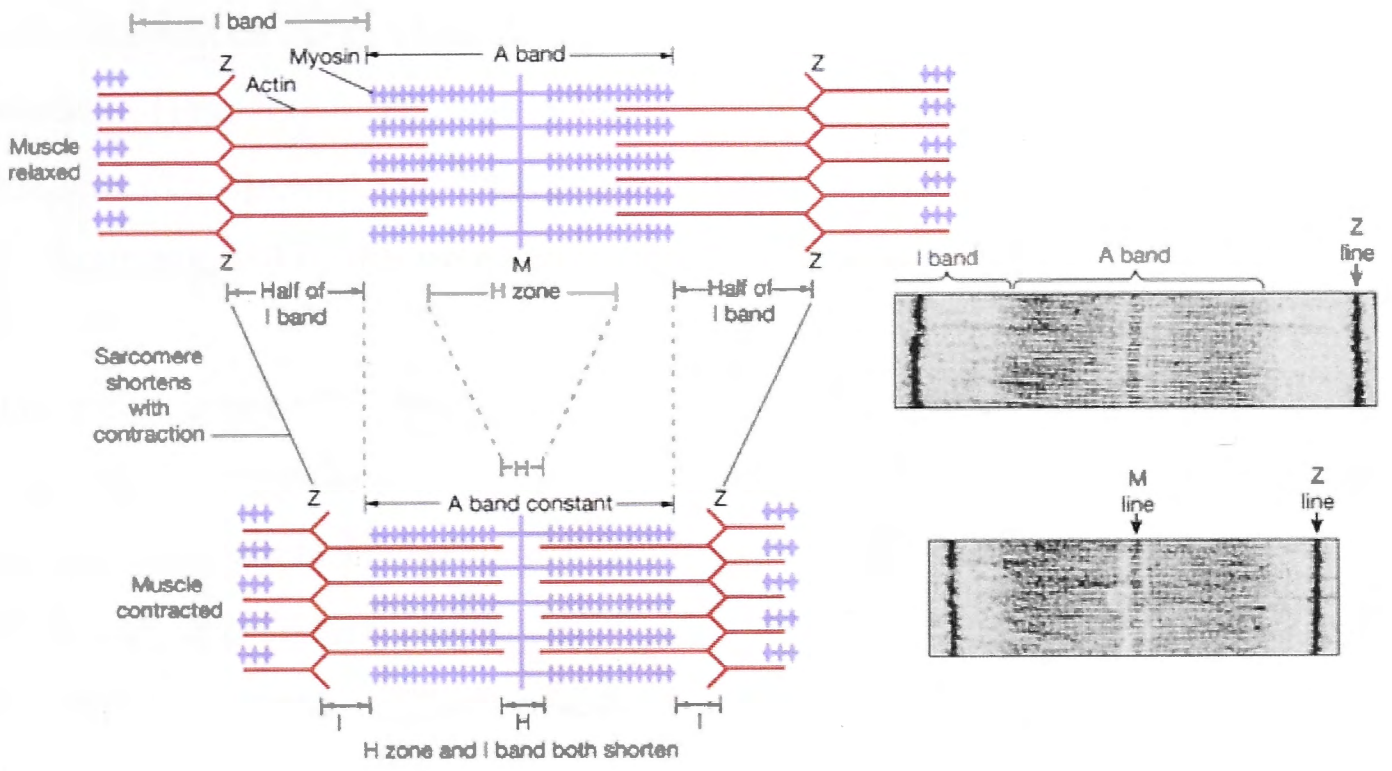

Figure 1.7: Changes in the sarcomere during contraction

1.3.4 Sarcoplasmic reticulum and Transverse tubules

Skeletal muscle fibers contain two sets of intracellular tubules that participate in the regulation of contraction. They are the sarcoplasmic reticulum (SR) and transverse tubules (t-tubules).

The SR is a modified smooth endoplasmic reticulum and it surrounds the myofibril closely. Most of the tubules run longitudinally along the myofibril forming connecting branches in the H zone, others referred to as terminal cisternae form swollen perpendicular connections at the A band – I band junction (see **Figure 1.8**). The major function of the SR is to regulate intracellular levels of Ca^{2+}. It stores Ca^{2+} and releases it upon stimulation for contraction.

At each A band – I band junction, the sarcolemma forms invaginations that extends deep into the cell interior, forming elongated tubules referred to as transverse tubules (t-tubules). The effect of the presence of the t-tubule network is to increase the surface area of fiber. The lumen of the t-tubule is continuous with the extracellular matrix. T-tubules allow action potentials that originate on the cell surface to move rapidly into the interior of the muscle fiber thereby facilitating a quicker response time. A surface potential would only release Ca^{2+} at the surface

of the fiber and it would take the Ca^{2+} ions >1000 times longer to reach the center of the fiber by diffusion through the cytosol than it would take the action potential traveling down the t-tubule membrane and releasing Ca^{2+} deep in the fiber.

A t-tubule encircles each sarcomere as it passes from one myofibril to the next. Along the length, the t-tubule is flanked by two terminal cisternae forming an intracellular junction called a triad (Franzini-Armstrong et al. 1999) (see **Figure 1.8**).

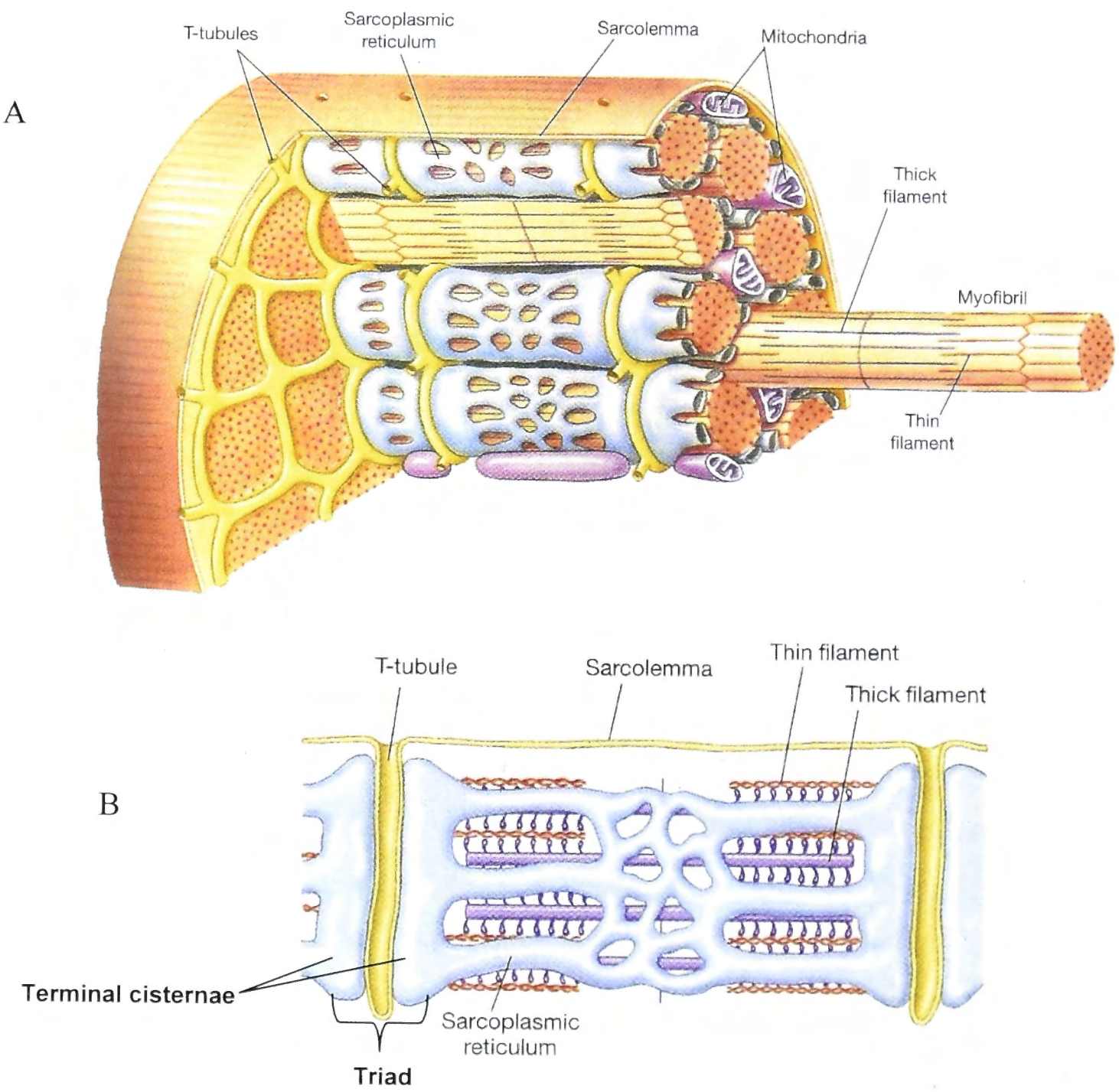

Figure 1.8: T-tubular network and sarcoplasmic reticulum (SR). (**A**) The t-tubular network and sarcoplasmic reticulum in relation to the other internal structures of the muscle fiber. (**B**) A closer view of the arrangement of the t-tubular network and the SR. Adapted from (Silverthorn 1998).

1.3.4.1 Calcium release units

The t-tubule flanked by two terminal cisternae, as mentioned above, is referred to as a triad, but that is not the only configuration between the t-tubules and SR. Sometimes the t-tubule is associated with only one terminal cisterna, in which case, the junction is referred to as a dyad. When the SR forms a junction between the SR and the surface membrane, it is referred to as a

peripheral coupling. Triads, dyads and peripheral couplings are functionally equivalent and they are collectively referred to as calcium release units (CRUs) (Franzini-Armstrong et al. 1999). In developing muscle and in the myotendinous junction of adult muscle fibers, pentads and heptads (two or three t-tubule elements with three or four elements of terminal cisternae closely alligned) can also be found (Yamashita et al. 2007). So CRUs are formed by apposed junctional domains of the sarcoplasmic reticulum and of t-tubules or sarcolemma. In skeletal muscle, the most common CRU is the triad. The CRU is essential for muscle function as it is the site of one of the steps in excitation contraction coupling (EC coupling) – the rapid release of calcium from the calcium store (SR) in response to the depolarization of the sarcolemma and t-tubules (Franzini-Armstrong 1973; Franzini-Armstrong and Jorgensen 1994; Flucher and Franzini-Armstrong 1996; Protasi et al. 1998; Franzini-Armstrong et al. 1999). The process of EC coupling will be discussed in further detail in Section 1.4.2.

The electron micrograph of a triad showed in **Figure 1.9** clearly shows the two terminal cisternae flanking the t-tubule in the center. There are also darker structures visible that span the gap between the t-tubule and the terminal cisternae (indicated by arrows). These darker structures were first referred to as foot structures but have since been shown to be the cytoplasmic assembly of the ryanodine receptor (RyR) (Kawamoto et al. 1986; Campbell et al. 1987; Imagawa et al. 1987; Inui et al. 1987b; Lai et al. 1988). The RyR will be discussed in more detail in Section 1.5

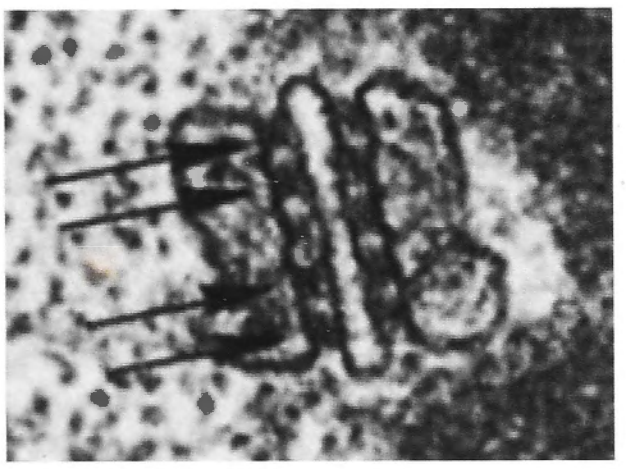

Figure 1.9: Electron micrograph of muscle from the hind legs of *Rana pipiens* showing the triad. Arrows indicate foot structures - adapted from (Franzini-Armstrong 1973).

The RyR is one of many proteins involved in EC coupling. The depolarization of the t-tubular membrane has to be communicated to the RyR is some way. For this purpose the RyR1 has recruited a voltage sensor in the t-tubular membrane in the form of an L-type voltage gated Ca^{2+} channel, the dihydropyridine receptor (DHPR). In skeletal muscle the communication between the DHPR and the RyR is a physical interaction with the signal communicated via conformational changes in the proteins. The DHPR will be discussed in more detail in Section 1.6.

A further term used to describe this system is the "couplon". A couplon is defined as a functional grouping of RYRs and DHPRs (and other SR proteins) which may act in concert during EC coupling. (Rios and Stern 1997; Stern et al. 1997). With this definition, a triad contains two couplons (one on either side of the t-tubule) and dyads and peripheral couplings are made up of one couplon.

During development the formation of CRUs, the close association between SR and t-tubules/sarcolemma, referred to as docking, is the first step (Franzini-Armstrong 2010). Small SR cisternae are docked at the sarcolemma before RyRs and DHPRs are detectable (Franzini-Armstrong et al. 1991). There is evidence that the docking protein junctophilin is directly involved in this process (Takeshima et al. 2000). Docking occurs without the presence of any of the following proteins; RyR1 (Takekura et al. 1995a), DHPR (Flucher et al. 1993; Felder et al. 2002), calsequestrin (Knollmann et al. 2006), triadin (Shen et al. 2007) and junctin (Franzini-Armstrong 2010). Docking is an essential step for the assembly of CRUs in skeletal muscle, in the absence of junctophilin, expression of RyR1 and DHPR is not sufficient to form CRUs (Takekura et al. 1995b).

Although the RyR and DHPRs have to be in close proximity to each other in order to interact, as shown above, each does not require the presence of the other to be retained in the CRUs. Another protein, perhaps junctophilin, must trap them within the CRU once they reach the site (Franzini-Armstrong 2010). Once within the CRU, the component proteins cluster into their characteristic assemblies.

In mammalian skeletal muscle, the junctional gap is occupied by two rows of feet (RyR1s) therefore every foot has a side that faces the junctional gap and one facing the myofibrils (Franzini-Armstrong et al. 1999). Two geometrical factors are constant in all types of CRUs, the size of the junctional gap separating the SR from the t-tubule/sarcolemma (approximately the size of the foot) and the tight ordered clustering of feet. In skeletal muscle the RyRs are arranged in a tetragonal disposition with a center-to-center distance of about 29nm. (Ferguson et al. 1984; Block et al. 1988; Saito et al. 1988; Franzini-Armstrong et al. 1999)

1.3.4.2 The arrangement of RYRs and DHPR in the CRUs

RyR1s, as stated above, form a two-rowed regular array in the CRUs with their corners overlapping. In skeletal muscle, the DHPRs are clustered into groups of four DHPRs (tetrads) overlaying every other RyR1 (see **Figure 1.10**) (Ferguson et al. 1984; Block et al. 1988; Franzini-Armstrong and Kish 1995; Serysheva 2004). The four DHPRs making up the tetrad are arranged in such a way that they correspond to the four subunits of the RyR1. The fact that

tetrad formation is unique to skeletal muscle provides structural evidence supporting the mechanical nature of interaction between the DHPR and RyR1 during EC coupling (Block et al. 1988). Even though the RyR is not involved in targeting the DHPR to the CRU, tetrads only form in the presence of RyR1, suggesting that anchoring to RyR1 is necessary for positioning DHPRs into tetrads (Protasi et al. 1998).

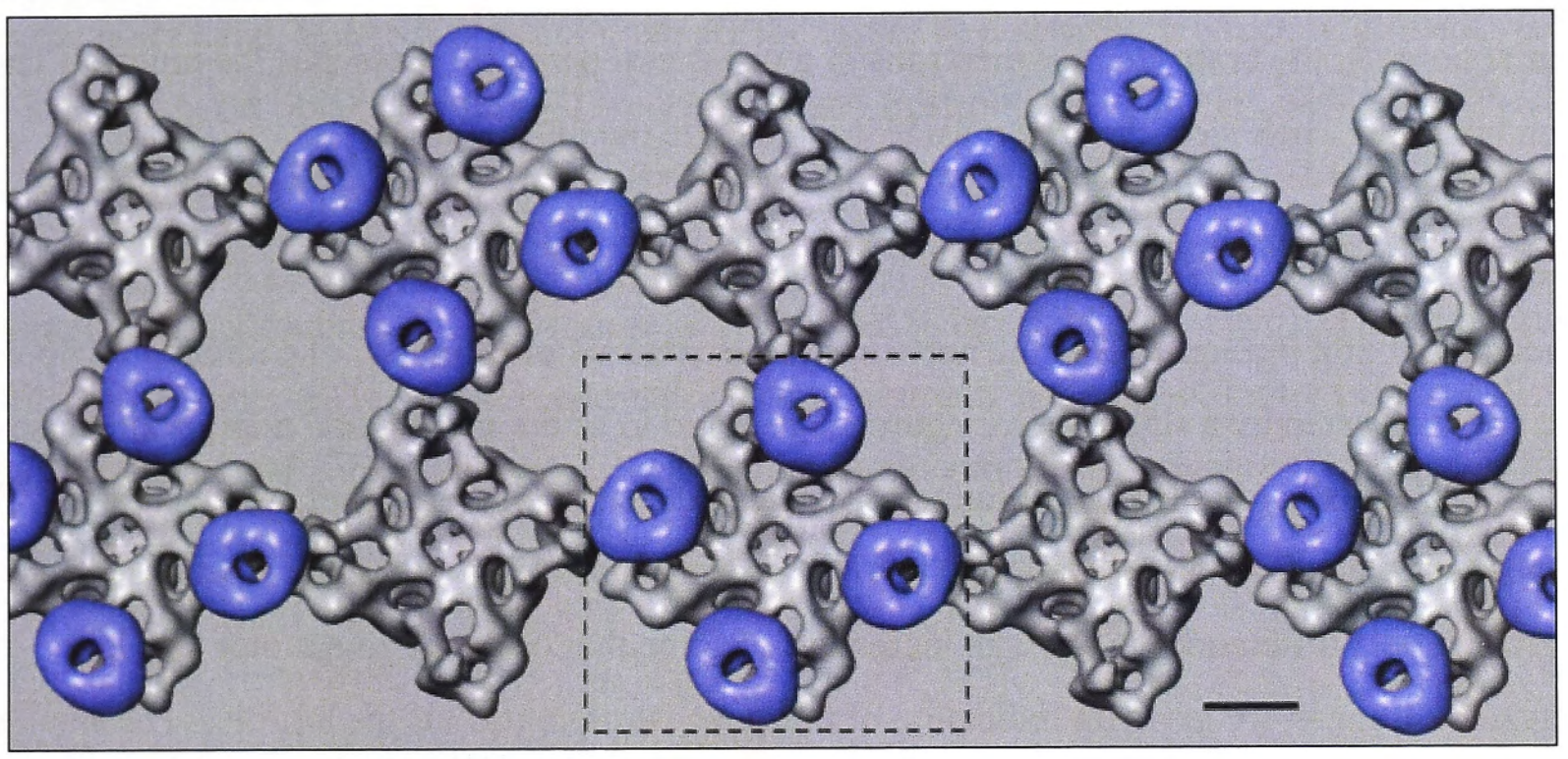

Figure 1.10: Model of physical coupling between RyR1 and DHPR in skeletal muscle based on freeze-fracture studies and using 3D reconstruction of two Ca^{2+} channels, generated by electron cryomicroscopy and single particle reconstruction. The model shows two arrays of RyRs overlaid by arrays of DHPRs grouped into tetrads. The scale bar represents 100Å. From (Serysheva 2004).

How the RyRs that are not associated with DHPRs are activated during EC coupling is still not fully understood. One theory is that the Ca^{2+} released from the RyRs that are associated with the DHPRs activate the unassociated RyRs through a calcium induced calcium release (CICR) mechanism. There are, however, a few problems with this theory as the rate of Ca^{2+} release by CICR under physiological conditions is too low. This will be discussed in more detail in Section 1.4.2 that deals with EC coupling. Another theory involves the coordinated activities of multiple channels possibly though coupled gating. Coupled gating describes the simultaneous opening and closing of multiple RyR channels (Marx et al. 1998; Lehnart et al. 2003) that occurs through their physical contact at their corners and seems to be facilitated by FKBP12 (see **Figure 1.10** and Section 1.4.2 and 1.5.3.2).

1.4 Physiology of skeletal muscle fibers

1.4.1 The motor unit and neuromuscular junction

1.4.1.1 The motor unit

Every muscle is served by a motor nerve, which in turn consists of axons of up to hundreds of motor neurons whose cell bodies are clustered in a motor nucleus in the spinal cord or brain stem. The axon of each motor neuron exits the spinal cord through the ventral root or through a cranial nerve in the brain stem. It then runs in a peripheral nerve till it reaches the muscle. The axon branches when it reaches the muscle, to innervate the muscle fibers.

A motor unit consists of a motor neuron and the muscle fibers it innervates. It is the basic fundamental unit through which the nervous system controls movement. The number of fibers that are innervated by a single motor neuron is referred to as the innervation number. It varies with muscle type and function. In human skeletal muscle the range for average innervation number stretches from 5 (eye muscles) to 1800 (leg muscles). Differences in innervation number reflect differences in average increment of force that occur when a motor unit is activated. It therefore gives an indication of the fineness of control of the muscle. The smaller the innervation number, the finer the control achieved by varying the number of motor units activated. The muscle fibers of a single motor unit are distributed throughout the muscle and fibers from different motor units are therefore intermingled. When a motor neuron transmits an action potential, all the muscle fibers it innervates contract and because they are spread throughout the muscle, it causes a weak contraction of the entire muscle.

The force exerted by a muscle depends on the number of motor units activated, but it also depends on the properties of the active motor units. The relevant properties are:

- Contraction speed
- Maximal force
- Fatigability

These properties are assessed by examining the time course and force exerted by individual motor units in response to the number and rate of action potentials evoked.

A motor unit's response to a single action potential is referred to as a twitch (as is the response of one or all fibers in the muscle to one electrical stimulus) and the time it takes for the twitch to reach its peak force is the contraction time. The contraction time is measure of the contraction speed of fibers that make up a motor unit. A slow-twitch motor unit has a long contraction time (e.g. 38ms in rat soleus muscle) and fast-twitch motor units have a shorter contraction time (e.g. 12ms in rat extensor digitorum longus, EDL muscle) (Close 1967). A rapid series of

action potentials cause overlapping twitches and is known as a tetanic contraction or tetanus. The force exerted during tetanus depends on the extent that the twitches overlap and summate and the innervation number. The force varies with the contraction time of the motor units involved as well as the frequency of the action potentials. Maximal force is reached at different action potential frequencies for fast- and slow-twitch motor units. Slow-twitch motor units produce small forces (e.g. 2.34-3.53N in rat soleus) (Larsson and Edstrom 1986), but are resistant to fatigue. These motor units are the first to be activated during voluntary contraction. On the other hand, fast-twitch motor units are the last to be activated, produce large forces (e.g. 11.9-15.0N in rat tibialis anterior - TA) (Larsson and Edstrom 1986) and are easy to fatigue. In a study of human motor units in toe extensors (EDL, extensor hallucis longis- EHL, extensor digitorum brevis – EDB) contraction forces of 6.3-78.1 mN were measured as well as an average contraction time of 74ms (range of 50-107ms) (Macefield et al. 1996). The order in which motor units are recruited is correlated with motor unit size (size of motor neuron cell body, diameter and conducting velocity of motor neuron axon and amount of force muscle fibers can exert).

1.4.1.2 The neuromuscular junction

The branches of the axons from the motor neurons that form the motor units end in a number of terminals, each of which forms an elliptical neuromuscular junction (NMJ) along the surface of a single muscle fiber. Each muscle fiber has only one NMJ located approximately midway along its length. The axon terminal and muscle fiber are about 50nm apart, separated by the synaptic cleft and are situated in a shallow depression in the sarcolemma. At this point, the sarcolemma is further invaginated into deep and regular folds, called post-junctional folds. The motor nerve terminal is specialized for the neurotransmitter, acetylcholine (ACh), release. Within the axon terminal are synaptic vesicles containing ACh that cluster adjacent to specialized structures of the presynaptic membrane, called active zones. ACh receptors are highly concentrated, with a density of about 12000 receptors per μm^2 (Shigemoto et al. 2010), close to the outermost part of the post-junctional fold. When the nerve impulse reaches the axon terminal, depolarization opens voltage gated Ca^{2+} channels on the presynaptic membrane, which triggers the fusion of the synaptic vesicles with the presynaptic membrane and the release of ACh into synaptic cleft. ACh binds to ACh receptors on sarcolemma, which triggers depolarization of sarcolemma. A layer of connective tissue called basal lamina sheaths each muscle fiber and contains the enzyme acetylcholinesterase. After ACh binds to receptors, its effects are terminated by its enzymatic breakdown by acetylcholinesterase to acetate and choline. This prevents continued muscle fiber contractions in absence of additional nerve stimulation.

The binding of ACh to its ligand gated ACh receptors opens the ion channel which is permeable to a number of cations including Na^+ and K^+. When the ACh receptor opens, the resting membrane potential (-70 to -90mV) is close to the K^+ equilibrium potential (-98mV) and far from the Na^+ equilibrium potential (+67mV) and therefore the biggest driving force is on Na^+ ions which move down their concentration gradient into the muscle fiber causing a local and transient depolarisation of the sarcolemma. Initially the depolarization is a local event (end plate potential) but when depolarization reaches a threshold, an action potential is invoked which spreads in all directions across from the NMJ across the sarcolemma, opening voltage gated Na^+ channels in adjacent areas of the sarcolemma and down the t-tubules. The Na^+ channels inactivate and voltage gated K^+ channels open allowing K^+ to flow down its concentration gradient out of the fiber, reducing the membrane potential to a value near the K+ equilibrium potential (repolarization). The repolarization occurs untill the resting membrane potential is restored, after which, the Na^+/K^+ ATPase pump restores the ionic concentrations to resting levels by exchanging Na^+ inside the fiber for K^+ outside the fiber.

1.4.2 Excitation contraction coupling

The term EC coupling refers to the process whereby an action potential travelling along the sarcolemma and down the t-tubular membrane is converted into cross-bridge cycling and contraction of the muscle. However, it is also used more narrowly to describe the process occurring between sarcolemmal depolarization and Ca^{2+} release from the SR. Central to this process is the functional interaction between the DHPR in the t-tubular membrane and the RyR in the membrane of the SR. EC coupling differs in skeletal muscle and in cardiac muscle.

1.4.2.1 Skeletal muscle excitation contraction coupling

When the action potential is propagated along the sarcolemma and down the t-tubules, the change in the electrical field across the membrane caused by the movement of Na+ ions across the membrane causes the five to six positively charged residues that make up the voltage sensor in the DHPR to move outward under the influence of this electric field (Schneider and Chandler 1973; Rios and Brum 1987; Tanabe et al. 1987; Numa et al. 1990; Serysheva 2004; Catterall 2011). The movement of the charged residues causes a conformational change that is somehow relayed to the RyRs via a physical interaction (Tanabe et al. 1988; Numa et al. 1990; Paolini et al. 2004; Catterall 2011). The DHPR is a functional Ca^{2+} channel in itself and the charge movement within this molecule changes, allowing the ion channel pore to enter an open state and Ca^{2+} to enter the muscle fiber. This Ca^{2+} influx across the sarcolemma is small and very slow (Lamb and Walsh 1987; Field et al. 1988) and it is not necessary for EC coupling in adult vertebrate skeletal muscle (Rios and Pizarro 1991; Dulhunty 1992; Melzer et al. 1995). In fact skeletal type EC coupling can occur in the absence of extracellular Ca^{2+}. Interestingly, neonatal

vertebrate skeletal muscle is more like cardiac muscle as it requires the inflow of Ca^{2+} for full contraction (Dangain and Neering 1991; Melzer et al. 1995). The physical interaction between the DHPR and the RyR (discussed in more detail in Section 1.6) activates the RyR, which allows Ca^{2+} to be released into the cytoplasm resulting in muscle contraction (see Section 1.4.2). The Ca^{2+} released into the sarcoplasm is pumped back into the SR by the sarcoplasmic, endoplasmic Ca-ATPase (SERCA) that is located in the SR membrane. This lowers the cytoplasmic Ca^{2+} level allowing relaxation of the muscle fiber (see **Figure 1.11**).

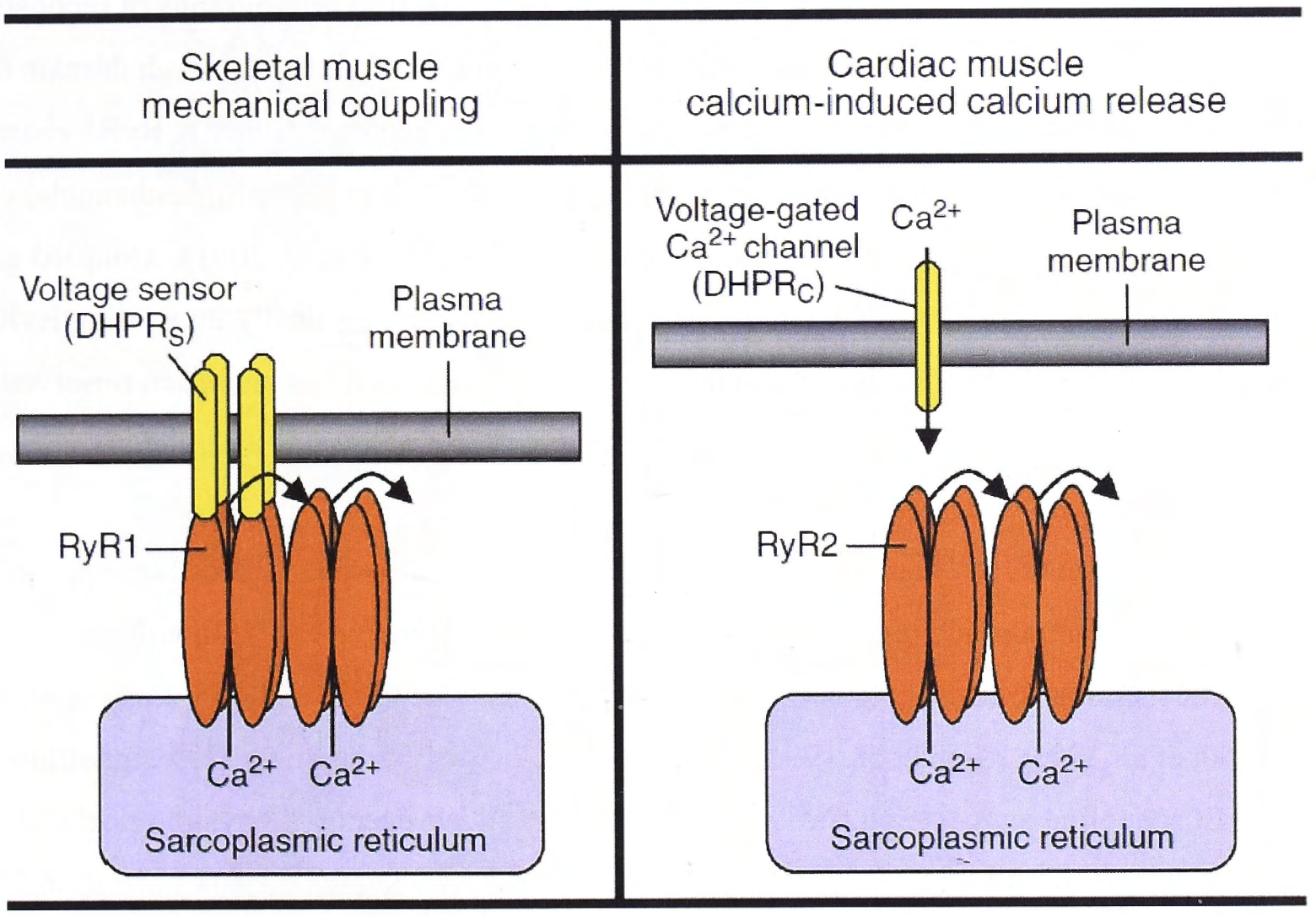

Figure 1.11: A comparison between EC coupling in skeletal and cardiac muscle. In skeletal muscle (left panel), the DHPR sense the sarcolemmal depolarisation and transmit a conformational change to the RyR1 causing the channel to open and release Ca^{2+} from the SR. Ca^{2+} influx through the DHPR is not required. RyR1 channel snot associated with a DHPR tetrad may either be activated by Ca2+ release from a neighbouring RyR1 or, more likely, by transmission of the conformational change through physical interactions between RyR1 within the array. In cardiac muscle (right panel), DHPRs are activated by sarcolemmal depolarization and allow Ca^{2+} influx into the cytoplasm. The Ca^{2+} entering the cell activate RyR2 channels allowing Ca^{2+} release from the SR. Neighbouring RyR2 channels may in turn be activated by Ca^{2+} flowing from the SR (Zissimopoulos and Lai 2007).

The RyR and DHPR, as mentioned in Section 1.3.4.2, are arranged in a very ordered way in the skeletal muscle CRUs. The DHPR forms tetrads and associates with every other RyR1 in the CRU. The mechanism whereby the RyRs that are not associated with a DHPR tetrad are activated during EC coupling remains unclear with CICR as one possible theory and another theory that of a physical coupling between RyR1 at the overlapping corners in the array. Ca^{2+} release induced by the direct action of Ca^{2+} through the voltage activated RyR1channel on neighbouring channels does not seem to significantly contribute to Ca^{2+} release during EC coupling as the rate of Ca^{2+} released by CICR under physiological conditions is too low (Endo

1984; Endo 2009). RyR inhibition by physiological 1mM concentrations of Mg^{2+} also provides a stumbling block for CICR as Mg^{2+} inhibition is maintained in the presence of activating Ca^{2+} concentrations (Meissner 1994). The relief of Mg^{2+} inhibition is suggested as a fundamental part of EC coupling in response to signal transmission from the DHPR to RyR in skeletal muscle (Endo 1985; Lamb and Stephenson 1990; Lamb and Stephenson 1991). There is also evidence that Ca^{2+} activation of the RyR1 is not necessary for the initiation of skeletal type EC coupling (O'Brien et al. 2002). Therefore the transmission of the EC coupling activation signal from the DHPR-associated RyR1s to their neighbouring DHPR-unassociated RyR1s probably occurs through a physical coupling. Image processing of electron micrographs of reconstituted RyR1 arrays in vitro showed that adjacent RyR1 tetramers are interlocked though domain 6 located at the corner of the clamp region (see Section 1.5.1) (Yin et al. 2005a). RyR1 channel recordings in lipid bilayer experiments show synchronous openings of multiple channels, which suggests the occurrence of coupled gating (Marx et al. 1998; Marx et al. 2001). Coupled gating is consistent with intermolecular interactions occurring between physically interacting RyR1s in lipid bilayers. Coupled gating is not a unique feature of RyRs, as it has also been observed in IP_3R (Dargan et al. 2002) and KcsA potassium channels (Molina et al. 2006).

Ca^{2+} sparks are small, brief and highly localized releases of Ca^{2+} which can occur spontaneously, but at much higher frequencies during depolarisation and with voltage dependence similar to that of the activation of Ca^{2+} release (Baylor et al. 1983; Pape et al. 1995; Tsugorka et al. 1995; Klein et al. 1996). Numerous studies of intracellular Ca^{2+} signalling during EC coupling suggest that Ca^{2+} sparks are the basic unit events of physiological Ca^{2+} release (Cheng et al. 1993; Cannell et al. 1995; Klein et al. 1996). Each spark corresponds to a multiple RyR1-channel opening event and appears to have a preferred amplitude. This suggests that Ca^{2+} sparks involve a cohort of a specific number of RyR channels opening and closing in a coordinated synchronous manner (Gonzalez et al. 2000; Rios et al. 2001).

The proposed mechanism for coordinated activation of adjacent RyR1s in an array involves the following (see **Figure 1.12**) (Yin et al. 2005a; Yin et al. 2008). At rest, the DHPRs and RyR1 are in the closed conformation. Upon depolarization of the sarcolemma and t-tubular membrane, there is a simultaneous movement of charge in the four DHPRs in one tetrad. The DHPR charge movement is transmitted to the directly associated RyR1 and induces a conformational change and activation of the RyR1. This activation is transmitted to the RyR1s that are physically coupled to the activated RyR1 in the array, inducing them to open synchronously. In this way, a single DHPR tetrad would be able to activate five RyRs synchronously (the RyR1 associated with the DHPR and the four surrounding RyRs in the array), which is consistent with the proposed four to six activated RyRs requires to generate a single Ca^{2+} spark (Gonzalez et al. 2000; Rios et al. 2001).

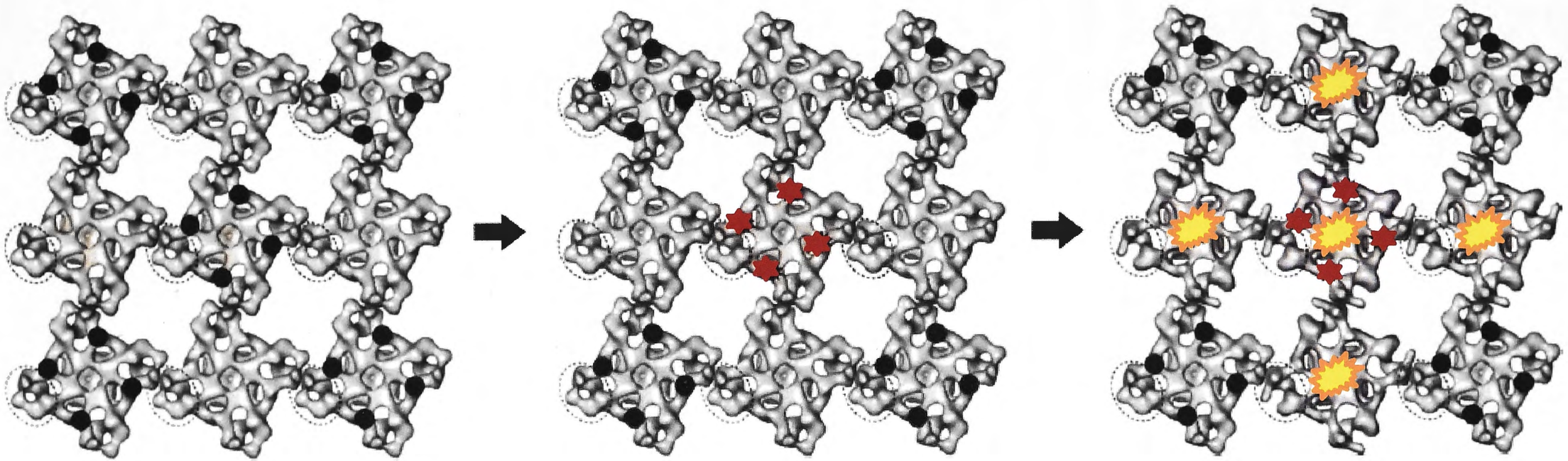

Figure 1.12: Proposed mechanism of activation of Ca^{2+} release during a Ca^{2+} release event in skeletal muscle. In the resting state, the DHPRs (group of four black filled circles) and RyRs are in the closed state (left panel). Upon depolarization of the sarcolemma, one tetrad is activated (group of four red stars) to produce a conformational change (middle panel). The DHPR conformational change is transmitted to the RyR1 associated with the tetrad through a physical interaction and induces a conformational change and activation in the RyR1 (yellow star). As the RyRs in the array are physically coupled, the conformational change would be instantly relayed to the neighbouring RyR1 that are not associated with a tetrad, inducing them to open synchronously (right panel). Adapted from (Yin et al. 2005a).

1.4.2.2 Cardiac muscle excitation contraction coupling

Cardiac EC coupling does not involve a physical interaction between the DHPR and the RyR. The activation of the cardiac isoform of the DHPR upon sarcolemmal and t-tubular membrane depolarization causes the Ca^{2+} channel pore to open, allowing Ca^{2+} to flow into the cytoplasm. The Ca^{2+} entering the cell binds to the RyR2 in the SR membrane , activating the RyR Ca^{2+} release channel and allowing Ca^{2+} to flow into the cytoplasm from the SR. There is approximately one-tenth as many DHPRs as RyR2s but that is all that is required to allow sufficient Ca^{2+} entry to activate all the RyR2s. The rise in cytoplasmic Ca^{2+} concentration activates the contractile proteins as with skeletal muscle. The Ca^{2+} is subsequently taken up into the SR by SERCA and extruded from the cell by the Na^{+}/Ca^{2+} exchanger on the sarcolemma, allowing the muscle to relax (Lamb 2000; Zissimopoulos and Lai 2007). Cardiac muscle CRUs are mostly diads (Franzini-Armstrong 1999) and although the DHPR and RyR2 are in close proximity to each other, the DHPRs do not form tetrads but are randomly distributed with respect to the RyR2 arrays (Carl et al. 1995a; Sun et al. 1995; Protasi et al. 1996). An opening of a single cardiac DHPR channel triggers the calcium release from 4-6 RyR2 channels (Wang et al. 2001) (see **Figure 1.11**).

1.4.3 Cross-bridge cycling

The sliding filament theory described in Section 1.3.3 relies on mechanical work performed by the globular myosin heads and requires ATP for energy. The binding of the myosin head to the actin filament forms a cross bridge and the sequence of detachment, activation and attachment of myosin heads to actin filaments is referred to as cross-bridge cycling. Cross-bridge formation (attachment of myosin heads to actin) requires Ca^{2+}. The active (myosin-binding) sites on the actin filament in a relaxed muscle fiber, when intracellular levels of calcium ions are low, are physically blocked by tropomyosin molecules. As Ca^{2+} levels rise, the ions bind to regulatory sites on troponin. Each troponin molecule can bind up to four Ca^{2+} ions. To allow availability of the active sites on the actin filament, troponin C must bind two calcium ions, change shape, and then roll tropomyosin into the groove of the actin helix, away from the myosin binding sites. Once binding sites on actin are exposed, cross bridge cycling can occur. Cross-bridge cycling is the series of events during which myosin heads pull thin filaments toward the centre of the sarcomere. Before the myosin head can bind to actin it binds to ATP. The ATPase activity of the myosin head cleaves the ATP but leaves the resulting ADP and phosphate ion (P_i) bound to the head. In this state, the head extends perpendicular toward the actin filament ready to bind to the active sites on actin. Cross bridge cycling involves the following steps:

- Step 1: *Cross bridge formation* – the energized myosin head attaches to actin myofilament, forming a cross bridge.

- Step 2: *The power stroke* – ADP and P_i are released and the myosin head pivots and bends, changing to its bent, low energy shape. This results in the actin filament sliding toward the M line.
- Step 3: *Cross bridge detachment* – After a new ATP molecule attaches to the myosin at the site where ADP was released, the link between myosin and actin weakens, and the myosin head detaches (the cross bridge "breaks").
- Step 4: *Cocking of myosin head* – As ATP is again hydrolysed to ADP and Pi, the myosin head returns to its pre-stroke high-energy or "cocked" position ready to bind to actin once more.

Cross-bridge cycling and thus the sliding of the thin filament continues as long as the calcium signal and enough ATP are present. The force that a muscle fiber can exert depends on the number of cross-bridges formed and also the force produced by each cross-bridge. Both factors are influenced by the Ca^{2+} concentration in the cytoplasm, the amount of overlap between the thick and thin filaments and the velocity with which the filaments slide over each other. The release and uptake of Ca^{2+} in response to a single action potential occurs so quickly that there is not enough time for all the potential cross-bridges to form and therefore only some of them are formed. The peak force of a twitch is less that the maximal force of the muscle for this reason. Maximal force can be achieved only when a series of action potentials sustains the Ca^{2+} concentration in the cytoplasm, allowing for maximum cross bridge formation.
When SERCA pumps the Ca^{2+} from the cytoplasm into the SR, troponin changes back to its original shape and tropomyosin moves back over the active sites, blocking them from myosin. The contraction ends and the muscle fiber relax. Contracting muscle routinely shortens by 30-35% of its total resting length, so each myosin cross bridge attaches and detaches many times during a single contraction and the actin filament does not slide backwards because there are always some myosin heads attached to actin.

1.5 The ryanodine receptor

Structures were observed in skeletal muscle in the early 1970s in electron micrographs as large electron dense masses (feet) spanning the junctional gap between the SR membrane and the t-tubules (Franzini-Armstrong 1973) were later found to be RyRs. Intact RyR molecules were isolated and purified in skeletal muscle and the purified receptors incorporated into lipid bilayers as functional Ca^{2+} channels with characteristics identical to the Ca^{2+} release channels previously identified in the heavy SR (Kawamoto et al. 1986; Campbell et al. 1987; Imagawa et al. 1987; Inui et al. 1987b; Lai et al. 1987; Lai et al. 1988). The RyR gained its name because the plant alkaloid Ryanodine, found in the *Ryania speciosa*, a plant from Central and South America, binds to it very specifically.

Three isoforms of RyR are expressed in mammals: RyR1, RyR2 and RyR3. RyR1 was first detected in skeletal muscle (Takeshima et al. 1989; Zorzato et al. 1990), RyR2 in cardiac muscles (Nakai et al. 1990; Otsu et al. 1990) and RyR3 was found in the brain (Hakamata et al. 1992). They are each encoded by a distinct gene (RYR1, RYR2 and RYR3), residing on three different chromosomes. RYR1 is located on chromosome 19q13.2 and spans 104 exons, RYR2 is located on chromosome 1q43 and spans 102 exons and RYR3 is located on chromosome 15q13.3-14 and spans 103 exons (Lanner et al. 2010). The three mammalian isoforms share about 70% homology (Hakamata et al. 1992) with the highest sequence identity present in the carboxy-terminal end (Hakamata et al. 1992; Zissimopoulos and Lai 2007). Three major regions of diversity are termed D1-3. D1 lies between residues 4254 and 4631 in the skeletal sequence, D2 between residues 1342 and 1404 and D3 between residues 1872 and 1923. D2 is essential for the mechanical interaction between RyR1 and DHPR (Sorrentino and Volpe 1993; Yamazawa et al. 1997; Perez et al. 2003b).

RyR1 is predominantly expressed in skeletal muscle (Takeshima et al. 1989; Zorzato et al. 1990) but is also found in smooth muscle (Neylon et al. 1995) stomach, kidney, thymus (Nakai et al. 1990), cerebellar Purkinje cells, adrenal glands, ovaries and testis (Marks et al. 1989; Takeshima et al. 1989; Furuichi et al. 1994; Giannini et al. 1995; Ottini et al. 1996) as well as B-lymphocytes (Vukcevic et al. 2010). RyR2 is predominantly expressed in cardiac muscle (Nakai et al. 1990; Ottini et al. 1996), but is also found to be the predominant isoform in the brain (Kuwajima et al. 1992; Lai et al. 1992a; Nakanishi et al. 1992; Sharp et al. 1993; Furuichi et al. 1994). RyR2 is also found in the stomach, kidney, adrenal glands, ovaries, thymus and lungs(Giannini et al. 1995). RyR3 is more widely expressed including in hippocampal neurons, thalamus, Purkinje cells, corpus striatum (Hakamata et al. 1992; Lai et al. 1992a; Furuichi et al. 1994), skeletal muscle (Marks et al. 1989) (especially during development (Conti et al. 2005; Perez et al. 2005) and in the adult diaphragm), smooth muscle cell of the coronary vasculature, lung, kidney, ileum, jejunum, spleen, stomach, uterus, ureter, urinary bladder and oesophagus (Giannini et al. 1992; Hakamata et al. 1992; Giannini et al. 1995; Neylon et al. 1995; Ottini et al. 1996).

Non-mammalian vertebrate (birds, amphibians, reptiles, fish) skeletal muscle contain two RyR isoforms referred to as α and β (Airey et al. 1990; Olivares et al. 1991; Lai et al. 1992b; Murayama and Ogawa 1992; O'Brien et al. 1993). The β-isoform is homologous to RyR3 and the α-isoform to RyR1 (Oyamada et al. 1994; Giannini et al. 1995; Conti et al. 1996). The RyR1 and RyR3 isoforms (α and β) are present in equal amounts in non-mammalian skeletal muscle with both isoforms found in the triads (Airey et al. 1990; Olivares et al. 1991; Lai et al. 1992b). Although RyR3 is present in mammalian skeletal muscle and found in the triadic

microsomal fraction, it is present at a 20- to 50-fold lower concentrations (Ledbetter et al. 1994; Giannini et al. 1995; Takeshima et al. 1995; Conti et al. 1996).

1.5.1 Structure

The RyR is the largest known ion channel, with four subunits of about 500kDa, it forms a homotetramer of about 2MDa. Because of its size and the fact that it is a membrane bound protein, a detailed atomic three dimensional structure is not available and the protein awaits crystallization. The structural information about the RyR that is available has been obtained with the use of cryo-electron microscopy (EM) (Radermacher et al. 1994; Serysheva et al. 1995; Jeyakumar et al. 1998; Sharma et al. 1998; Wagenknecht and Samso 2002; Samso et al. 2005; Serysheva et al. 2005; Samso et al. 2006; Serysheva et al. 2008; Hamilton and Serysheva 2009; Samso et al. 2009), comparative modelling (Welch et al. 2004) and recently x-ray crystallography of sections of the RyR (Amador et al. 2009; Lobo and Van Petegem 2009; Tung et al. 2010).

The RyR has a quatrefoil or cloverleaf-shaped structure when seen from above (i.e. looking down from the t-tubule membrane) and seen from the side has a mushroom shape with the cytoplasmic assembly forming the "cap" (27nm x 27nm x 12 nm) and the "stalk" made up of the smaller square shaped transmembrane assembly measuring about 12 x 12nm where it attaches to the cytoplasmic assembly and with a length of around 7nm (see **Figure 1.13**). The quatrefoil structure arises from the symmetrical arrangement of the four subunits. The cytoplasmic assembly consists of 15 distinct domains (1, 2a, 2b, 3, 4, 5, 6, 7a, 7b, 8a, 8b, 9, 10, 11 and 12) per subunit that can be mapped onto morphological units called the clamp, handle, column and the central rim (see **Figure 1.14**). The clamp is found on the corners of the cytoplasmic assembly and is formed by domains 5, 7a, 7b, 8b, 9 and 10 from one subunit and domains 6 and 8a from the adjacent subunit. The clamps are connected through the handle that surrounded the central rim, which is connected to the transmembrane assembly via the column. The handle is formed by domains 3 and 4, the central rim by domains 1, 2a and 2b and the column by domains 11 and 12 (Serysheva et al. 2008). In between these domains are numerous cavities that facilitate interactions with solvent, small molecules and protein modulators. The molecule has the architecture of scaffolding that allows for mechanical linkage between the SR membrane and the t-tubules but also allow solutes (Ca^{2+}) to flow through it easily.

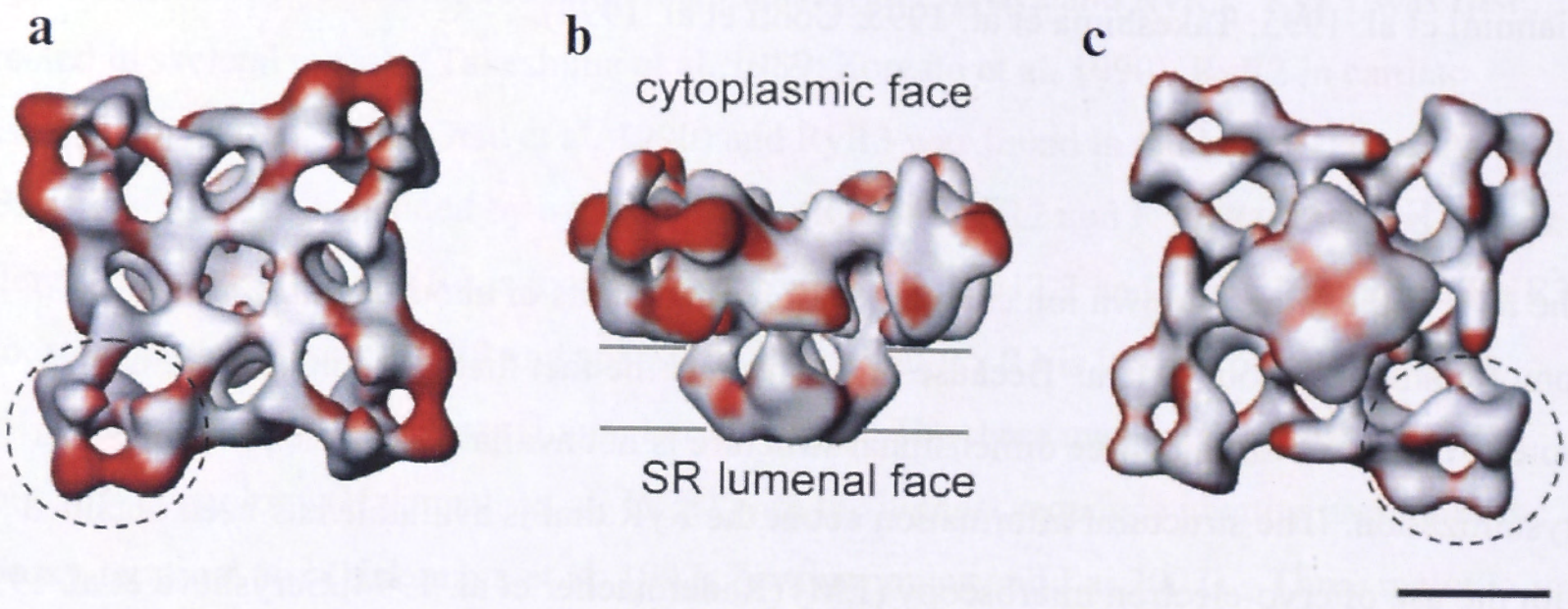

Figure 1.13: Three dimensional reconstruction of RyR1in the closed confirmation at a resolution of 25-30Å. Regions that differ between the open and closed states are shown in red. The structure is shown from the (a) top (view from cytoplasm), (b) the side view (b) and (c) from the bottom (view from the SR lumen). The dashed circles indicate the clamp regions. The scale bar represents 100Å. Adapted from (Serysheva 2004).

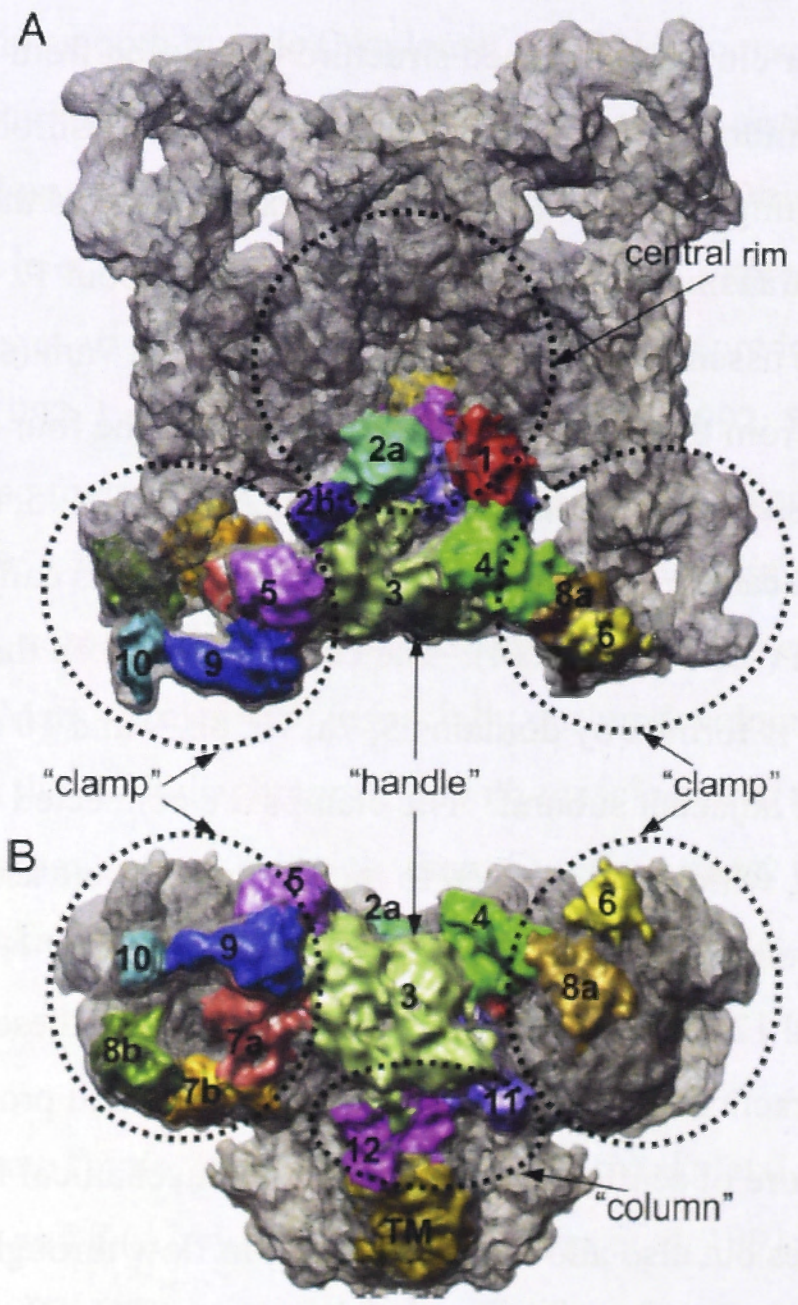

Figure 1.14: A 9.6Å resolution cryo-EM map of the RyR1 showing the numbering of the globular domains on the cytoplasmic assembly from (A) the top view (view from cytoplasm) and (B) the side view. The clamp, handle and column and central rim morphological units have also been indicated. (Serysheva et al. 2008)

The clamps undergo major conformational changes during the opening and closing of the channel (see **Figures 1.13 and 1.15**) (Serysheva 2004; Serysheva et al. 2008; Samso et al. 2009) and are likely to participate in inter molecular interactions between neighbouring RyRs (Yin et al. 2005a; Yin et al. 2005b; Yin et al. 2008). They are also the sites of interactions with modulators (Wagenknecht et al. 1994; Wagenknecht et al. 1996; Wagenknecht et al. 1997; Samso and Wagenknecht 2002; Samso et al. 2006; Sharma et al. 2006). The transmembrane domain also undergoes conformational changes during the opening and closing of the channels as to be expected. It seems to undergo dilation and constriction quite like a camera diaphragm (Serysheva et al. 1999). The transmembrane assembly is rotated at 4° with respect to the cytoplasmic assembly during the open conformation of the channel (Orlova et al. 1996; Serysheva et al. 1999; Sharma et al. 2000).

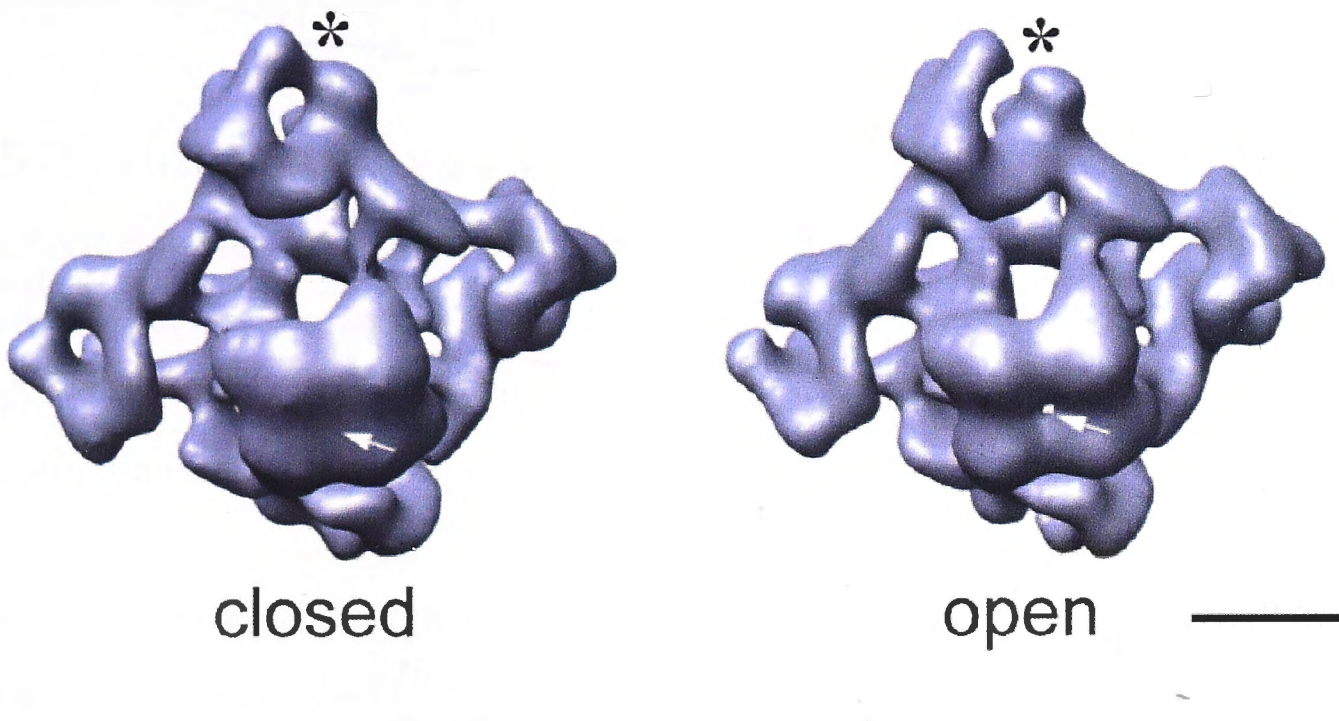

Figure 1.15: 3D reconstructions of the RyR1 in the closed (left) and in the open (right) stateat a resolution of 25-30Å. The clamp domains are marked with an asterisk and the presence and absence of a channel opening in the transmembrane regions with an arrow. The scale bar represents 100Å. (Serysheva 2004)

Hydropathy plots of the primary sequence of the RyR1 indicates a large hydrophilic N-terminal region, which corresponds to the cytoplasmic assembly, and a smaller mostly hydrophobic C-terminal region which corresponds to the transmembrane assembly and with a sequence that is the most conserved among the RyR isoforms (Takeshima et al. 1989; Nakai et al. 1990; Otsu et al. 1990; Zorzato et al. 1990; Hakamata et al. 1992; Tunwell et al. 1996). Two topology models, of 4 transmembrane (TM) (Takeshima et al. 1989) or 10TM segments (Zorzato et al. 1990), were first proposed. Since then a lot of experimental work has been done (Marty et al. 1994; Grunwald and Meissner 1995; Tunwell et al. 1996; Du et al. 2002; Du et al. 2004; Ludtke et al. 2005) and the latest model of the transmembrane topology is based on a revised 10TM model and can be seen in **Figure 1.16**. The RyR1 pore structure in the closed position resolved at 9.6Å (Ludtke et al. 2005) shows at least 5 α-helices within the membrane spanning region. The structure can be seen in **Figure 1.17**. Helix 1 is likely to correspond to M10 and was

assigned as the inner, pore-lining helix with the gating hinge, whereas helix 2 likely corresponds to M9 or pore loop and contains a sequence analogous to the selectivity filter in K^+ channels and is therefore possibly the selectivity filter for RyR1 (Ludtke et al. 2005).

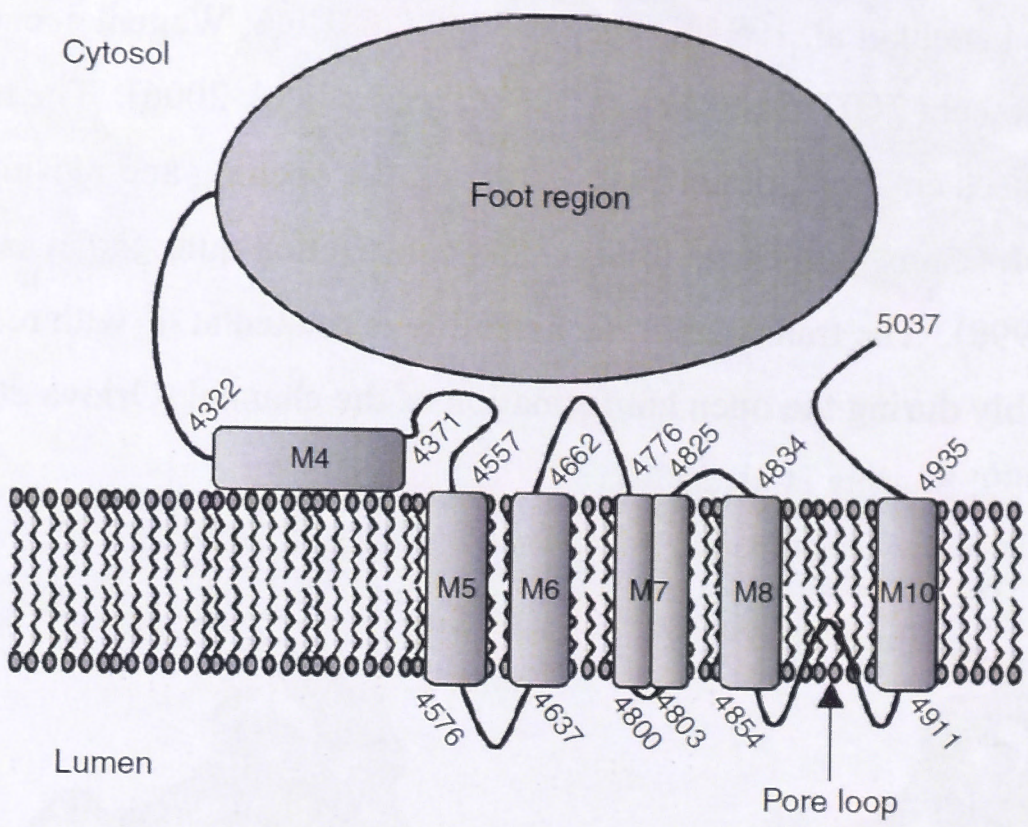

Figure 1.16: Model of the membrane topology of the RyR. The model is based on the 10TM model but revised with late experimental evidence. Hydrophobic sequences M5, M6, M8 and M10 span the membrane once. M7 is shown as a transmembrane hairpin and M4 resides parallel to the SR membrane on the cytoplasmic side. Hydrophobic domain M9 dips inside the lipid bilayer from the luminal side to form the pore loop and selectivity filter. The residues marked on the model correspond to rabbit RyR1. (Zissimopoulos and Lai 2007)

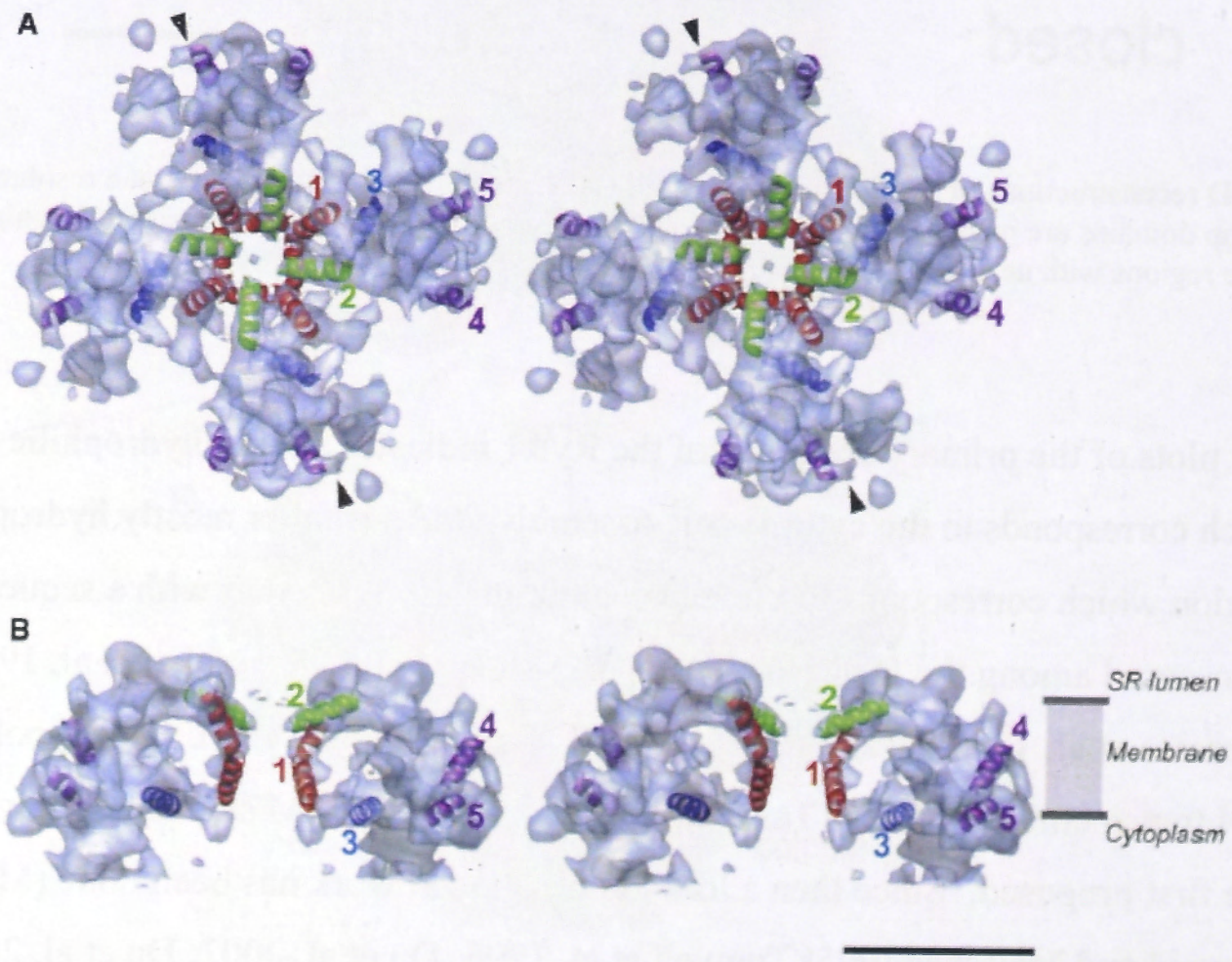

Figure 1.17: The putative helices in the RyR1 membrane spanning region at a resolution of 9.6Å. (A) Stereo view of the membrane spanning region view from the SR luminal side along the symmetry axis. The helices are shown in red (inner helix), green (pore helix), blue and purple. (B) Side view perpendicular to the symmetry axis showing two of the four subunits of RyR1 with annotated helices showing the relative positions of the putative α helices within the SR membrane. The scale bar indicates 50Å. (Ludtke et al. 2005)

The binding sites for two proteins that closely associates with the RyR and alter channel gating, namely calmodulin (CaM) and FKBP12 have been localized by cryo-EM. The differences in shape between the RyR1 by itself and bound to the proteins were used to identify the binding sites (Wagenknecht et al. 1997) and the results showed that both CaM and FKBP12 are situated further than 10nm away from the pore. This suggests that conformational changes can be transmitted over long distances between the binding sites and the channel pore.

Two studies have solved high-resolution crystal structures (2.5Å) of portions of the N-terminal region of the RyR1 (Amador et al. 2009; Tung et al. 2010). The first study crystalized the N-terminal 210 residues and the second study the N-terminal residues 1-559. The first 210 residues were found to adopt a β trefoil fold structure, and residues 1-559 were found to fold into three distinct domains that were arbitrarily termed A, B and C, forming a vestibule around the central rim of the channel.

1.5.2 Interactions with other proteins

The RyR serves as a scaffold for other proteins and cofactors and are often complexed with several accessory proteins to form an intricate multiprotein array. Apart from its interactions with the DHPR, the RyR's other binding partners include proteins such as FKBP12, calmodulin, junctin, triadin, calsequestrin and several kinases.

The interactions between the DHPR and the RyR1 will be discussed in the section dealing with the DHPR in more detail (Section 1.6).

1.5.2.1 FKBP12

FKBP stands for FK506 binding protein. The proteins form part of the immunophilin family of highly conserved proteins that bind immunosuppressive drugs like rapamycin and FK506. FKBPs are named according to their molecular weight and are expressed in most tissues. They are involved in a number of biochemical processes such as protein folding, receptor signalling, protein trafficking and transcription (Lanner et al. 2010). FKBP12 and FKBP12.6 have been shown to physically interact with all three isoforms of RyR, but they have different expression levels in different tissues (Chelu et al. 2004). FKBP12 is sometimes referred to as calstabin 1 and FKBP12.6 as calstabin 2. Both isoforms of FKBP have peptidyl-prolyl *cis-trans* isomerase activity and consists of 108 residues with 85% homology (Kay 1996). They have nearly identical structures as determined by X-ray crystallography (Michnick et al. 1991; Van Duyne et al. 1991; Deivanayagam et al. 2000). Co-immunoprecipitation and co-purification assays as well as GST-FKBP affinity chromatography have shown that RyR1 binds both FKBP12 and FKBP12.6 with similar affinities (Collins 1991; Jayaraman et al. 1992; Timerman et al. 1995;

Timerman et al. 1996; Qi et al. 1998). Because FKBP12 is more abundant in skeletal muscle, native RyR1 is isolated as a complex with mostly FKBP12.

FKBP12 binds to the RyR1 with a stoichiometry of four FKBP12 molecules to one RyR1tetramer with one FKBP12 molecule associated with each subunit of RyR1 (Jayaraman et al. 1992). Mutation analysis has shown three residues (Q3, R18 and M49) on FKBP12 to be important for the interaction with RyR1 (Lee et al. 2004a), but that isomerase activity is not necessary for the interaction with RyR1 (Timerman et al. 1995). The RyR1-FKBP12 interaction is a high affinity, conformation sensitive, interaction. Strong FKBP12 binding occurs when RyR1 is in its open state (Kd of about 1nM), but the RyR1's closed configuration enhances this binding even further (approximately 4-5 orders of magnitude) (Jones et al. 2005). The RyR1-FKBP12 interaction is unaffected by temperature or pH, but is sensitive to ionic strength (Mackrill et al. 2001). The binding site of FKBP12 to RyR1 has been visualized with cryo-EM along the edge of the of the cytoplasmic assembly on domain 3 in the handle region, about 12nm away from the channel entrance (Wagenknecht et al. 1997). A later study found two interaction sites between FKBP12 and RyR1 (Samso et al. 2006). A portion of the β-sheet of FKBP12 interacts with domain 9 and the intersection of domain 3, 5 and 9. Loop 87-90 of the FKBP12 molecule binds with domain 3 of RyR1 (see **Figure 1.18**).

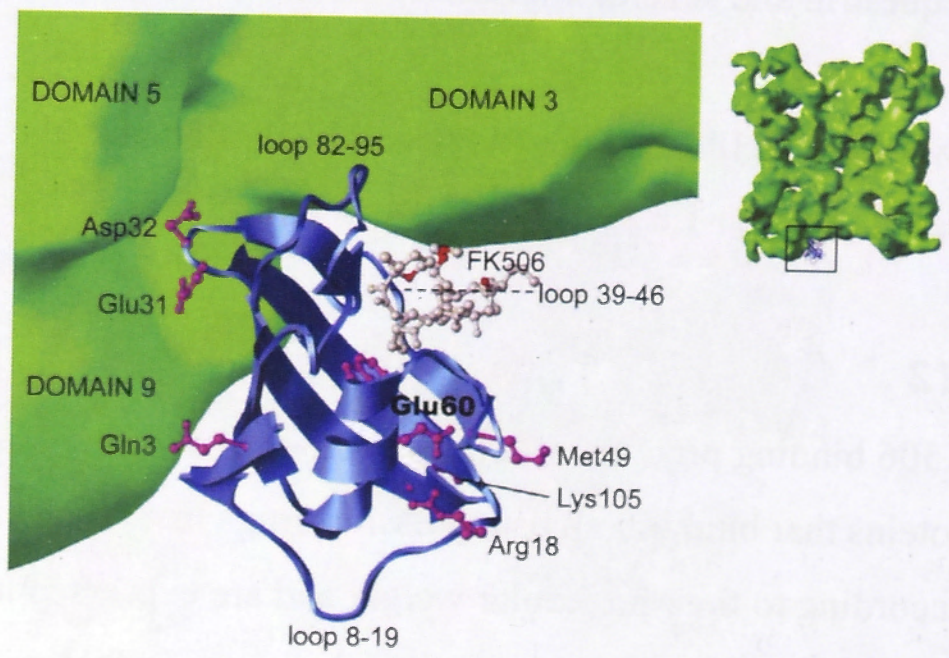

Figure 1.18: Detail of the proposed interaction between RyR1 and FKBP12. RyR1 (green) is shown with FKBP12 (blue) and FK506 (gray). Interaction with domain 3, 5 and 9 can be seen (Samso et al. 2006).

Functionally, FKBP12 stabilizes RyR1in the closed and open conformation. In the absence of FKBP12 channels show an increased open probability with extended openings to subconductance levels (partial openings to less than the full current amplitude) as well as increased sensitivity to Ca^{2+} or caffeine activation and reduced sensitivity to Mg^{2+} inhibition (Timerman et al. 1993; Ahern et al. 1994; Brillantes et al. 1994; Mayrleitner et al. 1994; Timerman et al. 1995; Ahern et al. 1997; Barg et al. 1997; Qi et al. 1998). The subconductance levels are multiples of ¼ of the total conductance of the channel which might indicate that the

subunits can act semi-independently, but coordinate to allow maximum current amplitude (Franzini-Armstrong and Protasi 1997).

The action of FKBP12 on RyR1 is thought to maintain RyR1 in the closed state at low cytosolic Ca^{2+} concentrations or after inactivation, and to stabilize the RyR1in a high conductance state during channel activation. This enables a steeply increasing and large cytosolic Ca^{2+} transient that is necessary for activation of contraction (Lehnart et al. 2003). An additional role for the FKBP12's regulation of RyR activity is that of the facilitation of coupled gating. Coupled gating is the simultaneous opening and closing of multiple channels as opposed to independent stochastic gating of channels (Lehnart et al. 2003). Coupled gating depends on the close special organization of RyR complexes and is suggested to occur only in the presence of FKBP12. This mechanism has been suggested as way in which the RyRs that are not associated with DHPRs can be activated during skeletal type EC coupling (Marx et al. 1998; Lehnart et al. 2003; Yin et al. 2005a; Yin et al. 2005b; Yin et al. 2008).

1.5.2.2 Calsequestrin, triadin and junctin

The efficiency of calcium release during EC coupling is dependent, among other things, upon the activity of RyR1 and the amount of calcium stored in the SR. These two factors, however, are interdependent because the amount of calcium in the calcium store affects the activity of the RyR1, partially through the action of the calcium binding protein, calsequestrin (CSQ), in the lumen of the SR (Beard et al. 2002; Beard et al. 2005; Wei et al. 2006) and the activity of the RyR1 in turn affects the level of calcium in the SR.

CSQ has high capacity and low affinity for Ca^{2+} which makes it an efficient Ca^{2+} binding and storage protein (MacLennan and Wong 1971; Ikemoto et al. 1972; Beard et al. 2009a). The binding of Ca^{2+} to CSQ effectively allows the total Ca^{2+} concentration in the SR to be in excess of 20mM, while the free Ca^{2+} concentration remains at around 1mM (MacLennan and Wong 1971). CSQ undergoes conformational changes upon changes in Ca^{2+} concentration so that its conformation is highly dependent upon the Ca^{2+} concentration and ionic strength of its environment. It has the highest Ca^{2+} binding capacity as a polymer which occurs at Ca^{2+} concentrations $\geq$1mM (physiological free Ca^{2+} concentration in SR) (Fryer and Stephenson 1996). CSQ has a C-terminal tail domain with a high density of acidic residues and forms a Ca^{2+} binding pocket when CSQ polymerises (Wang et al. 1998; Beard et al. 2009b). CSQ as a polymer is visible in electron micrographs as electron-dense material in the terminal cisternae of the SR anchored near the luminal face of the RyR1(Franzini-Armstrong 1999)

Skeletal muscle has two isoforms of CSQ that are expressed and coded for by different genes (Scott et al. 1988; Fliegel et al. 1990). CSQ1 (skeletal isoform) is the only isoform expressed in

fast-twitch skeletal muscle (Biral et al. 1992; Damiani and Margreth 1994), while slow-twitch skeletal muscle also express CSQ2 (cardiac isoform) as a minor transcript together with CSQ1. The two isoforms share 86% homology (Fliegel et al. 1987; Scott et al. 1988). The major difference being in the C-terminal with CSQ2 having an extended, highly acidic C-terminal tail.

Functionally, CSQ1 inhibits RyR1(Beard et al. 2002; Wei et al. 2009) and CSQ acts as a luminal Ca^{2+} sensor for RyR (Beard et al. 2004; Gyorke et al. 2004; Wei et al. 2006; Qin et al. 2008) and is anchored to the junctional face of the SR membrane by its interactions with two integral SR proteins, triadin and junctin (Guo and Campbell 1995; Zhang et al. 1997).

Triadin and junctin are thought to be closely involved in the inhibitory interaction between CSQ1 and RyR1 as this interaction is only seen when RyR1 channels have triadin and junctin associated (Beard et al. 2002; Wei et al. 2009). In the absence of triadin and junctin, CSQ1 enhances RyR1 channel activity probably by binding directly to the RyR1 (Szegedi et al. 1999; Beard et al. 2002), showing that the normal inhibitory action of CSQ1 on RyR1 requires the presence of triadin and junctin.

Triadin was originally identified by Caswell et al and Kim et al (Kim et al. 1990; Caswell et al. 1991) and was isolated from skeletal muscle as a 95kDa membrane glycoprotein (Brandt et al. 1990). At a later stage the primary sequence and structure of skeletal triadin was deduced from its cDNA sequence. An intrinsic membrane protein of about 705 residues was predicted, containing a short cytoplasmic N-terminus, a single membrane-spanning domain, and a long intraluminal C-terminal domain (Knudson et al. 1993a; Knudson et al. 1993b). There are multiple isoforms of triadin in both skeletal muscle and in cardiac muscle, but they are all encoded by a single gene (Trdn) and undergo alternative splicing give rise to the multiple isoforms (Knudson et al. 1993b; Guo et al. 1996; Kobayashi and Jones 1999; Marty et al. 2000; Vassilopoulos et al. 2005). Skeletal muscle has four isoforms labelled according to their molecular weights (Trisk 95, 51, 49 and 32). Trisk 95 is the predominant isoform in skeletal muscle (Caswell et al. 1991; Knudson et al. 1993a; Knudson et al. 1993b; Marty et al. 1995; Taske et al. 1995; Kobayashi and Jones 1999; Thevenon et al. 2003; Shen et al. 2007). All of triadin's isoforms share identical sequences between residues 1-264, but have unique C-terminal regions. Triadin forms oligomers through disulphide bonds (Caswell et al. 1991).

Triadin interacts with RyR1 through both the cytoplasmic and luminal domains of triadin. The cytoplasmic binding site to RyR1 involves residues 18-46 and is Ca^{2+} dependent (optimal Ca^{2+} concentration <10μM) (Groh et al. 1999). The luminal RyR1 binding site involves a triadin sequence of alternating positive and negative residues located between residues 210-224 known as the KEKE motif (Realini et al. 1994; Jones et al. 1995; Kobayashi et al. 2000; Lee et al.

2004b). These KEKE residues interact with the RyR1 at the most C-terminal luminal loop (M8-M10 loop) where three charged residues are important for the interaction (D4878, D4907 and E4908) (Guo and Campbell 1995; Lee et al. 2004b; Goonasekera et al. 2007). Trisk 49 and 32 do not bind RyR1 although they contain both the cytoplasmic binding domain and the KEKE motif (Vassilopoulos et al. 2005).

Junctin is a 26kDa non-catalytic splice variant of the aspartate-β-hydroxylase gene. It is an integral membrane protein found in the junctional SR of both skeletal and cardiac muscle and has a structure similar to that of triadin. It has a short, 21 residue cytoplasmic N-terminal domain, a single transmembrane domain and a highly charged luminal domain which is highly enriched with KEKE motifs. It is not glycosylated and does not form disulphide-linked oligomers (Jones et al. 1995). Junctin binds to RyR and triadin through its luminal domain in a Ca^{2+} independent manner, but binding to CSQ is disrupted by either low or high Ca^{2+} concentrations (Zhang et al. 1997). The binding site for junctin on RyR1 is different to that of triadin as mutating the three residues important for triadin binding does not abolish junctin binding to RyR1 (Goonasekera et al. 2007).

Because of junctin and triadin's structural similarity and the ability of both to interact with CSQ and RyR1, they were presumed to be functionally redundant and were clumped together as CSQ anchoring proteins. It has since been shown that triadin and junctin have independent functions in regulating RyR1. When triadin binding to RyR1 is abolished by the mutation of the three RyR1 residues important for its binding, EC coupling and Ca^{2+} release from the SR are modified even though junctin binding remains intact (Goonasekera et al. 2007). Trisk 95 enhances [^{3}H]ryanodine binding to recombinant RyR channels and triadin or junctin added independently to the luminal side of purified RyR1 in planar lipid bilayer studies, each increase the open probability of the channel (Goonasekera et al. 2007; Wei et al. 2009). Wei et al also showed that junctin alone is responsible for normal CSQ1 regulation of RyR1 (Wei et al. 2009), however, there is mention of Ca^{2+} imaging studies in junctin-null mice showing nearly wild type phenotype with no significant alteration in skeletal SR content and a small but significant increase in resting cytoplasmic Ca^{2+} concentration (Perez 2011; Boncompagni et al. 2012). Another study by Yuan et al, however, found an increased SR content in junctin null cardiomyocytes (Yuan et al. 2009). Therefore junctin's role in the SR remains to be fully unveiled. Triadin-null myotubes show significant dysregulation of Ca^{2+} homeostasis indicating that triadin is a key functional component of Ca^{2+} homeostasis in skeletal muscle (Perez 2011; Boncompagni et al. 2012).

1.5.2.3 Calmodulin

Calmodulin (CaM) is part of the EF-hand family of Ca^{2+} sensing proteins. It is a ubiquitous, highly conserved protein of 17kDa with a high affinity for Ca^{2+}. Calmodulin participates in a number of Ca^{2+} signalling processes that regulate various mechanisms including growth, proliferation and movement. It has a dumbbell-shaped structure with N-terminal and C-terminal globular domains which are linked by a flexible linker. The N-terminal and C-terminal domains each contains two EF hand Ca^{2+} binding motifs. Calcium free calmodulin is referred to as apocalmodulin (apo-CaM) and binding of Ca^{2+} causes conformational changes to the molecule (Porter Moore et al. 1999a; Chin and Means 2000; Zissimopoulos and Lai 2007).

Calmodulin binds to all three RyR isoforms with nanomolar affinity both in its calcium bound and apo-CaM form (Porter Moore et al. 1999a; Fruen et al. 2000; Rodney et al. 2000; Balshaw et al. 2001; Yamaguchi et al. 2005). As with FKBP12, four CaM molecules bind to one RyR molecule (one for each subunit) at high and low Ca^{2+} concentrations (Chen and MacLennan 1994; Menegazzi et al. 1994; Yang et al. 1994; Tripathy et al. 1995). The CaM binding site involves residues 3614-3643 on the RyR1 (rabbit sequence) (Takeshima et al. 1989; Porter Moore et al. 1999b; Yamaguchi et al. 2003; Zhang et al. 2003). The CaM/RyR1 binding site has also been visualized by cryo-EM as with FKBP12 and is situated approximately 10nm from the putative channel pore in clefts formed by domains 3, 4 and 7 (Wagenknecht et al. 1997). Cryo-EM studies found that Ca^{2+}-CaM and apo-CaM bind to overlapping but spatially distinct locations on the RyR1 with the centres of mass of the two forms of CaM differing by 3-4nm (Wagenknecht et al. 1997; Samso and Wagenknecht 2002). However, a subsequent study employing FRET to investigate the binding of Ca^{2+}-CaM and apo-CaM to the RyR1 found no difference in Ca^{2+}-CaM and apo-CaM binding sites (Cornea et al. 2009). The different sites of binding have since been confirmed by cryo-EM using a mutated CaM with its four Ca^{2+} binding sites rendered incapable of binding Ca^{2+} (Huang et al. 2012). The different results obtained by FRET and cryo-EM may possibly be explained by the location of the fluorophores on CaM and how it changes its conformation upon binding to Ca^{2+} and further investigation is need to resolve this matter.

CaM has a Ca^{2+}-dependent biphasic effect of RyR1 activity. CaM activates RyR1 at low nanomolar Ca^{2+} levels, but at Ca^{2+} concentrations higher than 1μM, it inhibits the RyR1 (Meissner 1986; Smith et al. 1989; Fuentes et al. 1994; Tripathy et al. 1995; Rodney et al. 2000; Fruen et al. 2003). CaM binding to RyR1, however, is not essential for EC coupling as mutation of its binding site to RyR1 did not affect voltage-induced calcium release (O'Connell et al. 2002). CaM does, however, bind to and regulate the DHPR α_{1s} calcium current so it may contribute to EC coupling through this interaction (Tang et al. 2002; Ohrtman et al. 2008).

Apart from CaM, a number of other EF-hand containing proteins have been shown to interact with RyR, including calumenin and S100A1. S100A1 competes with CaM for the binding site on the RyR. The role for these proteins in vivo is, however, still not clear (Jung et al. 2006; Wright et al. 2008).

1.5.2.4 Glutathione S-transferase (GST)

Glutathione S-transferases are a major group of detoxification enzymes (Hayes and Pulford 1995). Some of the members of this family have been shown to modulate RyR calcium release from skeletal and cardiac muscle. The effects thusfar defined are muscle specific with GSTs having a strong inhibitory action on RyR2 and a weaker activation of RyR1. The first member of the GST family shown to have an effect on RyR activity was the GST-omega class protein. Other members of the GST family examined were found to have similar actions to GST-omega. They include GSTA1-1, the muscle specific GSTM2-2 and the CLIC2 (**c**hloride **i**ntracellular **c**hannel type 2) protein (Dulhunty et al. 2001; Board et al. 2004; Dulhunty et al. 2005; Liu et al. 2009). Modulation of RyRs is probably a ubiquitous function of the GST family but the muscle specific GSTM2-2, which is strongly expressed in skeletal and cardiac muscle is the most physiologically relevant GST in terms of RyR modulation.

Structurally, GSTs have distinct N-terminal and C-terminal domains. The N-terminal domain forms a thioredoxin fold made up of three α-helices and four antiparallel β-strands. Most of the residues involved in glutathione (GSH) binding are found in this domain. The C-terminal domain has a bundle of five to six helices that are connected with unstructured loops. The overall fold of the C-terminal domain is conserved but it is generally more variable than the N-terminal domain thereby allowing different substrates to be accommodated by different isoforms (Dulhunty et al. 2011).

As stated above, the general modulation of GSTs on cytoplasmic side of RyRs involves the inhibition of RyR2 and activating RyR1 channels (Dulhunty et al. 2001; Board et al. 2004; Dulhunty et al. 2005; Liu et al. 2009). CLIC2, however is an exception as it inhibits both RyR1 and RyR2 in bilayer studies (Board et al. 2004). Modulation effects are mild and occur within a physiological range of open probabilities. RyR2 inhibition for example does not abolish RyR2 activity but is reduced 40-60% of control activity, while RyR1 activation by GSTs is by a factor of about 2 and not to maximal activity. RyR1 therefore remains responsive to modulation by other agents.

1.5.3 Non-protein modulators of RyR1 function

Not only is the RyR involved in protein interactions that modulate its function, there are also some smaller non-protein molecules that significantly influence RyR function. Some of the molecules discussed here are normally present in cells (Ca^{2+}, Mg^{2+} and ATP), whereas others do not occur in muscle cells naturally and are substances commonly used to study RyR function (caffeine, ryanodine, ruthenium red).

Ruthenium red is an inorganic dye used in histology and it completely blocks CICR (Ohnishi 1979; Miyamoto and Racker 1981; Meissner 1984; Smith et al. 1986; Ma 1993). It is often used as a tool to check for RyR-dependent Ca^{2+} leaks from the SR as well as identifying RyR at the end of lipid bilayer experiments.

1.5.3.1 Ca^{2+}, Mg^{2+}, and ATP

Ca^{2+} is thought to be the "physiological" RyR channel activator as other RyR ligands cannot activate the channel in the absence of Ca^{2+}, or Ca^{2+} is necessary for some ligands to have their full effect (Zucchi and Ronca-Testoni 1997). Cytosolic Ca^{2+} has a biphasic effect on RyR1 channel activity (Meissner et al. 1986; Smith et al. 1986; Pessah et al. 1987; Bull and Marengo 1993; Percival et al. 1994; Meissner et al. 1997). RyR1 is activated above 100nM Ca^{2+} with a maximal activation between 10-100μM. Millimolar Ca^{2+} concentrations almost completely inhibit RyR1. The bell shaped cytosolic Ca^{2+}-dependence curve suggests the existence of high-affinity Ca^{2+}-binding sites on RyR1 that stimulate the channel and low-affinity inhibitory binding sites. Ca^{2+} alone, however, cannot fully activate the RyR1 and other agonists are therefore still able to modulate RyR1 activity in the presence of Ca^{2+}. It has also been shown that RyR1 has considerable functional heterogeneity with respect to Ca^{2+} regulation, which may be due to differences in the redox state between individual channels (Ma 1995; Copello et al. 1997; Marengo et al. 1998). Recombinant RyR1 expressed in HEK293 cells showed Ca^{2+}-dependence properties similar to native channels (Chen et al. 1997) and is therefore a suitable model for native channels.

Luminal Ca^{2+} also has an effect on the RyR as demonstrated by single channel recordings (Sitsapesan and Williams 1994b; Sitsapesan and Williams 1995; Tripathy and Meissner 1996; Gyorke and Gyorke 1998; Xu and Meissner 1998; Laver et al. 2004) and the rate of Ca^{2+} release from the SR that is sensitive to Ca^{2+} store content (Donoso et al. 1995; Lamb et al. 2001a). Increasing the luminal Ca^{2+} concentration increases RyR1 channel activity by increasing its sensitivity to its cytosolic agonists (Ca^{2+}, ATP and caffeine) and by alleviating Mg^{2+} inhibition (Sitsapesan and Williams 1995; Tripathy and Meissner 1996; Xu and Meissner 1998). The luminal Ca^{2+} concentration, however, has a threshold where, if reached, it can cause a decrease in channel activity (Tripathy and Meissner 1996). The mechanism of activation by luminal Ca^{2+}

can involve Ca^{2+} binding on the luminal side of the RyR (Sitsapesan and Williams 1994b; Sitsapesan and Williams 1995; Gyorke and Gyorke 1998) and/or the cytosolic Ca^{2+} regulatory sites activated by Ca^{2+} flowing through the pore from the luminal solution (Tripathy and Meissner 1996; Xu and Meissner 1998). Both mechanisms are probably operational with luminal Ca^{2+} altering the cytosolic Ca^{2+} regulatory sites' affinity through an allosteric effect if only one channel is present. In RyR1 arrays, luminal Ca^{2+} flowing through one channel might interact with cytosolic regulatory sites on neighbouring channels (Laver et al. 2004). The luminal Ca^{2+} sensor is an intrinsic RyR property (luminal Ca^{2+} regulatory sites) as purified RyR channels that are not associated with CSQ, triadin and junctin are regulated by luminal Ca^{2+} (Ching et al. 2000), but CSQ, triadin and junctin are also involved (Gyorke et al. 2004; Beard et al. 2005) in conveying sensitivity to luminal Ca^{2+} to the RyR, by modifying the intrinsic RyR response.

Mg^{2+} is a very strong inhibitor of the RyR. It inhibits the RyR1 in a dose-dependent manner, with complete inhibition occurring at millimolar concentrations of Mg^{2+} (Meissner et al. 1986; Smith et al. 1986; Pessah et al. 1987; Lamb and Stephenson 1994; Laver et al. 1997a; Copello et al. 2002; Laver et al. 2004). Since Mg^{2+} has a cytoplasmic concentration of about 1mM, Mg^{2+} inhibition may be a significant mechanism for keeping the RyR1 in the closed state until activation during EC coupling. Mg^{2+} inhibits RyR1 activity in the absence of Ca^{2+} (Laver et al. 2004). It has also been suggested that it competes with Ca^{2+} for high affinity Ca^{2+}-stimulatory sites, having the opposite effect to Ca^{2+} upon binding to these sites, as well as the low affinity inactivation sites (Laver et al. 1997a). Mg^{2+} has a binding affinity to the Ca^{2+} binding sites comparable to that of Ca^{2+} (Laver et al. 1997a; Liu et al. 1998; Copello et al. 2002). In skeletal muscle, the inhibition of Ca^{2+} release by Mg^{2+} seems to be modulated by depolarisation, which decreased the affinity of RyR1 to Mg^{2+} (at least the RyR1 associated with DHPRs) (Lamb and Stephenson 1994; Ritucci and Corbett 1995).

The adenine nucleotides (ATP, ADP, AMP and cyclic-AMP) as well as adenine (but not adenosine) activate RyR1 channel activity (Meissner et al. 1986; Smith et al. 1986; Pessah et al. 1987; Rousseau et al. 1988). ATP is a potent agonist of RyR1 at millimolar concentrations (Meissner 1984; Meissner et al. 1986; Smith et al. 1986; Pessah et al. 1987; Laver et al. 2001). RyR1 is activated by ATP even at low nanomolar Ca^{2+}concentrations and a combination of micromolar Ca^{2+} and millimolar ATP concentrations further increase RyR1 channel activity. ATP has been suggested to increase RyR1 sensitivity to Ca^{2+} activation, decrease RyR1 sensitivity to Ca^{2+} inactivation and Mg^{2+} inhibition (Meissner et al. 1986; Meissner et al. 1997). ATP and other adenine nucleotides seems to interact with the RyR1 at a molecular site that is different from (although interacting with) the Ca^{2+}-binding and Mg^{2+}- binding site. Two putative binding sites have been identified in RyR1 by sequence analysis. The sites contain the

nucleotide binding motif GXGXXG (Takeshima et al. 1989; Zorzato et al. 1990). Labelling the putative binding site with a photoaffinity analogue of ATP showed a molar ratio of 1:1 with the subunits of the RyR1(Zarka and Shoshan-Barmatz 1993).

1.5.3.2 Caffeine

Millimolar concentrations of caffeine activate the RyR through a ligand binding, and do not cause sarcolemmal depolarization. It facilitates CICR in skinned skeletal fibers even at inhibiting Mg^{2+} concentrations (Weber 1968; Weber and Herz 1968; Endo et al. 1970; Delay et al. 1986; Rousseau et al. 1986; Meissner and Henderson 1987; Ikemoto et al. 1991). RyR activation by caffeine is Ca^{2+} dependent and inhibited by ryanodine (Fabiato 1985; Rousseau et al. 1988; Rousseau and Meissner 1989). Caffeine may have two modes of action. At relatively low concentrations less than 2mM () the effect of caffeine is dependent on Ca^{2+} being present and therefore its action may be to increase the sensitivity of the Ca^{2+} activation site. However, at higher caffeine concentrations, the RyR channels are activated in the absence of Ca^{2+} and with different kinetics to Ca^{2+} activation alone or in combination with caffeine, though the permeability remains the same (Sitsapesan and Williams 1990).

1.5.3.3 Ryanodine

As mentioned before, ryanodine is a plant alkaloid that binds to the RyR with such high specificity that it has been used in its initial identification and lends its name to it. Its action on the RyR is complex. In the whole animal and when applied to intact muscle, ryanodine can produce either intense contracture, which is accelerated by muscle activity, or flaccidity (Franzini-Armstrong and Protasi 1997). The reason for this contradictory effect lies in the direct dual action ryanodine elicits on RyR that is concentration-dependent (Fairhurst and Jenden 1966; Fleischer et al. 1985; Pessah et al. 1985; Sutko et al. 1985; Smith et al. 1988; Lai et al. 1989; Zimanyi et al. 1992). Low and high concentrations of ryanodine have opposite effects on the RyR. At low concentrations (<10μM), ryanodine locks the RyR into a partially open subconductance state (Rousseau et al. 1987; Smith et al. 1988). This effect is strongly dependent on the RyR being in its open state as it selectively binds to the RyR in the open state (Pessah et al. 1985; Michalak et al. 1988; Lai and Meissner 1989; Chu et al. 1990a). This is facilitated by a high affinity binding site for ryanodine that is better accessible in the open channel (Zimanyi and Pessah 1991). As the concentration of ryanodine is increased, the affinity of RyRs for ryanodine decreases (Pessah et al. 1985; Michalak et al. 1988; McGrew et al. 1989) through allosteric negative interactions between four binding sites (one per monomer). The first ryanodine molecule binds with high affinity to the open channel and reduces the binding affinity of ryanodine to the other sites. With each subsequent binding of ryanodine to a binding site, the affinities of the remaining sites are lowered. When one ryanodine molecule per monomer is

bound, the channel enters a long lived state in which ryanodine is occluded and the channel is totally blocked (Carroll et al. 1991; Pessah and Zimanyi 1991; Buck et al. 1992).

1.5.4 Post-translational modifications

As the RyR is such a large protein, it is subject to quite a number of post translational modifications such as phosphorylation, oxidation and nitrosylation.

Both the skeletal and cardiac RyRs are substrates for serine/threonine protein kinases. In particular cAMP-dependent protein kinase (PKA), Ca^{2+}/calmodulin-dependent protein kinase II (CaMKII) and to a lesser extent cGMP-dependent protein kinase (PKG) (Takasago et al. 1989; Chu et al. 1990b; Takasago et al. 1991; Witcher et al. 1991; Hohenegger and Suko 1993; Suko et al. 1993). Dephosphorylation is catalysed mainly by protein phosphatase 1 (PP1) and 2A (PP2A) (Marx et al. 2000; Marx et al. 2001). CaMKII co-purifies with the RyR though direct association (Chu et al. 1990b; Hohenegger and Suko 1993; Currie et al. 2004). The association of PKA, PP1 and PP2A with RyR seems take place indirectly through anchoring proteins (Marx et al. 2001). Most of the emphasis in the field of phosphorylation has been on RyR2. There is therefore not as much information about phosphorylation of RyR1. One site for phosphorylation has been identified for RyR1 at S2843 and all three kinases phosphorylate this site to different degrees, with PKA showing the highest phosphorylation of this site, followed by PKG and then CaMKII (Suko et al. 1993). Functionally, the phosphorylation of the RyR activates the channel by increasing the sensitivity to Ca^{2+} activation and substantially reduced Mg^{2+} inhibition (Takasago et al. 1989; Takasago et al. 1991; Hain et al. 1994; Hain et al. 1995; Mayrleitner et al. 1995; Patel et al. 1995; Valdivia et al. 1995; Marx et al. 2000; Uehara et al. 2002; Reiken et al. 2003; Carter et al. 2006).

Oxidative modifications of thiol residues in cysteines, such as S-nitrosylation, S-glutathionylation and disulphide oxidation, can modulate the skeletal and cardiac RyR (Xu et al. 1998; Eu et al. 2000; Aracena et al. 2003; Aracena et al. 2005; Sanchez et al. 2005; Sun et al. 2008). Endogenous redox modulators regulate the RyR. Reduced glutathione inhibits the RyR, but oxidized glutathione stimulates the RyR (Zable et al. 1997; Xia et al. 2000). Reactive oxygen species (ROS) such as hydrogen peroxide and superoxide anion radical activate the RyR (Boraso and Williams 1994; Favero et al. 1995; Kawakami and Okabe 1998; Zima et al. 2004). Nitric oxide has also been suggested as an important physiological modulator of RyR function, but results are somewhat contradictory (Meszaros et al. 1996; Stoyanovsky et al. 1997; Xu et al. 1998; Eu et al. 2000; Aracena et al. 2003; Cheong et al. 2005). However, most of the studies show an activation of the RyR by NO and contradictory results may be due to different experimental conditions such as NO donor concentrations. Recently, NO-induced Ca^{2+} release

through RyR1 was shown to occur in cerebellar Purkinje cells (Kakizawa et al. 2012; Kakizawa 2013; Kakizawa et al. 2013) suggesting that, at least in Purkinje cells, the activation of RyR1 by NO is the more plausible scenario.

There is evidence for at least three classes of functional cysteines that modulate RyRs and the activity of the RyR has been correlated to the number of free thiols (Aghdasi et al. 1997; Sun et al. 2001). Under physiological conditions, the number of free thiols on the RyR1 is high (about 48 per subunit) and this is associated with low channel activity. Oxidation of about 10 thiols did not substantially affect channel activity, but the oxidation of about 15 additional thiols increased channel activity reversibly. Further oxidation of approximately 10 additional thiol groups caused the channel to be irreversibly inactivated (Sun et al. 2001). Oxidation of thiol groups the RyR channel's sensitivity to Ca^{2+} activation (Marengo et al. 1998; Xia et al. 2000; Sun et al. 2001; Oba et al. 2002; Bull et al. 2003). It also increases the RyR sensitivity to ATP activation and decreases its sensitivity to Mg^{2+} inhibition (Donoso et al. 2000; Oba et al. 2002; Aracena et al. 2003; Bull et al. 2003). Protein-protein interactions are also affected by oxidation with the formation of intrasubunit and intersubunit cross-links within the RyR1 (Wu et al. 1997) as well as complexes with triadin (Liu et al. 1994), CaM (Kawakami and Okabe 1998; Moore et al. 1999; Zhang et al. 1999; Eu et al. 2000; Aracena et al. 2005)and FKBP12 (Aracena et al. 2005) being affected.

1.5.5 Alternative splicing

Futatsugi et al (Futatsugi et al. 1995) investigated the possibility that splice variants of the RyR exist, as the Inositol triphosphate receptor (IP_3R), which shares several structural features with the RyR, and had been shown to have splice variants in the N-terminal and modulatory regions (Nakagawa et al. 1991; Schell et al. 1993). Futatsugi et al found two alternatively spliced regions localized in a modulatory region of the RyR1. They called the two regions ASI and ASII. The ASI region contains 15bp that are included in the ASI(+), or excluded in the ASI(-), RyR1 variants. ASII involves the inclusion and exclusion of 18bp and also generated two variants ASII(+) and ASII(-). The exclusion of the ASI and ASII base pairs result in the absence of 5 or 6 amino acid residues respectively. In the ASI region, this corresponds to Ala^{3481}-Gln^{3485} and in the ASII region Val^{3865}-Asn^{3870} in rabbit RyR1. Each of the splice variants involves the inclusion/exclusion of an exon.

Analysis of splicing patterns by Futatsugi et al. revealed a molar ratio of ASI(+):ASI(-) to be roughly 3:1 in skeletal muscle. Only ASI(+) is found in the cerebrum and cerebellum. They also found that during the stages of development, the splicing pattern of ASI in muscle changed dramatically. In the embryonic period, only ASI(-) was detected and the proportion of ASI(+)

increased gradually with development. Both ASII(+) and ASII(-) was detected in skeletal muscle and cerebrum with molar ratios of ASII(+):ASII(-) about 10:1 in skeletal muscle and more than 10:1 in the cerebrum. The cerebellum only showed the presence of ASII(+). The splicing pattern of ASII in muscle also changed dramatically during development. After birth ASII(-) abruptly became predominant. The ratio of ASII(+):ASII(-) increased gradually until three weeks after birth (Futatsugi et al. 1995).

Kimura et al (Kimura et al. 2005) later found that the ASI splicing pattern is different in patients suffering from myotonic dystrophy type 1 (DM1). DM1 is a debilitating multisystemic disorder caused by a CTG repeat expansion in the DMPK gene. Several genes have been found to undergo aberrant splicing and contribute to the symptoms of the disease. Kimura et al investigated whether RyR1 also undergoes aberrant splicing. In normal subjects, ASI(+)RyR1 was the major splice variant, while in cultured myotubes, ASI(-)RyR1 was the dominant splice variant. This is consistent with the findings of Futasugi et al. In patients with DM1, ASI(-) was significantly increased compared to age-matched controls, although the degree of aberrant splicing was variable. In some patients, the splice pattern was not discernably different from control, whereas in other cases, there was 100% ASI(-). ASII(-)RyR1 splice variants in DM1 patients were similar to control. Kimura et al also performed functional studies using [^{3}H]ryanodine binding and lipid bilayer techniques. They found the channel activity of ASI(-)RyR1 to be less than that of ASI(+)RyR1, but that their biphasic Ca^{2+} dependence of ryanodine binding was similar. In lipid bilayers, the open probability of ASI(-)RyR1 was lower than ASI(+)RyR1. They also showed that caffeine induced Ca^{2+} release from ASI(+)RyR1 and ASI(-)RyR1 was similar but that there was a significantly higher incidence of Ca^{2+} oscillations in ASI(+)RyR1 during the application of 10mM caffeine. This is indicative of a less active ASI(-)RyR1 channel (Kimura et al. 2005).

In a subsequent study, Kimura et al (Kimura et al. 2007) investigated the possibility that the ASI region may be involved an inter-domain interaction. Residues 3495-3502, which are close to the ASI region, had been shown to influence binding of the DHPR β_{1a} subunit, which is involved in EC coupling in skeletal myotubes (Cheng et al. 2005). In their investigation, Kimura et al made use of peptides corresponding to sequences surrounding the variably spliced regions (ASI and ASII). The peptide corresponding to ASI(+)RyR1 was called PASI(+), ASI(-)RYR1 was called PASI(-) and so on. Both PASI peptides significantly increased [^{3}H]ryanodine binding to native SR vesicles as well as purified RyR1 over a range of Ca^{2+} concentrations (100nM to 10μM). The increase in [^{3}H]ryanodine binding was significantly greater with PASI(-) than with PASI(+). The peptides induced the greatest increase in [^{3}H]ryanodine binding at 100nM Ca^{2+} with the [^{3}H]ryanodine binding declining with increased Ca^{2+} concentrations. Neither PASII(+) nor PASII(-) had any effect on [^{3}H]ryanodine binding.

The PASI peptides also increased Ca^{2+} release from SR vesicles in a dose-dependent manner with PASI(-) releasing significantly more Ca^{2+} at concentrations between 10 and 50μM than PASI(+). When Kimura et al repeated their [^{3}H]ryanodine binding studies using recombinant ASI(+)RyR1 and ASI(-)RyR1 rather than native RyR1 from SR, their results again showed the PASI peptides activating RyR1 with PASI(-) inducing the greatest relative activation. PASI(-) activated ASI(-)RyR1 at lower concentrations than ASI(+)RyR1. These results together led Kimura et al to propose a model in which an inter-domain interaction between the ASI region and a binding partner stabilizes the closed state of the RYR1 and upon binding. The PASI peptides abolish this interaction, resulting in channel activation. They also proposed that ASI(-)RyR1 interacts more strongly with its binding partner than ASI(+)RyR1, causing ASI(-)RyR1 to dwell more in the closed state. Upon disruption of this interaction, the removal of the stronger interaction in ASI(-)RyR1 causes a greater relative channel activation. The peptides corresponding to ASII had no effect on channel activity which either suggests that this region does not participate in an inter-domain interaction, or if it does, the site is not accessible to the peptides.

Kimura et al then went on to investigate the effects of the ASI region on EC coupling (Kimura et al. 2009). In recording Ca^{2+} currents through the DHPR and Ca^{2+} release from the SR under voltage clamp conditions in dyspedic (RyR1-null) myotubes expressing either ASI(+)RyR1 or ASI(-)RyR1, Kimura et al found that voltage-induced Ca^{2+} release during EC coupling was significantly increased in ASI(-)RyR1 expressing myotubes. The magnitude and voltage dependence of the L-type currents were similar in ASI(-)RyR1 and ASI(+)RyR1 expressing myotubes as well as wild type myotubes (endogenously expressing RyR1). This indicates that DHPR expression and RyR1 association are similar for ASI(+)RyR1 and ASI(-)RyR1 and correlates with previous results (Kimura et al. 2005; Kimura et al. 2007). Kimura et al then tested SR Ca^{2+} content and Ca^{2+} release from the SR in ASI(+)RyR1 and ASI(-)RyR1 expressing dyspedic myotubes. The authors used another RyR1 specific agonist, 4-choloro-m-cresol (4-cmc) to induce Ca^{2+} release from the SR. They found that in contrast to voltage-induced Ca^{2+} release (EC coupling), but consistent with previous single channel data, 4-cmc induced Ca^{2+} release was significantly reduced in ASI(-)RyR1 expressing myotubes. Kimura et al then investigated the possibility that the different effects observed during EC coupling with the splice variants may be due to the secondary structure of the greater ASI domain (including the basic residues that serves as the β_{1a} subunit binding site). The authors therefore compared the structure of the PASI peptides using circular dichroism (CD) and nuclear magnetic resonance (NMR). They found that their structures are very similar and therefore suggest that the functional differences are not due to structural differences between ASI(+)RyR1 and ASI(-)RyR1. They also showed that the basic residues that were incorporated into the PASI

peptides were essential for the activation of RyR1 by the PASI peptides. When three of the basic residues were mutated to alanine or lysine, RyR1 activation was significantly reduced.

1.5.6 Mutations of the RyR1 causing disease

Because the RyR is such a large protein there are many possibilities for mutations and many have been associated with three clinically distinct muscle disorders, namely Malignant Hyperthermia (MH), Central Core Disease (CCD) and Multi-minicore Disease (MmD) (Treves et al. 2005).

MH is an autosomal dominant pharmacogenetic disorder of skeletal muscle first described by Denborough and Lovell in 1960 (Denborough and Lovell 1960). The clinical manifestations are triggered in pre-disposed individuals by inhalation of anaesthetics (e.g. halothane) or by depolarising muscle relaxants (e.g. succinylcholine). The manifestations include a rapid increase in body temperature, muscle rigidity, tachycardia, hypercapnia, cyanosis, rhabdomyolisis and myoglobinuria (Denborough and Lovell 1960; MacLennan and Phillips 1992; Denborough 1998; Miller 2009). MH is a life-threatening disease if not recognised and treated shortly after onset with the RyR antagonist, dantrolene (Zhao et al. 2001; Paul-Pletzer et al. 2002; Krause et al. 2004).

CCD is a congenital myopathy involving structural changes of the muscle fibers (Magee and Shy 1956). It is usually inherited as an autosomal dominant disease, but two cases of recessive CCD has also been reported (Jungbluth et al. 2002; Romero et al. 2003). CCD is characterized by hypotonia during infancy, proximal weakness, delayed motor development and reduced muscle bulk (Magee and Shy 1956; Isaacs et al. 1975; Shuaib et al. 1987). CCD is diagnosed with histological identification of large, well demarcated, centrally located cores that lack mitochondria and do not stain with histological dyes for oxidative enzymes. In longitudinal sections, the core area covers a considerable length of mostly the slow-twitch muscle fibers (Greenfield et al. 1958; Shuaib et al. 1987; Hayashi et al. 1989; Sewry et al. 2002).

MmD is a non-progressive congenital myopathy and it is inherited autosomal recessively. Infants are typical hypotonic at birth, present distal joint laxity, ophtalmoplegia and arthrogyposis. Progressive scoliosis and respiratory problems are common, with most patients requiring mechanical ventilation. Multiple small cores can occur in both slow-twitch and fast-twitch fibers, but unlike CCD, the cores do not run the entire length of the fiber (Ferreiro et al. 2002; Treves et al. 2005; Zissimopoulos and Lai 2007).

More than 100 different RyR1 mutations have so far been associated with MH, CCD and MmD (Treves et al. 2005; Zissimopoulos and Lai 2007; Capes et al. 2011). They are mostly associated with RyR1 mutations, but also with small, in-frame deletions or out-of-frame insertions. The mutations cluster in three regions on RyR1: the N-terminus, the central domain and the C-terminal domain containing the channel pore. There are, however, mutations outside these regions and they will probably increase as more mutations are found and better sequency methods become available. These same three regions are involved in arrythmogenic diseases in RyR2, which might suggest common mechanisms of action. Mutations on the RYR1 gene are the only mutations, so far, linked to CCD. MH mutations are mostly on RYR1, but there are also MH-causing mutations in the gene coding for the DHPR α_{1s} subunit (Ali et al. 2003). Only a minority of MmD cases are due to RYR1 mutations, with the majority of cases caused by a mutation on the selenoprotein gene (SEPN1) (Ferreiro et al. 2002). MH-linked mutation are mostly in the N-terminal and central domains of the RyR1 and CCD-linked mutations predominate in the C-terminal domain, however, mutations for MH and CCD are found in all three regions. Some mutations cause both MH and CCD (Quane et al. 1993; Zhang et al. 1993; Jurkat-Rott et al. 2000; McCarthy et al. 2000; Treves et al. 2005).

Studies on the effects of MH and CCD indicate that RyR1 mutations in the N-terminal and central domain as well as the C-terminal domain result in higher sensitivity to RyR1 agonists such as caffeine and halothane, as well as to sarcolemmal depolarisation. The mutant channels also show reduced sensitivity to inactivation by Mg^{2+} and Ca^{2+} (Gallant and Lentz 1992; Otsu et al. 1994; Treves et al. 1994; Laver et al. 1997b; Owen et al. 1997; Tong et al. 1997; Censier et al. 1998; Dietze et al. 2000; Avila and Dirksen 2001; Yang et al. 2003; Wehner et al. 2004; Chelu et al. 2006). Mutant RyR1 channels show increased basal activity at rest to a variable extent, which can result in higher resting cytoplasmic Ca^{2+} concentrations and lower Ca^{2+} store content. Lower Ca^{2+} store content leads to a reduced magnitude of Ca^{2+} release and therefore muscle weakness (Censier et al. 1998; Tong et al. 1999; Avila and Dirksen 2001; Tilgen et al. 2001; Avila et al. 2003b; Zorzato et al. 2003; Dirksen and Avila 2004; Brini et al. 2005; Chelu et al. 2006). CCD-linked mutations have the highest effect on Ca^{2+} store depletion. Disruption of interdomain interactions involved in stabilizing the channel in the closed state has also been suggested in MH (Yamamoto et al. 2000; Lamb et al. 2001b; Shtifman et al. 2002; Yamamoto and Ikemoto 2002; Kobayashi et al. 2004; Bannister and Ikemoto 2006; Lobo and Van Petegem 2009).

1.6 The dihydropyridine receptor (DHPR)

In muscle, the major Ca^{2+} currents have a high voltage of activation, large single channel conductance, slow voltage-dependent inactivation, marked up-regulation by PKA

phosphorylation pathways and specific inhibition by Ca^{2+} antagonist drugs such as dihydropyridines, phenylalkylamines and benzothiasepines (Reuter 1979; Tsien et al. 1988). These Ca^{2+} currents are known as L-type because they have slow voltage dependent inactivation and are therefore long lasting (Tsien et al. 1988; Catterall 2011). Due to the L-type Ca^{2+} channel's specific interaction with dihydropyridines, it is also referred to as the dihydropyridine receptor (DHPR).

The different types of voltage gated Ca^{2+} channels are primarily defined by different α_1 subunits. Ten different α_1 subunits have been characterized by cDNA cloning and functional expression in mammalian cell lines and *Xenopus* oocytes. These can be divided into three structurally and functionally related families; Ca_V1, Ca_V2, and Ca_V3 (Snutch and Reiner 1992; Ertel et al. 2000) (See **Table 1.1**). For the purposes of this thesis, the Ca_V1 family of α_1 subunits, in particular the skeletal muscle isoform $Ca_V1.1$ (α_{1s}) and cardiac muscle isoform $Ca_V1.2$ (α_{1c}) will be discussed.

Table 1.1: Subunit composition and function of Ca^{2+} channel types. Adapted from (Catterall 2011)

Ca^{2+} current type	α_1 Subunits	Specific blocker	Principle physiological function
L	$Ca_V1.1$	DHPs	EC coupling in skeletal muscle, regulation of transcription
	$Ca_V1.2$	DHPs	EC coupling in cardiac and smooth muscle, endocrine secretion, neuronal Ca^{2+} transients in cell bodies and dendrites, regulation of enzyme activity, regulation of transcription
	$Ca_V1.3$	DHPs	Endocrine secretion, cardiac pacemaking, neuronal Ca2+ transients in cell bodies and dendrites, auditory transduction
	$Ca_V1.4$	DHPs	Visual transduction
N	$Ca_V2.1$	ω-CTx-GVIA	Neurotransmitter release, dendritic Ca^{2+} transients
P	$Ca_V2.2$	ω-Agotoxin	Neurotransmitter release, dendritic Ca^{2+} transients
R	$Ca_V2.3$	SNX-482	Neurotransmitter release, dendritic Ca^{2+} transients
T	$Ca_V3.1$	None	Pacemaking and repetitive firing
	$Ca_V3.2$		Pacemaking and repetitive firing
	$Ca_V3.3$		

Abbreviations: DHP, dihydropyridine; ω-CTx-GVIA, ω-conotoxin GVIA from the cone snail *Conus geographus*; SNX-482, a synthetic version of a peptide toxin from the tarantula *Hysterocrates gigas*.

1.6.1 Structure and function

The skeletal DHPR is heteropentameric comprising of α_1, α_2, β, γ, and δ subunits (Curtis and Catterall 1984; Curtis and Catterall 1986; Flockerzi et al. 1986; Hosey et al. 1987; Leung et al. 1987; Striessnig et al. 1987; Takahashi et al. 1987). A structural model based on analysis of biochemical properties, glycosylation and hydrophobicity of the five subunits includes a principle transmembrane α1subunit of 190kDa in association with a disulphide-linked $\alpha_2\delta$ dimer of 170kDa, an intracellular β subunit of 55kDa and a transmembrane γ subunit of 33kDa (Takahashi et al. 1987) (see **Figure 1.19**)

The α_1 subunit contains about 2000 residues and its predicted transmembrane structure is similar to the pore-forming α subunit of voltage-gated sodium and potassium channels (Tanabe et al. 1987; Tempel et al. 1987; Hille 2001) (see **Figure 1.19**). The amino acid sequence is organised into four repeated domains (I-IV), which each contains six transmembrane segments (S1-6) and a membrane associated loop between transmembrane segment S5 and S6 (Takahashi et al. 1987). The S5 and S6 helices together with the S5-S6 linker loop from each of the four repeated domains is believed to form the Ca^{2+} channel pore. The S4 segment of each repeat contains an ordered pattern of five to six positively charged residues and is the voltage sensor (Aggarwal and MacKinnon 1996; Seoh et al. 1996; Catterall 2010). The β subunit has predicted α-helices but no transmembrane segments (Ruth et al. 1989). The γ subunit is a glycoprotein with four transmembrane segments (Jay et al. 1990). The α_2 subunit is an extracellular extrinsic membrane glycoprotein attached to the membrane through disulphide linkage to the δ subunit (Gurnett et al. 1996). The δ and α_2 subunits are coded for by the same gene and the mature forms of the two subunits are produced by posttranslational proteolytic processing and disulphide linkage (De Jongh et al. 1990). Initially the δ subunit was assumed to be anchored to the membrane via a single transmembrane segment, but recent work argues persuasively that further posttranslational processing actually cleaves the predicted transmembrane segment and replaces it with a glycophosphatidylinostiol membrane anchor (Davies et al. 2010). Ablation of either $\alpha_2\delta$ or γ subunit expression has only modest effects on channel current density (Freise et al. 2000; Held et al. 2002; Ursu et al. 2004; Obermair et al. 2005; Gach et al. 2008; Obermair et al. 2008). The main function of $\alpha_2\delta$ so far identified is to slow activation kinetics of the α_{1s} subunit (Obermair et al. 2005; Gach et al. 2008; Obermair et al. 2008), while that of the γ subunit is to cause a depolarizing shift in the voltage-dependence of channel activation (Freise et al. 2000; Held et al. 2002; Ursu et al. 2004). The broader physiological significance of the effect of these two subunits is not clear. Although the α_1 subunit carries the characteristic pharmacological and functional properties for voltage sensing, ion permeability and drug binding of the DHPR, all the subunits are required for complete receptor function (Tanabe et al. 1988; McDonald et al. 1994; Melzer et al. 1995; Catterall 2000).

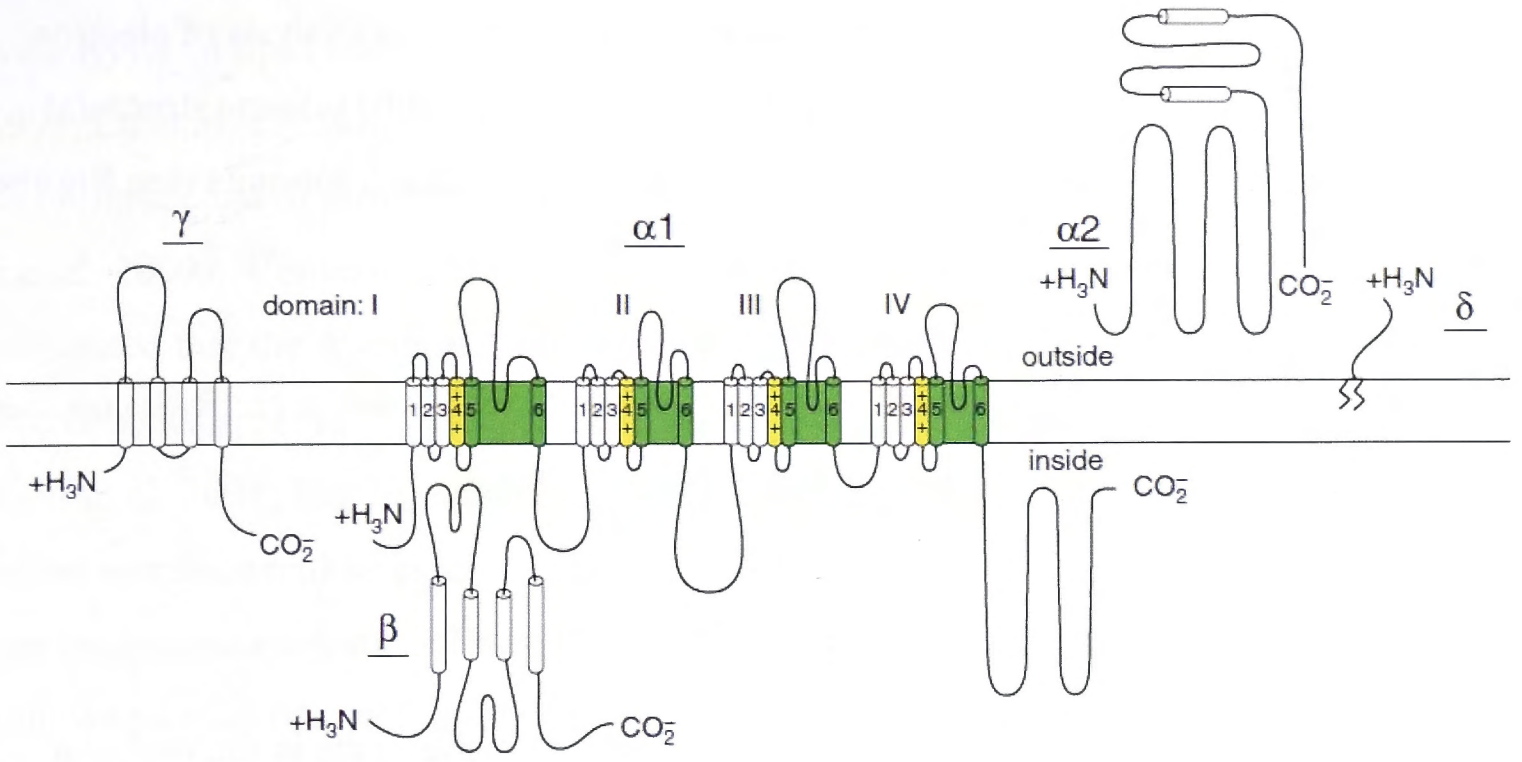

Figure 1.19: Subunit structure of the DHPR illustrated as transmembrane folding models. Predicted α-helices are shown as cylinders. The length of lines correlated approximately to the lengths of the polypeptide segments represented. The zigzag line on the δ subunit illustrates its glycophosphatidyl-inositol anchor.

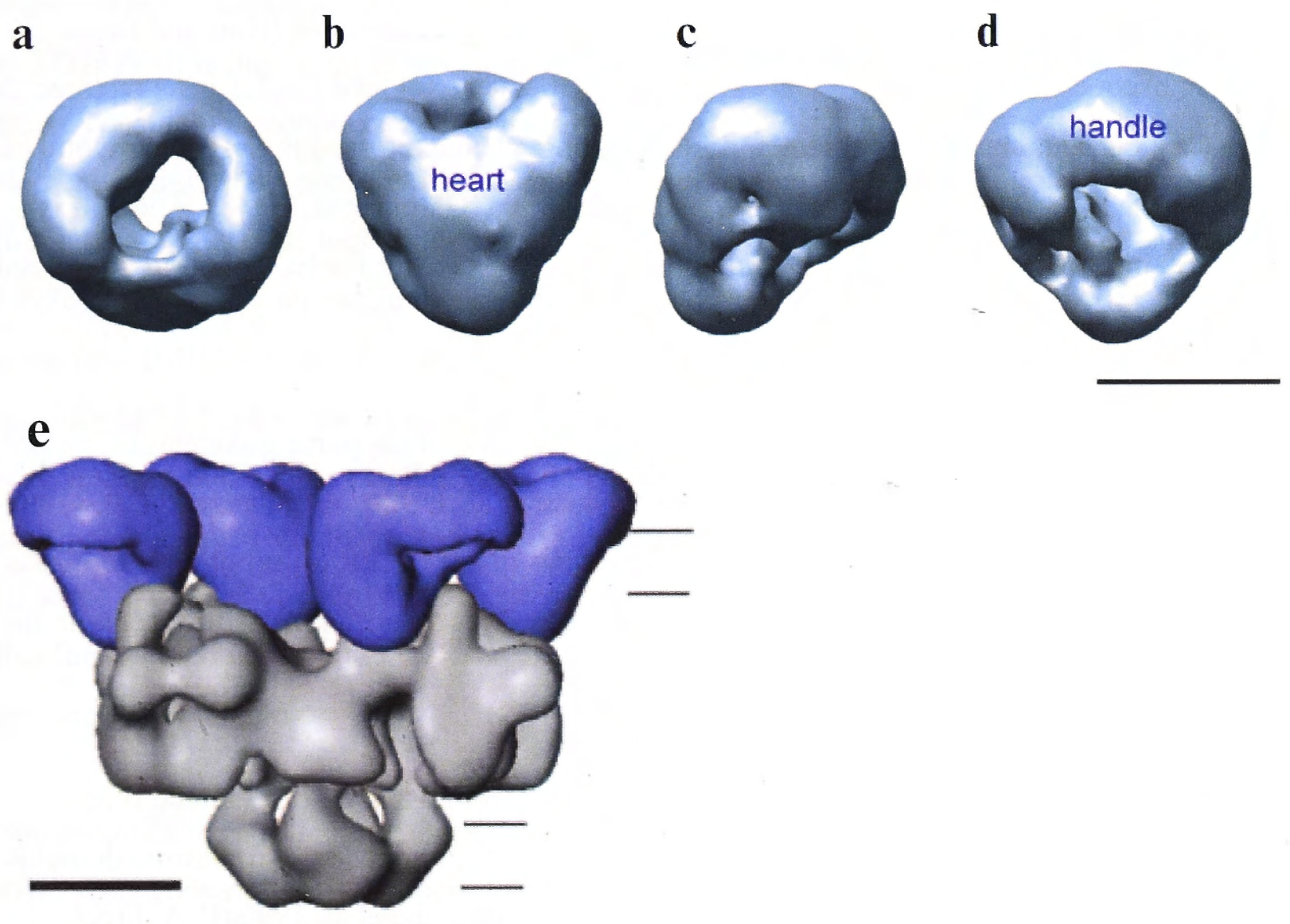

Figure 1.20: 30Å resolution 3D structure obtained by cryo-electron microscopy and single particle reconstruction. The structure is shown in four different views: (a) top view; (b) front view by 90° rotation along the horizontal axis of the top view in (a); (c) and (d) are views obtained by stepwise rotation of the view in (b) along the vertical axis by 90°. The handle-shaped structure and the upper lobes of the heart-shaped region were proposed to account for the extracellular channel region and to include the α_2 subunit. Thus the heart shaped region includes the voltage-sensitive transmembrane region of the DHPR and the cytoplasmic β_{1a} subunit.(e) Shows the side view of RyR1 coupled with the DHPR tetrad. Horizontal lines indicate the approximate position of the surface and SR membranes. The scale bar represents 100Å. Adapted from (Serysheva et al. 2002; Serysheva 2004).

Apart from the predicted structure of the DHPR discussed above, there are only low resolution structural models that have been developed from image reconstitution analysis of electron micrographs (Serysheva et al. 2002; Wang et al. 2002; Wolf et al. 2003). Some structural features of the 3D model have been associated with the α_{1s}, β_{1a} and $\alpha_2\delta$ subunits (see **Figure 1.20**).

The structure and function of the skeletal α_{1s} and β_{1a} subunits with specific emphasis on skeletal type EC coupling will be discussed in more detail below.

1.6.1.1 α_{1s} subunit

Schneider and Chandler demonstrated intramembrane charge movements in the t-tubular membrane (Schneider and Chandler 1973) which led to the hypothesis that release of Ca^{2+} from the SR is controlled by a voltage sensor in the t-tubular membrane physically interacting with RyR1. The voltage sensor was later identified as the DHPR when it was observed that dysgenic myotubes, which lack the DHPR α_{1s} subunit , did not have the DHP-sensitive voltage gated Ca^{2+} current, charge movements or EC coupling (Beam et al. 1986) and that charge movement and EC coupling were inhibited in parallel by the DHPR antagonist nifedipine (Rios and Brum 1987). Subsequently it was shown that expression of the newly cloned $Ca_V1.1$ gene restored the L-type Ca^{2+} current, charge movement and EC coupling when expressed in dysgenic myotubes (Tanabe et al. 1988; Adams et al. 1990; Tanabe et al. 1990a; Garcia et al. 1994). Today it is universally believed that the DHPR α_{1s} subunit is the voltage sensor for EC coupling in skeletal muscle.

The skeletal muscle DHPR is the only L-type channel capable of supporting skeletal EC coupling (Tanabe et al. 1990b; Garcia et al. 1994; Nakai et al. 1998b; Kasielke et al. 2003) and it is believed that one or more of the intracellular regions of the DHPR α_{1s} subunit (N-terminus, C-terminus, cytoplasmic loops I-II, II-II and II-IV) either directly or indirectly interact with the cytoplasmic assembly of the RyR1.

The II-II loop of the α_{1s} subunit was first identified as a major contributor to skeletal type EC coupling with the use of chimeric DHPRs consisting of the individual α_{1s} cytoplasmic domains within the highly conserved background of the α_{1c} subunit (Tanabe et al. 1990a). A direct interaction between the full length α_{1s} II-III loop and RyR1 was subsequently detected (Lu et al. 1994). A peptide corresponding to the α_{1s} II-III loop activated purified RyR1 in lipid bilayers and increased [^{3}H]ryanodine binding in isolated skeletal SR vesicles. Two regions of interest on the II-III loop were studied intensively. The first corresponds to residues 681-690 and was arbitrarily named the A region and the second corresponds to residues 720-765 and was named

the C region (El-Hayek et al. 1995). A peptide corresponding to the A region was shown to activate RyR1 in lipid bilayers and increase [^{3}H]ryanodine binding in SR vesicles (El-Hayek et al. 1995; Lu et al. 1995; El-Hayek and Ikemoto 1998; Dulhunty et al. 1999) and that, in vitro, it binds to the second of three SPRY domains on RyR1 which encompasses residues 1085-1208 (Cui et al. 2009). Contrastingly, in dysgenic myotubes expressing modified α_{1s} subunits demonstrated that the A region is not essential for skeletal type EC coupling *in situ* (Nakai et al. 1998b; Grabner et al. 1999; Proenza et al. 2000b; Ahern et al. 2001a; Ahern et al. 2001b; Wilkens et al. 2001; Flucher et al. 2002; Lorenzon et al. 2004; Papadopoulos et al. 2004). The C-region was shown to be essential to produce skeletal type EC coupling in further chimeric studies in dysgenic myotubes (Nakai et al. 1998b) and a peptide corresponding to this region was shown to modify RyR1 activity in lipid bilayer studies and [^{3}H]ryanodine binding assays (Saiki et al. 1999; Haarmann et al. 2003; Haarmann et al. 2005). The C region was named the "critical domain" and a subsequent study proposed that residues 744-751 within this domain adopt a random coil conformation that enables α_{1s} to interact with other junctional proteins. The corresponding residues in α_{1c} form a putative α-helix that inhibits such interactions (Haarmann et al. 2003; Kugler et al. 2004; Cui et al. 2009). This study identified four residues to be responsible for stopping the formation of an α-helix in the α1s II-III loop (A739, F741, P742 and D744). It is important at this stage to point out that the α_{1s} and α_{1c} II-III loops share more than a considerable sequence similarity (Wilkens et al. 2001) and therefore some conserved elements required for conformational coupling may remain masked. Leong and MacLennan found that the α_{1s} II-III loop binds to residues 922-1112 of RyR1 (Leong and MacLennan 1998a) and that this interaction was dependent on positively charged residues K667 and K682 within the II-III loop. In contrast, residues 719-767 of the critical domain interacts weakly with residues 1837-2168 of the RyR1 in a yeast two-hybrid assay, while no interaction was found with residues 666-709 on the II-III loop in parallel experiments (Proenza et al. 2002). The conflicting results from these studies may reflect that a particular conformational state of the II-III loop, that cannot be replicated *in vitro,* may be required in order to interact with the RyR1, or that the interactions with the RyR1 is of very low affinity, as crucial physiological interactions frequently are (Bannister 2007).

Some studies have found that there is some residual EC coupling in dysgenic myotubes expressing constructs missing both the A and C regions (Ahern et al. 2001b) and that a component of EC coupling is lost in chimeras with only the α_{1s} II-III loop in a α_{1c} background compared to chimeras with all the intracellular α_{1s} domains in a α_{1c} background (Carbonneau et al. 2005). Although the importance of the II-III loop for skeletal type EC coupling is well accepted, a broader view of multiple contacts between the DHPR and RyR1 might be closer to the truth and consistent with studies showing multiple regions of RyR1 involved in EC coupling

(Nakai et al. 1998a; Proenza et al. 2002; Protasi et al. 2002; Perez et al. 2003a; Perez et al. 2003b; Sheridan et al. 2006).

The C-terminus of the α_{1s} subunit is subject to proteolytic cleaving at residue A1664 (De Jongh et al. 1989; Hulme et al. 2005) although cleaving at this site does not seem to affect the ability of the α_{1s} subunit to couple to RyR1 in dysgenic myotubes (Beam et al. 1992). Deletions upstream from this site progressively diminish DHPR surface expression as this region contains a PDZ domain (residues 1543-1647) that is critical for targeting of the α_{1s} subunit to the triad junction (Flucher et al. 2000; Proenza et al. 2000a). The important role of the C-terminus is clear, but attempts to show the role of this region in DHPR trafficking have been unsuccessful (Flucher et al. 2002; Wilkens and Beam 2003). Biochemical approaches identified direct interactions between RyR1 with the α_{1s} C-terminus in binding directly to RyR1 and in reducing [^{3}H]ryanodine binding (Slavik et al. 1997; Sencer et al. 2001). It also seems that the presence of the RyR1 puts conformational pressure on the α_{1s} C-terminus (Lorenzon et al. 2004; Papadopoulos et al. 2004).

The α_{1s} III-IV loop has not drawn so much experimental attention for a possible role in EC coupling, despite its identification as the only site for DHPR-linked MH mutations (R1086H and R1086C) (Monnier et al. 1997). Dysgenic myotubes expressing DHPRs with the R1086H mutation showed increased sensitivity to pharmacological (caffeine) and physiological (membrane depolarization) stimuli, suggesting a negative allosteric contribution of the III-IV loop in coupling to RyR1 (Weiss et al. 2004). Evidence for binding between the III-IV loop and residues 922-1112 on the RyR1 is also consistent with a possible role for the α_{1s} III-IV loop in the basic EC coupling mechanism as The II-III and III-IV loops bind to contiguous and possibly overlapping sites on the RyR1 (Leong and MacLennan 1998b).

The N-terminus of the α_{1s} subunit seems not to be involved in EC coupling (Tanabe et al. 1990a; Bannister and Beam 2005; Carbonneau et al. 2005).

1.6.1.2 β_{1a} subunit

There are four voltage-gated Ca^{2+} channel β subunit ($Ca_V\beta$) genes with various splice variants for each gene (Ruth et al. 1989; Hullin et al. 1992; Perez-Reyes et al. 1992; Castellano et al. 1993a; Castellano et al. 1993b). The skeletal muscle isoform, $Ca_V\beta_{1a}$, is uniquely associated with $Ca_V1.1$. All the $Ca_V\beta$ isoforms possess a common structure consisting of five domains (see **Figure 1.21**). Homology modelling and X-ray crystallography have shown an Src homology domain (SH3) and a guanylate kinase (GK)-like domain making up the core of the β subunit. The core is highly conserved among the four isoforms (Chen et al. 2004; Opatowsky et al. 2004;

Van Petegem et al. 2004), while the connecting region between the core domains (Hook region) and the N- and C-termini are unconserved and subject to alternative splicing. The core of the β subunits is similar to the membrane-associated guanylate kinases (MAGUKs), a group of scaffolding proteins containing several protein-protein interaction domains and involved in the assembly of multiprotein complexes (Hanlon et al. 1999; Dolphin 2003).

No published crystal structure for the β_{1a} subunit is available, but the core of other β subunit isoforms that have been crystalized and share significant homology with the β_{1a} subunit core, show that the GK domain of the β subunit interacts with the alpha interaction domain (AID) located in the α_1 subunit I-II loop with high affinity (low nanomolar range) (Chen et al. 2004; Opatowsky et al. 2004; Richards et al. 2004; Van Petegem et al. 2004). Two other lower-affinity β subunit interactions sites have also been identified on the N- and C-terminal domains of the α_1 subunit (Qin et al. 1997; Walker et al. 1999; Stephens et al. 2000)

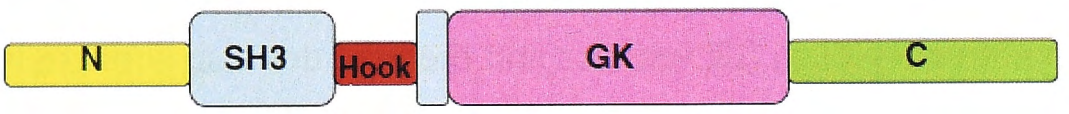

Figure 1.21: A schematic representation of the domain modules of $Ca_V\beta$. The SH3 and GK domains are conserved in all β subunit isoforms with the greatest sequence variability observed in the N- and C termini and the Hook region (Karunasekara et al. 2009).

The β_{1a} subunit is essential for DHPR function (Gregg et al. 1996; Strube et al. 1996). It facilitates trafficking of the α_{1s} subunit to the plasma membrane, but the specific targeting of the assembled DHPR to the junctional membrane is dependent on the α_{1s} subunit (Neuhuber et al. 1998; Bichet et al. 2000; Schredelseker et al. 2005; Leuranguer et al. 2006). In mammals the absence of the β_{1a} subunit is fatal at birth due to respiratory failure and myotubes from β_{1a}-null mice are incapable of EC coupling (Gregg et al. 1996; Strube et al. 1996). The β_{1a} subunit is essential for efficient tetrad formation. The β_{1a}-null zebra fish mutant *relaxed* embryo displays randomly positioned α_{1s} subunits at the junctional membranes, whereas the transgenic overexpression of β_{1a} in these *relaxed* mutant embryos restored the tetradic arrays (Schredelseker et al. 2005). The rescue of tetrads is unique to the β_{1a} subunit (Schredelseker et al. 2009). This suggests that the β_{1a} subunit may be the molecular "glue" that hold the tetrad together by linking the α_{1s} subunit to RyR1 (Bannister et al. 2013).

The functional significance of the β subunit SH3 domain remains unclear. SH3 domains are typically protein interaction domains that mediate the assembly of protein complexes through proline-rich recognition sites such as PXXP or XPPPX (McPherson 1999). Possible binding

sites have been identified in the II-III loop and C-terminal of the α_{1a} subunit (Dubuis et al. 2006). Interestingly, as discussed above (Section 1.6.1.1) the II-III loop has been shown to be important for EC coupling. A recent study using chimeras of the β_{1a} and β_3 expressed in *relaxed* zebra fish mutants have shown the importance of the SH3 domain and C-terminus of the β1a subunit for charge movement and EC coupling restoration (Dayal et al. 2013) suggesting cooperativity between the SH3 and C-terminal domains in inducing a proper conformational change in the α_{1a} subunit crucial for its voltage sensing function to operate. This resonates with the suggestion above that the β_{1a} subunit may be the molecular "glue" that hold the tetrad together. The SH3 domain of the β_{2a} subunit has also been shown to bind to dynamin and mediate endocytosis of the DHPR α_{1c} subunit in *Xenopus* oocytes (Gonzalez-Gutierrez et al. 2007).

In vitro binding studies have shown a possible direct interaction site between the C –terminus of the β_{1a} subunit and the RyR1. Specifically, a cluster of positively charged residues (3495-3502) on the cytoplasmic assembly of RyR1 is close to the ASI region as discussed in Section 1.5.5 (Cheng et al. 2005). Peptides corresponding the 35 most distal residues of the β_{1a} C-terminus (490-524) bind to native RyR1 in SR vesicles and the peptides also activate RyR1 directly in lipid bilayer and [^{3}H]ryanodine binding assays. The full length β_{1a} subunit was also shown to activate the RyR1 in lipid bilayers (Rebbeck et al. 2011; Karunasekara et al. 2012). However, the β_{1a} subunit does not seem to bind to the RyR1 in dysgenic myotubes (Neuhuber et al. 1998; Papadopoulos et al. 2004; Leuranguer et al. 2006) suggesting, not surprisingly, that if an association between RyR1 and β_{1a} exists *in vivo*, the presence of α_{1s} is required (Bannister et al. 2013).

1.6.2 Orthograde and retrograde coupling

The triggering of the release of calcium from the SR though the interaction of the DHPR and RyR has been discussed in Section 1.4.2. This coupling (DHPR-to-RyR) is referred to as orthograde coupling. Interestingly, the signalling interaction between DHPR and RYR is often bi-directional. The calcium conducting properties of the DHPR are strongly influenced by its functional association with RyR. The ability of the RyR to alter DHPR channel behaviour is referred to as retrograde coupling (RyR-to-DHPR) (Nakai et al. 1996; Dirksen 2002). The nature of the bi-directional signal can be chemical (cardiac muscle) or mechanical (skeletal muscle).

In cardiac muscle, retrograde signalling is in the form of calcium-independent inactivation (Brehm and Eckert 1978; Kass and Sanguinetti 1984; Lee et al. 1985). Calcium release from the SR acts as a negative feedback mechanism for cardiac EC coupling by promoting calcium-

dependent inactivation of the DHPR and thereby reducing subsequent calcium influx and release (Sham et al. 1995; Adachi-Akahane et al. 1996). Calmodulin acts as a Ca^{2+} sensor for the DHPR to facilitate calcium-dependent inactivation and interacts with the C-terminal tail of the α_{1c} subunit (Peterson et al. 1999; Zuhlke et al. 1999; Pate et al. 2000; Zuhlke et al. 2000).

The retrograde signal in skeletal muscle does not occur through chemical feedback, but rather involves an allosteric modulation of the DHPR through the DHPR/RyR1 mechanical interaction involved in orthograde coupling (Nakai et al. 1996; Grabner et al. 1999; Avila and Dirksen 2000). The calcium conducting properties of the DHPR are strongly dependent on the presence of RyR1 (Nakai et al. 1996; Avila and Dirksen 2000). RyR1 increases the ratio of maximal L-type channel conductance to charge movement, indicating that DHPRs not associated with RyR1 function poorly as a Ca^{2+}-permeable L-type channel (Nakai et al. 1996; Dirksen 2002). The α_{1s} II-III loop, important in orthograde coupling (above), is also important for retrograde coupling (Grabner et al. 1999). Multiple RyR1 regions are involved with retrograde coupling (Nakai et al. 1998a) suggesting that two-or more regions from different parts of the RyR1 primary sequence may come together to form and interaction domain for the DHPR α_{1s} II-III loop when the RyR1 is folded.

1.7 Muscle fiber type

Muscles are heterogeneous with respect to a number of characteristics. Whole muscles themselves differ in size, shape, anatomical position as well as function. The fibers that make up the muscle are also heterogeneous with different metabolic as well as contraction characteristics. In addition, the motor units of the skeletal muscle system are heterogeneous in nerve stimulus frequency and also in the fiber-type content.

1.7.1 Four major fiber types

Since the first half of the 19th century skeletal muscles have been distinguished on the basis of their colour (red/white) and their contractile properties (fast/slow). Until around 1968-1970, mammalian skeletal muscle was classified as (Needham 1926):

- Fast twitch muscles with glycolytic metabolism, specialized for phasic activity and identified as white muscle
- Slow twitch muscles, rich in myoglobin and oxidative enzymes, specialized for more continuous activity and called red muscles

At the end of the 1960s and as a result of four different lines of evidence, a more complex scheme emerged. The first line of evidence correlated histochemical and physiological studies

of individual motor units. The second was electron microscopy of fast and slow skeletal muscle. The third was a novel procedure for myosin ATPase histochemistry and lastly, biochemical studies on oxidative and glycolytic enzymes in different muscles (Schiaffino and Reggiani 2011). Edstrom and Kugelberg used stimulation of single motor axons in rat fast TA muscles to characterize single motor units according to its twitch properties. They then used periodic acid-Schiff (PAS) staining (stain for glycogen) to indicate changes in glycogen levels after induced glycogen depletion in those fibers thereby identifying the fibers in cryo-sections. Subsequently oxidative metabolism of the fibers were assessed by enzyme histochemistry for succinate dehydrogenase (SDH) (Edstrom and Kugelberg 1968). Their results showed that motor units are homogenous in fiber type composition. Motor units composed of small SDH negative fibers or large SDH positive fibers were both fast-twitch, but they differed with respect to fatigue resistance. A spectrum of motor units with intermediate SDH staining and fatigue resistance was detected in TA muscle. Similar results were found in rat extensor digitorum longus (EDL), a muscle known to contain essentially only fast twitch motor units (Close 1967; Schiaffino et al. 1970). Enzyme histochemical procedures for myosin ATPase led to the identification of two fast twitch fiber populations, type 2A and 2B, abundant in fast-twitch muscle , but distinct from type 1 fibers predominant in slow twitch muscle (Guth and Samaha 1969; Brooke and Kaiser 1970). This was confirmed using both myosin ATPase and SDH staining, with the type 2A fibers staining strongly for SDH and being fatigue resistant whereas type 2B fibers stained weakly for SDH and was fatigable (Burke et al. 1971). The fatigue resistance of type 2A fibers is lower than that of type 1 fibers. It was subsequently shown that type 2A and 2B fibers have high levels of glycolytic enzymes, in spite of their differences in oxidative enzyme content and this led to the further classification of slow-twitch oxidative (type 1), fast-twitch oxidative glycolytic (type 2A) and fast-twitch glycolytic fibers (type 2B) (Peter et al. 1972). The different fiber types each express different myosin heavy chain (MyHC) isoforms (see **Table1.2**). Due to the central role myosin plays as molecular motor in the muscle fibers as well as the existence of several MyHC isoforms that are differentially expressed in the fibers, MyHC is the most useful marker available for fiber typing (Schiaffino and Reggiani 2011).

A third fast fiber type with a MyHC composition different from 2A and 2B fibers was identified and named type 2X (Schiaffino et al. 1988; Schiaffino et al. 1989). Type 2X motor units have twitch properties similar to 2A and 2B with a fatigue resistance intermediate between type 2A and 2B (Larsson et al. 1991). Rat skeletal type 2X fibers have moderate to strong SDH staining (Schiaffino et al. 1989; Larsson et al. 1991) with a maximal shortening velocity intermediate between 2A and 2B fibers (Bottinelli et al. 1991; Bottinelli et al. 1994). It was also shown that there is a spectrum of fiber types with a pure or hybrid MyHC the following composition: 1, 1/2A, 2A, 2A/2X, 2X, 2X/2B and 2B (Gorza 1990; Pette and Staron 1990; DeNardi et al. 1993;

Bottinelli et al. 1994). Human muscles do not express the gene for MyHC-2B (although MYH4 is present in the genome) and the fibers that were typed 2B according to myosin ATPase staining are in fact 2X fibers based on MyHC composition (Smerdu et al. 1994). The 2X fibers in humans have the lowest level of SDH activity compared to all other fibers types. There are therefore important differences to consider in extrapolating results from mice and rats to humans.

Developing muscles express different MyHC isoforms (MyHC-emb and MyHC-neo) but fully developed mammal limb and trunk muscles contain the four major fiber types discussed above. There are, however, several other muscle groups with specialized functions and fiber types different from those seen in limb and trunk muscles. Atypical muscle fibers are present in head and neck muscles, particularly the extraocular muscles, jaw muscles, middle ear muscles, laryngeal muscles (Schiaffino and Reggiani 2011).

Table 1.2: The complete panel of sarcomeric MyHC isoforms with their corresponding genes and expression pattern. Adapted from (Rossi et al. 2010; Schiaffino and Reggiani 2011)

Protein	Genes	Expression
MyHC-2A	MYH2	Fast-twitch 2A fibers
MyHC-2B	MYH4	Fast-twitch 2B fibers
MyHC-2X	MYH1	Fast-twitch 2X fibers
MyHC-α	MYH6	Heart and jaw muscle
MyHC-β/slow	MYH7	Heart and slow-twitch fibers
MyHC-Neo	MYH8	Developing muscle
MyHC-emb	MYH3	Developing muscle
MyHC-EO	MYH13	Extraocular muscle
MyHC-slow/tonic	MYH14/7b	Extraocular muscle
MyHC-15	MYH15	Extraocular muscle
MyHC-M	MYH16	Jaw muscle

1.7.2 Functional significance of fiber type diversity

The nervous system employs the ability of skeletal muscle to generate force and movement for a variety of tasks that for simplicity can be reduced to three main types: postural joint stabilization, long-lasting and repetitive activity (respiration, locomotion, chewing) and fast, generally powerful action (jumping, kicking, biting). Muscle fibers have adapted to suite each

task. Motor units with specific firing patterns must be connected to fibers with the correct functional properties for proper muscle function. Motor neuron firing patterns can determine the properties of the fibres that they innervate and this is also the basis of fiber type remodelling discussed in Section 1.7.9 (Schiaffino and Reggiani 2011).

Three distinct firing patterns in rat motor units have been detected (Hennig and Lomo 1985). Motor units consisting of slow and fatigue resistant fibers are characterized by a persistent activity (300000-500000 impulses/24h) with long lasting trains (300-500s) and relatively low frequency of firing (~20Hz). Motor units consisting of fast fibers have an intermittent but higher frequency of firing and can be divided into two groups. The first has a modest amount of activity per day (300-10000 impulses/24h), high discharge frequency (70-90Hz) and short duration of trains (<3s). This group presumably corresponds to type 2B fibers. The second group has a similar discharge frequency (50-80Hz), but has much greater activity per day (90000-250000 impulses/24h) and relatively long train duration (60-240s), which presumably corresponds to type 2A and 2X fibers (see **Figure 1.22** for summary). The motor neuron and motor unit muscle fiber properties integrate well in terms of firing pattern, contraction parameters and fatigue resistance (Kugelberg and Edstrom 1968; Burke et al. 1971; Burke et al. 1973).

Firing patterns	Median firing frequency (Hz)	Longest train duration (s)	Impulses per 24 hrs	Time on per 24 hrs
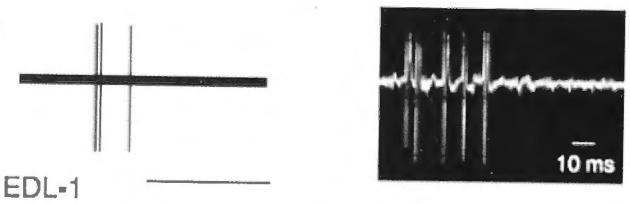	69-91	0.8-3.9	2600-11200	0.5-3 min
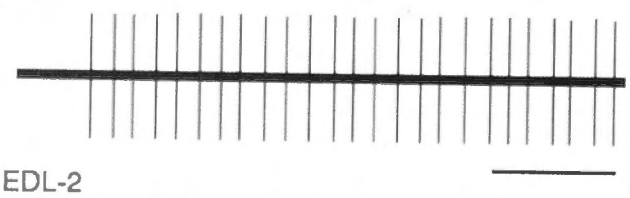	48-83	59-141	89500-243100	23-72 min
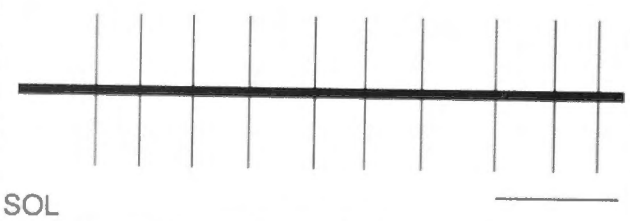	18-21	290-548	309500-495800	5.3-8.4 hrs

Figure 1.22: Firing patterns of three classes of motor units identified in rat fast EDL and slow Soleus muscles. EDL-1 and EDL-2 presumably corresponds to motor units consisting of 2B and 2A fibers respectively (Hennig and Lomo 1985; Schiaffino and Reggiani 2011).

1.7.3 Fiber type differences in EC coupling

Skeletal muscle fibers are very specialized in their control of intracellular Ca^{2+}. Different fiber types are characterized by distinct levels of resting Ca^{2+} concentration and kinetics of Ca^{2+} transients induced by action potentials. Ca^{2+} transient kinetics are correlated with the dynamic properties of muscle fibers. Fast twitch fibers for example have a faster Ca^{2+} transient, faster cross-bridge kinetics and thus a shorter time to peak tension and half relaxation (Schiaffino and Reggiani 2011).

1.7.3.1 Resting Ca^{2+}, Ca^{2+} transients and Ca^{2+} release from the SR

The cytosolic free Ca^{2+} concentration at rest is higher in slow-twitch than fast-twitch fibers (Gailly et al. 1993; Carroll et al. 1997; Carroll et al. 1999; Fraysse et al. 2003; Fraysse et al. 2006). Values of 50-60nM have been reported in rodent slow-twitch fibers, in contrast to 30nM in fast-twitch fibers. Sreter et al. first hypothesised that the resting Ca^{2+} concentration could influence fiber phenotype (Sreter et al. 1987). This was subsequently confirmed experimentally using rabbit myotube cultures to show that an increase of resting Ca^{2+} concentration induced a fast-to-slow fiber type transformation (Kubis et al. 1997).

Calcium transients reach a higher peak in fast-twitch fibers than slow-twitch fibers (Eusebi et al. 1980; Fryer and Stephenson 1996; Carroll et al. 1997; Baylor and Hollingworth 2003). The SR volume is larger in fast-twitch fibers compared to slow-twitch (Schiaffino et al. 1970; Luff and Atwood 1971) and an inverse relation between terminal cisternae fraction volume and time to peak tension has been observed in rat motor units (Liu et al. 2005).

Ca^{2+} release from slow-twitch fibers is less inhibited by cytosolic Mg^{2+} (Stephenson et al. 1998) and the responsiveness of slow-twitch fibers to caffeine-induced calcium release is greater than in fast-twitch fibers (Isaacson et al. 1970; Salviati and Volpe 1988; Fraysse et al. 2003). Ca^{2+} release is first detected with 0.2mM caffeine in rat soleus but requires 1mM in EDL (Fryer and Stephenson 1996). In fast twitch fibers, the threshold for caffeine response becomes lower when the SR is maximally loaded, but this does not occur in slow-twitch fibers (Bortolotto et al. 2001). Neonatal muscles are also more responsive to caffeine than adult muscles (Bertocchini et al. 1997). RyR3 is present in postnatal muscle, and may determine the features of Ca^{2+} release (Bertocchini et al. 1997), but in adult muscle RyR1 is the predominant Ca^{2+} release channel. The differences in Ca^{2+} release from the different adult fiber types therefore, is not due to different RyR1 isoforms. It might be determined by other factors such as post-translational modifications (phosphorylation, oxidative state) (Ruehr et al. 2003; Isaeva et al. 2005), interactions with other proteins (DHPR, calmodulin, FKBP12, CSQ) and the amount of Ca^{2+}

available in the terminal cisternae (slow-twitch fiber SR is maximally loaded but fast-twitch fiber SR is not) (Schiaffino and Reggiani 2011).

The amount of Ca^{2+} release by a single action potential is greater in fast-twitch than in slow-twitch fibers (Baylor and Hollingworth 2003). This is correlated with the abundance of RyR1 channels, which in fast-twitch fibers is more than twice that in slow-twitch fibers (Franzini-Armstrong et al. 1988) and in the different fraction of RyR channels coupled to DHPRs. The ratio of DHPR to RyR1 is lower in slow-twitch fibers (Delbono and Meissner 1996; Baylor and Hollingworth 2003). CICR may play a role in the slow twitch kinetics of slow-twitch fibers. Slow-twitch fibers may therefore be partly reminiscent of cardiac muscle. Interestingly, the same MyHC isoform expressed in type 1 (slow-twitch) fibers is also expressed in the heart (see **Table 1.2**) and the DHPR α_{1c} subunit is expressed in soleus and diaphragm but not in EDL (Pereon et al. 1998). RyR3, which is activated by CICR, is also expressed at higher levels in soleus and diaphragm (Flucher et al. 1999; Sorrentino and Reggiani 1999; Rossi et al. 2001; Conti et al. 2005).

As discussed in Section 1.5.2.2, CSQ influences RyR1 channel activity, and there are two isoforms of CSQ expressed in skeletal muscle. Fast-twitch fibers express CSQ1, whereas slow-twitch fibers express CSQ1 and CSQ2. CSQ content is greater in fast-twitch than in slow-twitch fibers (Leberer et al. 1988), which is probably related to the larger volume of SR in fast-twitch muscles. A quantitative analysis of CSQ content in murine fibers showed concentrations of 36μM in fast-twitch fibers (CSQ1 only) and 11μM in slow-twitch fibers (CSQ1 and CSQ2) (Murphy et al. 2009). CSQ plays a role in fiber type diversity. Firstly, CSQ buffers Ca^{2+} in the SR lumen and as CSQ1 binds up to 80 Ca^{2+} molecules per molecule and CSQ2 binds up to 60, CSQ1 contributes to the fast-twitch SR's greater Ca^{2+} store content. Secondly, it modulates Ca^{2+} release because of its interaction with RyR1 (Beard et al. 2004).

1.7.3.2 Cytosolic Ca^{2+} buffers

The Ca^{2+} transient declines faster in fast-twitch fibers compared to slow-twitch. The rate of decline of the Ca^{2+} transient is determined by the Ca^{2+} removal mechanisms (SERCA etc.) and binding of Ca^{2+} to cytoplasmic buffers. The major cytoplasmic Ca^{2+} buffers are parvalbumin, troponin C (TnC) and calmodulin. (Schiaffino and Reggiani 2011).

Parvalbumin is expressed in fast-twitch fibers at concentrations of ~1mM but is virtually absent in slow-twitch fibers (Celio and Heizmann 1982; Gundersen et al. 1988; Campbell et al. 2001). Parvalbumin is specifically expressed in type 2B and 2X fibers but not in type 2A fibers (Fuchtbauer et al. 1991). Functionally, parvalbumin quickly lowers the cytoplasmic Ca^{2+}

concentration after the Ca^{2+} release from the SR (Schwaller et al. 1999) allowing the fiber to relax faster. The Ca^{2+} bound to the parvalbumin dissociates and is returned to the SR slowly causing a tail in the Ca^{2+} transient detectable only in fast-twitch fibers (Klein et al. 1991).

TnC, which is involved in cross-bridge cycling (see Section 1.4.3) is present in the myofibril at a concentration of ~60μM with two reported isoforms (Salviati et al. 1984; Schiaffino and Reggiani 1996; Schiaffino and Reggiani 2011). TnC-fast expressed in fast-twitch fibers has four Ca^{2+} binding sites (two high affinity and two low affinity), whereas TnC-cardiac-slow, expressed in slow twitch fibers, lacks one of the low affinity binding sites. Thus TnC's contribution to Ca^{2+} buffer capacity is greater in fast-twitch fibers than slow-twitch (240μM vs. 180μM).

1.7.3.3 Ca^{2+} uptake by the SR

Early studies suggested that Ca^{2+} uptake occurs faster in fast-twitch fibers than in slow-twitch because of the greater SR surface area, parvalbumin as cytosolic Ca^{2+} buffer and the presence of specific transport proteins, (Sreter and Gergely 1964; Margreth et al. 1972; Salviati et al. 1982). SERCA1 is exclusively expressed in fast-twitch skeletal muscle fibers, whereas SERCA2 is expressed in slow-twitch fibers, cardiac muscle, smooth muscle and non-muscle tissue (Periasamy and Kalyanasundaram 2007). However, when expressed in COS cells, SERCA1 and SERCA2 have identical kinetics and transport rate (Lytton et al. 1992), so the diversity in Ca^{2+} uptake rate must be due to other factors such as the density of the pumps, presence of SERCA regulatory subunits or free Ca^{2+} gradient (Schiaffino and Reggiani 2011). The mitochondrion might also contribute to the Ca^{2+} uptake diversity seen in different fiber types due to different levels of ATP production and uptake of Ca^{2+} into the mitochondrion (see Section 1.7.3.4). The oxidation state of SERCA is another factor that could contribute to Ca^{2+} uptake rate as SERCA is vulnerable to redox modification. Oxidation of free-thiol groups on SERCA reduces its activity (Hidalgo and Donoso 2008).

SERCA pump density is greater (5-6 fold) in fast-twitch fibers than slow-twitch (Leberer and Pette 1986; Everts et al. 1989; Wu and Lytton 1993). Type 2B fibers have the highest SERCA density (Krenacs et al. 1989). This may be due to the SR volume and surface area being larger in fast-twitch fibers but could also be due to a greater concentration of SERCA pumps per unit area of SR (Dulhunty et al. 1987). Ca^{2+} uptake by SERCA is affected by extraluminal regulatory proteins that are bound to the pump as well as intraluminal proteins. SERCA2 is modulated by the phosphorylation state of the regulatory subunit phospholamban (Kirchberber et al. 1975; Tada and Kirchberger 1976; Kugelberg and Thornell 1983; Vangheluwe et al. 2005). As in cardiac muscle, phospholamban probably also inhibits SERCA2 in a

phosphorylation-dependent manner in slow-twitch muscle. Sarcolipin associates with SERCA1 in fast-twitch fibers and reduces Ca^{2+} pump activity, however, its regulatory role is less well defined (Vangheluwe et al. 2005). Due to the SR's larger volume in fast-twitch fibers, and greater abundance of CSQ, it is filled only to 35% of its capacity at resting cytoplasmic free Ca^{2+}. Therefore any increase of cytoplasmic Ca^{2+} results in fast and effective uptake into the SR (Dawson et al. 1987; Fryer and Stephenson 1996). In slow fibers, however, the SR is completely saturated with Ca^{2+} at resting cytoplasmic Ca^{2+} concentrations (Fryer and Stephenson 1996). Therefore the reuptake of cytoplasmic Ca^{2+} following a Ca^{2+} transient is slowed by a back inhibition of SERCA as SR Ca^{2+} binding sites become saturated (Inesi and de Meis 1989)

1.7.3.4 Contribution of mitochondria to Ca^{2+} homeostasis

Mitochondria, in addition to their energy supply role, play a role in modulating cytoplasmic free Ca^{2+} concentration. In skeletal muscle fibers, mitochondria are either subsarcolemmal, clustered beneath the sarcolemma, or they are intermyofibrilar and embedded among the myofibrils, (Ogata and Yamasaki 1985). The intermyofibrilar mitochondria are located in transversal rows close to the CRUs at the I-A band edge where they are closely associated with terminal cisternae (Vendelin et al. 2005; Dirksen 2009). In type 1 and 2A fibers there is an additional longitudinal row of mitochondria. Ca^{2+} enters the mitochondrion mainly through a Ca^{2+}-uniporter (MCU) (De Stefani et al. 2011). MCUs have a low affinity for Ca^{2+} (1-10μM), however they transport Ca^{2+} into mitochondria that are located near RyRs and are exposed to microdomains of high Ca^{2+} concentration (Rizzuto and Pozzan 2006; Franzini-Armstrong 2007). Mitochondria take up Ca^{2+} during contraction and rapidly release it during relaxation (Rudolf et al. 2004). The increase in mitochondrial Ca^{2+} is delayed by a few milliseconds following the cytoplasmic Ca^{2+} transient. Ca^{2+} entry into the mitochondrion is an important signal for mitochondrial function (Satrustegui et al. 2007; Gellerich et al. 2010), and could also help in calcium homeostasis by providing a calcium buffer. Indeed, there is some evidence that mitochondrial contribute differentially to Ca^{2+} homeostasis slow- and fast-twitch fibers. Inhibition of mitochondrial Ca^{2+} uptake shows that mitochondria do not play an active role in promoting relaxation in fast-twitch fibers, but play a significant role in the mitochondria-rich slow-twitch fibers (Gillis 1997). There is also some evidence that the protein compliment of mitochondria differs between fast- and slow-twitch fibers, which suggests that mitochondria can be specialized not just for energy metabolism, but also calcium regulation (Racay et al. 2006).

1.7.3.5 Response of myofibrils to Ca^{2+}

The troponin subunits and tropomyosin have distinct isoforms expressed in skeletal muscle (Schiaffino and Reggiani 1996). The response of the myofibrillar apparatus to Ca^{2+}

concentration is often expressed as the relation between tension developed and free Ca^{2+} concentration as a log value (pCa) giving the tension-pCa curve (see **Figure 1.23**). The threshold for activation is lower in slow-twitch than in fast-twitch fibers, but the steepness of the slope is greater in fast-twitch fibers (Schiaffino and Reggiani 2011).

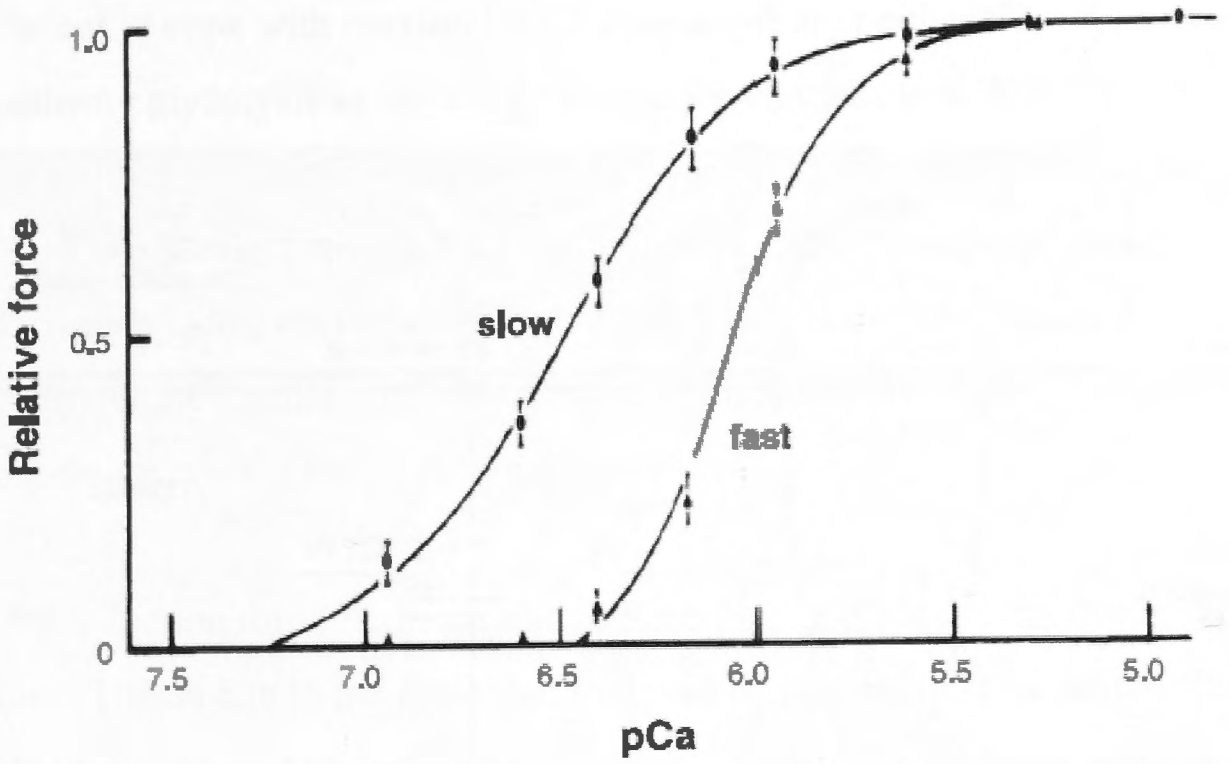

Figure 1.23: Modulation of active tension and rate of tension development be free calcium concentration (expressed as pCa = -log[Ca^{2+}]). The slow fibers were from rat soleus and the fast from rat EDL. The slow-twitch fibers have a lower threshold and slope compared to fast-twitch fibers (Schiaffino and Reggiani 2011)

In summary, compared to slow-twitch fibers, fast-twitch fibers are characterized by the following:

- Lower cytoplasmic free Ca^{2+} concentration due to more powerful cytoplasmic Ca^{2+} buffering
- Reduced Ca^{2+} entry from extracellular space
- Ability to release and take up larger amounts of Ca^{2+} in a shorter time due to a more developed SR, more SERCA, RyR1 and CSQ and more Ca^{2+} stored in the SR
- A steeper tension-pCa curve

1.7.4 Energy supply

The energy supply in terms of oxidative or glycolytic metabolism is extensively reviewed by Schiaffino and Reggiani (Schiaffino and Reggiani 2011) and only a brief summary is given below (see **Figure 1.24**).

The metabolic diversity among fibers becomes apparent when contractile activity starts. Upon activation, the energy consumption in muscle fibers increases roughly 1000-fold due to ATP hydrolysed by myofibrillar ATPase as well as SERCA. In human muscle, during high intensity

contractions, 1.5mM/s of ATP is consumed in slow-twitch muscle (37°C) and up to 7mM/s in fast-twitch muscle. ATP stores and phosphocreatine provide energy to support contractile activity for a few seconds, and for a longer period in slow-twitch fibers than for fast-twitch fibers. Therefore, even on a short time scale, fast-twitch fibers can generate more power, but contract for a shorter time than slow-twitch fibers.

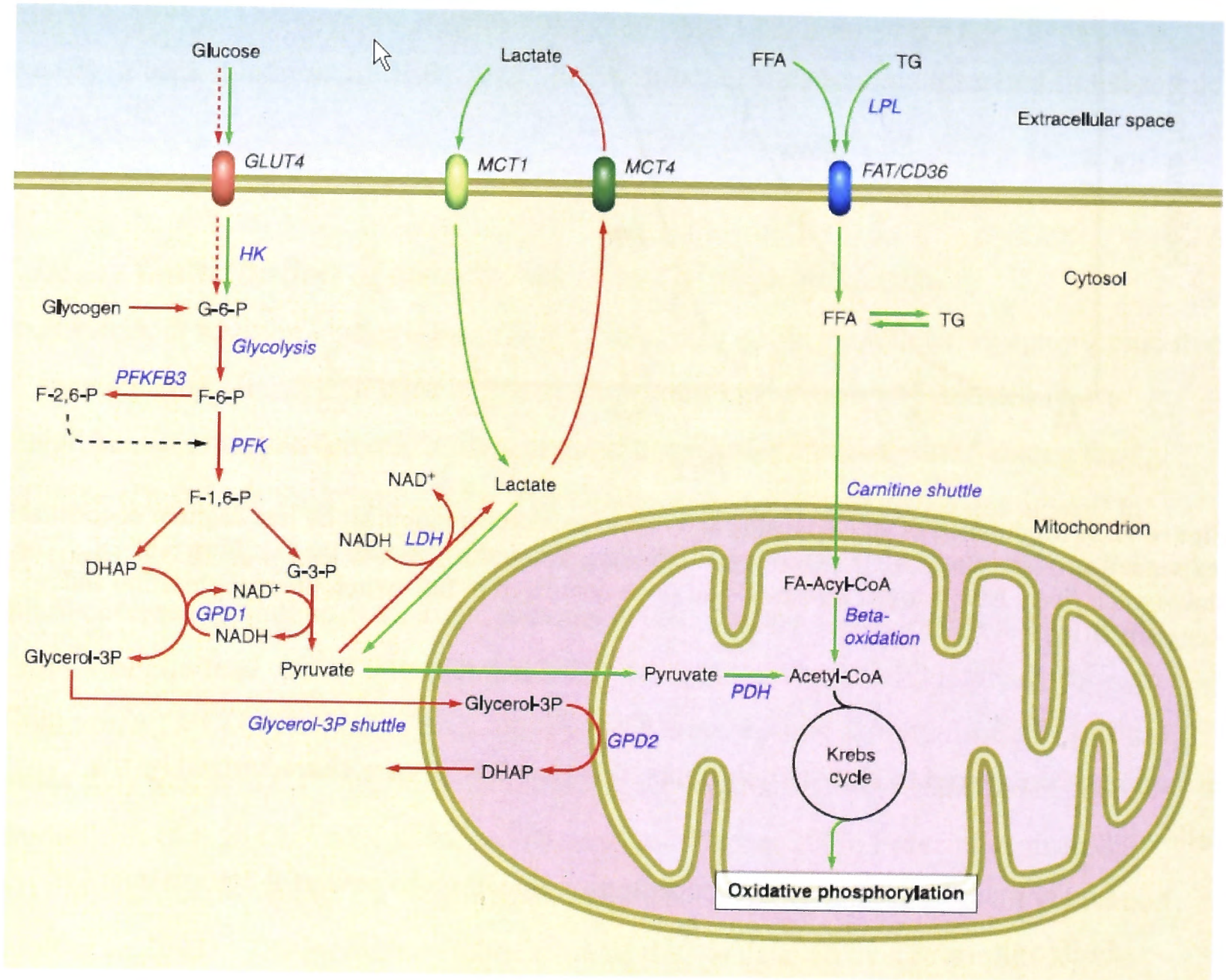

Figure 1.24: Scheme showing some differences in glucose, lactate and fatty metabolism between fat and slow twitch muscle fibers. Pathways prevalent in fast twitch muscle are shown in red arrows, whereas pathways prevalent in slow-twitch are shown in green arrows. The abbreviations stand for the following: DHAP, dihydroxyacetone phosphate; GLUT4, flucose transporter 4; F-6-P, fructose-6-phosphate; FAT/CD36, fatty acid translocase; FFA, free fatty acids; F-1,6-P, fructose-1,6-bisphosphate; F-2-6-P, fructose-2,6-bisphosphate; G-3-P, glyceraldehyde-3-phosphate; G-6-P, glucose-6-phosphate; GPD1, glycerolphosphate dehydrogenase 1 (cytoplasmic); GPD2, glycerolphosphate dehydrogenase 2 (mitochondrial); HK, hexokinase; LDH, lactate dehydrogenase; MCT1, monocarboxylic acid transporter 1; MCT4, monocarboxylic acid transporter 4; PDH, pyruvate dehydrogenase; PFK, phosphofructokinase; MCT4, monocarboxylic acid transporter 4; PDH, pyruvate dehydrogenase; PFK, phosphofructokinase; PFKFB3, phosphofructokinase-fructose bisphosphatase 3; TG, triglycerides (Schiaffino and Reggiani 2011).

Creatine kinase supports immediate ATP regeneration with assistance from adenylate kinase. Adenylate kinase is more active and leads to more AMP accumulation in fast-twitch fibers compared to slow-twitch. AMP deaminase, which is more abundant in fast-twitch fibers, converts AMP to IMP. IMP causes a greater activation of glycogenolysis. On the other hand

AMP activates AMP kinase which is more active in slow-twitch fibers and therefore causes a greater glucose uptake and β-oxidation than in fast-twitch fibers.

ATP production through glycolysis is more effective in fast-twitch than slow-twitch fibers because glycolytic activity is about twice as high in fast-twitch fibers. This, however, is not sufficient to cope with maximal ATP consumption in either fiber type and therefore sets a limit to pathway glycolysis as an energy source for contractile activity. Pyruvate produced through glycolysis can either be converted to lactate and exported, or it can be decarboxylated to acetyl-CoA. The balance between the two options is shifted towards acetyl-CoA in slow-twitch fibers and towards lactate in fast-twitch. Different lactate dehydrogenase isoforms and pyruvate dehydrogenase regulation via pyruvate dehydrogenase kinase and pyruvate dehydrogenase phosphatase control the switch in the pathway.

ATP production through the oxidative Krebs-cycle is more effective in slow-twitch fibers than in fast. This is due to the greater mitochondrial density in slow-twitch fibers and greater Krebs-cycle fuelling based on β-oxidation, which is three time higher in slow-twitch fibers. Mitochondrial activity is also regulated differently in slow- and fast-twitch fibers with differences in the effects of ADP stimulation (more effective in fast-twitch fibers) and creatine stimulation (more effective in slow-twitch fibers). Once mitochondrial respiration and ATP production are activated in slow-twitch fibers, they achieve a complete energy balance (ATP consumption is covered by ATP production). This never occurs in fast-twitch fibers.

1.7.5 Variations in muscle fiber types in relation to species, gender and individual polymorphism

1.7.5.1 Species diversity

Body size is a major determining factor in muscle fiber type composition. Muscles from small mammals like mice consist mainly of type 2X and 2B fibers and they abound in oxidative enzymes. Muscle from larger mammals like humans consists mainly of type 1 and 2A fibers but they contain lower levels of oxidative enzymes (Schiaffino and Reggiani 2011). Energy metabolism per unit body mass is inversely related to body size (Kleiber's law) therefore the metabolic activity in smaller species is higher than in larger animals (Kleiber 1947). This is reflected in the volume of muscle fiber occupied by mitochondria and the density of capillary vessels (Hoppeler et al. 1981). For example, in the common shrew, which is the smallest mammalian species, muscles are composed of exclusively type 2X and 2B fibers (Savolainen and Vornanen 1995) with a mitochondrial volume of 35% of the fiber. In humans however, mitochondria make up about 2-5% of fiber volume (Howald et al. 1985). Muscle fiber diameter

and maximum shortening velocity are also related to body size in that muscles from smaller animals are smaller diameter and have a faster shortening velocity (Rome et al. 1990; Seow and Ford 1991; Pellegrino et al. 2003; Toniolo et al. 2005; Marx et al. 2006) (Gauthier and Padykula 1966), although there are exceptions. Tension development is also faster in both in fast-twitch and slow-twitch fibers from small animals (Close 1965), and consequently the stimulation frequency necessary to obtain fused tetanic contraction is higher in smaller animals than in larger animals. For example, in humans, a maximal force is attained at about 50Hz, whereas rats need more than 100Hz for fast motor units and more than 70Hz for slow motor units to achieve fused tetanic contraction (Macefield et al. 1996; Piotrkiewicz and Celichowski 2007).

1.7.5.2 Gender diversity

There is obvious gender diversity in skeletal muscle mass when it comes to humans and this is dependent on the increased testosterone levels in men after puberty. The MyHC fiber type profile, however, is essentially similar in men and women but there is a higher ratio of type 2 to type1 fiber mass in men. This could be because of the hypertrophy of type 2 fibers induced by testosterone (Welle et al. 2008; Schiaffino and Reggiani 2011). There are also differences in metabolic properties such as lipid metabolism in muscle from women and men (Kiens 2006). Women use more lipids in exercise than men, which could also be because they have a higher ratio of type 1 to type 2 fibers. However, the factors responsible for gender differences in muscle metabolism are not known.

1.7.5.3 Individual diversity

Human skeletal muscle composition shows significant individual variation. For example in a study on fiber type composition of human vastus lateralis (Simoneau and Bouchard 1989), type 1 fibers were found to vary from 15-85% in a large cohort of individuals including sedentary and physically active individual of both sexes. 25% of individuals had either less than 35% or more than 65% of type 1 fibers. Muscle biopsies from monozygotic and dizygotic twins have shown that almost 50% of this variance is associated with genetic factors (Simoneau and Bouchard 1995). Muscle biopsies from athletes also show marked variation in fiber type profile. Sprint athletes have a tendency towards type 2 dominance and endurance athletes towards type 1. However, the extent to which training or genetic endowment influence this is not known (Costill et al. 1976; Andersen et al. 2000).

1.7.6 Fiber type diversification during muscle development

Muscle fiber type diversification is observed from the early developmental stages and it is initially independent of neural influence (Condon et al. 1990b). In mouse embryos, before E16,

all muscle fibers express both MyHC-emb and MyHC-β/slow (Narusawa et al. 1987; Condon et al. 1990a; Lyons et al. 1990). At E16, fiber type diversity is first observed with some of the primary fiber generation losing MyHC-β/slow expression for MyHC-neo. The two primary generation fiber populations turn into fast–twitch fibers (MyHC-emb and MyHC-neo expressing) or slow-twitch fibers (MyHC-emb and MyHC-β/slow) (Condon et al. 1990a). New, secondary generation fibers are also formed, expressing MyHC-emb and MyHC-neo. Fiber diversification occurs independently of neural influence and during the early stages of synaptogenesis. Matching between motor neuron types and muscle fiber types must occur because early motor units are largely homogenous in fiber type even during the period when they are polyneuronally innervated (Thompson et al. 1984).

During the first weeks after birth, four major changes take place in fiber type and MyHC composition in rat and mouse muscles:

- The progressive disappearance of MyHC-emb and MyHC-neo (lost more slowly in type 2A fibers) (Schiaffino et al. 1989).
- The upregulation of adult MyHC genes and the accumulation of MyHC-2A, -2X and -2B in fast-twitch fibers (DeNardi et al. 1993).
- Some fast-twitch muscle in mice (TA, plantaris) contain a proportion of type 1 fibers that disappear during postnatal development (Whalen et al. 1984; Agbulut et al. 2003).
- Some slow-twitch muscle in rats (soleus) have some type 2A fibers which are progressively transformed into type 1 fibers with concomitant transformation of type 2 to type 1 motor units (Kugelberg 1976).

The developmental MyHCs disappear during the first 2-4 weeks of postnatal development staring in type 2B fibers, then type 2X and later type 2A fibers (Schiaffino et al. 1989).

1.7.7 Fiber type in regenerating skeletal muscle

The satellite cells (muscle stem cells) responsible for muscle regeneration differ from the embryonic muscle precursor cells present at prenatal development. They also differ from the satellite cell involved in muscle growth during the early postnatal development stage. At first, developmental MyHC isoforms are expressed during regeneration (Sartore et al. 1982; Schiaffino et al. 1986; d'Albis et al. 1988). This is switched to adult isoforms under control of nerve activity. A widely used model for regeneration is the rat soleus which undergoes rapid regeneration after injury. If innervation is present, the regenerating fibers acquire the typical slow-twitch profile within a week. The fast-twitch gene program which seems to be the default, is activated in denervated regenerating muscle (Whalen et al. 1990; Esser et al. 1993). Functional innervation of regenerating fibers starts 3-5 days after injury and causes a rapid downregulation in MyHC-2B and -2X with an upregulation in MyHC-slow (Jerkovic et al.

1997). A slow motor neuron stimulation frequency is the switch in MyHC expression (Kalhovde et al. 2005). Satellite cells from adult mammalian muscle tend to form fibers with a phenotype reflecting their fiber type of origin, which suggest that there is satellite cell heterogeneity (Dusterhoft and Pette 1993; Wehrle et al. 1994; Barjot et al. 1995; Rosenblatt et al. 1996; Huang et al. 2006). This might also be because of transcription factors influenced by the fiber type milieu they find themselves in.

1.7.8 Fiber type remodelling

Skeletal muscle is very adaptable in response to changes in use. Its adaptations include changes in fiber size, fiber type as well as changes in muscle force and fatigue resistance (Pette and Staron 1997). Adult skeletal muscle can be induced to switch fiber type by changes in nerve activity, loading (increasing the force that a muscle must support or overcome e.g. weight training) or hormonal influences.

The effect nerve activity has on fiber type is mediated by specific impulse patterns (Pette and Vrbova 1999; Schiaffino and Reggiani 2011; Jorquera et al. 2013). A phasic high-frequency electrical stimulation can induce a slow-to-fast switch. This pattern resembles the firing pattern of fast neurons and the direction of fiber type change is 1→2A→2X→2B. Muscle unloading caused by hind limb suspension as well as hyperthyroidism can also cause a slow-to-fast fiber type switch in muscle. A fast-to-slow switch can be induced by electrical stimulation resembling the firing pattern of slow motor neurons (tonic low frequency). The direction of switching is 2B→2X→2A→1. Muscle overloading due to loss of synergistic muscles as well as hypothyroidism can also cause a fast-to-slow switch. The changes in any given muscle are dictated by the original fiber type of the muscle and intrinsic differences between muscles that determine their range of adaptations. Fast muscle has the capacity to adapt mostly in the fast range (2B↔ 2X↔ 2A) and slow muscles in the range 1↔ 2A↔ 2X (Ausoni et al. 1990).

Muscles undergoing fiber type transformation very frequently have hybrid fibers with mixed MyHC composition. This is due to the slow turnover of myosin (Schiaffino et al. 1988; Ausoni et al. 1990; Caiozzo et al. 1998). In humans, endurance-trained individuals have increased 1/2A hybrid fibers, whereas sedentary individuals have increased 2A/2X fibers (Klitgaard et al. 1990a).

During postnatal development and regeneration, a default nerve-activity independent muscle fiber differentiation program pathway activates the fast-gene program. However, slow-motor neuron activity induces slow gene program during postnatal development (Butler-Browne and Whalen 1984; Esser et al. 1993). Once established, the slow gene program is not readily

reversed in adult fibers and can persist for a long time even in denervated muscle. Physiological adaptation to increased activity, such as endurance exercise, induces a switch to a more oxidative fast phenotype (2X→2A in humans, 2B→ 2X→ 2A in rats and mice), but no significant switch to type 1 muscle fibers (Ausoni et al. 1990; Allen et al. 2001).

1.8 Sarcopenia

Sarcopenia is the age related loss of muscle mass and strength. It has also been associated with other serious conditions such as insulin resistance, osteoporosis, obesity, arthritis, and metabolic syndromes (Boden et al. 1993; Colman et al. 1995; Marcus 1995; Coin et al. 2000; Roubenoff 2000). In addition, the decay of the neuromuscular system due to age results in diminished force production, reduced speed of contraction, problems with maintaining balance, an increased risk of accidental falls, struggling to rise from seated positions and slowed walking (Lennmarken et al. 1985; Young et al. 1985; Einsiedel and Luff 1992; Hakkinen et al. 1996; Lindle et al. 1997; Izquierdo et al. 1999; Vaillancourt et al. 2003). Together, these outcomes can have a negative effect on quality and quantity of life. The causes of sarcopenia are multidimensional involving alterations in the central and peripheral nervous system, hormonal, nutritional, immunological and physical activity changes (Narici and Maffulli 2010). For the purposes of this thesis, the focus will be on structural and functional changes involving and affecting EC coupling.

1.8.1 Structural changes

Muscle undergoes significant structural changes during aging. From about the age of 50, whole muscle size decreases at a rate of roughly 1% per year. The result is that from the age of 50 to the age of 80yr, there is a reduction of 30% in whole muscle size (Lexell et al. 1988; Marcell 2003; Goodpaster et al. 2006). The proportions of protein, collagen and fat also change. As protein (contractile tissue) is lost, it is replaced by fat and collagen (Rice et al. 1989; Overend et al. 1992). The muscle mass decline with age in humans appears to be primarily due to a loss in the number of fibers (Eddinger et al. 1985; Lexell et al. 1988) and although early studies suggested that fiber size decreases, especially in type 2 fibers, more recent longitudinal reports suggest that fiber size is preserved in humans (Aniansson et al. 1992; Frontera et al. 2008).

1.8.1.1 Changes in fiber type

The loss of muscle mass seen with aging is due to atrophy of the muscle fibers and especially of fast-twitch fibers. Lexell et al showed that type II fibers experience a 26% decline in cross-sectional area between 20 and 80yr while the size of type I fibers did not atrophy significantly

(Lexell et al. 1988). This fiber type-specific reduction in size is seen in humans as well as animals (Lexell et al. 1983; Ansved and Larsson 1989; Holloszy et al. 1991; Coggan et al. 1992). However in humans although fiber atrophy contributes to the whole muscle's decrease in size, the main factor is the decrease in fiber number with age. In humans between the age of 52 and 77, there is a 35% decrease in fiber number within the whole muscle (Lexell et al. 1986). There appears to be a difference between species in the fiber specificity of the decrease in in muscle fiber numbers. A number of investigations show that humans loose equal amount of fast- and slow-twitch fibers during the aging process (Lexell et al. 1983; Lexell et al. 1988; Ansved and Larsson 1990). However, there seems to be a selective loss in fast-twitch fibers in rodent muscle in aging (Ishihara et al. 1987; Kanda and Hashizume 1989; Ansved and Larsson 1990). In rodents and humans, aging results in the whole muscle size and mass being comprised of a higher percentage of slow-twitch fibers. For rodents this would be the natural outflow of selective loss in fast-twitch fibers, but for humans this is unexpected as equal numbers of fast- and slow-twitch fibers are lost. The reason for the increase in slow-twitch content in aging human muscle is due to the age related atrophy of muscle fibers being more severe in fast-twitch fibers, therefore the proportion of muscle mass made up by slow-twitch fibers is significantly increased even though the fiber number ratio between fast-and slow does not change (Larsson et al. 1978; Essen-Gustavsson and Borges 1986; Lexell et al. 1988).

1.8.1.2 Changes in CRU structure

Boncompagni et al (Boncompagni et al. 2006) studied the ultrastructure and geometry of the CRUs in human vastus lateralis and gluteus medius biopsies from male and female subjects between the age of 28 and 83. They found that in mature skeletal muscle from young individuals, the CRUs were located almost exclusively opposite the sarcomere I-A junctions, one on each side of the Z-line. The CRUs were frequent and fairly evenly distributed, oriented transversely with respect to the long axis of the myofibrils. The feet (RyR1) were located in two parallel rows on either side of the t-tubule. Dyads as well as longitudinal triads and dyads were extremely rare. Several differences were observed in aged muscle specimens. The overall number of junctions was lower and the average CRU density per unit area significantly decreased. While the CRUs were uniformly distributed in fibers from younger muscle, the density of the CRUs in fibers from aged muscle was variable with areas completely devoid of CRUs. The junctions in the aged muscle were also more variable. The frequency of dyads and junctions with a large transverse profile (showing more than two feet on each side of the t-tubule) were higher in aged muscle. The frequency of longitudinal t-tubules was also increase in the aged muscle samples. Significantly, the size of the junctional gap between the SR and t-tubule, however, remained unchanged. The aged muscle CRUs often appeared disordered (although recognizable from their location near the A-I junction), with disordered junctions

usually in areas of low CRU density. It was suggested that they might represent a stage in the disassembly of CRUs.

1.8.2 Changes in motor units and neuromuscular junctions

1.8.2.1 Structural and functional changes in motor units

The decrease in the number of fibers with age is, as might be expected, directly linked with a loss of motor neurons. A number of mechanisms have been proposed to explain age-related loss of muscle fibers. One particularly involves the denervation of fibers caused by motor neuron cell death (Vandervoort 2002; Jones et al. 2009; Siu and Alway 2009; Deschenes et al. 2010). There have been reports of fewer of motor neuron axons present in the ventral roots of aged spinal cords and a greater number of the remaining axons displaying axonal degeneration. One study showed that among humans aged 60 and over, there were 25% fewer motor neurons compared to younger individuals (Tomlinson and Irving 1977). The remaining healthy neurons were significantly smaller in aged spinal cords. This is important because smaller neurons are capable of innervating fewer fibers than larger neurons (Kawamura et al. 1977; Tomlinson and Irving 1977; Mittal and Logmani 1987).

The current understanding of age-related remodelling of the motor units (Deschenes 2011) states that, during the degeneration of motor units the fibers innervated by the affected neuron become abandoned and no longer receives neural input. This process is compensated for, to some degree, by nerve terminal sprouting of the remaining healthy neurons to re-innervate the abandoned muscle fibers. Aging, however, also results in a reduced capacity for motor neuron sprouting and therefore the capacity for reinnervation of abandoned fibers is reduced (Jacob and Robbins 1990; Robbins 1992). This age related denervation/reinnervation process leads to greater clustering of reinnervated fibers and the death of fibers that are not successfully reinnervated (Larsson et al. 1978; Larsson and Edstrom 1986; Lexell and Downham 1991). Another effect of this process is that unlike the motor units of young adults, where all the fibers are of the same fiber type, different fiber types are dispersed in aging motor units, although they still display one dominant fiber type (Edstrom and Larsson 1987). The presence of more than one type of muscle fiber in a motor unit has become the hallmark of aging motor units.

With age-related remodelling of motor units, the muscle is left with fewer, but larger motor units. The innervation ratio of motor units is increased and therefore the remaining motor neurons activate a greater number of muscle fibers. Also, whether it is through the selective loss of fast motor neurons seen in animals or a greater atrophy of fast-twitch fibers seen in humans, the result is a greater portion of the aged muscle being composed of slow-twitch

muscle (Brown 1972; Lexell et al. 1983; Lexell et al. 1988; Klitgaard et al. 1989). This has physiological and functional implications for the muscle.

The natural consequence of structural changes in motor units is functional change in the affected muscles. A number of investigations have found that in humans 60 years and above, there is a steady decline in strength, at an annual rate of about 1.5% (Vandervoort and McComas 1986; Lindle et al. 1997; Rantanen et al. 1998; Deschenes 2004). This is seen in both men and women in muscles of both the upper and lower body (Young et al. 1984; Young et al. 1985; Lynch et al. 1999; Deschenes 2004). One of the main reasons for age-related decrease in muscle strength is the decrease in the number of motor units in affected muscles (Brown 1972; Campbell et al. 1973; Stalberg and Fawcett 1982; Galea 1996). Although aging reduces muscle mass, motor unit number and specific tension (force produced relative to fiber size) (Frontera et al. 2000; Gonzalez et al. 2003), the strength of individual motor units seems to increase in aging. It has been shown in humans that the age-related decline in the motor unit number of a muscle exceeds that muscle's decrease in maximal force production and that the strength expressed by surviving motor units is amplified (Doherty et al. 1993). This provides some compensation for the loss of motor units. Another functional implication of the change in motor-units with age is that the contractile velocity of the muscle fiber decreases due to more slow-twitch fibers in the whole muscle (Krivickas et al. 2001; Yu et al. 2007). However, age-induced changes in motor neuron conduction rate and alterations in the Ca^{2+} handling during contraction contribute to the reduction in contractile velocity and power (Campbell et al. 1973; Edstrom and Larsson 1987; Ansved and Larsson 1989; Sugiura and Kanda 2004; Deschenes 2011). Increased fatigue resistance with aging is another consequence of increased slow-twitch fiber content (Lanza et al. 2004; Dalton et al. 2010). However the reported effect of aging on fatigue resistance can vary due to differences in the way fatigue is measured (Kent-Braun et al. 2002; Yoon et al. 2008; Callahan et al. 2009). Whether the motor units themselves show improved fatigue resistance depends on the type of motor unit examined. While aging has no significant impact on slow-twitch motor units, fast-twitch motor units show decreased resistance to fatigue with aging (Kanda and Hashizume 1989; Sugiura and Kanda 2004; Lochynski et al. 2008). **Table 1.3** gives a summary of the age related adaptations of whole muscles and their motor units (Deschenes 2011).

Table 1.3 Summary of age-related adaptations of whole muscles and their motor units (Deschenes 2011)

	Whole Muscle	Motor Unit
Size	Decrease	Increase
Number of muscle fibers	Decrease	Increase
Maximal force production	Decrease	Increase
Specific tension (force/size)	No change or decrease	Decrease
Contractile velocity	Decrease	Decrease
Fatigue resistance	Increase (depending on test protocol)	No change (slow-twitch) or decrease (fast-twitch

1.8.2.2 Structural and functional changes in neuromuscular junctions

There is evidence that remodelling of the NMJ occur throughout our lifetime (Banker et al. 1983; Kelly and Robbins 1986; Wigston 1990a; Wigston 1990b; Hill et al. 1991; Robbins 1992), and that this natural remodelling is amplified with age and results in significant structural synaptic modifications. Reports show that modifications of the NMJ may possibly cause the modifications in muscle fibers such as atrophy and fiber type composition (Deschenes et al. 2010). Age-related modifications of the NMJ include elevations in nerve terminal branching (Courtney and Steinbach 1981; Oda 1984; Robbins and Fahim 1985; Andonian and Fahim 1987), and at the same time a sharp decline in vesicle density resulting in a decrease in stored ACh in aged nerve endings (Fahim and Robbins 1982; Deschenes and Wilson 2003). The reduced neurotransmitter is associated with a decrease in the number of active zones (ACh release sites) in the presynaptic terminals. Typically, the size of the neural endings and the number of branches within are related to axon thickness. However, even though the nerve terminal branching is elevated, the axons of the aged motor neurons were no larger in diameter (Prakash and Sieck 1998). This suggests that age-related NMJ changes do not originate in the spinal cord, but are initiated by changes at the neuromuscular apparatus. In fact there is evidence that the expedited denervation/reinnervation process that characterizes aging begins the NMJ and progresses in a retrograde (terminal to spinal cord) direction causing the axon to degenerate and ultimately resulting in the death of the neuron cell body (Ansved and Larsson 1990; Dupuis et al. 2009). The NMJ degeneration may be rooted in mitochondrial dysfunction in the nerve terminal which increases cellular toxicity association with excess ROS production (Seo et al. 2008; Dupuis et al. 2009; Jang et al. 2010) and reduced ATP synthesis (Kujoth et al. 2006; Safdar et al. 2010), which is needed for vesicular and neurotransmitter recycling.

Changes in the pre-synaptic nerve terminal are accompanied by alterations at the post-synaptic endplate. The overall area of the motor endplate enlarges in aged NMJ with a more dispersed AChR distribution (Fahim and Robbins 1982; Rosenheimer and Smith 1985; Prakash and Sieck 1998; Deschenes et al. 2010). There is also increased architectural uncoupling of pre- and post-synaptic features (Fahim and Robbins 1982; Prakash and Sieck 1998). This less stable, more fragile relationship between pre- and post-synaptic components of the NMJ, leads to a greater incidence of neuromuscular transmission failure during continuous stimulation (Smith 1979; Smith 1984). **Table 1.4** gives a summary of the morphological response of the NMJ to aging.

Table 1.4: Summary of morphological adaptations of the NMJ to aging. Adapted from (Deschenes 2011)

Pre-synaptic	Post-synaptic
↑ complexity of nerve terminal branching	↑ incidence of abandoned synaptic gutters
↑ nerve terminal branch number	↑dispersion of ACh receptors
↑ total nerve terminal branch length	↑ length of endplate
↑ planar area of nerve terminal branching	↑ total area of endplate
↑ area of ACh vesicle clusters	↑ perimeter length around endplate
↓ total number of ACh vesicles	↑incidence of pre- and post-synaptic uncoupling

The structural changes in NMJs related to age are naturally linked to functional changes in neurotransmission across the synapse. The larger nerve terminal number and area in aged NMJs are accompanied by an increased neurotransmitter release upon stimulation resulting in higher sarcolemmal endplate potential amplitude (Kelly and Robbins 1986; Bhattacharyya et al. 1994; Fahim 1997). This, however, leads to an earlier depletion of neurotransmitter and therefore increased neurotransmission failure.

1.8.3 Changes in EC coupling (EC uncoupling)

Although loss of muscle mass would reduce muscle strength, the loss in muscle strength is greater than can be accounted for by the loss in mass (Lynch et al. 1999). *In vitro* studies in single human muscle fibers have also shown a decrease in specific force (force/cross sectional area) with age (Frontera et al. 2000). This suggests that the intrinsic force-generating capacity of skeletal muscle per contractile unit may be impaired in aging mammals. Some of the suggested mechanisms involved in this process include alterations to the EC coupling process (Delbono et al. 1995; Renganathan et al. 1997; Wang et al. 2000) and decreased actin-myosin cross-bridge stability (Lowe et al. 2002).

Delbono et al (Delbono et al. 1995) first investigated the possibility that the reduction in specific force seen in aging muscle may be due to alterations in the EC coupling Ca^{2+} release process. Their study was specific to fast-twitch fibers as fast-twitch fibers showed the most significant degree of hypo-atrophy with aging in mixed fiber type composition muscles (Coggan et al. 1992). Delbono et al found that the fast-twitch fibers from the aged human subjects (65-75yr) had a reduced smaller average fiber diameter than the younger cohort (25-35yr). The maximal DHPR charge movement, normalized to membrane capacitance was reduced in the aged muscle with no change in voltage dependence or charge distribution. They also found DHPR Ca^{2+} current amplitude was reduced in aged muscle, again with no change in voltage dependence. The peak voltage-induce Ca^{2+} transient from the SR was reduced in aged muscle and this was not due to SR store depletion. These results suggested that the DHPR-dependent Ca^{2+} release underlying EC coupling is less in aged fast twitch muscle. This group coined the term EC uncoupling to describe the defects in transmission of membrane depolarization to SR Ca^{2+} release that are responsible for decreased specific force (Payne and Delbono 2004). Reduced DHPR change movement during EC coupling could indicate fewer DHPRs and/or dysfunctional DHPR with age. The reduced SR Ca^{2+} release could be the result of fewer DHPRs, dysfunctional DHPR, fewer RyR1 and/or dysfunctional RyR1. A number of subsequent studies investigated the expression of EC coupling proteins and are discussed below in Section 1.8.3.1.

In addition to the changes discussed above, the cytoplasmic free Ca^{2+} concentration is increased in both slow-twitch soleus and fast-twitch EDL muscles from old rats (Fraysse et al. 2006). In addition, a population of aging mouse skeletal muscle fibers has an external Ca^{2+} dependent component to EC coupling indicated by reduced voltage-induced Ca^{2+} transients in fibers in the absence of external Ca^{2+} (Payne et al. 2004). Interestingly, regenerating skeletal muscle and developing muscle go through similar stages in which effective EC coupling and contraction are partially dependent on external Ca^{2+} (Louboutin et al. 1995; Louboutin et al. 1996), and there is an accompanying transient expression of the DHPR α_{1c} subunit (Pereon et al. 1997). The expression of the DHPR α_{1c} diminishes as the expression of DHPR α_{1s} increases over time as muscle regeneration proceeds. As denervation and reinnervation occur in aged muscle with accompanying regeneration it is tempting to speculate that there is a shift towards cardiac EC coupling in aged muscle. However, one subsequent study found that external Ca^{2+} but not Ca^{2+} influx is needed to maintain force in repetitive fiber electrical stimulation of single fibers from aging mouse muscle (Payne et al. 2004). It is therefore unlikely that CICR plays a role in EC coupling in aged mice. The authors found that the external Ca^{2+} dependence is due to sodium channels modification with age, with the absence of external Ca^{2+} leading to a failure in in action potential generation.

Muscle weakness in aged muscle could also be due to modification of the RyR1. Oxidation and S-nitrosylation of RyR1 in aged muscle dissociates FKBP12 from the RyR1 causing an increase RyR1 activity and therefore "leaky" channels (Andersson et al. 2011). Stabilizing the RyR1/FKBP12 binding reduced this calcium leak from the SR, enhanced Ca^{2+} release from the SR, increased specific force and increased exercise capacity in aged mice.

1.8.3.1 DHPR and RyR1 expression in aged muscle tissue

It seems that there is a general change in protein expression (O'Connell et al. 2007) as well as protein turnover (Ferrington et al. 1998) in muscle with age. Changes in expression levels of DHPR and RyR1 are associated with loss of specific muscle force with age and this underlies the EC uncoupling hypothesis.

1.8.3.1.1 The RyR1

There are conflicting reports regarding the expression of RyR1 with age. A decrease in RyR1 levels has been reported in mixed and fast-twitch fibers in rats and mice with age using [^{3}H]ryanodine binding (Renganathan et al. 1997; Renganathan et al. 1998). However, other [^{3}H]ryanodine binding and immunoblot studies report no change in RyR1 expression in fast- and slow-twitch muscle from aged rats (Damiani et al. 1996; Margreth et al. 1999; O'Connell et al. 2008). In terms of the EC uncoupling hypothesis, the ratio of DHPR to RyR1 is likely to be more important than absolute expression levels in rodents.

1.8.3.1.2 The DHPR α_{1s} subunit

The report by Delbono et al (Delbono et al. 1995) showing reduced DHPR charge movement and SR Ca^{2+} transients in aged human muscle fast-twitch fibers was subsequently confirmed in fast-twitch fibers of aging mice (Wang et al. 2000). [^{3}H]PN200-110binding to DHPR α_{1s} in rat and mouse muscle shows reduced DHPR α_{1s} expression with age in mixed, slow-twitch and fast-twitch muscles (Renganathan et al. 1997; Renganathan et al. 1998). This was confirmed by immunoblot of aging rabbit and rat muscle (Ryan et al. 2000; Ryan et al. 2003; O'Connell et al. 2008). The DHPR/RyR1 ratio in adult rat EDL of ~1 suggests that every fourth RyR1 is linked to a DHPR tetrad. In soleus muscle this ratio is lower (~0.4) and indicates every 12th RyR1 is linked to a DHPR tetrad (Delbono and Meissner 1996; Renganathan et al. 1997). In aged muscle the ratio decreases to 0.26 in soleus and 0.68 in EDL muscle. This indicates that more DHPR uncoupled RyR1s are present in older rat muscle and supports the EC uncoupling hypothesis. Significantly, insulin growth factor-1 (IGF-1) enhances DHPR α_{1s} expression and prevents the age-related decline in DHPRα_{1s} expression and muscle force (Renganathan et al. 1998; Delbono 2000; Zheng et al. 2002).

In human muscle, however, there is apparently no decrease in DHPR α_{1s} with age (Ryan et al. 2003). The alterations in CRU structure seen in aged human muscle showed that the total number of CRUs was decreased, but that the average size of the RyR1 feet arrays are increased to compensate for this loss (Boncompagni et al. 2006). In human muscle therefore, it may be more a case of altered structure and arrangement of the EC coupling apparatus than the expression of the protein that cause the EC uncoupling.

1.8.3.1.3 The DHPR β_{1a} subunit

As discussed previously in Section 1.6.1.2, the DHPR β_{1a} subunit plays an important role in EC coupling as it is required for the trafficking of the DHPR α_{1s} subunit to the sarcolemma, formation of tetrads as well as regulating L-type Ca^{2+} current and supporting a fraction of EC coupling. In addition, the SH3 domain of the β_{2a} subunit has been shown to bind to dynamin and mediate endocytosis of the DHPR α_{1c} subunit in *Xenopus* oocytes (Gonzalez-Gutierrez et al. 2007). The effect of aging on the DHPR β_{1a} subunit expression was investigated by Taylor et al (Taylor et al. 2009). They reported a significant increase in β_{1a} expression with age in mice both in mixed muscles and fast-twitch muscles. They also found that over expression of the β_{1a} subunit in TA muscles of mice caused a decrease in α_{1s} subunit expression and decline in specific force. Introducing siRNA against the β_{1a} subunit and thereby reducing its expression in aged mice showing a decrease in charge movement restored the charge movement levels to control. These results suggest a possible role for β_{1a} in the reduction in α_{1s} subunit expression reported in rodents. However, the increased expression of β_{1a} has not been investigated in humans.

Chapter 2: Materials and Methods

2.1 Materials

2.1.1 List of chemicals and reagents

All chemicals and reagents used were of analytical grade.

CHEMICAL	MANUFACTURER
1,2-Bis (2-Aminophenoxy)ethane-N,N,N',N'-tetraacetic acid (BAPTA)	Sigma-Aldrich, USA
10bp DNA ladder	Invitrogen, Life Technologies, USA
10mM dNTP Mix	Invitrogen, Life Technologies, USA
2-Mercaptoethanol	Sigma-Aldrich, USA
2-Propanol (Isopropanol)	AnalaR Normapur, VWR International, USA
Acetic acid	AnalaR Normapur, VWR International, USA
Acetone	Univar, USA
Acrylamide	Bio-Rad Laboratories, USA
Adenosine 5'-triphosphate disodium salt hydrate (ATP-Na_2)	Sigma-Aldrich, USA
Agar	Difco Laboratories, USA
Albumin from bovine serum (BSA) lyophilized powder	Sigma-Aldrich, USA
Ammonium persulphate (APS)	Sigma-Aldrich, USA
Ampicillin	Sigma-Aldrich, USA
BCA protein assay Kit	Thermo Scientific Pierce Protein Biology Products, Thermo Scientific, USA
Benzamidine	Sigma-Aldrich, USA
Bolt® LDS Sample Buffer (4x)	Life Technologies, USA
Bolt® MES SDS running buffer (20x)	Life Technologies, USA
Bolt® MOPS SDS running buffer (20x)	Life Technologies, USA
Bolt® Sample Reducing Agent (10x)	Life Technologies, USA
Boric acid	AnalaR Normapur, VWR International, USA
Brilliant Blue R	Sigma-Aldrich, USA
Bromophenol blue	Sigma-Aldrich, USA
$CaCl_2$	Univar, USA

CHEMICAL	MANUFACTURER
Calpain inhibitor I	Sigma-Aldrich, USA
Calpain inhibitor II	Sigma-Aldrich, USA
Cesium hydroxide (CsOH)	Sigma-Aldrich, USA
Cesium methanesulfonate – $CsCH_3O_3S$ (CsMS)	Sigma-Aldrich, USA
Chloroform	Sigma-Aldrich, USA
CsCl	Sigma-Aldrich, USA
DC Plus Protein Assay Kit	Bio-Rad Laboratories, USA
Dimethyl sulfoxide (DMSO)	Sigma-Aldrich, USA
Dithiothreitol (DTT)	Sigma-Aldrich, USA
Ethanol	EMSURE, Merck Millipore, Germany
Ethidium Bromide	Sigma-Aldrich, USA
Ethylene glycol-bis(2-aminoethylether)-N,N,N',N'-tetraacetic acid (EGTA)	Sigma-Aldrich, USA
Ethylenediaminetetaacetic acid disodium salt dihydrate (EDTA-Na_2)	Sigma-Aldrich, USA
Foetal Calf Serum (FCS)	Sarana Australia Animal Serum Manufacturers, Australia
Glycerol	Univar, USA
Glycine	AMRESCO LLC, USA
Goat α-mouse IgG-HRP antibody	Santa Cruz Biotechnology Inc, USA
Goat α-rabbit IgG-HRP antibody	Santa Cruz Biotechnology Inc, USA
Guanidine hydrochloride (GuHCl)	AMRESCO LLC, USA
HiSpeed Plamid Maxi Kit	QIAGEN, Netherlands
Imidazole	Sigma-Aldrich, USA
Isopropyl β-D-1-thiogalactopyranoside (IPTG)	Sigma-Aldrich, USA
KCl	Chem-Supply, Australia
KOD Hotstart DNA polymerase	Novagen, Merck Millipore, Germany
Leupeptin	Sigma-Aldrich, USA
Luria Broth	JCSMR media, Australia
Luria Broth (LB)	JCSMR media, Australia
Methanol	EMSURE, Merck Millipore, Germany
Minimum Essential Medium (MEM)	Invitrogen, Life Technologies, USA
N,N,N',N',-Tetramethylethylenediamine (TEMED)	Bio-Rad Laboratories, USA
N,N,N',N'-Tetraethylsulfamide (TES)	Sigma-Aldrich, USA

CHEMICAL	MANUFACTURER
Na^2HPO_4	AnalaR Normapur, VWR International, USA
NaCl	Merck Millipore, Germany
NaH_2PO_4	AnalaR Normapur, VWR International, USA
n-Decane	Sigma-Aldrich, USA
Oligo dT 12-18 primer	Invitrogen, Life Technologies, USA
Pepstatin A	Sigma-Aldrich, USA
Phosphate Buffered Saline (PBS)	JCSMR media, Australia
Phosphatidylcholine (PC)	Avanti polar lipids, USA
Phosphatidylethanolamine (PE)	Avanti polar lipids, USA
Phosphatidylserine (PS)	Avanti polar lipids, USA
Phynylmethylsulfonylfluoride (PMSF)	Sigma-Aldrich, USA
Pierce ECL Western Blotting Substrate	Thermo Scientific Pierce Protein Biology Products, Thermo Scientific, USA
Precast 4-12% Novex® Bolt® Bis-Tris gels	Life Technologies, USA
Precast 4-15% Bio-Rad Tris-Gly gels	Bio-Rad Laboratories, USA
Precision Plus Protein Dual Colour Prestained Standard	Bio-Rad Laboratories, USA
Primers for PCR (human)	GeneWorks, Australia
Primers for PCR (mouse and rat)	Integrated DNA Technologies, USA
Protease inhibitor cocktail, EDTA free	Roche, Switzerland
PSN 1000x antibiotic cocktail	JCSMR media, Australia
QIAprep spin Miniprep Kit	QIAGEN, Netherlands
RNaseOUT™	Invitrogen, Life Technologies, USA
RNeasy mini Kit	QIAGEN, Netherlands
Ruthenium red	Sigma-Aldrich, USA
Silver Stain Plus Kit	Bio-Rad Laboratories, USA
Skim milk powder	Woolworths, Australia
Sodium dodecyl sulphate (SDS)	Sigma-Aldrich, USA
Sucrose	Chem-Supply, Australia
SuperScript®III Reverse Transcriptase Kit	Invitrogen, Life Technologies, USA
Tris	Sigma-Aldrich, USA
Tris–HCl	Sigma-Aldrich, USA
TRIzol®	Invitrogen, Life Technologies, USA
TWEEN® 20	AMRESCO LLC, USA
Urea	Sigma-Aldrich, USA
α-$Ca_V1.2$ ACC-003 polyclonal antibody	Alemone labs, Israel

CHEMICAL	MANUFACTURER
α-DHPR α_{1a} IIID5E1 monoclonal antibody	Developmental Studies Hybridoma Bank, USA
α-DHPR β_{1a} VD2(1)B12 monoclonal antibody	Developmental Studies Hybridoma Bank, USA
α-FKBP12 (H-5) monoclonal antibody	Santa Cruz Biotechnology Inc, USA
α-RyR1 34C monoclonal antibody	Developmental Studies Hybridoma Bank, USA

2.1.2 Buffers and Solutions

All buffers and solutions were made up using water that has been sequentially passed through a 10mU filter, 5mU filter, activated carbon and a reverse osmosis (RO) system. The water from the RO system was then filtered through a MilliQ unit (Merck Millipore, Germany). This process produces water at 18.2 mΩ.

Some buffers were made up at higher concentrations to serve as stock solutions. The dilution factor is indicated in front of the buffers affected e.g 10x Buffer A has to be diluted 1 in 10 to make 1x Buffer A.

2.1.2.1 Buffers and solutions used in expression and purification of the full length DHPR β_{1a}-subunit

2.1.2.1.1 10x Buffer A

0.5M sodium phosphate pH8, 3M NaCl.

2.1.2.1.2 DHPR β_{1a} Resuspension Buffer

8M Urea, 5mM Imidazole, 12mM 2-Mercaptoethanol, 1x Buffer A pH 8.0, 10% Glycerol.

2.1.2.1.3 DHPR β_{1a} Elution Buffer

8M Urea, 500mM Imidazole, 12mM 2-Meraptoethanol, 1x Buffer A pH8, 10% Glycerol.

2.1.2.1.4 Sample Buffer for DHPR β_{1a} Purification

0.06M Tris-HCl pH 6.8, 2% (w/v) SDS, 5% (v/v) 2-Mercaptoethanol, 10% (v/v) Glycerol, 0,025% (w/v) Bromophenol blue.

2.1.2.1.5 10x Electrophoresis Running Buffer

0.25M Tris, 1.95M Glycine, 1% (w/v) SDS.

2.1.2.1.6 DHPR β_{1a} Purification Prepcell Gel Recipe

Resolving gel: 25% (v/v) 1.5M Tris-HCl pH 8.8 stock
7% (v/v) Acrylamide/Bis-acrylamide (37.5:1)
0.5% (w/v) APS
0.125% (v/v) TEMED

Stacking gel: 25% (v/v) 0.5M Tris-HCl pH 6.8 stock
6% (v/v) Acrylamide/Bis-acrylamide (37.5:1)
0.5% (w/v) APS
0.125% (v/v) TEMED

2.1.2.2 Buffers and solutions used in MyHC analysis

2.1.2.2.1 MyHC Homogenizing Buffer

20mM Imidazole pH7.2, 150mM KCl, 0.2mM EDTA-Na_2.

2.1.2.2.2 MyHC Resuspending Buffer

50mM Tris-HCL pH7.4, 150mM NaCl.

2.1.2.2.3 5x MyHC Resolving Gel Buffer

1M Tris-HCl pH 8.8, 0.5M Glycine.

2.1.2.2.4 5x MyHC Stacking Gel Buffer

0.35M Tris-HCl pH 6.7, 20mM EDTA-Na_2.

2.1.2.2.5 20x MyHC Electrophoresis Running Buffer

1M Tris, 1.5M Glycine, 1% (w/v) SDS.

2.1.2.2.6 3x MyHC Sample buffer

0.24M Tris-HC pH 6.8, 60% (v/v) Glycerol , 6% (w/v) SDS, 150mM DTT, 0.01% (w/v) Bromophenol blue.

2.1.2.2.7 MyHC Gel Recipe

Resolving gel: 35% (v/v) Glycerol
8% (v/v) Acrylamide/Bis-acrylamide (99:1)
0.4% (w/v) SDS
20% (v/v) 5xMyHC Resolving gel buffer
0.1% (w/v) APS
0.05% (v/v) TEMED

Stacking gel: 30% (v/v) Glycerol
4% (v/v) Acrylamide/Bis-acrylamide (49:1)
0.4% (w/v) SDS
20% (v/v) 5x MyHC Stacking gel buffer
0.01% (w/v) APS
0.05% (v/v) TEMED

2.1.2.3 Microsomal vesicle homogenizing buffer

300mM Sucrose, 5mM Imidazole pH 7.4.

2.1.2.4 2x HBS

140mM NaCl, 1.5mM Na_2HPO_4, 5mM HEPES.

2.1.2.5 Bilayer solutions

2.1.2.5.1 *Trans* Solution

20mM CsCl, 30mM $CsCH_3O_3S$, 1mM $CaCl_2$, 10mM TES.

2.1.2.5.2 *Cis* Solution

20mM CsCl, 230mM $CsCH_3O_3S$, 1mM $CaCl_2$, 10mM TES.

2.1.2.5.3 Perfusion Solution

20mM CsCl, 230mM $CsCH_3O_3S$, 10μM $CaCl_2$, 10mM TES

2.1.2.6 Buffers and solutions used in SDS-PAGE and Immunoblot

2.1.2.6.1 10x Electrophoresis Running Buffer

0.25M Tris, 1.95M Glycine, 1% (w/v) SDS.

2.1.2.6.2 4x Sample Buffer

200mM Tris-HCl pH 6.8, 8% (w/v) SDS, 0.05M EDTA-Na_2, 40% (v/v) glycerol, 0.588M 2-Mercaptoethanol, 0.08% (w/v) Bromophenol Blue.

2.1.2.6.3 Immunoblot Transfer Buffer

37mM Tris, 140mM Glycine, 20% (v/v) Methanol.

2.1.2.6.4 Coomassie Brilliant Blue stain

0.1% (w/v) Brilliant Blue R, 10% (v/v) Acetic acid, 40% (v/v) Ethanol.

2.1.2.6.5 Destain Solution

5% (v/v) Acetic acid, 20% (v/v) Ethanol.

2.1.2.7 Buffers and solutions used for vertical DNA gels

2.1.2.7.1 10x TBE Buffer

0.89M Tris pH 8.2, 0.91M Boric acid, 0.025M EDTA-Na_2.

2.1.2.7.2 DNA Gel Recipe

Resolving gel: 10% (v/v) Acrylamide / Bis acrylamide (29:1)
0.4% (w/v) SDS
10% (v/v) 10x TBE buffer
0.075% (w/v) APS
0.05% (v/v) TEMED

No stacking gel used

2.1.2.7.3 2x Sucrose DNA Loading Dye

60% (w/v) sucrose, 15mM EDTA-Na_2, 0.025% (w/v) Bromophenol Blue.

2.1.2.8 Buffers and Solutions from JCSMR Media

2.1.2.8.1 1000x PSN Antibiotic Cocktail

30.072g/L Penicillin G, 50g/L Streptomycin Sulphate, 50g/L Neomycin Sulphate

2.1.2.8.2 Luria Broth (LB)

10g/L Tryptone, 5g/L Yeast Extract, 10g/L NaCl

2.1.2.8.3 Minimum Essential Medium F15 Eagles

9.61g/L F15 MEM powder (Gibco, Lif Technologies, USA), 2.2g/L $NaHCO_3$, pH6.8-7.5

2.1.2.8.4 Phosphate Buffered Saline (PBS)

8g/L NaCl, 1.25g/L $Na_2HPO_4.2H_2O$, 0.3535g/L $NaH_2PO_4.H_2O$

2.2 Methods

2.2.1 DNA extraction

2.2.1.1 DNA extraction for transformation of bacterial cells

5ml of Luria Broth (LB) (JCSMR Media, Australia) containing 100µg/ml ampicillin was inoculated with BL21(DE3) *Escherichia coli* (*E. coli)* cells containing the plasmid of interest and incubated overnight at 37°C with agitation. Plasmid DNA was extracted using the QIAprep spin Miniprep Kit (QIAGEN, Netherlands) following manufacturer's instructions and quantified using a Nanodrop ND-1000 (Thermo Scientific, USA) spectrophotometer.

2.2.1.2 DNA extraction for transfection of mammalian cells

A starter culture was prepared by inoculating 5ml of LB (JCSMR Media, Australia) containing 100µg/ml ampicillin with DH5α *E. coli* cells containing the plasmid of interest and incubated for 8-9hr at 37°C with agitation. The 5ml starter culture was then added to 200ml LB containing 100µg/ml ampicillin and incubated overnight at 37°C with agitation. Plasmid DNA was extracted using the HiSpeed Plamid Maxi Kit (QIAGEN, Netherlands) following manufacturer's instructions and quantified using a Nanodrop ND-1000 (Thermo Scientific, USA) spectrophotometer.

2.2.2 Transformation of competent cells

Competent cells were prepared using the calcium chloride method (Sambrook and Russell 2001), and 100µl aliquots were snap frozen on dry ice. Cells were stored at -70°C until further use.

Competent cells were transformed by adding 1ng of plasmid DNA to 100µl of competent cells, mixing by carefully pipetting up and down on ice. The mixture was then incubated on ice for 30min. The plasmid/competent cell mixture was then exposed to a heat shock by spreading the mixture onto a pre-heated (37°C) LB agar plate containing 100µg/ml ampicillin and the plate was incubated over night at 37°C.

2.2.3 Protein expression in bacterial cells

The full length murine DHPR β1a-subunit was expressed in a pHUE vector (**Figure 2.1**) (Baker et al. 1994; Karunasekara 2011; Rebbeck et al. 2011) which attaches a 6xHis-ubiquitin tag to the protein.

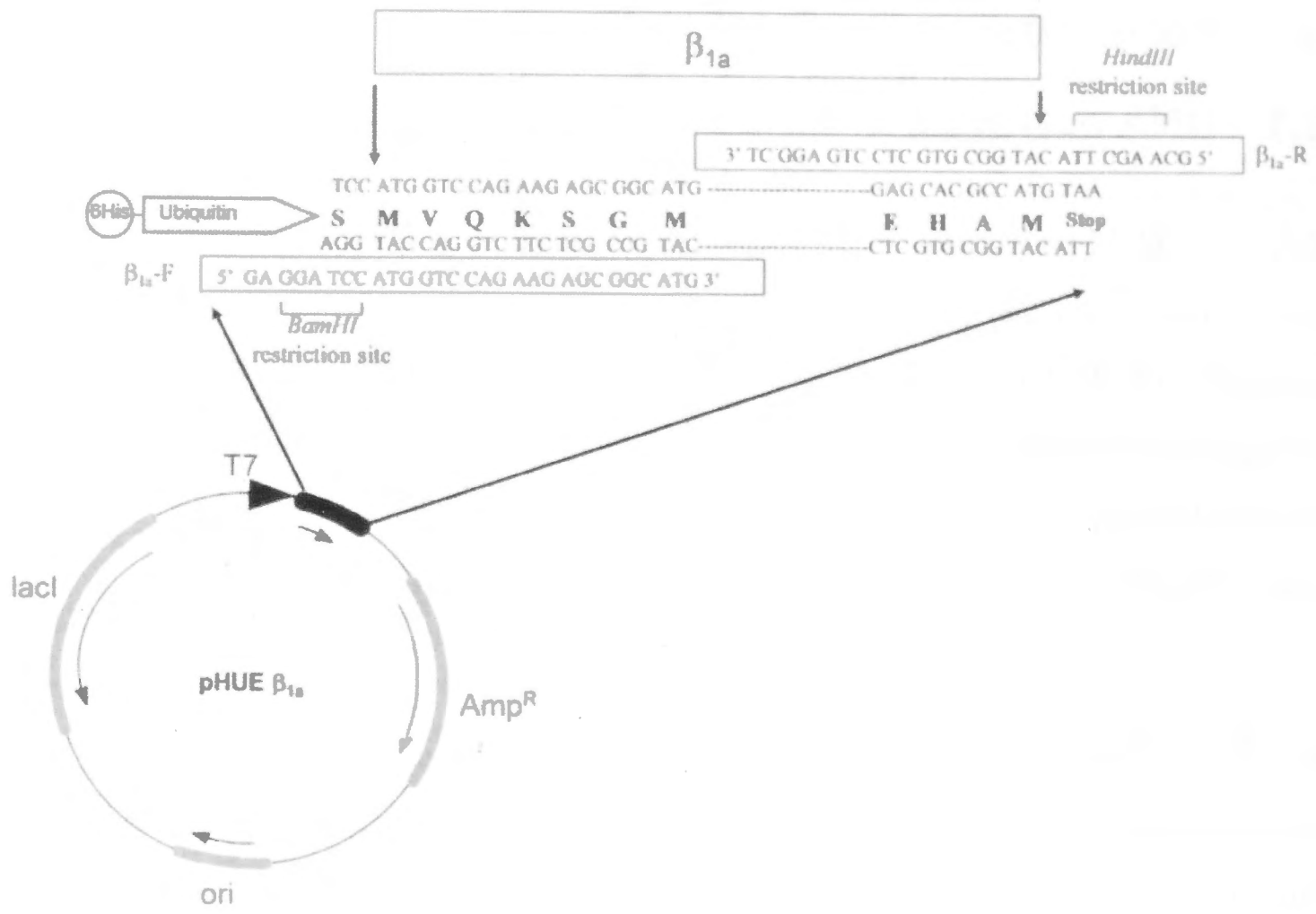

Figure 2.1 DHPR β_{1a}/pHUE construct (Karunasekara 2011; Rebbeck et al. 2011). The murine sequence of the DHPR β_{1a}- subunit was used.

An LB agar plate containing 100µg/ml ampicillin was streaked with DHPR β_{1a}/pHUE in BL21(DE3) *E. coli* and incubated overnight at 37°C. A single colony from this plate was then inoculated into 40ml of LB containing 100µg/ml ampicillin and incubated with agitation at 37°C overnight. 5ml of the starter culture was then inoculated into 400ml of LB containing 100µg/ml in a 2 litre flask. 6 such flasks were prepared and incubated with agitation at 37°C until OD_{600} (optical density at 600nm) reached approximately 0.8-1.0 (Cary 100 UV-vis spectrophotometer). Protein expression was initiated with the addition of 0.1mM IPTG to each flask. The flasks were then incubated at 37°C with agitation for 2hr. The culture was then centrifuged in 500ml Drypin bottles (Du Pont Instruments, USA) at 5000rpm (4400g) at 4°C for

20min. A Sorval RC-5B Refrigerated Superspeed Centrifuge, (Du Pont Instruments, USA) was used with a SLA-3000 rotor. The pellets were stored at -20°C until further use.

The initial purification steps of the expressed β_{1a}-subunit was carried out by immobilized metal affinity chromatography (IMAC) using a Ni-NTA agarose resin produced in-house according to (Hochuli 1990).

2.2.4 Protein purification by IMAC (immobilized metal affinity chromatography)

As this is a denaturing purification, all steps were carried out at room temperature unless otherwise specified because proteases will be denatured and risk of protein breakdown at room temperature is minimal. The *E. coli* pellet obtained from the procedure described in section 2.2.3 was thawed on ice and resuspended in 40ml of DHPR β_{1a} resuspension buffer (Section 2.1.2.1.2). Cells were lysed by sonication on ice using 5 bursts of 30s at 300W with a 30s cooling period between bursts (Branson Sonifier, USA). The cell lysate was centrifuged in 50ml polycarbonate tubes (Du Pont Instruments, USA), using a SS34 rotor (Sorval RC-5B Refrigerated Superspeed Centrifuge, Du Pont Instruments, USA) at 15000rpm (10000g) for 40min at 4°C.

The supernatant was added to 50% slurry of Ni-NTA agarose resin pre-equilibrated in resuspension buffer. A Ni-NTA agarose bed volume of 2ml was used. The mixture of agarose and supernatant was incubated on a rotating wheel at 4°C for 1hr. Subsequently, the mixture was centrifuged at 1500rpm (453g) in a benchtop centrifuge (Eppendorf Centrifuge Model 5810R, Eppendorf, USA) for 5min at 4°C to spin down the resin. The supernatant was discarded and the resin washed three times by centrifugation with 50ml of resuspension buffer. After the final wash, the resin was transferred to a 10ml polypropylene column and the protein eluted with DHPR β_{1a} elution buffer (Section 2.1.2.1.3). 15ml of eluate was collected and diluted to a final volume of 45ml with 1x Buffer A (Section 2.1.2.1.1) in order to dilute the urea concentration to 2.6M to preserve the activity ubiquitin protease cleaving enzyme.

The 6xHis-ubiquitin tag was removed by digesting the expressed β_{1a} with an ubiquitin-specific protease, Usp2cc, in the presence of 1mM DTT. The protease was added at a ratio of 1:200 (v/v) and incubated at 30°C overnight.

The digested sample was concentrated to approximately 2ml using a 10kDa cutoff AMICON® Ultra filter concentrator (Merck Millipore, Germany) following the manufacturer's instructions.

2.2.5 Protein purification by preparative denaturing polyacrylamide gel electrophoresis (SDS-PAGE)

After the initial purification of the expressed DHPR β_{1a}-subunit the protein was purified by preparative denaturing polyacrylamide gel electrophoresis (PAGE) using the Bio-Rad Prep Cell model 491 (Bio-Rad laboratories, USA).

A 10cm, 7% Tris-glycine resolving gel and a 2cm, 6% stacking gel (Section 2.1.2.1.6) was poured on to the 2.8cm diameter assembly tube of the Prep Cell apparatus according to the manufacturer's instructions.

The partially purified concentrated 2ml DHPR β_{1a} sample obtained at the end of the protocol described in the previous section (2.2.4) was mixed with 1ml sample buffer (2.1.2.1.4) and boiled for 5min. The sample was then loaded onto the preparative gel. The Prep Cell apparatus was assembled according to the manufacturer's instructions and electrophoresis was carried out at 4°C at a constant current of 40mA and 1x Electrophoresis Running buffer (2.1.2.1.5) was used both as the running buffer and as the elution buffer. 4ml fractions were collected after the dye front eluted (Bio-Rad Model 2128 Fraction Collector, Bio-Rad Laboratories, USA).

The collected fractions were analysed on 4-15% Precast Tris-glycine polyacrylamide gels (Section 2.2.12) and the fractions containing the band of interest pooled. Ice cold acetone was added to the pooled fraction at a ratio of 4:1 (v/v) to precipitate the protein from the buffer containing SDS. The proteins were precipitated overnight at -20°C. Subsequently the protein was centrifuged at 4000rpm (Eppendorf Centrifuge Model 5810R, Eppendorf, USA) at 4°C for 30min and the supernatant removed. A vacuum desiccator was used to remove excess acetone. The dried protein sample was then dissolved in 1x Buffer A (Section 2.1.2.1.1) containing 6M guanidine hydrochloride. The sample was then refolded to its native form by dialysis into 1x Buffer A at 4°C overnight. The refolded protein was quantified and aliquots were stored at -70°C until further use.

2.2.6 Protein Quantitation

2.2.6.1 BCA assay

The concentration of the expressed full length DHPR β_{1a}-subunit was determined using the BCA assay (Smith et al. 1985) according to the manufacturer's instructions for microplates (Thermo Scientific Pierce BCA protein assay kit, Thermo Scientific, USA). The assay measures the formation of Cu^{+} form Cu^{2+} by the Biuret complex in alkaline solutions of proteins

using bicinchonic acid (BCA). The absorbance at 562nm was measured as primary wavelength with a reference wavelength of 750nm using an EL 800 Universal Microplate Reader (Bio-Tek Instruments, USA).

2.2.6.2 DC protein assay

The total protein concentration in muscle homogenates and in microsomal vesicles was determined using the Bio-Rad DC Protein assay (Bio-Rad Laboratories, USA). This assay is similar to the Lowry assay (Lowry et al. 1951). It is based on the reaction of protein with an alkaline copper tartrate solution and Folin reagent, which produces reduced species that have a characteristic blue colour. The assay was conducted according to the manufacturer's instructions for microplates. The absorbance at 650nm was measured as primary wavelength with a reference wavelength at 405nm using an EL 800 Universal Microplate Reader (Bio-Tek Instruments, USA).

2.2.7 Protein expression in mammalian cells

The full length splice variants of the rabbit RyR1, ASI(+)RyR1 and ASI(-)RyR1 were expressed in a pCIneo vector (**Figure 2.2**) in HEK293 cells which do not naturally express RyR1 in levels detectable by standard immunoblot analysis (Querfurth et al. 1998). The recombinant constructs were kindly donated by Prof R. T. Dirksen (Kimura et al. 2007).

HEK293 cells were grown in minimum essential medium (MEM) (JCSMR Media, Australia) with 10% foetal calf serum (FCS) and 0.1% PSN antibiotic cocktail (JCSMR Media, Australia) at 37°C with 5% CO_2. HEK293 cells were transfected using the calcium-phosphate method (Sambrook and Russell 2001). T175 flasks (cell culture flasks with a surface area of 175cm^2 for cell adhesion) were plated at 50% confluency 24h before transfection. The cells were given fresh growth medium 3h before transfection. For each T175 flask, the calcium phosphate precipitate was prepared in the following manner. All dropping was done using a P1000 Pipetman®, Gilson Inc., USA. One drop from 0.75ml 2M $CaCl_2$ was added to a volume of sterile MilliQ (Merck Millipore, Germany) water. The volume of water is determined by the concentration of the plasmid DNA. As the final volume of plasmid DNA and water must be 1.2825ml per flask and 80µg of plasmid DNA is needed per flask, the volume of water used is 1.2825 minus the volume of plasmid DNA that contains 80µg of DNA. The plasmid DNA (80µg per flask) was then added to the water drop for drop. The remaining 2M $CaCl_2$ was then added to the mixture drop for drop. The $CaCl_2$/plasmid DNA/water mixture was subsequently added to 1.5ml 2x HBS (Section 2.1.2.4) drop for drop, while agitating the 2x HBS with a motorised pipette (Eppendorf Easypet, Eppendorf, USA). The resulting mixture was incubated for 45min at room temperature to allow the formation of the calcium phosphate precipitate. The

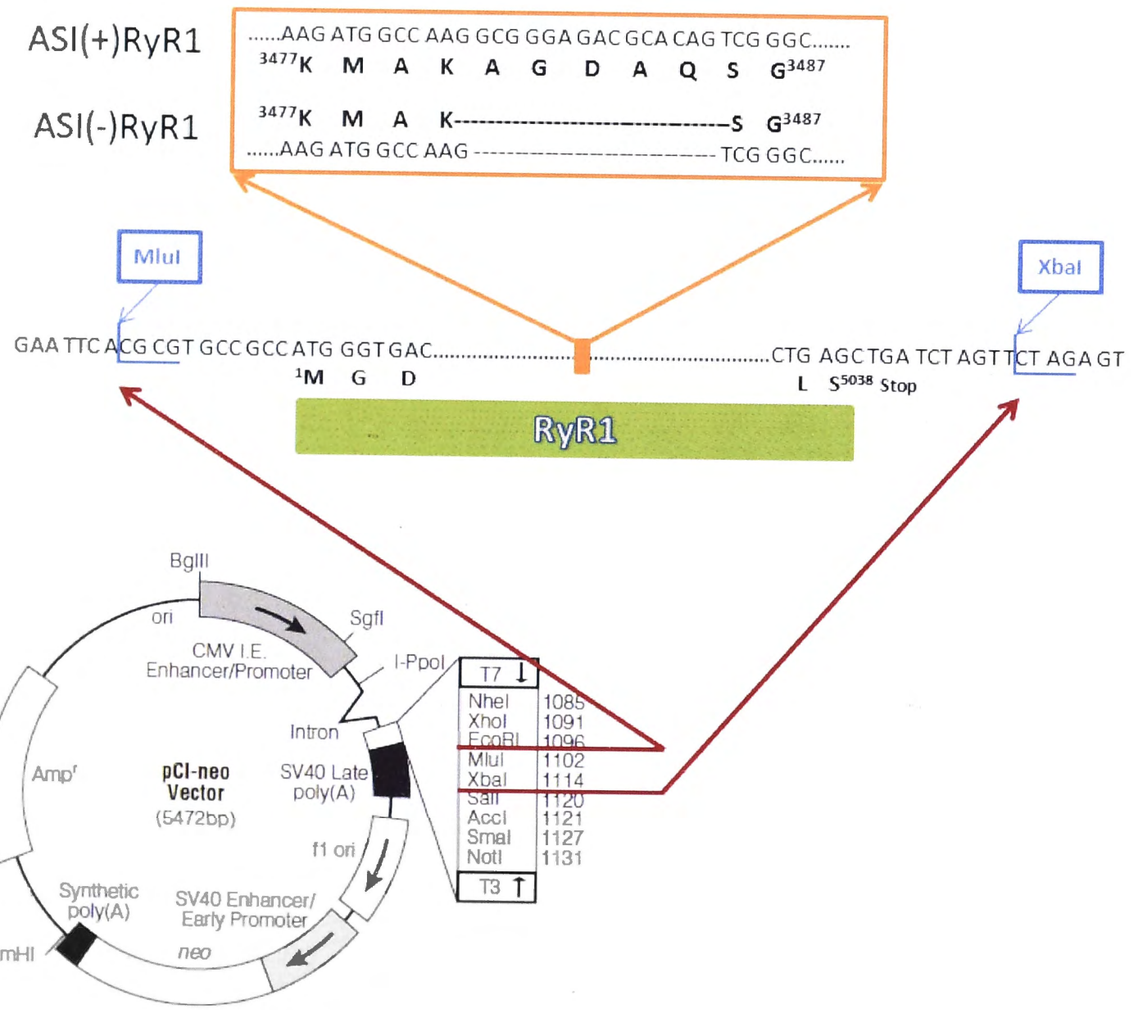

Figure 2.2 Diagram showing the ASI(+)RyR1 and ASI(-)RyR1 in pCI-neo constructs. ASI(-)RyR1 does not contain residues ^{3480}AGDAQ^{3485} which is indicated by the dashed line between ^{3479}K and ^{3486}S

mixture was then added to the 175cm^2 flask containing the HEK293 cells and incubated at 37°C in 5% CO_2 for 24h. The medium containing the DNA calcium phosphate precipitate was then removed and replaced with fresh medium after which the cells were incubated for another 24h and then harvested.

The transfected HEK293 cells were removed from the 175cm^2 flask using cell scrapers and the growth medium with the suspended cells were centrifuged at 1000rpm (169g) for 20min at room temperature using a Hettich Universal 16 Centrifuge (Hettich Lab technology, Germany) with a model 1617 swing-out rotor. The supernatant was removed and the cell pellet stored at -70°C until further processed.

2.2.8 Preparation of microsomal vesicles from HEK 293 cells

As this is a native preparation, all steps were carried out at 4°C, so as to reduce the activity of proteases. The transfected cell pellet was resuspended in microsomal vesicle homogenizing buffer (Section 2.1.2.3) with a protease inhibitor cocktail (Roche, Switzerland). The cells were homogenized using a motorised homogenizer (IKA® T10 basic ULTRA-TURRAX®, IKA Works, Germany) on setting 2, using the plastic probe. The cells were homogenised twice for 5s. The homogenate was then transferred to a 2ml eppendorf tube and centrifuged at 12000rpm (11752g) for 20min at 4°C (Eppendorf 5415C Microcentrifuge, Eppendorf, USA). The supernatant was discarded and an equal volume of homogenizing buffer added to the pellet. The pellet was then homogenized again three times for 5s and the homogenate transferred to Beckman Coulter ultracentrifuge tubes for use with Beckman Coulter TLA120.2 rotor (Beckman Coulter, USA). The homogenate was then centrifuged at 46000rpm (75126g) for 2hr at 4°C (Beckman Coulter Optima MAX ultracentrifuge, Beckman Coulter, USA). The supernatant was removed and the pellet resuspended in 300µl of homogenising buffer using a potter homogenizer. The homogenate was then sonicated for 2 bursts of 5s at 300W (Branson Sonifier, USA). Aliquots were snap frozen in liquid nitrogen and stored at -70°C until further use.

2.2.9 Collection of muscle tissue

2.2.9.1 Rabbit muscle

New Zealand White Rabbits were euthanized with Pentobarbitone Sodium (325mg/ml) administered intravenously at a dose rate of 1ml/2kg using Lignonocaine to pre-load the wing infusion set according to the ethically approved protocol A2012/01 (ethical approval obtained from The Australian National University Animal Experimentation Ethics Committee). The back and leg fast twitch muscles were removed and immediately rinsed in PBS containing 2mM

EGTA. Subsequently, excess fat and connective tissue was removed and the muscle diced into approximately 50g pieces. The muscle was then snap-frozen in liquid nitrogen and stored at -70°C until further processed.

2.2.9.2 Human muscle

Human muscle was collected at John James Calvary Hospital theatre, Deakin, ACT, Australia with ethical approval ETH.9/07.865 obtained from ACT Health Human Research Ethics Committee and Protocol 2013/307 obtained from the ANU Human Ethics Committee. Muscle tissue samples were collected in collaboration with Prof P.N. Smith from patients undergoing knee and hip replacements. Vastus medialis tissue samples were from patients undergoing knee replacements. Gluteus medius and gluteus minimus samples were from patients undergoing hip replacements. The muscle tissue sample was rinsed in PBS containing 2mM EGTA, excess fat and connective tissue was removed and cut into approximately 80mg pieces. The muscle was then snap-frozen in liquid nitrogen and stored at -70°C until further processed

2.2.9.3 Rat muscle

5 week old and 1 year old male Wistar rats were euthanized with CO_2 gas according to the ethically approved protocol A2011/022 (ethical approval obtained from The Australian National University Animal Experimentation Ethics Committee). Soleus and extensor digitorum longus (EDL) muscles were removed from both hind legs of the rats, briefly rinsed in PBS containing 2mM EGTA and snap frozen in liquid nitrogen. Muscle was stored at -70°C until further processed.

2.2.10 Homogenization of muscle tissue

2.2.10.1 For MyHC analysis

All steps in this protocol were performed at 4°C. Muscle was thawed on ice in 1ml of cold MyHC homogenizing buffer (Section 2.1.2.2.1) with protease inhibitor cocktail (Roche, Switzerland). Muscle was homogenized 3 times for 5s with a motorized homogenizer (IKA® T10 basic ULTRA-TURRAX®, IKA Works, Germany) on setting 5, using the metal probe. The homogenate was transferred to 2ml eppendorf tubes and centrifuged at 12000 rpm (11752 g) for 20min at 4°C (Eppendorf 5415C Microcentrifuge, Eppendorf, USA). The supernatant was discarded and the pellet resuspended in 100-200µl MyHC resuspending buffer (Section 2.1.2.2.2) using a potter homogenizer. The protein concentration of the homogenates was determined using the DC protein assay (Bio-Rad Laboratories, USA) as described in section

2.2.6.2. The concentration of the homogenates was then adjusted to 0.4mg/ml and aliquots were snap-frozen in liquid nitrogen until further use.

2.2.10.2 For Immunoblot

All steps in this protocol were performed at 4°C. Muscle was thawed on ice in 1ml of cold Microsomal vesicle homogenizing buffer (Section 2.1.2.3) with protease inhibitors (1μM pepstatin A, 1μM leupeptin, 1μM benzamidine, 0.7mM PMSF, 3μM calpain inhibitor I, 3μM calpain inhibitor II). Muscle was homogenized 3 times for 5s with a motorized homogenizer (IKA® T10 basic ULTRA-TURRAX®, IKA Works, Germany) on setting 5, using the metal probe. The protein concentration of the homogenates was determined using the DC protein assay (Bio-Rad Laboratories, USA) as described in section 2.2.6.2. Aliquots were snap frozen in liquid nitrogen and stored at -70°C until further use.

2.2.11 Isolation of SR microsomal vesicles from muscle tissue (rabbit)

Native skeletal muscle SR vesicles were isolated from back and leg muscles of New Zealand white rabbits. Muscle was collected as described in Section 2.2.9.1. The isolation procedure was carried out by Ms Suzy Pace and Joan Stivala from the JCSMR Muscle Research Group, based on the method described by (Inui et al. 1987a), with modifications (Ahern et al. 1994; Ahern et al. 1997).

Muscle was homogenized in a Waring commercial blender (Waring Products, USA) in Microsomal vesicle homogenizing buffer (Section 2.1.2.3) with protease inhibitors (1μM pepstatin A, 1μM leupeptin, 1μM benzamidine, 0.7mM PMSF, 3μM calpain inhibitor I, 3μM calpain inhibitor II) using a muscle to buffer ratio of 1:5 (w/v). The muscle was homogenized for 1min and then centrifuged at 9000rpm (12296g) for 20min at 4°C using a SLA1500 rotor (Sorval RC-5B Refrigerated Superspeed Centrifuge, Du Pont Instruments, USA). The supernatant was discarded and the pellet resuspended in the same volume of homogenizing buffer with protease inhibitors. The sample was then homogenized again for 1min followed by the centrifugation step described above.

The supernatant from the second centrifugation step was then filtered through four layers of cotton gauze and centrifuged at 30000rpm (70409g) using a Type 45 Ti rotor (Beckman Coulter Optima XE-100 Ultracentrifuge, Beckman Coulter, USA) for 1-2hr. The pellet was collected and resuspended in 45ml homogenizing buffer with protease inhibitors using a Dounce Teflon homogenizer (Edwards Instruments, Australia). Several millilitres of the sample was loaded

onto a discontinuous sucrose density gradient consisting of the following sucrose layers; 4ml 45% (w/v), 7ml 38% (w/v), 7ml 34% (w/v), 7ml 32% (w/v) and 4ml 27% (w/v). The sucrose solutions were prepared in a diluting buffer containing 20mM imidazole, pH 7.4 and the protease inhibitors stipulated above. The sucrose gradient was centrifuged at 20000rpm (49123g) overnight at 4°C using a SW 32 rotor (Beckman Coulter Optima XE-100 Ultracentrifuge, Beckman Coulter, USA). Sucrose density bands at the 34-38% interface (band 3) and the 38-45% interface (band 4) were collected and diluted with two volumes of diluting buffer. The diluted fractions were then centrifuged at 32000rpm (80110g) for 1hr at 4°C using a Type 45 Ti rotor (Beckman Coulter Optima XE-100 Ultracentrifuge, Beckman Coulter, USA). The pellet was resuspended in homogenizing buffer with protease inhibitors to a final concentration of about 20mg/ml and aliquots were snap-frozen in liquid nitrogen and stored at -70°C until further use.

2.2.12 Preparation of microsomal vesicles from muscle tissue (human and rat)

All steps in this protocol were performed at 4°C. Muscle was thawed on ice in 1.8ml cold Microsomal vesicle homogenizing buffer (Section 2.1.2.3) with protease inhibitors (1μM pepstatin A, 1μM leupeptin, 1μM benzamidine, 0.7mM PMSF, 3μM calpain inhibitor I, 3μM calpain inhibitor II). Muscle was homogenized 3 times for 5s with a motorized homogenizer (IKA® T10 basic ULTRA-TURRAX®, IKA Works, Germany) on setting 5, using the metal probe. The homogenate was transferred to 2ml eppendorf tubes and centrifuged at 12000rpm (11752g) for 20min at 4°C (Eppendorf 5415C Microcentrifuge, Eppendorf, USA). The supernatant was removed and an equal volume of homogenizing buffer with protease inhibitors added to the pellet. The pellet was then homogenized on setting 3 of the motorized homogenizer for 5s and the resulting homogenate centrifuged at 12000 rpm (11752 g) for 20min at 4°C (Eppendorf 5415C Microcentrifuge, Eppendorf, USA). The supernatant was then transferred to Beckman Coulter ultracentrifuge tubes for use with Beckman Coulter TLA100.3 rotor (Beckman Coulter, USA) and centrifuged at 43000rpm (78486g) for 2hr at 4°C (Beckman Coulter Optima MAX ultracentrifuge, Beckman Coulter, USA). The supernatant was removed and the pellet resuspended in 150μl homogenizing buffer with protease inhibitors with a potter homogenizer which was used to resuspend the pellet. The protein concentration of the microsomal vesicles was determined using the DC protein assay (Bio-Rad Laboratories, USA) as described in section 2.2.6.2. Aliquots were snap-frozen in liquid nitrogen and stored at -70°C until further use.

2.2.13 Denaturing (SDS) Polyacrylamide Gel Electrophoresis (SDS-PAGE)

2.2.13.1 General

One-dimensional SDS-PAGE was used to resolve proteins in muscle homogenate and microsomal vesicle samples. SDS-PAGE was performed using either 4-15% Tris-Glycine precast Bio-Rad gels in a Mini-PROTEAN® Tetra Cell system (Bio-Rad Laboratories, USA) or 4-12% Bis-Tris precast Novex® Bolt® gels in a Bolt® Mini Gel Tank system (Life Technologies, USA). Sample preparation for each system is described below (Sections 2.2.13.1.1 and 2.2.13.1.2). Precision Plus Protein Dual Colour Prestained Standard (Bio-Rad Laboratories, USA) was used as protein marker. Upon completion of electrophoresis, gels were either used in immunoblotting or stained using Coomassie Brilliant Blue stain (Section 2.1.2.6.4) for at least 40min with gentle agitation on a platform shaker followed by destaining in Destain Solution (Section 2.1.2.6.4) with gentle agitation on a platform shaker until the background was clear and protein bands visable. Stained gels were dried between cellophane sheets in a gel drying solution containing 20% (v/v) ethanol and 2% (v/v) glycerol. Gels were documented by digital imaging using a Gel Doc XR System (Bio-Rad Laboratories, USA) with Quantity One 1-D analysis Software (Bio-Rad Laboratories, USA).

2.2.13.1.1 Sample preparation for use on 4-15% Tris-Glycine precast Bio-Rad gels

Samples were mixed with 4x Sample Buffer (Section 2.1.2.6.2) and heated at 60°C for 10min. Samples were then loaded onto the gel and the gel run at 200V in 1x Electrophoresis Running Buffer (Section 2.1.2.6.1) until the dye front reached the bottom of the gel.

2.2.13.1.2 Sample preparation for use on 4-12% Bis-Tris precast Novex® Bolt® gels

Samples were mixed with 10x Bolt® Sample Reducing Agent and 4x Bolt® LDS Sample Buffer and heated at 70°C for 10min. Samples were loaded onto the gel and the gel run at 165V in 1x Bolt® MOPS SDS running buffer (Life Technologies, USA) until the dye front reached the bottom of the gel.

2.2.13.2 MyHC analysis

One-dimensional SDS-PAGE was used to analyse MyHC isoforms present in muscle. The method has been modified from (Talmadge and Roy 1993; Mizunoya et al. 2008). 0.75 mm and 1.5mm thick 8% polyacrylamide MyHC gels were cast (Section 2.1.2.2.7) allowing 1h for polymerization of the resolving gel before the stacking gel was cast. The gels were stored in 1x MyHC Electrophoresis Running Buffer (Section 2.1.2.2.5) overnight to allow for complete

polymerization. Homogenate prepared according to method described in Section 2.2.10.1 was mixed with 3x MyHC Sample Buffer (Section2.1.2.2.6) and boiled for 2min. 3µg of protein was loaded onto the gel and gels were run for at 140V for 20hr at 4°C using a Mini-PROTEAN 3 cell (Bio-Rad Laboratories, USA). Precision Plus Protein Dual Colour Prestained Standard (Bio-Rad Laboratories, USA) was used as a protein marker. 1x MyHC Electrophoresis Running buffer was used in the outer buffer dam, whereas 8x MyHC Electrophoresis Running buffer with 0.12% (v/v) 2-Mercaptoethanol was used in the inner buffer dam. After completion of electrophoresis, the gels were stained using a Silver Stain Plus Kit (Bio-Rad Laboratories, USA) according to manufacturer's instructions. Stained gels were dried between cellophane sheets in a gel drying solution containing 20% (v/v) ethanol and 2% (v/v) glycerol. Gels were documented by digital imaging using a Gel Doc XR System (Bio-Rad Laboratories, USA) with Quantity One 1-D analysis Software (Bio-Rad Laboratories, USA).

2.2.14 Immunoblot

After electrophoresis, gels were equilibrated in cold Immunoblot Transfer Buffer (Section 2.1.2.6.3) for 15min. Proteins were transferred onto a 0.45µm pore PVDF membrane (Merck Millipore, USA or Thermo Scientific, USA) using a Mini Trans-Blot® Electrophoretic Transfer Cell (Bio-Rad Laboratories, USA). The membrane was prepared by soaking it sequentially for at least 1min in methanol, MilliQ water and then cold Transfer Buffer. The membrane was left in cold Transfer Buffer until used. The membrane was placed on the gel containing the proteins to be transferred and sandwiched between Extra Thick Western Blotting Filter Paper (Thermo Scientific, USA) and fiber pads and secured in the plastic gel holder cassette. The assembled cassette was the placed in the gel tank containing cold Transfer buffer in such a way that the membrane was placed on the anode side of the gel. Transfer was performed at 100V for 1h at room temperature with continuous stirring of the buffer. After 1h, the voltage was increased till a current of about 0.5A was reached and the protein transferred for another 30min or until the current reached 0.8A (which ever occur first).

Following transfer, the membrane was washed twice for 5min with PBS (JCSMR Media, Australia) and blocked for 1hr at room temperature in either 5% (w/v) skim milk in PBS or 3%BSA (w/v) in PBS (depending on the primary antibody used) with agitation on a platform shaker. After blocking, the membrane was washed 4 times for 10min with 0.05% (v/v) TWEEN® 20 in PBS (TPBS). The membrane was then cut into appropriate sections and incubated with the appropriate primary antibody overnight at 4°C. A list of primary antibodies with the blocking agent for each one used is listed in **Table 2.1**.

Table 2.1: Primary antibodies used for detecting proteins (see Section 2.1.1 for manufacturer)

Antibody	Blocking solution used
α-$Ca_V1.2$ ACC-003 polyclonal antibody	3% BSA (w/v) in PBS
α-DHPR α_{1a} IIID5E1 monoclonal antibody	5% skim milk (w/v) in PBS
α-DHPR β_{1a} VD2(1)B12 monoclonal antibody	5% skim milk (w/v) in PBS
α-FKBP12 (H-5) monoclonal antibody	5% skim milk (w/v) in PBS
α-RyR1 34C monoclonal antibody	5% skim milk (w/v) in PBS

After this incubation, the membrane was washed again 4 times for 10min in TPBS and then incubated with the appropriate secondary antibody for 2h at room temperature. Upon completion of the incubation, the membrane was washed 4 times for 10min in TPBS and then once in PBS for 5min before treating it with Pierce ECL Western Blotting Substrate (Thermo Scientific Pierce Protein Biology Products, USA) for 5min. The treated membrane was exposed to X-ray film (FUJI Medical X-ray Film, FUJIFILM Corporation, Japan) and manually developed. Developed films were documented by digital imaging using a Gel Doc XR System (Bio-Rad Laboratories, USA) with Quantity One 1-D analysis Software (Bio-Rad Laboratories, USA).

2.2.14.1 Reprobing of Immunoblot

The membrane was rehydrated for 1min in methanol and then rinsed with MilliQ water before it was placed in 50ml of stripping solution (40ml PBS, 350µl 2-Mercaptoethanol, 10ml 10% (w/v) SDS) and heated at 50°C for 1h. The membrane was then washed 3-5x in PBS until the 2-Mercaptoethanol could no longer be smelled, and then blocked in either 5% (w/v) skim milk in PBS or 3%BSA (w/v) in PBS (depending on the primary antibody used) for 1h at room temperature with agitation on a platform shaker.

After blocking, the membrane was washed 6 times for 10min with 0.05% (v/v) TWEEN® 20 in PBS (TPBS) and then incubated with the appropriate primary antibody overnight at 4°C. After this incubation, the membrane was washed again 6 times for 10min in TPBS and then incubated with the appropriate secondary antibody for 2h at room temperature. Upon completion of the incubation, the membrane was washed 6 times for 10min in TPBS and then once in PBS for 5min before treating it with Pierce ECL Western Blotting Substrate (Thermo Scientific Pierce Protein Biology Products, USA) for 5min. The treated membrane was exposed to X-ray film (FUJI Medical X-ray Film, FUJIFILM Corporation, Japan) and manually developed. Developed films were documented by digital imaging using a Gel Doc XR System (Bio-Rad Laboratories, USA) with Quantity One 1-D analysis Software (Bio-Rad Laboratories, USA).

2.2.15 Planar lipid bilayer studies

2.2.15.1 Lipid mixture

Bilayers were made using an artificial phospholipid mixture consisting of phosphatidylethanolamine, phosphatidylserine and phosphatidylcholine at a ratio of 5:3:2 respectively. The lipids were obtained in chloroform and the lipid mixture is dried under a stream of nitrogen gas. The mixture is then redissolved in n-decane at a final concentration of 50mg/ml.

2.2.15.2 Bilayer solutions

The solutions used in bilayer experiments are described in Section 2.1.2.5. Each solution was adjusted to a pH of 7.4 with 4M CsOH. BAPTA is a Ca^{2+} chelator and was used to accurately control the Ca^{2+} concentrations <100μM. The purity of BAPTA as well as Ca^{2+} concentrations of solutions was accessed using a Ca^{2+} electrode.

Cs^+ rather than Ca^{2+} was used as current carrier for a number of reasons. Firstly, the Ca^{2+} conductance of 100-200mM Ca^{2+} through the RyR1 is much lower than that for 100-200mM Cs^+, so that use of Ca^{2+} as the current carrier and would reduce the signal to noise level 5 fold (Sitsapesan and Williams 1994a). Secondly, Ca^{2+} has a physiological modulatory effect on RyR1 activity at concentrations between ~100nM and 1mM, and is varied experimentally within this range (Meissner et al. 1986). Cs^+ does not have a modulatory action (Laver 2001). Thirdly, Cs^+ has a low conductance through SR K^+ channels and therefore effectively blocks them by dominantly competing with other cations (Cukierman et al. 1985). $CH_3O_3S^-$ is used as the major anion because it blocks SR Cl^- channels, due to their low permeability to the anion (Laver 2001).

2.2.15.3 Bilayer apparatus setup

Miller and Racker (Miller and Racker 1976) discovered that SR vesicles isolated from muscle could be fused with artificial lipid bilayers thereby incorporating ion channels into artificial membranes. The bilayer apparatus consists of two interconnected solution filled chambers formed when of a lipophilic Delrin cup is fitted snugly into the back compartment of a two compartment Teflon mould (**Figure 2.3**). The Delrin cup contains an aperture of 150-200μm. The chamber to which the microsomal vesicles are added is referred to as the *cis* chamber and the other chamber is the *trans* chamber.

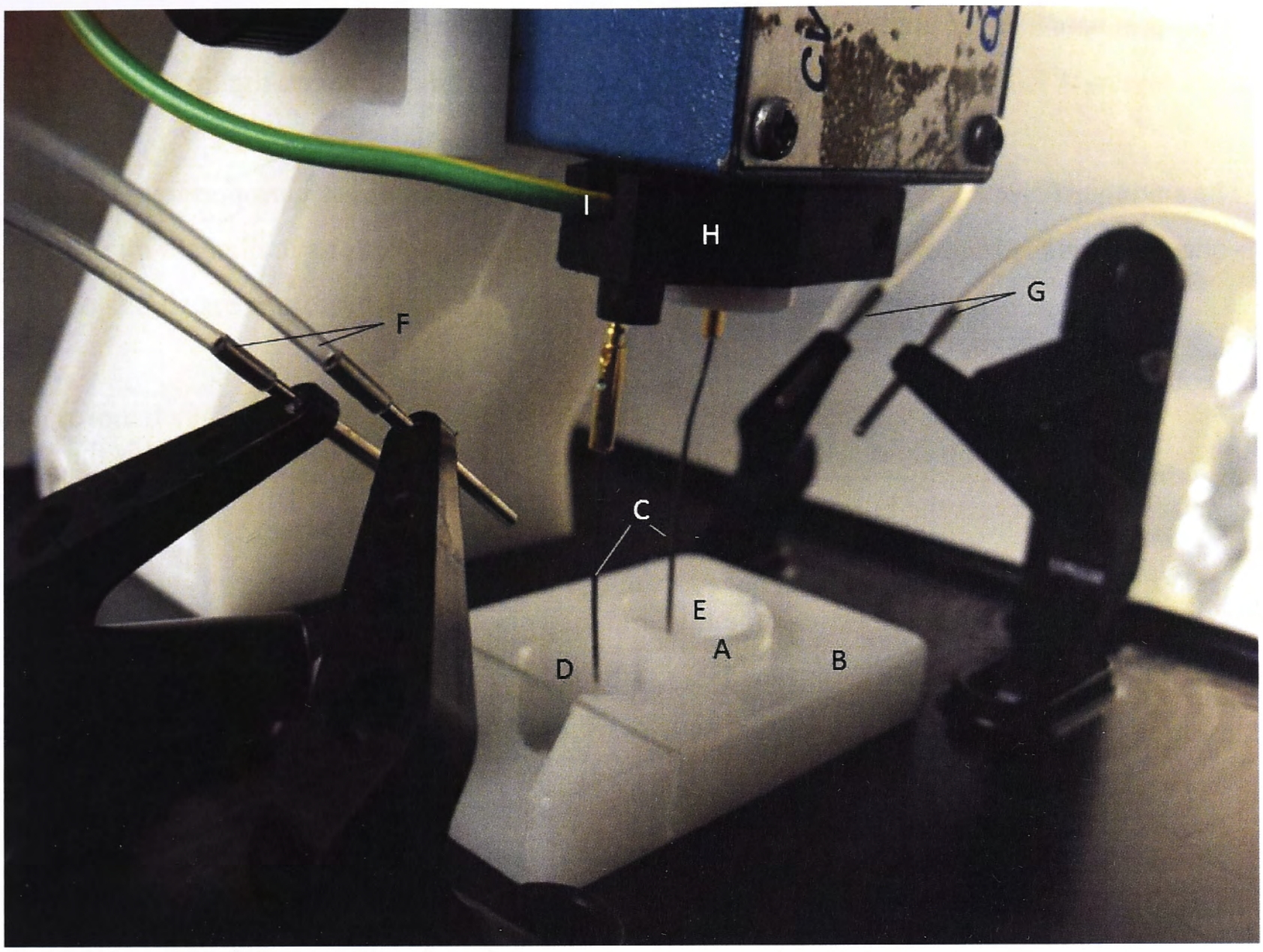

Figure 2.3 Bilayer apparatus setup showing the Delrin cup (A) inside the Teflon mould (B) with the electrodes (C) on either side of the aperture. The perfusion tubes for the *cis* chamber (front chamber - D) can be seen in front of the mould (F) and those for the *trans* chamber (back chamber - E) is located behind the mould (G). The electrodes are attached to the head stage (H) with the grounding wire (green - I) attached to the *cis* electrode visible.

The *cis* chamber was filled with 0.85ml *cis* solution (Section 2.1.2.5.2) and the *trans* chamber with 0.85ml *trans* solution (Section 2.1.2.5.1). The lipid mixture describe in Section 2.2.15.1 is painted over the aperture with a flame polished glass rod and the bilayers forms spontaneously as the surface active lipids aggregate into monolayers at the oil-water interfaces and the n-decane drains away from the two monolayers thus allowing the formation of the bilayer (Laver 2001). At times it was necessary to apply gentle pressure on the side of the aperture to induce the draining of the n-decane. The thickness of the bilayer was monitored by observing changes in the bilayer capacitive current amplitude when a 1V/s triangular voltage ramp is applied across the bilayer. The voltage ramp was generated by a custom built ramp generator (JCSMR workshop, Canberra, Australia). Due to the bilayer's ability to separate ions across an electrical insulator (bilayer), it has capacitive properties (Hille 2001). The relationship between capacitance of the lipid bilayer and membrane areas is described by **Equation 2.1**.

Equation 2.1

$$C = \varepsilon \times \frac{A}{d}$$

Where C is the capacitance, ε is the dielectric constant of n-decane between the lipid monolayers, A is the area of the lipid bilayer and d is the distance between the lipid monolayers.

The amount of charge stored by the lipid bilayer as a capacitor is directly proportional to the voltage across the bilayer indicated by **Equation 2.2** below.

Equation 2.2

$$Q = C \times V$$

Where Q is the charge stored on the lipid bilayer, C is the capacitance and V is the voltage across the bilayer.

When the area and distance between the lipid monolayers are constant, the capacitance of the lipid bilayer is constant (see **Equation 2.1**). If the voltage across the bilayer is altered, the resulting capacitive current is described by **Equation 2.3** below.

Equation 2.3

$$\frac{dQ}{dt} = I_c = C \times \frac{dV}{dt}$$

Where dQ/dt is the change in charge over time, I_c is the capacitive current, C is the capcitance, and dV/dt is the change in voltage over time.

When **Equation 2.1** and **Equation 2.3** are combined, the resulting equation is **Equation 2.4** (below).

Equation 2.4

$$I_c = \varepsilon \times \frac{A}{d} \times \frac{dV}{dt}$$

Where I_c is the capacitive current, ε is the dielectric constant of n-decane, A is the area of the lipid bilayer, d is the distance between the lipid monolayers and dV/dt is the change in voltage over time.

Therefore if the thickness of the bilayer (d) is decreased when a triangular voltage ramp is applied across it, the size of the capacitve current (I_c) increases due to the fact that the capacitive current is inversely proportional to the thickness of the bilayer as seen in **Equation 2.4**.

The Teflon mould fits snugly into a custom built bilayer box (JCSMR Workshop, Canberra, Australia) that also holds the CV 201A headstage (Axon Instruments, USA) that connects the two silver chloride coated silver electrodes immersed in the *cis* and *trans* solutions to the bilayer amplifier (Axon Instruments, USA) **(Figure 2.3).** To reduce the junction potential between the solutions and the electrodes, the ends of the electrodes were immersed in salt agar bridges. Agar bridges were made form a mixture of 2% (w/v) agar powder and 250mM CsCl injected

into 30cm lengths of 1.47mm laboratory tubing (Dow Corning Corporation, USA). Once the agar set, the tubing was cut into 1.5-2cm lengths and stored in 250mM CsCl at 4°C.

The *cis* chamber was grounded and the *trans* chamber was voltage clamped at +40mV or -40mV with the help of an Axopatch 200A Integrated Patch Clamp (Axon Instruments, USA). The potentials are expressed according to standard physiological convention V_{cis} - V_{trans}.

Microsomal vesicles containing RyR1 were added to the *cis* chamber at a concentration of about 20µg/ml. In order to promote vesicle incorporation the following steps were taken. Firstly, an osmotic gradient was created across the bilayer by having different Cs^+ concentrations on either side of the bilayer (250mM Cs^+ in *cis* chamber vs. 50mM Cs^+ in the *trans* chamber). Secondly, the *cis* solution contained a high Ca^{2+} concentration (1mM) as fusion of the vesicles with the bilayer is dependent on a Ca^{2+} concentration greater than 0.5mM (Miller and Racker 1976) . Thirdly, the *cis* solutions was vigorously stirred thereby increasing the probability that vesicles could come into contact with the bilayer to fuse (Laver 2001). Generally channels incorporate with their cytoplasmic surface facing the *cis* solution. This was confirmed by the addition of 2mM ATP-Na_2 to the *cis* chamber, which, if the RyR1 is incorporated in the correct way, would increase channel activity (see Section 1.5.4.1) and by decreasing the Ca^{2+} in the *cis* chamber from 1mM to 10µM which will also cause an increase in RyR1 channel activity (see Section 1.5.4.3).

2.2.15.4 Channel recordings

The current across the bilayer, indicating channel incorporation into the lipid bilayer, and channel activity was recorded using an in-house acquisition program BLM1. Activity was recorded throughout the experiment at 5kHz and the current was filtered with a low pass 8-pole Bessel filter at 1kHz integrated in the Axopatch 200A Integrated Patch Clamp (Axon Instruments, USA). The bilayer box is surrounded by a grounded faraday cage on an air table to reduce electrical noise.

After the commencement of recording, 200mM $CsCH_3O_3S$ was added to the *trans* chamber in order to have symmetrical solutions on either side of the bilayer with respect to Cs^+, Cl^- and $CH_3O_3S^-$. The voltage across the bilayer was alterated between +40mV and -40mV every 30s thoughout the experiment. The solutions were stirred for 15-20s after which 4min of activity () was recorded. The Ca^{2+} concentration was then lowered to 10µM by perfusing the *cis* chamber with 5ml *cis* solution containing 10µM Ca^{2+} (Section 2.1.2.5.3). Control activity was recorded for 8min. 10nM full length DHPR β_{1a} in dialysis buffer (or an equal volume of dialysis buffer alone in buffer control experiments) was added to the *cis* chamber and stirred for 15-20s.

Activity was recorded for 8min alternating between +40mV and -40mV every 30s. The concentration of full length β1a was then increased to 50nM (or an equal volume of dialysis buffer alone in buffer control experiments) in the *cis* chamber and stirred for 15-20s. Activity was recorded for 8min. 2mM ATP-Na_2 was then added to the *cis* chamber and stirred for 15-20s. Activity was recorded for 4min. Lastly, 20μM Ruthenium Red was added to the *cis* chamber and stirred for 15-20s. Activity was recorded for 4min. The recording was then terminated. Experiments were conducted at 20±2°C.

2.2.15.5 Data analysis

Single and multiple channel parameters were obtained using an in-house software program, Channel 2 (developed by P.W. Gage and M. Smith, John Curtin School of Medical Research, Canberra, Australia). The channel parameters were measured from 90s of channel activity at each potential for each experimental condition.

The following parameters were determined:

Open probability (P_o)	=	$T_{open}/T_{total\ time}$
Fractional Mean Current (I'f)	=	I'/I_{max}
Mean open time (T_o; ms)	=	T_{open}/n
Mean closed time (T_c; ms)	=	T_{closed}/n
Open frequency (F_o)	=	$n/T_{total\ time}$

Where T_{open} is the total channel open time; $T_{total\ time}$ is the total duration of the analysed record; I' is the mean current; I_{max} is the maximal current of channel openings in the analysed record; T_{closed} is the total channel closed time; and n is the total number of channel openings.

I'f is approximately equal to P_o and it has been shown that P_o and I'f values obtained from a single channel record with a high open probability these values are very similar (Beard et al. 2008). P_o most accurately quantifies RyR1 activity when only a single channel is present in the recording, however, when more than one channel is present I'f is the more accurate quantification method. Since these quantification methods yield approximately equal values, all channel activity (I'f and P_o) is expressed as P_o in this thesis. To measure P_o, a threshold was set outside baseline noise level at about 20% of the maximum open conductance, currents exceeding this threshold was perceived as open. I_{max} was measured from the baseline which was the mean of the baseline noise. The close threshold was placed above baseline noise. Slow baseline variation was corrected for using an in-house program Baseline2 (developed by D.R. Laver).

Statistical analysis was done with paired and unpaired student's t-tests as appropriate and a $P \leq 0.05$ was deemed statistically significant

2.2.16 .RNA extraction from muscle tissue

Muscle was thawed in 1ml TRIzol® reagent (Invitrogen, Life Technologies, USA) and homogenized using a motorised homogenizer (IKA® T25 ULTRA-TURRAX®, IKA Works, Germany). The homogenate was incubated for 5min at room temperature to permit complete dissociation of the nucleoprotein complex. 200µl of chloroform was added and the samples shaken vigorously by hand for 15s. The samples were then incubated for 3min at room temperature and subsequently centrifuged at 12126rpm (12000g) for 15min at 4°C (Eppendorf 5415C Microcentrifuge, Eppendorf, USA). The mixture separates into a lower red phenol-chloroform phase, an interphase and a colourless upper aqueous phase. The aqueous phase, containing the extracted RNA, was removed and the RNeasy Mini Kit (QIAGEN, Netherlands) according manufacturer's instructions, used to clean the RNA. The resultant RNA was then treated with the TURBO DNA-free™ Kit (Ambion, Life Technologies, USA) according to manufacturer's instructions to remove any DNA contamination. The RNA concentration was determined using a Nanodrop ND-1000 (Thermo Scientific, USA) spectrophotometer.

2.2.17 Production of cDNA

RT-PCR was performed using the SuperScript™ III Reverse Transcriptase Kit (Invitrogen, Life Technologies, USA) according to manufacturer's instructions. Oligo(dT)$_{12-18}$ primers (Invitrogen, Life Technologies) were used and the reaction was performed at 50°C for 60min, followed by a 15min incubation at 70°C (PTC-200 DNA Engine , MJ Research, USA)

2.2.18 PCR

PCR was performed using KOD Hot start DNA Polymerase Kit (Novagen, Merck Millipore, Germany) according to manufacturer's instructions. The mixture was cycled 35 times in a PTC-200 DNA Engine (MJ Research, USA). The following cycling parameters were used:

Parameter	Time (s)	Temperature (°C)
Initialization	120	95
Denaturation	20	95
Annealing	10	62
Extension	10	70

The sequences for human and mouse primers were the same as the primers used by Kimura et al (Kimura et al. 2005) to amplify the ASI region on the RyR1. The rat primers were designed with thanks by Dr Angelo Theodoratos of the Molecular Genetics Group, John Curtin School of Medical Research, The Australian National University. The sequences for primers used were:

Human (forward): 5'-GACAACAAAAGCAAAATGGC-3'

Human (reverse): 5'-CTTGGTGCGTTCCTGGTCCG-3'

Mouse (forward): 5'-GACAATAAGAGCAAAATGGC-3'

Mouse (reverse): 5'-CTTGGTGCGTTCCTGATCTG-3'

Rat (forward): 5'-ACTGGATAATGCAGCCTTCC-3'

Rat (reverse): 5'-CTTGGTGCGTTCCTGGTC-3'

2.2.19 Visualization of DNA on vertical polyacrylamide gels

As the PCR product had a maximum length of 69bp, vertical polyacrylamide gels were used to visualize the DNA. 10% Polyacrylamide gels were cast (Section 2.1.2.7.2) and left to polymerise for 60min. 15µl of PCR product was mixed with 2x Sucrose DNA loading dye (Section 2.1.2.7.3) and loaded onto the gel. The gel was run at 100V at 4°C in 1x TBE buffer (Section 2.1.2.7.1) till the dye reached ¾ down the gel using a Mini-PROTEAN 3 cell (Bio-Rad Laboratories, USA). The gel was subsequently stained with 0.5µg/ml Ethidium Bromide in 1x TBE buffer for 30min. DNA bands were visualized under UV light using a Gel Doc XR System (Bio-Rad Laboratories, USA) with Quantity One 1-D analysis Software (Bio-Rad Laboratories, USA).

Chapter 3: Fiber type distribution of muscle samples

3.1 Introduction

Muscles differ in regard to their fiber type distribution. This is part of the muscle's adaption to its function (see Chapter 1, for a detailed description). Muscles used for short bursts of large movements tend to have more type II fibers than muscles involved mostly in stabilizing joints and posture, which have more type I fibers. Humans have only muscles containing a mixture of fiber types. Rats on the other hand have fiber type specific muscles. Rat soleus is often used as a representative of slow twitch muscle whereas rat EDL is used as a representative fast twitch muscle (Schiaffino and Reggiani 2011). The developmental MyHC isoforms disappear during the first 2-4 weeks of postnatal development in rodents (Schiaffino et al. 1989). Although rats are sexually mature from about 6wk they reach musculoskeletal maturity by about 7mo and are considered senecent from 18-20mo (Quinn 2005). In humans, changes related to sarcopenia occur from about 50-60yr of age (Larsson et al. 1979; Hakkinen et al. 1995).

Muscle fiber type distribution can shift towards a more oxidative fiber type distribution or a more glycolytic fiber type depending on its use. Certain exercise training regimes, or stimulating muscle with rates of electrical stimulation that mimic the motor neuron firing patterns during exercise can facilitate these fiber type shifts (Pette and Vrbova 1999; Schiaffino and Reggiani 2011; Jorquera et al. 2013). Muscle wasting conditions can also cause fiber type shifts. Some are from slow-to-fast (e.g. Spinal cord injury, denervation, microgravity) and others are from fast-to-slow (e.g. fasting, glucocorticoid administration, type 1 diabetes, cachexia) (Schiaffino et al. 2013). Sarcopenia has also been suggested to be accompanied by a fast-to-slow fiber type switch. In the majority of studies investigating changes in size fibers of specific types, (usually in the vastus lateralis), the conclusion is that type 2 fiber size is reduced with increasing age, whereas the size of type 1 fibers is much less, if at all, affected (Lexell 1995; Porter et al. 1995). When examining the proportions of each fiber type with age in human vastus lateralis, both type 1 and type 2 fibers appear to be reduced to a similar extent. When the proportion of type 2 fibers and their mean area were expressed as the relative type 2 area, the negative correlation between age and type 2 fiber contribution was much stronger (Lexell 1995; Porter et al. 1995). In other words, the cross sectional area of the muscle occupied by type 2 fibers was significantly reduced with increasing age due to a combined effect of reduced fiber size and fewer fibers. In rodents, however, there seems to be a selective loss in fast-twitch

fibers during aging (Ishihara et al. 1987; Kanda and Hashizume 1989; Ansved and Larsson 1990). In both rodent and humans, aging results in the muscle mass being comprised of a higher percentage of slow-twitch muscle. For rodents this would be the natural outflow of selective loss in fast-twitch fibers. Conversely, for humans this is, as discussed above, due to the age related atrophy of muscle fibers being more severe in fast-twitch fibers, so that the proportion of muscle mass made up of slow-twitch fibers is significantly increased even though the ratio between the numbers of fast- and slow-twitch fibers does not change (Larsson et al. 1978; Essen-Gustavsson and Borges 1986; Lexell et al. 1988; Lexell 1995).

As mentioned above, most of the studies involving fiber type distribution in humans have been done on the vastus lateralis muscle (Lexell 1995). The fiber type distribution of this muscle (as well as most other muscles in humans) varies depending on the depth within the muscle, with the surface of the muscle having fewer type 1 fibers present than deeper in the muscle (Johnson et al. 1973). Less information is available regarding fiber type distribution shifts in other muscles with age, with some data available about biceps brachii (Klitgaard et al. 1990b; Grimby 1995). There are no reports of the effect of aging on the gluteus medius, gluteus minimus or vastus medialis which are examined in the work reported in this thesis.

3.2 Aim

To determine the fiber type distribution of the muscle samples obtained from human gluteus medius, gluteus minimus and vastus medialis as well as muscle obtained from rat soleus and EDL as positive controls. This work was done in order to investigate any changes that might occur during aging, as well as to facilitate correlations between fiber type distribution and the results of analyses of other aspects of the muscles presented in later chapters of this thesis.

3.3 Quantitative and statisctical analysis

Quantitative analysis was done after digital images of gels were made by determining the density of each MyHC band with the use of Quantity One software from Bio-Rad Laboratories, USA. Statistical analysis of differences in fiber type distribution was done with ANOVA using Fisher's post-hoc test where differences were deemed significant when $P<0.05$. The Pearson correlation coefficient was used to determine significant correlations between fiber type and age. Correlations were deemed significant when the coefficient differed significantly from 0 with a $P< 0.05$.

3.4 Results

3.4.1 Human muscle

Muscle samples were obtained from human donors and were fiber typed in terms of MyHC isoform using SDS-PAGE (as described in Sections 2.2.10.1 and 2.2.13.2). This was done in order to investigate whether there is a fiber type shift with age in humans and in order to correlate fiber type with all other analysis done on the muscle. Representative examples of the silver stained gels are shown in **Figure 3.1A**. A breakdown of the human samples received is given in **Table 3.1**.

Table 3.1: Breakdown of the human samples received from 40 donors

Gluteus medius		Gluteus minimus		Vastus medialis	
Female	51	Female	51	Female	54
Female	52	Female	52	Female	56
Female	76	Female	58	Female	57
Female	84	Female	61	Female	62
		Female	66	Female	64
		Female	70	Female	64
		Female	71	Female	65
		Female	74	Female	74
		Female	79		
		Female	82		
		Female	85		
Male	72	Male	45	Male	59
		Male	47	Male	66
		Male	52	Male	69
		Male	56	Male	71
		Male	59	Male	73
		Male	60	Male	77
		Male	61		
		Male	69		
		Male	70		
		Male	72		

3.4.1.1 Densitometry results

The density of each of the MyHC bands were determined and expressed as a percentage of the total amount of MyHC present. There were 40 donors in total and 4 repeats were done for each muscle sample. The average percentage of each fiber type for female and male donors <60yr and ≥60yr are given in **Table 3.2** and are represented graphically in **Figure 3.2**.

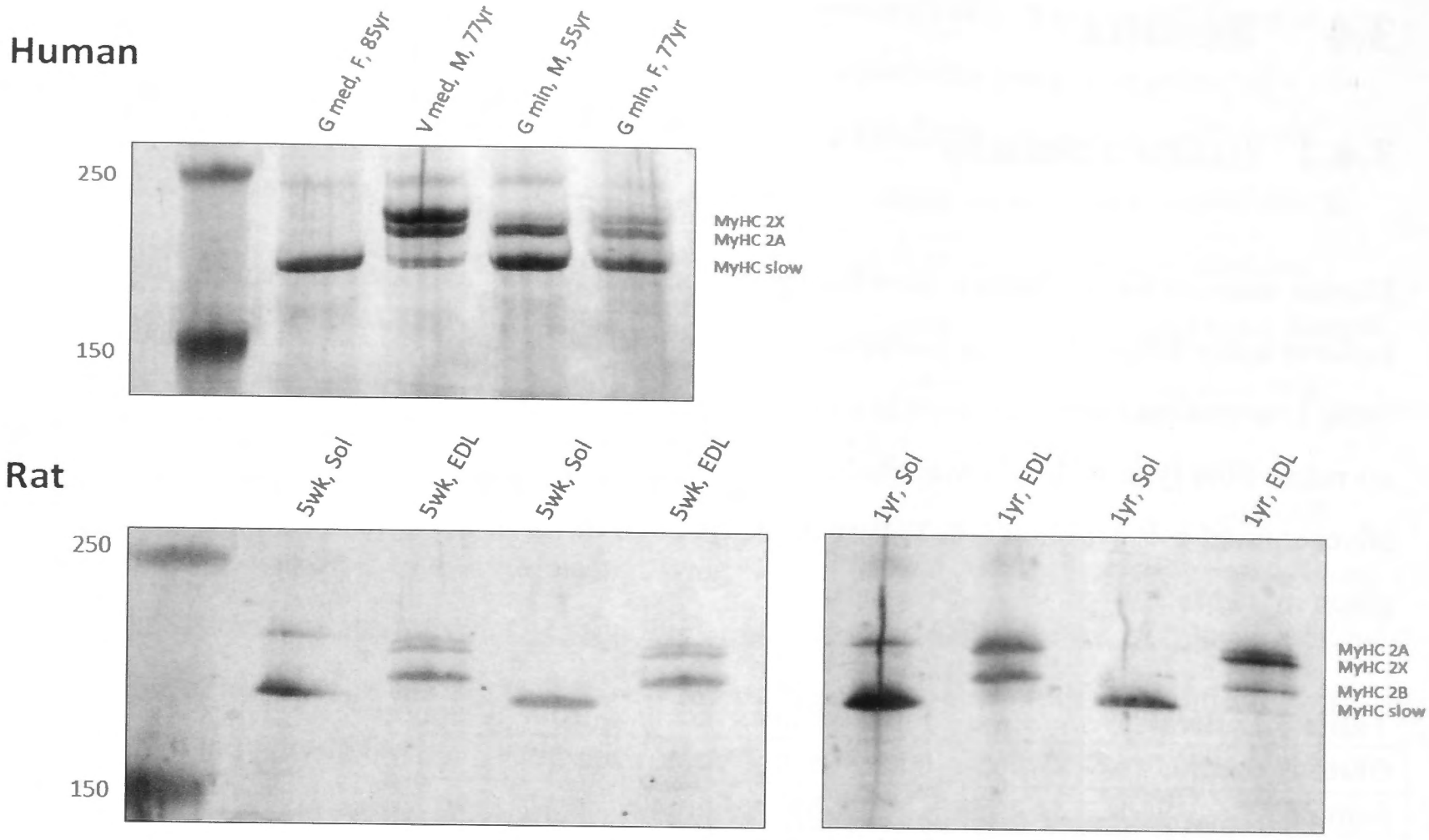

Figure 3.1: Examples of silver stained MyHC SDS-PAGE with the 250 and 150kDa markers indicated. (**A**) Human muscle from four different donors (G med – gluteus medius, V med – vastus medialis, G min - gluteus minimus, F – female, M – male, yr – years). (**B**) Rat soleus and EDL muscle (So - soleus, wk – weeks, yr – years).

Table 3.2: Fiber type distribution for each human muscle sample per age group. Values are averages of the fiber type as a percentage of the total MyHC present (n – number of observations, sem – standard error of the mean, * significantly different to <60yr $P \leq 0.05$, # significantly different to female $P \leq 0.05$).

			n	Type 1		Type 2A		Type 2X	
				mean	±sem	mean	±sem	mean	±sem
Gluteus medius	female	<60yr	8	41.9	2.2	31.8	2.1	26.2	3.4
		≥60yr	8	72.6*	5.4	16.0*	3.4	11.4*	2.2
	male	<60yr	0	----	----	----	----	----	----
		≥60yr	4	78.2	4.4	15.3	4.2	6.5	0.5
Gluteus minimus	female	<60yr	12	63.9	4.8	28.1	3.8	8.1	2.6
		≥60yr	32	61.5	3.3	24.1	1.8	14.4*	1.9
	male	<60yr	19	55.9	3.5	30.7	2.2	13.4	1.8
		≥60yr	19	57.0	3.1	32.4#	1.5	10.6	2.0
Vastus medialis	female	<60yr	12	25.1	2.1	35.8	1.9	39.2	3.6
		≥60yr	17	33.9	2.7	41.9	1.9	24.2*	2.1
	male	<60yr	4	31.0	1.6	40.8	2.2	28.2#	2.2
		≥60yr	20	26.0	1.7	38.7	1.1	35.2#	1.9

3.4.1.2 *Fiber type vs. muscle*

The three source muscles differed significantly from each other with regards to fiber type distribution when age and gender groups are compared, with four exceptions. 1) The percentage of type 2A fibers in gluteus minimus and gluteus medius from females <60yr did not differ significantly. 2) The percentage of type 2A fibers did not differ significantly between vastus medialis and gluteus medius from females <60yr. 3) In females ≥60 yr there was no significant difference in the percentage of type 2X fibers between gluteus minimus and gluteus medius. 4) The percentage of type 2X fibers did not differ significantly in males ≥60yr between gluteus minimus and gluteus medius (see **Table 3.3)**. Muscle samples taken from the vastus medialis had the highest percentage of type 2 fibers with type 2A and 2X contributing to varying degrees in the different age and gender groups (see **Table 3.2**). Gluteus medius and gluteus minimus had a higher percentage type 1 fibers, with gluteus medius having the highest percentage of type 1 fibers, with the exception of the <60yr female group, which has a lower percentage type 1 fibers than gluteus minimus.

3.4.1.3 *Fiber type vs. age*

The fiber type distribution of donors <60yr and ≥60yr of age within each muscle were compared (see **Table 3.2** and **Figure 3.2**). As there was only one male donor of gluteus medius muscle, no age group comparison could be made for male gluteus medius subjects. In the gluteus medius muscle, there was a significant difference in all three fiber types in between female donors <60 and ≥60 years of age. The percentage of type 1 fibers were significantly higher in the older age group (72.6±5.4%) compared to the younger age group (41.9±2.15%). The type 2A and 2X fiber percentages were significantly lower in the older age group (16.0±3.4 and 11.4±2.2% respectively) compared to the younger age group (31.8±2.1% and 26.2±3.4% respectively). Gluteus minimus muscle showed less change with age, with the only significant difference in fiber type distribution between age groups being the percentage 2X fibers in the ≥60 yr female group that is significantly larger (14.4±1.9%) than the younger age group (8.1±2.6%). There were no significant differences in fiber type distribution with age in muscle from male gluteus minimus donors. In vastus medialis there was also only one significant difference between the different age groups for each gender. The type 2X fiber percentage was significantly lower in females ≥60yr (24.2±2.1%) compared to the younger age group (39.2±3.6%). There was again no difference between the male age groups for vastus medialis donors. However, there was only one donor younger than 60yr and he was 59yr old.

Table 3.3: Comparison matrix to show significant difference ($P<0.05$) between fiber type distribution in muscle obtained from gluteus medius, gluteus minimus and vastus medialis. Red shading indicates the muscle indicated in the column heading is significantly lower than the muscle indicated in the row heading, whereas green shading indicates the muscle indicated in the column heading is significantly greater than the muscle indicated in the row heading. No shading indicates no significant difference.

Female <60yr	Gluteus medius			Vastus medialis		
Gluteus minimus	1	2A	2X	1	2A	2X
Vastus medialis	1	2A	2X			
Female ≥60yr	Gluteus medius			Vastus medialis		
Gluteus minimus	1	2A	2X	1	2A	2X
Vastus medialis	1	2A	2X			
Male <60yr	Gluteus medius			Vastus medialis		
Gluteus minimus				1	2A	2X
Male ≥60yr	Gluteus medius			Vastus medialis		
Gluteus minimus	1	2A	2X	1	2A	2X
Vastus medialis	1	2A	2X			

The fiber type distribution was correlated with age for each of the three muscles separated according to gender. The Pearson correlation coefficient was determined and used as an indicator for correlation. Correlations were regarded as significant if they differed significantly ($P<0.05$) from 0 (see **Figure 3.3**). Again, due to the presence of only one male donor of gluteus medius muscle, only a correlation between female subjects and age was done in this muscle. There was a strong positive correlation between age and type 1 fibers with the accompanying negative correlation for both type 2X and 2A fibers in female gluteus medius donors (**Figure 3.3A, F**). Among gluteus minimus muscle donors, there was no significant correlation with fiber type distribution and age in females (**Figure 3.3 B, F**) or males (**Figure 3.3 C, F**). In female vastus medialis donors a significant positive correlation between age and type 1 fiber percentage and the accompanying significant negative correlation between type 2X fiber percentage and age was found No significant correlation between the percentage of type 2A

fibers and age was seen (**Figure 3.3 D, F**). In male donors of vastus medialis muscle, there was a significant negative correlation between age and type 1 fiber percentage with an accompanying significant positive correlation between age and type 2X fiber percentage. The type 2A fiber percentage showed no significant correlation with age (**Figure 3.3 E, F**).

3.4.1.4 Fiber type vs. gender

The fiber type distribution of each gender age group was compared in the three muscle groups. Although there was only one male gluteus medius donor (72 yr old), his fiber type distribution did not differ significantly from the female gluteus medius donors in the ≥60yr age group (**Figure 3.2A**). Among gluteus minimus muscle donors, a significant difference was found in the average percentage of type 2A fibers in the ≥60yr female group (24.1±1.8%) compared to the ≥60yr male group (32.4±1.5%) (**Figure 3.2B**). The vastus medialis donors showed a significant difference in average type 2X percentage between male and female donors for each age group. In the <60yr age group, the male donors had a lower average percentage of type 2X fibers (28.2±2.2%) compared to the female donors (39.2±3.6%) and in the ≥60yr age group, the male donors had a larger percentage type 2X fibers (35.2±1.9%) compared to the female donors (24.2±2.1%) (**Figure 3.2C**).

The correlations of individual fiber type distributions with age were compared between the two gender groups for each muscle. In gluteus minimus donor muscle, there was no significant correlation between fiber type distribution and age in either of the two gender groups (**Figure 3.3 B, C, and F**). In muscle from vastus medialis donors, the fiber type distribution in the two gender groups showed opposing patterns with regards to age. The female donors showed a significant positive correlation in type 1 fiber percentage with age, an accompanying significant negative correlation between type 2X fiber percentage and age, but no significant correlation between age and type 2A fiber percentage (**Figure3.3 D, F**). Male donors showed a significant positive correlation in type 2X fiber percentage with age, an accompanying significant negative correlation between type 1 fiber percentage and age, and no significant correlation between age and type 2A fiber percentage (**Figure3.3 E, F**). Comparison between gender groups in gluteus medius donors could not be done as there was only one male donor.

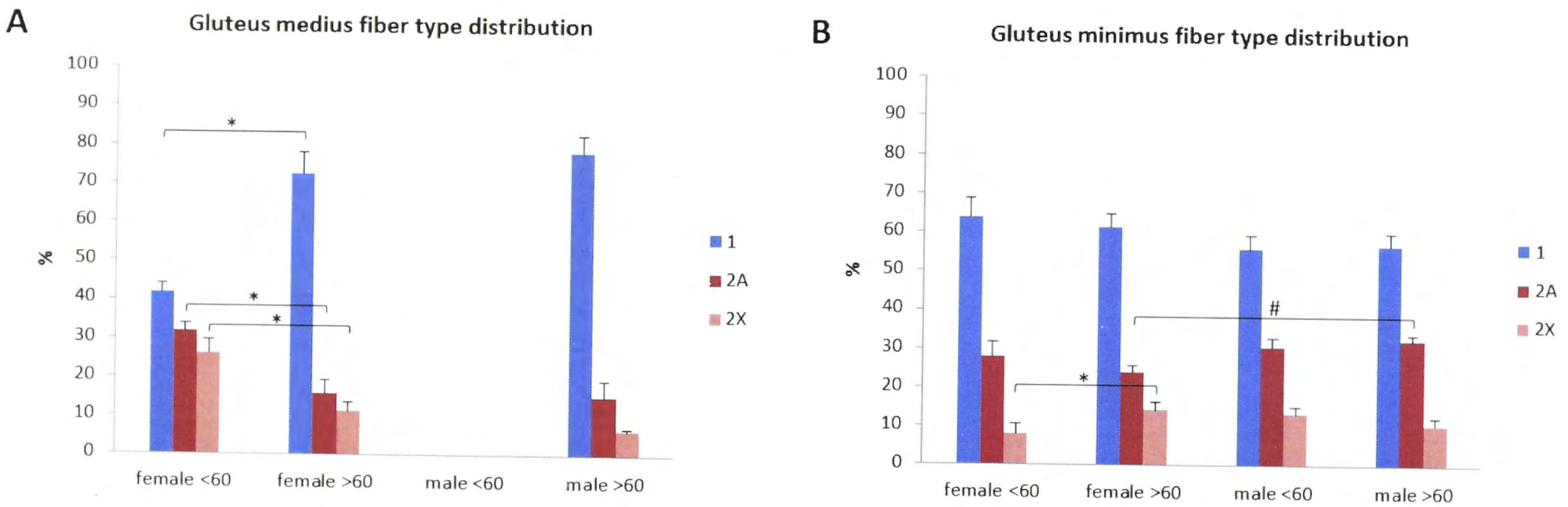

Figure 3.2: Fiber type distribution of muscle samples [gluteus medius (A), gluteus minimus (B) and vastus medialis (C)] obtained from human donors. The donors have been grouped into younger than 60yr or 60yr and over for each gender. Type 1 fiber percentage is given in blue whereas the red hues represent the percentage type 2 fibers (2A in red, 2X in pink). * Significant difference between age groups of same gender $P<0.05$, # Significant difference between genders of same age group $P<0.05$

A

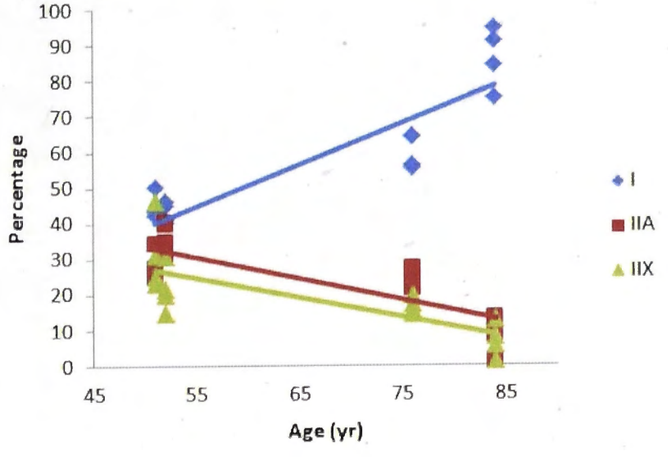

B

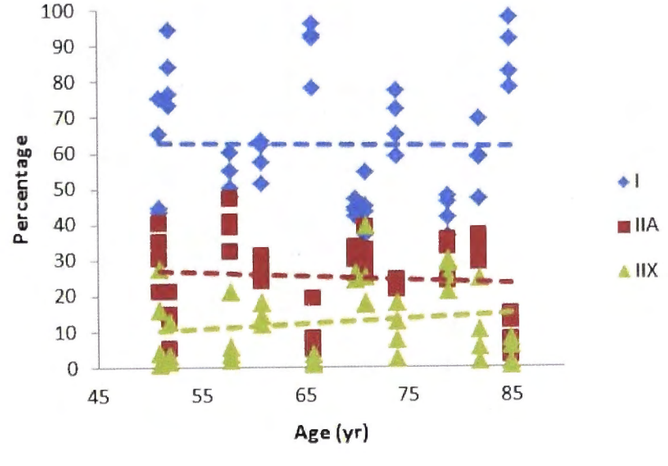

C

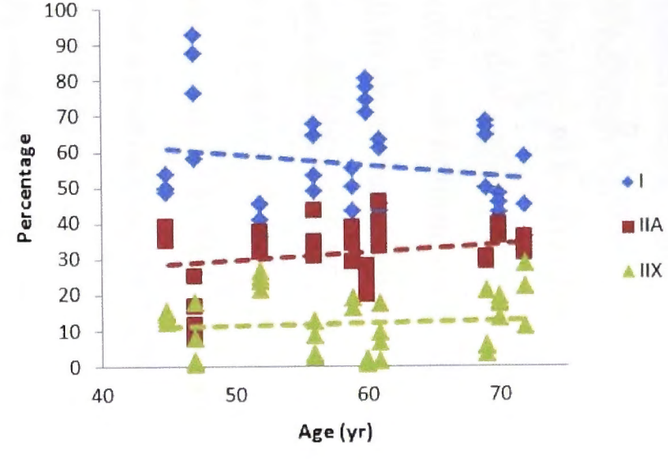

D

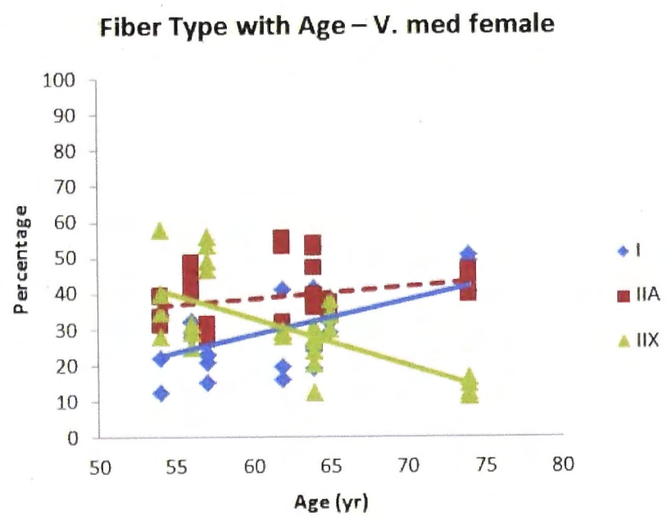

E

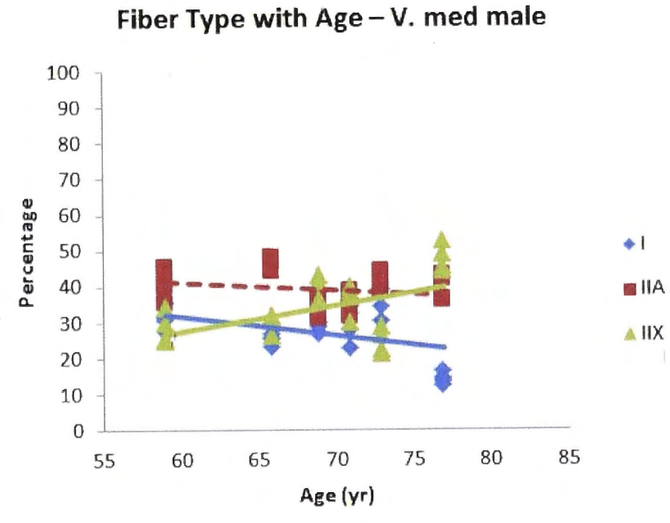

F

Pearson Correlation Coefficient			
Muscle	Fiber type	Female	Male
G. med	1	**0.896**	
	2A	**-0.810**	
	2X	**-0.754**	
G. min	1	-0.027	-0.193
	2A	-0.105	0.257
	2X	0.155	0.080
V. med	1	**0.589**	**-0.425**
	2A	0.276	-0.243
	2X	**-0.669**	**0.503**

Figure 3.3: Correlation between age and fiber type for each muscle group obtained from human donors separated by gender [(**A**) gluteus medius, (**B-C**) gluteus minimus, and (**D-E**) vastus medialis]. Significant correlations are indicated by a solid line, whereas correlations that are not significant are indicated by dashed lines. The Pearson correlation coefficient for each correlation between fiber type and age is given in (F) with number in bold significantly different from 0 ($P<0.05$

3.4.2 Rat muscle

Soleus and EDL muscle obtained from three 5wk old and three 1yr old male Wistar rats were also fiber-typed in terms of MyHC isoform using SDS-PAGE (as described in Sections 2.2.10.1 and 2.2.13.2). This was done as a positive control in order to confirm that the methods used here would reproduce the fiber type shifts reported for rats during maturation and aging of skeletal muscle. The decision to use rats in this study was made in the latter stages of the study. As a result the rats used here could not be maintained for sufficient time to fall into the senescent age group and only reached an age of about 1yr, however other rats have been retained for a further 6 to 8 months and will be studied in the next year. The choice of using 5wk old rats was made based on availability at the time. The 5wk old rats are not adult rats and therefore represent a juvenile age group, whereas the 1year old rats would be consistent with middle aged humans (Quinn 2005) but merely an adult group. The changes occurring in rats during 5wk and 1yr of age are therefore not considered here as age-related changes, but as developmental changes and are compared as such to developmental changes reported in the literature. Examples of the silver stained gels are shown in **Figure 3.1B**.

3.4.2.1 Densitometry results

In rats, the soleus muscle contains type 1 and 2A fibers whereas, the EDL muscle contains type 2A, 2X and 2B fibers (Schiaffino and Reggiani 2011). Soleus and EDL muscle from of three 5wk old and three 1yr old male rats were used and the fiber typing was repeated 4 times for each rat. The density of each of the MyHC bands were determined and depicted as a percentage of the total amount of MyHC present. The average percentage of each fiber type of the soleus and EDL muscles is given in **Table 3.4** and shown graphically in **Figure 3.4**.

Table 3.4: Fiber type distribution for each rat muscle sample per age group. Values are averages of the fiber type as a percentage of the total MyHC present (n – number of observations, sem – standard error of the mean, * significantly different to 5wk old of the same muscle $P \leq 0.05$, # significantly different to soleus of the same age group).

		n	Type 1		Type 2A		Type 2X		Type 2B	
			mean	±sem	mean	±sem	mean	±sem	mean	±sem
Soleus	5wk	12	83.8	2.9	16.3	2.9				
	1yr	12	90.2	3.2	9.8	3.2				
EDL	5wk	12			20.3	1.3	29.7	0.9	46.0	3.1
	1yr	12			29.6*#	1.4	43.7*	1.2	18.9*	2.0

3.4.2.2 Fiber type vs. muscle

As discussed above in Section 3.4.2.1, rat soleus muscle consists of type 1 and 2A fibers whereas rat EDL consist only of type 2 fibers in the form of 2A, 2X and 2B. Therefore, only

type 2A fibers are common to the two muscles. A comparison of the percentage of type 2A fibers in soleus and EDL muscle for each age group reveals that there was a significant difference between 1yr old rats with the soleus muscle containing 9.8±3.2% and the EDL muscle containing 29.6±1.4%. There was no significant difference in type 2A fiber percentages between soleus and EDL muscle in 5wk old rats.

3.4.2.3 Fiber type vs. age

The fiber type distribution for each muscle was compared between age groups. No significant difference was found in fiber type distribution in soleus muscle of 5wk old rats compared to 1yr old rats. In marked contrast, the EDL muscle fiber type distribution was significantly different for each fiber type. The 1yr old rats had a higher percentage of type 2A and 2X fibers (29.6±1.4% and 43.7±1.2% respectively) than 5wk old rats (20.3±1.3% and 29.7±0.9% respectively). In contrast, 1yr old EDL has a relatively fewer type 2B fibers (18.9±2.0%) compared to 5wk old rats (46.0±3.1%) (see **Figure 3.4**)

3.5 Discussion

3.5.1 Human muscle

Obtaining human samples for muscle research is always a challenge and the samples mostly consist of muscle biopsies or autopsies. The human muscle obtained for the work done in this thesis namely, vastus medialis, gluteus minimus and gluteus medius has not been the subject of studies of fiber type distribution as a function of age. Therefore the work described in this chapter provides new insight into fiber type distribution changes with age in different muscle groups. Because the muscles samples were obtained from hip and knee replacement operations, the age distribution available for sampling was limited as it is more likely that a knee or hip replacement will be needed later in life than in younger subjects. The youngest donor was 45yr and the lack of young donors could influence the results as the difference in age between samples was small. Although an attempt was made to obtain equal numbers of samples from each muscle for every age group this was not always possible. Consequently there was only one male gluteus medius donor and also only one male younger than 60 who donated vastus medialis muscle. The results, although insightful, have to be regarded in the light of small sample numbers and large individual variation. Although it can be assumed that all the subjects were sedentary because a knee or hip replacement was necessary, no information about their activity during the course of their lives was available, and this could have contributed to individual variation.

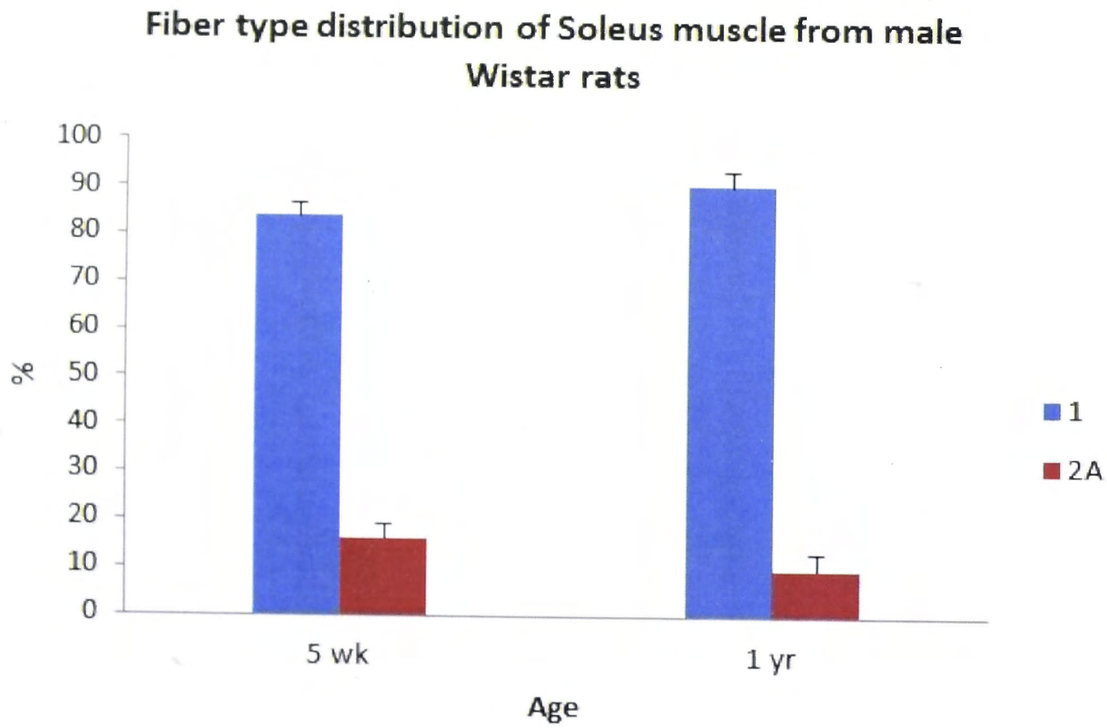

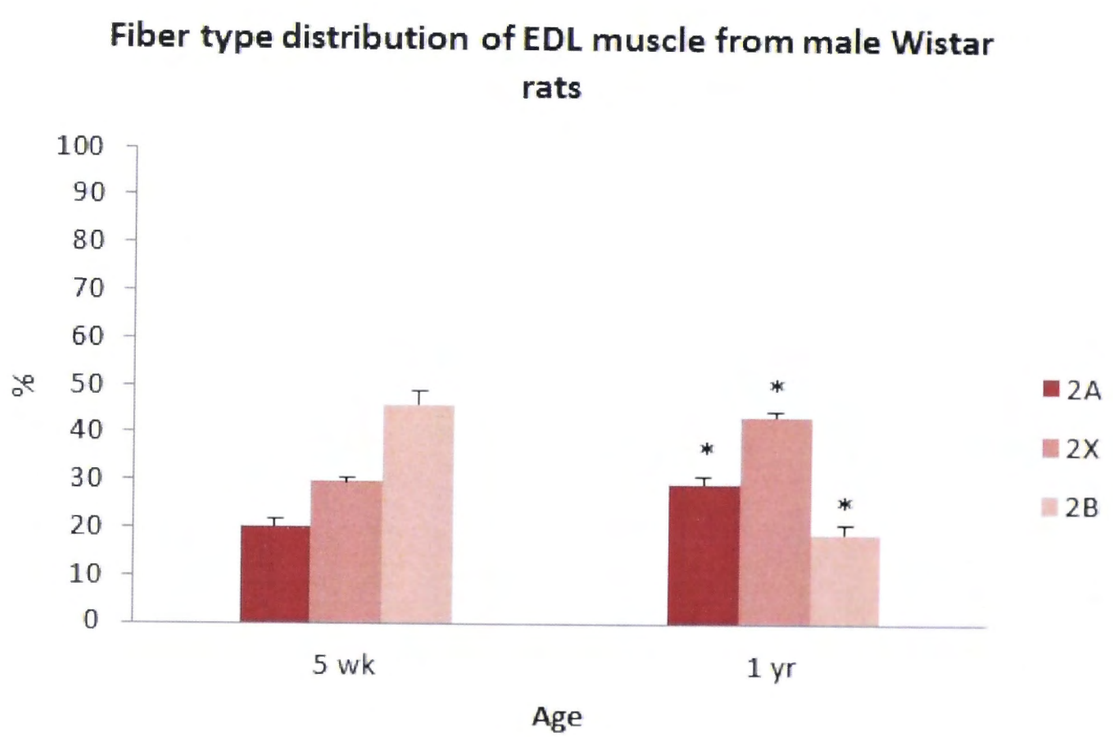

Figure 3.4: The fiber type distribution using MyHC isoform as indication for soleus and EDL muscle of 5wk and 1yr old male Wistar rats. The different fiber types are represented as a percentage of the total MyHC present on the gel with (**A**) showing the fiber type distribution for soleus muscle and (**B**) the fiber type distribution for EDL muscle. Type 1 fibers percentage is shown in blue, whereas the percentage type 2 fiber types are shown in red hues with 2A in red, 2X in dark pink en 2B in light pink. * Significantly different to 5wk ($P<0.05$).

3.5.1.1 *Fiber type vs. muscle*

Most of the studies by others on human muscle have been done on biopsies from the vastus lateralis muscle. Consequently, much of the available data on human muscle changes with age are based on results from this muscle. The vastus lateralis muscle is responsible for extending and stabilizing the knee. Muscles that are involved in short bursts of large movement, e.g. gluteus maximus, tend to have roughly an equal distribution of type 1 and type 2 fibers. The gluteus maximus, is the most powerful muscle in the human body for example (Marieb and Hoehn 2010), and it has 52% type 1 fibers and 47% type 2 fibers in young (17-30yr) male adult subjects (Johnson et al. 1973). The vastus lateralis and vastus medialis are also muscles that fall in this short burst/large movement group and have a similar fiber type distribution. Although samples from the surface contained less type 1 fibers (37.8% vastus lateralis and 43.7% vastus medialis) than from deeper in the muscle (46.9% vastus lateralis and 61.5% vastus medialis) in the study by Johnson et al (Johnson et al. 1973). The results from the work done in this thesis showed a lower percentage (25.1-33.9%) of type 1 fibers in general (see **Table 3.2**) for vastus medialis than the study by Johnson et al. However, Johnson et al used autopsy samples and myosin ATPase staining to determine the fiber type of their muscle samples, which could account for the variation in results. Johnson et al stained cross-sections of musle samples, selected three areas at random and counted a total of 200 fibers which were then classified as type 1 or type 2 according to their level of staining. The percentages of different fiber types reported by Johnson et al were therefore a reflection of the number of fibers of each fiber type. The results discussed in this chapter were obtained through the homogenization of muscle samples and the determination of the fraction of each fiber type based on separation of the MyHC isoforms on SDS-PAGE. There is therefore no information about single fibers, but the results reflect what fraction of the whole muscle could be attributed to each fiber type. In human vastus lateralis it has been shown that the number of fibers of each fiber type were reduced to a similar extent with age but that the mean cross sectional area of the type 2 fibers were reduced more than type 1 fibers (Lexell 1995; Porter et al. 1995). In other words, aging results in the muscle mass being comprised of a higher percentage of slow-twitch muscle. As the work discussed in this thesis investigates fiber type distribution changes with age, the use of MyHC isoforms separated on SDS-PAGE in determining fiber type distribution would be more useful than counting the amount of fibers on a cross-section.

The gluteus minimus and gluteus medius samples in general contained more type 1 fibers than type two fibers with the exception of the <60yr of age female group of gluteus medius donors, which contained 41.9% type 1 fibres. In general the three muscles studied here differed significantly from each other in terms of fiber type distribution with some exceptions (see **Table 3.3**). Gluteus minimus and gluteus medius are both involved in the stabilization of the pelvis

during walking, pointing the toes inwards and lifting the leg sideways (Marieb and Hoehn 2010). They are mostly used in their pelvis stabilizing function and this is consistent with the higher percentage type 1 fibers seen in these muscles.

3.5.1.2 Fiber type vs. age

As mentioned above, most of the work done on changes in fiber type distribution with age has involved the vastus lateralis and I have been unable to find any studies thus far on changes in fiber type distribution in gluteus minimus and gluteus medius muscle with age. Although the gluteus medius and gluteus minimus have a similar function in the pelvic stabilization during walking, their fiber type distribution is significantly different from each other and the correlation between fiber type distribution and age is also significantly different between the two muscles. The female gluteus medius muscle donors <60yr age group had a lower percentage type 1 fibers (41.9%) than the corresponding group in gluteus minimus donors (63.9%). However, in the ≥60yr age group of gluteus medius donors, the percentage type 1 fibers was significantly higher and was also significantly higher than the corresponding gluteus minimus donor group (see **Table 3.2** and **Figure 3.2**). The percentage of type 1 fibers was not significantly different in the two age groups of the female gluteus minimus donors. Therefore, the female gluteus medius showed a very strong positive correlation with age and the percentage of type 1 fibers, whereas the female gluteus minimus showed no correlation in this regard (see **Figure 3.3**). The male gluteus minimus also did not have a correlation between age and fiber type distribution. It is interesting to note that two muscles that have similar functions have a very different response to age. It is unfortunate that there were not enough male donors of gluteus medius to correlate fiber type distribution with age.

Although there was no correlation between fiber type distribution and age in gluteus minimus from female donors, there was a significant difference in percentage type 2X fibers between the <60yr age group (8.1%) and the ≥60yr age group (14.4%), but the percentage of type 1 fibers was not significantly different (see **Table 3.2** and **Figure 3.2**). Although one would expect the percentage of type 2A fibers to be lower because the percentage of type 2X fibers is larger and there was no change in percentage of type 1 fibers, this is not the case. However, there is a trend towards a lower type 2A fiber percentage in female gluteus minimus donors of the ≥60yr age group (28.1% vs. 24.1%), although the difference is not significant. This lack of significant change in type 2A fibers may be a consequence of the low sample size.

The vastus medialis results showed a significant difference between percentage of type 2X fibers in the female <60yr age group (39.2%) and the ≥60yr age group (24.2%), again with no significant difference in the percentage of type 2A or type 1 fiber (see **Table 3.2** and **Figure**

3.2). However, there is a strong trend towards a higher percentage of type 1 fibers in the older age group. In correlating age with fiber type distribution, there is a significant positive correlation between age and type 1 fiber percentage with an accompanying negative correlation between age and type 2X fiber percentage (see **Figure 3.3**). With regard to the vastus medialis muscle from male donors, there was no significant difference between the age groups. However, there was a significant positive correlation between age and type 2X fiber percentage with a corresponding negative correlation in type 1 fiber percentage. The fact that there was only one male vastus medialis donor below the age of 60yr, could contribute to the lack significance between the younger and older age group as the mean value for the younger age group (28.18%) was lower than that of the older age group (35.24%). The decrease in the percentage of type 1 fibers and the increase in the percentage of type 2X fibers in male vastus medialis is unexpected as most previous studies on vastus lateralis have shown a reduced contribution of type 2 fibers to muscle mass due to atrophy, resulting in a higher type 1 fiber content in the muscle (Lexell 1995; Porter et al. 1995). The increased percentage of type 2X fibers found here is therefore surprising and in contrast to female vastus medialis donors. Together with the gluteus minimus and gluteus medius muscle results, the vastus medialis results regarding fiber type distribution and age points to a diverse response from different muscles to aging. Importantly the results emphasise the importance of taking care when extrapolating results obtained in vastus lateralis muscle to all muscles in the human body.

3.5.1.3 Fiber type vs. gender

A comparison of gender and fiber type distribution in gluteus medius was not possible due to the limited sample size. The percentage of type 2A fibres in gluteus minimus muscles from donors in the ≥60yr age group was significantly less than in the muscle from male donors (24.1% and 32.4% respectively) (see **Table 3.2** and **Figure 3.2**). Again, there was no significant difference in the other fiber types although there was a trend towards lower values for type 1 fibers in muscle from males (61.5% female and 56.1% male) and type 2X fibers (14.4% female vs. 10.6% male). The younger age group of gluteus minimus donors showed no significant difference between fiber type distribution in male and female donors and there was no correlation between age and fiber type distribution in gluteus minimus from male and female donors (see **Figure 3.3**).

Vastus medialis muscle showed significant differences in the percentage of type 2X fibers between male and female donors in both age groups (see **Table 3.2** and **Figure 3.2**). In the younger age group, male donors had lower percentage of type 2X fibers (28.18% vs. 39.17%) and in the older age group the male donors had a larger percentage of type 2X fibers (35.24% vs. 24.24%). There were no significant age-related differences in the other fiber types to

account for the different fraction of type 2Xfibers. The correlation between age and fiber type distribution among vastus medialis muscles showed opposing patterns in male and female donors (see **Figure 3.3**) with muscles from female donors having the expected significant positive correlation between percentage of type 1 fibers and age with a corresponding negative correlation between type 2X fiber percentage and age. Muscles from male donors however, showed exactly the opposite trend with a significant positive correlation between the percentage of type 2X fibers and age and a corresponding negative correlation between the percentage of type 1 fibers and age.

The lack of clear pattern in fiber type distribution when comparing the corresponding age groups in the different sexes could be attributed to the high degree of individual variability present in human muscle apparent in **Figures 3.2** and **3.3** and also reported by others (Lexell 1995; Schiaffino and Reggiani 2011). The muscles discussed responded differently not just with age but also between male and female donors. This may be due individual variability, but might suggest a more complex response to age than commonly reported for vastus lateralis.

3.5.2 Rat muscle

As explained in Section 3.4.2, the 5wk old rats are not adult rats and represent a juvenile age group, whereas the 1yr old rats would be consistent with middle age humans (Quinn 2005) and do not represent an aged group. They represent an adult group. The changes occurring in rats during 5wk and 1yr of age are therefore developmental changes and are compared as such to developmental changes reported in the literature.

3.5.2.1 Fiber type vs. muscle

The fiber type distributions found for soleus and EDL muscles from the rats where consistent with earlier reports of fiber type distributions, reviewed in (Schiaffino and Reggiani 2011). The soleus muscle consisted of type 1 and 2A fibers and the EDL muscle consisted of type 2A, 2X and 2B fibers. The percentage of type1 fibers in soleus muscle (83.8% in 5wk old and 90.2% in 1yr old rats) (see **Table 3.4**) is very similar to the percentage of type 1 fibers reported for soleus muscle in young adult (17-30yr) male human subjects (86.4% on the surface and 89% deeper in the muscle) (Johnson et al. 1973). Unfortunately the study by Johnson et al did not include data for EDL muscle for comparison and no other reports for human EDL could be found.

3.5.2.2 Fiber type vs. age

No developmental MyHC isoforms were present in the 5wk old rat muscle, indicating that the transition to adult MyHC isoforms was complete. Although the skeletal muscle from 5wk old

rats contains the adult MyHC isoforms, the muscle will still continue to grow and mature until they reach musculoskeletal maturity at an age of about 7mo.

No significant difference was found in soleus fiber type distribution between 5wk old rats and 1yr old rats. The EDL muscle fiber type distribution showed significant differences between the 5wk and 1yr old rats for each of the three type 2 fiber types with a lower percentage of type 2B fibers in the 1yr old rats (18.9% 1yr vs. 46.0% 5wk) and a higher percentage of type 2X (43.7% 1yr vs. 29.7% 5wk) and and 2A fibers (29.6% 1yr vs. 20.3% 5wk) (see **Table 3.4** and **Figure 3.4**). This indicates a shift towards more a oxidative type 2 profile in the 1yr old rats compared to the 5wk old rats and is consistent with previous reports reviewed in (Schiaffino and Reggiani 2011).

3.6 Conclusion

Very little data regarding the response of human muscles other than vastus lateralis to age is available in the literature due to the accessibility of vastus lateralis for muscle biopsies. The work presented here has contributed to this gap in our knowledge base. The findings point to a rather complex and varied response of the different human muscles studied with regards to age with no clear pattern emerging across the muscle. This suggests that it is necessary to be cautious in extrapolating data obtained from vastus lateralis to all other muscles in the human body. Humans show large variability between individuals regarding fiber type distribution as well as muscle response to aging which makes establishing patterns more difficult and point to the need of large subject numbers in order to obtain significant data. However, significant correlations between age and fiber type distribution were found for female gluteus medius, female vastus medialis and male vastus medialis. The fiber type distribution of the rat soleus and EDL muscle was consistent with previous reports and the rat results therefore validate the measurements in humans (i.e. human results do not reflect experimental errors).

Chapter 4: ASI splice variant ratio in muscle

4.1 Introduction

Zorzato et al reported in 1994 that they found two RyR1 transcripts present in rabbit skeletal muscle (Zorzato et al. 1994). The two RyR1 transcripts differed with 5 amino acids and seemed to be due to the alternative splicing of a 15bp exon. The different transcripts were present in slow- and fast-twitch muscle and in different stages of fast-twitch muscle development and it suggested that there are two RyR1 isoforms present in mammalian skeletal muscle. This was followed up by a study from Futatsugi et al in 1995 showing two alternatively spliced regions in the RyR1 which they called alternatively spliced region I (ASI) and alternative spliced region II (ASII) respectively (Futatsugi et al. 1995). The region they called ASI corresponded to the alternative spliced region described by Zorzato et al. Futatsugi et al used the muscle of the hind limbs of mice to show that there is more RyR1 splice variants containing the 5 amino acid residues (ASI(+)RyR1) than RyR1 that does not have the 5 amino acid residues (ASI(-)RyR1) in adult skeletal muscle of mice (ratio of about 3:1) and suggested that ASI is a developmentally spliced area. In juvenile and embryonic muscle, the ASI(-)RyR1 splice variant predominated.

In 1998, Bastide and Mounier showed that there is no difference in the properties of the Ca^{2+} release channels from slow-and fast-twitch muscle in terms of conductance, sensitivity to caffeine and the bell shaped Ca^{2+} activation curve between a pCa of 7 to 3 in muscle from Rhesus monkeys (Bastide and Mounier 1998). Interestingly, they found that about 18% of the RyR1 from slow-twitch preparations showed a very high activity level. They concluded that the differences seen in Ca^{2+} release kinetics in fast- and slow-twitch muscle is not due to different intrinsic properties of the RyR1 Ca^{2+} release channel, but due to the co-expression of RyR isoforms and the relative amounts of the RyR1 expressed in slow- and fast-twitch muscle, but did not mention ASI.

Kimura et al did a series of studies involving the ASI region of the RyR1 (Kimura et al. 2005; Kimura et al. 2007; Kimura et al. 2009). Their main findings were firstly, that there was a change in the ASI(+)RyR1:ASI(-)RyR1 ratio in muscle from humans suffering from myotonic dystrophy type 1, with there being an increase in the level of ASI(-)RyR1 transcripts (Kimura et al. 2005). Secondly, they found that peptides corresponding the ASI region activate RyR1 possibly by interrupting an inhibitory interdomain interaction and with ASI(-)RyR1 being activated the most by its corresponding peptide (Kimura et al. 2007). Thirdly, they found that the ASI splice variants showed different levels of activation during EC coupling, with ASI(-)RyR1 being activated more than ASI(+)RyR1 during EC coupling (Kimura et al. 2009).

With the ASI region being close to a binding site for the DHPR β_{1a} subunit on the RyR1 (Sections 1.5.5 and 1.6.1 above), and the necessity for the β_{1a} subunit to be present for successful EC coupling, it was suggested that the ASI region may be involved in EC coupling through influencing β_{1a} subunit binding.

A characteristic of aging muscle is the increased denervation and reinnervation of muscle fibers (Deschenes 2011). During long-term denervation of skeletal muscles, the regenerated muscle fibers do not undergo complete maturation, and morphologically resemble myotubes (Dedkov et al. 2001) with juvenile isoforms of proteins. Therefore the starting hypothesis for the work in this chapter was that the juvenile splice variant (ASI(-)RyR1) may be upregulated in aged muscle.

4.2 Aim

To investigate the splice variant transcript levels of the ASI region (ASI(+)RYR1 vs. ASI(-)RyR1) in muscle from human and rat subjects and correlate it with age and fiber type distribution.

4.3 Quantitative and statistical analysis

The density of the visualized PCR product bands were determined using Quantity One 1-D analysis Software (Bio-Rad Laboratories, USA) and represented as a percentage of the total PCR product for the ASI region present. Statistical analysis was done using ANOVA with Fisher's post hoc test ($P<0.05$) and Pearson correlations. Correlations were deemed significant if the correlation coefficient (R) differed significantly from 0 ($P<0.05$).

4.4 Results

4.4.1 Human muscle

To investigate splice variant ratio of RyR1 ASI region, RT-PCR analysis of spliced transcripts was performed on each of the skeletal muscle samples from 40 human donors (see **Table 3.1** for breakdown of donors). The total RNA was extracted from the muscle samples (as described in Section 2.2.16). Two of the samples had too low a yield of RNA to merit its further use and it was decided to continue without these samples due to the limited quantity of muscle received from each donor. RT-PCR was performed on all samples at the same time in the same apparatus to ensure the same conditions for all samples (as described in Sections 2.2.17 - 2.2.19). The ASI region of the RYR1 gene was amplified using primers specific for this region

(Kimura et al. 2005). The RT-PCR products were 69bp and 54bp for ASI(+)RyR1 and ASI(-)RyR1 respectively An example of the visualized RT-PCR product for some of the human donors is represented in **Figure 4.1**.

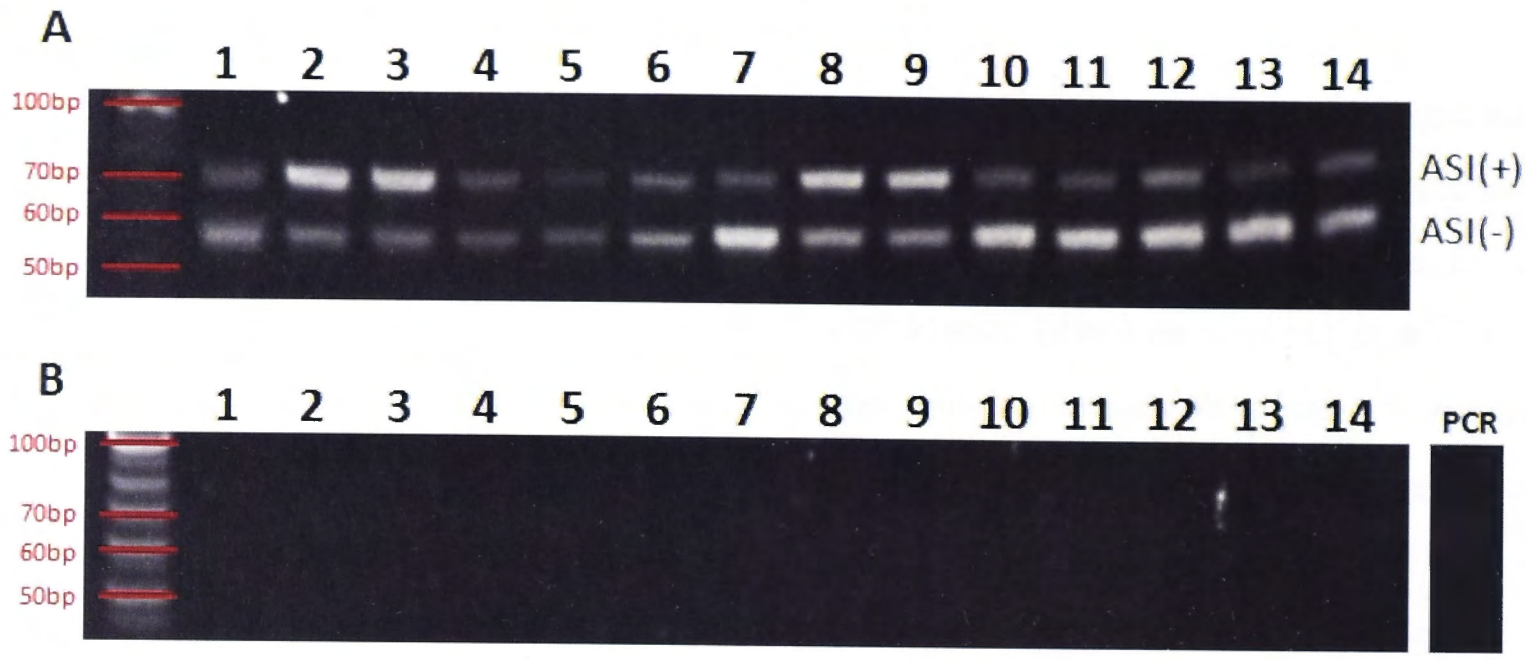

Lane	Muscle	Sex	Age
1	Gluteus minimus	F	51
2	Vastus medialis	F	54
3	Vastus medialis	M	71
4	Gluteus medius	F	76
5	Gluteus minimus	M	60
6	Gluteus minimus	F	74
7	Gluteus minimus	F	58
8	Vastus medialis	M	59
9	Vastus medialis	M	73
10	Gluteus minimus	F	52
11	Gluteus medius	F	52
12	Gluteus minimus	F	61
13	Gluteus minimus	F	66
14	Gluteus minimus	F	79

Figure 4.1: Examples of the RT-PCR product of the splice variant analysis of the RyR1 ASI region. (**A**) RT-PCR product from 14 of the human muscle donor samples. The ASI(+)RyR1 and ASI(-) RyR1 RT-PCR products are 69bp and 54bp respectively. (**B**) Negative controls of the RT-PCR reaction for each of the samples in (A) PCR – negative control for the PCR reaction containing no cDNA template.

To ensure that the band intensity for each sample was a true reflection of the ASI(+):ASI(-) ratio and that the PCR reaction was not saturated, two representative samples of a high ASI(+)RyR1 level, equal ASI(+RyR1) and ASI(-)RyR1 levels as well as a high ASI(-) level

were selected and the PCR repeated. The reaction was allowed to run for 28 cycles, 32 cycles and 35 cycles for each sample. The visualized PCR product is shown in **Figure 4.2**.

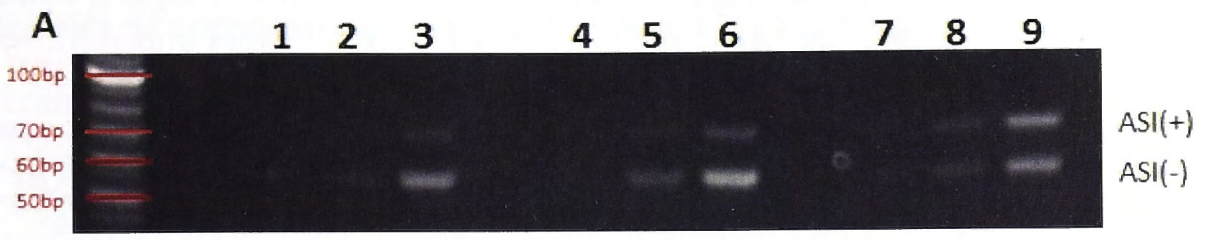

Lane	Muscle	Sex	Age	PCR Cycles
1	G. med	F	85	28
2				32
3				35
4	G. min	F	66	28
5				32
6				35
7	G. med	F	76	28
8				32
9				35

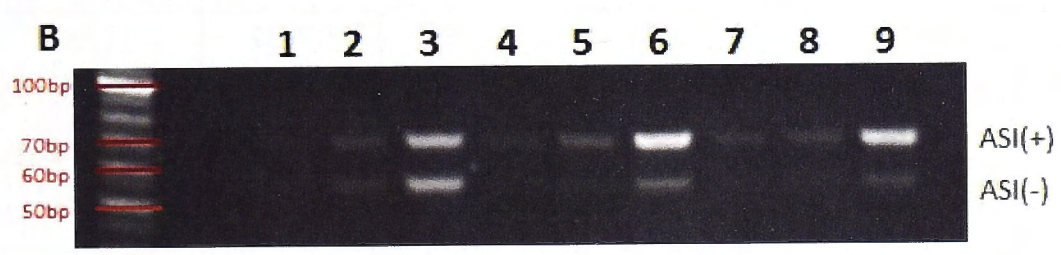

Lane	Muscle	Sex	Age	PCR Cycles
1	G. min	M	61	28
2				32
3				35
4	V. med	M	77	28
5				32
6				35
7	V. med	F	57	28
8				32
9				35

Figure 4.2: Experiment to show that PCR reaction was not saturated at 35 cycles and that differences seen in band density is a true reflection of ratio of ASI(+)RyR1 and ASI(-)RyR1 mRNA present in the muscle. ASI(+)RyR1 PCR poduct is 69bp and ASI(-)RyR1 PCR product is 54bp. (**A**) Lanes 1-3 and 4-6 shows the PCR product at 28, 32 and 35 PCR cycles for two samples with a higher ASI(-)RyR1 product level. Lanes 7-9 shows the PCR product at 28, 32 and 35 PCR cycles of a sample with roughly equal levels of ASI(+)RyR1 and ASI(-)RyR1 product. (**B**) Lanes 1-3 shows the PCR product at 28, 32 and 35 cycles of a sample with roughly equal levels of ASI(+)RyR1 and ASI(-)RyR1 product. Lanes 4-6 and 7-9 shows the PCR product at 28, 32 and 35 cycles of two samples with a higher level of ASI(+)RyR1 product.

4.4.1.1 Densitometry results

The density of the visualized RT-PCR product was determined and expressed as a percentage of the total RT-PCR product of the RyR1 ASI region present for each sample. The densitometry result for each sample as well as their corresponding fiber type distribution is shown in **Table 4.1**.

Table 4.1: Densitometry results of the PCR product of the amplified ASI region for the human donors with their corresponding fiber type distribution. Values are averages of the fiber type as a percentage of the total MyHC present. The values for type 2A and 2X are given separately (grey fill) as well as together as type 2. Blue fill highlights muscle having high percentages of type 1 fibers and ASI(-) RyR1. Pink fill highlights muscle having high percentages of Type 2 fibers and ASI(+) RyR1.

Muscle	Sex	Age	Type 1	Type 2A	Type 2X	Type 2	%ASI(+)	%ASI(-)
Gluteus medius	F	52	42.82	35.91	21.27	57.18	23.16	76.84
		76	59.65	24.15	16.20	40.35	47.16	52.84
		84	85.64	7.82	6.54	14.36	14.99	85.01
	M	72	78.25	15.29	6.46	21.75	30.43	69.57
Gluteus minimus	F	51	58.04	32.00	9.95	41.96	29.22	70.78
		52	81.77	13.33	4.90	18.23	24.93	75.07
		58	52.95	39.44	7.61	47.05	25.10	74.90
		61	58.16	26.68	15.15	41.84	31.25	68.75
		66	89.22	9.31	1.47	10.78	17.50	82.50
		70	44.11	31.51	24.38	55.89	22.35	77.65
		71	44.60	30.79	24.61	55.40	36.82	63.18
		74	67.88	22.26	9.86	32.12	41.89	58.11
		79	42.93	31.07	26.00	57.07	31.90	68.10
		82	58.10	31.80	10.10	41.90	20.93	79.07
		85	87.05	9.28	3.67	12.95	33.44	66.56
	M	45	49.96	36.30	13.74	50.04	42.54	57.46
		47	78.41	14.93	6.66	21.59	54.37	45.63
		52	41.76	34.31	23.93	58.24	33.05	66.95
		56	58.34	35.03	6.63	41.66	33.81	66.19
		59	49.46	33.63	16.90	50.54	20.71	79.29
		60	75.77	23.03	1.20	24.23	32.74	67.26
		61	52.91	38.60	8.49	47.09	51.75	48.25
		69	62.05	29.26	8.69	37.95	30.44	69.56
		70	45.27	37.84	16.89	54.73	37.72	62.28
		72	46.20	33.54	20.25	53.80	45.34	54.66
Vastus medialis	F	54	25.14	35.15	39.72	74.86	70.84	29.16
		56	29.93	42.97	27.09	70.07	57.53	42.47
		57	20.14	29.16	50.70	79.86	82.77	17.23
		62	25.02	46.58	28.40	74.98	61.25	38.75
		64	33.42	41.18	25.40	66.58	53.04	46.96
		64	31.99	46.96	21.05	68.01	53.97	46.03
		74	44.66	42.11	13.23	55.34	42.24	57.76
	M	59	31.00	40.82	28.18	69.00	57.58	42.42
		66	24.78	45.33	29.89	75.22	62.40	37.60
		69	27.66	33.55	38.79	72.34	78.26	21.74
		71	28.88	35.16	35.95	71.12	69.57	30.43
		73	34.99	40.76	24.25	65.01	59.03	40.97
		77	13.80	38.87	47.33	86.20	80.19	19.81

4.4.1.2 *RyR1 ASI splice variant levels vs. age*

The percentage of ASI(+)RyR1 transcript present was correlated with the ages of the donors and the Pearson correlation coefficient determined to establish correlation. As the percentage ASI(-)RyR1 transcript correlation is just the reciprocal of the ASI(+)RyR1 correlation, only the ASI(+)RyR1 transcript correlation is shown. No significant correlation between age and percentage ASI(+)RyR1 transcript was found (see **Figure 4.3A**). When the data was sorted according to muscle and gender and then correlated with age, the only significant correlation between age and the percentage ASI(+)RyR1 transcript was found in muscle from female vastus medialis donors (R =0.791). No significant correlation between age and the percentage ASI(+)RyR1 transcript was found in muscle from gluteus medius, gluteus minimus or male vastus medialis donors (see **Figure 4.3B-D**).

4.4.1.3 *RyR1 ASI splice variant levels vs. muscle and fiber type distribution*

The percentage of ASI(+)RyR1 transcript was then correlated with the different fiber type percentages of the muscle from each of the donors. A strong positive correlation (R=0.781) was found when the percentage ASI(+)RyR1 transcript was plotted against the percentage type 2X fibers in the muscle of each of the donors (see **Figure 4.4A**). The correlation between percentage ASI(+)RyR1 transcript and percentage type 2A fibers (R=0.461) was not as strong as in the case of type 2X fibers, but still a significant positive correlation (see **Figure 4.4B**). When the type 2X and 2A fiber components were combined into a type 2 fiber group and plotted against the percentage of ASI(+)RyR1 transcript, a strong positive correlation was found (R=0.725) with a corresponding strong negative correlation between percentage ASI(+)RyR1 transcript and type 1 fiber percentage (R=-0.725) (see **Figure 4.4C&D**). Comparison of the mean ASI(+)RyR1 transcript percentage of the three different muscles samples were taken from, showed a significant difference ($P<0.01$) between vastus medialis and both gluteus medius and gluteus minimus (see **Figure 4.5B**).

4.4.1.4 *RyR1 ASI splice variant levels vs. gender*

The percentage of ASI(+)RyR1 transcript was separated into gender groups and the means for each group compared. There was no significant difference in the percentage of ASI(+)RyR1 transcript between female and male donors (see **Figure 4.5A**). When the percentage of ASI(+)RyR1 transcript was separated according to muscle and gender and the means of each group compared, the only significant difference found was between the male and female donors of gluteus minimus (see **Figure 4.5C-E**). No significant difference was found between the gender groups of the vastus medialis muscle donors. A mean comparison between gluteus medius gender groups was not possible as there was only one male donor.

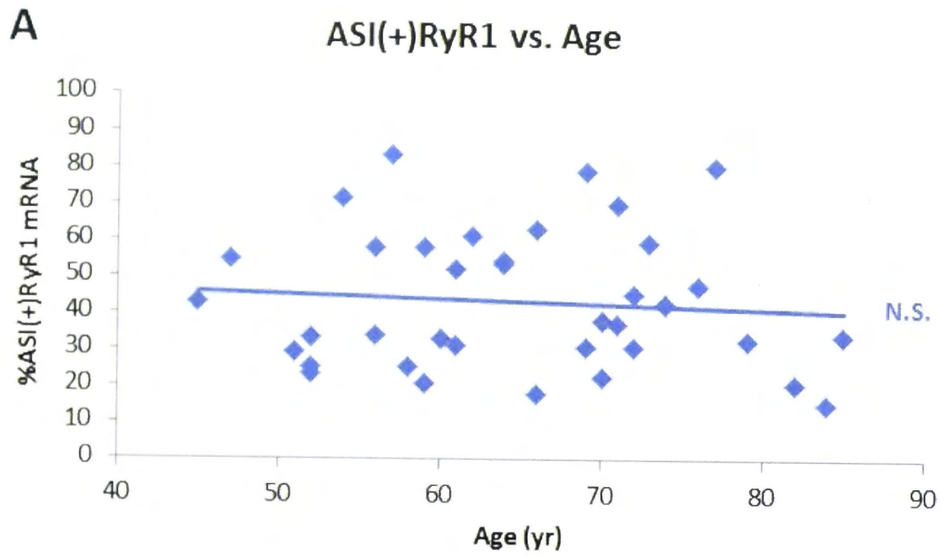

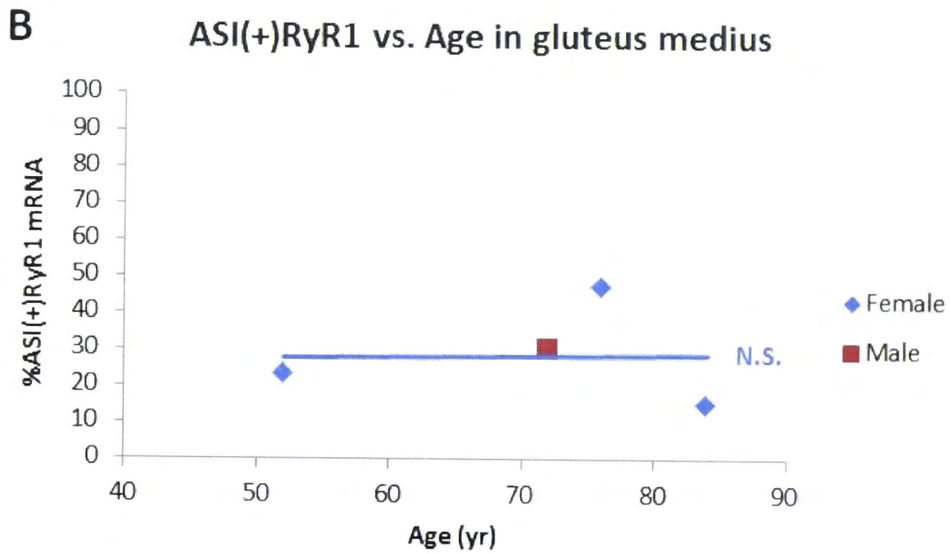

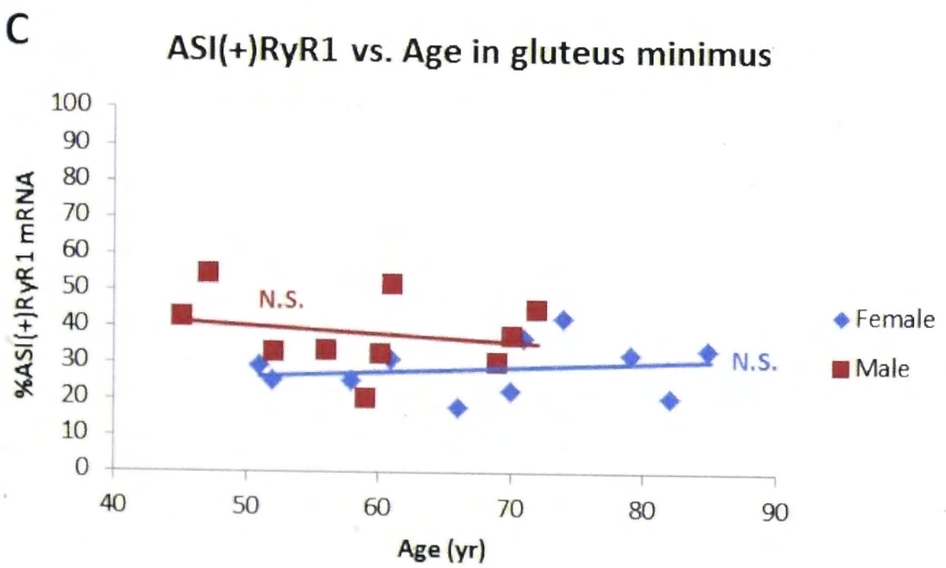

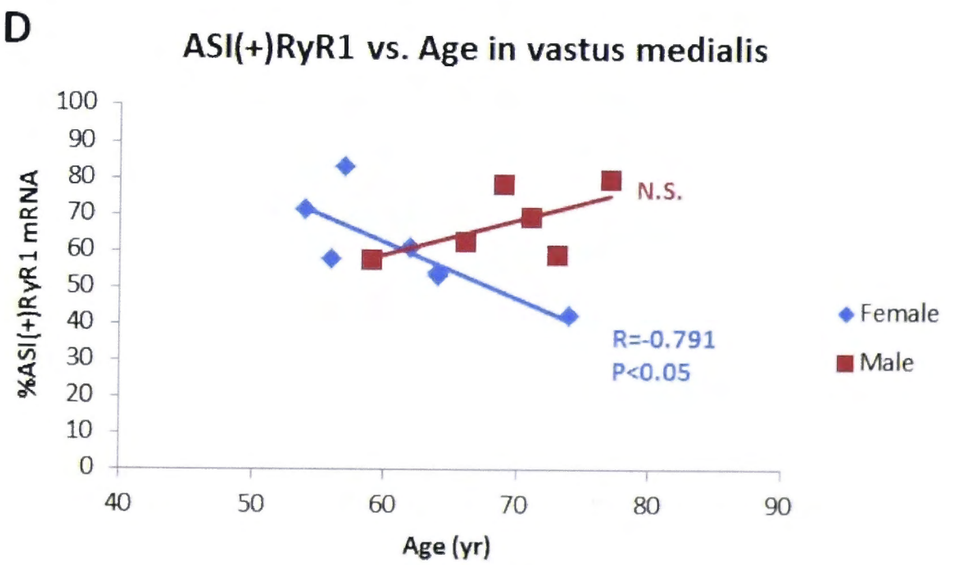

Figure 4.3: Correlation between age and percentage of ASI(+)RyR1 transcript in muscle from human gluteus medius, gluteus minimus and vastus medialis muscle. (**A**) Correlation between age and percentage of ASI(+)RyR1 transcript for all the donors. (**B**) Correlation between age and percentage of ASI(+)RyR1 transcripts of gluteus medius donors sorted according to gender. (**C**) Correlation between age and percentage of ASI(+)RyR1 transcript of gluteus minimus donors sorted according to gender. (**D**) Correlation between age and percentage of ASI(+)RyR1 transcript of vastus medialis sorted according to gender. N.S. = Correlation not significant, R = Pearson correlation coefficient

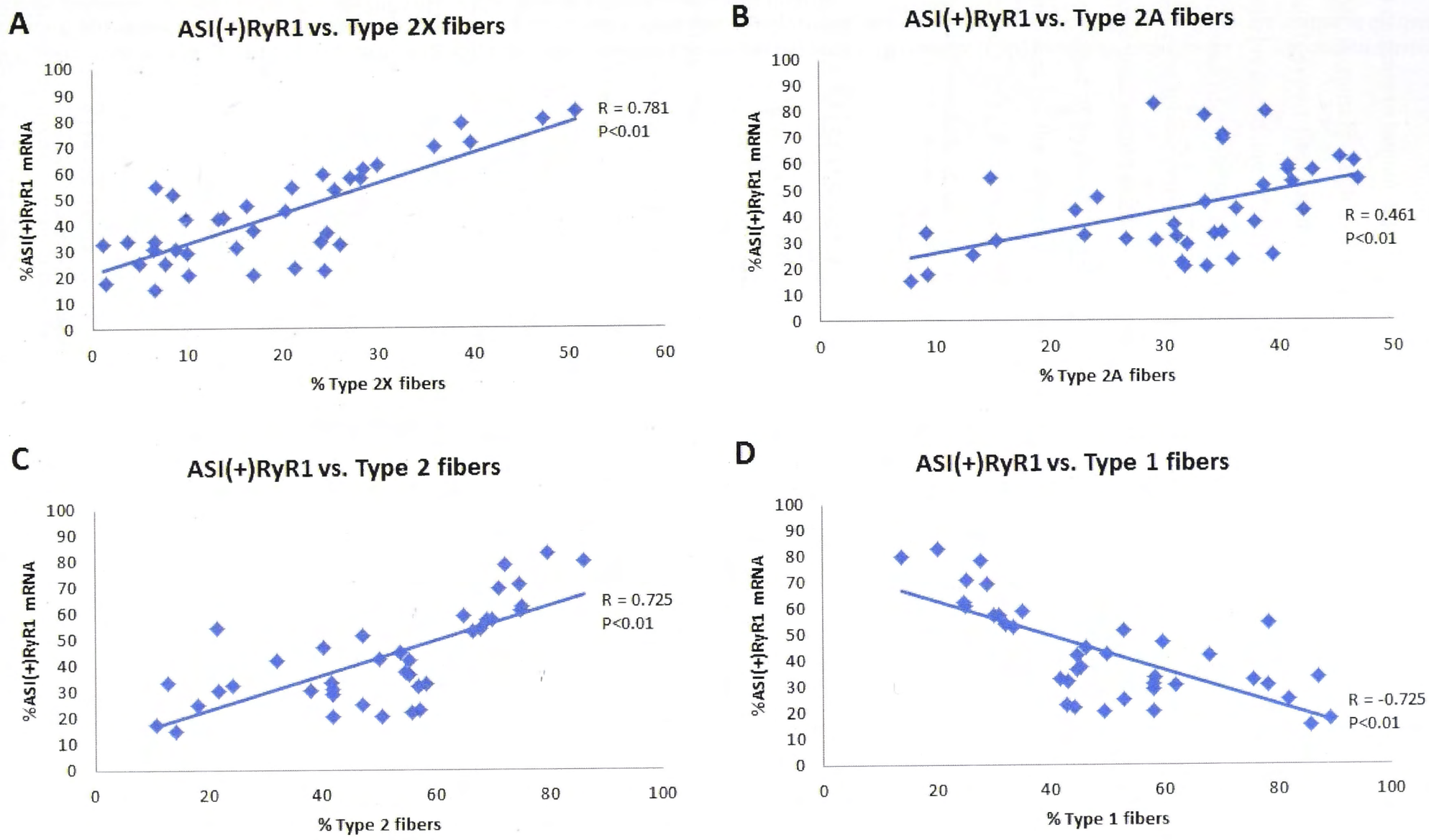

Figure 4.4: Correlation between fiber type percentage and percentage of ASI(+)RyR1 transcript present. (A) Correlation between percentage of ASI(+)RyR1 transcript and type 2X fiber percentage for all the donors. (B) Correlation between percentage of ASI(+)RyR1 transcript and percentage of type 2A fiber for all the donors. (C) Correlation between percentage ASI(+)RyR1 transcript and percentage of type 2 fiber for all donors. (D) Correlation between percentage of ASI(+)RyR1 transcript and percentage of type 1 fiber for all donors. N.S. = No significant correlation, R = Pearson correlation coefficient.

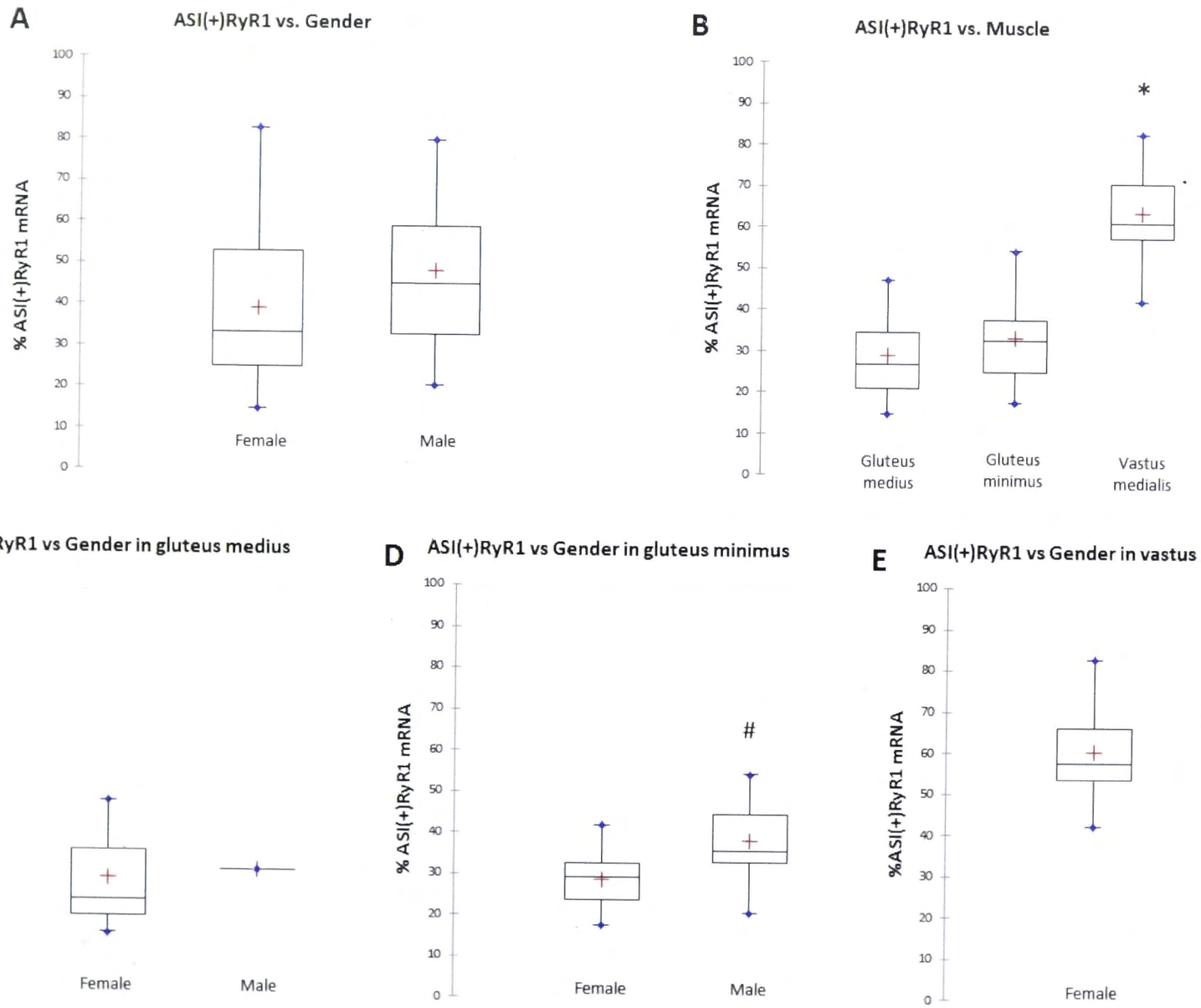

Figure 4.5: Boxplots of the percentage of ASI(+)RyR1 transcript in muscle from human donors sorted according to (**A**) gender, (**B**) muscle, (**C-D**) gender for each muscle. + = Mean percentage ASI(+)RyR1 transcript , the top and bottom margins of the box indicates the third and first quartile of the data set respectively, and the line in the middle of the box indicates the median of the data set. * Significantly different from gluteus medius and gluteus minimus ($P<0.01$). # Significantly different from female ($P<0.05$).

4.4.2 Rat muscle

In contrast to human muscles that mostly contain a mixture of fiber types, rats have fiber type specific muscles such as the EDL, which consists of only type 2 fibers and soleus, which is mostly type 1 fibers with some type 2A fibers. It is therefore useful to determine whether muscles consisting of only type 2 fibers would express only ASI(+)RyR1. The complete sequence of the rat RYR1 gene is not available on the NCBI databases. It was therefore decided to use the mouse primer sequence used by Kimura et al (Kimura et al. 2005) instead. The PCR using these mouse primers, however, was unsuccessful. The RNA was checked for degradation and found to be intact. A rat sequence for RYR1 was found on the Ensembl Genome Browser database, but the sequence was quite different from rabbit, human and mouse sequences. Primers using that rat sequence were designed but the PCR was again unsuccessful. It was decided due to time constraints not to pursue this further.

4.5 Discussion

4.5.1 RyR1 ASI splice variant levels vs. age

The hypothesis underlying the investigation of ASI splice variant transcript levels in muscle was there would be an increased level of the juvenile splice variant in aged muscle. This was based on observations that denervation and reinnervation occur at higher frequencies in aged muscle (Deschenes 2011) and the fact that the regenerated muscle fibers do not always completely mature (Dedkov et al. 2001). However this hypothesis was not proven. When the percentage ASI(+)RyR1 transcript of all the muscles was plotted against donor age, there was no significant correlation (see **Figure 4.3A**). When the data was separated according to muscle type and donor gender and the percentage of ASI(+)RyR1 transcript plotted against age , the only significant correlation was found in female vastus medialis muscle (see **Figure 4.3B-D**) with the percentage of ASI(+)RyR1 transcript showing a negative correlation with age ($R = -0.791$). The coefficient of determination (R^2) for this correlation is 0.626 which indicates that 62.6% of the variance in the percentage of ASI(+)RyR1 transcript could be explained by variance in age. This is interesting as there was also a negative correlation found between female vastus medialis donors and percentage of type 2X fiber type with a correlation coefficient (R) of -0.669 and R^2 value of 0.447 (see **Figure 3.3D&F**). However, in female gluteus medius, where a similar strong negative correlation between type 2X fibers and age was seen, no significant correlation between age and the percentage of ASI(+)RyR1 transcript was found (see **Figure 4.3B** and **Figure 3.3A&F**). There is also no significant correlation between the percentage of ASI(+)RyR1 transcript and age in male vastus medialis donors. Interestingly, a positive correlation between the percentage of type 2X fiber type and age was found in male vastus

medialis donors ($R = 0.503$, $R^2 = 0.253$) (see **Figure 3.3E&F**). One can therefore not say that a higher percentage of type 2X fiber is necessary to see the negative correlation between age and ASI(+)RyR1 transcript and age seen in female vastus medialis donors, as the male donors of this muscle do not show the same correlation. This result once again speaks of a more complex mechanism with multiple factors contributing to age related changes in muscle.

4.5.2 RyR1 ASI splice variant level vs. muscle and fiber type

When Zorzato et al showed the presence of two splice variants in both slow- and fast-twitch muscle they did not indicate the proportion or ratio of the transcript levels in either, as they used different primers and PCR reaction for the different splice variants (Zorzato et al. 1994). Futsasugi et al used the hind limb muscles of mice which is mostly fast-twitch muscle to show their adult ASI splice variant ratio of 3:1 ASI(+)RyR1 to ASI(-)RyR1 (Futatsugi et al. 1995). Kimura et al used vastus lateralis muscle biopsies to show that the same 3:1 ratio of ASI(+)RyR1 to ASI(-)RyR1 in normal adult human skeletal muscle (Kimura et al. 2005). Here I have shown for the first time that the levels of ASI(+)RyR1 and ASI(-)RyR1 transcripts are consistently influenced by fiber type with a strong positive correlation between ASI(+)RyR1 and the percentage of type 2 fibers in muscle from human donors ($R=0.725$, $R^2=0.525$) with a corresponding strong negative correlation between the percentages of ASI(+)RyR1 transcript and type 1 fibers ($R=-0.725$, $R^2=0.525$) (see **Figure 4.4C&D**). When the type 2 fibers were separated into type 2X and type 2A fibers, the correlation with the percentage of ASI(+)RyR1 transcript was the strongest with the percentage of type 2X fibers ($R=0.781$, $R^2=0.610$) with a weaker correlation between the percentages of type 2A fibers and ASI(+)RyR1 transcript ($R=0.461$, $R^2=0.212$) (see **Figure 4.4A&B**). This result points to a muscle fiber type specific distribution of the RyR1 splice variants with ASI(+)RyR1 being the type 2 fiber splice variant and ASI(-)RyR1 being the ASI(-)RyR1 splice variant. The use of vastus lateralis as muscle source by Kimura et al therefore becomes significant in interpreting the shift of ASI splice variant ratio observed in DM1 patients (Kimura et al. 2005) as it has been shown that vastus lateralis muscle from DM1 patients has a type 1 fiber dominance (64%) (Andersen et al. 2013), whereas vastus lateralis from healthy subjects show type 1 fibers constituting only 37.8 - 46.9% and therefore these muscle have a type 2 fiber type dominance (Johnson et al. 1973). **The higher level of ASI(-)RyR1 transcript observed by Kimura et al may therefore be due to a fiber type shift rather than a perturbed RyR1 splicing in the ASI region.** In the DM1 disease mechanism, RNAs with expanded CUG repeats bind to Muscleblind-like 1 (MBNL1) protein with high affinity, resulting in its sequestration in nuclear foci. MBNL1 acts as a regulator of splicing and microRNAs (miRNAs) processing and its sequestration leads to a loss of its activity (Miller et al. 2000; Warf and Berglund 2007; Yuan et al. 2007; Rau et al. 2011; Tang et al. 2012). This leads to misregulated alternative splicing and other changes of the

muscle transcriptome, which could in fact affect one of several steps in fiber type regulation signalling pathways causing this change in fiber type distribution observed in vastus lateralis of DM1 patiens. In fact, one of the mechanisms involved in coordinated fast and slow gene programs makes use of muscle specific miRNAs (Schiaffino and Reggiani 2011) and could possibly be one of the mechanisms affected in DM1.

In the results discussed in this chapter, the gluteus medius and gluteus minimus, which have a higher % of type 1 fibers, shows a significantly lower level of ASI(+)RyR1 transcript than vastus medialis which has a higher percentage of type 2 fibers (see **Figure 4.5B**). This result supports the hypothesis that ASI splice variants are fiber type specific. In this regard it would have been interesting to have determined the ASI splice variant levels in rat EDL muscle, as it contains no type 1 fibers. The concept of having different RyR1 isoforms in slow- and fast-twitch fibers is not novel, as it has been shown in skeletal muscle of fish that there are two RyR1 isoforms specific to fast- and slow-twitch muscle (Franck et al. 1998; Morrissette et al. 2000). However, the presence of fiber type specific RyR1 isoforms in amphibian, avian and mammalian skeletal muscle has not been shown and therefore the presence of fiber-type specific RyR1 splice variants in humans is a novel finding. The physiological significance of ASI(+)RyR1 in type 2 fibers and ASI(-)RyR1 in type 1 fibers will be discussed in the general discussion chapter (Chapter 7).

It remains to be determined whether individual fibers express only one splice variant, or whether (as with myosin isoforms), regions of the multinucleate fiber can express different isoforms, so that an individual fiber may have a higher percentage of one or the other isoform. It is also not known whether a fiber that contains both splice variants would have homotetrameric or heteroterameric RyR1s containing just one splice variant per RyR1 or a various hybrids consisting of different combination of the two splice variants. The latter is most probably the case as have been demonstrated with co-expression of WT and mutant RyR1s in HEK cells (Xu et al. 2008). This will be discussed more in the general discussion chapter (Chapter 7).

4.5.3 RyR1 ASI splice variant level vs. gender

No significant difference was found in the percentage of ASI(+)RyR1 transcript between the muscles of male and female donors, (see **Figure 4.5A**). When the donors were separated according to muscle and then gender, the only significant difference in ASI(+)RyR1 transcript found was between female (28.67%) and male donors (30.43%) of gluteus minimus (see **Figure 4.5 C-E**) ($P<0.05$). This was probably due to the significant difference ($P<0.01$) in type

2A fiber type percentage between the gender groups in gluteus minimus muscle (female 25.17% vs. male 31.55%) rather than gender differences in the percentage of ASI(+)RyR1 transcript.

4.6 Conclusion

The level of RyR1 ASI splice variants in human muscle is not affected by age as was originally hypothesised. However, a novel finding is that the levels of ASI splice variant in human muscle correlates with fiber type distribution. It seems therefore that the splice variants are fiber type specific isoforms of the RyR1. Different RyR1isoforms in slow-twitch and fast-twitch fibers have been shown in fish, but this is the first time that this is shown in mammalian skeletal muscle.

Chapter 5: EC coupling protein expression with age

5.1 Introduction

Sarcopenia is the age related loss of muscle mass and strength. Although loss of muscle mass would reduce muscle strength, the loss in muscle strength is greater than can be accounted for by the loss in mass (Lynch et al. 1999). One of the suggested mechanisms involved in the loss of muscle strength is alterations to the EC coupling process (Delbono et al. 1995; Renganathan et al. 1997; Wang et al. 2000).

Delbono et al (Delbono et al. 1995) first investigated the possibility that the reduction in specific force seen in aging muscle may be due to alterations in the EC coupling Ca^{2+} release process. Delbono et al coined the term "EC uncoupling" to describe the defects in transmission of membrane depolarization to SR Ca^{2+} release that are responsible for decreased specific force with aging (Payne and Delbono 2004). The observed reduction in DHPR charge movement during EC coupling could indicate fewer DHPRs and/or dysfunctional DHPRs with age. The reduced SR Ca^{2+} release observed could be the result of fewer DHPRs, dysfunctional DHPR, fewer RyR1 and/or dysfunctional RyR1. It seems that there is a general change in protein expression (O'Connell et al. 2007) as well as protein turnover (Ferrington et al. 1998) in muscle with age. Changes in expression levels of the DHPR and RyR1 are associated with loss of specific muscle force with age and this could underlie the EC uncoupling hypothesis.

There are conflicting reports regarding the expression of RyR1 in aging muscle. A decrease in RyR1 levels has been reported in mixed and fast-twitch fibers in rats and mice with age based on [^{3}H]ryanodine binding (Renganathan et al. 1997; Renganathan et al. 1998). However, other [^{3}H]ryanodine binding and immunoblot studies report no change in RyR1 expression in fast- and slow-twitch muscle from aged rats (Damiani et al. 1996; Margreth et al. 1999; O'Connell et al. 2008). In terms of the EC uncoupling hypothesis, the ratio of DHPR to RyR1 is likely to be more important than absolute expression levels in rodents because it is the increase in RyR1 unassociated with DHPR that is the basis for this hypothesis. In the work discussed in this chapter both RyR1 expression and the DHPR α_{1s}/RyR1 expression ratio are investigated with respect to age and sex.

The results reported by Delbono et al (Delbono et al. 1995) showing reduced DHPR charge movement and SR Ca^{2+} transients in aged human fast-twitch fibers were subsequently confirmed in fast-twitch fibers of aging mice (Wang et al. 2000). [^{3}H]PN200-110 binding to

DHPR α_{1s} in rat and mouse muscle indicates reduced DHPR α_{1s} expression with age in mixed, slow-twitch and fast-twitch muscles (Renganathan et al. 1997; Renganathan et al. 1998). This was confirmed by immunoblot of aging rabbit and rat muscle (Ryan et al. 2000; Ryan et al. 2003; O'Connell et al. 2008). The DHPR/RyR1 ratio in adult rat EDL of ~1 suggests that every fourth RyR1 may be linked to a DHPR tetrad. In soleus muscle this ratio is lower (~0.4) and could mean that every 12th RyR1 is linked to a DHPR tetrad (Delbono and Meissner 1996; Renganathan et al. 1997). In aged muscle the ratio decreases to 0.26 in soleus and 0.68 in EDL muscle. Therefore more DHPR uncoupled RyR1s may be present in older rat muscle and this would support the EC uncoupling hypothesis. In human muscle, however, there is apparently no decrease in DHPR α_{1s} with age (Ryan et al. 2003). The alterations in CRU structure seen in aged human muscle showed that the total number of CRUs decrease, but that the average size of the RyR1 feet arrays increase to compensate for the loss of CRUs (Boncompagni et al. 2006). In human muscle therefore, it may be more a case of altered structure and arrangement of the EC coupling apparatus than the expression of the protein that cause the EC uncoupling. In the work discussed in this chapter, the level of α_{1s} expression is also investigated.

The DHPR β_{1a} subunit plays an important role in EC coupling as it is required for the trafficking of the DHPR α_{1s} subunit to the sarcolemma (Neuhuber et al. 1998; Bichet et al. 2000; Schredelseker et al. 2005; Leuranguer et al. 2006), formation of tetrads (Schredelseker et al. 2005) as well as regulating L-type Ca^{2+} current and supporting a fraction of EC coupling (Gregg et al. 1996; Strube et al. 1996). In addition, the SH3 domain of the β_{2a} subunit has been shown to bind to dynamin and mediate endocytosis of the DHPR α_{1c} subunit in *Xenopus* oocytes (Gonzalez-Gutierrez et al. 2007). The effect of aging on the DHPR β_{1a} subunit expression was investigated by Taylor et al (Taylor et al. 2009). They reported a significant increase in β_{1a} expression with age in mice both in mixed muscles and fast-twitch muscles (TA and EDL). They also found that over expression of the β_{1a} subunit in TA muscles of mice caused a decrease in α_{1s} subunit expression and decline in specific force. Introducing siRNA against the β_{1a} subunit and thereby reducing its expression in aged mice showing a decrease in charge movement restored the charge movement to control levels. These results suggest a possible role for β_{1a} in the reduction in α_{1s} subunit expression reported in rodents. However, the increased expression of β_{1a} has not been investigated in humans and has been attempted in the work discussed in this chapter.

The cytoplasmic free Ca^{2+} concentration is increased in both slow-twitch soleus (22%) and fast-twitch EDL muscles (76%) from old rats (Fraysse et al. 2006). A population of aging mouse skeletal muscle fibers demonstrates an external Ca^{2+} dependent component to EC coupling, indicated by reduced voltage-induced Ca^{2+} transients in fibers in the absence of external Ca^{2+} (Payne et al. 2004). Interestingly, regenerating muscle and developing skeletal muscle go

through similar stages in which effective EC coupling and contraction are partially dependent on external Ca^{2+} (Louboutin et al. 1995; Louboutin et al. 1996), and there is an accompanied transient expression of the DHPR α_{1c} subunit (Pereon et al. 1997). The expression of the DHPR α_{1c} diminishes as the expression of DHPR α_{1s} increases over time as muscle regeneration proceeds. As aged muscle show increased denervation and reinnervation and therefore also undergo regeneration, it could be possible that there may a shift towards cardiac EC coupling in aged muscle. However, a subsequent study found that external Ca^{2+} but not Ca^{2+} influx is required to maintain force in repetitive fiber electrical stimulation of single fibers from aging mouse muscle (Payne et al. 2004). If this is generally true, it is unlikely that CICR plays a role in EC coupling in aged mice. In fact, the authors contributed the external Ca^{2+} dependence to sodium channel modification with age that leads to a failure in action potential generation in the absence of external Ca^{2+}. However, the expression of the DHPR α_{1c} in aging human skeletal muscle has not been investigated. In the work discussed in this chapter the α_{1c}/RyR1 expression ratio is examined in human skeletal muscle.

Muscle weakness in aged muscle could also be due to the modification of RyR1. Oxidation and S-nitrosylation of RyR1 in aged muscle dissociates FKBP12 from the RyR1 causing an increase RyR1 activity and therefore "leaky" channels (Andersson et al. 2011). Stabilizing RyR1/FKBP12 binding reduced this calcium leak from the SR, enhanced Ca^{2+} release from the SR, increased specific force and increased exercise capacity in aged mice. In the results discussed in this chapter, the expression of FKBP12 with age in humans as well as the FKBP12/RyR1 ratio has been investigated.

5.2 Aim

To investigate the expression levels of RyR1, DHPR α_{1s}, DHPR β_{1a} and FKBP12 as well as the DHPR α_{1s}/RyR1, DHPR α_{1c} /RyR1, and FKBP12/RyR1 expression ratios in muscle obtained from human and rat subjects.

5.3 Quantitative and statistical analysis

Stained gels and developed films were documented by digital imaging using a Gel Doc XR System (Bio-Rad Laboratories, USA) and band intensity measured using Quantity One 1-D analysis Software (Bio-Rad Laboratories, USA). For muscle homogenate immunoblots, the band density was normalised to the density of the total protein in the same sample on a Coomassie stained gel (see **Figure 5.1**). This was done as most proteins used as loading standards in muscle immunoblot (e.g. actin, MyHC and glyceraldehyde 3-phophate dehydrogenase - GAPDH) show a change in expression in humans with age (Gelfi et al. 2006). For microsomal vesicle immunoblots, the protein band intensity was normalised to that of the

RyR1 because the ratio of the expression of the specific proteins relative to that of the RyR1 was of interest.

Statistical analysis was done using ANOVA, student's t-test ($P \leq 0.05$) and Pearson correlations. Correlations were deemed significant if the correlation coefficient (R) differed significantly from 0 ($P \leq 0.05$).

5.4 Results

In order to determine if all the proteins of interest were present in microsomal vesicles, the different fractions obtained during the preparation of microsomal vesicles for a human muscle sample were probed for RyR1, DHPR α_{1s}, DHPR β_{1a}, and FKBP12. The results showed that most of the β_{1a} subunit is lost during with the first centrifugation step (see **Figure 5.2**) and that there is very little β_{1a} present in the final microsomal vesicles. It was therefore decided to use the muscle homogenate in the investigation of the expression levels of the proteins.

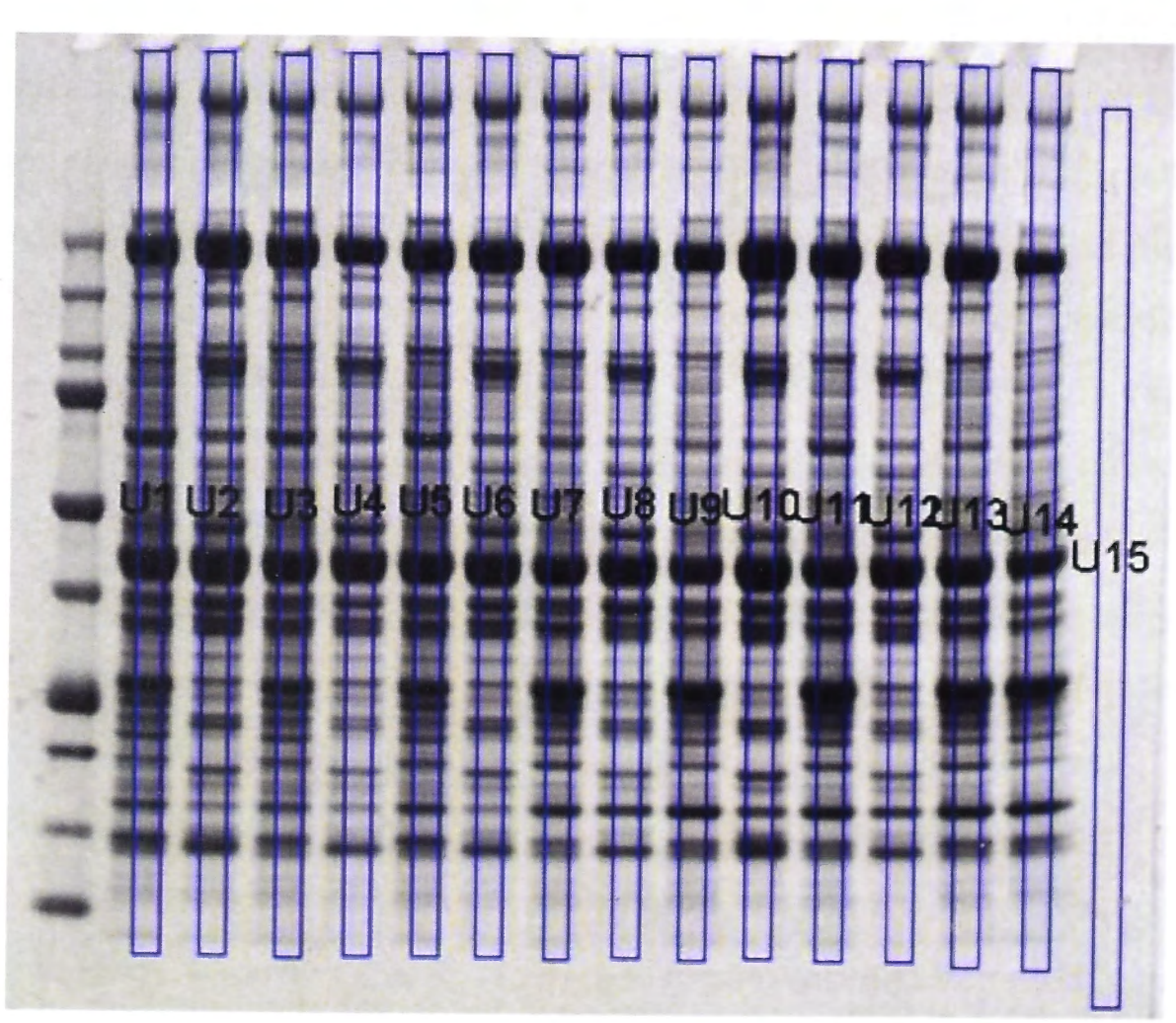

Figure 5.1: Example of muscle homogenate SDS-PAGE showing areas used to determine density of total protein (U1-U14). U15 was used as background (in each case the whole lane was scanned including bands and regions between bands?)

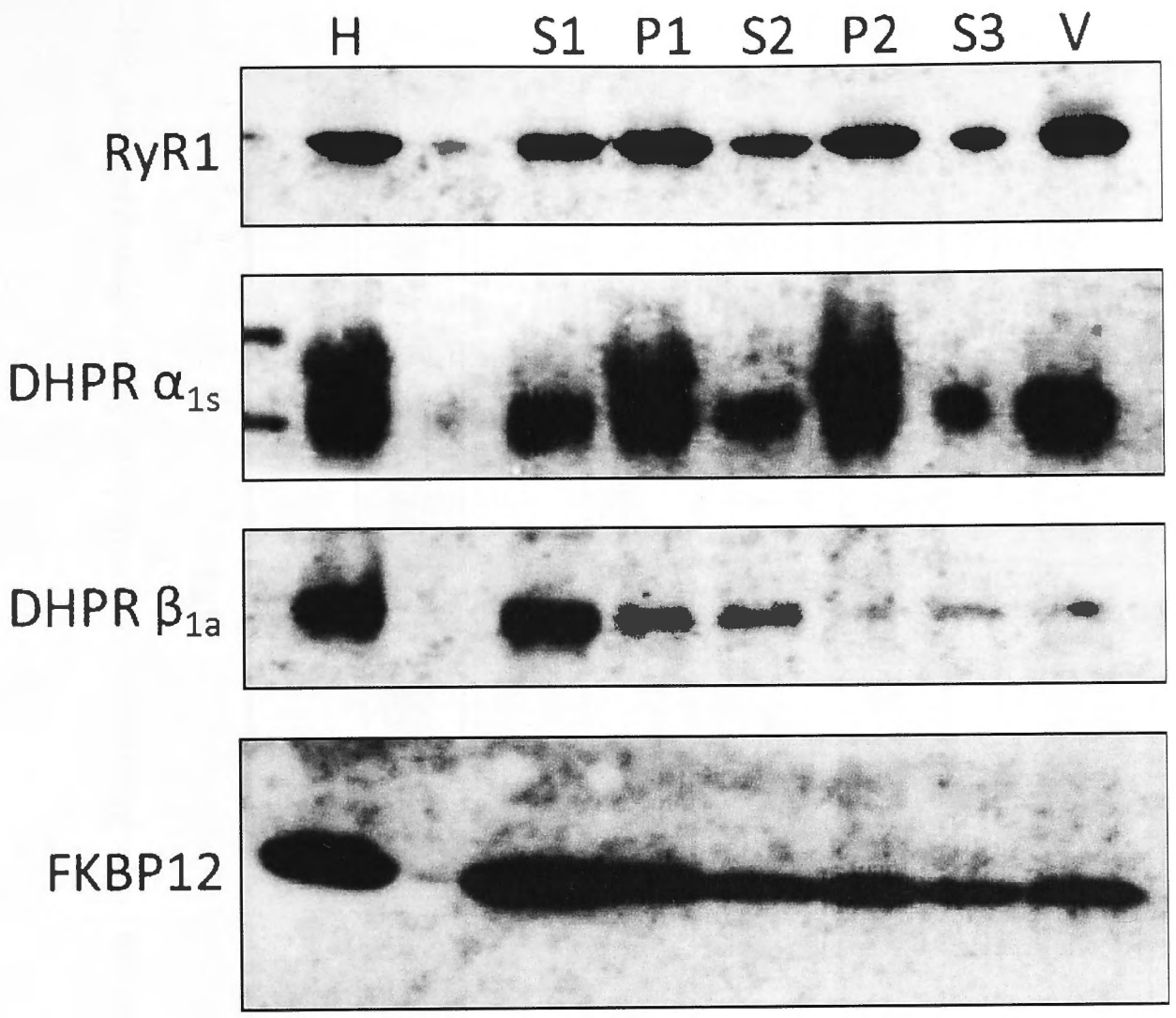

Figure 5.2: Immunoblot of human muscle microsomal vesicle preparation fractions, probed for RyR1, DHPR α_{1s}, DHPR β_{1a} and FKBP12. H – homogenate, S1 – supernatant from first centrifugation step , P1 – pellet from first centrifugation step, S2 – supernatant from second centrifugation step, P2 – pellet from second centrifugation step, S3 supernatant from final centrifugation step and V – microsomal vesicles.

The expression levels of RyR1, DHPR α_{1s}, DHPR β_{1a} and FKBP12 was investigated in human (gluteus medius, gluteus minimus and vastus medialis) and rat (soleus and EDL) muscle homogenate using immunoblot and densitometry (as described in Sections 2.2.9 – 2.2.14). At least four repeats on two different immunoblots (two per blot) were done for each muscle homogenate sample. The density for the resulting bands was determined and normalised to total protein as described in section 5.1.5. **Figure 5.3** gives an example of the muscle homogenate immunoblots for the human and rat muscle samples. As not all the FKBP12 present in the muscle homogenate will be associated with RyR1, microsomal vesicles were used to investigate the FKBP12/RyR1 level for the different muscle samples. The α_{1s}/RyR1 and α_{1c}/RyR1 levels were also investigated in microsomal vesicles. The expression levels of DHPR α_{1s}, DHPR α_{1c}, and FKBP12 were determined in microsomal vesicles prepared from human (gluteus medius, gluteus minimus and vastus medialis) and rat (soleus and EDL) muscle. As the DHPR α_1 subunits are of similar molecular weight, the membrane was first probed for α_{1s} and then stripped and reprobed for α_{1c} in cases where both proteins were probed for on one blot. At least four repeats on two different immunoblots (two per blot) were done for each microsomal vesicle sample and the density of the resulting bands determined. The density was normalised to the RyR1 density. **Figure 5.4** gives an example of the microsomal vesicle immunoblots for the human and rat muscle samples.

Chapter 5

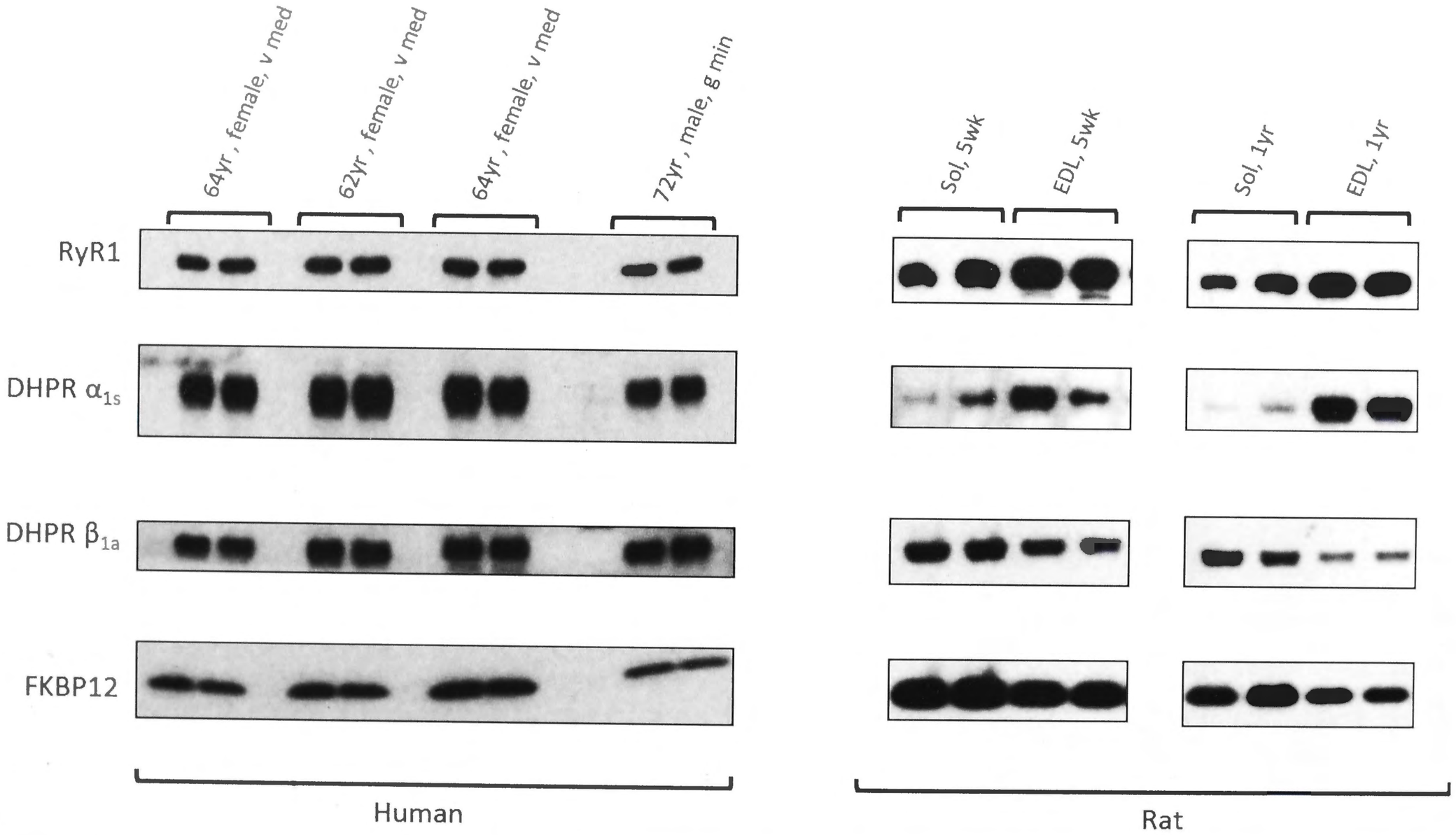

Figure 5.3: Example of immunoblots of muscle homogenates. The human muscle blot is shown on the left and the rat muscle blot on the right (v med – vastus medialis, g min – gluteus minimus, Sol – Soleus, EDL- extensor digitorum longus).

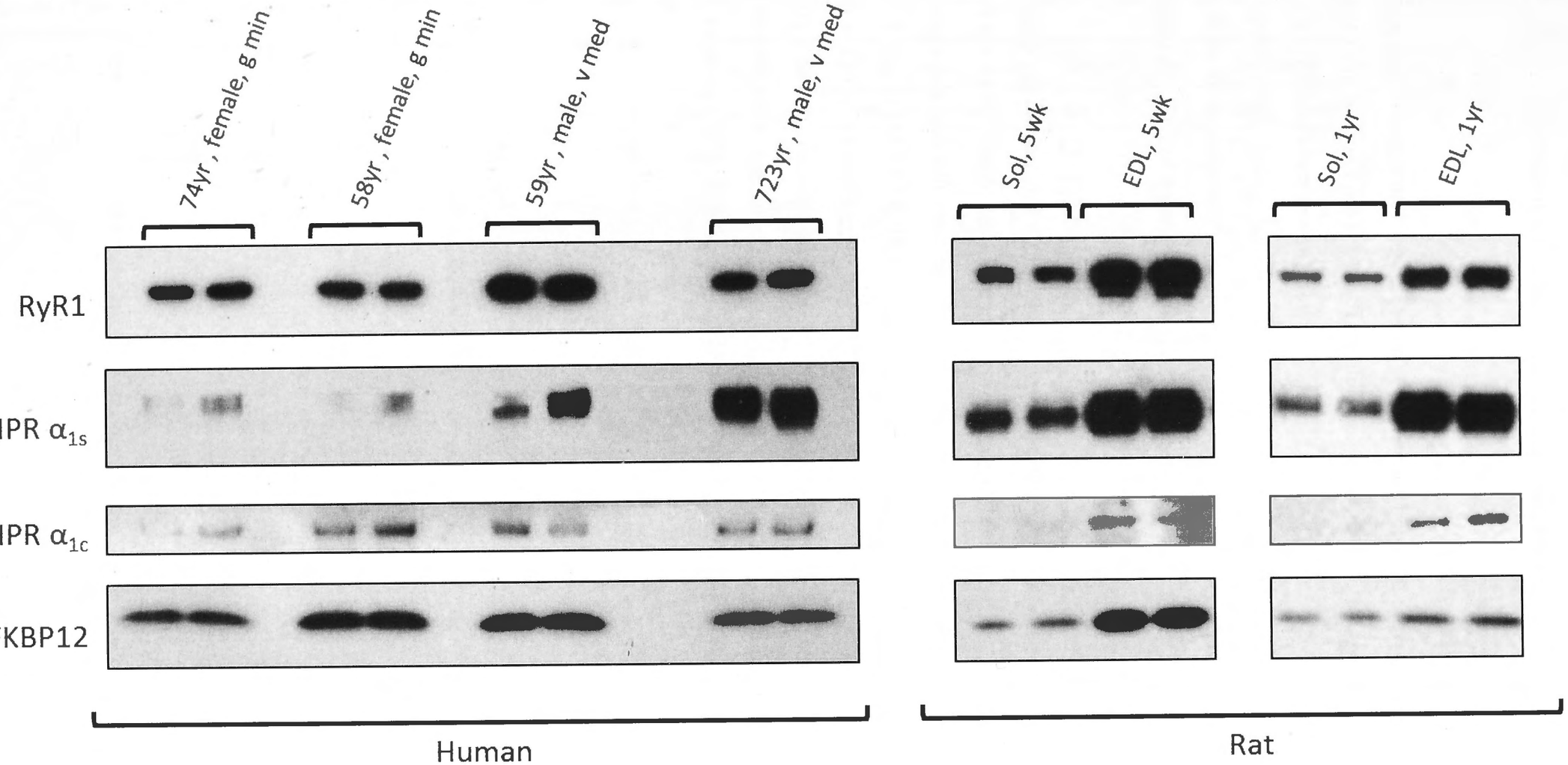

Figure 5.4: Example of immunoblots of microsomal vesicles prepared from muscle samples. The human muscle blot is shown on the left and the rat muscle blot on the right (v med – vastus medialis, g min – gluteus minimus, Sol – Soleus, EDL- extensor digitorum longus).

5.4.1 Human muscle

A breakdown of the human donors has been given in **Table 3.1** of Chapter 3.

5.4.1.1 Densitometry results

The human muscle results were grouped according to muscle, and donor gender and age (<60yr or ≥60yr). As most of the changes in muscle associated with age seem to occur after the 6th decade (Vandervoort and McComas 1986; Lindle et al. 1997; Rantanen et al. 1998; Deschenes 2004), the donors younger than 60yr were considered as the control group. The average density of the protein bands relative to total protein determined in muscle homogenate for each group is given in **Table 5.2** and the average density of the protein bands relative to RyR1 determined in microsomal vesicles for each group is given in **Table 5.3.**

The expression level of the DHPR α_{1s} subunit was then plotted as a function of the expression levels of RyR1 (both normalised to total protein) in the muscle homogenate for all the muscle donors (**Figure 5.5A**). The same was done for the DHPR β_{1a} subunit and then the expression levels of the two DHPR subunits were also correlated (**Figure 5.5B&C**). There was a significant positive correlation ($P<0.01$) between the DHPR α_{1s} density and that of the RyR1 with a correlation coefficient of 0.889. The DHPR β_{1a} subunit density also showed a significant positive correlation ($P<0.01$) with that of the RyR1, although the correlation coefficient was lower ($R=0.435$). The two DHPR subunits also showed a significant ($P<0.01$) positive correlation with $R=0.542$.

Table 5.1: The average density of the protein bands relative to total protein in human muscle homogenate. Donors were grouped according to muscle, gender and age (<60yr or ≥60yr) (sem – standard error of the mean, n – number of observations, * significantly different from <60yr age group of same muscle, $^{\#}$ significantly different from female of same muscle, $^{+}$ significantly different from female of same age group and muscle, ‡ significantly different from gluteus medius, † significantly different from gluteus minimus)

				RyR1		DHPR α_{1s}		DHPR β_{1a}		FKBP12	
			n	mean	±sem	mean	±sem	mean	±sem	mean	±sem
gluteus medius	female	<60	8	0.57	0.09	0.58	0.11	0.81	0.13	1.00	0.09
		≥60	8	1.23*	0.14	0.95*	0.12	1.09	0.19	1.31*	0.06
		combined	16	0.90	0.12	0.77	0.09	0.95	0.12	1.15	0.07
	male	<60	0	-	-	-	-	-	-	-	-
		≥60	4	1.02	0.09	0.55^{+}	0.11	0.63^{+}	0.07	1.21	0.13
		combined	4	1.02	0.09	0.55	0.11	0.63$^{\#}$	0.07	1.21	0.13
	f and m combined		20	0.92	0.10	0.72	0.08	0.89	0.10	1.16	0.06
gluteus minimus	female	<60	12	0.73	0.05	0.91	0.10	0.78	0.13	1.01	0.10
		≥60	32	0.88	0.08	0.92	0.08	0.96	0.06	1.28*	0.08
		combined	44	0.84	0.06	0.91	0.06	0.91	0.06	1.21	0.07
	male	<60	20	1.16^{+}	0.12	1.17	0.12	1.24^{+}	0.08	1.02	0.10
		≥60	20	0.81*	0.11	0.95	0.10	1.18	0.13	1.19	0.10
		combined	40	0.99	0.09	1.06	0.08	1.21$^{\#}$	0.08	1.11	0.07
	f and m combined		84	0.91	0.05	0.98‡	0.05	1.05	0.05	1.16	0.05
vastus medialis	female	<60	12	1.31	0.10	1.12	0.06	0.63	0.09	0.97	0.09
		≥60	20	1.44	0.15	1.44	0.17	0.92*	0.10	1.21	0.15
		combined	32	1.39	0.10	1.32	0.11	0.81	0.08	0.70	0.10
	male	<60	4	1.64	0.12	1.41^{+}	0.07	0.79	0.07	0.84	0.12
		≥60	20	1.91	0.32	1.93	0.34	1.04	0.14	1.30	0.36
		combined	24	1.91	0.27	1.93	0.29	1.04	0.12	1.30	0.30
	f and m combined		56	1.62‡†	0.13	1.58‡†	0.14	0.91	0.07	1.20	0.14

Table 5.2: The average density of the protein bands relative to that of RyR1 in microsomal vesicles from human muscle donors. Donors were grouped according to muscle, gender and age (<60yr or ≥60yr) (sem – standard error of the mean, n – number of observations, * significantly different from <60yr age group of same muscle, # significantly different from female of same muscle, + significantly different from female of same age group and muscle, † significantly different from gluteus minimus).

			DHPR α_{1s}/RyR1			DHPR α_{1c}/RyR1			FKBP12/RyR1		
			mean	±sem	n	mean	±sem	n	mean	±sem	n
gluteus medius	female	<60	0.94	0.23	10	1.07	0.51	8	2.01	0.22	10
		≥60	0.69	0.10	8	0.51	0.06	8	0.82*	0.12	10
		combined	0.83	0.14	18	0.79	0.26	16	1.07	0.14	20
	male	<60	-	-	-	-	-	-	-	-	-
		≥60	0.51	0.10	4	1.03+	0.13	4	0.59	0.11	4
		combined	0.51	0.10	4	1.03	0.13	4	0.59#	0.11	4
	f and m combined		0.77	0.12	22	0.83	0.21	20	0.99	0.12	24
gluteus minimus	female	<60	1.05	0.15	12	0.74	0.19	12	1.08	0.10	14
		≥60	0.73	0.12	39	0.36	0.04	37	0.81*	0.04	51
		combined	0.81	0.10	51	0.45	0.06	49	0.86	0.04	65
	male	<60	1.09	0.13	25	0.65	0.15	26	1.04	0.10	28
		≥60	1.27+	0.12	19	0.51	0.14	20	1.00+	0.06	24
		combined	1.17#	0.09	44	0.59	0.10	47	1.02	0.06	53
	f and m combined		0.98	0.07	95	0.52	0.06	96	0.94	0.04	118
vastus medialis	female	<60	1.10	0.13	12	0.91	0.13	12	0.94	0.02	12
		≥60	0.89	0.11	20	1.02	0.12	26	0.76*	0.05	36
		combined	0.97	0.08	32	0.99	0.09	38	0.80	0.04	48
	male	<60	1.12	0.11	4	0.35+	0.07	5	0.96	0.09	6
		≥60	1.01	0.12	19	0.77*	0.16	20	0.83	0.05	22
		combined	1.03	0.10	23	0.67#	0.13	26	0.86	0.05	28
	f and m combined		1.00	0.06	55	0.86†	0.08	64	0.82†	0.03	76

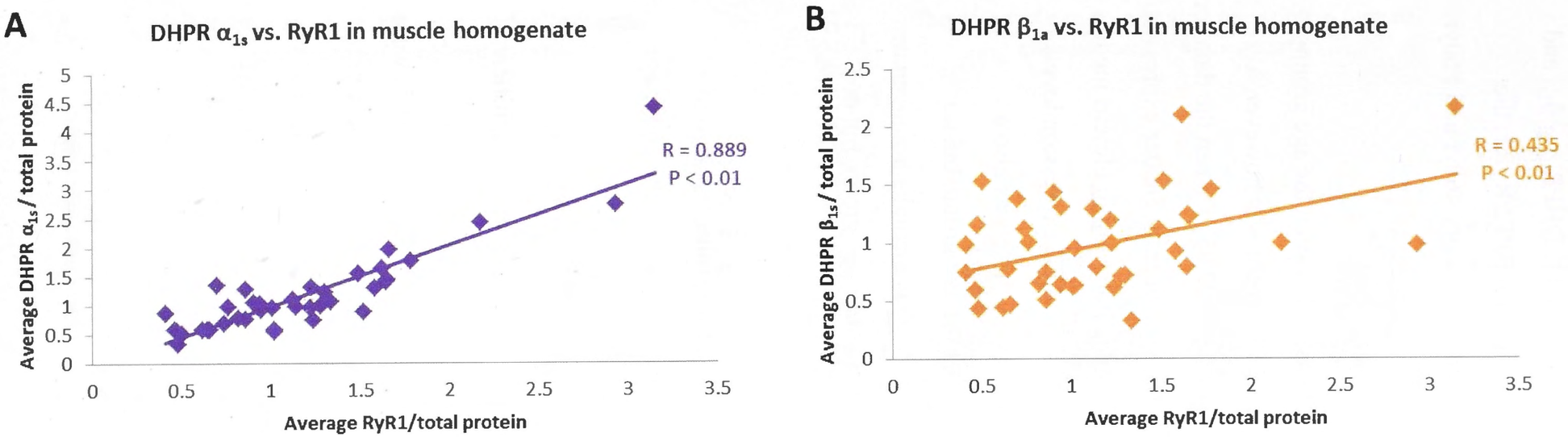

Figure 5.5: Correlation between the expression levels of the DHPR subunits and RyR1 in the human muscle homogenates, normalized to total protein. (**A**) Expression levels of the DHPR α_{1s} subunit plotted against that of RyR1. (**B**) Expression levels of the DHPR β_{1a} subunit plotted against that of RyR1. (**C**) Expression levels of the DHPR β_{1a} subunit plotted against that of the α_{1s} subunit.

5.4.1.2 The effect of age on protein expression levels

5.4.1.2.1 Comparing the means

In order to investigate the effect of age on the expression levels of RyR1, DHPR α_{1s}, β_{1a}, and FKBP12 as well as the expression ratios of α_{1s}/RyR1, α_{1c}/RyR1 and FKBP12/RyR1, the densitometry data obtained from the immunoblots were grouped into donors <60yr and ≥60yr. The mean was determined for each group (**Table 5.2** and **5.3**).

There was no significant difference in RyR1, α_{1s}, and β_{1a} expression between the age groups when the data for all three muscles were combined (**Figure 5.6A**). There was however, a significantly higher expression of FKBP12 in the ≥60yr age group ($P \leq 0.05$). When the data for the different muscles was plotted separately (**Figure 5.6 B-D**), significantly greater expression levels of RyR1 and FKBP12 ($P \leq 0.05$) were observed in the ≥60yr age group in gluteus medius muscle homogenates. No significant differences were found in α_{1s} and β_{1a} expression levels in this muscle (**Figure 5.6B**). In gluteus minimus muscle homogenates, there was also a significantly greater FKBP12 expression level ($P \leq 0.05$) in the ≥60yr age group, but no difference in RyR1, α_{1s} or β_{1a} expression levels (**Figure 5.6C**). Vastus medialis homogenates showed a significantly higher α_{1s} and β_{1a} expression ($P \leq 0.05$) in ≥60yr age group, but no difference in RyR1 and FKBP12 expression (**Figure 5.6D**).

Combining the microsomal immunoblot densitometry data of the three muscles showed a significantly lower ($P \leq 0.05$) α_{1s}/RyR1 and FKBP12/RyR1 expression ratio in the ≥60yr age group (**Figure 5.7A**) but no difference in the α_{1c}/RyR1 expression ratio.
When the data from the three muscles were separated, a significantly lower ($P \leq 0.05$) FKBP12/RyR1 ratio was observed in gluteus medius microsomal vesicles, but no significant difference in the α_{1s}/RyR1 or α_{1c}/RyR1 ratios (**Figure 5.7B**). In the gluteus minimus microsomal vesicles significantly lower ratios of FKBP12/RyR1 and α_{1c} /RyR1 ($P \leq 0.05$) were observed in ≥60yr donors with no significant difference in the α_{1s}/RyR1 ratio (**Figure 5.7C**). The vastus medialis microsomal vesicles showed a significantly lower FKBP12/RyR1 ratio ($P \leq 0.05$) in the ≥60yr age group with no significant difference in the α_{1s}/RyR1 and α_{1c}/RyR1 e ratios (**Figure 5.7D**).

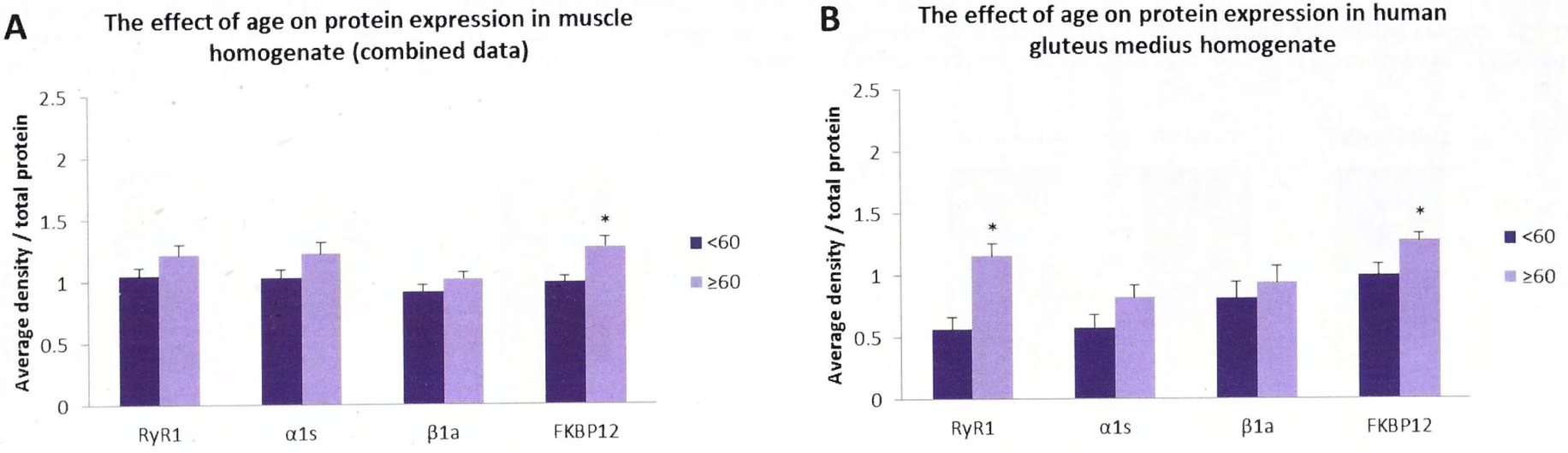

* Significantly different from <60 (P≤0.05)

Figure 5.6: A comparison of expression levels of RyR1, DHPR α_{1s}, DHPR β_{1a} and FKBP12 in muscle homogenate of human donors <60yr and ≥60yr. (**A**) The protein expression levels in muscle homogenate where data from all three muscles were combined. (**B**) The protein expression levels in gluteus medius muscle homogenate. (**C**) The protein expression levels in gluteus minimus muscle homogenate. (**D**) The protein expression levels in vastus medialis muscle homogenate.

A The effect of age on protein expression in human muscle microsomal vesicles (combined)

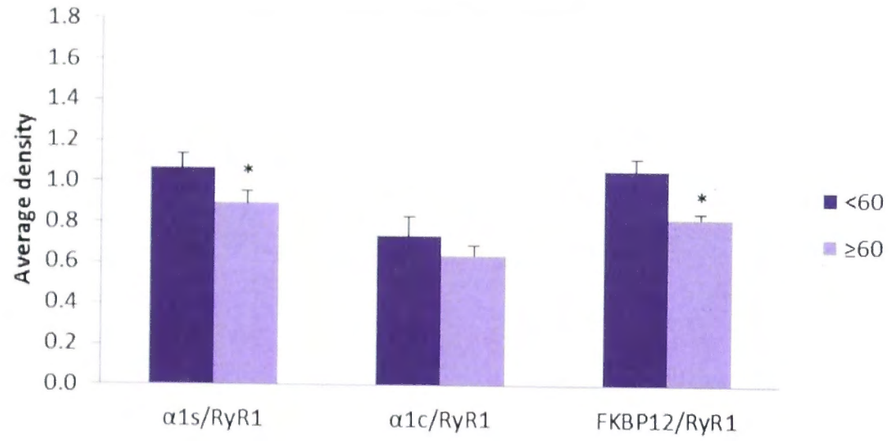

* Significantly different from <60 (P≤0.05)

B The effect of age on protein expression in human gluteus medius microsomal vesicles

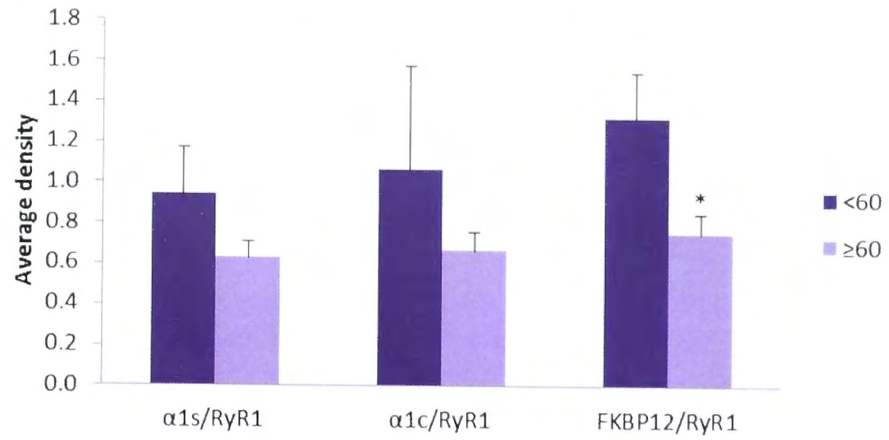

C The effect of age on protein expression in human gluteus minimus microsomal vesicles

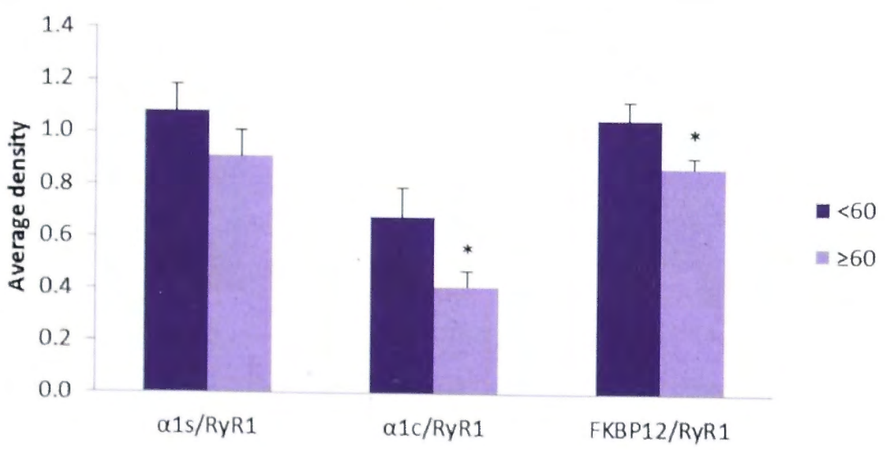

D The effect of age on protein expression in human vastus medialis microsomal vesicles

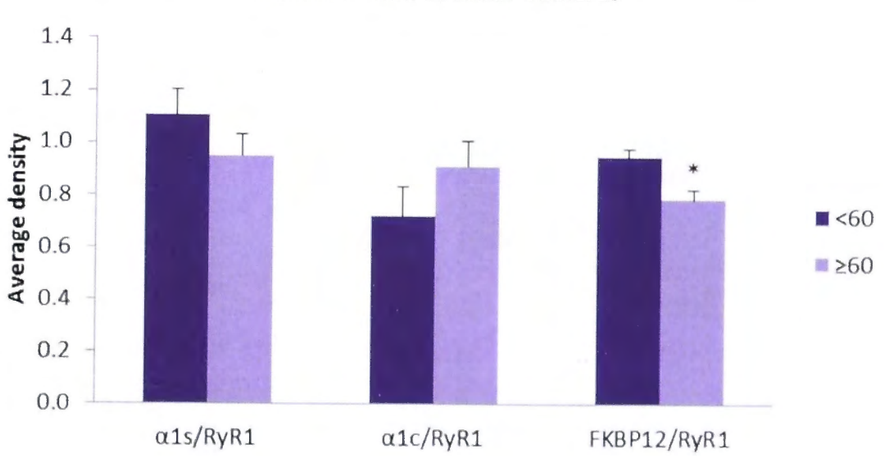

Figure 5.7: A comparison of DHPR α_{1s} / RyR1, DHPR α_{1c} / RyR1 and FKBP12 / RyR1 expression ratios in microsomal vesicles prepared from muscle of human donors <60yr and ≥60yr. (**A**) The protein expression ratios in microsomal vesicles where data from all three muscles were combined. (**B**) The protein expression ratios in gluteus medius microsomal vesicles. (**C**) The protein expression ratios in gluteus minimus microsomal vesicles. (**D**) The protein expression ratios in vastus medialis microsomal vesicles.

In order to determine if the effect of age on the expression levels are different between male and female donors, the densitometry results for the muscle homogenate and microsomal vesicle immunoblots were grouped firstly into the <60yr and ≥60yr age groups and then each age group was separated into male and female donors (see **Table 5.2** and **5.3**). As there was only one male gluteus medius donor, only the female gluteus medius donors are considered.

The muscle homogenates from female gluteus medius showed a significantly greater ($P \leq 0.05$) expression level of RyR1, α_{1s} and FKBP12 in the ≥60yr age group. No difference was seen in β_{1a} expression levels between the age groups (**Figure 5.8A**). In female gluteus minimus muscle homogenate a significantly greater level ($P \leq 0.05$) of FKBP12 was observed in the ≥60yr age group with no significant difference in the expression levels of RyR1, α_{1s} and β_{1a} (**Figure 5.8B**). However, in the male gluteus minimus muscle homogenate, there was a significantly lower expression ($P \leq 0.05$) of RyR1 in the ≥60yr age group with no difference in the α_{1s}, β_{1a} and FKBP12 expression levels (**Figure 5.8D**). The female vastus medialis muscle homogenates a significantly greater expression level ($P \leq 0.05$) of β_{1a} was observed in the ≥60yr age group whereas there was no difference in the RyR1, α_{1s} and FKBP12 expression levels (**Figure 5.8C**). No significant difference in any of the proteins' expression levels were observed in male vastus medialis muscle homogenate (**Figure 5.8E**).

The data obtained from female gluteus medius microsomal vesicles showed a significantly lower ($P \leq 0.05$) FKBP12/RyR1 ratio in the ≥60yr age group. No difference was observed in the α_{1s}/RyR1 and α_{1c}/RyR1 expression ratios (**Figure 5.9A**). Female gluteus minimus microsomal vesicles showed similar results with only the FKBP12/RyR1 being significantly lower ($P \leq 0.05$) in the ≥60yr age group (**Figure 5.9B**). The male gluteus minimus microsomal vesicles showed no difference in any of the ratios investigated (**Figure 5.9D**). The female vastus medialis microsomal vesicles also showed a significantly lower ($P \leq 0.05$) FKBP12/RyR1 ratio with no difference in the α_{1s}/RyR1 and α_{1c}/RyR1 ratios (**Figure 5.9C**). The male vastus medialis microsomal vesicles, however, showed a significantly higher α_{1c}/RyR1 ratio ($P \leq 0.05$) with no difference in α_{1s}/RyR1 or FKBP12/RyR1 ratios (**Figure 5.9E**).

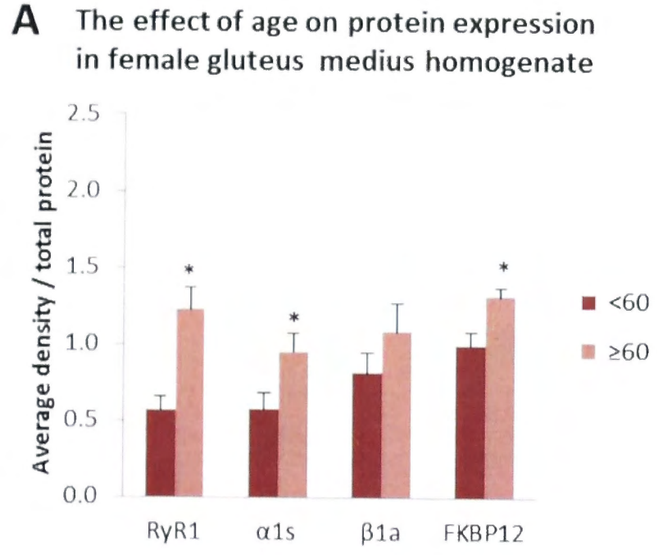

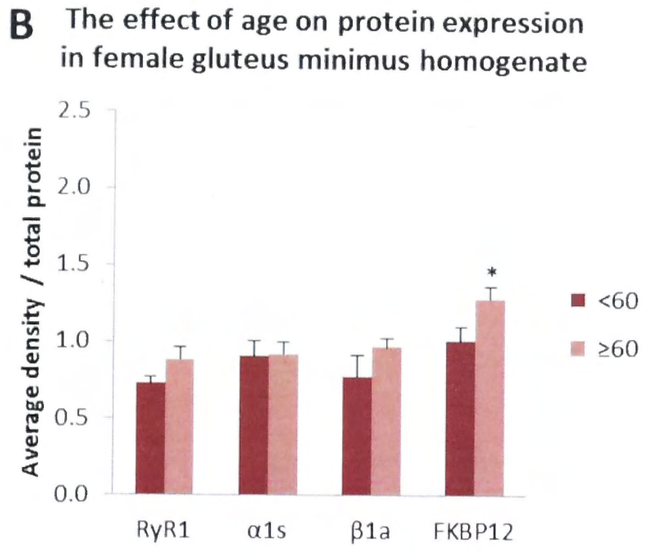

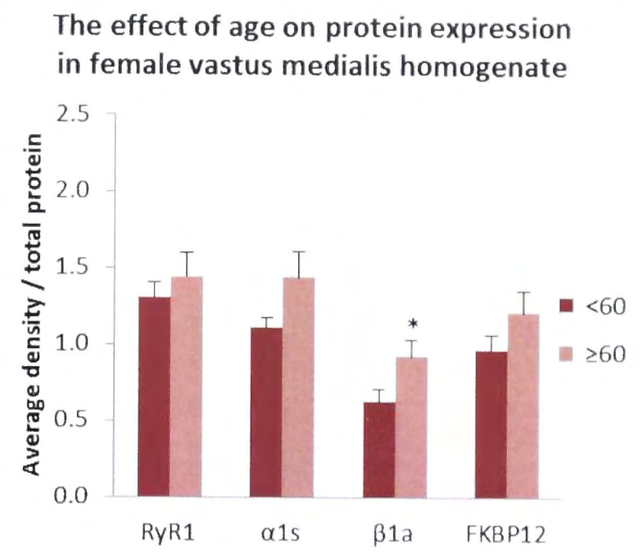

* Significantly different from <60 (P≤0.05)

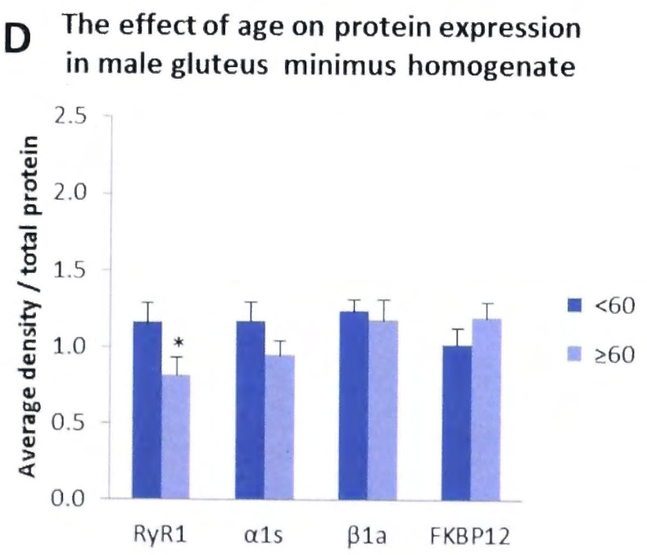

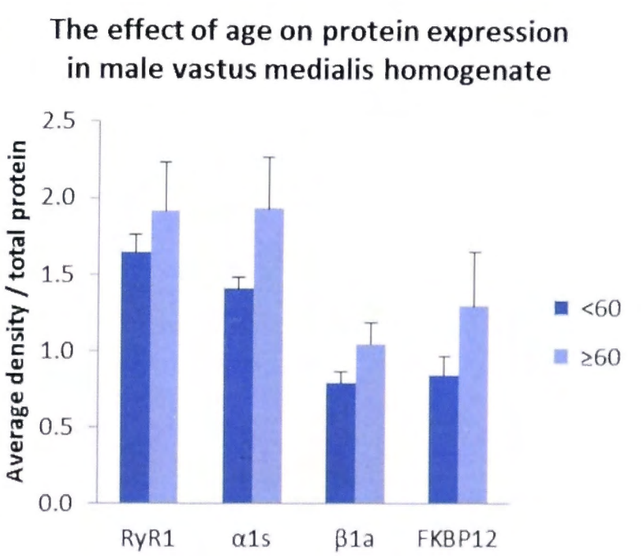

Figure 5.8: A comparison of expression levels of RyR1, DHPR α_{1s}, DHPR β_{1a} and FKBP12 in muscle homogenate of male and female human donors <60yr and ≥60yr. (**A**) The protein expression levels in muscle homogenate from female gluteus medius. (**B**) The protein expression levels in female gluteus minimus muscle homogenate. (**C**) The protein expression levels in female vastus medialis muscle homogenate. (**D**) The protein expression levels in male gluteus minimus muscle homogenate. (**E**) The protein expression levels in male vastus medialis muscle homogenate.

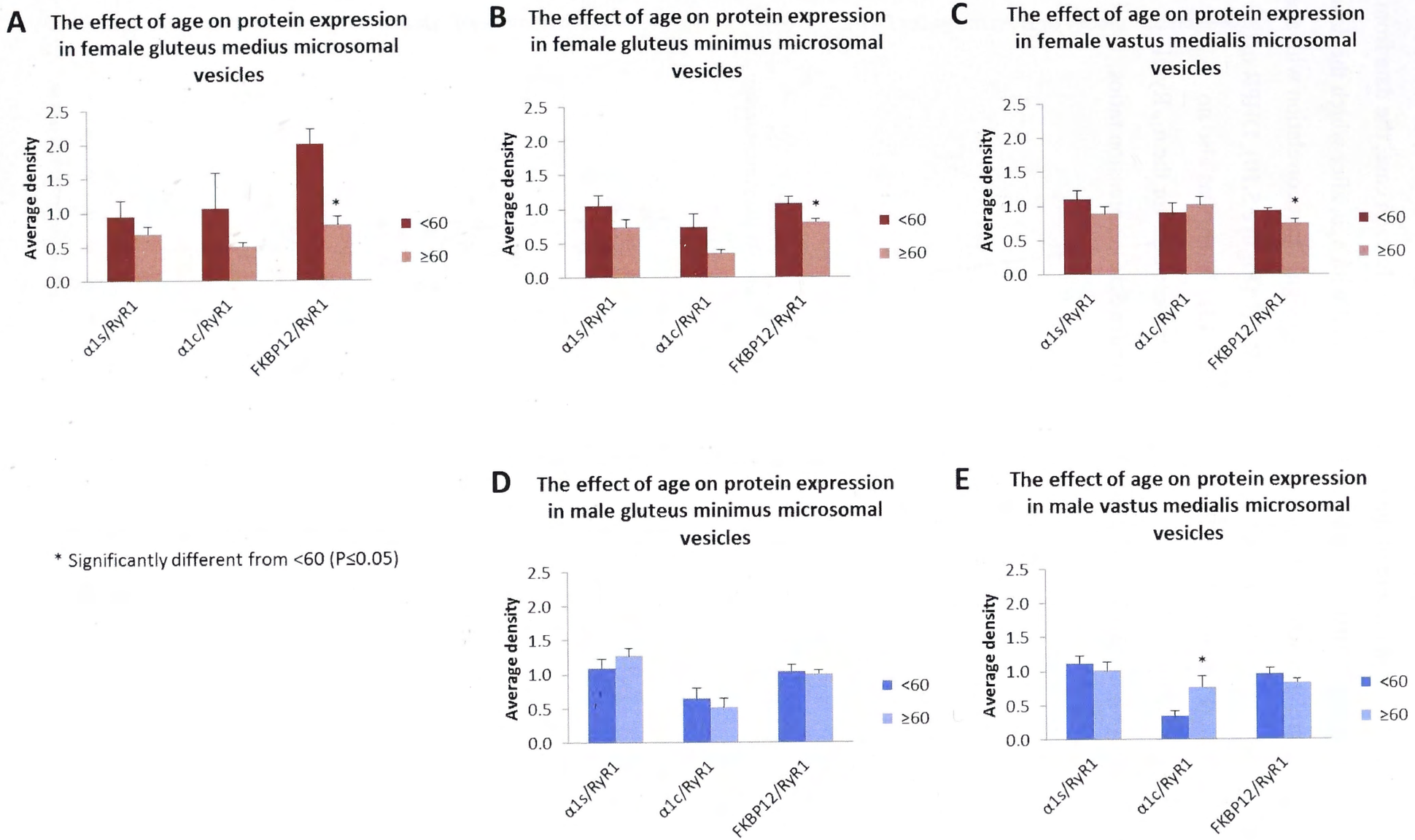

Figure 5.9: A comparison of DHPR α_{1s} / RyR1, DHPR α_{1c} / RyR1 and FKBP12 / RyR1 expression ratios in microsomal vesicles prepared from muscle of male and female human donors <60yr and ≥60yr. (**A**) The protein expression ratios in female gluteus medius microsomal vesicles. (**B**) The protein expression ratios in female gluteus minimus microsomal vesicles. (**C**) The protein expression ratios in female vastus medialis microsomal vesicles. (**D**) The protein expression ratios in male gluteus minimus microsomal vesicles. (**E**) The protein expression ratios in male vastus medialis microsomal vesicles.

5.4.1.2.2 Correlations

To further investigate the effect of age on the expression levels of RyR1, α_{1s}, β_{1a}, FKBP12 as well as the expression ratios of α_{1s}/RyR1, α_{1c}/RyR1 and FKBP12/RyR1, the average density for each protein was plotted against the age of their respective donors. In each case, the data from the three different muscles was first combined and the correlated with age, after which the data for each muscle was correlated separately with age as well. No significant correlation with age was found either in the combined data or separated data for RyR1 (**Figure 5.10**), DHPR α_{1s} (**Figure 5.11**), DHPR β_{1a} (**Figure 5.12**) of FKBP12 (**Figure 5.13**). There was also no significant correlation with age in the combined or separated muscle data for the α_{1s}/RyR1 (**Figure 5.14**), α_{1c}/RyR (**Figure 5.15**) or FKBP12/RyR1 (**Figure 5.16**) expression ratios.

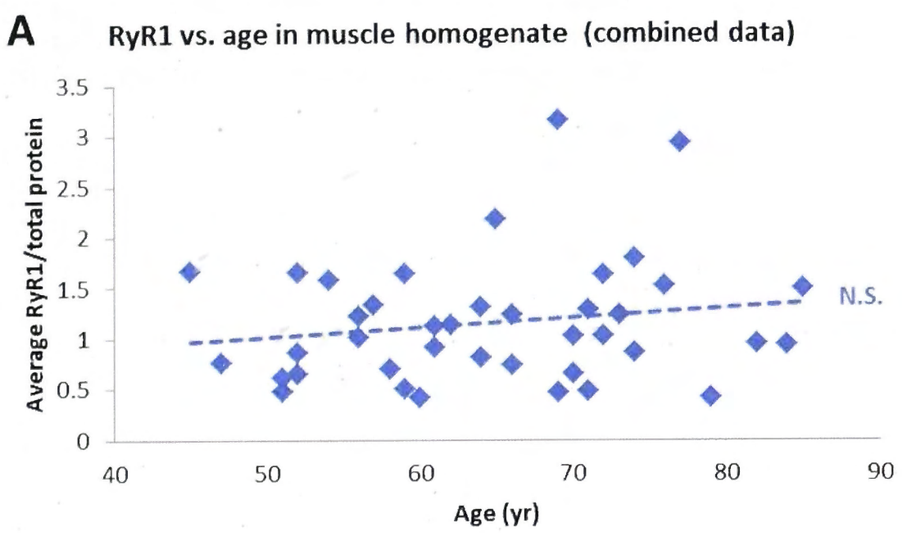

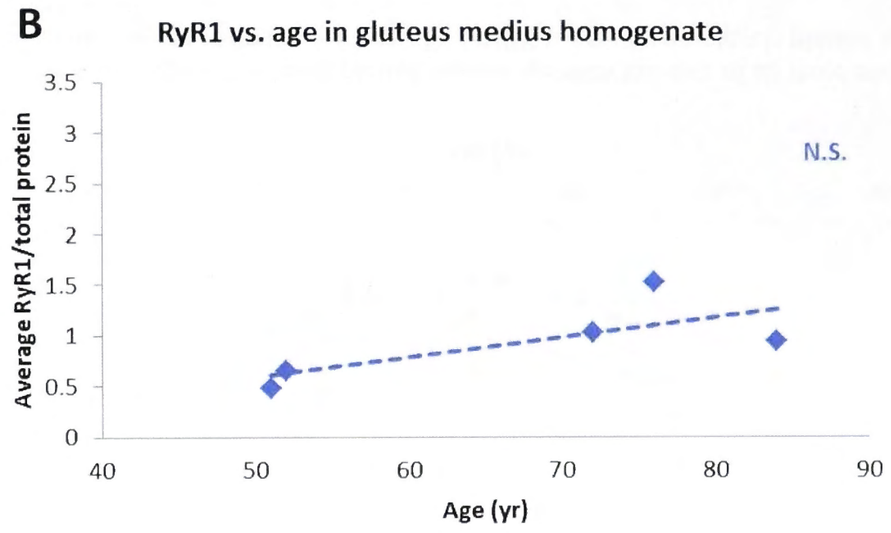

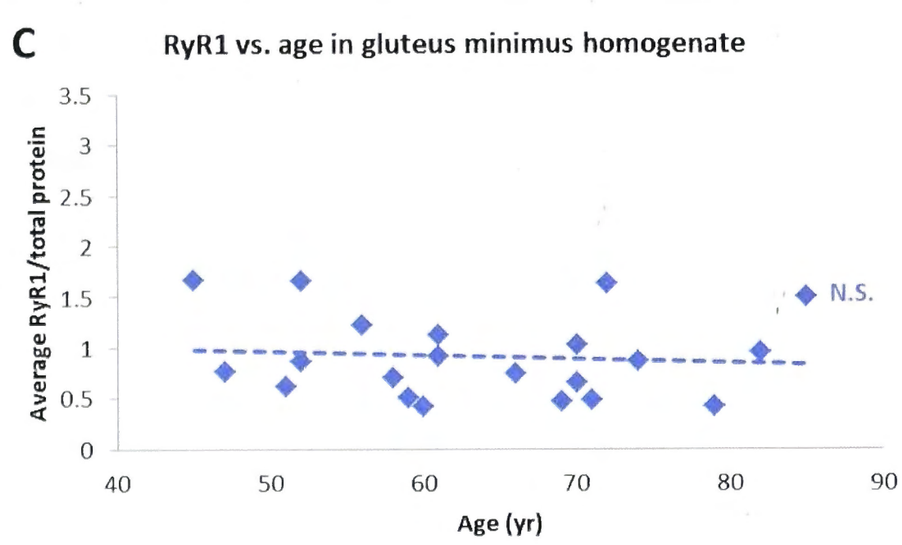

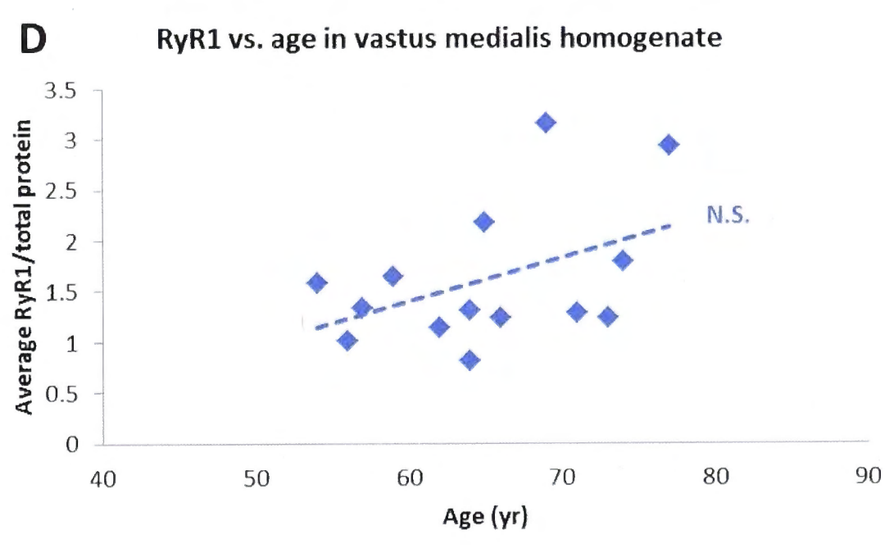

Figure 5.10: The correlation between RyR1 expression levels and the age of the human donors. (**A**) RyR1 expression levels plotted against age with the data of all three muscles combined. (**B**) RyR1 expression levels plotted against age in gluteus medius. (**C**) RyR1 expression levels plotted against age in gluteus minimus. (**D**) RyR1 expression levels plotted against age in vastus medialis (Dashed line indicates no significant correlation and is also indicated by N.S, R – correlation coefficient).

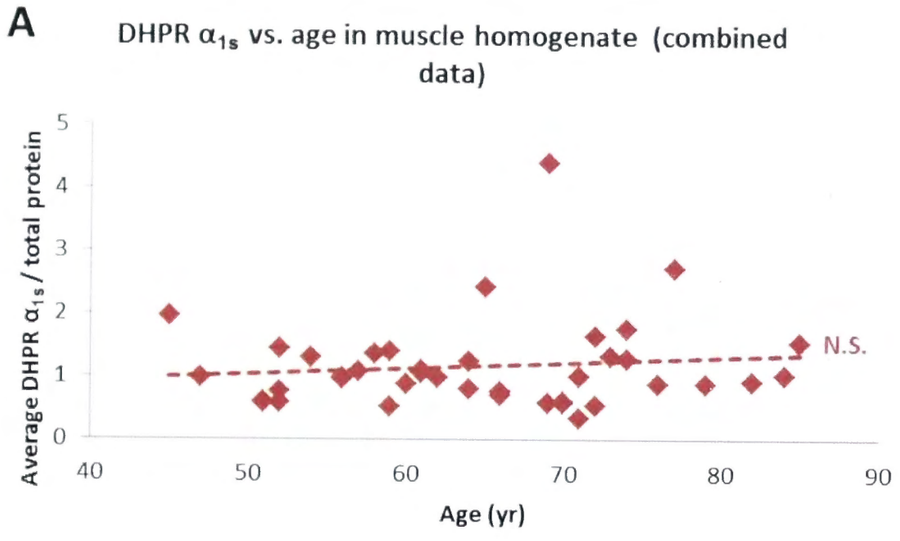

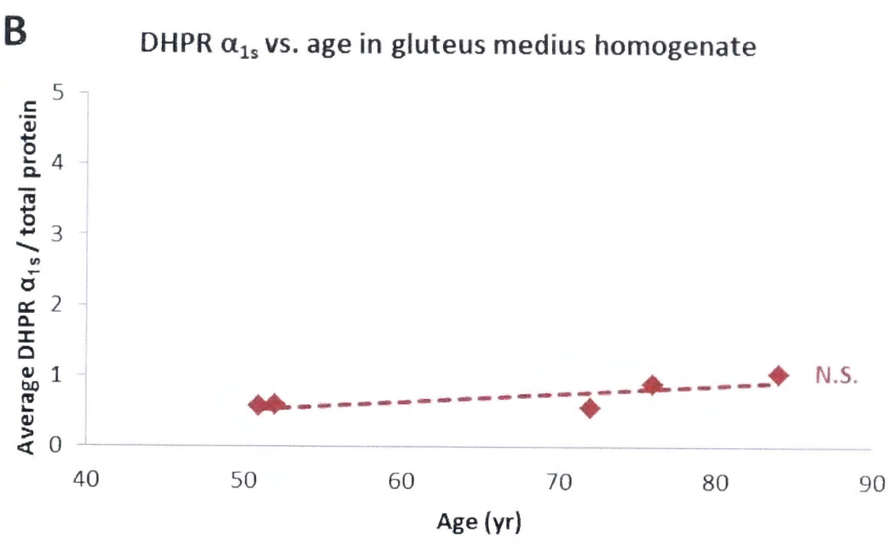

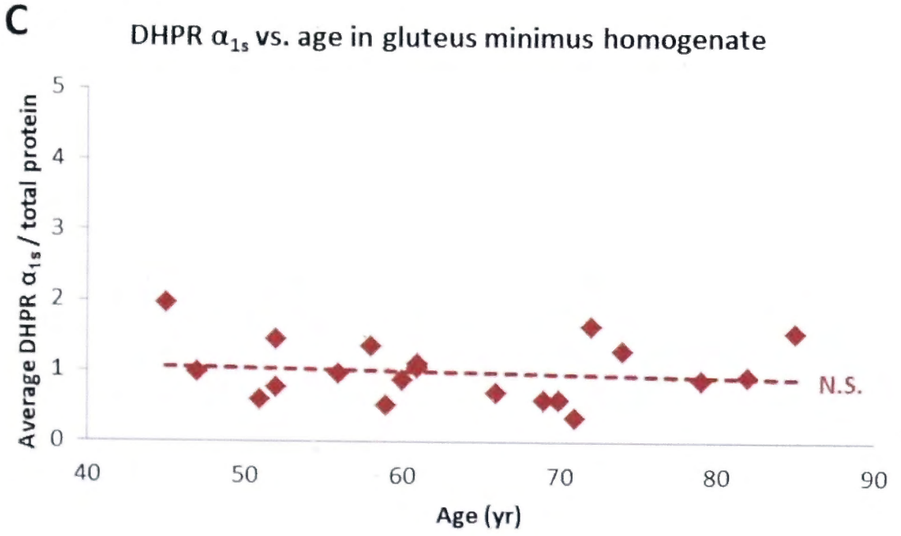

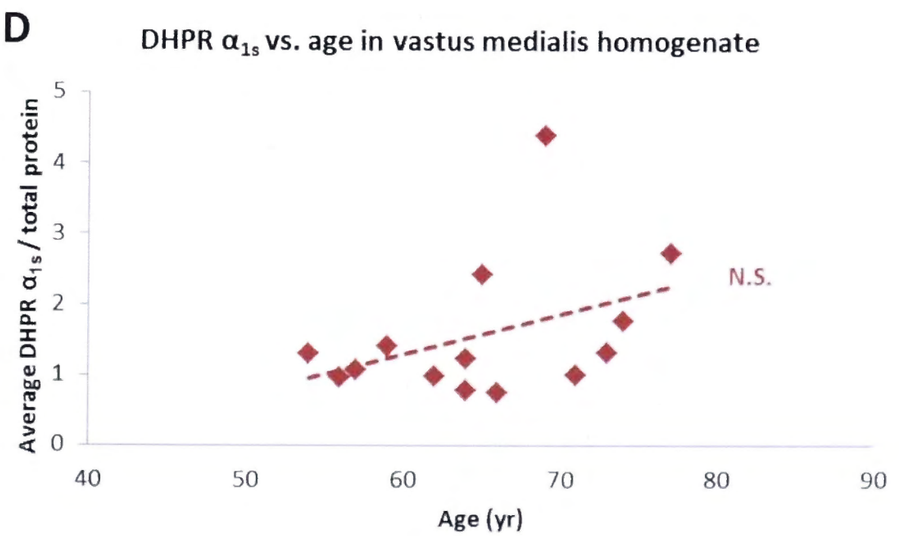

Figure 5.11: The correlation between DHPR α_{1s} expression levels and the age of the human donors. (**A**) DHPR α_{1s} expression levels plotted against age with the data of all three muscles combined. (**B**) DHPR α_{1s} expression levels plotted against age in gluteus medius. (**C**) DHPR α_{1s} expression levels plotted against age in gluteus minimus. (**D**) DHPR α_{1s} expression levels plotted against age in vastus medialis (A dashed line indicates no significant correlation and is also indicated by N.S. R – correlation coefficient).

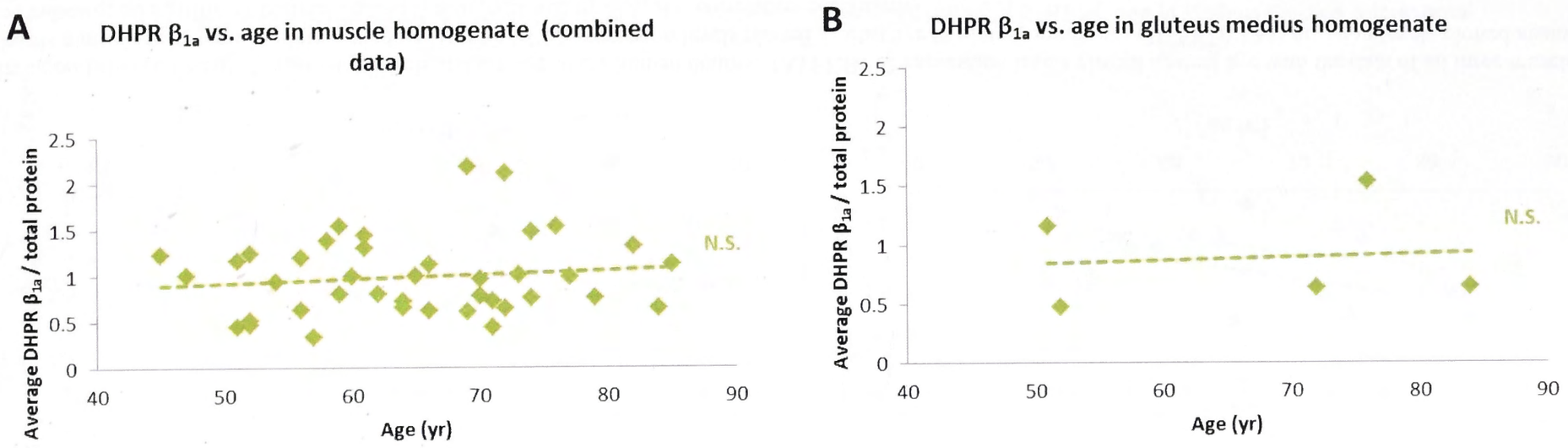

Figure 5.12: The correlation between DHPR β_{1a} expression levels and the age of the human donors. (**A**) DHPR β_{1a} expression levels plotted against age with the data of all three muscles combined. (**B**) DHPR β_{1a} expression levels plotted against age in gluteus medius. (**C**) DHPR β_{1a} expression levels plotted against age in gluteus minimus. (**D**) DHPR β_{1a} expression levels plotted against age in vastus medialis. (Dashed line indicates no significant correlation and is also indicated by N.S, R – correlation coefficient).

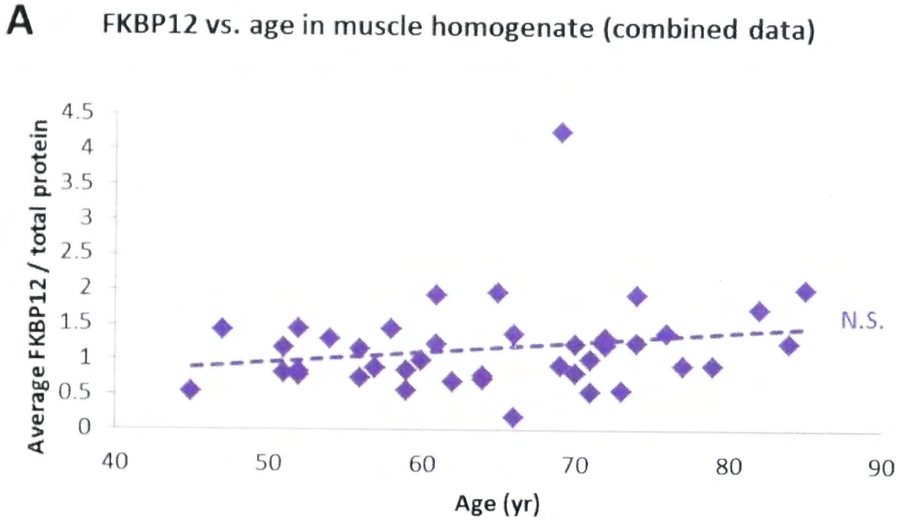

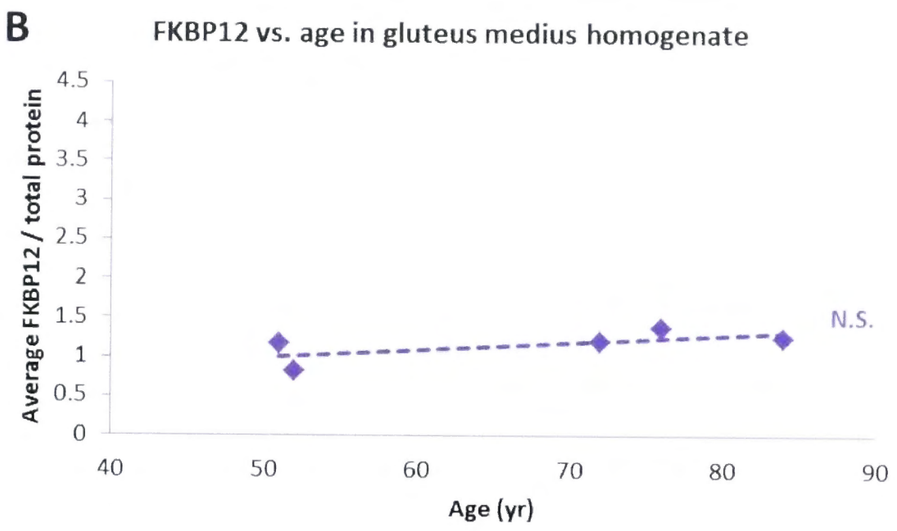

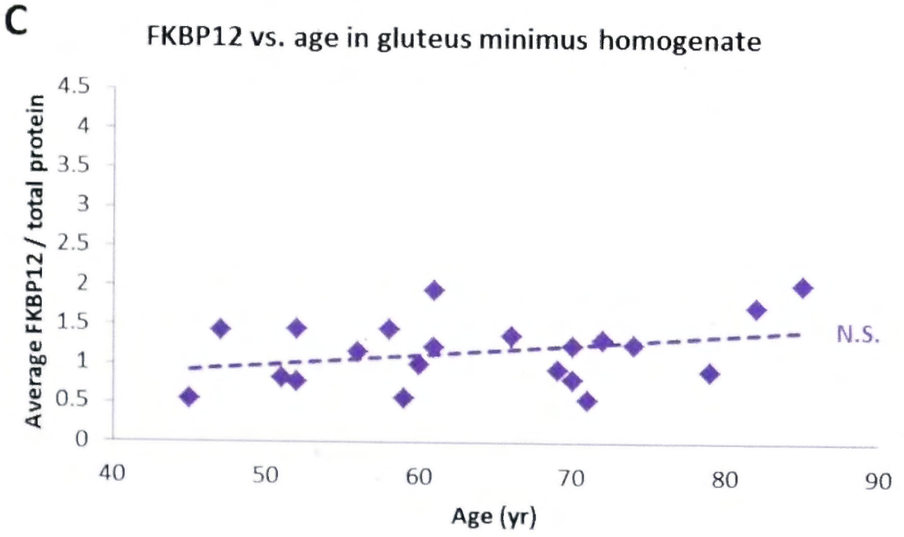

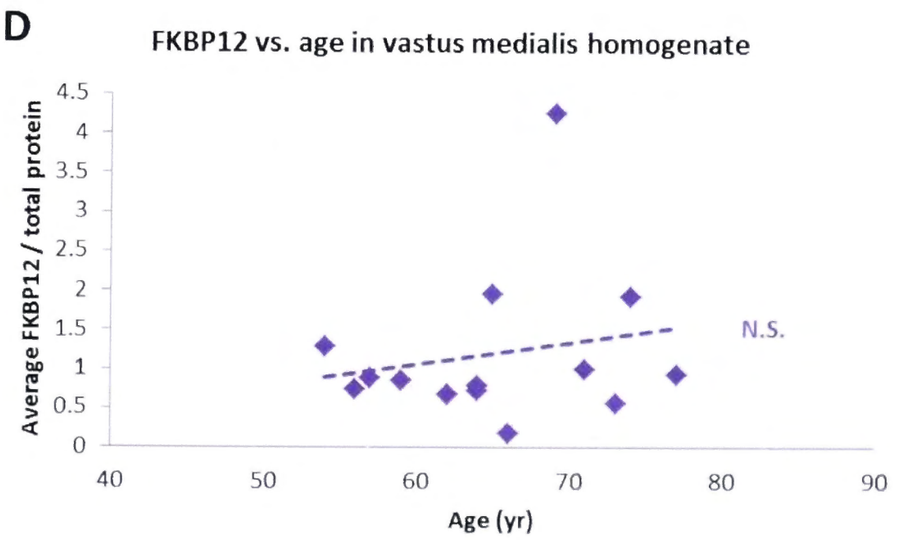

Figure 5.13: The correlation between FKBP12 expression levels and the age of the human donors. (**A**) FKBP12 expression levels plotted against age with the data of all three muscles combined. (**B**) FKBP12 expression levels plotted against age in gluteus medius. (**C**) FKBP12 expression levels plotted against age in gluteus minimus. (**D**) FKBP12 expression levels plotted against age in vastus medialis. (Dashed line indicates no significant correlation and is also indicated by N.S, R – correlation coefficient).

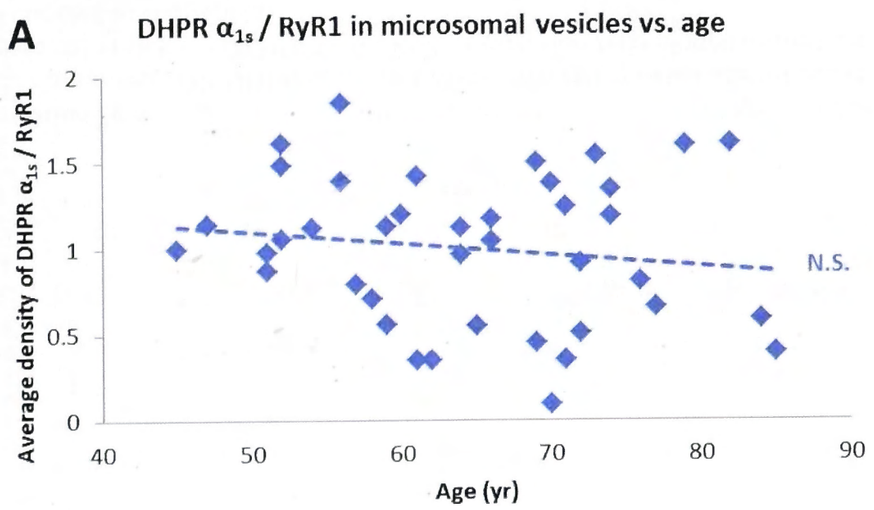

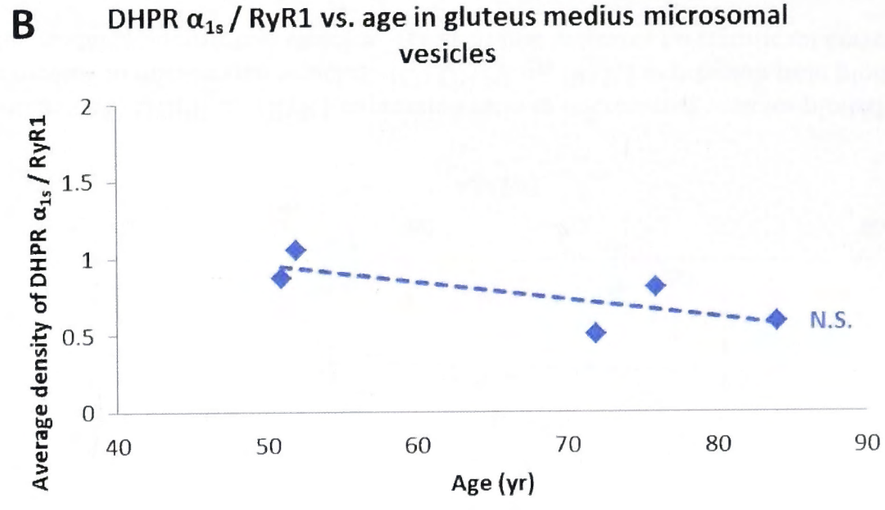

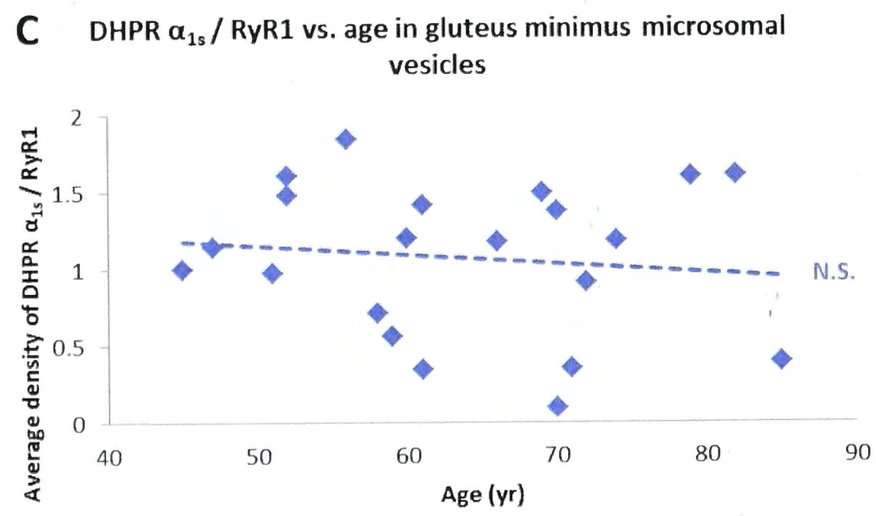

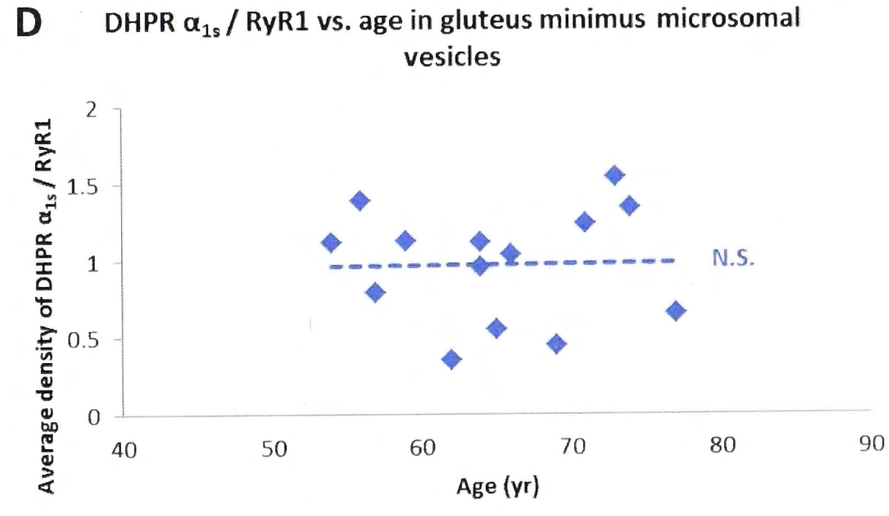

Figure 5.14: The correlation between the DHPR α_{1s} /RyR1 expression ratio and the age of the human donors. (**A**) DHPR α_{1s} /RyR1 expression ratio in microsomal vesicles plotted against age with the data of all three muscles combined. (**B**) DHPR α_{1s} /RyR1 expression ratio plotted against age in gluteus medius microsomal vesicles. (**C**) DHPR α_{1s} /RyR1 expression ratio plotted against age in gluteus minimus microsomal vesicles. (**D**) DHPR α_{1s} /RyR1 expression ratio and plotted against age in vastus medialis microsomal vesicles. (Dashed line indicates no significant correlation and is also indicated by N.S, R – correlation coefficient).

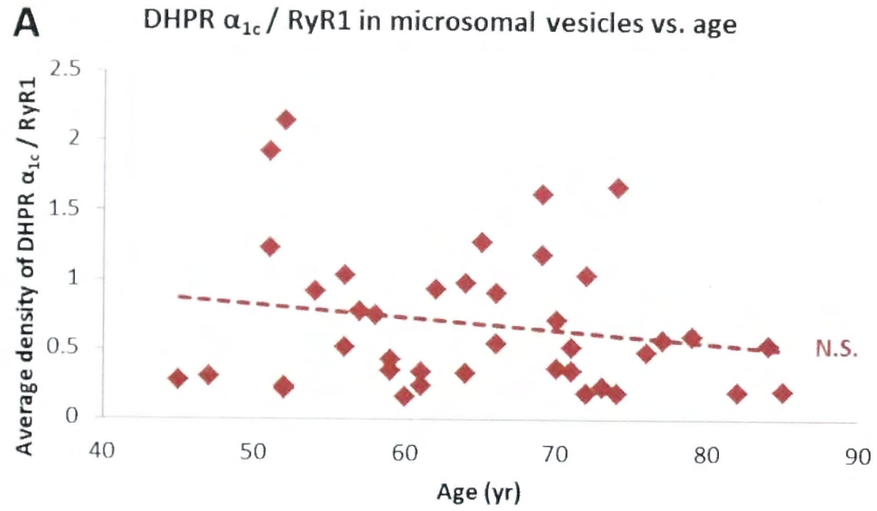

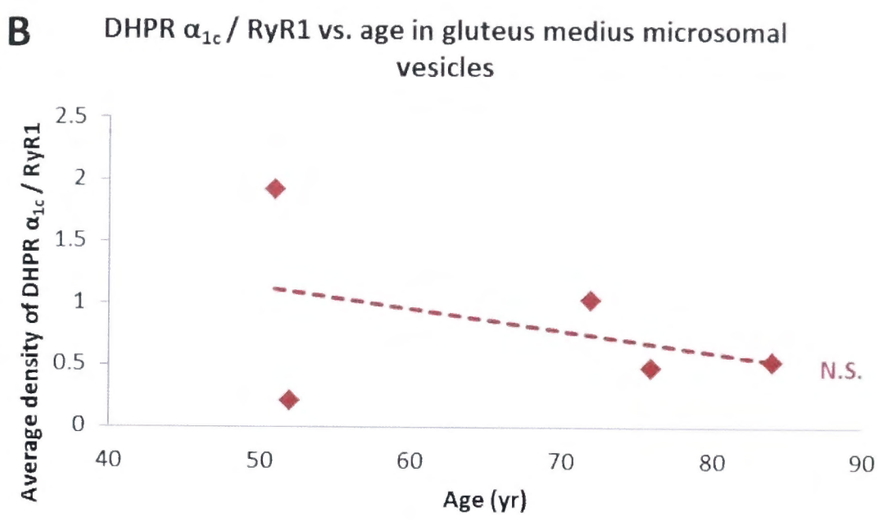

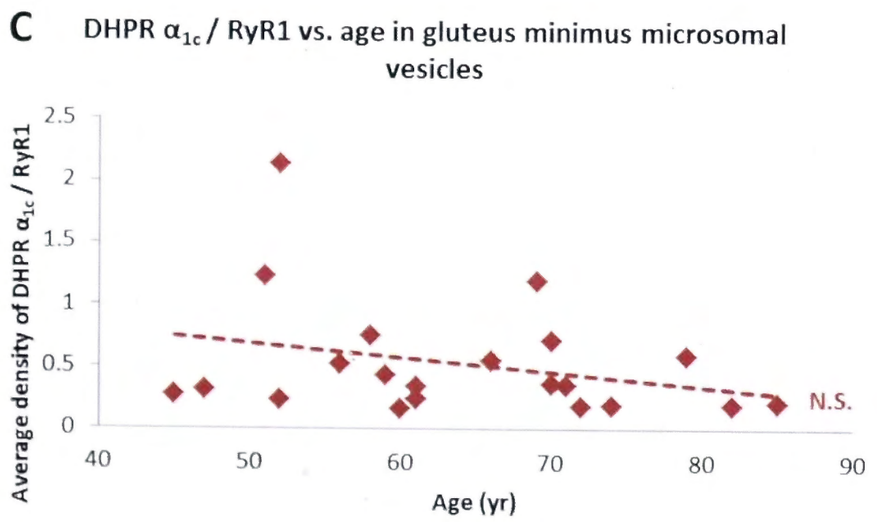

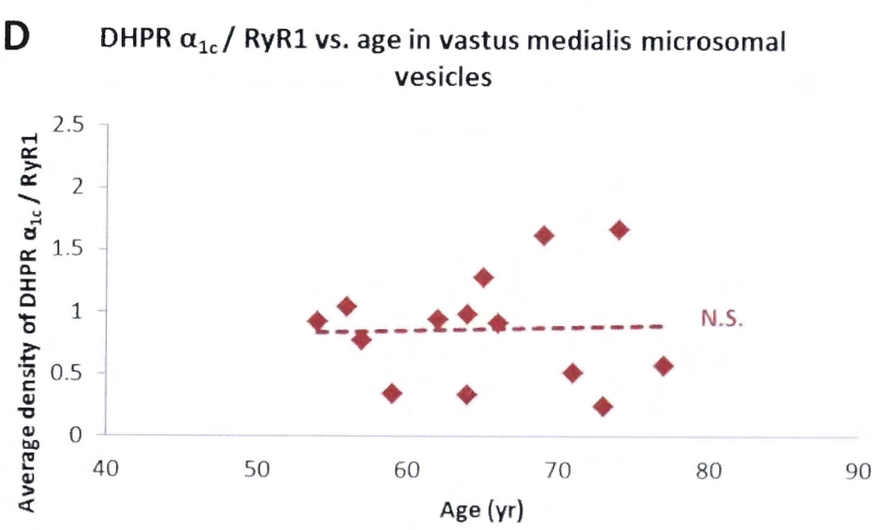

Figure 5.15: The correlation between the DHPR α_{1c} /RyR1 expression ratio and the age of the human donors. (**A**) DHPR α_{1c} /RyR1 expression ratio in microsomal vesicles plotted against age with the data of all three muscles combined. (**B**) DHPR α_{1c} /RyR1 expression ratio plotted against age in gluteus medius in microsomal vesicles. (**C**) DHPR α_{1c} /RyR1 expression ratio plotted against age in gluteus minimus microsomal vesicles. (**D**) DHPR α_{1c} /RyR1 expression ratio plotted against age in vastus medialis microsomal vesicles. (Dashed line indicates no significant correlation and is also indicated by N.S, R – correlation coefficient).

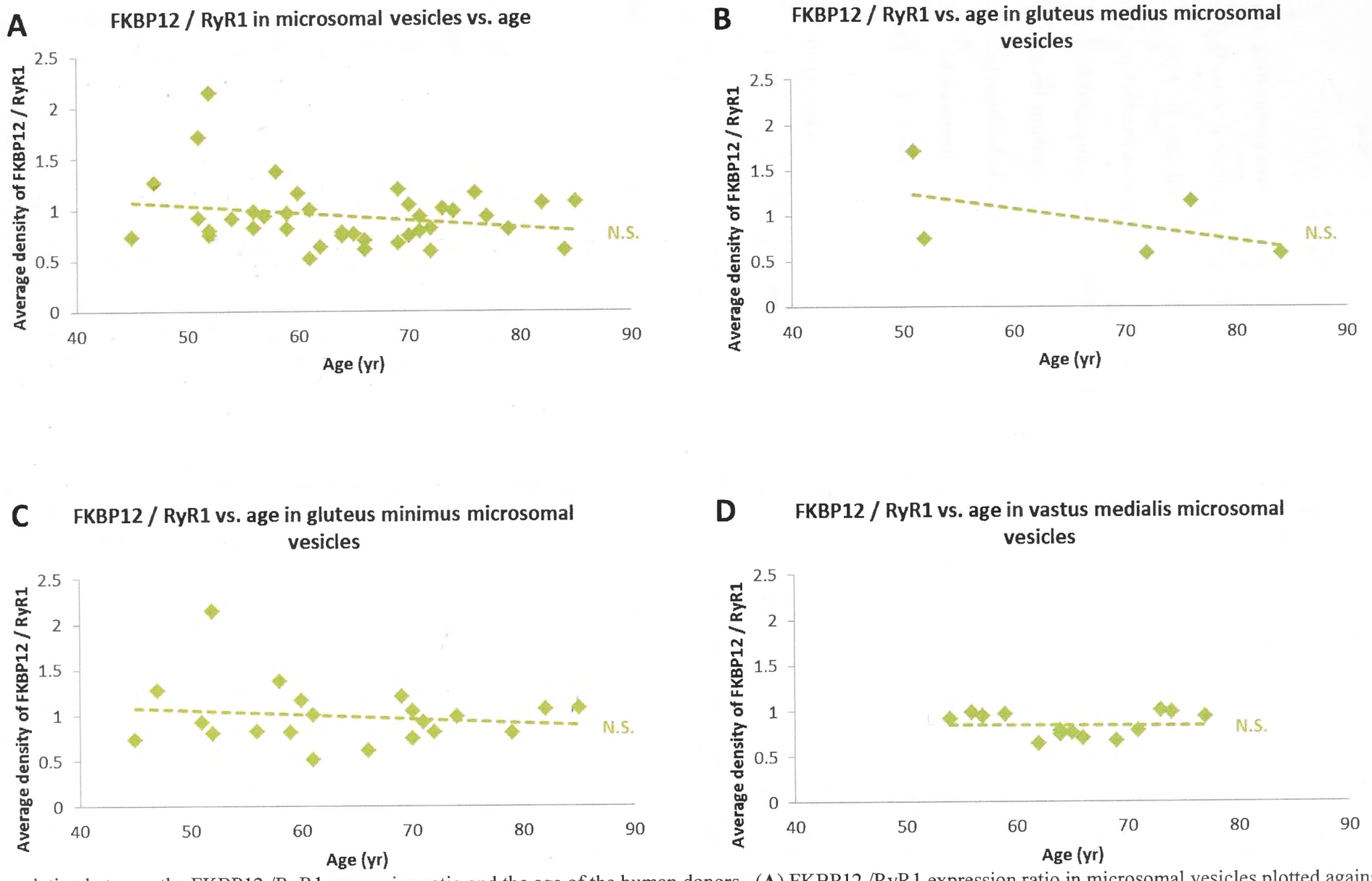

Figure 5.16: The correlation between the FKBP12 /RyR1 expression ratio and the age of the human donors. (**A**) FKBP12 /RyR1 expression ratio in microsomal vesicles plotted against age with the data of all three muscles combined. (**B**) FKBP12 /RyR1 expression ratio plotted against age in gluteus medius in microsomal vesicles. (**C**) FKBP12 /RyR1 expression ratio plotted against age in gluteus minimus microsomal vesicles. (**D**) FKBP12 /RyR1 expression ratio plotted against age in vastus medialis microsomal vesicles. (Dashed line indicates no significant correlation and is also indicated by N.S, R – correlation coefficient).

5.4.1.3 The effect of gender on protein expression levels

In order to investigate whether the donor's gender influenced the protein expression levels and ratios of the proteins under investigation, the donors were grouped into male and female bins and the mean density (**Tables 5.2 and 5.3**) for each protein compared.

When the data obtained from the muscle homogenates of all three muscles were combined, there was a significantly greater expression ($P \leq 0.05$) of RyR1, α_{1s} and β_{1a} in male donors than in female donors with no difference in FKBP12 expression (**Figure 5.17A**). The data from each muscle was then compared separately. In the muscle homogenates from gluteus medius muscle, there was a significantly lower expression of β_{1a} ($P \leq 0.05$) in the male donors compared to the female. There was, however, no difference in the RyR1, α_{1a} and FKBP12 expression levels between male and female donors (**Figure 5.17B**). The gluteus minimus muscle homogenate showed a significantly higher expression level of β_{1a} ($P \leq 0.05$) in male donors compared to female, again with no difference in RyR1, α_{1a} or FKBP12 expression levels between the genders (**Figure 5.17C**). The muscle homogenate from vastus medialis showed no significant difference between male and female donors in any of the protein expression levels investigated (**Figure 5.17D**).

In the combined muscle data from the microsomal vesicles there was a significantly larger α_{1a}/RyR1 expression ratio ($P \leq 0.05$) in male donors than female donors with no difference in the α1c/RyR1 or FKBP12/RyR1 ratios (**Figure 5.18A**). When the data for each muscle was compared separately, the microsomal vesicles from gluteus medius muscle showed a significantly smaller FKBP12/RyR1 ratio ($P \leq 0.05$) in male donors compared to female donors. No difference was observed in the α_{1s}/RyR1 or α_{1c}/RyR1 ratios (**Figure 5.18B**). The gluteus minimus microsomal vesicles showed a significantly greater α_{1s}/RyR1 ratio in male donors ($P \leq 0.05$) but no difference in the α_{1c}/RyR1 or FKBP12/RyR1 ratios (**Figure 5.18C**). And finally, the microsomal vesicles of the vastus medialis donors showed a significantly lower α1c/RyR1 ratio in male donors with no difference in α_{1s}/RyR1 or FKBP12/RyR1 ratios (**Figure 5.18D**).

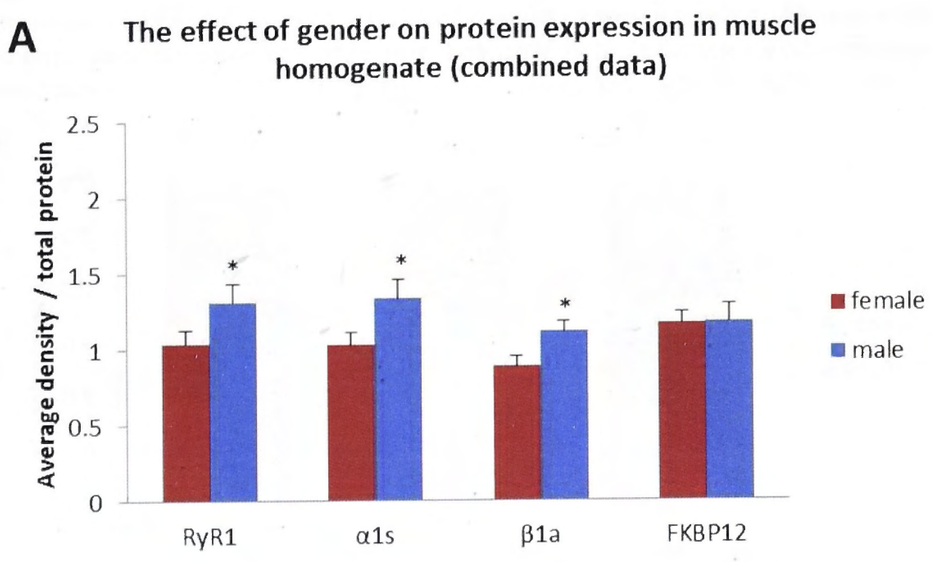

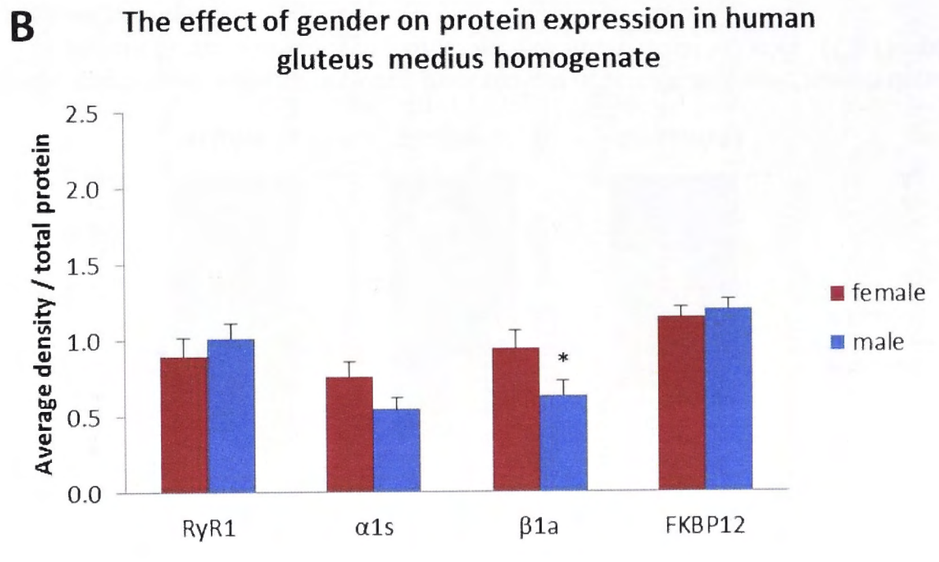

* Significantly different from female (P≤0.05)

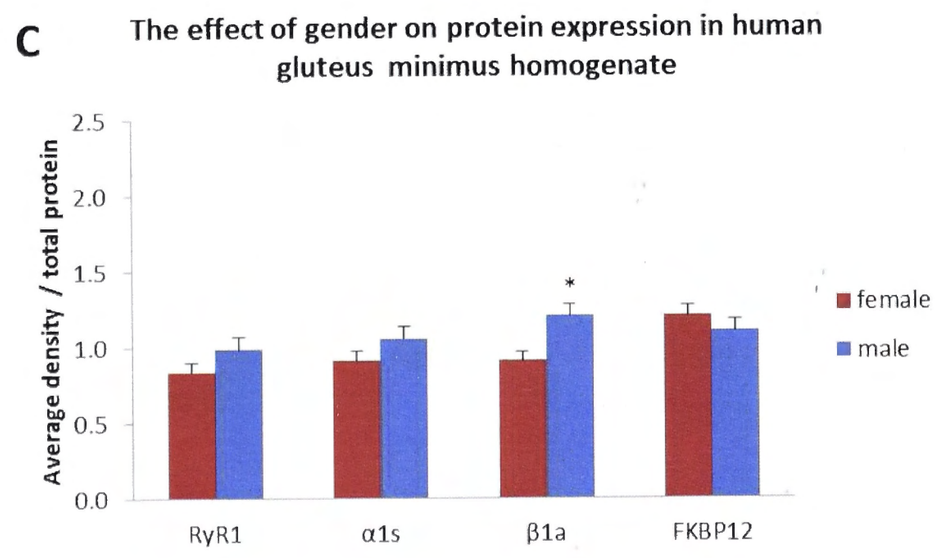

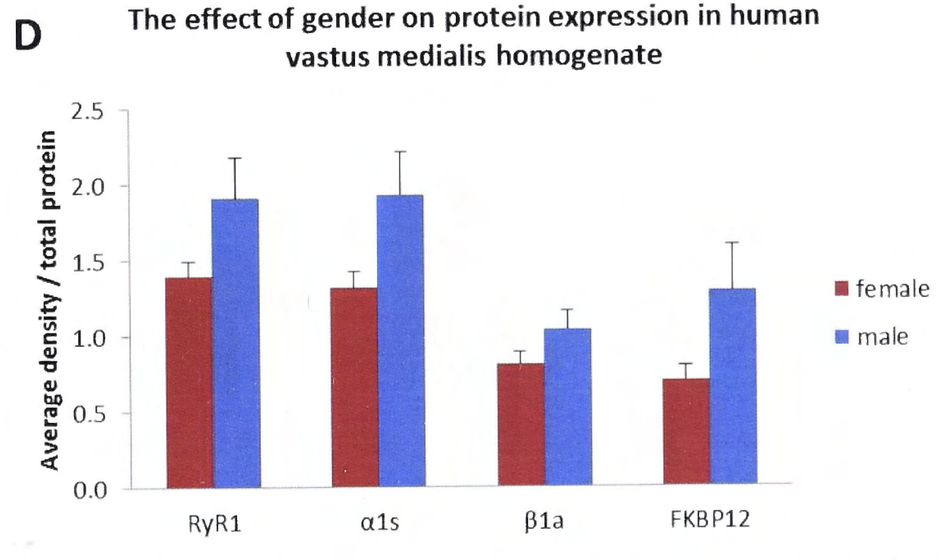

Figure 5.17: A comparison of expression levels of RyR1, DHPR α_{1s}, DHPR β_{1a} and FKBP12 in muscle homogenate of female and male human donors. (**A**) The protein expression levels in muscle homogenate where data from all three muscles were combined. (**B**) The protein expression levels in gluteus medius muscle homogenate. (**C**) The protein expression levels in gluteus minimus muscle homogenate. (**D**) The protein expression levels in vastus medialis muscle homogenate.

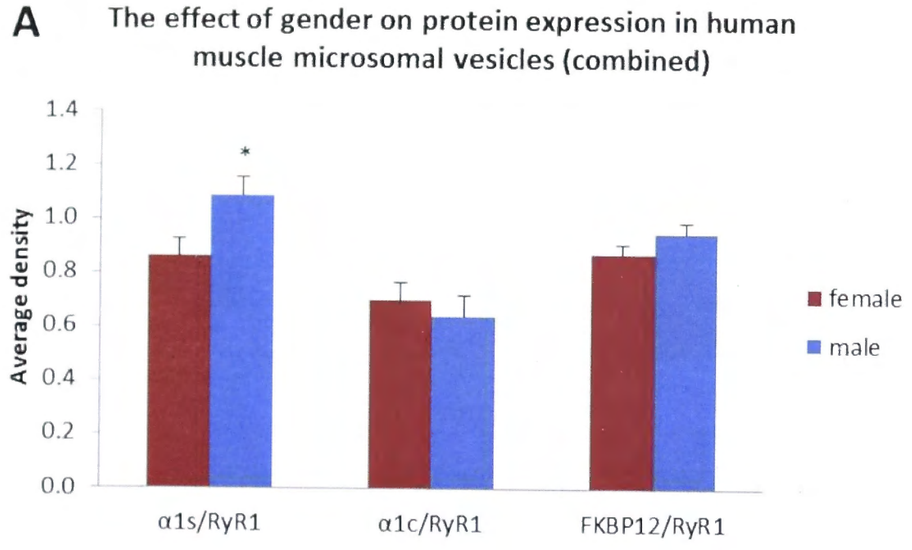

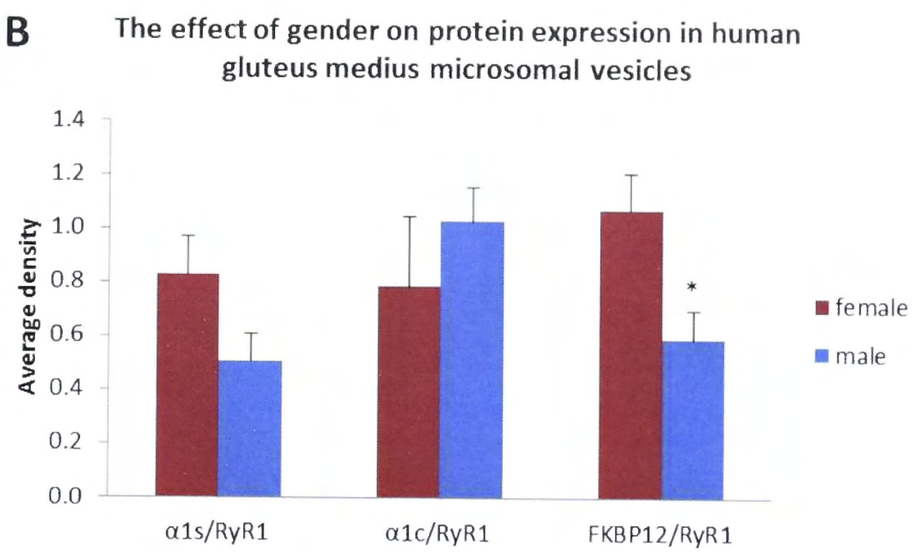

* Significantly different from female (P≤0.05)

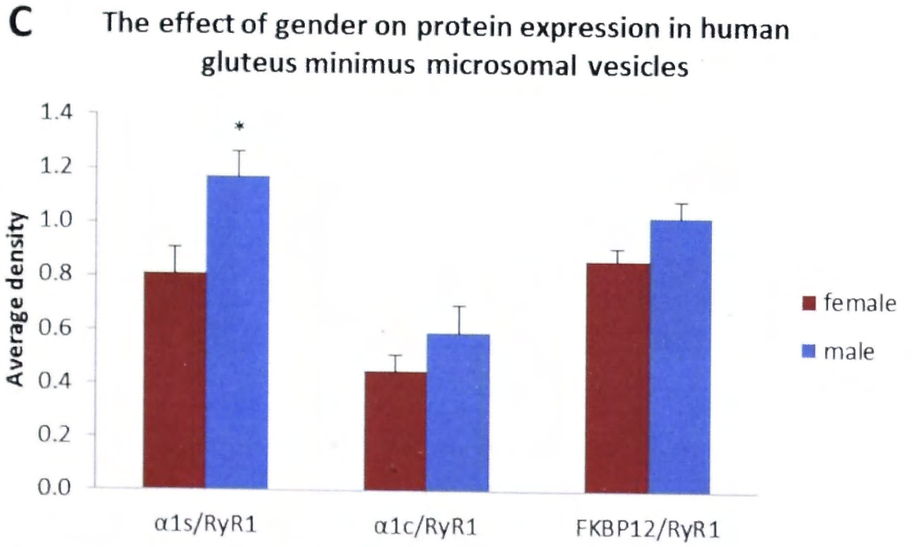

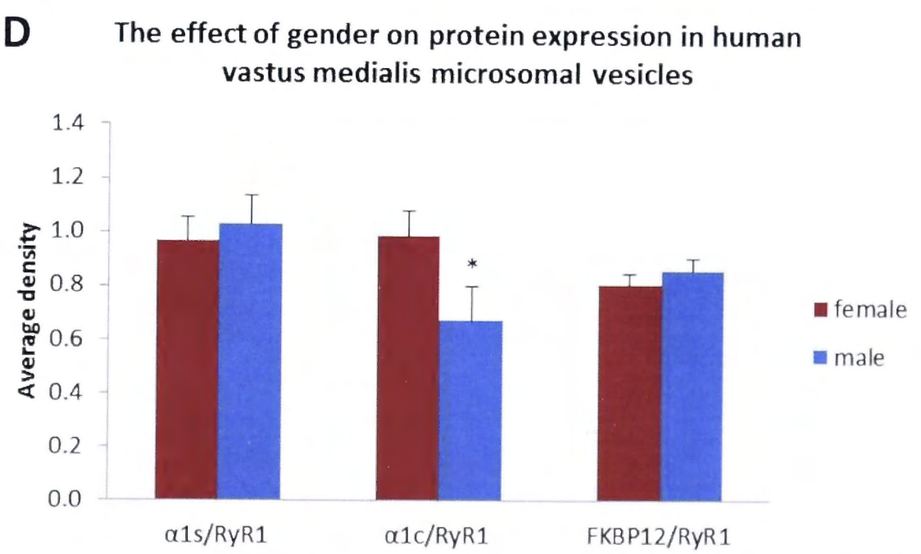

Figure 5.18: A comparison of DHPR α_{1s} / RyR1, DHPR α_{1c} / RyR1 and FKBP12 / RyR1 expression ratios in microsomal vesicles prepared from muscle of female and male human donors. (**A**) The protein expression ratios in microsomal vesicles where data from all three muscles were combined. (**B**) The protein expression ratios in gluteus medius microsomal vesicles. (**C**) The protein expression ratios in gluteus minimus microsomal vesicles. (**D**) The protein expression ratios in vastus medialis microsomal vesicles.

The data for each muscle was then further grouped according to the age of the donors into <60yr or ≥60yr old (**Tables 5.2 and 5.3**). As the single gluteus medius male donor was >60yr, only the ≥60yr donors were considered for this muscle. A significantly lower level of α_{1s} and β_{1a} expression was observed in the male donor compared to the female donors (P≤0.05). No difference was observed in RyR1 or FKBP12 expression levels (**Figure 5.19A**). The muscle homogenate from gluteus minimus donors <60yr showed a significantly greater RyR1 and β_{1a} expression level in male donors compared to female (P≤0.05) with no significant difference in α_{1s} or FKBP12 levels (**Figure 5.19B**). The ≥60yr gluteus minimus muscle homogenate showed no significant difference between male and female donors in any of the protein expression levels investigated (**Figure 5.19C**). The muscle homogenate from vastus medialis donors <60yr showed a significantly greater α_{1s} expression level (P≤0.05) in male donors with no difference in RyR1, β_{1a} or FKBP12 levels (**Figure 5.19D**). However, there was no significant difference in expression levels between ≥60yr female and male vastus medialis donors for any of the proteins investigated (**Figure 5.19E**).

When the microsomal immunoblot data from each muscle was similarly grouped into age groups to compare the expression ratios in male and female donors of each age group, the ≥60yr gluteus medius group showed a significantly larger α_{1c}/RyR1 ratio in the male donor compared to the female donors (P≤0.05) and no significant difference in the α_{1s}/RyR1 or FKBP12/RyR1 ratios (**Figure 5.20A**). The microsomal vesicles from <60yr gluteus minimus donors showed no difference between male and female donors in any of the expression ratios investigated (**Figure 5.20B**), however the ≥60yr group showed significantly larger α_{1s}/RyR1 and FKBP12/RyR1 ratios (P≤0.05) with no difference in the α_{1c}/RyR1 ratio (**Figure 5.20C**). Finally, a significantly smaller α_{1c}/RyR1 expression ratio was observed in male vastus medialis microsomal vesicles from <60yr donors (P≤0.05) with no difference in α_{1s}/RyR1 or FKBP12/RyR1 ratios (**Figure 5.20D**). There was also no difference in any of the expression ratios investigated in ≥60yr vastus medialis donors (**Figure 5.20E**).

Chapter 5

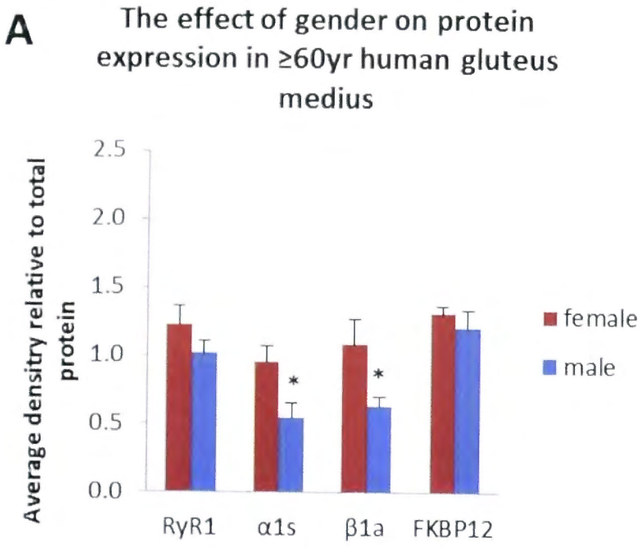

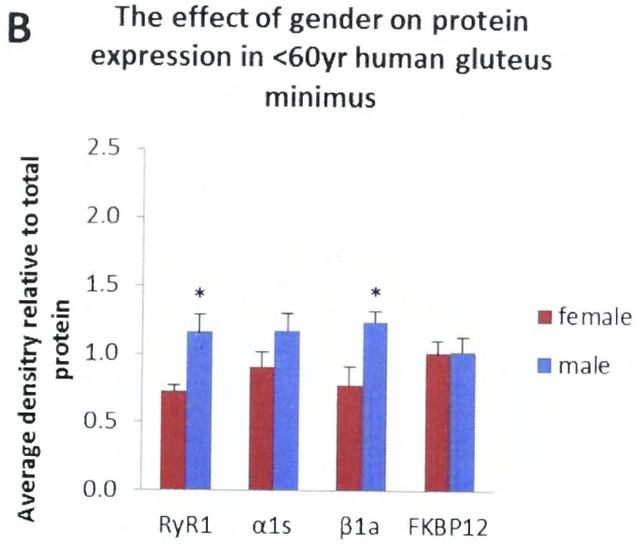

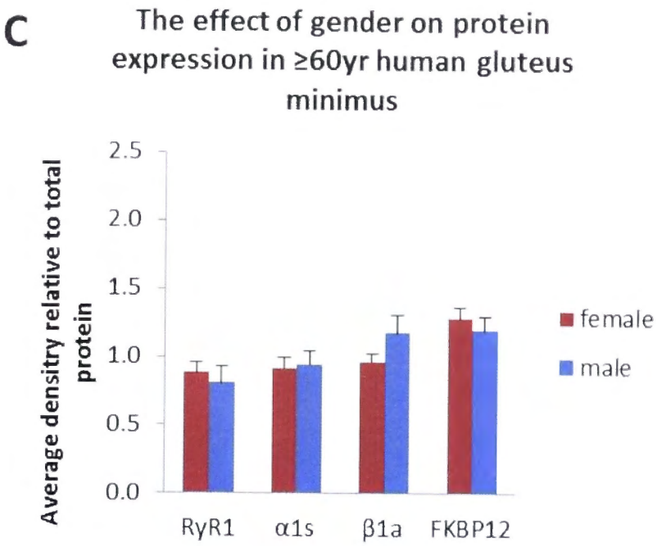

* Significantly different from female (P≤0.05)

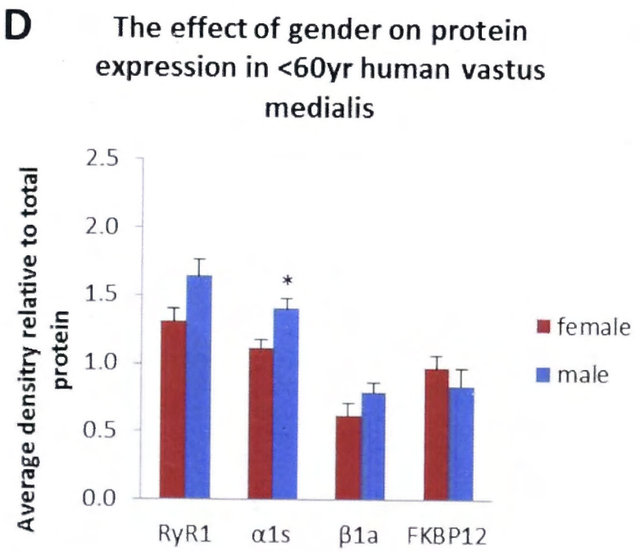

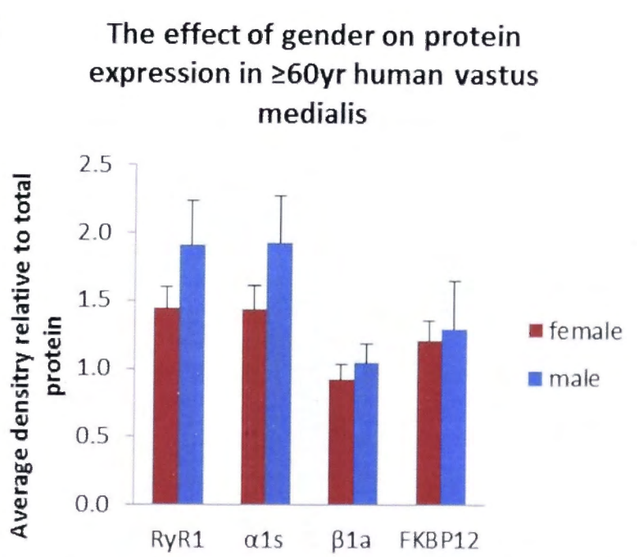

Figure 5.19: A comparison of expression levels of RyR1, DHPR α_{1s}, DHPR β_{1a} and FKBP12 in muscle homogenate of <60yr and ≥60yr male and female human donors. (**A**) The protein expression levels in muscle homogenate from ≥60yr gluteus medius. (**B**) The protein expression levels in <60yr gluteus minimus muscle homogenate. (**C**) The protein expression levels in ≥60yr gluteus minimus muscle homogenate. (**D**) The protein expression levels in <60yr vastus medialis muscle homogenate. (**E**) The protein expression levels in ≥60yr vastus medialis muscle homogenate.

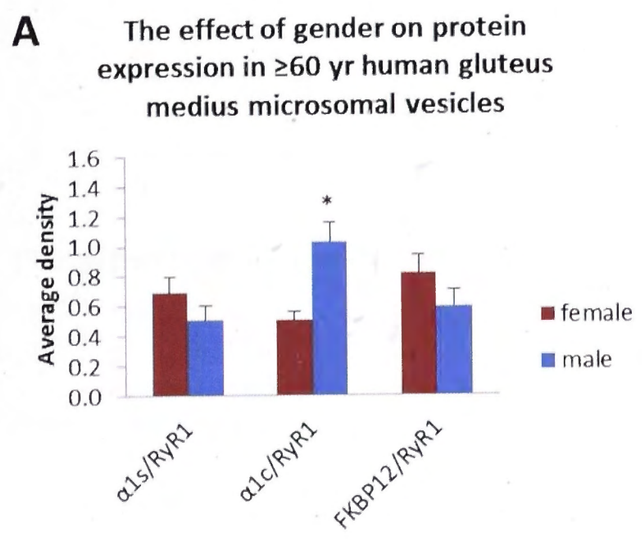

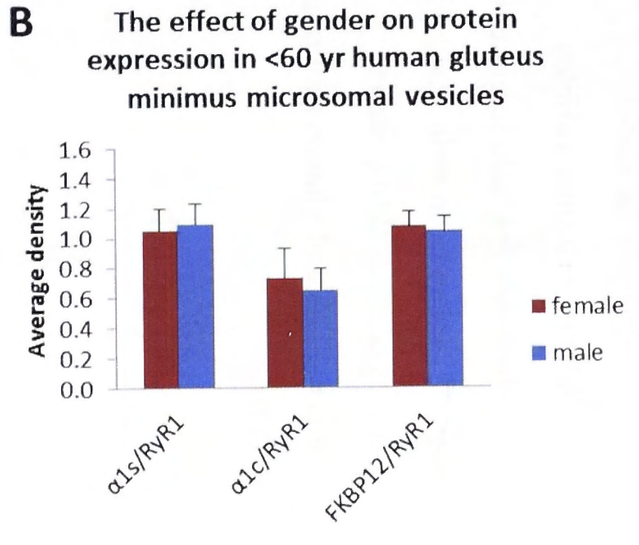

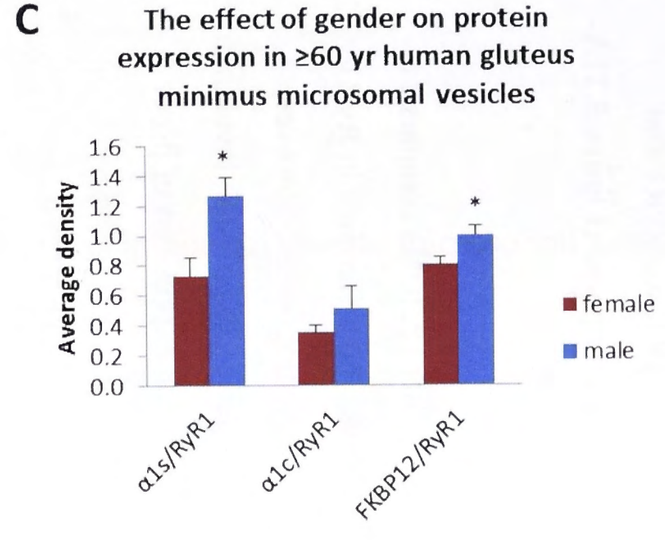

* Significantly different from female (P≤0.05)

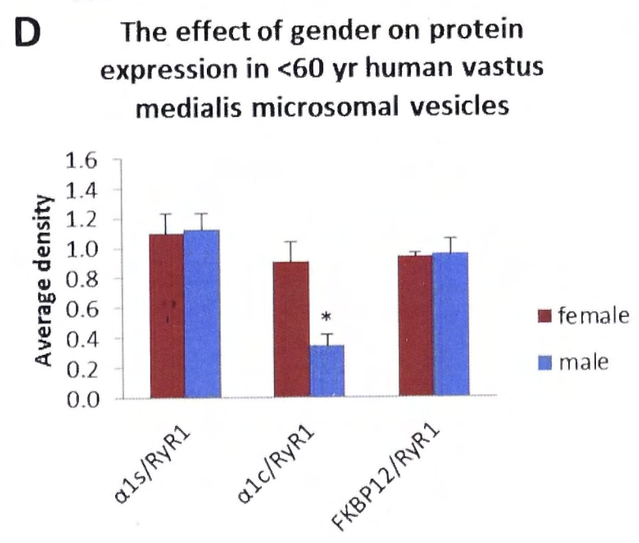

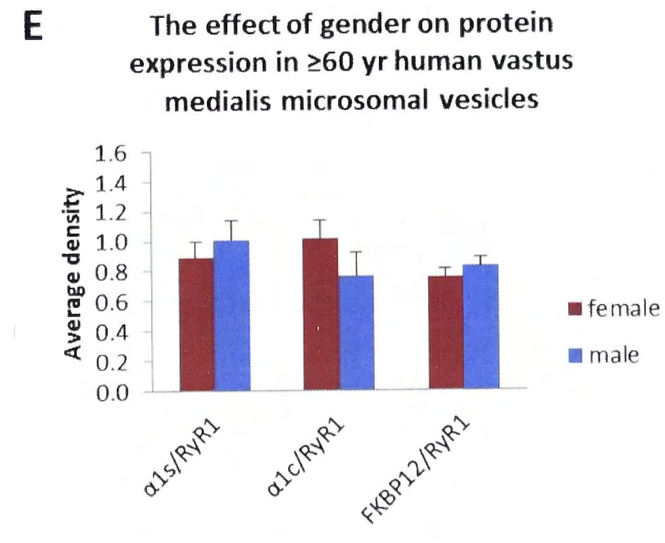

Figure 5.20: A comparison of DHPR α_{1s} / RyR1, DHPR α_{1c} / RyR1 and FKBP12 / RyR1 expression ratios in microsomal vesicles prepared from muscle of <60yr and ≥60yr male and female human donors. (**A**) The protein expression ratios in ≥60yr gluteus medius microsomal vesicles. (**B**) The protein expression ratios in <60yr gluteus minimus microsomal vesicles. (**C**) The protein expression ratios in ≥60yr gluteus minimus microsomal vesicles. (**D**) The protein expression ratios in <60yr vastus medialis microsomal vesicles. (**E**) The protein expression ratios in ≥60yr vastus medialis microsomal vesicles.

5.4.1.4 Protein expression levels and ratios in the different human muscles

The mean expression level of RyR1, DHPR α_{1s}, DHPR β_{1a} and FKBP12 for each muscle was determined (**Table 5.2**) as well as the mean expression ratio of α_{1s}/RyR1, α_{1c}/RyR1 and FKBP12/RyR1 (**Table 5.3**). The means for each muscle were then compared (**Figure 5.21A-B**).

RyR1 and α_{1s} expression in vastus medialis were significantly greater ($P \leq 0.01$) compared to their expression in gluteus medius and gluteus minimus. There was no difference in RyR1 expression between gluteus medius and gluteus minimus muscle homogenates, however, gluteus minimus muscle homogenates showed a significantly larger α_{1s} expression level than gluteus medius. There was also no significant difference in the mean expression of β_{1a} or FKBP12 between the three muscles (**Figure 5.21A**).

There was no significant difference between the mean α_{1s}/RyR1 ratio between the muscles, . The α_{1c}/RyR1 ratio was significantly larger ($P \leq 0.05$) in vastus medialis microsomal vesicles than gluteus minimus, however, there was no significant difference between the ratio in gluteus medius and vastus medialis microsomal vesicles. The FKBP12/RyR1 expression ratio was significantly smaller ($P \leq 0.05$) in vastus medialis microsomal vesicles compared to gluteus minimus. No significant difference was observed between gluteus medius and gluteus minimus, neither between gluteus medius and vastus medialis (**Figure 5.21B**).

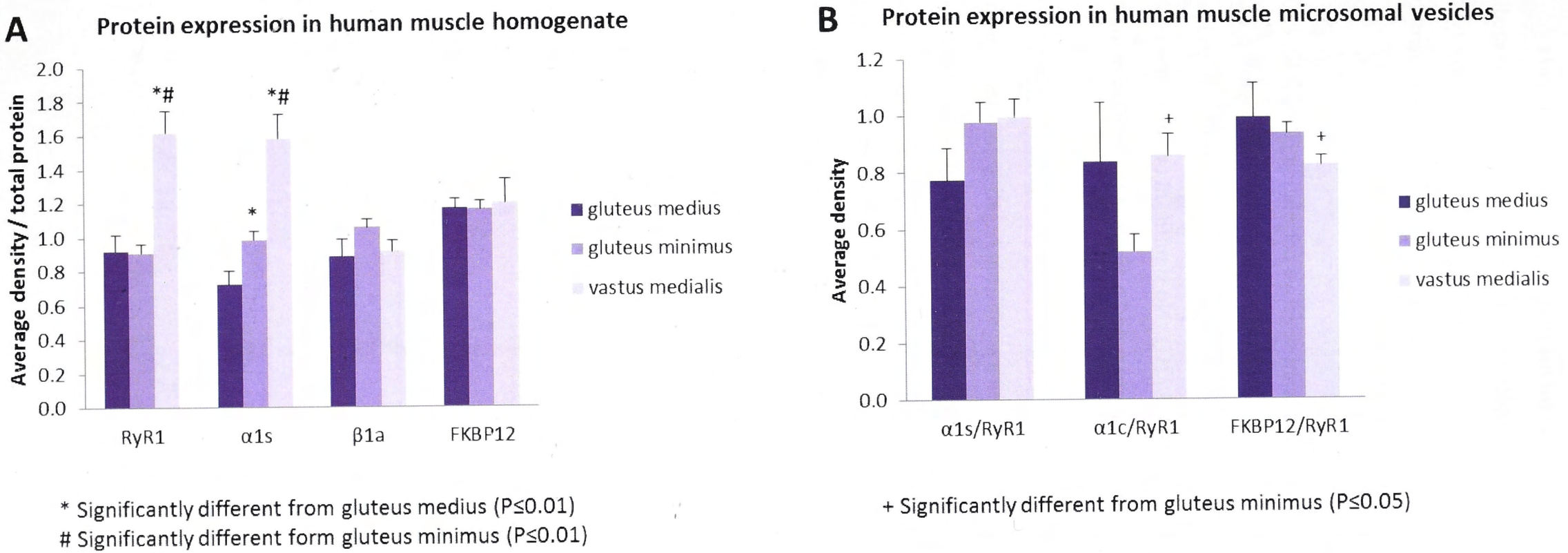

Figure 5.21: A comparison of expression levels of RyR1, DHPR α_{1s}, DHPR β_{1a} and FKBP12 in the muscle homogenates of the different muscles (A). A comparison of DHPR α_{1s} / RyR1, DHPR α_{1c} / RyR1 and FKBP12 / RyR1 expression ratios in microsomal vesicles prepared from the different muscles (B).

5.4.1.5 *The effect of fiber type on protein expression levels*

Because the mean expression level of RyR1 and α_{1s} were higher in vastus medialis compared to the gluteal muscles, and vastus medialis muscles have a greater percentage type 2 fibers, the average density of each protein was correlated with the average percentage of type 1, 2A and 2X fibers in the muscle for each respective donor.

The RyR1 expression showed a significant negative correlation ($R=-0.442$, $P\leq0.01$) with the percentage type 1 fibers in the muscle from the respective donors (**Figure 5.22A**) with an accompanying significant positive correlation between RyR1 expression and percentage of type 2X fibers ($R=0.521$, $P\leq0.01$) (**Figure 5.22C**). No significant correlation was observed between RyR1 expression level and the percentage type 2A fibers in the respective muscle (**Figure 5.22B**).

DHPR α_{1s} expression levels also showed a significant negative correlation with the percentage type 1 fibers in the respective muscle ($R=-0.325$, $P\leq0.05$) (**Figure 5.23A**) and a significant positive correlation with the percentage type 2X fibers in the respective muscle ($R=0.382$, $P\leq0.05$) (**Figure 5.23C**). No significant correlation was observed between α_{1s} expression level and the percentage type 2A fibers of the respective muscle (**Figure 5.23B**).

No significant correlation between DHPR β_{1a} expression and fiber type was found (**Figure 5.24 A-C**). There was also no significant correlation between FKBP12 expression (**Figure 5.25**), or the α1s/RyR1 (**Figure 5.26**), α1c/RyR1 (**Figure 5.27**) or FKBP12/RyR1 (**Figure 5.28**) ratios and fiber type.

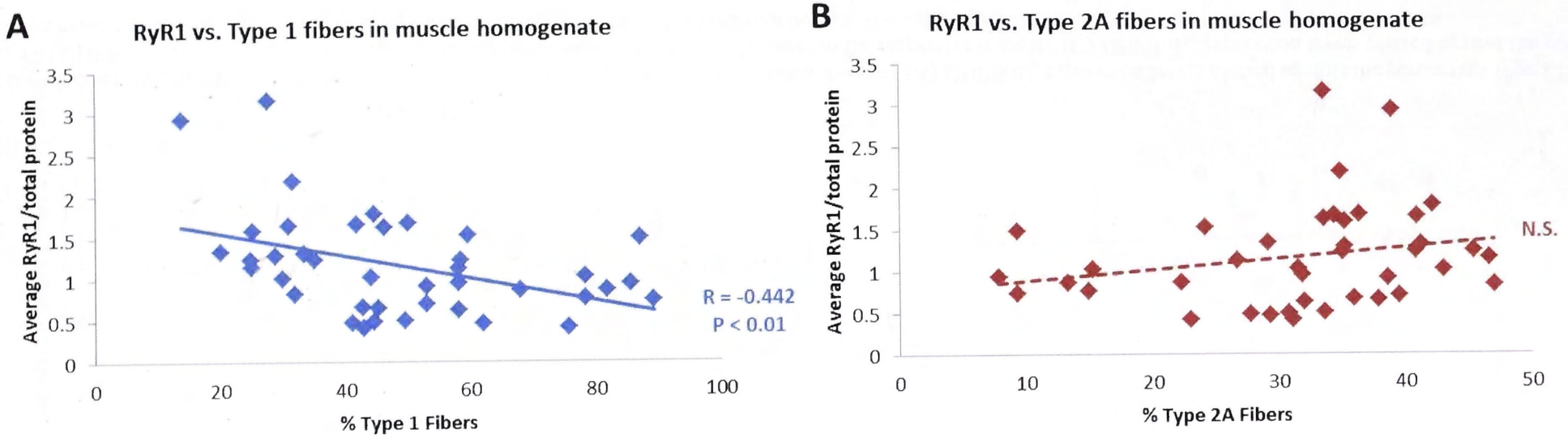

Figure 5.22: The correlation between RyR1 expression levels and the fiber type of the human donor muscle. (A) RyR1 expression levels plotted against the percentage type 1 fibers in the respective muscle. (B) RyR1 expression levels plotted against percentage type 2A muscle fibers in the respective muscle. (C) RyR1 expression levels plotted against the percentage type 2X fibers in the respective muscle. (A dashed line indicates no significant correlation and is also indicated by N.S. R – correlation coefficient).

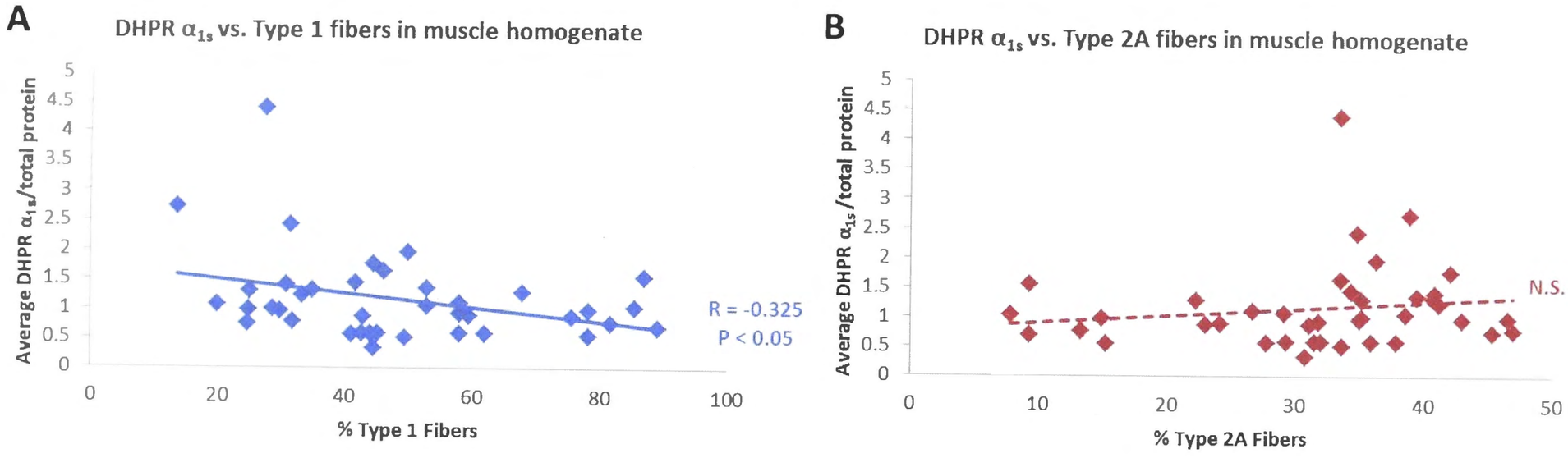

Figure 5.23: The correlation between DHPR α_{1s} expression levels and the fiber type of the human donor muscle. (**A**) DHPR α_{1s} expression levels plotted against the percentage type 1 fibers in the respective muscle. (**B**) DHPR α_{1s} expression levels plotted against the percentage type 2A muscle fibers in the respective muscle. (**C**) DHPR α_{1s} expression levels plotted against the percentage type 2X fibers in the respective muscle. (Dashed line indicates no significant correlation and is also indicated by N.S, R – correlation coefficient).

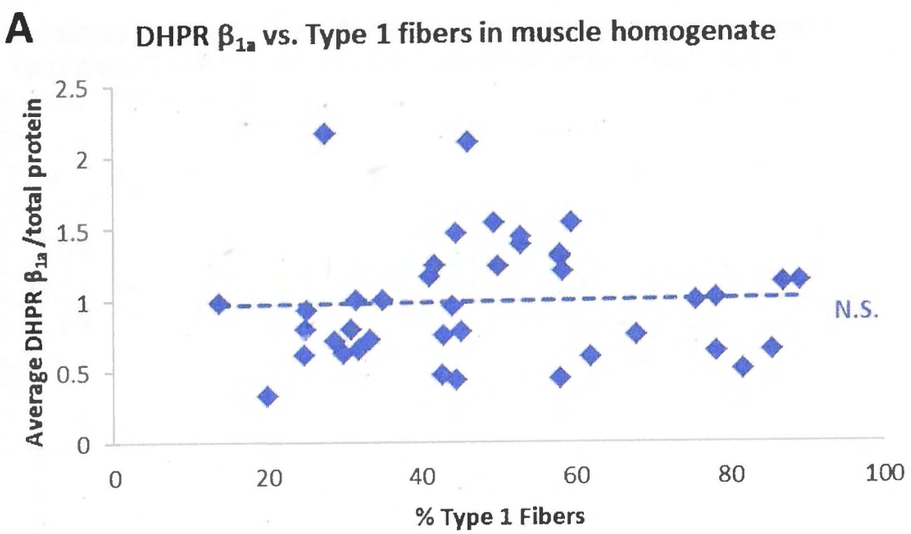

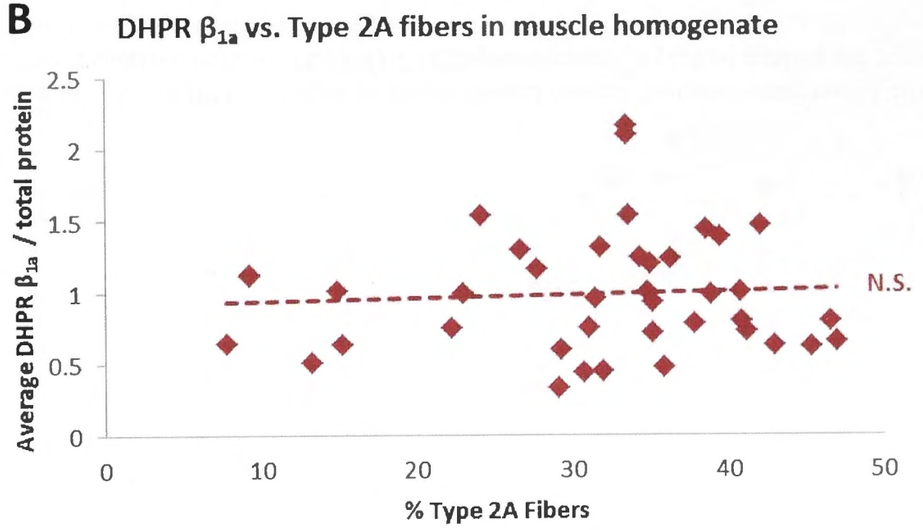

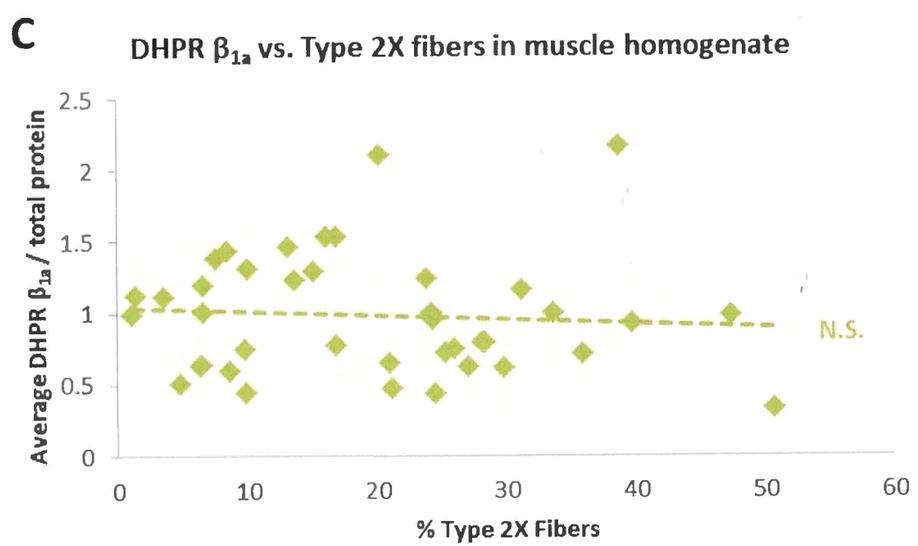

Figure 5.24: The correlation between DHPR β_{1a} expression levels and the fiber type of the human donor muscle. (**A**) DHPR β_{1a} expression levels plotted against the percentage type 1 fibers in the respective muscle. (**B**) DHPR β_{1a} expression levels plotted against the percentage type 2A muscle fibers in the respective muscle. (**C**) DHPR β_{1a} expression levels plotted against the percentage type 2X fibers in the respective muscle. (Dashed line indicates no significant correlation and is also indicated by N.S, R – correlation coefficient).

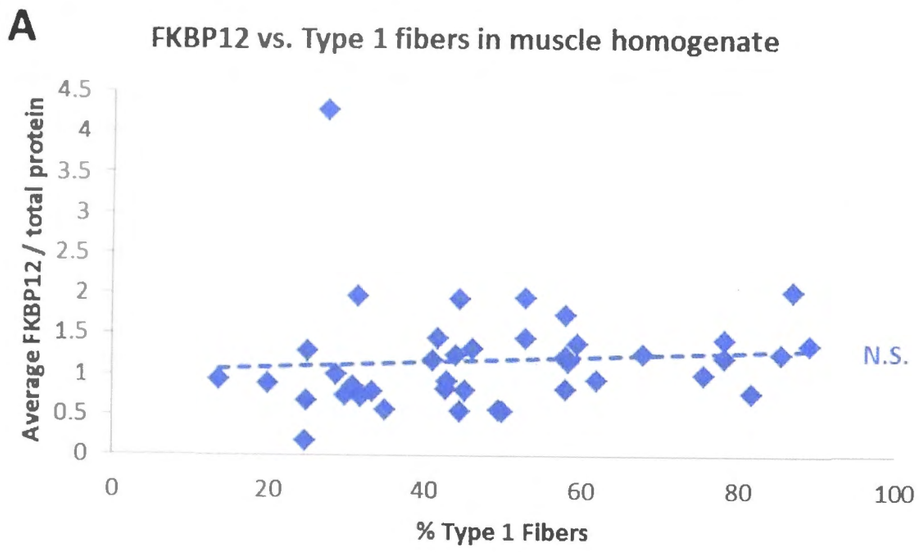

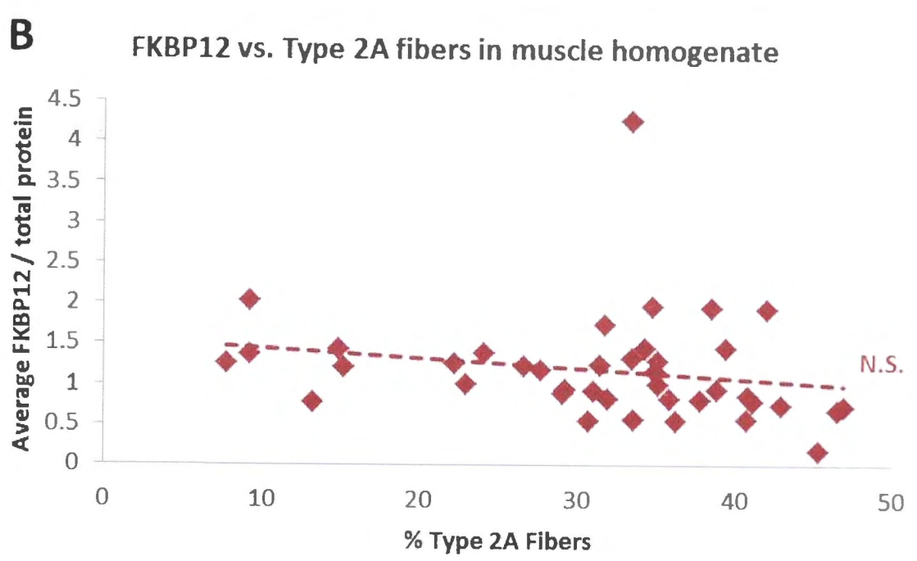

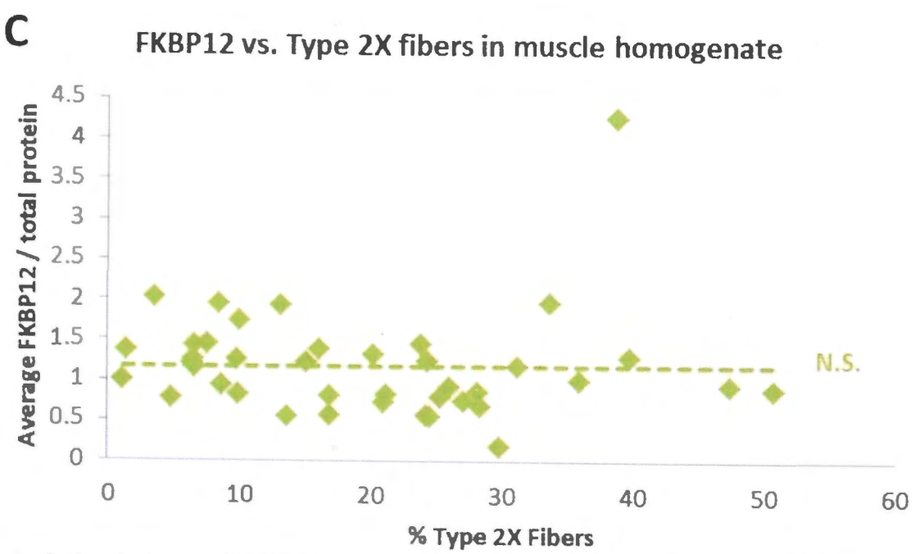

Figure 5.25: The correlation between FKBP12 expression levels and the fiber type of the human donor muscle. (**A**) FKBP12 expression levels plotted against the percentage type 1 fibers in the respective muscle. (**B**) FKBP12 expression levels plotted against the percentage type 2A muscle fibers in the respective muscle. (**C**) FKBP12 expression levels plotted against the percentage type 2X fibers in the respective muscle. (Dashed line indicates no significant correlation and is also indicated by N.S, R – correlation coefficient).

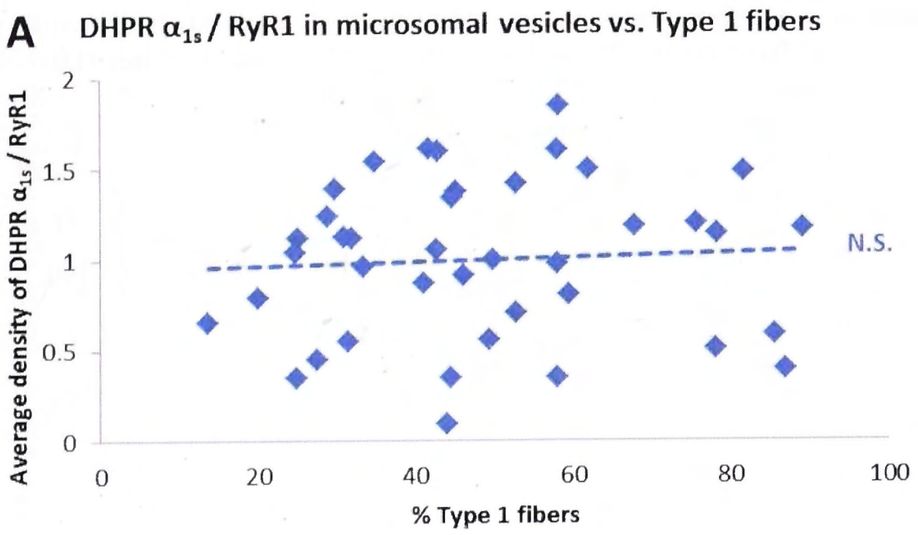

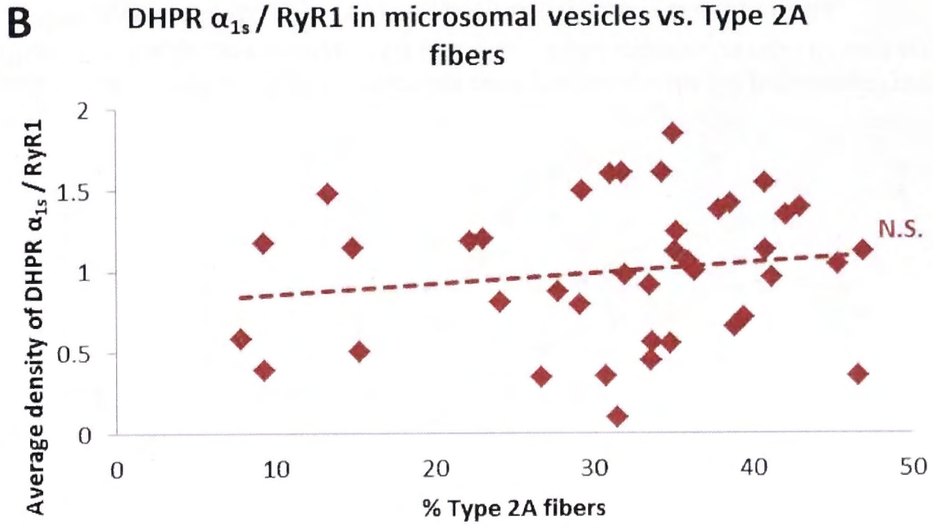

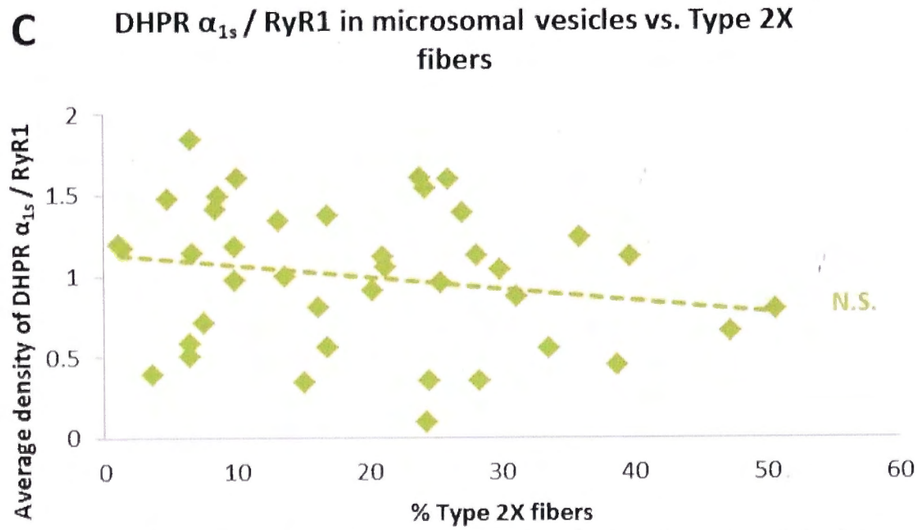

Figure 5.26: The correlation between α_{1s}/RyR1 expression ratio and the fiber type of the human donor muscle. (**A**) DHPR α_{1s}/RyR1 expression ratio plotted against the percentage type 1 fibers in the respective muscle. (**B**) DHPR α_{1s}/RyR1 expression ratio plotted against the percentage type 2A muscle fibers in the respective muscle. (**C**) DHPR α_{1s}/RyR1 expression ratio plotted against the percentage type 2X fibers in the respective muscle. (Dashed line indicates no significant correlation and is also indicated by N.S, R – correlation coefficient).

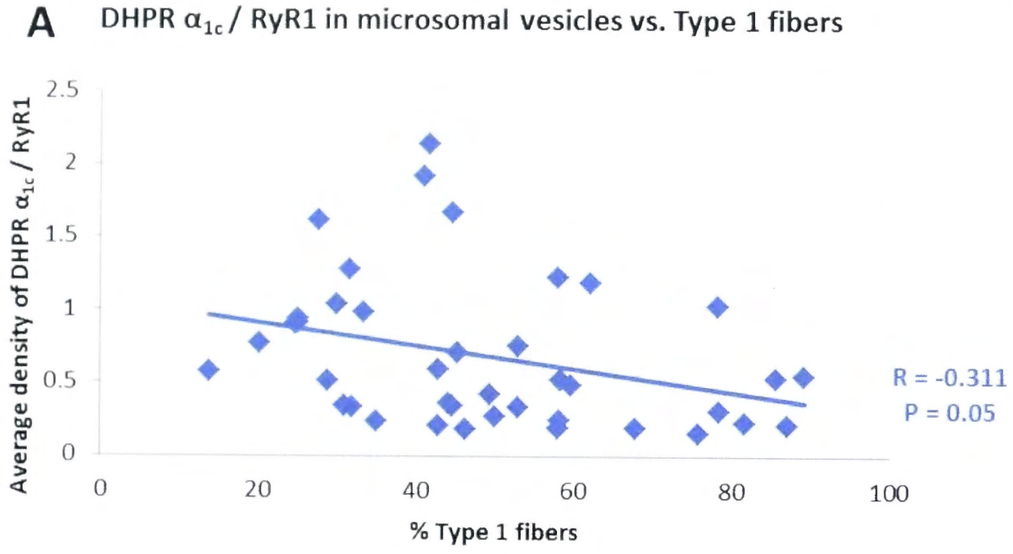

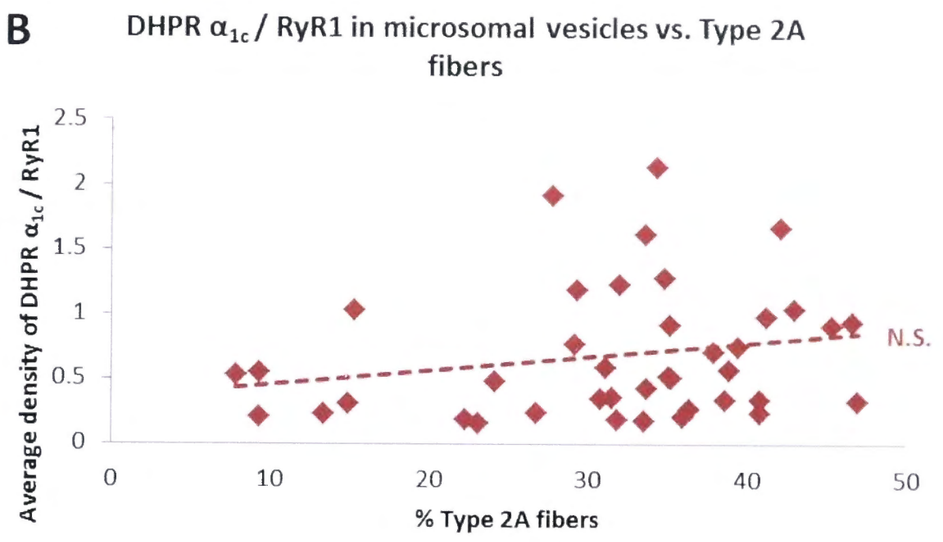

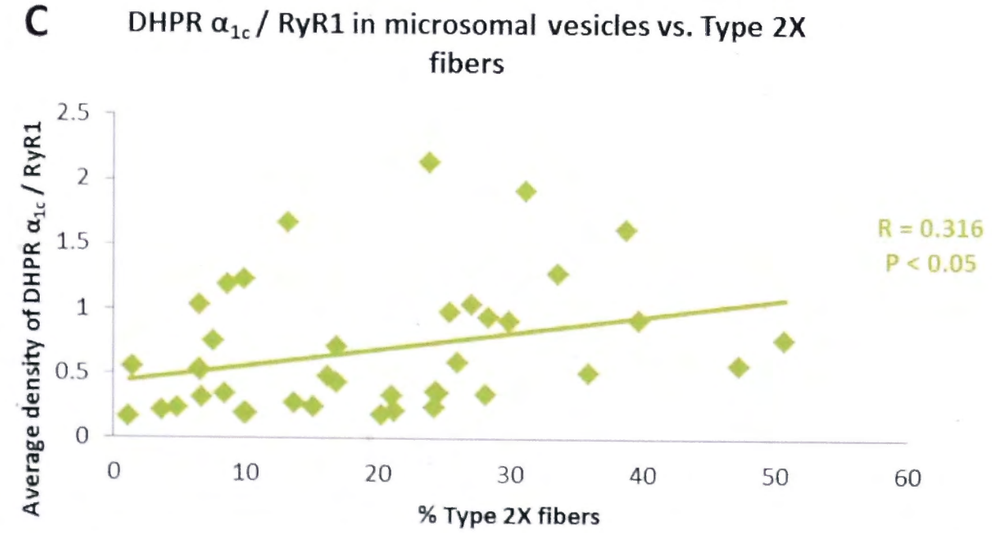

Figure 5.27: The correlation between α_{1c}/RyR1 expression ratio and the fiber type of the human donor muscle. (**A**) DHPR α_{1c}/RyR1 expression ratio plotted against the percentage type 1 fibers in the respective muscle. (**B**) DHPR α_{1c}/RyR1 expression ratio plotted against the percentage type 2A muscle fibers in the respective muscle. (**C**) DHPR α_{1c}/RyR1 expression ratio plotted against the percentage type 2X fibers in the respective muscle. (Dashed line indicates no significant correlation and is also indicated by N.S, R – correlation coefficient).

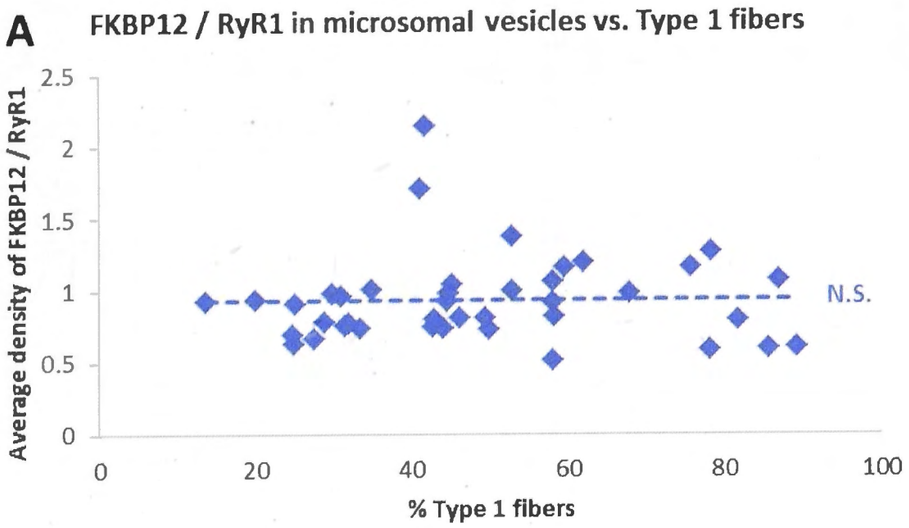

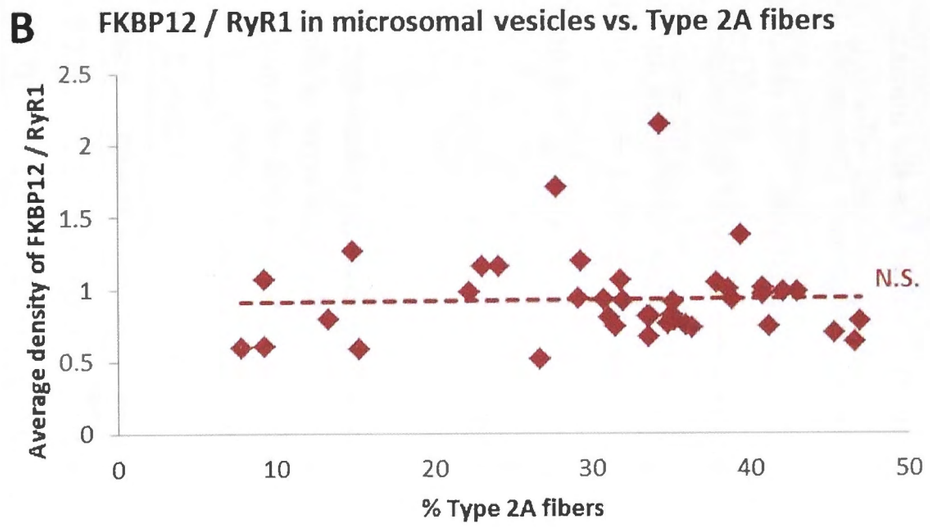

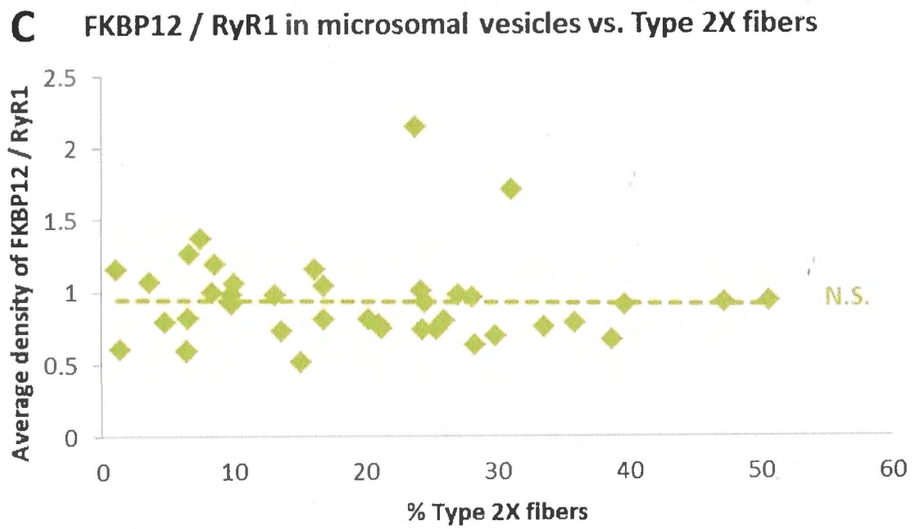

Figure 5.28: The correlation between FKBP12/RyR1 expression ratio and the fiber type of the human donor muscle. (**A**) FKBP12/RyR1 expression ratio plotted against the percentage type 1 fibers in the respective muscle. (**B**) FKBP12/RyR1 expression ratio plotted against the percentage type 2A muscle fibers in the respective muscle. (**C**) FKBP12/RyR1 expression ratio plotted against the percentage type 2X fibers in the respective muscle. (Dashed line indicates no significant correlation and is also indicated by N.S, R – correlation coefficient).

5.4.2 Rat muscle

5.4.2.1 Densitometry results

Rat muscles were examined as a positive control due to the variability observed in the human data. The average density of the protein bands obtained from muscle homogenate immunoblots relative to total protein were determined for each muscle of the two rat age groups. The results are given in **Table 5.4**. The average density of the protein bands relative to RyR1 determined in microsomal vesicles for each muscle from the two rat age groups were also determined and the results are given in **Table 5.5**.

Table 5.3: The average density of the protein bands relative to total protein in rat soleus and EDL muscle homogenate from 5wk and 1yr old rats. (sem – standard error of the mean, n – number of observations, * significantly different from 5wk old of same muscle P≤0.05, # significantly different from Sol of same age group P≤0.05).

			RyR1		DHPR α_{1s}		DHPR β_{1a}		FKBP12	
		n	mean	±sem	mean	±sem	mean	±sem	mean	±sem
5wk	Soleus	12	0.59	0.05	0.38	0.07	0.91	0.04	1.21	0.09
	EDL	12	1.23#	0.05	0.93#	0.13	0.67#	0.03	1.23	0.11
1yr	Soleus	12	0.68	0.05	0.77*	0.07	0.64*	0.07	1.09	0.08
	EDL	12	1.40#	0.07	1.89*#	0.12	0.38*#	0.05	0.87*	0.06

Table 5.4: The average density of the protein bands relative to that of RyR1 in microsomal vesicles from rat soleus and EDL muscle obtained from 5k and 1yr old rats. (sem – standard error of the mean, n – number of observations, * significantly different from 5wk old of same muscle P≤0.05, # significantly different from Sol of same age group P≤0.05).

		DHPR α_{1s} / RyR1			DHPR α_{1c} / RyR1			FKBP12/RyR1		
		mean	±sem	n	mean	±sem	n	mean	±sem	n
5wk	Soleus	0.84	0.14	12	0.05	0.02	6	0.72	0.26	12
	EDL	1.33#	0.07	12	0.32	0.67	6	0.12	0.06	12
1yr	Soleus	2.25*	0.36	12	0.14*	0.03	12	0.36	0.05	12
	EDL	1.67*	0.07	12	0.35#	0.04	12	0.47*	0.03	12

The expression level of the DHPR α_{1s} subunit was correlated with the expression levels of RyR1 in the rat muscle homogenate to validate the results obtained from the immunoblots (**Figure 5.29A**). The data obtained from the two age groups as well as the two muscles types were combined in this correlation. The DHPR β_{1a} subunit was also correlated with RyR1 expression in a similar fashion (**Figure 5.29B**) and then the expression levels of the two DHPR subunits were correlated (**Figure 5.29C**). There was a significant positive correlation ($P<0.01$) between the DHPR α_{1s} density and that of the RyR1 with a correlation coefficient of 0.710. The DHPR β_{1a} subunit density showed a significant negative correlation ($P<0.01$) with that of the RyR1 ($R = -0.395$). The two DHPR subunits also showed a significant ($P<0.01$) negative correlation with $R = -0.420$.

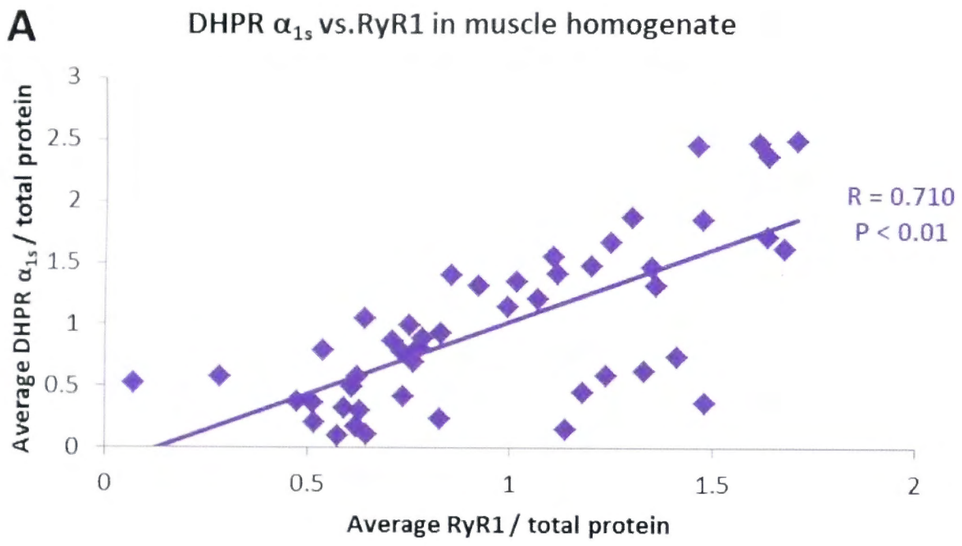

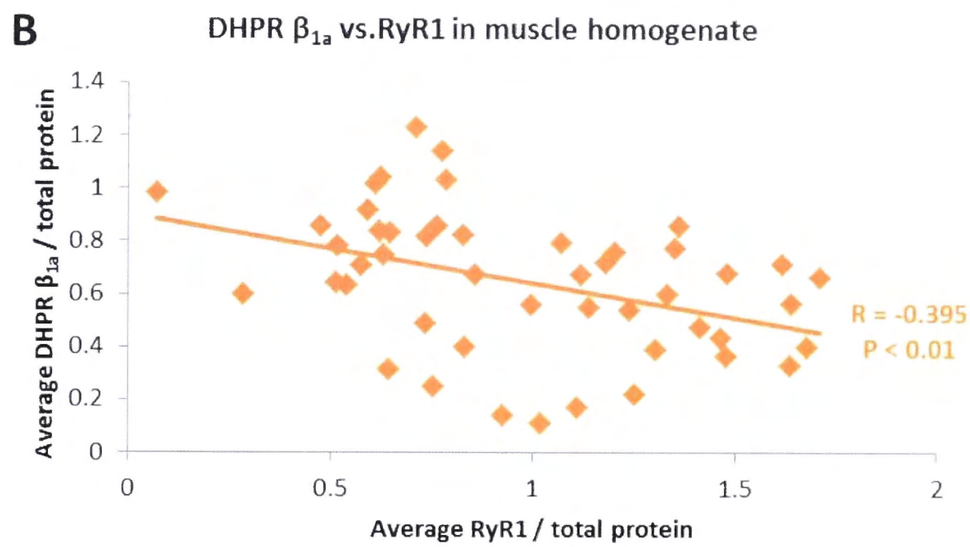

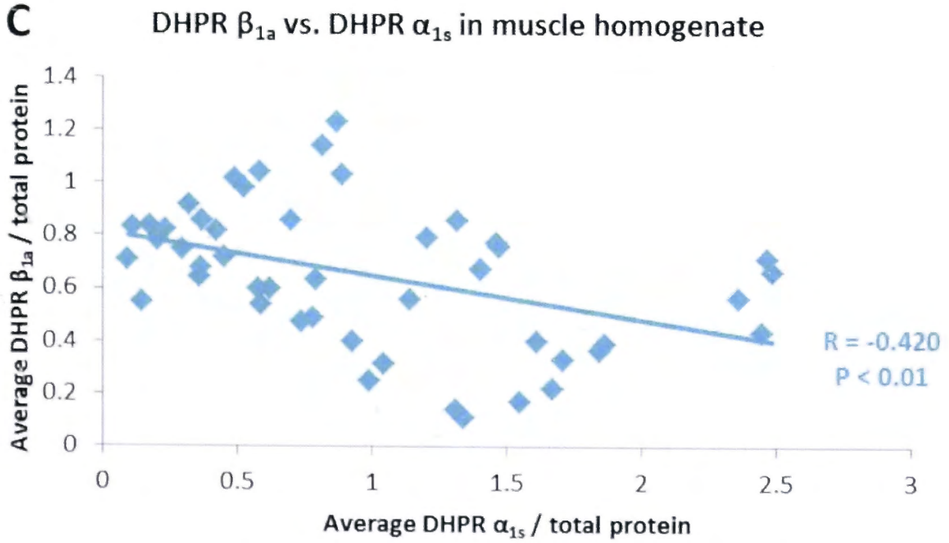

Figure 5.29: The correlation between the expression levels of the DHPR subunits and RyR1 in the rat muscle homogenates. (**A**) DHPR α_{1s} subunit expression levels plotted against that of the RyR1. (**B** DHPR β_{1a} subunit expression levels plotted against that of the RyR1. (**C**) DHPR β_{1a} subunit expression levels plotted against that of the α_{1s} subunit.

5.4.2.2 *The effect of age on protein expression levels*

In order to investigate the change in protein expression with the age of the rat, the average expression levels of RyR1, DHPR α_{1s}, DHPR β_{1a} and FKBP12 in rat muscle homogenate as well as the α_{1s}/RyR1, α_{1c}/RyR1 and FKBP12/RyR1 ratios in microsomal vesicles were compared between the 5wk old and 1yr old rats.

In the muscle homogenate from soleus, a significantly greater α_{1s} expression was observed in the 1yr old rats ($P \leq 0.05$). However, the β_{1a} expression was significantly lower in the 1yr old rats ($P \leq 0.05$). No significant age difference was found in RyR1 or FKBP12 expression (**Figure 5.30A**). When the protein levels between the rat age groups were compared in EDL, a significantly greater α_{1s} expression was observed in 1yr old rats ($P \leq 0.05$). The β1a and FKBP12 expression levels, however, where significantly lower ($P \leq 0.05$) in 1yr old rats. No significant difference between 5wk and 1yr old rats RyR1 expression was found in EDL muscle (**Figure 5.30B**).

The soleus microsomal vesicles showed a significantly larger α_{1s}/RyR1 and α_{1c}/RyR1 ratios in 1yr old rats compared to the 5wk old rats ($P \leq 0.05$) but no significant difference in FKBP12 expression (**Figure 5.30C**). In EDL microsomal vesicles, there was a significantly larger α_{1s}/RyR1 expression ratio in 1yr old rats but a significantly lower FKBP12/RyR1 ratio compared to 5wk old rats ($P \leq 0.05$). No difference was found in the α_{1c}/RyR1 eratio (**Figure 5.30D**).

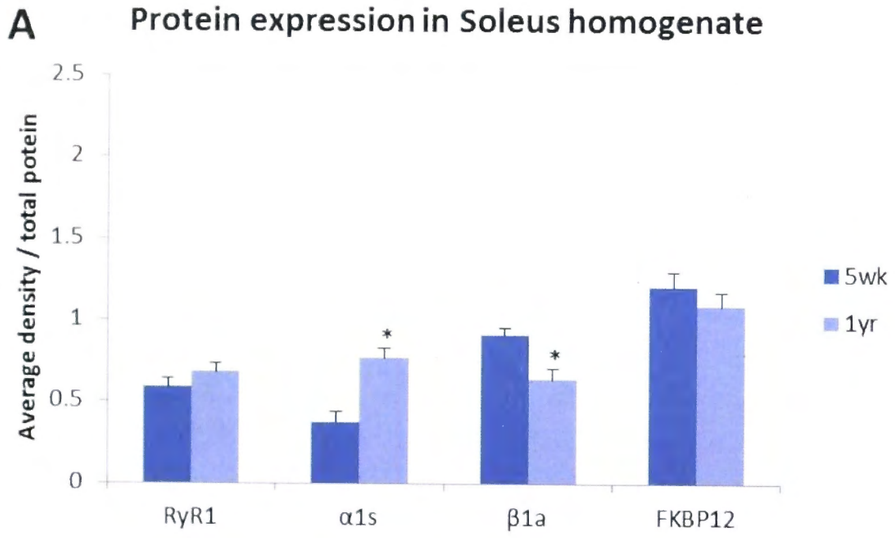

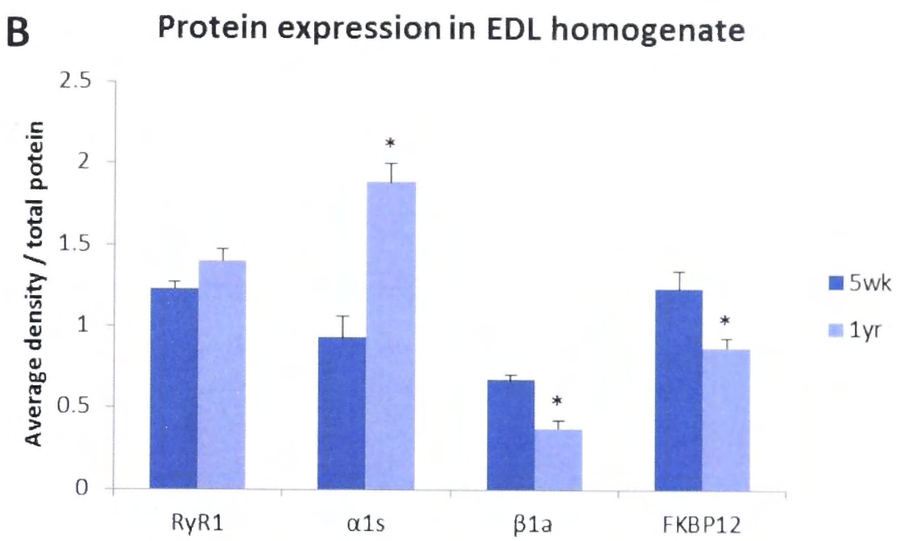

* Significantly different from 5wk (P≤0.05)

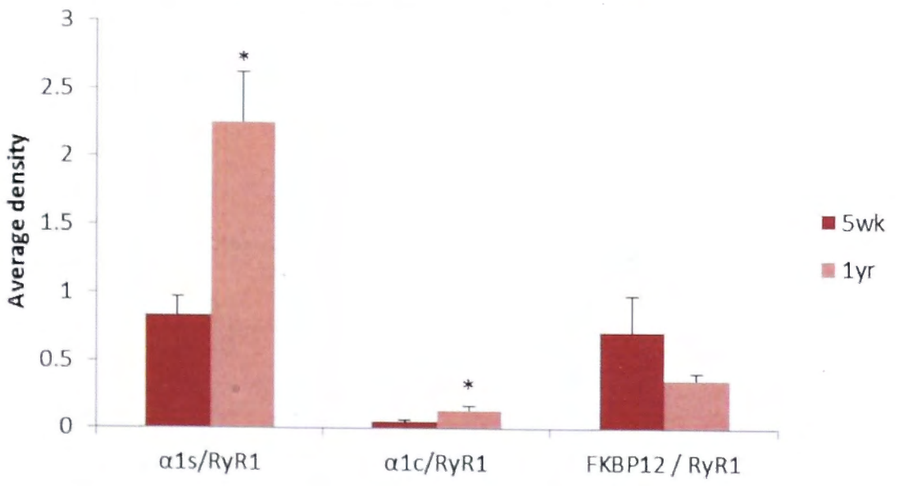

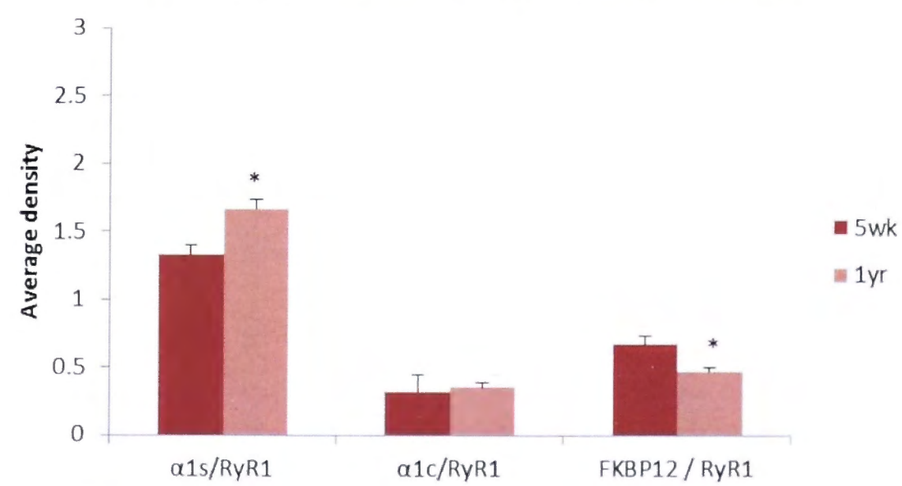

Figure 5.30: The effect of age on protein expression levels and ratios in rat homogenate and microsomal vesicles from soleus and EDL muscle. (**A**) The protein expression levels in soleus muscle homogenate from 5wk and 1yr old rats. (**B**) The protein expression levels in EDL muscle homogenate from 5wk and 1yr old rats. (**C**). The protein expression ratios in soleus microsomal vesicles from 5wk and 1yr old rats. (**D**) The protein expression ratios in EDL microsomal vesicles from 5wk and 1yr old rats.

5.4.2.3 The effect of muscle type on protein expression levels

In order to investigate differences in protein expression as a result of the rat muscle used, the average levels of RyR1, DHPR α_{1s}, DHPR β_{1a} and FKBP12 in rat muscle homogenate as well as the α_{1s}/RyR1, α_{1c}/RyR1 and FKBP12/RyR1 ratios in microsomal vesicles were compared between the 5wk old rat soleus and EDL muscle as well as the 1yr old rat soleus and EDL muscle.

The 5wk old rat EDL muscle homogenate showed significantly greater RyR1 and α_{1s} expression compared to the soleus muscle ($P \leq 0.05$). The β_{1a} expression was significantly lower in EDL muscle homogenate compared to soleus in 5wk old rats. No difference in FKBP12 expression was observed (**Figure 5.31A**). In 1yr old rat muscle homogenate, similar results were observed. RyR1 and α_{1s} expression were significantly higher in EDL ($P \leq 0.05$), β1a expression significantly lower ($P \leq 0.05$) and there was no difference in FKBP12 expression (**Figure 5.31B**).

Comparing the soleus and EDL microsomal vesicle data in 5wk rats showed a significantly larger α_{1s}/RyR1 expression ratio in EDL muscle ($P \leq 0.05$) with no difference in the α_{1c}/RyR1 or FKBP12/RyR1 ratios (**Figure5.31C**). In 1yr old rats, there was a significantly larger α_{1c}/RyR1 expression ratio in EDL ($P \leq 0.05$) with no difference in α_{1s}/RyR1 or FKBP12/RyR1 ratios (**Figure 5.31D**).

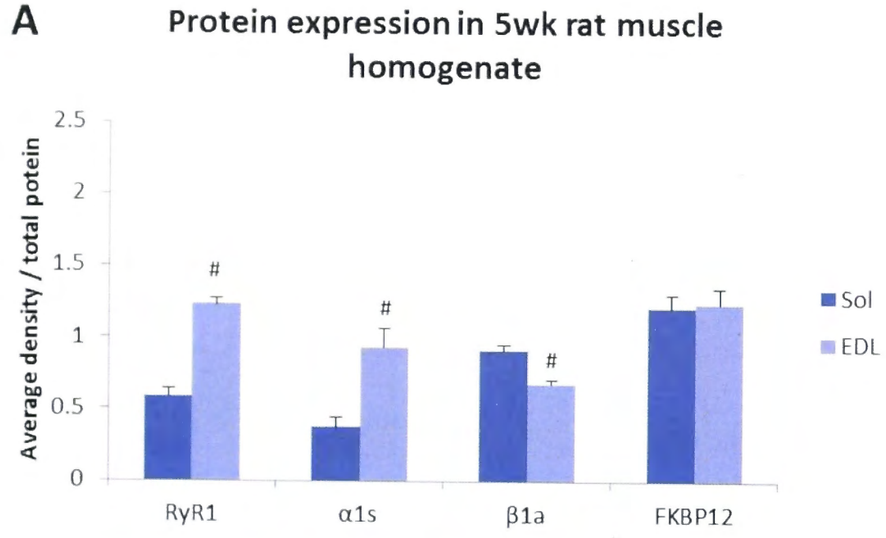

Significantly different from Sol (P≤0.05)

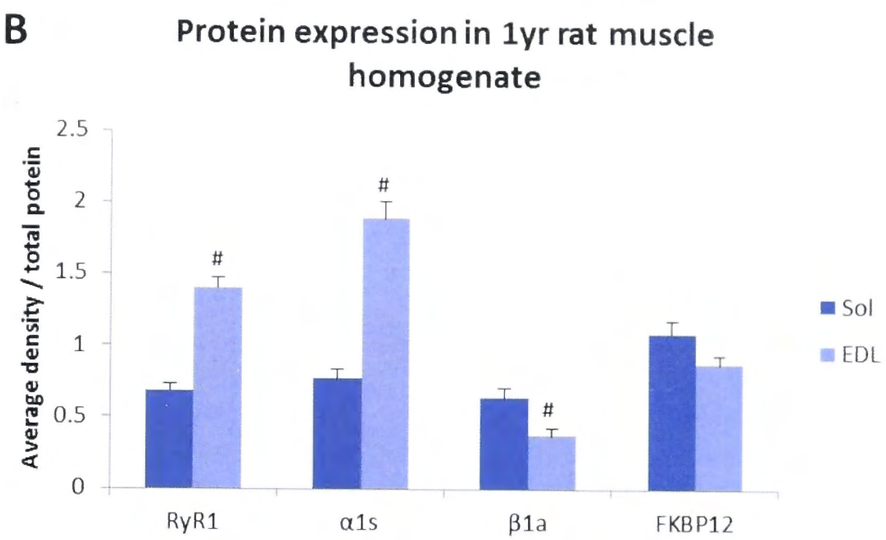

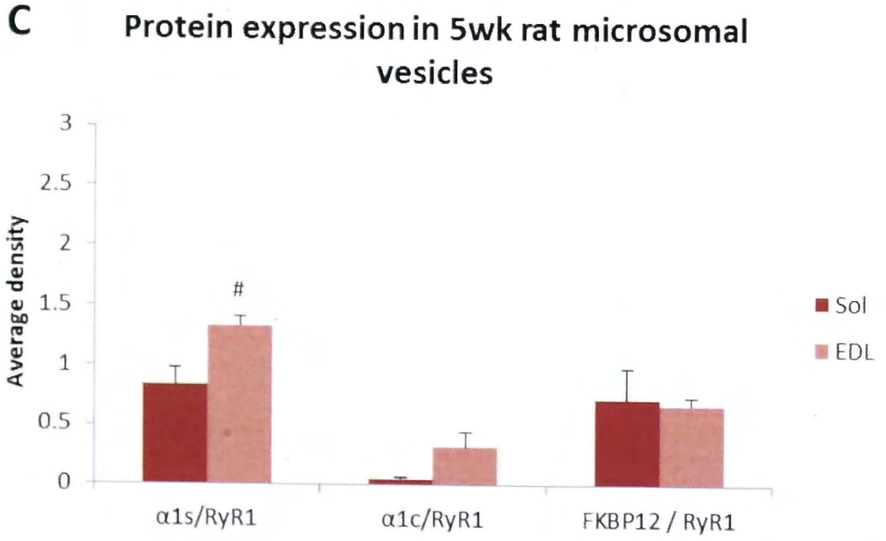

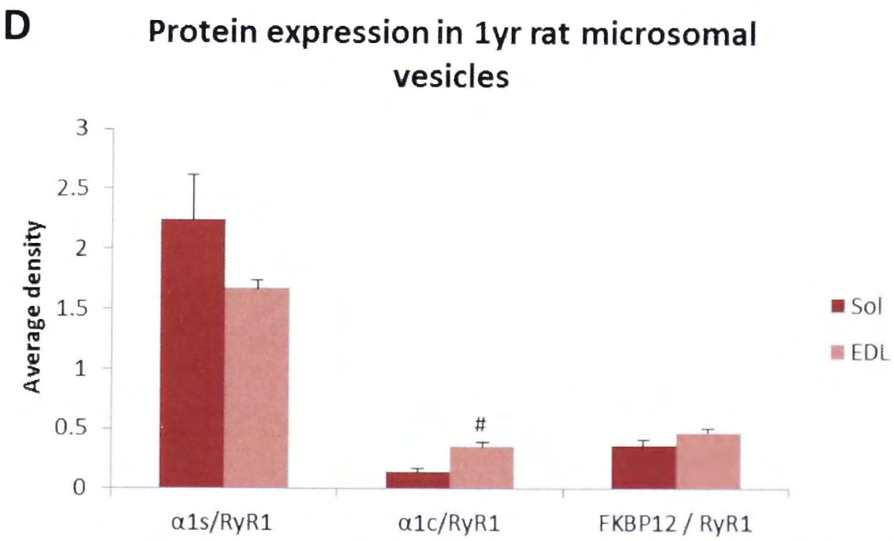

Figure 5.31: The effect of muscle type on protein expression levels and ratios in muscle homogenates and microsomal vesicles from 5wk and 1yr old rats. (**A**) The protein expression levels in soleus and EDL muscle homogenate from 5wk old rats. (**B**) The protein expression levels in soleus and EDL muscle homogenate from 1yr old rats. (**C**) The protein expression levels in soleus and EDL microsomal vesicles from 5wk old rats. (**D**) The protein expression levels in soleus and EDL microsomal vesicles from 1yr old rats.

5.5 Discussion

5.5.1 Human muscle

5.5.1.1 Muscle samples

Obtaining samples is a limiting factor to any study involving humans. In the work described in this chapter, all the possible human samples that became available in the allotted time frame were collected without a filtering system. In total 40 muscle samples were collected, however, they were sourced from three different muscles with the donor cohort consisting of males and females. The sample number for each muscle was not ideal, especially the gluteus medius muscle which were donated by only five individuals, one of which was male. Due to the nature of the sample collection, which was during hip and knee replacements, the age of the donors are also skewed towards older people, the youngest sample being from a 45yr old. There are therefore no donors in the 20-30 year age range which is normally considered to be the control age group for studies involving aged muscle. However, as most of the changes in muscle associated with age seem to occur after the 6^{th} decade (Vandervoort and McComas 1986; Lindle et al. 1997; Rantanen et al. 1998; Deschenes 2004), the donors younger than 60yr were considered as the control group.

5.5.1.2 Correlations between RyR1, DHPR α_{1s} and DHPR β_{1a}

The expression levels of RyR1, α_{1s} and β_{1a} in human muscle homogenate (measured as the average density of the protein bands obtained with immunoblots normalised to total protein) were correlated with each other. The significant positive correlation between α_{1s} and RyR1 expression (R= 0.889) is consistent with a close association between the DHPR and RyR1 in the skeletal muscle CRUs. In fact most of the DHPR is found in the junctional t-tubules (Yuan et al. 1991; Carl et al. 1995b; Jorgensen 1998), which would imply that the α_{1s} and RyR1 expression levels should correlate positively. When the correlation coefficient is squared to obtain the coefficient of determination (R^2), a value of 0.79 is obtained which indicates a strong correlation in expression between these two proteins.

The significant positive correlation (R=0.435) between β_{1a} and RyR1 is also to be expected as the β1a subunit forms part of the DHPR that is closely associated with the RyR1. However, what is surprising is that the correlation is not as strong. The R^2 for this correlation is 0.19 which indicates a moderate correlation. Therefore the variance in the RyR1 expression level can only account for 19% of the variance in β_{1a} expression level whereas it could account for 79% of the variance of the α_{1s} expression level.

The significant positive correlation between the two DHPR subunits (R=0.542) is also to be expected as they form part of the complete DHPR subunit complex. Again the strength of the

correlation is interesting as one would also expect it to be as strong as that of the RyR1 and α_{1s}. However, the R^2 value for this correlation is 0.29 and although statistically this indicates a strong correlation, only 29% of the variance in β_{1a} expression can be accounted for by the variance in α_{1s} and might indicate that there is a cohort of β_{1a} not associated with α_{1s} in the muscle homogenate. This is also consistent with the observation that the β_{1a} subunit is lost during the first centrifugation step in the preparation of microsomal vesicles, although the imidazole in the homogenizing buffer could also cause a dissociation of the β_{1a} subunit from the α_{1s} subunit. Witcher et al (Witcher et al. 1995) described the presence of non-associated β_{1a} subunits in skeletal muscle homogenate which is consistent with the lower than expected correlation between α_{1s} and β_{1a} subunits in muscle homogenate described in this chapter.

5.5.1.3 Effect of age on protein expression levels and ratios

5.5.1.3.1 RyR1

The general pattern emerging when the RyR1 expression levels between the <60yr and ≥60yr age groups are compared is that there is no difference in its expression between these age groups. There are three exceptions to this. The first is in gluteus medius homogenate where a significantly larger RyR1 expression level was observed in the ≥60yr age group (**Figure 5.6B**). However, as the sample size for this muscle in particular is very small (n=2 for <60yr and n=3 for >60yr) caution should be applied when interpreting this data. Secondly, when the male and female muscle donors are considered separately, the female gluteus medius shows the same larger RyR1 expression level in the ≥60yr age group as when the genders were combined (**Figure5.8B**). As only one of the 5 gluteus medius donors were male, the RyR1 expression levels for the combined gender gluteus medius and the female only gluteus medius muscle homogenate are essentially the same result and again reflect the small sample size.

Thirdly, male gluteus minimus muscle homogenate showed a significantly lower RyR1 expression level in the ≥60yr age group (**Figure 5.8D**). However, the male gluteus minimus group was the only human muscle group that showed this result and therefore an exception to the general RyR1 expression pattern observed in most of the muscle homogenate data.

When RyR1 expression levels were plotted over the entire range of ages, the correlation with the age of the respective donors confirms the general pattern observed when the mean values for the age groups were compared. There was no significant correlation between RyR1 expression and the age of the respective donors when the data from all the muscle combined were considered. There was also no significant correlation when the data from the three muscles were considered separately. Even the gluteus medius, which showed a significantly higher

RyR1 expression in the ≥60yr age group when comparing the means of the age groups, showed no significant correlation between RyR1 expression and age.

These results together suggest that in human muscle, there is no change in RyR1 expression with age, which is consistent with previous [^{3}H]ryanodine binding and immunoblot studies showing no change in RyR1 expression in aged rats (Damiani et al. 1996; Margreth et al. 1999; O'Connell et al. 2008).

5.5.1.3.2 DHPR α_{1s}

As with RyR1 expression discussed above, the general pattern emerging when comparing the mean α_{1s} expression level in <60yr and ≥60yr donors is that there is no difference in the expression of α_{1s} between the age groups. In this case there are two exceptions to the general pattern.

Firstly, muscle homogenate from vastus medialis showed a significantly larger α_{1s} expression level in the ≥60yr age group (**Figure 5.6D**). When the male and female data for this muscle is separated, the significance of the difference is lost (**Figure 5.8C&E**) although there are trends in both cases towards a higher expression level in the older age group. It seems that combining the data from the two genders provided a large enough observation number to make the difference significant. The higher α_{1s} expression is similar to the higher RyR1 expression in older vastus medialis (above). However, the larger expression level observed in the older age group is in contrast to all previous studies regarding α_{1s} expression which have shown a decrease in α_{1s} expression if a change was observed at all (Delbono et al. 1995; Renganathan et al. 1997; Renganathan et al. 1998; Ryan et al. 2000; Wang et al. 2000; Ryan et al. 2003; O'Connell et al. 2008). It is also difficult to explain the higher α_{1s} expression in terms of the structural changes that aging muscle undergoes with age as if anything, there are less CRUs in aging muscle and the t-tubular network is less orderly structured (Boncompagni et al. 2006). As there were only 4 vastus medialis donors younger than 60yr, the higher expression seen in the older age group could be attributed again to insufficient sampling.

Secondly, when the mean expression level of α_{1s} was compared between the age groups in males and females separately, a significantly greater expression of α_{1s} was also observed in the female gluteus medius muscle homogenate (**Figure 5.8A**). However, the addition of the data from the single male gluteus medius donor removes the significance of the difference observed in the female gluteus medius alone (**Figure 5.6B**). This suggests that the small sample size of the gluteus medius muscle cohort may be causing this anomalous result.

When α_{1s} expression was plotted over the entire range of ages, the correlation of α_{1s} expression with the age of the respective donors is consistent with the general pattern observed when the means of the age groups were compared. No significant correlation was found between α_{1s} expression and the age of the respective donors when the data from all three muscles were combined or correlated separately (**Figure 5.11**). Specifically, the vastus medialis muscle homogenate that showed a significantly larger α_{1s} expression in ≥60yr age group compared to the <60yr age group, showed no significant correlation with age.

These results together suggest that in human muscle, there is no change in DHPR α_{1s} expression in aging muscle, which is consistent with the study by Ryan et al (Ryan et al. 2003).

5.5.1.3.3 The α_{1s}/RyR1 ratio

The principal underlying the EC uncoupling hypothesis of reduced muscle strength in aging muscle is the ratio of the DHPR α_{1s} subunit to RyR1 that is reduced in aging muscle, leading to an increased number of RyR1s not associated with DHPR and an "uncoupling" between the voltage sensor and Ca^{2+} release channel of EC coupling (Payne and Delbono 2004).

The investigation into the α_{1s}/RyR1 expression ratio in microsomal vesicles prepared from human muscle described in this chapter showed a lower α_{1s}/RyR1 expression in the ≥60yr age group when the data from all three muscles are combined (**Figure 5.7A**). However, when the data from the three muscles are considered separately, there is no significant difference between the two age groups, although a trend towards a lower mean in the ≥60 age group is observed (**Figure 5.7B-D**). Similarly when the data from the male and female donors of each muscle is considered separately, a trend towards a lower mean in the ≥60yr age group is observed in all the groups except the male gluteus minimus. These results together may once again suggest that only when the data from all the donors are combined, the observation number is large enough to make the difference between the means of the two age groups significant.

However, when the α_{1s}/RyR1 expression ratio is plotted against the age of each donor, there is no significant correlation between this ratio and age in the combined data from all three muscles (**Figure 5.14A**), or in the muscles separately (**Figure 5.14B-D**). It may well be that an increased samples size may lead to a significant correlation, but this is speculation. Together with the results from muscle homogenates showing no change in RyR1 or α_{1s} expression with age, the microsomal vesicle data suggest that there is no change in the α_{1s}/RyR1 expression ratio with age in human muscle. This confirms the suggestion that the reduced muscle strength observed in aging human muscle may be more a case of altered structure and arrangement of the EC coupling apparatus than the expression of the protein.

5.5.1.3.4 The α_{1c}/RyR1 ratio

The cardiac DHPR α_{1c} subunit has been shown to be expressed in adult rat soleus, EDL and diaphragm of rats and developing muscle from mice (Chaudhari and Beam 1993; Pereon et al. 1997; Pereon et al. 1998). The work described in this chapter also shows for the first time cardiac DHPR expression in adult human skeletal muscle. The DHPR α_{1c}/RyR1 ratio did not seem to change with age as the general pattern observed in results from microsomal vesicle immunoblots shows no significant difference between the <60 yr and ≥60yr age groups of human donors. This is the case when the data from all three muscles are combined (**Figure 5.7A**), when the data from the muscles are considered separately (**Figure 5.7B-D**) as well as when the male and female donor data for each muscle is considered separately (**Figure 5.9**). There are two exceptions to this general pattern. The first is a significantly lower α_{1c}/RyR1 ratio in the ≥60yr age group of gluteus minimus microsomal vesicles (**Figure 5.7C**). The second is a significantly larger α_{1c}/RyR1 ratio in the ≥60yr age group in male vastus medialis vesicles (**Figure 5.9E**). In both cases there is no apparent explanation for the significant differences. The fact that there was no significant correlation between the α_{1c}/RyR1 and the age of the respective donors in either the combined muscle data or the data from the muscles considered separately suggests that the two exceptions discussed above might be due to the large variation observed between humans in combination with sample size and that generally the data suggests that there is no change in the α_{1c}/RyR1 ration with age in humans.

5.5.1.3.5 DHPR β1a

As with RyR1 and α_{1s} expression discussed above, the β_{1a} subunit expression shows a general pattern of no difference between the age groups of human donors (**Figures 5.6 and 5.8**) with one exception. The muscle homogenate from vastus medialis showed a larger β_{1a} expression in the ≥60yr age group (**Figure 5.6D**). When the female and male donors for this muscle are considered separately, the female muscle homogenate shows a similar significantly larger β_{1a} expression in the older age group (**Figure 5.8C**) and the although the male muscle homogenate showed no significant difference, there was a trend toward a higher expression in the older age group (**Figure 5.8E**). As the vastus medialis was the only muscle showing this increase in β_{1a} expression, and it contains higher percentage fast-twitch fibers, it may be that the increase in β_{1a} expression seen in this muscle with age is fiber type related. However, the study by Taylor et al (Taylor et al. 2009) showing an increase in β_{1a} expression with age in mice found the increase in expression less pronounced in tibialis anterior and EDL muscles which contain only fast twitch muscle. When β_{1a} expression was correlated with age in the work described in this thesis, there was no significant correlation found when the muscle data was combined (**Figure 5.12A**) or when the data from different muscles were correlated separately (**Figure 5.12B-D**). Even in the vastus medialis there was no significant correlation between age and β_{1a} expression (**Figure**

5.12D). These results together suggest that in contrast to the results found in mice by Taylor et al, there is no change in β_{1a} expression with age in humans. However, further investigation into this matter involving larger sample sizes is warranted because the vastus medialis results indicate possible differences between fiber types in β_{1a} expression with age.

5.5.1.3.6 FKBP12

FKBP12 expression in muscle homogenates shows a general pattern of increased expression in the ≥60yr age group (**Figure 5.6 and 5.8**). The vastus medialis muscle homogenate does not show a significant difference between the <60 and ≥60yr age groups, but there is a trend towards a larger FKBP12 expression in the older age group (**Figure 5.6D**). The standard error of the mean (sem) is larger for this data set showing more variability in the data and may be why the difference is not significant. When the male and female donors are considered separately, there is again a loss in significance in the difference between the age groups in male gluteus minimus and male vastus medialis donors (**Figure 5.8D&E**), but both these groups show a trend towards a larger FKBP12 expression and the small sample size in addition to the larger sem may be why the difference is not significant in these two groups. Interestingly, FKBP12 inhibits the mTOR signalling pathway in muscle, which is involved in muscle growth (Kang et al. 2008; Schiaffino et al. 2013). An increased FKBP12 expression in aging muscle may therefore contribute to the reduction in muscle mass observed in aging muscle.

However, the when FKBP12 expression is considered over the individual ages, in the combined muscle data as well as the data from the muscles considered individually, there is no significant correlation between FKBP12 expression and age (**Figure 5.13**). Again this may be due to the variability in the data. However, the significant differences in the average data suggest that the question merit further investigation with a larger sample size to determine the effect of aging on FKBP12 expression.

5.5.1.3.7 The FKBP12/RyR1 ratio

Not all of the FKBP12 present in muscle homogenate is associated with the RyR1 as FKBP12 is involved in various cellular pathways (Kang et al. 2008). In an attempt to investigate the level of FKBP12 associated with RyR1, the level of FKBP12 expression in microsomal vesicles relative to the expression of RyR1 in microsomal vesicles was investigated. As there is an increase in oxidation and S-nitrosylation of RyR1 in aging muscle which could lead to dissociation of FKBP12 from RyR1 (Andersson et al. 2011), a decreased FKBP12/RyR1 ratio might be expected in aging muscle.

When the average FKBP12/RyR1 expression ratio in human muscle microsomal vesicles were compared between <60yr aged donors and ≥60yr old donors, a general pattern of a smaller FKBP12/RyR1 ratio in the older age group emerged. This was the case when the data from the three muscles were combined as well as considered separately (**Figure 5.7**). Separating the data from male and female donors for each muscle showed similar results when the <60yr old donors were compared with ≥60yr old donors (**Figure 5.9**). Although the microsomal vesicles from male gluteus minimus and male vastus medialis showed no significant difference, the male vastus medialis data also showed a trend towards a lower FKBP12/RyR1 ratio in the older age group. These results are consistent with the hypothesis that there is less FKBP12 associated with RyR1 in aging muscle. However, when the FKBP12/RyR1 ratio was plotted against the age of the respective donors, no significant correlation was observed either in the combined data from all three muscles or when the data from each muscle was correlated separately (**Figure 5.16**). However the significant differences between the average data for the two age groups again point towards a need for further investigation into this matter.

5.5.1.4 Gender differences in protein expression levels and ratios

The data obtained from the muscle homogenate and microsomal vesicle immunoblots were also compared between male and female donors to investigate whether there was a difference in protein expression between the genders.

In the combined data from all three muscles, the male donor muscle homogenate showed a significantly larger RyR1, DHPR α_{1s}, and DHPR β_{1a} expression level compared to the female muscle homogenates (**Figure 5.17**). However, when the data from the three muscles were considered separately, no significant difference was observed between male and female donors with the exception of the β1a subunit expression level in gluteus medius and gluteus minimus. In the gluteus medius muscle homogenate there was a significantly lower expression of β_{1a} in the male donor compared to the female donors (**Figure 5.17B**). Seeing that there is only one male donor of gluteus medius muscle, the sample size is not large enough for the differences in protein expression between male and female donors of gluteus medius to be significant. The gluteus minimus muscle homogenate showed the same significantly larger β_{1a} expression in male donors that was observed when the data from all three muscles were combined (**Figure 5.17C**).

When the data from each muscle were separated into <60yr old donors and ≥60yr old donors and the expression levels of the proteins compared between the male and female donors (**Figure 5.19**), the sample sizes become too small for most of the differences seen in the combine muscle data to be significant. Once again the gluteus medius sample size is too small to contribute

significantly to the question of whether there is a difference in male and female donor protein expression.

In comparing male and female donor expression ratios in microsomal vesicles, a significantly larger α_{1s}/RyR1 ratio is observed in male donors when the data from all three muscles are combined (**Figure 5.18A**). When the muscles are considered separately, the gluteus minimus donor microsomal vesicles show a similar greater α_{1s}/RyR1 ratio in male donors (**Figure 5.18C**) and although the difference isn't significant, the α_{1s}/RyR1 ratio in male vastus medialis microsomal vesicles showed a trend towards a higher expression ratio (**Figure 5.18D**). Once more the gluteus medius muscle sample size was too small to be included gender differences in protein expression in this muscle. When the data from the microsomal vesicles of each muscle were grouped into <60yr and ≥60yr old donors and the expression ratios compared between male and female donors (**Figure 5.21**), the sample size of each group once more was too small to provide meaningful information.

5.5.1.5 Muscle differences in protein expression levels and ratios

The average expression levels of each of the proteins investigated were compared between the three muscles to investigate whether the muscle source would have an effect on the observed expression level of each protein. This was done for the data obtained from muscle homogenates as well as microsomal vesicles.

In the muscle homogenates, the vastus medialis muscle exhibited a significantly greater RyR1 and α1s expression level compared to the gluteal muscles (**Figure 5.21A**). Seeing that vastus medialis has a larger percentage fast-twitch fibers than slow-twitch, and that fast-twitch fibers generally have a larger and more developed SR and t-tubular network (Schiaffino and Reggiani 2011), the larger RyR1 and α_{1s} expression levels in vastus medialis is probably due to the fiber type composition of the muscle. Interestingly, there was no difference in the β_{1a} expression levels between the muscles even though it forms part of the DHPR in the skeletal muscle CRU and is essential for the formation of tetrads. This is consistent with the lower than expected correlation between the α_{1s} and β_{1a} expression levels discussed in section 5.3.1.2. The fact that there is no significant difference in β_{1a} and FKBP12 expression levels between the three muscles also suggests that the expression of these proteins are not fiber type dependent.

In the microsomal vesicles, there was no significant difference in the α_{1s}/RyR1 expression ratio between the three muscles (**Figure 5.21B**). The higher fast-twitch content in vastus medialis therefore did not show a larger α_{1s}/RyR1 ratio compared to the gluteal muscles which have a higher slow-twitch content. This is in contrast to the Renganathan et al study on rat muscle

(Renganathan et al. 1997) in which they found a higher α1s/RyR1 ratio in fast twitch muscle (EDL) compared to slow twitch muscle (soleus).

The microsomal vesicles from vastus medialis did, however, show a significantly larger α_{1c}/RyR1 ratio and significantly lower FKBP12/RyR1 ratio compared to gluteus minimus (**Figure 5.21B**). This may also be attributed to the fiber type composition difference between the muscles. The effect of fiber type on protein expression will be discussed further in section 5.3.1.6 below.

5.5.1.6 The effect of fiber type distribution on protein expression levels and ratios

In order to investigate whether the fiber type composition of the samples from the donors had an effect on the protein expression levels and ratios investigated, the average RyR1, DHPR α_{1s}, DHPR β1 and FKBP12 expression level as well as the α_{1s}/RyR1, α_{1c}/RyR1 and FKBP12/RyR1 expression ratios for each donor sample were correlated to the percentage type1, type 2A and type 2X fibers present in the sample.

The significant positive correlation between the RyR1 (R=0.521) and α_{1s} (R=0.382) expression levels and the percentage type 2X fibers in the muscle samples (**Figures 5.22 and 5.23**) is consistent with the suggestion that the greater expression of these two proteins seen in vastus medialis is related to fiber type composition. The lack of significant correlation with β_{1a} and FKBP12 expression levels and fiber type (**Figures 5.24 and 5.25**) is also consistent with the suggestion that the β_{1a} and FKBP12 expression levels are not related to fiber type.

There was no significant correlation between the fiber type composition of the muscle samples and the α_{1s}/RyR1 or FKBP12/RyR1 expression ratios in microsomal vesicles (**Figures 5.26 and 28**). The significantly lower FKBP12/RyR1 ratio seen in vastus medialis compared to gluteus minimus therefore is not due to fiber type composition. However, there was a moderate significant positive correlation (R=0.316, R^2=0.10) between the percentage type 2X fibers in the muscle samples and the α_{1c}/RyR1 ratio (**Figure 5.27**), which indicates that the larger α_{1c}/RyR1 ratio observed in vastus medialis microsomal vesicles compared to gluteus minimus may also be due to the fiber type composition of the muscle. This in contrast to a study by Pereon et al showing a less intense immunohistochemical α_{1c} response in rat EDL compared to soleus and diaphragm (Pereon et al. 1998). Fast-twitch muscle has a more developed t-tubular network than slow-twitch muscle and has more DHPR as a result. It may be that if a certain percentage of the DHPR present in muscle is of the cardiac type, it may result in the fast-twitch fibers having a larger level of α_{1c} present due it having more DHPR to begin with.

5.5.2 Rat muscle

5.5.2.1 Muscle samples

In the time constraints for the work described in this chapter, there was not time for rats to be maintained for sufficient time to fall into the senescent age group. The decision to use rats in this study was made in the light of the variability in the human data and was thus made in the latter stages of the study. As a result the rats used here only reached an age of about 1yr, however other rats have been retained for a further 6 to 8 months and will be studied in the next year. The choice of 5wk old rats was made based on availability at the time. All the rats used in this study were male.

The 5wk old rats are not adult rats and therefore represent a juvenile age group, whereas the 1year old rats would be consistent with middle aged humans (Quinn 2005) and therefore represent an adult age group and not a senescent age group.

5.5.2.2 Correlations between RyR1, DHPR α_{1s} and DHPR β_{1a}

The expression levels of RyR1, α_{1s} and β_{1a} in rat muscle homogenate (indicated by the average density of the protein bands obtained with immunoblots normalised to total protein) were correlated with each other.

As with human muscle homogenate, the expected strong significant positive correlation between the DHPR α_{1s} expression level and that of the RyR1 ($R=0.710$, $R^2=0.50$) was observed in rat muscle homogenate. However, the DHPR β_{1a} expression level showed a surprizinglymoderate significant negative correlation with the RyR1 ($R=-0.395$, $R^2=0.16$) and DHPR α_{1s} ($R=-0.420$, $R^2=0.18$) expression levels. This indicates that the more α_{1s} is present in the muscle homogenate, the less β_{1a} is present and vice versa. Although this result is in contrast to the correlation found between the DHPR subunits in human muscle discussed in section 5.3.1.2, a study by Taylor et al showed a similar inverse relationship between α_{1s} and β_{1a} in mice (Taylor et al. 2009). When the β_{1a} subunit was overexpressed, the α_{1s} expression decreased.

Clearly, the expression of the DHPR subunits show different patterns in humans and rodents indicating again that caution is required when extrapolating results obtained in rodents to humans.

5.5.2.3 The effect of age on protein expression levels and ratios

As there is no senescent age group in the rats the muscle was sourced from, this section will not be about the changes in protein expression within aging muscle. However, the results show

differences in expression between juvenile rat muscle and "middle aged" adult rat muscle. The protein expression levels and ratios in soleus and EDL muscle homogenates and microsomal vesicles were compared between the 5wk and 1yr old rats.

There was no difference in RyR1 expression levels between the age groups in either soleus or EDL but both muscles showed a trend towards a higher RyR1 expression in 1yr old rats. The α_{1s} expression level was significantly larger in the 1yr old rats in both these muscles (**Figure 5.30A-B**). The α_{1s}/RyR1 expression ratio in the microsomal vesicles prepared from the soleus and EDL muscles also show a significantly larger ratio in 1yr old rats compared to 5wk (**Figure 5.31A-B**). The larger in α_{1s} expression in 1yr old rats is probably due to the more developed t-tubular network in adult muscle (Luff and Atwood 1971; Baldwin 1984; Takekura et al. 1994).

Interestingly, the β_{1a} expression level in muscle homogenate from soleus and EDL muscle was significantly lower in 1yr old rats compared to 5wk. This is in contrast with the findings of the study by Taylor et al that showed an increase in β_{1a} expression across the lifespan of mice (Taylor et al. 2009). The study does not investigate the α_{1s} expression in these mice over the same time period so it is not known whether the expression of the α_{1s} decreased as the β_{1a} expression increased across the lifespan of the mice. They do, however, show that the over expression of β_{1a} decreases α_{1s} expression in adult mice. The exact relationship between α_{1s} and β_{1a} expression levels in different mammalian species remains unclear and suggests that there may be significant differences even among rodents.

The FKBP12 expression levels remained unchanged in the soleus muscle between 5wk and 1yr old rats (**Figure 5.30A**), however, FKBP12 expression was significantly lower in 1yr old EDL muscle homogenate (**Figure 5.30B**). The implications of the lower FKBP12 expression in the adult EDL muscle remains unclear as FKBP12 is involved in a number of cellular signalling pathways. The FKBP12 associated with RyR1 seems to be reduced as well as the FKBP12/RyR1 ratio in 1yr old EDL is significantly lower than 5wk old EDL (**Figure 5.31B**). Although there was no significant difference in the soleus FKBP12/RyR1 ratio between the age groups, there was a trend towards a lower ratio in the 1yr old rats (**Figure 5.31A**). This may suggests that the RyR1 in the 1yr old rats are already more oxidized and S-nitrosylated than the RyR1 in 5wk old rats causing a dissociation of some of the FKBP12 from RyR1.

5.5.2.4 Muscle differences in protein expression levels and ratios

The protein expression levels and ratios in the 5wk and 1yr old rats muscle homogenates and microsomal vesicles were compared between soleus and EDL.

As expected there were significantly larger levels of RyR1 and α_{1s} in the EDL of both age groups compared to the soleus (**Figure 5.30C-D**). This is consistent with the larger and more developed SR and t-tubular network present in fast-twitch fibers compared to slow-twitch fibers (Flucher 1992; Schiaffino and Reggiani 2011). The 5wk old rats showed a significantly larger α_{1s}/RyR1 ratio in EDL muscle, but that difference is no longer present in the 1yr old rats (**Figure 5.31C-D**).

The higher level of α_{1c} present in EDL muscle of 1yr old rats (**Figure 5.31D**) is in contrast to a study by Pereon et al showing a less intense immunohistochemical α_{1c} response in adult rat EDL compared to soleus and diaphragm (Pereon et al. 1998). As discussed in section 5.3.1.6, it may be that if a certain percentage of the DHPR present in muscle is of the cardiac type, the more developed t-tubular network present in fast-twitch muscle with a larger amount of DHPR present may therefore have a larger level of α_{1c} present than slow-twitch which has less DHPR to begin with.

The significantly lower β_{1a} expression level observed in the EDL muscle homogenates from both age groups (**Figure 5.30C-D**) seems to be consistent with the increased α_{1s} expression observed in the EDL of both age groups as well as the negative correlation between the α_{1s} and β_{1a} expression levels. Therefore the higher α_{1s} expression in EDL coincides with a lower expression of β_{1a} in this muscle.

There was no difference in the FKBP12 expression levels or FKBP12/RyR1 expression ratio between soleus and EDL muscle in either age group (**Figure 5.30C-D and 5.31C-D**). This seems to suggest that FKBP12 expression and association with RyR1is not affected by the fiber type or source of the muscle in rats and is consistent with the correlations between FKBP12 expression and FKBP12/RyR1 ratio with fiber type composition done on human muscle discussed in section 5.3.1.6 that found no correlation.

5.6 Conclusion

The investigation into changes of EC coupling proteins with age in human muscle has shown no change in expression of the proteins with age in humans. Differences in protein expression in rodents and humans that came to light in this study emphasises once more the importance of caution in extrapolating data obtained in studies with rodent to humans.

Chapter 6: The response of RyR1 ASI splice variants to DHPR β_{1a} in lipid bilayers

6.1 Introduction

The RyR1 undergoes alternative splicing in two regions, namely alternatively spliced region I (ASI) and alternative spliced region II (ASII) (Zorzato et al. 1994; Futatsugi et al. 1995) as discussed in Chapter 4. The ASI region is of interest as it is located close to a cluster of positively charged residues (3495-3502) identified as a possible direct interaction site between the C –terminus of the β_{1a} subunit and the RyR1 see (Cheng et al. 2005). Peptides corresponding the 35 most distal residues of the β_{1a} C-terminus (490-524) bind to native RyR1 in SR vesicles and the peptides as well as the full length β_{1a} subunit also activate RyR1 directly in lipid bilayer and [^{3}H]ryanodine binding assays (Rebbeck et al. 2011; Karunasekara et al. 2012).

The ASI splice variants differ with respect to 5 amino acids, Ala^{3481}-Gln^{3485}, that are either present (ASI(+)RyR1) or absent (ASI(-)RyR1) (Futatsugi et al. 1995). Analysis of splicing patterns by Futatsugi et al. revealed a molar ratio of ASI(+):ASI(-) to be roughly 3:1 in adult mouse skeletal muscle (Futatsugi et al. 1995). Kimura et al performed functional studies on the ASI splice variants using [^{3}H]ryanodine binding and lipid bilayer techniques (Kimura et al. 2005). They found the channel activity of ASI(-)RyR1 to be less than that of ASI(+)RyR1, but that their biphasic Ca^{2+} dependence of ryanodine binding was similar. In lipid bilayers, the open probability of ASI(-)RyR1 was lower than ASI(+)RyR1. They also showed, in RyR1-null myotubes expressing ASI(-) or ASI(+) RyR1, that caffeine induced Ca^{2+} release through ASI(+)RyR1 and ASI(-)RyR1 was similar but that there was a significantly higher incidence of Ca^{2+} oscillations in ASI(+)RyR1 during the application of 10mM caffeine. These results are indicative of a less active ASI(-)RyR1 channel (Kimura et al. 2005).

In a subsequent study, Kimura et al investigated the effects of the ASI region on EC coupling. Recording Ca^{2+} currents through the DHPR and Ca^{2+} release from the SR under voltage clamp conditions in dyspedic (RyR1-null) myotubes expressing either ASI(+)RyR1 or ASI(-)RyR1 (Kimura et al. 2009). They found that voltage-induced Ca^{2+} release during EC coupling was significantly increased in the ASI(-)RyR1 expressing myotubes. The magnitude and voltage dependence of the L-type currents were similar in ASI(-)RyR1 and ASI(+)RyR1 expressing myotubes as well as wild type myotubes (endogenously expressing RyR1). This result indicates

that DHPR expression and RyR1 association are similar for ASI(+)RyR1 and ASI(-)RyR1. Kimura et al then tested SR Ca^{2+} content and Ca^{2+} release from the SR in ASI(+)RyR1 and ASI(-)RyR1 expressing dyspedic myotubes. The authors used another RyR1 specific agonist, 4-choloro-m-cresol (4-cmc) to induce Ca^{2+} release from the SR. They found that in contrast to voltage-induced Ca^{2+} release (EC coupling), 4-cmc induced Ca^{2+} release was significantly reduced in ASI(-)RyR1 expressing myotubes. Together these results suggest that the two splice variants respond differently to two types of triggers. Exogenous triggers (caffeine and 4-cmc) elicit a decreased response from ASI(-)RyR1 compared to ASI(+)RyR1, whereas the endogenous DHPR-mediated depolarization-dependent trigger evoked an increased response in ASI(-)RyR1 compared to ASI(+)RyR1.

Because the β_{1a} subunit activates RyR1 in lipid bilayer studies, and the possible β_{1a} binding site close to the ASI region on the RyR1 it was interesting to see whether there is a difference in activation of the RyR1 ASI splice variants by the β_{1a} subunit in lipid bilayers.

6.2 Aim

To investigate the response of ASI(+)RyR1 and ASI(-)RyR1 recombinant channels to 10nM and 50nM full length recombinant DHPR β_{1a} subunit in the presence of 10μM Ca^{2+} (see Sections 2.1 – 2.8 for preparation of recombinant proteins).

6.3 Results

6.3.1 Establishing that an ion channel is a RyR1

The response of RyR1 to Ca^{2+} concentration, ATP and ruthenium red have been well established and can be used to confirm of the identity and orientation of channels in lipid bilayers (Meissner 1994). In the work described in this chapter, the response of channel activity to the change of the free Ca^{2+} concentration of the *cis* solution from 1mM to 10μM was used to confirm that the channel was a RyR1 as well as its correct orientation in the bilayer. When the *cis* Ca^{2+} concentration is reduced from 1 mM to 10μM an increase in channel activity is expected as 1 mM Ca^{2+} inhibits RyR1, while 10μM Ca^{2+} is a maximally activating concentration (Meissner et al. 1986; Smith et al. 1986; Smith et al. 1988) (also see Section 1.5.4.1). At the end of the experiment, the sequential addition of ATP and ruthenium red further confirmed the identity and orientation of the channel. The addition of ATP to the *cis* solution should increase RyR1 channel activity if the cytoplasmic side of the channel faces the *cis* solution (Meissner et al. 1986; Smith et al. 1986; Smith et al. 1988) (also see Section 1.5.4.1) and ruthenium red added to the *cis* solution should inhibit the RyR1 channel activity (Smith et al. 1988; Ma 1993) (also see

Section 1.5.4). If ruthenium red is added to the cytoplasmic side of the RyR1 it causes a fast flicker block of the channel, whereas its addition to the luminal side of the RyR1 causes a reduction in single channel amplitude (Ma 1993). As ruthenium red irreversibly inhibits the RyR1, it is added at the end of the experiment. **Figure 6.1** shows the representative channel traces for each condition described above.

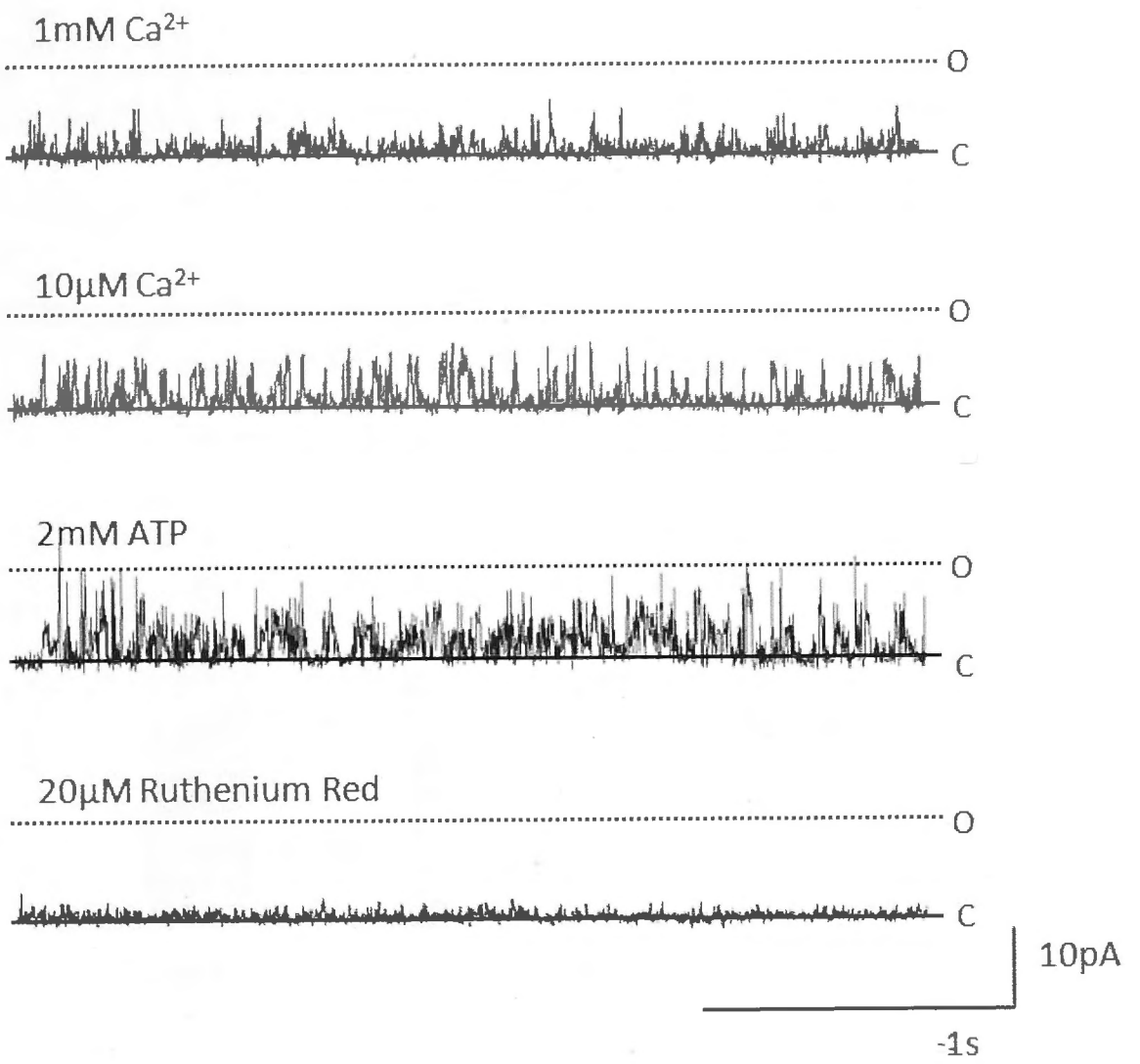

Figure 6.1: Representative channel traces showing RyR1 activity in conditions used to confirm the identity of the channel. (C – indicates level when channel is closed, O – indicates level when channel is fully open)

6.3.2 Response of RyR1 to buffer solution

Previous studies involving the response of RyR1 to the full length recombinant DHPR β_{1a} subunit (Karunasekara 2011; Rebbeck et al. 2011) used a buffer exchange protocol in order to change the β_{1a} phosphate buffer to the *cis* solution, as high concentrations of β_{1a} requiring significant volumes of stock solution were tested. As very small volumes of β_{1a} solution were added to the *cis* solution in this study, the buffer was not changed. To ensure that the buffer solution alone did not affect RyR1 channel activity, volumes of buffer equivalent to the volumes added with β_{1a} were added to the *cis* solution and RyR1 channel activity recorded and analysed (as described in Section 2.2.15). Due to the difficulty experienced in getting recombinant channel incorporation, native RyR1 (SR microsomal vesicles) isolated from rabbit muscle (as described in Section 2.2.11) were used for these control experiments. Representative traces of each condition as well as the mean P_o for each condition is shown in **Figure 6.2A-B** and **Table 6.1**.

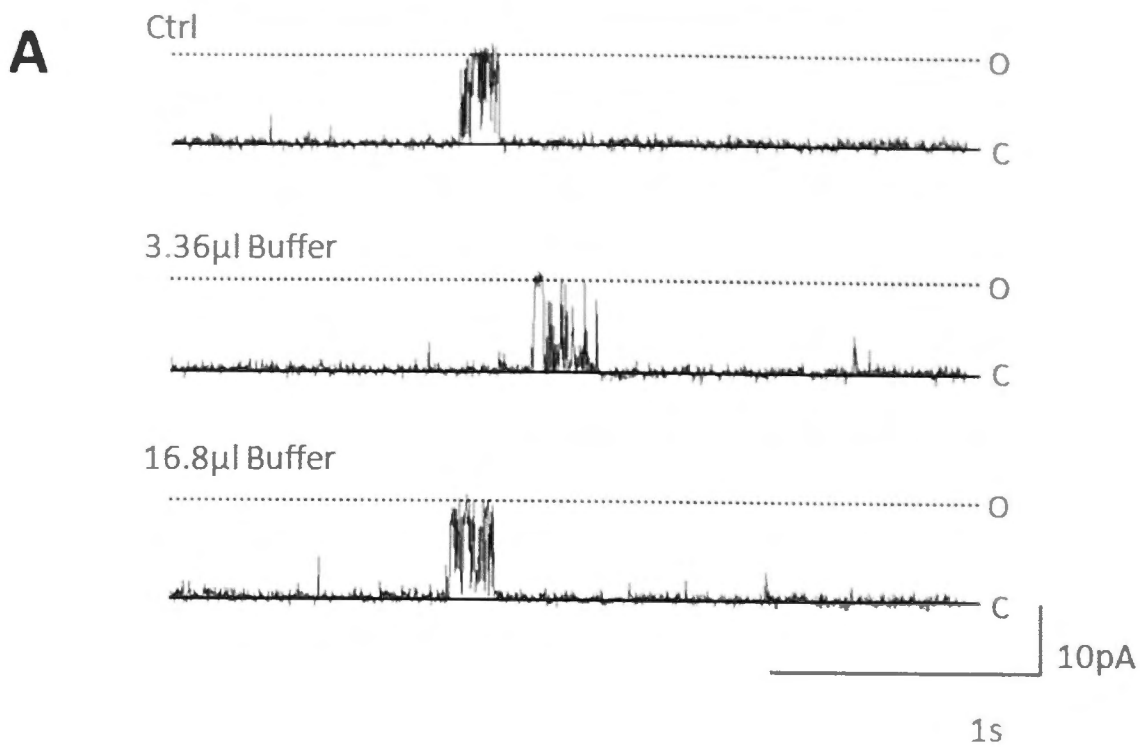

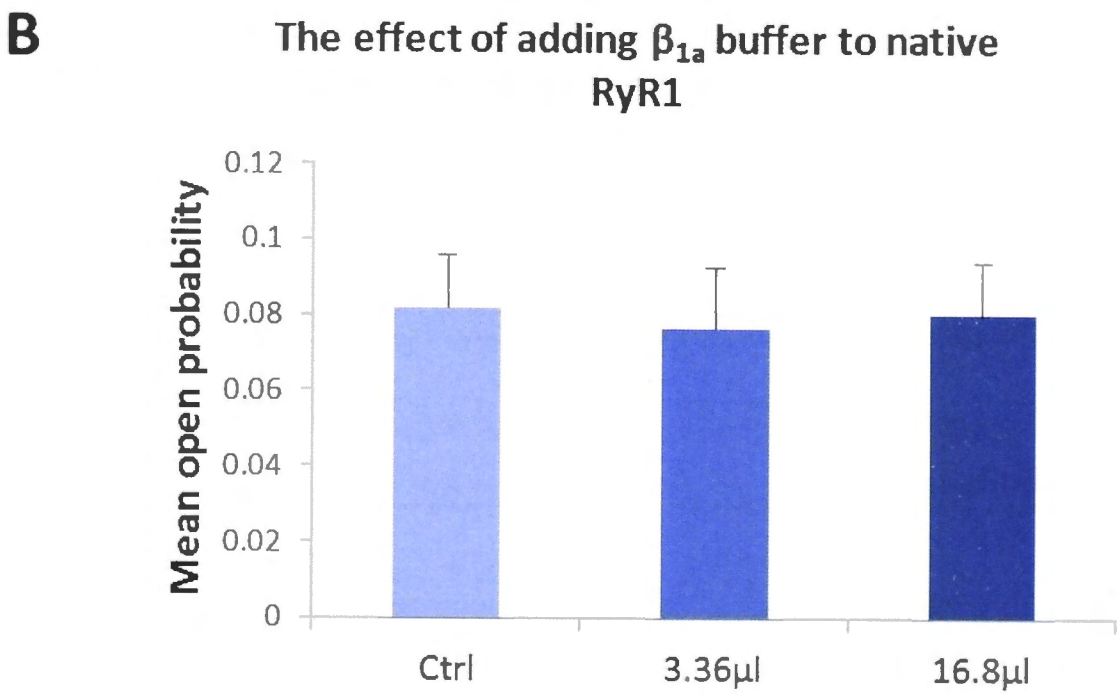

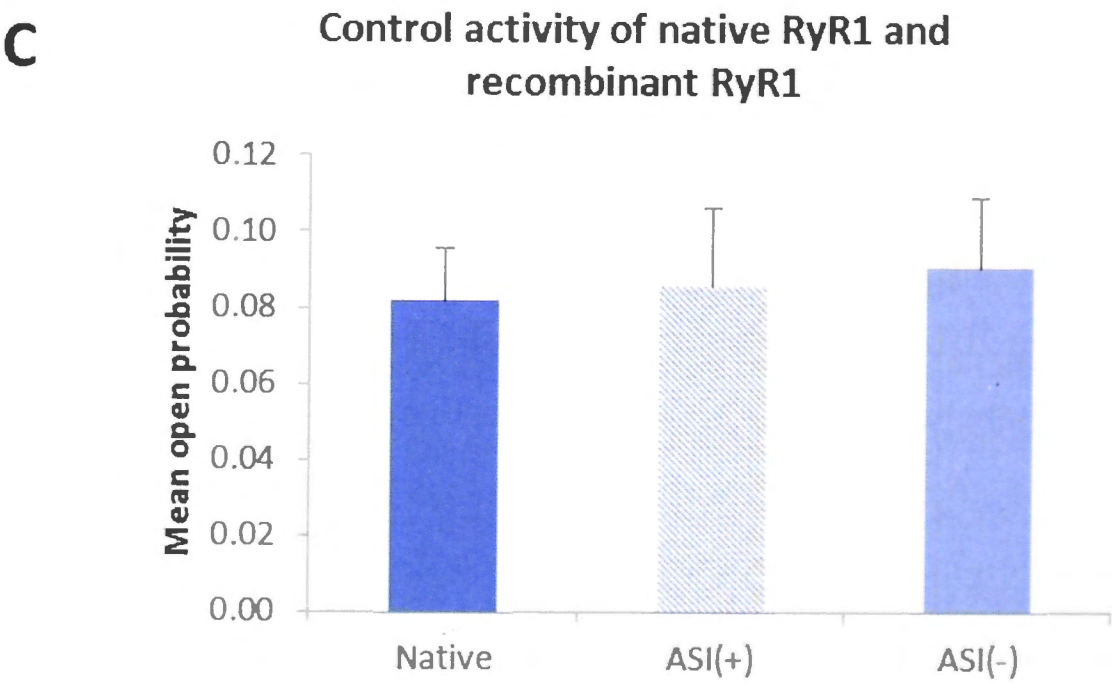

Figure 6.2: The addition of equivalent volumes of the β_{1a} buffer alone has no effect on RyR1 channel activity. (**A**) Representative channel traces of ctrl activity, activity after the addition of 3.36µl buffer (volume of β_{1a} solution added to *cis* chamber when 10nM β_{1a} is added) , and activity after the addition of a total volume of 16.8µl buffer (total volume of β_{1a} solution added to *cis* chamber after the concentration of β_{1a} is increased to 50nM). (**B**) The mean open probability for each condition (n=10). (**C**) The control channel activity of native RyR1 is not different from that of the recombinant RyR1 control channel activity.

Table 6.1: Mean RyR1 open probability after the addition of β_{1a} buffer to the *cis* chamber (n=10). (sem – standard error of the mean).

Volume Buffer added	0µl		3.36µl		16.8µl	
Channel open probability	mean	±sem	mean	±sem	mean	±sem
	0.082	0.014	0.077	0.016	0.080	0.014

In the 5 experiments performed, there was no statistically significant difference in P_o between +40mV and -40mV for any of the conditions and therefore the P_o data obtained at +40mV and -40mV were combined for each condition respectively giving n=10 observations. The mean control P_o of native RyR1 was compared to the mean control P_o of the recombinant RyR1s and found to be similar (**Figure 6.2C**).

6.3.3 Response of Recombinant channels to the DHPR β_{1a}-subunit

6.3.3.1 Effect of the DHPR β_{1a} subunit on P_o

In order to investigate the response of the RyR1 ASI splice variants to β_{1a} added to the cytoplasmic side of the RyR1 in lipid bilayers, recombinant ASI(+)RyR1 or ASI(-)RyR1 was incorporated into lipid bilayers and exposed to 10nM and 50nM β_{1a} in the *cis* solution. These particular β_{1a} concentrations were used as they have previously been shown to maximally activate native RyR1 in lipid bilayers (Rebbeck et al. 2011). The respective channel activities were analysed and P_o determined (as described in Section 2.2.15). There was no difference in activity recorded between +40mV and -40mV at any stage of the experiment and the data obtained at the +40mV and -40mV were combined for each experiment, giving n=10-12 observations for each condition. The mean P_o values for each condition are given in **Table 6.2** for the two splice variants respectively and representative traces for each condition are given in **Figure 6.3A**.

Table 6.2: The mean P_o of ASI(+)RyR1 and ASI(-)RyR1 before and after the addition of DHPR β_{1a} to the *cis* solution (n=10-12). (sem – standard error of the mean, * significantly different to control)

	Ctrl		10nM β_{1a}		Ctrl		50nM β_{1a}	
	mean	±sem	mean	±sem	mean	±sem	mean	±sem
ASI(+)RyR1	0.085	0.211	0.295 *	0.065	0.111	0.026	0.311 *	0.071
ASI(-)RyR1	0.091	0.019	0.204 *	0.044	0.097	0.022	0.239 *	0.049

10nM and 50nM β1a increased the channel activity of ASI(+)RyR1 as well as ASI(-)RyR1 significantly ($P \leq 0.05$) compared to control activity.

The mean relative P_o for each condition was determined as a log value. The mean $\log_{10}$ relative P_o is the average of the differences between the $\log_{10} P_o$ after the addition of β_{1a} and the $\log_{10} P_o$

before the addition of β_{1a}. The mean relative P_o for each condition is given in **Table 6.3** for the two splice variants respectively and shown graphically in **Figure 6.3B**.

Table 6.3: The mean relative P_o (log rel P_o) of ASI(+)RyR1 and ASI(-)RyR1 after the addition of 10nM and 50nM β1a to the *cis* solution (n=10-12). (sem – standard error of the mean, * significantly different from ASI(-)RyR1)

	10nM β_{1a}		50nM β_{1a}	
	mean	±sem	mean	±sem
ASI(+)RyR1	0.646*	0.083	0.520	0.114
ASI(-)RyR1	0.369	0.063	0.433	0.084

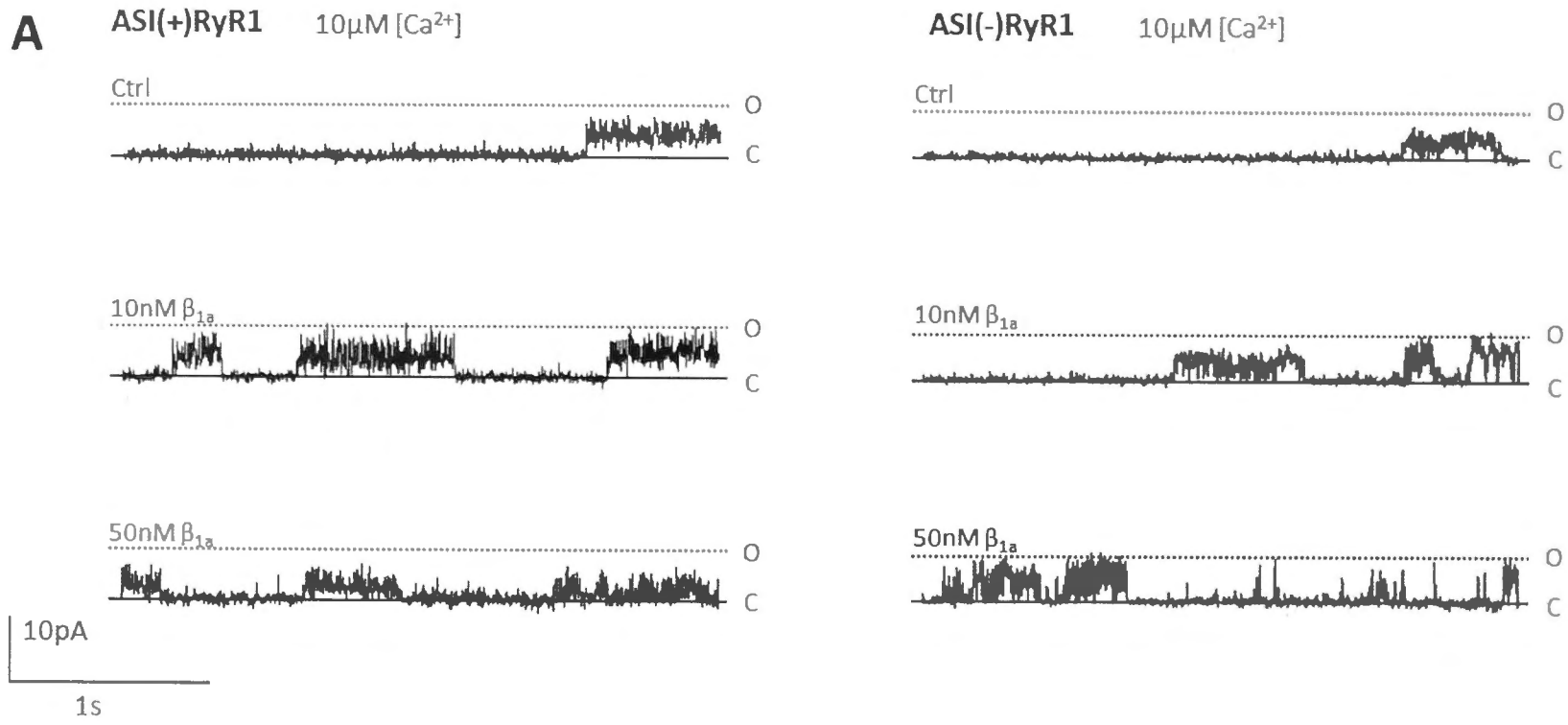

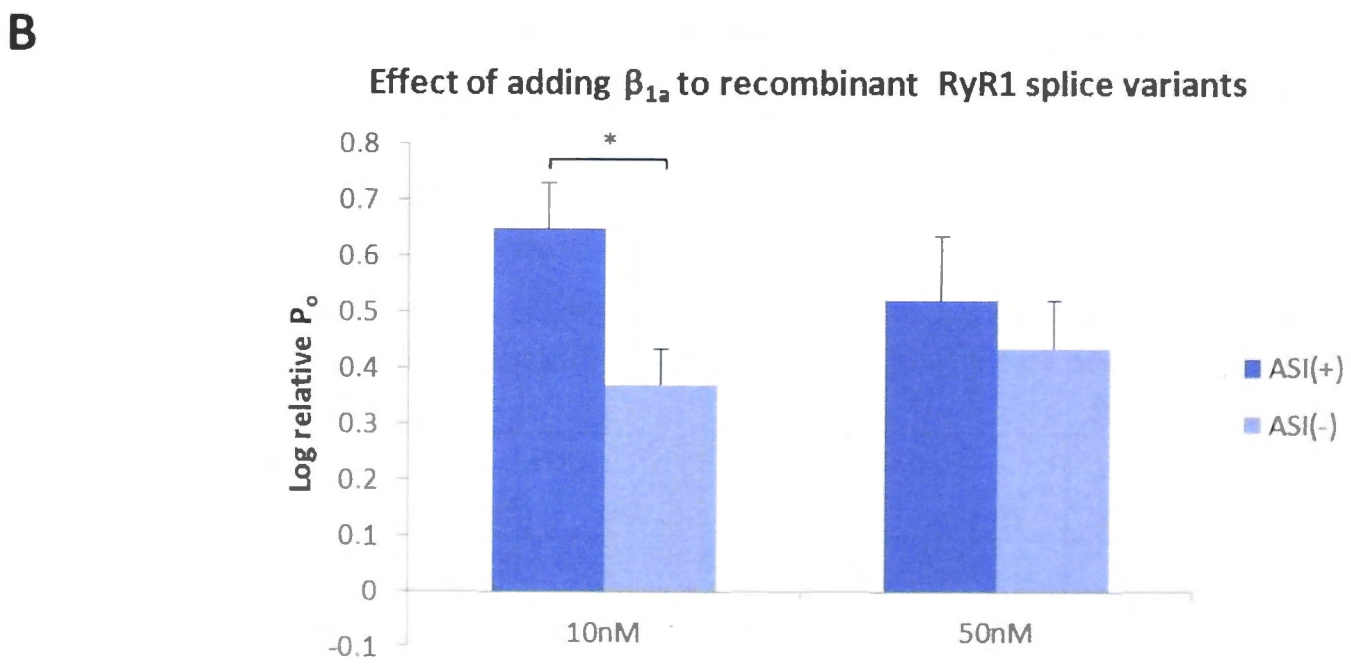

Figure 6.3: The effect of adding DHPR β_{1a} to the recombinant RyR1 ASI splice variants. (**A**) Representative traces of ASI(+)RyR1 (left) and ASI(-)RyR1 (right) showing control activity, activity after the addition of 10nM β1a and activity after the addition of 50nM β1a. (O – level at which channel is fully open, C- level at which channel is closed). (**B**) The mean relative open probability of ASI(+)RyR1 and ASI(-)RyR1 treated with 10nM and 50nM β_{1a} given as the log value. Log relative P_o is the average of differences between the $\log_{10}$ of P_o in the presence of the β_{1a} subunit ($\log P_{oB}$) and $\log_{10}$ of the control P_o ($\log P_{oC}$) for each channel, with P_o measured over 90s. (* significantly different $P \leq 0.05$).

The activation due to the addition of 10nM β_{1a} was significantly larger in ASI(+)RyR1 compared to ASI(-)RyR1. However, this difference in activation is not seen with the addition of 50nM β_{1a} to the splice variants respectively. There was also no difference in the relative P_o between 10nM and 50nM β_{1a} added in either ASI(+)RyR1 or ASI(-)RyR1. More concentrations were not tested due to time constraints. However, the smaller increase in activity at 10nM β_{1a} could indicate a shift in the activation curve for ASI(-)RyR1 to slightly higher β_{1a} concentrations.

6.3.3.2 Effect of the DHPR β_{1a}-subunit on T_o and T_c

Channels from both the recombinant RyR1 ASI splice variants showed simple gating and complex gating (**Figure 6.4**). The mean T_o and T_c can be determined meaningfully for channels showing simple gating, however in the channels showing complex gating with long periods of sub-conductance openings, determining mean T_o and T_c does not give meaningful results. The analysis of the gating properties of these recombinant channels therefore was not possible and is discussed further in Section 7.5.3.

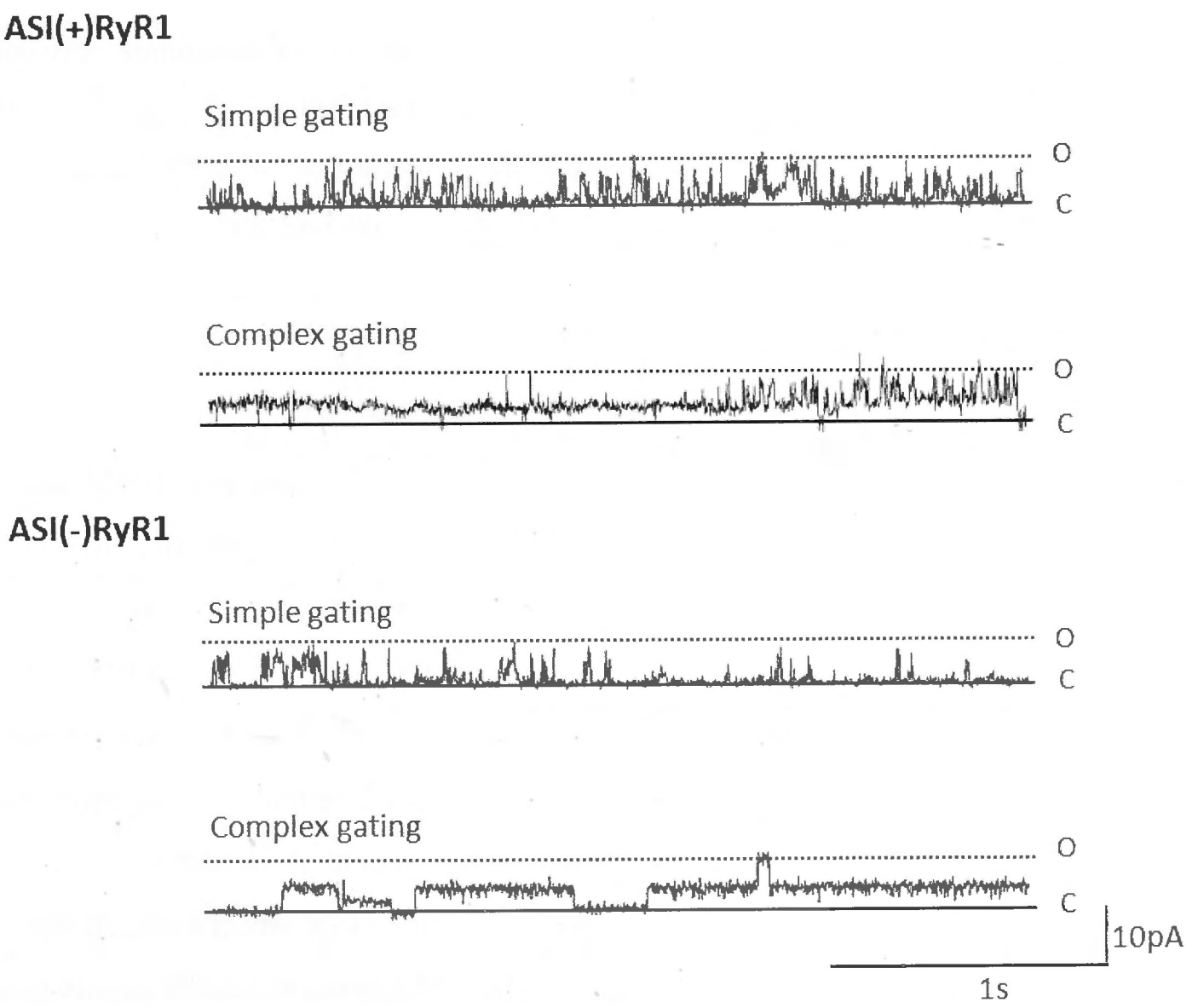

Figure 6.4: Representative traces of ASI(+)RyR1 and ASI(-)RyR1 showing simple and complex gating occurring in both splice variants (O – level at which channel is fully open, C- level at which channel is fully closed).

6.4 Discussion

6.4.1 Control channel activity of recombinant channels

The control channel activity of the recombinant channels was similar to the control activity of native RyR1 under similar conditions (**Figure 6.2C**). There was no difference between the average control open probability of ASI(+)RyR1 and ASI(-)RyR1 (**Table 6.2** and **Figure 6.2C**). This is in contrast to lipid bilayer studies by Kimura et al showing a higher P_o for ASI(+)RyR1 channels than for ASI(-)RyR1 (Kimura et al. 2005). There are several possible reasons for the discrepancy in findings between Kimura et al and the work described in this chapter including the following. Kimura et al recorded channel activity in the presence of 100μM free Ca^{2+} in their *cis* solution, whereas 10μM Ca^{2+} was used in the worked describe in this chapter. The preparation of microsomal vesicles was also different. Kimura et al solubilized the microsomal protein obtained after homogenisation under reducing conditions (with 1mM DTT) using 1.5% CHAPS and purified the RyR1 using sucrose gradient centrifugation after which they reconstituted the RyR1 into proteoliposomes by removing CHAPS through dialysis. In the work described in this chapter, RyR1 was not solubilized or purified and no reducing agent was present in any of the steps. After two centrifugation steps the pellet was resuspended and sonicated briefly. Any or all of these differences in preparation methods as well as differences in free Ca^{2+} concentrations used bilayer experiments could contribute to the difference between findings of Kimura et al and the results discussed in this chapter. Due to the difficulty experienced in incorporation of recombinant channels and time constraints, these differences could not be explored further.

6.4.2 DHPR β_{1a} activation of recombinant channels

The DHPR β_{1a} subunit activated the ASI(+)RyR1 and ASI(-)RyR1 significantly at 10nM and 50nM β_{1a} concentrations with no difference in the level of activation between the two β_{1a} concentrations (**Table 6.2, 6.3** and **Figure 6.3B**). This is consistent with previous findings by Rebbeck et al with native RyR1 showing maximal activation of the channel by the full length β_{1a} subunit as well as a peptide corresponding to the last 35 amino acids of the C-terminal tail of β_{1a} at concentrations ranging from 10-100nM (Rebbeck et al. 2011). The authors suggested that the β_{1a} subunit may contribute to an EC-coupling pathway. Kimura et al showed that ASI(-)RyR1 was activated more during EC coupling than ASI(+)RyR1 (Kimura et al. 2009). Due to the close proximity of a possible β_{1a} binding site to the ASI region, the work in this study was done to investigate a possible difference in activation of ASI(+)RyR1 and ASI(-)RyR1 by the β_{1a} subunit. There was indeed a difference in the level of activation of the ASI splice variants by β_{1a} at a concentration of 10nM with ASI(+)RyR1 activated significantly more than ASI(-)RyR1 (**Table 6.3** and **Figure 6.3B**). The difference in activation level between

ASI(+)RyR1 and ASI(-)RyR1 is not significant at 50nM β_{1a} although there is a trends towards a higher ASI(+)RyR1 relative P_o. Although the higher activation of ASI(+)RyR1 by 10nM β_{1a} is consistent with other agonists of RyR1, caffeine and 4-cmc (Kimura et al. 2005; Kimura et al. 2009), it does not support the hypothesis that the increased activation during EC coupling seen in ASI(-)RyR1 compared to ASI(+)RyR1 may be due to the contribution of the β_{1a} subunit to EC coupling. The sequence difference between ASI(+)RyR1 and ASI(-)RyR1 is 5 residues. This suggests that the direct activation of RyR1 through agonists occurs through a similar mechanism that is different from the mechanisms involved during EC coupling and which causes ASI(+)RyR1 to be activated more than ASI(-)RyR1. In the case of the DHPR mediated activation of the RyR1 during EC coupling it has been suggested that multiple regions of the RyR1 and DHPR are involved, and it may be that the combination of all the sites can produce a different outcome with the ASI splice variants so that the ASI(-)RyR1 is activated more.

Kimura et al investigated the possibility that the ASI region was involved in an inhibitory interdomain interaction with the use of peptides corresponding to the ASI region from $^{3471}T - G^{3500}$ (Kimura et al. 2007). In that study it was found that the peptide corresponding to the ASI(-)RyR1 sequence were more effective in activating both splice variants, but that ASI(-)RyR1 was activated the most. This together with other findings showing a less active ASI(-)RyR1 suggests that the ASI(-)RyR1 has a stronger inhibitory inter domain interaction than ASI(+)RyR1. It seems possible then that the mechanism involved in EC coupling disrupts this inhibitory interdomain interaction giving rise to the higher activation of the ASI(-)RyR1, but that the mechanism involving activation by agonists does not disrupt this inhibitory interaction and activates the RyR1 differently, giving rise to the ASI(+)RyR1 being activated more.

Due to time constraints, more concentrations of β_{1a} were not tested here. However, the smaller increase in activity at 10nM β_{1a} could indicate a shift in the activation curve for ASI(-)RyR1 to slightly higher β_{1a} concentrations. However the difference may be due to the fact that there was also a trend towards reduced activation of ASI(+) with 50nM β_{1a}. It is notable that higher concentrations of β_{1a} tend to produce less activation of native RyR1 under some circumstances (R. Rebbeck, personal communication). Therefore this possible difference in activation by β_{1a} observed between the ASI RyR1 splice variants *in vitro* merits further investigation.

It is important to note that it is not known whether RyR1s in vivo consists of only ASI(+)RyR1 or ASI(-)RyR1 subunits or whether they are hybrids of both splice variants to different degrees. The latter however seems the most likely in the light of results obtained in a study by Xu et al in which they co-expressed a mutant and WT RyR1 in HEK cells (Xu et al. 2008) resulting in heterotetramers RyR1s consisting of WT and mutant subunits. The implications of this will be discussed further in the final discussion chapter (Chapter 7).

6.4.3 Recombinant channel gating

The analysis of the gating properties (T_o and T_c) of the recombinant ASI(+)RyR1 and ASI(-)RyR1 was hindered by the presence of very long substate openings with brief openings to the fully open state in both splice variants (**Figure 6.4**). In vivo the Ca^{2+} flux through the channel during Ca^{2+} release is what is of importance and therefore the fractional mean current (I'f) was used as a measure for channel activity in channels exhibiting this type of gating. An increased conductance due to channels opening more to the fully open state would be reflected in the I'f value whereas the P_o would show only that the channel is open or closed. A more sophisticated analysis of channel gating such as that provided by HMM (Hidden Markov Model) (Chung and Gage 1998) was not considered to be warranted given the small differences observed between the two channel types and time restraints. The substate openings may be due to the absence of FKBP12 associated with the RyR1 and although some FKBP12 expression was detected by immunoblot in transfected HEK cells, it not known whether the FKBP is associated with the RyR1. RyR1 in muscle fibers is also associated with a number of other proteins e.g. CSQ, triadin and junctin, whereas the RyR1s expressed in HEK cells lack these associated proteins and could also contribute to the complex gating observed. Again due to time constraints, this could not be fully investigated and merits further investigation.

6.5 Conclusion

The DHPR β_{1a} subunit activated the recombinant ASI RyR1 splice variants significantly in lipid bilayer studies with the ASI(+)RyR1 isoform showing a higher activation by 10nM β1a than ASI(-)RyR1 isoform. The implications of this difference in ASI RyR1 splice variant activation by β_{1a} observed *in vitro* to differences between activation of ASI splice variants during EC coupling remains unclear and merits further investigation.

Chapter 7: Discussion

7.1 Summary

The work presented in this thesis was performed in an attempt to investigate factors associated with changes in human and rat muscle function with age. Several properties of muscle samples obtained from human and rat donors were analysed. Firstly expression of proteins essential in skeletal muscle type EC coupling was investigated with respect to age. Secondly fiber type distribution in muscles from donors of different ages was investigated, as well as ASI RyR1 splice variant ratios. Finally, the recombinant ASI RyR1 splice variants were expressed in HEK cells and their single channel properties assessed, as well as their response to activation by the recombinant β_{1a} subunit of the DHPR. The principle findings were as follows:

1. Fiber type distribution with age.
    a. *Human*: The human muscles investigated responded differently to age in regard to their fiber type distribution. The gluteus medius and gluteus minimus samples, although both containing a high percentage type 1 fibers, displayed different changes with age. Gluteus medius muscle samples showed an increase in the percentage type 1 fibers with age, whereas there was no change in fiber type distribution with age in gluteus minimus muscle samples. Vastus medialis samples, containing more type 2 fibers than type 1, showed opposite age-related changes in male and female donors to age, with female samples showing an increase in the percentage type 1 fibers in samples from older donors whereas samples from male donors showed a decrease in the percentage type 1 fibers with age.
    b. *Rat*: Not unexpectedly, a general shift towards a more oxidative fiber type distribution was observed in EDL muscles from the 1 year old rats relative to the juvenile 5 week old rats. No change in fiber type distribution was observed in soleus muscles.

2. EC coupling protein expression with age.

    The expression of RyR1, DHPR α_{1s}, DHPR α_{1c}, DHPR β_{1a} and FKBP12 proteins was investigated.

    a. *Human*: No change in expression levels with age was observed in any of the proteins examined in any of the human muscle samples. Differences in the means of α_{1s}/RyR1 and FKBP12/RyR1 ratios were observed between donors <60yr and ≥60yr. Although, no significant correlation was found when these ratios were

plotted against age, the difference between the <60yr and ≥60yr ratios indicates that these aspects merit further investigation. An age-independent positive correlation between the level of RyR1 and α_{1s}, RyR1 and β_{1a} as well as α_{1s} and β_{1a} expression levels were observed. Also independent of age, the level of RyR1 and α_{1s} expression as well as the α_{1c}/RyR1 ratio correlated positively with the percentage type 2X fiber in the muscle samples. In contrast there was no correlation between the β_{1a} and FKBP12 levels or the α_{1a}/RyR1 and FKBP12/RyR1 ratios and fiber type distribution. Notably, the presence of DHPR α_{1c} in adult human skeletal muscle was shown for the first time.

b. *Rat*: Contrary to what has been reported in mice, the level of β_{1a} expression was not higher in 1yr old rats compared to the juvenile 5wk old rats, but was in fact, lower. A positive correlation between the levels of RyR1 and α_{1s} was observed, and negative correlations between RyR1 and β_{1a} as well as α_{1s} and β_{1a} were observed.

3. ASI RyR1 splice variant analysis.

   a. *Human*: There was no correlation between the ASI RyR1 splice variants and age. However, a novel and important finding was that there was a positive correlation between the percentage ASI(+)RyR1 and the percentage type 2 fibers in the human muscle samples as well as a positive correlation between amounts of ASI(-) and fraction of type 1 fibres.

   b. *Rat:* Unfortunately the RYR1 sequence of rat is not known and the primers designed and used in the RT-PCR analysis were unsuccessful. Thus the generality of splice variant distribution across species and in muscle with dominant fiber types could not be examined.

4. Recombinant ASI RyR1 splice variant activation by DHPR β_{1a}.

   Both ASI(+)RyR1 and ASI(-)RYR1 channels were activated significantly by 10nM and 50nM DHPR β_{1a}. No significant difference in activation was observed between 10nM and 50nM β_{1a} for the same splice variant, however, when ASI(+)RyR1 and ASI(-)RyR1 channels were compared, 10nM β_{1a} activated ASI(+)RyR1 channels significantly more than ASI(-)RyR1 channels.

7.2 Muscle diversity

Humans, unlike inbred laboratory animals, show a high level of genetic variation and this necessitates large sample numbers in order to identify differences due to environmental or other factors apart from genetic variation. Most of the previous work involving changes in human muscle with age was performed on vastus lateralis muscle biopsies due to easy access for

voluntary biopsy. In contrast, in the work presented in this thesis, gluteus medius, gluteus minimus and vastus medialis were investigated and the results showed that the different muscles respond differently to age in regard to fiber type distribution. This indicates therefore that not only is there variability between individuals, there is also variability depending on the particular muscle studied. It is therefore important to investigate muscles other than the vastus lateralis when investigating changes in function and strength with age. This could give more insight into the extent to which a muscle's function might influence the level of atrophy and functional loss that may be associated with aging.

7.3 EC coupling protein expression with age

EC uncoupling has been proposed to be one process that contributes to the decay in skeletal muscle force with aging (Delbono et al. 1995). It was suggested from levels of dihydropyridine and ryanodine binding, that the number of RyR1 that were not physically coupled to DHPRs increased with age in rats (Renganathan et al. 1997), and this is consistent with the changes in DHPR activity and Ca^{2+} release from the SR observed in aged human muscle (Delbono et al. 1995). The decrease in DHPR α_{1s} expression with age in rodents has also been confirmed in several other studies (Ryan et al. 2000; Ryan et al. 2003; O'Connell et al. 2008). However, this reduction in DHPR α_{1s} with age was not seen in humans by Ryan et al (Ryan et al. 2003) or in the work described in Chapter 5, where no change in DHPR α_{1s} expression in aged human muscle was found. The changes reported by Delbono et al in DHPR activity and SR Ca^{2+} release in aged human muscle therefore is likely not to be due to reduced expression of DHPR α_{1s} and possibly not due to changes in RyR1/DHPR coupling as RyR1 expression was also unaltered in the aged human muscle examined in the present study and described in Chapter 5. It is possible that different methods used in studying the levels of DHPR and RyR1 could contribute to differences in findings. Ryanodine binding to RyR1 is subject to the activity level of the channel (Chu et al. 1990a) and could influence results. The determination of protein levels by binding of radioligands or immunoblots does not directly measure DHPR/RyR1 coupling and the assumption that all the DHPR detected by these methods are associated with RyR1 could be an overestimation of the actual numbers of coupled RyRs. Whatever the case may be, the mechanism of EC uncoupling cannot be translated from rodents to humans without modification. It may be that in humans other factors such as post-translational modifications of proteins, and also changes in muscle and CRU structure observed in aged muscle (Boncompagni et al. 2006) could account for the changes in DHPR activity and Ca^{2+} release observed by Delbono et al in aged human muscle. In fact the FKBP12/RyR1 disassociation due to oxidation of RyR1 shown by Andersson et al (Andersson et al. 2011), could account for at least some of the reduced Ca^{2+} release observed in aged human muscle. Results discussed in Chapter 5 showed that although there was no significant correlation between age and the

FKBP12/RyR1 ratio in microsomal vesicles from human muscle, there was a significantly lower FKBP12/RyR1 ratio in donors ≥60yr compared to <60yr in all three muscles studied. This suggests that there might be a reduction in the amount of FKBP12 associated with RyR1 in aged muscle, so that this aspect of the RyR macromolecular complex merits further investigation.

The increase in β_{1a} expression over the lifetime of mice shown by Taylor et al (Taylor et al. 2009) was not observed here in humans or rats (Chapter 5). In the human muscle investigated in the work described in this thesis, there was a positive correlation between the expression level of α_{1s} and β_{1a}, which is in contrast to the findings in mice where increased expressions of β_{1a} lead to a decreased α_{1a} level (Taylor et al. 2009). Curiously, a negative correlation between α_{1s} and β_{1a} expression levels was observed in the rat muscle studied here and this is consistent with the mice studied by Taylor et al. The rat results however, differ from the mouse findings in that a decrease in β_{1a} expression was observed in the 1yr old rats compared to the 5wk old rats, whereas Taylor et al found an increase in β_{1a} expression as the mice aged. They found a twofold increase in β_{1a} expression in TA and EDL of 6mo old mice compared to 2mo and a threefold increase in 14 mo compared to 6mo old mice. It seems therefore that the expression of DHPR subunits differs even among rodents and also between rodents and humans, emphasising the importance of caution in applying findings from rodents to human muscle.

7.4 ASI RyR1 splice variant distribution and function

The ASI region has, since its description and characterisation by Futatsugi et al and subsequently by Kimura et al, been thought of as a developmentally spliced region with the ASI(-)RyR1 splice variant being the juvenile isoform and ASI(+)RyR1 being the adult isoform (Futatsugi et al. 1995; Kimura et al. 2005; Kimura et al. 2007; Kimura et al. 2009). The hypothesis in this thesis was that there might be a higher level of ASI(-)RyR1 present in aged muscle. Formulation of this hypothesis was based on the Futatsugi/Kimura observations together with the fact that increased denervation and reinnervation associated with aged muscle leads to higher levels of juvenile isoforms of muscle proteins. The presence of the juvenile isoforms has been attributed to incomplete maturation of regenerated muscle (Dedkov et al. 2001). As shown in Chapter 4, this hypothesis proved to be incorrect. There was no correlation between the percentage ASI(-)RyR1 mRNA present and the age of the human muscle donors. Never-the-less the study led to important insights into the expression of the ASI splice variants.

The investigations by Futatsugi et al and Kimura et al involved muscles consisting predominantly of fast-twitch fibers. These muscles were human vastus lateralis and hindlimb muscle from mice. In these muscles there was a ASI(+)RyR1:ASI(-)RyR1 ratio of 3:1 in adult muscle. In Chapter 4, it was shown for the first time that the levels of ASI(+)RyR1 and

ASI(-)RyR1 transcripts are influenced by the fiber type distribution of three human muscles that had not previously been investigated and having various percentages of fibers of each type. A strong positive correlation was found between the percentage ASI(+)RyR1 transcripts and the percentage type 2 fibers present in the muscle. In the muscle having the highest percentage of fast-twitch fibers (vastus medialis), the correlation with the percentage ASI(+)RyR1 transcripts was the strongest with type 2X fibers, which in humans are the fast glycolytic fibers. This strongly suggests a fiber type specific distribution of the ASI RyR1 splice variants rather than a developmentally spliced region. This was reinforced by the gluteus medius and gluteus minimus muscles, which have predominantly slow-twitch fibers, found to have the highest level of ASI(-)RyR1 transcripts.

It is not known at this stage whether individual muscle fibers contain both splice variants or whether the post transcriptional splicing is regulated in such a way that only one splice variant is present per fibre. It has been shown that some muscle fibres co-express MyHC isoforms and that these fibres show contractile properties intermediate to fibers expressing only one MyHC isoforms (Rivero et al. 1998; Rhee et al. 2004; Cvetko et al. 2012; Lamboley et al. 2013). Individual slow twitch fibers express both isoforms of CSQ while fast twitch fibers express only CSQ1 and it has been suggested that the differential expression of CSQ in fast-and slow-twitch fibers probably facilitates optimal contractile function in the individual fiber types (Lamboley et al. 2013). This could also be true for the ASI RyR1 splice variants. It may also be that the fibers always contain both splice variants, but that it is the ratio between the two that is regulated to facilitate optimal contractile function in the individual fibers. A further level of complexity is added when one considers that the RyR1 is a tetramer and that if both splice variants are present in the fiber, the RyR1s would most likely be a heterotetramer consisting of various combinations of the splice variants. Xu et al showed that the co-expression of WT RyR1 and a mutant RyR1 in HEK cells produced RyR1s that exhibited a range of phenotypes intermediate between the WT phenotype and the mutant, and developed a model in which the detailed characteristics depended on the ratio of WT to mutant subunit present in each tetramer (Xu et al. 2008). This would suggest that if both ASI(+)RyR1 and ASI(-)RyR1 are present in a fiber, that the RyR1s would be heterogeneous with regards to its subunit composition and RyR1 channels would exhibit a range of functional characteristics between that of ASI(+)RyR1 only and ASI(-)RyR1 only.

Kimura et al showed a lower open probability in recombinant ASI(-)RyR1 compared to ASI(+)RyR1 in lipid bilayers in the presence of 100μM Ca^{2+} (Kimura et al. 2005). However the results discussed in Chapter 6 showed no difference in the open probability of the recombinant splice variant channels and the open probability was also similar with the open probability of native RyR1 under similar experimental conditions (10μM Ca^{2+}). In both instances, the Ca^{2+}

concentration reflects the concentration during muscle contraction and not the resting cytoplasmic Ca^{2+} concentration in muscle fibers. In vivo, the low resting cytoplasmic Ca^{2+} concentration of 50-100nM, together with the presence of 1mM Mg^{2+} (Konishi 1998; Hall and Guyton 2011), which strongly inhibits RyR1, would result in the RyR1 having a very low open probability under resting conditions (Meissner et al. 1986; Smith et al. 1986). During EC coupling, RyR1 is activated through a physical interaction with the DHPR. Kimura et al have shown that ASI(-)RyR1 expressing dyspedic myotubes are activated to a greater extent than ASI(+)RyR1 expressing myotubes during EC coupling (Kimura et al. 2009). The cytoplasmic Ca^{2+} concentration rises to levels as high as 20μM during muscle contraction (Hall and Guyton 2011). This is within the Ca^{2+} concentration range used in the experiments discussed in Chapter 6. It is possible that the mechanism involved in activation of the RyR1 during EC coupling causes an increased activation in the ASI(-)RyR1 compared to ASI(+)RyR1. In contrast in the isolated bilayer situation, a different mechanism dominates and determines the greater activation of ASI(+)RyR1 by β_{1a} than ASI(-)RyR1. It is relevant that Rebbeck et al showed that the β_{1a} C-tail peptide containing the last 35 residues of the C-terminal region of β_{1a} had no effect on the RyR1 at 100nM Ca^{2+} and its maximum activation effect on the RyR1 occurred at 1-10μM Ca^{2+} (Rebbeck et al. 2011). If we assume that the β_{1a} subunit plays a role in EC coupling, these findings could be taken together to suggests an initial activation of RyR1 through the EC coupling mechanism when cytoplasmic Ca^{2+} concentration is initially low (100nM) with a subsequent modulation by the β_{1a} as the concentrations of Ca^{2+} increases to micromolar levels. In the initial activation by the EC coupling mechanism, ASI(-)RyR1 is activated more than ASI(+)RyR1, whereas as Ca^{2+} concentration increases the second mechanism dominates so that the ASI(+)RyR1 is activated more than ASI(-)RyR1. Kimura et al suggested a mechanism by which the ASI(-)RyR1 could be activated more during EC coupling. Based on the results of their single channel studies, they hypothesised that the ASI region is involved in an inhibitory interdomain interaction and that the ASI(-)RyR1 inhibitory interaction is stronger than the ASI(+)RyR1 (Kimura et al. 2007; Kimura et al. 2009). A peptide corresponding to the ASI region (including the 5 basic residues thought to interact with β_{1a}) was used to disrupt this inter domain interaction and it was found that the activation by the peptide was strongest in the ASI(-)RyR1. This suggests that the EC coupling activation mechanism could work through a disruption of this stronger interdomain interaction, allowing ASI(-)RyR1 to be activated more during EC coupling when expressed in dyspedic myotubes (Kimura et al. 2009).

There is a significant physiological importance of the ASI(-)RyR1 being activated more through the EC coupling mechanism and the ASI(+)RyR1 activated more through the subsequent modulation mechanism. This is in their differential presence in fast- and slow-twitch fiber as discussed in Chapter 4. Slow-twitch fibers have a less developed and smaller SR than fast twitch fibers (Schiaffino and Reggiani 2011) therefore also have less RyR1 (Renganathan et al.

1997). The increased activation of ASI(-)RyR1, which is present in slow-twitch fibers, during EC coupling may be an adaptation by the muscle to compensate for the reduced Ca^{2+} release capacity. The late EC coupling modulation mechanism that kicks in at micromolar concentrations may be a way that fast-twitch fibers, in which ASI(+)RyR1 is dominantly present, could allow for increased Ca^{2+} release if necessary, when stronger contraction is needed. If individual fibers were to express both splice variants, with the accompanying heterotetrameric RyR1s, this could produce an intermediate response allowing for muscles to be more adaptable to changes in contraction demands. As the correlation between the percentage ASI(+)RyR1 transcripts and type 2X fibers were the strongest (as discussed in Chapter 4), it could also be that the type 2A fibers, which have a metabolism and contractile properties intermediate between type 1 and 2X fibers, have both the splice variants present in various degrees of RyR1 heterotetramers which facilitates its intermediate contractile properties.

7.5 Future directions

7.5.1 Sample selection

Throughout the discussion of results in this thesis, the limited number of samples has been mentioned as a possible cause for statistically insignificant or anomalous results. It would therefore be beneficial for future studies involving human muscle to have larger sample numbers. Not only is sample number a factor to consider, but also the age range of these donors. In the investigation of the effect of age on muscle, an age group that of 20-30yr old donors would serve as a better control group as the <60yr age group used in this thesis.

In addition, a selective screening of donors in terms of their medical history would help in reducing variation in data. For example, anthracyclines, which is a commonly used treatment for various types of cancers can cause muscle fatigue that is not alleviated by a period of rest and is associated with impairment in skeletal muscle function (Morrow et al. 2002; Gilliam and St Clair 2011; Hayward et al. 2013). Muscle fatigue could have many contributing factors, one of which is oxidative stress (Allen et al. 2008) and the RyR1 is susceptible to oxidative modifications (Aracena-Parks et al. 2006) and could potentially be a mechanism whereby anthracyclines could cause muscle fatigue. Due to the fact that the RyR1 is affected by this family of drugs, it would be beneficial to analyse muscle from donors with a history of anthracycline treatment as a separate cohort.

Statins (3-hydroxy-3methylglutaryl coenzyme-A (HMG-CoA) reductase inhibitors) are cholesterol-lowering drugs effective in decreasing low-density lipoprotein (Evans and Rees 2002; Joy and Hegele 2009). They are commonly used and the majority of patients tolerate

statins well, however, up to 10% of patients display muscle-related symptoms including soreness, fatigue, and an increase in circulating levels of muscle specific proteins such as creatine kinase that results in statin-induced myopathy (SIM) (Evans and Rees 2002; Sathasivam and Lecky 2008; Venero and Thompson 2009). The mechanism underlying this condition is still unclear. One theory centres on the potential of statins to modulate intracellular Ca^{2+} homeostasis (Sirvent et al. 2008; Ghatak et al. 2010; Sirvent et al. 2012). The application of statins to healthy human fibers triggers a significant increase in cytoplasmic Ca^{2+} and it has been suggested that the Ca^{2+} release can be from both mitochondria and the SR (Inoue et al. 2003; Sirvent et al. 2005a; Sirvent et al. 2005b; Guis et al. 2006; Metterlein et al. 2010; Sirvent et al. 2012). Mutations in RyR1 have been found to underlie some instances of SIM, specifically malignant hypothermia related mutations (Guis et al. 2006; Metterlein et al. 2010). It would therefore be interesting to analyse muscle from donors treated with statins as a separate cohort.

Exercise history is another example of a factor which could be used in screening for donors. Donors that did extensive training for sport should also be analysed as a separate cohort because training alters muscle composition and physiology (Schiaffino and Reggiani 2011).

7.5.2 FKBP12/RyR1

The results of FKBP12/RyR1 expression ratio in muscle from human donors discussed in Chapter 5 showed some interesting inconsistencies. The comparison of the means of the <60yr and ≥60yr old age groups showed a significantly lower FKBP12/RyR1 ratio in the ≥60yr group when the data from the three muscles were combined as well as when the data from each muscle was considered separately. However, when the FKBP12/RyR1 ratio was plotted against the age of the donors, there was no significant correlation. A repeat of this investigation with a larger donor cohort is merited as the association of FKBP12 with the RyR1 is important for normal RyR activity, Ca^{2+} release and presumably for muscle function (Brillantes et al. 1994; Lamb and Stephenson 1996; Marx et al. 1998; Avila et al. 2003a; Tang et al. 2004). If more RyR1 are not associated with FKBP12 in aged muscle they would have a higher open probability with more substate opening levels. This would lead to an increased cytoplasmic resting Ca^{2+} concentration that could activate Ca^{2+} sensitive proteases such as μ-calpain (Murphy et al. 2012). It could also lead to a reduction in the Ca^{2+} released from the SR during EC coupling due to a reduction in the Ca^{2+} stored in the SR causing reduced muscle function (Andersson et al. 2011). The dissociation of FKBP12 from RyR1 has been implicated in muscle disease. Bellinger et al found an age-dependent increase in S-nitrosylation of RyR1 in a mouse model of Duchenne muscular dystrophy (mdx) that correlated with depletion of FKBP12 from RyR1 and the onset of muscular dystrophy in the mdx mice (Bellinger et al. 2009). They found that the

stabilization of the FKBP12-RyR1 complex improved grip strength and reduced muscle damage in the mdx mice. The FKBP12-RyR1 complex is therefore an important interaction for normal muscle function and dissociation of these proteins has deleterious effects on muscle.

7.5.3 ASI RyR1 splice variants

The level of ASI(+)RyR1 and ASI(-)RyR1 splice variant transcripts has been shown to be correlated with fiber type in Chapter 4. The distribution of ASI splice variants could not be confirmed in rat muscle as the rat sequence for RYR1 was not available on the NCBI databases. Unlike humans, rats have muscles that are fiber type specific such as the EDL, which contains only type 2 fibers. Unfortunately, attempts at splice variant analysis in rats were unsuccessful in the time constraints associated with this project. However, the determination of the rat sequence for RYR1 and RT-PCR of the ASI region in order to determine the ratio of ASI splice variant transcripts in a muscle containing only fast-twitch fibers would be valuable in the confirmation of the results discussed in Chapter 4. Investigating the splice variant transcript ratio in single fibers would shed light on whether a single fiber contains both splice variants or if only one of the two is present.

The activation of the recombinant ASI RyR splice variant channels by the DHPR β_{1a} subunit was investigated in Chapter 6 using lipid bilayer techniques. Concentrations of 10nM and 50nM β_{1a} were added to the channels. A difference in activation at 10nM β_{1a} between the splice variants could possibly suggest a shift in the activation curve for ASI(-)RyR1 by β_{1a} to slightly higher β_{1a}. Repeating these experiments using β_{1a} concentrations lower than 10nM and higher than 50nM would elucidate whether this is the case. The open probability of the recombinant channels before the addition of β_{1a} as shown in chapter 6, was much lower than that reported by Kimura et al (Kimura et al. 2005). There was also no difference in open probability between the splice variants in the results discussed in Chapter 6, in contrast to Kimura et al who reported that ASI(-)RyR1 had a significantly lower open probability than ASI(-)RyR1. A possible reason for the contradicting findings could be the Ca^{2+} concentration at which the investigations were done. Kimura et al used a *cis* free Ca^{2+} concentration of 100μM in their bilayer experiments whereas the experiments discussed in Chapter 6 used a *cis* free Ca^{2+} concentration of 10μM. A repeat of experiments using different Ca^{2+} concentrations would shed some light as to whether the difference in Ca^{2+} concentration was indeed the cause of the different findings by the work discussed in this thesis and Kimura et al. As Mg^{2+} and ATP are both present in the muscle fiber cytoplasm *in vivo* and modulate RyR1 activity (Meissner 1984; Smith et al. 1986; Konishi 1998), it would also be important to repeat the addition of β_{1a} to the recombinant channels under increased physiological ionic conditions with MgATP present. RyR1 is also sensitive to redox potential (Xia et al. 2000; Aracena et al. 2003) and therefore experiments in

which the redox potentials are regulated, as can be achieved with reduced glutathione and oxidized glutathione (GSH:GSSG) ratios, would also be prudent.

Although the bilayer method is the only method to reveal basic mechanisms, it will never be able to mimic the intracellular environment exactly or even remotely. It is therefore important to investigate mechanisms revealed through bilayer experiments in whole cells. It is not possible for example to study EC coupling directly in bilayer experiments as only the SR membrane is represented in the bilayer with an incorporated RyR1. The t-tubular membrane with the DHPR tetrad that would associate with the RyR1 in the triads of skeletal muscle is not present in bilayers. However, the direct effect of ionic conditions, associated proteins and pharmacological agents on RyR1 activity could be determined using the bilayer technique, which could then be further investigated in whole cells. The bilayer technique therefore allows for the simplification of a system in order to facilitate its investigation. If the limitations of this technique is kept in mind and combined with other investigative techniques it is a useful and informative technique for the study of RyR1. It would therefore be important to investigate the role of the DHPR β_{1a} subunit in the modulation of the ASI RyR1 splice variant activity in whole cells. An example of a possible way this could be attempted lies in a study by Garcia et al in which the effect of the β_{1a} subunit on single fibers from mouse flexor digitorum brevis (FDB) was investigated (Garcia et al. 2005). They found that the acute application of β_{1a} subunits increased the amount of Ca^{2+} released by an action potential. FDB is a predominantly fast-twitch muscle, and from the results discussed in Chapter 4, it would probably have predominantly ASI(+)RyR1, however this is still to be confirmed. Similar investigations into the effect of β_{1a} on fibers containing predominantly ASI(-)RyR1 could be attempted.

7.6 Conclusion

In this project an attempt was made to investigate changes in EC coupling protein expression in human muscle with aging . No changes in expression with age was found in the proteins investigated which is in contrast with findings in rodents (Renganathan et al. 1997; Taylor et al. 2009), but consistent with other studies done in humans (Ryan et al. 2003). A novel finding was that the ASI RyR1 splice variants show a fiber type specific distribution. Different RyR1 isoforms in slow and fast-twitch muscle have been shown in fish but not in amphibians, birds or mammals (Franck et al. 1998; Morrissette et al. 2000). Another novel finding was the expression of the cardiac DHPR α_{1c} in adult human skeletal muscle. The expression of the cardiac isoform has been shown in developing and regenerating muscle as well as adult rat soleus and diaphragm (Pereon et al. 1998)

References

Adachi-Akahane, S., L. Cleemann, et al. (1996). "Cross-signaling between L-type Ca2+ channels and ryanodine receptors in rat ventricular myocytes." J Gen Physiol **108**(5): 435-454.

Adams, B. A., T. Tanabe, et al. (1990). "Intramembrane charge movement restored in dysgenic skeletal muscle by injection of dihydropyridine receptor cDNAs." Nature **346**(6284): 569-572.

Agbulut, O., P. Noirez, et al. (2003). "Myosin heavy chain isoforms in postnatal muscle development of mice." Biol Cell **95**(6): 399-406.

Aggarwal, S. K. and R. MacKinnon (1996). "Contribution of the S4 segment to gating charge in the Shaker K+ channel." Neuron **16**(6): 1169-1177.

Aghdasi, B., J. Z. Zhang, et al. (1997). "Multiple classes of sulfhydryls modulate the skeletal muscle Ca2+ release channel." The Journal of biological chemistry **272**(6): 3739-3748.

Ahern, C. A., J. Arikkath, et al. (2001a). "Intramembrane charge movements and excitation-contraction coupling expressed by two-domain fragments of the Ca2+ channel." Proceedings of the National Academy of Sciences of the United States of America **98**(12): 6935-6940.

Ahern, C. A., D. Bhattacharya, et al. (2001b). "A component of excitation-contraction coupling triggered in the absence of the T671-L690 and L720-Q765 regions of the II-III loop of the dihydropyridine receptor alpha(1s) pore subunit." Biophys J **81**(6): 3294-3307.

Ahern, G. P., P. R. Junankar, et al. (1994). "Single channel activity of the ryanodine receptor calcium release channel is modulated by FK-506." FEBS letters **352**(3): 369-374.

Ahern, G. P., P. R. Junankar, et al. (1997). "Subconductance states in single-channel activity of skeletal muscle ryanodine receptors after removal of FKBP12." Biophys J **72**(1): 146-162.

Airey, J. A., C. F. Beck, et al. (1990). "Identification and localization of two triad junctional foot protein isoforms in mature avian fast twitch skeletal muscle." The Journal of biological chemistry **265**(24): 14187-14194.

Ali, S. Z., A. Taguchi, et al. (2003). "Malignant hyperthermia." Best practice & research. Clinical anaesthesiology **17**(4): 519-533.

Allen, D. G., G. D. Lamb, et al. (2008). "Skeletal muscle fatigue: cellular mechanisms." Physiol Rev **88**(1): 287-332.

Allen, D. L., B. C. Harrison, et al. (2001). "Cardiac and skeletal muscle adaptations to voluntary wheel running in the mouse." J Appl Physiol (1985) **90**(5): 1900-1908.

Amador, F. J., S. Liu, et al. (2009). "Crystal structure of type I ryanodine receptor amino-terminal beta-trefoil domain reveals a disease-associated mutation "hot spot" loop." Proc Natl Acad Sci U S A **106**(27): 11040-11044.

Andersen, G., M. C. Orngreen, et al. (2013). "Muscle phenotype in patients with myotonic dystrophy type 1." Muscle & nerve **47**(3): 409-415.

Andersen, J. L., P. Schjerling, et al. (2000). "Muscle, genes and athletic performance." Sci Am **283**(3): 48-55.

Andersson, D. C., M. J. Betzenhauser, et al. (2011). "Ryanodine receptor oxidation causes intracellular calcium leak and muscle weakness in aging." Cell Metab **14**(2): 196-207.

Andonian, M. H. and M. A. Fahim (1987). "Effects of endurance exercise on the morphology of mouse neuromuscular junctions during ageing." Journal of neurocytology **16**(5): 589-599.

Aniansson, A., G. Grimby, et al. (1992). "Compensatory muscle fiber hypertrophy in elderly men." J Appl Physiol (1985) **73**(3): 812-816.

Ansved, T. and L. Larsson (1989). "Effects of ageing on enzyme-histochemical, morphometrical and contractile properties of the soleus muscle in the rat." Journal of the neurological sciences **93**(1): 105-124.

References

Ansved, T. and L. Larsson (1990). "Quantitative and qualitative morphological properties of the soleus motor nerve and the L5 ventral root in young and old rats. Relation to the number of soleus muscle fibers." Journal of the neurological sciences **96**(2-3): 269-282.

Aracena-Parks, P., S. A. Goonasekera, et al. (2006). "Identification of cysteines involved in S-nitrosylation, S-glutathionylation, and oxidation to disulfides in ryanodine receptor type 1." The Journal of biological chemistry **281**(52): 40354-40368.

Aracena, P., G. Sanchez, et al. (2003). "S-glutathionylation decreases Mg2+ inhibition and S-nitrosylation enhances Ca2+ activation of RyR1 channels." The Journal of biological chemistry **278**(44): 42927-42935.

Aracena, P., W. Tang, et al. (2005). "Effects of S-glutathionylation and S-nitrosylation on calmodulin binding to triads and FKBP12 binding to type 1 calcium release channels." Antioxidants & redox signaling **7**(7-8): 870-881.

Ausoni, S., L. Gorza, et al. (1990). "Expression of myosin heavy chain isoforms in stimulated fast and slow rat muscles." J Neurosci **10**(1): 153-160.

Avila, G. and R. T. Dirksen (2000). "Functional impact of the ryanodine receptor on the skeletal muscle L-type Ca(2+) channel." J Gen Physiol **115**(4): 467-480.

Avila, G. and R. T. Dirksen (2001). "Functional effects of central core disease mutations in the cytoplasmic region of the skeletal muscle ryanodine receptor." The Journal of General Physiology **118**(3): 277-290.

Avila, G., E. H. Lee, et al. (2003a). "FKBP12 binding to RyR1 modulates excitation-contraction coupling in mouse skeletal myotubes." J Biol Chem **278**(25): 22600-22608.

Avila, G., K. M. O'Connell, et al. (2003b). "The pore region of the skeletal muscle ryanodine receptor is a primary locus for excitation-contraction uncoupling in central core disease." The Journal of General Physiology **121**(4): 277-286.

Baker, R. T., S. A. Smith, et al. (1994). "Protein expression using cotranslational fusion and cleavage of ubiquitin. Mutagenesis of the glutathione-binding site of human Pi class glutathione S-transferase." The Journal of biological chemistry **269**(41): 25381-25386.

Baldwin, K. M. (1984). "Muscle development: neonatal to adult." Exerc Sport Sci Rev **12**: 1-19.

Balshaw, D. M., L. Xu, et al. (2001). "Calmodulin Binding and Inhibition of Cardiac Muscle Calcium Release Channel (Ryanodine Receptor)." Journal of Biological Chemistry **276**(23): 20144-20153.

Banker, B. Q., S. S. Kelly, et al. (1983). "Neuromuscular transmission and correlative morphology in young and old mice." The Journal of physiology **339**: 355-377.

Bannister, J. P., M. D. Leo, et al. (2013). "The voltage-dependent L-type Ca2+ (CaV1.2) channel C-terminus fragment is a bi-modal vasodilator." The Journal of physiology **591**(Pt 12): 2987-2998.

Bannister, M. L. and N. Ikemoto (2006). "Effects of peptide C corresponding to the Glu724-Pro760 region of the II-III loop of the DHP (dihydropyridine) receptor alpha1 subunit on the domain- switch-mediated activation of RyR1 (ryanodine receptor 1) Ca2+ channels." Biochem J **394**(Pt 1): 145-152.

Bannister, R. A. (2007). "Bridging the myoplasmic gap: recent developments in skeletal muscle excitation-contraction coupling." J Muscle Res Cell Motil **28**(4-5): 275-283.

Bannister, R. A. and K. G. Beam (2005). "The alpha1S N-terminus is not essential for bi-directional coupling with RyR1." Biochemical and Biophysical Research Communications **336**(1): 134-141.

Barg, S., J. A. Copello, et al. (1997). "Different interactions of cardiac and skeletal muscle ryanodine receptors with FK-506 binding protein isoforms." The American journal of physiology **272**(5 Pt 1): C1726-1733.

Barjot, C., M. L. Cotten, et al. (1995). "Expression of myosin heavy chain and of myogenic regulatory factor genes in fast or slow rabbit muscle satellite cell cultures." J Muscle Res Cell Motil **16**(6): 619-628.

Bastide, B. and Y. Mounier (1998). "Single-channel properties of the sarcoplasmic reticulum calcium-release channel in slow- and fast-twitch muscles of Rhesus monkeys." Pflugers Archiv : European journal of physiology **436**(3): 485-488.

Baylor, S. M., W. K. Chandler, et al. (1983). "Sarcoplasmic reticulum calcium release in frog skeletal muscle fibres estimated from Arsenazo III calcium transients." The Journal of physiology **344**: 625-666.

Baylor, S. M. and S. Hollingworth (2003). "Sarcoplasmic reticulum calcium release compared in slow-twitch and fast-twitch fibres of mouse muscle." J Physiol **551**(Pt 1): 125-138.

Beam, K. G., B. A. Adams, et al. (1992). "Function of a truncated dihydropyridine receptor as both voltage sensor and calcium channel." Nature **360**(6400): 169-171.

Beam, K. G., C. M. Knudson, et al. (1986). "A lethal mutation in mice eliminates the slow calcium current in skeletal muscle cells." Nature **320**(6058): 168-170.

Beard, N. A., M. G. Casarotto, et al. (2005). "Regulation of ryanodine receptors by calsequestrin: effect of high luminal Ca2+ and phosphorylation." Biophys J **88**(5): 3444-3454.

Beard, N. A., D. R. Laver, et al. (2004). "Calsequestrin and the calcium release channel of skeletal and cardiac muscle." Prog Biophys Mol Biol **85**(1): 33-69.

Beard, N. A., M. M. Sakowska, et al. (2002). "Calsequestrin is an inhibitor of skeletal muscle ryanodine receptor calcium release channels." Biophys J **82**(1 Pt 1): 310-320.

Beard, N. A., L. Wei, et al. (2008). "Phosphorylation of skeletal muscle calsequestrin enhances its Ca2+ binding capacity and promotes its association with junctin." Cell Calcium **44**(4): 363-373.

Beard, N. A., L. Wei, et al. (2009a). "Ca(2+) signaling in striated muscle: the elusive roles of triadin, junctin, and calsequestrin." Eur Biophys J **39**(1): 27-36.

Beard, N. A., L. Wei, et al. (2009b). "Control of muscle ryanodine receptor calcium release channels by proteins in the sarcoplasmic reticulum lumen." Clin Exp Pharmacol Physiol **36**(3): 340-345.

Bellinger, A. M., S. Reiken, et al. (2009). "Hypernitrosylated ryanodine receptor calcium release channels are leaky in dystrophic muscle." Nat Med **15**(3): 325-330.

Bertocchini, F., C. E. Ovitt, et al. (1997). "Requirement for the ryanodine receptor type 3 for efficient contraction in neonatal skeletal muscles." EMBO J **16**(23): 6956-6963.

Bhattacharyya, B. J., K. Tsen, et al. (1994). "Age-induced alteration of neuromuscular transmission: effect of halothane." European journal of pharmacology **254**(1-2): 97-104.

Bichet, D., V. Cornet, et al. (2000). "The I-II loop of the Ca2+ channel alpha1 subunit contains an endoplasmic reticulum retention signal antagonized by the beta subunit." Neuron **25**(1): 177-190.

Biral, D., P. Volpe, et al. (1992). "Coexistence of two calsequestrin isoforms in rabbit slow-twitch skeletal muscle fibers." FEBS letters **299**(2): 175-178.

Block, B. A., T. Imagawa, et al. (1988). "Structural evidence for direct interaction between the molecular components of the transverse tubule/sarcoplasmic reticulum junction in skeletal muscle." J Cell Biol **107**(6 Pt 2): 2587-2600.

Board, P. G., M. Coggan, et al. (2004). "CLIC-2 modulates cardiac ryanodine receptor Ca2+ release channels." Int J Biochem Cell Biol **36**(8): 1599-1612.

Boden, G., X. Chen, et al. (1993). "Effects of age and body fat on insulin resistance in healthy men." Diabetes Care **16**(5): 728-733.

Boncompagni, S., L. d'Amelio, et al. (2006). "Progressive disorganization of the excitation-contraction coupling apparatus in aging human skeletal muscle as revealed by electron microscopy: a possible role in the decline of muscle performance." J Gerontol A Biol Sci Med Sci **61**(10): 995-1008.

Boncompagni, S., M. Thomas, et al. (2012). "Triadin/Junctin double null mouse reveals a differential role for Triadin and Junctin in anchoring CASQ to the jSR and regulating Ca(2+) homeostasis." PLoS One **7**(7): 2.

Boraso, A. and A. J. Williams (1994). "Modification of the gating of the cardiac sarcoplasmic reticulum Ca(2+)-release channel by H2O2 and dithiothreitol." The American journal of physiology **267**(3 Pt 2): H1010-1016.

Bortolotto, S. K., D. G. Stephenson, et al. (2001). "Caffeine thresholds for contraction in electrophoretically typed, mechanically skinned muscle fibres from SHR and WKY rats." Pflugers Arch **441**(5): 692-700.

Bottinelli, R., R. Betto, et al. (1994). "Maximum shortening velocity and coexistence of myosin heavy chain isoforms in single skinned fast fibres of rat skeletal muscle." J Muscle Res Cell Motil **15**(4): 413-419.

References

Bottinelli, R., S. Schiaffino, et al. (1991). "Force-velocity relations and myosin heavy chain isoform compositions of skinned fibres from rat skeletal muscle." J Physiol **437**: 655-672.

Brandt, N. R., A. H. Caswell, et al. (1990). "Molecular interactions of the junctional foot protein and dihydropyridine receptor in skeletal muscle triads." J Membr Biol **113**(3): 237-251.

Brehm, P. and R. Eckert (1978). "Calcium entry leads to inactivation of calcium channel in Paramecium." Science **202**(4373): 1203-1206.

Brillantes, A. B., K. Ondrias, et al. (1994). "Stabilization of calcium release channel (ryanodine receptor) function by FK506-binding protein." Cell **77**(4): 513-523.

Brini, M., S. Manni, et al. (2005). "Ca2+ signaling in HEK-293 and skeletal muscle cells expressing recombinant ryanodine receptors harboring malignant hyperthermia and central core disease mutations." The Journal of biological chemistry **280**(15): 15380-15389.

Brooke, M. H. and K. K. Kaiser (1970). "Muscle fiber types: how many and what kind?" Arch Neurol **23**(4): 369-379.

Brown, W. F. (1972). "A method for estimating the number of motor units in thenar muscles and the changes in motor unit count with ageing." Journal of neurology, neurosurgery, and psychiatry **35**(6): 845-852.

Buck, E., I. Zimanyi, et al. (1992). "Ryanodine stabilizes multiple conformational states of the skeletal muscle calcium release channel." The Journal of biological chemistry **267**(33): 23560-23567.

Bull, R. and J. J. Marengo (1993). "Sarcoplasmic reticulum release channels from frog skeletal muscle display two types of calcium dependence." FEBS letters **331**(3): 223-227.

Bull, R., J. J. Marengo, et al. (2003). "SH oxidation coordinates subunits of rat brain ryanodine receptor channels activated by calcium and ATP." American journal of physiology. Cell physiology **285**(1): C119-128.

Burke, R. E., D. N. Levine, et al. (1973). "Physiological types and histochemical profiles in motor units of the cat gastrocnemius." J Physiol **234**(3): 723-748.

Burke, R. E., D. N. Levine, et al. (1971). "Mammalian motor units: physiological-histochemical correlation in three types in cat gastrocnemius." Science **174**(4010): 709-712.

Butler-Browne, G. S. and R. G. Whalen (1984). "Myosin isozyme transitions occurring during the postnatal development of the rat soleus muscle." Dev Biol **102**(2): 324-334.

Caiozzo, V. J., M. J. Baker, et al. (1998). "Novel transitions in MHC isoforms: separate and combined effects of thyroid hormone and mechanical unloading." J Appl Physiol (1985) **85**(6): 2237-2248.

Callahan, D. M., S. A. Foulis, et al. (2009). "Age-related fatigue resistance in the knee extensor muscles is specific to contraction mode." Muscle & nerve **39**(5): 692-702.

Campbell, K. P., C. M. Knudson, et al. (1987). "Identification and characterization of the high affinity [3H]ryanodine receptor of the junctional sarcoplasmic reticulum Ca2+ release channel." J Biol Chem **262**(14): 6460-6463.

Campbell, M. J., A. J. McComas, et al. (1973). "Physiological changes in ageing muscles." Journal of neurology, neurosurgery, and psychiatry **36**(2): 174-182.

Campbell, W. G., S. E. Gordon, et al. (2001). "Differential global gene expression in red and white skeletal muscle." Am J Physiol Cell Physiol **280**(4): C763-768.

Cannell, M. B., H. Cheng, et al. (1995). "The control of calcium release in heart muscle." Science **268**(5213): 1045-1049.

Capes, E. M., R. Loaiza, et al. (2011). "Ryanodine receptors." Skelet Muscle **1**(1): 18.

Carbonneau, L., D. Bhattacharya, et al. (2005). "Multiple loops of the dihydropyridine receptor pore subunit are required for full-scale excitation-contraction coupling in skeletal muscle." Biophys J **89**(1): 243-255.

Carl, S. L., K. Felix, et al. (1995a). "Immunolocalization of sarcolemmal dihydropyridine receptor and sarcoplasmic reticular triadin and ryanodine receptor in rabbit ventricle and atrium." J Cell Biol **129**(3): 673-682.

Carl, S. L., K. Felix, et al. (1995b). "Immunolocalization of triadin, DHP receptors, and ryanodine receptors in adult and developing skeletal muscle of rats." Muscle Nerve **18**(11): 1232-1243.

Carroll, S., P. Nicotera, et al. (1999). "Calcium transients in single fibers of low-frequency stimulated fast-twitch muscle of rat." Am J Physiol **277**(6 Pt 1): C1122-1129.

Carroll, S., J. G. Skarmeta, et al. (1991). "Interdependence of ryanodine binding, oligomeric receptor interactions, and Ca2+ release regulation in junctional sarcoplasmic reticulum." Archives of biochemistry and biophysics **290**(1): 239-247.

Carroll, S. L., M. G. Klein, et al. (1997). "Decay of calcium transients after electrical stimulation in rat fast- and slow-twitch skeletal muscle fibres." J Physiol **501 (Pt 3)**: 573-588.

Carter, S., J. Colyer, et al. (2006). "Maximum phosphorylation of the cardiac ryanodine receptor at serine-2809 by protein kinase a produces unique modifications to channel gating and conductance not observed at lower levels of phosphorylation." Circulation research **98**(12): 1506-1513.

Castellano, A., X. Wei, et al. (1993a). "Cloning and expression of a neuronal calcium channel beta subunit." The Journal of biological chemistry **268**(17): 12359-12366.

Castellano, A., X. Wei, et al. (1993b). "Cloning and expression of a third calcium channel beta subunit." The Journal of biological chemistry **268**(5): 3450-3455.

Caswell, A. H., N. R. Brandt, et al. (1991). "Localization and partial characterization of the oligomeric disulfide-linked molecular weight 95,000 protein (triadin) which binds the ryanodine and dihydropyridine receptors in skeletal muscle triadic vesicles." Biochemistry **30**(30): 7507-7513.

Catterall, W. A. (2000). "Structure and regulation of voltage-gated Ca2+ channels." Annual review of cell and developmental biology **16**: 521-555.

Catterall, W. A. (2010). "Ion channel voltage sensors: structure, function, and pathophysiology." Neuron **67**(6): 915-928.

Catterall, W. A. (2011). "Voltage-gated calcium channels." Cold Spring Harb Perspect Biol **3**(8): a003947.

Celio, M. R. and C. W. Heizmann (1982). "Calcium-binding protein parvalbumin is associated with fast contracting muscle fibres." Nature **297**(5866): 504-506.

Censier, K., A. Urwyler, et al. (1998). "Intracellular calcium homeostasis in human primary muscle cells from malignant hyperthermia-susceptible and normal individuals. Effect Of overexpression of recombinant wild-type and Arg163Cys mutated ryanodine receptors." The Journal of clinical investigation **101**(6): 1233-1242.

Chaudhari, N. and K. G. Beam (1993). "mRNA for cardiac calcium channel is expressed during development of skeletal muscle." Dev Biol **155**(2): 507-515.

Chelu, M. G., C. I. Danila, et al. (2004). "Regulation of ryanodine receptors by FK506 binding proteins." Trends Cardiovasc Med **14**(6): 227-234.

Chelu, M. G., S. A. Goonasekera, et al. (2006). "Heat- and anesthesia-induced malignant hyperthermia in an RyR1 knock-in mouse." FASEB journal : official publication of the Federation of American Societies for Experimental Biology **20**(2): 329-330.

Chen, S. R., P. Leong, et al. (1997). "Single-channel properties of the recombinant skeletal muscle Ca2+ release channel (ryanodine receptor)." Biophysical Journal **73**(4): 1904-1912.

Chen, S. R. and D. H. MacLennan (1994). "Identification of calmodulin-, Ca(2+)-, and ruthenium red-binding domains in the Ca2+ release channel (ryanodine receptor) of rabbit skeletal muscle sarcoplasmic reticulum." Journal of Biological Chemistry **269**(36): 22698-22704.

Chen, Y. H., M. H. Li, et al. (2004). "Structural basis of the alpha1-beta subunit interaction of voltage-gated Ca2+ channels." Nature **429**(6992): 675-680.

Cheng, H., W. J. Lederer, et al. (1993). "Calcium sparks: elementary events underlying excitation-contraction coupling in heart muscle." Science **262**(5134): 740-744.

Cheng, W., X. Altafaj, et al. (2005). "Interaction between the dihydropyridine receptor Ca2+ channel beta-subunit and ryanodine receptor type 1 strengthens excitation-contraction coupling." Proc Natl Acad Sci U S A **102**(52): 19225-19230.

Cheong, E., V. Tumbev, et al. (2005). "Effects of pO2 on the activation of skeletal muscle ryanodine receptors by NO: a cautionary note." Cell Calcium **38**(5): 481-488.

Chin, D. and A. R. Means (2000). "Calmodulin: a prototypical calcium sensor." Trends in Cell Biology **10**(8): 322-328.

References

Ching, L. L., A. J. Williams, et al. (2000). "Evidence for Ca(2+) activation and inactivation sites on the luminal side of the cardiac ryanodine receptor complex." Circulation research **87**(3): 201-206.

Chu, A., M. Diaz-Munoz, et al. (1990a). "Ryanodine as a probe for the functional state of the skeletal muscle sarcoplasmic reticulum calcium release channel." Molecular pharmacology **37**(5): 735-741.

Chu, A., C. Sumbilla, et al. (1990b). "Specific association of calmodulin-dependent protein kinase and related substrates with the junctional sarcoplasmic reticulum of skeletal muscle." Biochemistry **29**(25): 5899-5905.

Chung, S. H. and P. W. Gage (1998). "Signal processing techniques for channel current analysis based on hidden Markov models." Methods Enzymol **293**: 420-437.

Close, R. (1965). "The relation between intrinsic speed of shortening and duration of the active state of muscle." J Physiol **180**(3): 542-559.

Close, R. (1967). "Properties of motor units in fast and slow skeletal muscles of the rat." J Physiol **193**(1): 45-55.

Coggan, A. R., R. J. Spina, et al. (1992). "Histochemical and enzymatic comparison of the gastrocnemius muscle of young and elderly men and women." Journal of gerontology **47**(3): B71-76.

Coin, A., G. Sergi, et al. (2000). "Bone mineral density and body composition in underweight and normal elderly subjects." Osteoporosis international : a journal established as result of cooperation between the European Foundation for Osteoporosis and the National Osteoporosis Foundation of the USA **11**(12): 1043-1050.

Collins, J. H. (1991). "Sequence analysis of the ryanodine receptor: Possible association with a 12K, FK506-binding immunophilin/protein kinase C inhibitor." Biochemical and Biophysical Research Communications **178**(3): 1288-1290.

Colman, E., L. I. Katzel, et al. (1995). "Weight loss reduces abdominal fat and improves insulin action in middle-aged and older men with impaired glucose tolerance." Metabolism: clinical and experimental **44**(11): 1502-1508.

Condon, K., L. Silberstein, et al. (1990a). "Development of muscle fiber types in the prenatal rat hindlimb." Dev Biol **138**(2): 256-274.

Condon, K., L. Silberstein, et al. (1990b). "Differentiation of fiber types in aneural musculature of the prenatal rat hindlimb." Dev Biol **138**(2): 275-295.

Conti, A., L. Gorza, et al. (1996). "Differential distribution of ryanodine receptor type 3 (RyR3) gene product in mammalian skeletal muscles." The Biochemical journal **316 (Pt 1)**: 19-23.

Conti, A., C. Reggiani, et al. (2005). "Selective expression of the type 3 isoform of ryanodine receptor Ca2+ release channel (RyR3) in a subset of slow fibers in diaphragm and cephalic muscles of adult rabbits." Biochem Biophys Res Commun **337**(1): 195-200.

Copello, J. A., S. Barg, et al. (1997). "Heterogeneity of Ca2+ gating of skeletal muscle and cardiac ryanodine receptors." Biophysical Journal **73**(1): 141-156.

Copello, J. A., S. Barg, et al. (2002). "Differential activation by Ca2+, ATP and caffeine of cardiac and skeletal muscle ryanodine receptors after block by Mg2+." The Journal of membrane biology **187**(1): 51-64.

Cornea, R. L., F. Nitu, et al. (2009). "FRET-based mapping of calmodulin bound to the RyR1 Ca2+ release channel." Proc Natl Acad Sci U S A **106**(15): 6128-6133.

Costill, D. L., J. Daniels, et al. (1976). "Skeletal muscle enzymes and fiber composition in male and female track athletes." J Appl Physiol **40**(2): 149-154.

Courtney, J. and J. H. Steinbach (1981). "Age changes in neuromuscular junction morphology and acetylcholine receptor distribution on rat skeletal muscle fibres." The Journal of physiology **320**: 435-447.

Cui, Y., H. S. Tae, et al. (2009). "A dihydropyridine receptor alpha1s loop region critical for skeletal muscle contraction is intrinsically unstructured and binds to a SPRY domain of the type 1 ryanodine receptor." Int J Biochem Cell Biol **41**(3): 677-686.

Cukierman, S., G. Yellen, et al. (1985). "The K+ channel of sarcoplasmic reticulum. A new look at Cs+ block." Biophysical journal **48**(3): 477-484.

Currie, S., C. M. Loughrey, et al. (2004). "Calcium/calmodulin-dependent protein kinase IIdelta associates with the ryanodine receptor complex and regulates channel function in rabbit heart." The Biochemical journal **377**(Pt 2): 357-366.

Curtis, B. M. and W. A. Catterall (1984). "Purification of the calcium antagonist receptor of the voltage-sensitive calcium channel from skeletal muscle transverse tubules." Biochemistry **23**(10): 2113-2118.

Curtis, B. M. and W. A. Catterall (1986). "Reconstitution of the voltage-sensitive calcium channel purified from skeletal muscle transverse tubules." Biochemistry **25**(11): 3077-3083.

Cvetko, E., P. Karen, et al. (2012). "Myosin heavy chain composition of the human sternocleidomastoid muscle." Ann Anat **194**(5): 467-472.

d'Albis, A., R. Couteaux, et al. (1988). "Regeneration after cardiotoxin injury of innervated and denervated slow and fast muscles of mammals. Myosin isoform analysis." Eur J Biochem **174**(1): 103-110.

Dalton, B. H., B. Harwood, et al. (2010). "Recovery of motoneuron output is delayed in old men following high-intensity fatigue." Journal of neurophysiology **103**(2): 977-985.

Damiani, E., L. Larsson, et al. (1996). "Age-related abnormalities in regulation of the ryanodine receptor in rat fast-twitch muscle." Cell Calcium **19**(1): 15-27.

Damiani, E. and A. Margreth (1994). "Characterization study of the ryanodine receptor and of calsequestrin isoforms of mammalian skeletal muscles in relation to fibre types." Journal of muscle research and cell motility **15**(2): 86-101.

Dangain, J. and I. R. Neering (1991). "Effect of low extracellular calcium and ryanodine on muscle contraction of the mouse during postnatal development." Canadian journal of physiology and pharmacology **69**(9): 1294-1300.

Dargan, S. L., E. J. Lea, et al. (2002). "Modulation of type-1 Ins(1,4,5)P3 receptor channels by the FK506-binding protein, FKBP12." The Biochemical journal **361**(Pt 2): 401-407.

Davies, A., I. Kadurin, et al. (2010). "The alpha2delta subunits of voltage-gated calcium channels form GPI-anchored proteins, a posttranslational modification essential for function." Proceedings of the National Academy of Sciences of the United States of America **107**(4): 1654-1659.

Dawson, J. M., K. R. Tyler, et al. (1987). "A comparison of the microcirculation in rat fast glycolytic and slow oxidative muscles at rest and during contractions." Microvasc Res **33**(2): 167-182.

Dayal, A., V. Bhat, et al. (2013). "Domain cooperativity in the beta1a subunit is essential for dihydropyridine receptor voltage sensing in skeletal muscle." Proc Natl Acad Sci U S A **110**(18): 7488-7493.

De Jongh, K. S., D. K. Merrick, et al. (1989). "Subunits of purified calcium channels: a 212-kDa form of alpha 1 and partial amino acid sequence of a phosphorylation site of an independent beta subunit." Proceedings of the National Academy of Sciences of the United States of America **86**(21): 8585-8589.

De Jongh, K. S., C. Warner, et al. (1990). "Subunits of purified calcium channels. Alpha 2 and delta are encoded by the same gene." The Journal of biological chemistry **265**(25): 14738-14741.

De Stefani, D., A. Raffaello, et al. (2011). "A forty-kilodalton protein of the inner membrane is the mitochondrial calcium uniporter." Nature **476**(7360): 336-340.

Dedkov, E. I., T. Y. Kostrominova, et al. (2001). "Reparative myogenesis in long-term denervated skeletal muscles of adult rats results in a reduction of the satellite cell population." Anat Rec **263**(2): 139-154.

Deivanayagam, C. C., M. Carson, et al. (2000). "Structure of FKBP12.6 in complex with rapamycin." Acta crystallographica. Section D, Biological crystallography **56**(Pt 3): 266-271.

Delay, M., B. Ribalet, et al. (1986). "Caffeine potentiation of calcium release in frog skeletal muscle fibres." The Journal of physiology **375**: 535-559.

Delbono, O. (2000). "Regulation of excitation contraction coupling by insulin-like growth factor-1 in aging skeletal muscle." J Nutr Health Aging **4**(3): 162-164.

Delbono, O. and G. Meissner (1996). "Sarcoplasmic reticulum Ca2+ release in rat slow- and fast-twitch muscles." J Membr Biol **151**(2): 123-130.

References

Delbono, O., K. S. O'Rourke, et al. (1995). "Excitation-calcium release uncoupling in aged single human skeletal muscle fibers." J Membr Biol **148**(3): 211-222.

DeNardi, C., S. Ausoni, et al. (1993). "Type 2X-myosin heavy chain is coded by a muscle fiber type-specific and developmentally regulated gene." J Cell Biol **123**(4): 823-835.

Denborough, M. (1998). "Malignant hyperthermia." The Lancet **352**(9134): 1131-1136.

Denborough, M. A. and R. R. H. Lovell (1960). "ANÆSTHETIC DEATHS IN A FAMILY." The Lancet **276**(7140): 45.

Deschenes, M. R. (2004). "Effects of aging on muscle fibre type and size." Sports medicine **34**(12): 809-824.

Deschenes, M. R. (2011). "Motor unit and neuromuscular junction remodeling with aging." Current aging science **4**(3): 209-220.

Deschenes, M. R., M. A. Roby, et al. (2010). "Remodeling of the neuromuscular junction precedes sarcopenia related alterations in myofibers." Experimental gerontology **45**(5): 389-393.

Deschenes, M. R. and M. H. Wilson (2003). "Age-related differences in synaptic plasticity following muscle unloading." Journal of neurobiology **57**(3): 246-256.

Dietze, B., J. Henke, et al. (2000). "Malignant hyperthermia mutation Arg615Cys in the porcine ryanodine receptor alters voltage dependence of Ca2+ release." The Journal of physiology **526 Pt 3**: 507-514.

Dirksen, R. T. (2002). "Bi-directional coupling between dihydropyridine receptors and ryanodine receptors." Front Biosci **7**: d659-670.

Dirksen, R. T. (2009). "Sarcoplasmic reticulum-mitochondrial through-space coupling in skeletal muscle." Appl Physiol Nutr Metab **34**(3): 389-395.

Dirksen, R. T. and G. Avila (2004). "Distinct effects on Ca2+ handling caused by malignant hyperthermia and central core disease mutations in RyR1." Biophysical Journal **87**(5): 3193-3204.

Doherty, T. J., A. A. Vandervoort, et al. (1993). "Effects of ageing on the motor unit: a brief review." Canadian journal of applied physiology = Revue canadienne de physiologie appliquee **18**(4): 331-358.

Dolphin, A. C. (2003). "Beta subunits of voltage-gated calcium channels." J Bioenerg Biomembr **35**(6): 599-620.

Donoso, P., P. Aracena, et al. (2000). "Sulfhydryl oxidation overrides Mg(2+) inhibition of calcium-induced calcium release in skeletal muscle triads." Biophysical Journal **79**(1): 279-286.

Donoso, P., H. Prieto, et al. (1995). "Luminal calcium regulates calcium release in triads isolated from frog and rabbit skeletal muscle." Biophysical Journal **68**(2): 507-515.

Du, G. G., G. Avila, et al. (2004). "Role of the sequence surrounding predicted transmembrane helix M4 in membrane association and function of the Ca(2+) release channel of skeletal muscle sarcoplasmic reticulum (ryanodine receptor isoform 1)." J Biol Chem **279**(36): 37566-37574.

Du, G. G., B. Sandhu, et al. (2002). "Topology of the Ca2+ release channel of skeletal muscle sarcoplasmic reticulum (RyR1)." Proc Natl Acad Sci U S A **99**(26): 16725-16730.

Dubuis, E., N. Rockliffe, et al. (2006). "Evidence for multiple Src binding sites on the alpha1c L-type Ca2+ channel and their roles in activity regulation." Cardiovasc Res **69**(2): 391-401.

Dulhunty, A., P. Gage, et al. (2001). "The glutathione transferase structural family includes a nuclear chloride channel and a ryanodine receptor calcium release channel modulator." J Biol Chem **276**(5): 3319-3323.

Dulhunty, A. F. (1992). "The voltage-activation of contraction in skeletal muscle." Progress in biophysics and molecular biology **57**(3): 181-223.

Dulhunty, A. F., M. R. Banyard, et al. (1987). "Distribution of calcium ATPase in the sarcoplasmic reticulum of fast- and slow-twitch muscles determined with monoclonal antibodies." J Membr Biol **99**(2): 79-92.

Dulhunty, A. F., R. Hewawasam, et al. (2011). "Regulation of the cardiac muscle ryanodine receptor by glutathione transferases." Drug metabolism reviews **43**(2): 236-252.

Dulhunty, A. F., D. R. Laver, et al. (1999). "Activation and inhibition of skeletal RyR channels by a part of the skeletal DHPR II-III loop: effects of DHPR Ser687 and FKBP12." Biophys J **77**(1): 189-203.

Dulhunty, A. F., P. Pouliquin, et al. (2005). "A recently identified member of the glutathione transferase structural family modifies cardiac RyR2 substate activity, coupled gating and activation by Ca2+ and ATP." The Biochemical journal **390**(Pt 1): 333-343.

Dupuis, L., J. L. Gonzalez de Aguilar, et al. (2009). "Muscle mitochondrial uncoupling dismantles neuromuscular junction and triggers distal degeneration of motor neurons." PLoS One **4**(4): e5390.

Dusterhoft, S. and D. Pette (1993). "Satellite cells from slow rat muscle express slow myosin under appropriate culture conditions." Differentiation **53**(1): 25-33.

Eddinger, T. J., R. L. Moss, et al. (1985). "Fiber number and type composition in extensor digitorum longus, soleus, and diaphragm muscles with aging in Fisher 344 rats." J Histochem Cytochem **33**(10): 1033-1041.

Edstrom, L. and E. Kugelberg (1968). "Histochemical composition, distribution of fibres and fatiguability of single motor units. Anterior tibial muscle of the rat." J Neurol Neurosurg Psychiatry **31**(5): 424-433.

Edstrom, L. and L. Larsson (1987). "Effects of age on contractile and enzyme-histochemical properties of fast- and slow-twitch single motor units in the rat." J Physiol **392**: 129-145.

Einsiedel, L. J. and A. R. Luff (1992). "Alterations in the contractile properties of motor units within the ageing rat medial gastrocnemius." Journal of the neurological sciences **112**(1-2): 170-177.

El-Hayek, R., B. Antoniu, et al. (1995). "Identification of calcium release-triggering and blocking regions of the II-III loop of the skeletal muscle dihydropyridine receptor." J Biol Chem **270**(38): 22116-22118.

El-Hayek, R. and N. Ikemoto (1998). "Identification of the minimum essential region in the II-III loop of the dihydropyridine receptor alpha 1 subunit required for activation of skeletal muscle-type excitation-contraction coupling." Biochemistry **37**(19): 7015-7020.

Endo, M. (1984). "Significance of calcium-induced release fo of calcium form the sarcoplasmic reticulum in skeletal muscle." Jikeikai Medical Journal **30**(Suppl 1): 123-130.

Endo, M. (1985). Calcium Release from Sarcoplasmic Reticulum. Current Topics in Membranes and Transport. B. Felix, Academic Press. **Volume 25:** 181-230.

Endo, M. (2009). "Calcium-induced calcium release in skeletal muscle." Physiol Rev **89**(4): 1153-1176.

Endo, M., M. Tanaka, et al. (1970). "Calcium induced release of calcium from the sarcoplasmic reticulum of skinned skeletal muscle fibres." Nature **228**(5266): 34-36.

Ertel, E. A., K. P. Campbell, et al. (2000). "Nomenclature of voltage-gated calcium channels." Neuron **25**(3): 533-535.

Ervasti, J. M. and K. J. Sonnemann (2008). "Biology of the striated muscle dystrophin-glycoprotein complex." Int Rev Cytol **265**: 191-225.

Essen-Gustavsson, B. and O. Borges (1986). "Histochemical and metabolic characteristics of human skeletal muscle in relation to age." Acta physiologica Scandinavica **126**(1): 107-114.

Esser, K., P. Gunning, et al. (1993). "Nerve-dependent and -independent patterns of mRNA expression in regenerating skeletal muscle." Dev Biol **159**(1): 173-183.

Eu, J. P., J. Sun, et al. (2000). "The skeletal muscle calcium release channel: coupled O2 sensor and NO signaling functions." Cell **102**(4): 499-509.

Eusebi, F., R. Miledi, et al. (1980). "Calcium transients in mammalian muscles." Nature **284**(5756): 560-561.

Evans, M. and A. Rees (2002). "Effects of HMG-CoA reductase inhibitors on skeletal muscle: are all statins the same?" Drug Saf **25**(9): 649-663.

Everts, M. E., J. P. Andersen, et al. (1989). "Quantitative determination of Ca2+-dependent Mg2+-ATPase from sarcoplasmic reticulum in muscle biopsies." Biochem J **260**(2): 443-448.

Fabiato, A. (1985). "Effects of ryanodine in skinned cardiac cells." Federation proceedings **44**(15): 2970-2976.

References

Fahim, M. A. (1997). "Endurance exercise modulates neuromuscular junction of C57BL/6NNia aging mice." Journal of applied physiology **83**(1): 59-66.

Fahim, M. A. and N. Robbins (1982). "Ultrastructural studies of young and old mouse neuromuscular junctions." Journal of neurocytology **11**(4): 641-656.

Fairhurst, A. S. and D. J. Jenden (1966). "The distribution of a ryanodine-sensitive calcium pump in skeletal muscle fractions." Journal of cellular physiology **67**(2): 233-238.

Favero, T. G., A. C. Zable, et al. (1995). "Hydrogen peroxide stimulates the Ca2+ release channel from skeletal muscle sarcoplasmic reticulum." The Journal of biological chemistry **270**(43): 25557-25563.

Felder, E., F. Protasi, et al. (2002). "Morphology and molecular composition of sarcoplasmic reticulum surface junctions in the absence of DHPR and RyR in mouse skeletal muscle." Biophys J **82**(6): 3144-3149.

Ferguson, D. G., H. W. Schwartz, et al. (1984). "Subunit structure of junctional feet in triads of skeletal muscle: a freeze-drying, rotary-shadowing study." The Journal of cell biology **99**(5): 1735-1742.

Ferreiro, A., S. Quijano-Roy, et al. (2002). "Mutations of the selenoprotein N gene, which is implicated in rigid spine muscular dystrophy, cause the classical phenotype of multiminicore disease: reassessing the nosology of early-onset myopathies." American journal of human genetics **71**(4): 739-749.

Ferrington, D. A., A. G. Krainev, et al. (1998). "Altered turnover of calcium regulatory proteins of the sarcoplasmic reticulum in aged skeletal muscle." J Biol Chem **273**(10): 5885-5891.

Field, A. C., C. Hill, et al. (1988). "Asymmetric charge movement and calcium currents in ventricular myocytes of neonatal rat." The Journal of physiology **406**: 277-297.

Fleischer, S., E. M. Ogunbunmi, et al. (1985). "Localization of Ca2+ release channels with ryanodine in junctional terminal cisternae of sarcoplasmic reticulum of fast skeletal muscle." Proc Natl Acad Sci U S A **82**(21): 7256-7259.

Fliegel, L., E. Newton, et al. (1990). "Molecular cloning of cDNA encoding a 55-kDa multifunctional thyroid hormone binding protein of skeletal muscle sarcoplasmic reticulum." The Journal of biological chemistry **265**(26): 15496-15502.

Fliegel, L., M. Ohnishi, et al. (1987). "Amino acid sequence of rabbit fast-twitch skeletal muscle calsequestrin deduced from cDNA and peptide sequencing." Proceedings of the National Academy of Sciences of the United States of America **84**(5): 1167-1171.

Flockerzi, V., H. J. Oeken, et al. (1986). "Purified dihydropyridine-binding site from skeletal muscle t-tubules is a functional calcium channel." Nature **323**(6083): 66-68.

Flucher, B. E. (1992). "Structural analysis of muscle development: transverse tubules, sarcoplasmic reticulum, and the triad." Dev Biol **154**(2): 245-260.

Flucher, B. E., A. Conti, et al. (1999). "Type 3 and type 1 ryanodine receptors are localized in triads of the same mammalian skeletal muscle fibers." J Cell Biol **146**(3): 621-630.

Flucher, B. E. and C. Franzini-Armstrong (1996). "Formation of junctions involved in excitation-contraction coupling in skeletal and cardiac muscle." Proc Natl Acad Sci U S A **93**(15): 8101-8106.

Flucher, B. E., N. Kasielke, et al. (2000). "The triad targeting signal of the skeletal muscle calcium channel is localized in the COOH terminus of the alpha(1S) subunit." The Journal of cell biology **151**(2): 467-478.

Flucher, B. E., H. Takekura, et al. (1993). "Development of the excitation-contraction coupling apparatus in skeletal muscle: association of sarcoplasmic reticulum and transverse tubules with myofibrils." Developmental biology **160**(1): 135-147.

Flucher, B. E., R. G. Weiss, et al. (2002). "Cooperation of two-domain Ca(2+) channel fragments in triad targeting and restoration of excitation- contraction coupling in skeletal muscle." Proceedings of the National Academy of Sciences of the United States of America **99**(15): 10167-10172.

Franck, J. P., J. Morrissette, et al. (1998). "Cloning and characterization of fiber type-specific ryanodine receptor isoforms in skeletal muscles of fish." The American journal of physiology **275**(2 Pt 1): C401-415.

Franzini-Armstrong, C. (1973). "Studies of the triad. IV. Structure of the junction in frog slow fibers." J Cell Biol **56**(1): 120-128.

Franzini-Armstrong, C. (1999). "The sarcoplasmic reticulum and the control of muscle contraction." FASEB J **13 Suppl 2**: S266-270.

Franzini-Armstrong, C. (2007). "ER-mitochondria communication. How privileged?" Physiology (Bethesda) **22**: 261-268.

Franzini-Armstrong, C. (2010). "RyRs: Their Disposition, Frequency, and Relationships with Other Proteins of Calcium Release Units." Current topics in membranes **66C**: 3-26.

Franzini-Armstrong, C., D. G. Ferguson, et al. (1988). "Discrimination between fast- and slow-twitch fibres of guinea pig skeletal muscle using the relative surface density of junctional transverse tubule membrane." J Muscle Res Cell Motil **9**(5): 403-414.

Franzini-Armstrong, C. and A. O. Jorgensen (1994). "Structure and development of E-C coupling units in skeletal muscle." Annu Rev Physiol **56**: 509-534.

Franzini-Armstrong, C. and J. W. Kish (1995). "Alternate disposition of tetrads in peripheral couplings of skeletal muscle." J Muscle Res Cell Motil **16**(3): 319-324.

Franzini-Armstrong, C., M. Pincon-Raymond, et al. (1991). "Muscle fibers from dysgenic mouse in vivo lack a surface component of peripheral couplings." Developmental biology **146**(2): 364-376.

Franzini-Armstrong, C. and F. Protasi (1997). "Ryanodine receptors of striated muscles: a complex channel capable of multiple interactions." Physiol Rev **77**(3): 699-729.

Franzini-Armstrong, C., F. Protasi, et al. (1999). "Shape, size, and distribution of Ca(2+) release units and couplons in skeletal and cardiac muscles." Biophys J **77**(3): 1528-1539.

Fraysse, B., J. F. Desaphy, et al. (2003). "Decrease in resting calcium and calcium entry associated with slow-to-fast transition in unloaded rat soleus muscle." FASEB journal : official publication of the Federation of American Societies for Experimental Biology **17**(13): 1916-1918.

Fraysse, B., J. F. Desaphy, et al. (2006). "Fiber type-related changes in rat skeletal muscle calcium homeostasis during aging and restoration by growth hormone." Neurobiol Dis **21**(2): 372-380.

Freise, D., B. Held, et al. (2000). "Absence of the gamma subunit of the skeletal muscle dihydropyridine receptor increases L-type Ca2+ currents and alters channel inactivation properties." J Biol Chem **275**(19): 14476-14481.

Frontera, W. R., K. F. Reid, et al. (2008). "Muscle fiber size and function in elderly humans: a longitudinal study." J Appl Physiol (1985) **105**(2): 637-642.

Frontera, W. R., D. Suh, et al. (2000). "Skeletal muscle fiber quality in older men and women." American journal of physiology. Cell physiology **279**(3): C611-618.

Fruen, B. R., J. M. Bardy, et al. (2000). "Differential Ca2+ sensitivity of skeletal and cardiac muscle ryanodine receptors in the presence of calmodulin." American Journal of Physiology - Cell Physiolog **279**(3): C724-C733.

Fruen, B. R., D. J. Black, et al. (2003). "Regulation of the RYR1 and RYR2 Ca2+ Release Channel Isoforms by Ca2+-Insensitive Mutants of Calmodulin†." Biochemistry **42**(9): 2740-2747.

Fryer, M. W. and D. G. Stephenson (1996). "Total and sarcoplasmic reticulum calcium contents of skinned fibres from rat skeletal muscle." The Journal of physiology **493 (Pt 2)**: 357-370.

Fuchtbauer, E. M., A. M. Rowlerson, et al. (1991). "Direct correlation of parvalbumin levels with myosin isoforms and succinate dehydrogenase activity on frozen sections of rodent muscle." J Histochem Cytochem **39**(3): 355-361.

Fuentes, O., C. Valdivia, et al. (1994). "Calcium-dependent block of ryanodine receptor channel of swine skeletal muscle by direct binding of calmodulin." Cell Calcium **15**(4): 305-316.

Furuichi, T., D. Furutama, et al. (1994). "Multiple types of ryanodine receptor/Ca2+ release channels are differentially expressed in rabbit brain." The Journal of neuroscience : the official journal of the Society for Neuroscience **14**(8): 4794-4805.

Futatsugi, A., G. Kuwajima, et al. (1995). "Tissue-specific and developmentally regulated alternative splicing in mouse skeletal muscle ryanodine receptor mRNA." Biochem J **305 (Pt 2)**: 373-378.

References

Gach, M. P., G. Cherednichenko, et al. (2008). "Alpha2delta1 dihydropyridine receptor subunit is a critical element for excitation-coupled calcium entry but not for formation of tetrads in skeletal myotubes." Biophys J **94**(8): 3023-3034.

Gailly, P., B. Boland, et al. (1993). "Critical evaluation of cytosolic calcium determination in resting muscle fibres from normal and dystrophic (mdx) mice." Cell Calcium **14**(6): 473-483.

Galea, V. (1996). "Changes in motor unit estimates with aging." Journal of clinical neurophysiology : official publication of the American Electroencephalographic Society **13**(3): 253-260.

Gallant, E. M. and L. R. Lentz (1992). "Excitation-contraction coupling in pigs heterozygous for malignant hyperthermia." The American journal of physiology **262**(2 Pt 1): C422-426.

Ganong, W. F. (1997). Review of medical physiology. Stamford, Conn., Appleton & Lange ; London : Prentice Hall International.

Garcia, J., T. Tanabe, et al. (1994). "Relationship of calcium transients to calcium currents and charge movements in myotubes expressing skeletal and cardiac dihydropyridine receptors." The Journal of General Physiology **103**(1): 125-147.

Garcia, M. C., E. Carrillo, et al. (2005). "Short-term regulation of excitation-contraction coupling by the beta1a subunit in adult mouse skeletal muscle." Biophys J **89**(6): 3976-3984.

Gauthier, G. F. and H. A. Padykula (1966). "Cytological studies of fiber types in skeletal muscle. A comparative study of the mammalian diaphragm." J Cell Biol **28**(2): 333-354.

Gelfi, C., A. Vigano, et al. (2006). "The human muscle proteome in aging." J Proteome Res **5**(6): 1344-1353.

Gellerich, F. N., Z. Gizatullina, et al. (2010). "The regulation of OXPHOS by extramitochondrial calcium." Biochim Biophys Acta **1797**(6-7): 1018-1027.

Ghatak, A., O. Faheem, et al. (2010). "The genetics of statin-induced myopathy." Atherosclerosis **210**(2): 337-343.

Giannini, G., E. Clementi, et al. (1992). "Expression of a ryanodine receptor-Ca2+ channel that is regulated by TGF-beta." Science **257**(5066): 91-94.

Giannini, G., A. Conti, et al. (1995). "The ryanodine receptor/calcium channel genes are widely and differentially expressed in murine brain and peripheral tissues." The Journal of cell biology **128**(5): 893-904.

Gilliam, L. A. and D. K. St Clair (2011). "Chemotherapy-induced weakness and fatigue in skeletal muscle: the role of oxidative stress." Antioxid Redox Signal **15**(9): 2543-2563.

Gillis, J. M. (1997). "Inhibition of mitochondrial calcium uptake slows down relaxation in mitochondria-rich skeletal muscles." J Muscle Res Cell Motil **18**(4): 473-483.

Gonzalez-Gutierrez, G., E. Miranda-Laferte, et al. (2007). "The Src homology 3 domain of the beta-subunit of voltage-gated calcium channels promotes endocytosis via dynamin interaction." J Biol Chem **282**(4): 2156-2162.

Gonzalez, A., W. G. Kirsch, et al. (2000). "Involvement of multiple intracellular release channels in calcium sparks of skeletal muscle." Proceedings of the National Academy of Sciences of the United States of America **97**(8): 4380-4385.

Gonzalez, E., M. L. Messi, et al. (2003). "Insulin-like growth factor-1 prevents age-related decrease in specific force and intracellular Ca2+ in single intact muscle fibres from transgenic mice." J Physiol **552**(Pt 3): 833-844.

Goodpaster, B. H., S. W. Park, et al. (2006). "The loss of skeletal muscle strength, mass, and quality in older adults: the health, aging and body composition study." J Gerontol A Biol Sci Med Sci **61**(10): 1059-1064.

Goonasekera, S. A., N. A. Beard, et al. (2007). "Triadin binding to the C-terminal luminal loop of the ryanodine receptor is important for skeletal muscle excitation contraction coupling." J Gen Physiol **130**(4): 365-378.

Gorza, L. (1990). "Identification of a novel type 2 fiber population in mammalian skeletal muscle by combined use of histochemical myosin ATPase and anti-myosin monoclonal antibodies." J Histochem Cytochem **38**(2): 257-265.

Grabner, M., R. T. Dirksen, et al. (1999). "The II-III loop of the skeletal muscle dihydropyridine receptor is responsible for the Bi-directional coupling with the ryanodine receptor." J Biol Chem **274**(31): 21913-21919.

Greenfield, J. G., T. Cornman, et al. (1958). "The prognostic value of the muscle biopsy in the floppy infant." Brain : a journal of neurology **81**(4): 461-484.

Gregg, R. G., A. Messing, et al. (1996). "Absence of the beta subunit (cchb1) of the skeletal muscle dihydropyridine receptor alters expression of the alpha 1 subunit and eliminates excitation-contraction coupling." Proc Natl Acad Sci U S A **93**(24): 13961-13966.

Grimby, G. (1995). "Muscle performance and structure in the elderly as studied cross-sectionally and longitudinally." J Gerontol A Biol Sci Med Sci **50 Spec No**: 17-22.

Groh, S., I. Marty, et al. (1999). "Functional interaction of the cytoplasmic domain of triadin with the skeletal ryanodine receptor." The Journal of biological chemistry **274**(18): 12278-12283.

Grunwald, R. and G. Meissner (1995). "Lumenal sites and C terminus accessibility of the skeletal muscle calcium release channel (ryanodine receptor)." The Journal of biological chemistry **270**(19): 11338-11347.

Guis, S., D. Figarella-Branger, et al. (2006). "In vivo and in vitro characterization of skeletal muscle metabolism in patients with statin-induced adverse effects." Arthritis Rheum **55**(4): 551-557.

Gundersen, K., E. Leberer, et al. (1988). "Fibre types, calcium-sequestering proteins and metabolic enzymes in denervated and chronically stimulated muscles of the rat." J Physiol **398**: 177-189.

Guo, W. and K. P. Campbell (1995). "Association of triadin with the ryanodine receptor and calsequestrin in the lumen of the sarcoplasmic reticulum." J Biol Chem **270**(16): 9027-9030.

Guo, W., A. O. Jorgensen, et al. (1996). "Biochemical characterization and molecular cloning of cardiac triadin." J Biol Chem **271**(1): 458-465.

Gurnett, C. A., M. De Waard, et al. (1996). "Dual function of the voltage-dependent Ca2+ channel alpha 2 delta subunit in current stimulation and subunit interaction." Neuron **16**(2): 431-440.

Guth, L. and F. J. Samaha (1969). "Qualitative differences between actomyosin ATPase of slow and fast mammalian muscle." Exp Neurol **25**(1): 138-152.

Gyorke, I. and S. Gyorke (1998). "Regulation of the cardiac ryanodine receptor channel by luminal Ca2+ involves luminal Ca2+ sensing sites." Biophysical Journal **75**(6): 2801-2810.

Gyorke, I., N. Hester, et al. (2004). "The role of calsequestrin, triadin, and junctin in conferring cardiac ryanodine receptor responsiveness to luminal calcium." Biophys J **86**(4): 2121-2128.

Haarmann, C. S., A. F. Dulhunty, et al. (2005). "Regulation of skeletal ryanodine receptors by dihydropyridine receptor II-III loop C-region peptides: relief of Mg2+ inhibition." Biochem J **387**(Pt 2): 429-436.

Haarmann, C. S., D. Green, et al. (2003). "The random-coil 'C' fragment of the dihydropyridine receptor II-III loop can activate or inhibit native skeletal ryanodine receptors." Biochem J **372**(Pt 2): 305-316.

Hain, J., S. Nath, et al. (1994). "Phosphorylation modulates the function of the calcium release channel of sarcoplasmic reticulum from skeletal muscle." Biophysical Journal **67**(5): 1823-1833.

Hain, J., H. Onoue, et al. (1995). "Phosphorylation modulates the function of the calcium release channel of sarcoplasmic reticulum from cardiac muscle." The Journal of biological chemistry **270**(5): 2074-2081.

Hakamata, Y., J. Nakai, et al. (1992). "Primary structure and distribution of a novel ryanodine receptor/calcium release channel from rabbit brain." FEBS letters **312**(2-3): 229-235.

Hakkinen, K., W. J. Kraemer, et al. (1996). "Bilateral and unilateral neuromuscular function and muscle cross-sectional area in middle-aged and elderly men and women." The journals of gerontology. Series A, Biological sciences and medical sciences **51**(1): B21-29.

References

Hakkinen, K., U. M. Pastinen, et al. (1995). "Neuromuscular performance in voluntary bilateral and unilateral contraction and during electrical stimulation in men at different ages." European journal of applied physiology and occupational physiology **70**(6): 518-527.

Hall, J. E. and A. C. Guyton (2011). Guyton and Hall textbook of medical physiology. Philadelphia, Pa., Saunders/Elsevier.

Hamilton, S. L. and Serysheva, II (2009). "Ryanodine receptor structure: progress and challenges." J Biol Chem **284**(7): 4047-4051.

Hanlon, M. R., N. S. Berrow, et al. (1999). "Modelling of a voltage-dependent Ca2+ channel beta subunit as a basis for understanding its functional properties." FEBS Lett **445**(2-3): 366-370.

Hayashi, K., R. G. Miller, et al. (1989). "Central core disease: ultrastructure of the sarcoplasmic reticulum and T-tubules." Muscle & nerve **12**(2): 95-102.

Hayes, J. D. and D. J. Pulford (1995). "The glutathione S-transferase supergene family: regulation of GST and the contribution of the isoenzymes to cancer chemoprotection and drug resistance." Crit Rev Biochem Mol Biol **30**(6): 445-600.

Hayward, R., D. Hydock, et al. (2013). "Tissue retention of doxorubicin and its effects on cardiac, smooth, and skeletal muscle function." J Physiol Biochem **69**(2): 177-187.

Held, B., D. Freise, et al. (2002). "Skeletal muscle L-type Ca(2+) current modulation in gamma1-deficient and wildtype murine myotubes by the gamma1 subunit and cAMP." The Journal of physiology **539**(Pt 2): 459-468.

Hennig, R. and T. Lomo (1985). "Firing patterns of motor units in normal rats." Nature **314**(6007): 164-166.

Hidalgo, C. and P. Donoso (2008). "Crosstalk between calcium and redox signaling: from molecular mechanisms to health implications." Antioxid Redox Signal **10**(7): 1275-1312.

Hill, R. R., N. Robbins, et al. (1991). "Plasticity of presynaptic and postsynaptic elements of neuromuscular junctions repeatedly observed in living adult mice." Journal of neurocytology **20**(3): 165-182.

Hille, B. (2001). Ion channels of excitable membranes. Sunderland, Mass. ; [Great Britain], Sinauer.

Hochuli, E. (1990). "Purification of recombinant proteins with metal chelate adsorbent." Genetic engineering **12**: 87-98.

Hohenegger, M. and J. Suko (1993). "Phosphorylation of the purified cardiac ryanodine receptor by exogenous and endogenous protein kinases." The Biochemical journal **296 (Pt 2)**: 303-308.

Holloszy, J. O., M. Chen, et al. (1991). "Skeletal muscle atrophy in old rats: differential changes in the three fiber types." Mechanisms of ageing and development **60**(2): 199-213.

Hoppeler, H., O. Mathieu, et al. (1981). "Design of the mammalian respiratory system. VI Distribution of mitochondria and capillaries in various muscles." Respir Physiol **44**(1): 87-111.

Hosey, M. M., J. Barhanin, et al. (1987). "Photoaffinity labelling and phosphorylation of a 165 kilodalton peptide associated with dihydropyridine and phenylalkylamine-sensitive calcium channels." Biochemical and Biophysical Research Communications **147**(3): 1137-1145.

Howald, H., H. Hoppeler, et al. (1985). "Influences of endurance training on the ultrastructural composition of the different muscle fiber types in humans." Pflugers Arch **403**(4): 369-376.

Huang, X., B. Fruen, et al. (2012). "Calmodulin-binding locations on the skeletal and cardiac ryanodine receptors." J Biol Chem **287**(36): 30328-30335.

Huang, Y. C., R. G. Dennis, et al. (2006). "Cultured slow vs. fast skeletal muscle cells differ in physiology and responsiveness to stimulation." Am J Physiol Cell Physiol **291**(1): C11-17.

Hullin, R., D. Singer-Lahat, et al. (1992). "Calcium channel beta subunit heterogeneity: functional expression of cloned cDNA from heart, aorta and brain." The EMBO journal **11**(3): 885-890.

Hulme, J. T., K. Konoki, et al. (2005). "Sites of proteolytic processing and noncovalent association of the distal C-terminal domain of CaV1.1 channels in skeletal muscle." Proc Natl Acad Sci U S A **102**(14): 5274-5279.

Huxley, A. F. and R. Niedergerke (1954). "Structural changes in muscle during contraction; interference microscopy of living muscle fibres." Nature **173**(4412): 971-973.

Ikemoto, N., B. Antoniu, et al. (1991). "Intravesicular calcium transient during calcium release from sarcoplasmic reticulum." Biochemistry **30**(21): 5230-5237.

Ikemoto, N., G. M. Bhatnagar, et al. (1972). "Interaction of divalent cations with the 55,000-dalton protein component of the sarcoplasmic reticulum. Studies of fluorescence and circular dichroism." The Journal of biological chemistry **247**(23): 7835-7837.

Imagawa, T., J. S. Smith, et al. (1987). "Purified ryanodine receptor from skeletal muscle sarcoplasmic reticulum is the Ca2+-permeable pore of the calcium release channel." J Biol Chem **262**(34): 16636-16643.

Inesi, G. and L. de Meis (1989). "Regulation of steady state filling in sarcoplasmic reticulum. Roles of back-inhibition, leakage, and slippage of the calcium pump." J Biol Chem **264**(10): 5929-5936.

Inoue, R., M. Tanabe, et al. (2003). "Ca2+-releasing effect of cerivastatin on the sarcoplasmic reticulum of mouse and rat skeletal muscle fibers." J Pharmacol Sci **93**(3): 279-288.

Inui, M., A. Saito, et al. (1987a). "Isolation of the ryanodine receptor from cardiac sarcoplasmic reticulum and identity with the feet structures." J Biol Chem **262**(32): 15637-15642.

Inui, M., A. Saito, et al. (1987b). "Purification of the ryanodine receptor and identity with feet structures of junctional terminal cisternae of sarcoplasmic reticulum from fast skeletal muscle." J Biol Chem **262**(4): 1740-1747.

Isaacs, H., J. J. Heffron, et al. (1975). "Central core disease. A correlated genetic, histochemical, ultramicroscopic, and biochemical study." Journal of neurology, neurosurgery, and psychiatry **38**(12): 1177-1186.

Isaacson, A., M. J. Hinkes, et al. (1970). "Contracture and twitch potentiation of fast and slow muscles of the rat at 20 and 37 C." Am J Physiol **218**(1): 33-41.

Isaeva, E. V., V. M. Shkryl, et al. (2005). "Mitochondrial redox state and Ca2+ sparks in permeabilized mammalian skeletal muscle." J Physiol **565**(Pt 3): 855-872.

Ishihara, A., H. Naitoh, et al. (1987). "Effects of ageing on the total number of muscle fibers and motoneurons of the tibialis anterior and soleus muscles in the rat." Brain research **435**(1-2): 355-358.

Izquierdo, M., J. Ibanez, et al. (1999). "Maximal strength and power characteristics in isometric and dynamic actions of the upper and lower extremities in middle-aged and older men." Acta physiologica Scandinavica **167**(1): 57-68.

Jacob, J. M. and N. Robbins (1990). "Differential effects of age on neuromuscular transmission in partially denervated mouse muscle." The Journal of neuroscience : the official journal of the Society for Neuroscience **10**(5): 1522-1529.

Jang, Y. C., M. S. Lustgarten, et al. (2010). "Increased superoxide in vivo accelerates age-associated muscle atrophy through mitochondrial dysfunction and neuromuscular junction degeneration." FASEB journal : official publication of the Federation of American Societies for Experimental Biology **24**(5): 1376-1390.

Jay, S. D., S. B. Ellis, et al. (1990). "Primary structure of the gamma subunit of the DHP-sensitive calcium channel from skeletal muscle." Science **248**(4954): 490-492.

Jayaraman, T., A. M. Brillantes, et al. (1992). "FK506 binding protein associated with the calcium release channel (ryanodine receptor)." The Journal of biological chemistry **267**(14): 9474-9477.

Jerkovic, R., C. Argentini, et al. (1997). "Early myosin switching induced by nerve activity in regenerating slow skeletal muscle." Cell Struct Funct **22**(1): 147-153.

Jeyakumar, L. H., J. A. Copello, et al. (1998). "Purification and characterization of ryanodine receptor 3 from mammalian tissue." The Journal of biological chemistry **273**(26): 16011-16020.

Johnson, L. R. and J. H. Byrne (2003). Essential medical physiology. Amsterdam ; London, Elsevier Academic Press.

Johnson, M. A., J. Polgar, et al. (1973). "Data on the distribution of fibre types in thirty-six human muscles. An autopsy study." J Neurol Sci **18**(1): 111-129.

Jones, J. L., D. F. Reynolds, et al. (2005). "Ryanodine receptor binding to FKBP12 is modulated by channel activation state." Journal of cell science **118**(Pt 20): 4613-4619.

Jones, L. R., L. Zhang, et al. (1995). "Purification, primary structure, and immunological characterization of the 26-kDa calsequestrin binding protein (junctin) from cardiac junctional sarcoplasmic reticulum." J Biol Chem **270**(51): 30787-30796.

Jones, T. E., K. W. Stephenson, et al. (2009). "Sarcopenia--mechanisms and treatments." Journal of geriatric physical therapy **32**(2): 83-89.

Jorgensen, A. O. (1998). Polarity and Development of The Cell Surface in Skeletal Muscle. Advances in Molecular and Cell Biology. E. E. Bittar and R. B. James, Elsevier. **Volume 26:** 157-199.

Jorquera, G., F. Altamirano, et al. (2013). "Cav1.1 controls frequency-dependent events regulating adult skeletal muscle plasticity." J Cell Sci **126**(Pt 5): 1189-1198.

Joy, T. R. and R. A. Hegele (2009). "Narrative review: statin-related myopathy." Ann Intern Med **150**(12): 858-868.

Jung, D. H., S. H. Mo, et al. (2006). "Calumenin, a multiple EF-hands Ca2+-binding protein, interacts with ryanodine receptor-1 in rabbit skeletal sarcoplasmic reticulum." Biochemical and Biophysical Research Communications **343**(1): 34-42.

Jungbluth, H., C. R. Muller, et al. (2002). "Autosomal recessive inheritance of RYR1 mutations in a congenital myopathy with cores." Neurology **59**(2): 284-287.

Jurkat-Rott, K., T. McCarthy, et al. (2000). "Genetics and pathogenesis of malignant hyperthermia." Muscle Nerve **23**(1): 4-17.

Kakizawa, S. (2013). "Nitric Oxide-Induced Calcium Release: Activation of Type 1 Ryanodine Receptor, a Calcium Release Channel, through Non-Enzymatic Post-Translational Modification by Nitric Oxide." Front Endocrinol (Lausanne) **4**: 142.

Kakizawa, S., T. Yamazawa, et al. (2012). "Nitric oxide-induced calcium release via ryanodine receptors regulates neuronal function." EMBO J **31**(2): 417-428.

Kakizawa, S., T. Yamazawa, et al. (2013). "Nitric oxide-induced calcium release: activation of type 1 ryanodine receptor by endogenous nitric oxide." Channels (Austin) **7**(1): 1-5.

Kalhovde, J. M., R. Jerkovic, et al. (2005). ""Fast" and "slow" muscle fibres in hindlimb muscles of adult rats regenerate from intrinsically different satellite cells." J Physiol **562**(Pt 3): 847-857.

Kanda, K. and K. Hashizume (1989). "Changes in properties of the medial gastrocnemius motor units in aging rats." Journal of neurophysiology **61**(4): 737-746.

Kandel, E. R. (2012). Principles of neural science. New York, McGraw-Hill.

Kang, C. B., Y. Hong, et al. (2008). "FKBP family proteins: immunophilins with versatile biological functions." Neurosignals **16**(4): 318-325.

Karunasekara, Y., A. F. Dulhunty, et al. (2009). "The voltage-gated calcium-channel beta subunit: more than just an accessory." Eur Biophys J.

Karunasekara, Y., R. T. Rebbeck, et al. (2012). "An alpha-helical C-terminal tail segment of the skeletal L-type Ca2+ channel beta1a subunit activates ryanodine receptor type 1 via a hydrophobic surface." FASEB J.

Karunasekara, Y. A. (2011). Interactions between the skeletal dihydropyridine receptor β subunit, the α_{1s} II-III loop and the ryanodine receptor. PhD, Australian National Univeristy.

Kasielke, N., G. J. Obermair, et al. (2003). "Cardiac-type EC-coupling in dysgenic myotubes restored with Ca2+ channel subunit isoforms alpha1C and alpha1D does not correlate with current density." Biophysical Journal **84**(6): 3816-3828.

Kass, R. S. and M. C. Sanguinetti (1984). "Inactivation of calcium channel current in the calf cardiac Purkinje fiber. Evidence for voltage- and calcium-mediated mechanisms." J Gen Physiol **84**(5): 705-726.

Kawakami, M. and E. Okabe (1998). "Superoxide anion radical-triggered Ca2+ release from cardiac sarcoplasmic reticulum through ryanodine receptor Ca2+ channel." Molecular pharmacology **53**(3): 497-503.

Kawamoto, R. M., J. P. Brunschwig, et al. (1986). "Isolation, characterization, and localization of the spanning protein from skeletal muscle triads." J Cell Biol **103**(4): 1405-1414.

Kawamura, Y., H. Okazaki, et al. (1977). "Lumbar motoneurons of man: I) number and diameter histogram of alpha and gamma axons of ventral root." Journal of neuropathology and experimental neurology **36**(5): 853-860.

Kay, J. E. (1996). "Structure-function relationships in the FK506-binding protein (FKBP) family of peptidylprolyl cis-trans isomerases." The Biochemical journal **314 (Pt 2)**: 361-385.

Kelly, S. S. and N. Robbins (1986). "Sustained transmitter output by increased transmitter turnover in limb muscles of old mice." The Journal of neuroscience : the official journal of the Society for Neuroscience **6**(10): 2900-2907.

Kent-Braun, J. A., A. V. Ng, et al. (2002). "Human skeletal muscle responses vary with age and gender during fatigue due to incremental isometric exercise." Journal of applied physiology **93**(5): 1813-1823.

Kiens, B. (2006). "Skeletal muscle lipid metabolism in exercise and insulin resistance." Physiol Rev **86**(1): 205-243.

Kim, K. C., A. H. Caswell, et al. (1990). "Identification of a new subpopulation of triad junctions isolated from skeletal muscle; morphological correlations with intact muscle." J Membr Biol **113**(3): 221-235.

Kimura, T., J. D. Lueck, et al. (2009). "Alternative splicing of RyR1 alters the efficacy of skeletal EC coupling." Cell Calcium **45**(3): 264-274.

Kimura, T., M. Nakamori, et al. (2005). "Altered mRNA splicing of the skeletal muscle ryanodine receptor and sarcoplasmic/endoplasmic reticulum Ca2+-ATPase in myotonic dystrophy type 1." Hum Mol Genet **14**(15): 2189-2200.

Kimura, T., S. M. Pace, et al. (2007). "A variably spliced region in the type 1 ryanodine receptor may participate in an inter-domain interaction." Biochem J **401**(1): 317-324.

Kirchberber, M. A., M. Tada, et al. (1975). "Phospholamban: a regulatory protein of the cardiac sarcoplasmic reticulum." Recent Adv Stud Cardiac Struct Metab **5**: 103-115.

Kleiber, M. (1947). "Body size and metabolic rate." Physiol Rev **27**(4): 511-541.

Klein, M. G., H. Cheng, et al. (1996). "Two mechanisms of quantized calcium release in skeletal muscle." Nature **379**(6564): 455-458.

Klein, M. G., L. Kovacs, et al. (1991). "Decline of myoplasmic Ca2+, recovery of calcium release and sarcoplasmic Ca2+ pump properties in frog skeletal muscle." J Physiol **441**: 639-671.

Klitgaard, H., O. Bergman, et al. (1990a). "Co-existence of myosin heavy chain I and IIa isoforms in human skeletal muscle fibres with endurance training." Pflugers Arch **416**(4): 470-472.

Klitgaard, H., A. Brunet, et al. (1989). "Morphological and biochemical changes in old rat muscles: effect of increased use." Journal of applied physiology **67**(4): 1409-1417.

Klitgaard, H., M. Mantoni, et al. (1990b). "Function, morphology and protein expression of ageing skeletal muscle: a cross-sectional study of elderly men with different training backgrounds." Acta physiologica Scandinavica **140**(1): 41-54.

Knollmann, B. C., N. Chopra, et al. (2006). "Casq2 deletion causes sarcoplasmic reticulum volume increase, premature Ca2+ release, and catecholaminergic polymorphic ventricular tachycardia." The Journal of clinical investigation **116**(9): 2510-2520.

Knudson, C. M., K. K. Stang, et al. (1993a). "Biochemical characterization of ultrastructural localization of a major junctional sarcoplasmic reticulum glycoprotein (triadin)." J Biol Chem **268**(17): 12637-12645.

Knudson, C. M., K. K. Stang, et al. (1993b). "Primary structure and topological analysis of a skeletal muscle-specific junctional sarcoplasmic reticulum glycoprotein (triadin)." J Biol Chem **268**(17): 12646-12654.

Kobayashi, S., T. Yamamoto, et al. (2004). "Antibody probe study of Ca2+ channel regulation by interdomain interaction within the ryanodine receptor." The Biochemical journal **380**(Pt 2): 561-569.

Kobayashi, Y. M., B. A. Alseikhan, et al. (2000). "Localization and characterization of the calsequestrin-binding domain of triadin 1. Evidence for a charged beta-strand in mediating the protein-protein interaction." The Journal of biological chemistry **275**(23): 17639-17646.

Kobayashi, Y. M. and L. R. Jones (1999). "Identification of triadin 1 as the predominant triadin isoform expressed in mammalian myocardium." The Journal of biological chemistry **274**(40): 28660-28668.

Konishi, M. (1998). "Cytoplasmic free concentrations of Ca2+ and Mg2+ in skeletal muscle fibers at rest and during contraction." Jpn J Physiol **48**(6): 421-438.

Krause, T., M. U. Gerbershagen, et al. (2004). "Dantrolene--a review of its pharmacology, therapeutic use and new developments." Anaesthesia **59**(4): 364-373.

Krenacs, T., E. Molnar, et al. (1989). "Fibre typing using sarcoplasmic reticulum Ca2+-ATPase and myoglobin immunohistochemistry in rat gastrocnemius muscle." Histochem J **21**(3): 145-155.

Krivickas, L. S., D. Suh, et al. (2001). "Age- and gender-related differences in maximum shortening velocity of skeletal muscle fibers." American journal of physical medicine & rehabilitation / Association of Academic Physiatrists **80**(6): 447-455; quiz 456-447.

Kubis, H. P., E. A. Haller, et al. (1997). "Adult fast myosin pattern and Ca2+-induced slow myosin pattern in primary skeletal muscle culture." Proc Natl Acad Sci U S A **94**(8): 4205-4210.

Kugelberg, E. (1976). "Adaptive transformation of rat soleus motor units during growth." J Neurol Sci **27**(3): 269-289.

Kugelberg, E. and L. Edstrom (1968). "Differential histochemical effects of muscle contractions on phosphorylase and glycogen in various types of fibres: relation to fatigue." J Neurol Neurosurg Psychiatry **31**(5): 415-423.

Kugelberg, E. and L. E. Thornell (1983). "Contraction time, histochemical type, and terminal cisternae volume of rat motor units." Muscle & nerve **6**(2): 149-153.

Kugler, G., R. G. Weiss, et al. (2004). "Structural requirements of the dihydropyridine receptor alpha1S II-III loop for skeletal-type excitation-contraction coupling." J Biol Chem **279**(6): 4721-4728.

Kujoth, G. C., C. Leeuwenburgh, et al. (2006). "Mitochondrial DNA mutations and apoptosis in mammalian aging." Cancer research **66**(15): 7386-7389.

Kuwajima, G., A. Futatsugi, et al. (1992). "Two types of ryanodine receptors in mouse brain: skeletal muscle type exclusively in Purkinje cells and cardiac muscle type in various neurons." Neuron **9**(6): 1133-1142.

Lai, F. A., M. Dent, et al. (1992a). "Expression of a cardiac Ca(2+)-release channel isoform in mammalian brain." The Biochemical journal **288 (Pt 2)**: 553-564.

Lai, F. A., H. Erickson, et al. (1987). "Evidence for a junctional feet-ryanodine receptor complex from sarcoplasmic reticulum." Biochemical and Biophysical Research Communications **143**(2): 704-709.

Lai, F. A., H. P. Erickson, et al. (1988). "Purification and reconstitution of the calcium release channel from skeletal muscle." Nature **331**(6154): 315-319.

Lai, F. A., Q. Y. Liu, et al. (1992b). "Amphibian ryanodine receptor isoforms are related to those of mammalian skeletal or cardiac muscle." The American journal of physiology **263**(2 Pt 1): C365-372.

Lai, F. A. and G. Meissner (1989). "The muscle ryanodine receptor and its intrinsic Ca2+ channel activity." Journal of bioenergetics and biomembranes **21**(2): 227-246.

Lai, F. A., M. Misra, et al. (1989). "The ryanodine receptor-Ca2+ release channel complex of skeletal muscle sarcoplasmic reticulum. Evidence for a cooperatively coupled, negatively charged homotetramer." The Journal of biological chemistry **264**(28): 16776-16785.

Lamb, G. D. (2000). "Excitation-contraction coupling in skeletal muscle: comparisons with cardiac muscle." Clin Exp Pharmacol Physiol **27**(3): 216-224.

Lamb, G. D., M. A. Cellini, et al. (2001a). "Different Ca2+ releasing action of caffeine and depolarisation in skeletal muscle fibres of the rat." J Physiol **531**(Pt 3): 715-728.

Lamb, G. D., G. S. Posterino, et al. (2001b). "Effects of a domain peptide of the ryanodine receptor on Ca2+ release in skinned skeletal muscle fibers." Am J Physiol Cell Physiol **281**(1): C207-214.

Lamb, G. D. and D. G. Stephenson (1990). "Control of calcium release and the effect of ryanodine in skinned muscle fibres of the toad." The Journal of physiology **423**: 519-542.

Lamb, G. D. and D. G. Stephenson (1991). "Effect of Mg2+ on the control of Ca2+ release in skeletal muscle fibres of the toad." The Journal of physiology **434**: 507-528.

Lamb, G. D. and D. G. Stephenson (1994). "Effects of intracellular pH and [Mg2+] on excitation-contraction coupling in skeletal muscle fibres of the rat." The Journal of physiology **478 (Pt 2)**: 331-339.

Lamb, G. D. and D. G. Stephenson (1996). "Effects of FK506 and rapamycin on excitation-contraction coupling in skeletal muscle fibres of the rat." J Physiol **494 (Pt 2)**: 569-576.

Lamb, G. D. and T. Walsh (1987). "Calcium currents, charge movement and dihydropyridine binding in fast- and slow-twitch muscles of rat and rabbit." The Journal of physiology **393**: 595-617.

Lamboley, C. R., R. M. Murphy, et al. (2013). "Endogenous and maximal sarcoplasmic reticulum calcium content and calsequestrin expression in type I and type II human skeletal muscle fibres." J Physiol **591**(Pt 23): 6053-6068.

Lanner, J. T., D. K. Georgiou, et al. (2010). "Ryanodine Receptors: Structure, Expression, Molecular Details, and Function in Calcium Release." Cold Spring Harb Perspect Biol.

Lanza, I. R., D. W. Russ, et al. (2004). "Age-related enhancement of fatigue resistance is evident in men during both isometric and dynamic tasks." Journal of applied physiology **97**(3): 967-975.

Lapidos, K. A., R. Kakkar, et al. (2004). "The dystrophin glycoprotein complex: signaling strength and integrity for the sarcolemma." Circ Res **94**(8): 1023-1031.

Larsson, L. and L. Edstrom (1986). "Effects of age on enzyme-histochemical fibre spectra and contractile properties of fast- and slow-twitch skeletal muscles in the rat." Journal of the neurological sciences **76**(1): 69-89.

Larsson, L., L. Edstrom, et al. (1991). "MHC composition and enzyme-histochemical and physiological properties of a novel fast-twitch motor unit type." Am J Physiol **261**(1 Pt 1): C93-101.

Larsson, L., G. Grimby, et al. (1979). "Muscle strength and speed of movement in relation to age and muscle morphology." Journal of applied physiology: respiratory, environmental and exercise physiology **46**(3): 451-456.

Larsson, L., B. Sjodin, et al. (1978). "Histochemical and biochemical changes in human skeletal muscle with age in sedentary males, age 22--65 years." Acta physiologica Scandinavica **103**(1): 31-39.

Laver, D. (2001). "The power of single channel recording and analysis: its application to ryanodine receptors in lipid bilayers." Clinical and experimental pharmacology & physiology **28**(8): 675-686.

Laver, D. R., T. M. Baynes, et al. (1997a). "Magnesium inhibition of ryanodine-receptor calcium channels: evidence for two independent mechanisms." The Journal of membrane biology **156**(3): 213-229.

Laver, D. R., G. K. Lenz, et al. (2001). "Regulation of the calcium release channel from rabbit skeletal muscle by the nucleotides ATP, AMP, IMP and adenosine." J Physiol **537**(Pt 3): 763-778.

Laver, D. R., E. R. O'Neill, et al. (2004). "Luminal Ca2+-regulated Mg2+ inhibition of skeletal RyRs reconstituted as isolated channels or coupled clusters." The Journal of General Physiology **124**(6): 741-758.

Laver, D. R., V. J. Owen, et al. (1997b). "Reduced inhibitory effect of Mg2+ on ryanodine receptor-Ca2+ release channels in malignant hyperthermia." Biophysical Journal **73**(4): 1913-1924.

Leberer, E., K. T. Hartner, et al. (1988). "Postnatal development of Ca2+-sequestration by the sarcoplasmic reticulum of fast and slow muscles in normal and dystrophic mice." Eur J Biochem **174**(2): 247-253.

Leberer, E. and D. Pette (1986). "Immunochemical quantification of sarcoplasmic reticulum Ca-ATPase, of calsequestrin and of parvalbumin in rabbit skeletal muscles of defined fiber composition." Eur J Biochem **156**(3): 489-496.

Ledbetter, M. W., J. K. Preiner, et al. (1994). "Tissue distribution of ryanodine receptor isoforms and alleles determined by reverse transcription polymerase chain reaction." The Journal of biological chemistry **269**(50): 31544-31551.

Lee, E. H., S. H. Rho, et al. (2004a). "N-terminal region of FKBP12 is essential for binding to the skeletal ryanodine receptor." The Journal of biological chemistry **279**(25): 26481-26488.

Lee, J. M., S. H. Rho, et al. (2004b). "Negatively charged amino acids within the intraluminal loop of ryanodine receptor are involved in the interaction with triadin." J Biol Chem **279**(8): 6994-7000.

Lee, K. S., E. Marban, et al. (1985). "Inactivation of calcium channels in mammalian heart cells: joint dependence on membrane potential and intracellular calcium." J Physiol **364**: 395-411.

Lehnart, S. E., F. Huang, et al. (2003). "Immunophilins and coupled gating of ryanodine receptors." Current topics in medicinal chemistry **3**(12): 1383-1391.

Lennmarken, C., T. Bergman, et al. (1985). "Skeletal muscle function in man: force, relaxation rate, endurance and contraction time-dependence on sex and age." Clinical physiology **5**(3): 243-255.

Leong, P. and D. H. MacLennan (1998a). "A 37-amino acid sequence in the skeletal muscle ryanodine receptor interacts with the cytoplasmic loop between domains II and III in the skeletal muscle dihydropyridine receptor." J Biol Chem **273**(14): 7791-7794.

Leong, P. and D. H. MacLennan (1998b). "The cytoplasmic loops between domains II and III and domains III and IV in the skeletal muscle dihydropyridine receptor bind to a contiguous site in the skeletal muscle ryanodine receptor." J Biol Chem **273**(45): 29958-29964.

Leung, A. T., T. Imagawa, et al. (1987). "Structural characterization of the 1,4-dihydropyridine receptor of the voltage-dependent Ca2+ channel from rabbit skeletal muscle. Evidence for two distinct high molecular weight subunits." The Journal of biological chemistry **262**(17): 7943-7946.

Leuranguer, V., S. Papadopoulos, et al. (2006). "Organization of calcium channel beta1a subunits in triad junctions in skeletal muscle." J Biol Chem **281**(6): 3521-3527.

Lexell, J. (1995). "Human aging, muscle mass, and fiber type composition." J Gerontol A Biol Sci Med Sci **50 Spec No**: 11-16.

Lexell, J., D. Downham, et al. (1986). "Distribution of different fibre types in human skeletal muscles. Fibre type arrangement in m. vastus lateralis from three groups of healthy men between 15 and 83 years." Journal of the neurological sciences **72**(2-3): 211-222.

Lexell, J. and D. Y. Downham (1991). "The occurrence of fibre-type grouping in healthy human muscle: a quantitative study of cross-sections of whole vastus lateralis from men between 15 and 83 years." Acta neuropathologica **81**(4): 377-381.

Lexell, J., K. Henriksson-Larsen, et al. (1983). "Distribution of different fiber types in human skeletal muscles: effects of aging studied in whole muscle cross sections." Muscle & nerve **6**(8): 588-595.

Lexell, J., C. C. Taylor, et al. (1988). "What is the cause of the ageing atrophy? Total number, size and proportion of different fiber types studied in whole vastus lateralis muscle from 15- to 83-year-old men." Journal of the neurological sciences **84**(2-3): 275-294.

Lindle, R. S., E. J. Metter, et al. (1997). "Age and gender comparisons of muscle strength in 654 women and men aged 20-93 yr." Journal of applied physiology **83**(5): 1581-1587.

Liu, D., R. Hewawasam, et al. (2009). "Dissection of the inhibition of cardiac ryanodine receptors by human glutathione transferase GSTM2-2." Biochemical pharmacology **77**(7): 1181-1193.

Liu, G., J. J. Abramson, et al. (1994). "Direct evidence for the existence and functional role of hyperreactive sulfhydryls on the ryanodine receptor-triadin complex selectively labeled by the coumarin maleimide 7-diethylamino-3-(4'-maleimidylphenyl)-4-methylcoumarin." Mol Pharmacol **45**(2): 189-200.

Liu, W., D. A. Pasek, et al. (1998). "Modulation of Ca(2+)-gated cardiac muscle Ca(2+)-release channel (ryanodine receptor) by mono- and divalent ions." The American journal of physiology **274**(1 Pt 1): C120-128.

Liu, Y., W. R. Randall, et al. (2005). "Activity-dependent and -independent nuclear fluxes of HDAC4 mediated by different kinases in adult skeletal muscle." J Cell Biol **168**(6): 887-897.

Lobo, P. A. and F. Van Petegem (2009). "Crystal structures of the N-terminal domains of cardiac and skeletal muscle ryanodine receptors: insights into disease mutations." Structure **17**(11): 1505-1514.

Lochynski, D., P. Krutki, et al. (2008). "Effect of ageing on the regulation of motor unit force in rat medial gastrocnemius muscle." Experimental gerontology **43**(3): 218-228.

Lorenzon, N. M., C. S. Haarmann, et al. (2004). "Metabolic biotinylation as a probe of supramolecular structure of the triad junction in skeletal muscle." J Biol Chem **279**(42): 44057-44064.

Louboutin, J. P., V. Fichter-Gagnepain, et al. (1995). "Comparison of contractile properties between developing and regenerating soleus muscle: influence of external calcium concentration upon the contractility." Muscle Nerve **18**(11): 1292-1299.

Louboutin, J. P., V. Fichter-Gagnepain, et al. (1996). "External calcium dependence of extensor digitorum longus muscle contractility during bupivacaine-induced regeneration." Muscle Nerve **19**(8): 994-1002.

Lowe, D. A., D. D. Thomas, et al. (2002). "Force generation, but not myosin ATPase activity, declines with age in rat muscle fibers." Am J Physiol Cell Physiol **283**(1): C187-192.

Lowry, O. H., N. J. Rosebrough, et al. (1951). "Protein measurement with the Folin phenol reagent." The Journal of biological chemistry **193**(1): 265-275.

Lu, X., L. Xu, et al. (1994). "Activation of the skeletal muscle calcium release channel by a cytoplasmic loop of the dihydropyridine receptor." The Journal of biological chemistry **269**(9): 6511-6516.

Lu, X., L. Xu, et al. (1995). "Phosphorylation of dihydropyridine receptor II-III loop peptide regulates skeletal muscle calcium release channel function. Evidence for an essential role of the beta-OH group of Ser687." J Biol Chem **270**(31): 18459-18464.

Ludtke, S. J., Serysheva, II, et al. (2005). "The pore structure of the closed RyR1 channel." Structure **13**(8): 1203-1211.

Luff, A. R. and H. L. Atwood (1971). "Changes in the sarcoplasmic reticulum and transverse tubular system of fast and slow skeletal muscles of the mouse during postnatal development." J Cell Biol **51**(21): 369-383.

Lynch, N. A., E. J. Metter, et al. (1999). "Muscle quality. I. Age-associated differences between arm and leg muscle groups." Journal of applied physiology **86**(1): 188-194.

Lyons, G. E., M. Ontell, et al. (1990). "The expression of myosin genes in developing skeletal muscle in the mouse embryo." J Cell Biol **111**(4): 1465-1476.

Lytton, J., M. Westlin, et al. (1992). "Functional comparisons between isoforms of the sarcoplasmic or endoplasmic reticulum family of calcium pumps." J Biol Chem **267**(20): 14483-14489.

Ma, J. (1993). "Block by ruthenium red of the ryanodine-activated calcium release channel of skeletal muscle." The Journal of General Physiology **102**(6): 1031-1056.

Ma, J. (1995). "Desensitization of the skeletal muscle ryanodine receptor: evidence for heterogeneity of calcium release channels." Biophysical Journal **68**(3): 893-899.

Macefield, V. G., A. J. Fuglevand, et al. (1996). "Contractile properties of single motor units in human toe extensors assessed by intraneural motor axon stimulation." J Neurophysiol **75**(6): 2509-2519.

Mackrill, J. J., S. O'Driscoll, et al. (2001). "Analysis of type 1 ryanodine receptor-12 kDa FK506-binding protein interaction." Biochemical and Biophysical Research Communications **285**(1): 52-57.

MacLennan, D. H. and M. S. Phillips (1992). "Malignant hyperthermia." Science **256**(5058): 789-794.

MacLennan, D. H. and P. T. Wong (1971). "Isolation of a calcium-sequestering protein from sarcoplasmic reticulum." Proceedings of the National Academy of Sciences of the United States of America **68**(6): 1231-1235.

Magee, K. R. and G. M. Shy (1956). "A new congenital non-progressive myopathy." Brain : a journal of neurology **79**(4): 610-621.

Marcell, T. J. (2003). "Sarcopenia: causes, consequences, and preventions." J Gerontol A Biol Sci Med Sci **58**(10): M911-916.

Marcus, R. (1995). "Relationship of age-related decreases in muscle mass and strength to skeletal status." The journals of gerontology. Series A, Biological sciences and medical sciences **50 Spec No**: 86-87.

Marengo, J. J., C. Hidalgo, et al. (1998). "Sulfhydryl oxidation modifies the calcium dependence of ryanodine-sensitive calcium channels of excitable cells." Biophysical Journal **74**(3): 1263-1277.

Margreth, A., E. Damiani, et al. (1999). "Sarcoplasmic reticulum in aged skeletal muscle." Acta Physiol Scand **167**(4): 331-338.

Margreth, A., G. Salviati, et al. (1972). "Early biochemical consequences of denervation in fast and slow skeletal muscles and their relationship to neural control over muscle differentiation." Biochem J **126**(5): 1099-1110.

Marieb, E. N. and K. Hoehn (2010). Human anatomy & physiology. San Francisco ; London, Benjamin Cummings.

Marks, A. R., P. Tempst, et al. (1989). "Molecular cloning and characterization of the ryanodine receptor/junctional channel complex cDNA from skeletal muscle sarcoplasmic reticulum." Proc Natl Acad Sci U S A **86**(22): 8683-8687.

Marty, I., M. Robert, et al. (1995). "Localization of the N-terminal and C-terminal ends of triadin with respect to the sarcoplasmic reticulum membrane of rabbit skeletal muscle." Biochem J **307 (Pt 3)**: 769-774.

Marty, I., D. Thevenon, et al. (2000). "Cloning and characterization of a new isoform of skeletal muscle triadin." J Biol Chem **275**(11): 8206-8212.

Marty, I., M. Villaz, et al. (1994). "Transmembrane orientation of the N-terminal and C-terminal ends of the ryanodine receptor in the sarcoplasmic reticulum of rabbit skeletal muscle." The Biochemical journal **298 Pt 3**: 743-749.

Marx, J. O., M. C. Olsson, et al. (2006). "Scaling of skeletal muscle shortening velocity in mammals representing a 100,000-fold difference in body size." Pflugers Arch **452**(2): 222-230.

Marx, S. O., K. Ondrias, et al. (1998). "Coupled gating between individual skeletal muscle Ca2+ release channels (ryanodine receptors)." Science **281**(5378): 818-821.

Marx, S. O., S. Reiken, et al. (2001). "Phosphorylation-dependent regulation of ryanodine receptors: a novel role for leucine/isoleucine zippers." The Journal of cell biology **153**(4): 699-708.

Marx, S. O., S. Reiken, et al. (2000). "PKA phosphorylation dissociates FKBP12.6 from the calcium release channel (ryanodine receptor): defective regulation in failing hearts." Cell **101**(4): 365-376.

Mayrleitner, M., R. Chandler, et al. (1995). "Phosphorylation with protein kinases modulates calcium loading of terminal cisternae of sarcoplasmic reticulum from skeletal muscle." Cell Calcium **18**(3): 197-206.

Mayrleitner, M., A. P. Timerman, et al. (1994). "The calcium release channel of sarcoplasmic reticulum is modulated by FK-506 binding protein: effect of FKBP-12 on single channel activity of the skeletal muscle ryanodine receptor." Cell Calcium **15**(2): 99-108.

McCarthy, T. V., K. A. Quane, et al. (2000). "Ryanodine receptor mutations in malignant hyperthermia and central core disease." Hum Mutat **15**(5): 410-417.

McDonald, T. F., S. Pelzer, et al. (1994). "Regulation and modulation of calcium channels in cardiac, skeletal, and smooth muscle cells." Physiological reviews **74**(2): 365-507.

McGrew, S. G., C. Wolleben, et al. (1989). "Positive cooperativity of ryanodine binding to the calcium release channel of sarcoplasmic reticulum from heart and skeletal muscle." Biochemistry **28**(4): 1686-1691.

McPherson, P. S. (1999). "Regulatory role of SH3 domain-mediated protein-protein interactions in synaptic vesicle endocytosis." Cellular signalling **11**(4): 229-238.

Meissner, G. (1984). "Adenine nucleotide stimulation of Ca2+-induced Ca2+ release in sarcoplasmic reticulum." The Journal of biological chemistry **259**(4): 2365-2374.

Meissner, G. (1986). "Evidence of a role for calmodulin in the regulation of calcium release from skeletal muscle sarcoplasmic reticulum." Biochemistry **25**(1): 244-251.

Meissner, G. (1994). "Ryanodine receptor/Ca2+ release channels and their regulation by endogenous effectors." Annu Rev Physiol **56**: 485-508.

Meissner, G., E. Darling, et al. (1986). "Kinetics of rapid Ca2+ release by sarcoplasmic reticulum. Effects of Ca2+, Mg2+, and adenine nucleotides." Biochemistry **25**(1): 236-244.

Meissner, G. and J. S. Henderson (1987). "Rapid calcium release from cardiac sarcoplasmic reticulum vesicles is dependent on Ca2+ and is modulated by Mg2+, adenine nucleotide, and calmodulin." The Journal of biological chemistry **262**(7): 3065-3073.

Meissner, G., E. Rios, et al. (1997). "Regulation of skeletal muscle Ca2+ release channel (ryanodine receptor) by Ca2+ and monovalent cations and anions." The Journal of biological chemistry **272**(3): 1628-1638.

Melzer, W., A. Herrmann-Frank, et al. (1995). "The role of Ca2+ ions in excitation-contraction coupling of skeletal muscle fibres." Biochimica et biophysica acta **1241**(1): 59-116.

Menegazzi, P., F. Larini, et al. (1994). "Identification and Characterization of Three Calmodulin Binding Sites of the Skeletal Muscle Ryanodine Receptor." Biochemistry **33**(31): 9078-9084.

Meszaros, L. G., I. Minarovic, et al. (1996). "Inhibition of the skeletal muscle ryanodine receptor calcium release channel by nitric oxide." FEBS letters **380**(1-2): 49-52.

Metterlein, T., F. Schuster, et al. (2010). "Statins alter intracellular calcium homeostasis in malignant hyperthermia susceptible individuals." Cardiovasc Ther **28**(6): 356-360.

Michalak, M., P. Dupraz, et al. (1988). "Ryanodine binding to sarcoplasmic reticulum membrane; comparison between cardiac and skeletal muscle." Biochimica et biophysica acta **939**(3): 587-594.

Michnick, S. W., M. K. Rosen, et al. (1991). "Solution structure of FKBP, a rotamase enzyme and receptor for FK506 and rapamycin." Science **252**(5007): 836-839.

Miller, C. and E. Racker (1976). "Ca++-induced fusion of fragmented sarcoplasmic reticulum with artificial planar bilayers." The Journal of membrane biology **30**(3): 283-300.

Miller, J. W., C. R. Urbinati, et al. (2000). "Recruitment of human muscleblind proteins to (CUG)(n) expansions associated with myotonic dystrophy." EMBO J **19**(17): 4439-4448.

Miller, R. D. (2009). Miller's anesthesia. Philadelphia, Pa. ; [Edinburgh], Churchill Livingstone.

Mittal, K. R. and F. H. Logmani (1987). "Age-related reduction in 8th cervical ventral nerve root myelinated fiber diameters and numbers in man." Journal of gerontology **42**(1): 8-10.

Miyamoto, H. and E. Racker (1981). "Calcium-induced calcium release at terminal cisternae of skeletal sarcoplasmic reticulum." FEBS letters **133**(2): 235-238.

Mizunoya, W., J. Wakamatsu, et al. (2008). "Protocol for high-resolution separation of rodent myosin heavy chain isoforms in a mini-gel electrophoresis system." Anal Biochem **377**(1): 111-113.

Molina, M. L., F. N. Barrera, et al. (2006). "Clustering and coupled gating modulate the activity in KcsA, a potassium channel model." The Journal of biological chemistry **281**(27): 18837-18848.

Monnier, N., V. Procaccio, et al. (1997). "Malignant-hyperthermia susceptibility is associated with a mutation of the alpha 1-subunit of the human dihydropyridine-sensitive L-type voltage-dependent calcium-channel receptor in skeletal muscle." Am J Hum Genet **60**(6): 1316-1325.

Moore, C. P., G. Rodney, et al. (1999). "Apocalmodulin and Ca2+ calmodulin bind to the same region on the skeletal muscle Ca2+ release channel." Biochemistry **38**(26): 8532-8537.

Morrissette, J., L. Xu, et al. (2000). "Characterization of RyR1-slow, a ryanodine receptor specific to slow-twitch skeletal muscle." American journal of physiology. Regulatory, integrative and comparative physiology **279**(5): R1889-1898.

Morrow, G. R., P. L. Andrews, et al. (2002). "Fatigue associated with cancer and its treatment." Support Care Cancer **10**(5): 389-398.

Murayama, T. and Y. Ogawa (1992). "Purification and characterization of two ryanodine-binding protein isoforms from sarcoplasmic reticulum of bullfrog skeletal muscle." Journal of biochemistry **112**(4): 514-522.

Murphy, R. M., T. L. Dutka, et al. (2012). "Ca2+-dependent Proteolysis of Junctophilin 1 and Junctophilin 2 in Skeletal and Cardiac Muscle." J Physiol.

Murphy, R. M., N. T. Larkins, et al. (2009). "Calsequestrin content and SERCA determine normal and maximal Ca2+ storage levels in sarcoplasmic reticulum of fast- and slow-twitch fibres of rat." The Journal of physiology **587**(Pt 2): 443-460.

Nakagawa, T., H. Okano, et al. (1991). "The subtypes of the mouse inositol 1,4,5-trisphosphate receptor are expressed in a tissue-specific and developmentally specific manner." Proceedings of the National Academy of Sciences of the United States of America **88**(14): 6244-6248.

Nakai, J., R. T. Dirksen, et al. (1996). "Enhanced dihydropyridine receptor channel activity in the presence of ryanodine receptor." Nature **380**(6569): 72-75.

Nakai, J., T. Imagawa, et al. (1990). "Primary structure and functional expression from cDNA of the cardiac ryanodine receptor/calcium release channel." FEBS letters **271**(1-2): 169-177.

Nakai, J., N. Sekiguchi, et al. (1998a). "Two regions of the ryanodine receptor involved in coupling with L-type Ca2+ channels." J Biol Chem **273**(22): 13403-13406.

Nakai, J., T. Tanabe, et al. (1998b). "Localization in the II-III loop of the dihydropyridine receptor of a sequence critical for excitation-contraction coupling." J Biol Chem **273**(39): 24983-24986.

Nakanishi, S., G. Kuwajima, et al. (1992). "Immunohistochemical localization of ryanodine receptors in mouse central nervous system." Neuroscience research **15**(1-2): 130-142.

Narici, M. V. and N. Maffulli (2010). "Sarcopenia: characteristics, mechanisms and functional significance." Br Med Bull **95**: 139-159.

Narusawa, M., R. B. Fitzsimons, et al. (1987). "Slow myosin in developing rat skeletal muscle." J Cell Biol **104**(3): 447-459.

Needham, D. M. (1926). "RED AND WHITE MUSCLE." Physiological Reviews **6**(1): 1-27.

Neuhuber, B., U. Gerster, et al. (1998). "Association of calcium channel alpha1S and beta1a subunits is required for the targeting of beta1a but not of alpha1S into skeletal muscle triads." Proc Natl Acad Sci U S A **95**(9): 5015-5020.

Neylon, C. B., S. M. Richards, et al. (1995). "Multiple types of ryanodine receptor/Ca2+ release channels are expressed in vascular smooth muscle." Biochemical and Biophysical Research Communications **215**(3): 814-821.

Numa, S., T. Tanabe, et al. (1990). "Molecular insights into excitation-contraction coupling." Cold Spring Harbor symposia on quantitative biology **55**: 1-7.

O'Brien, J., G. Meissner, et al. (1993). "The fastest contracting muscles of nonmammalian vertebrates express only one isoform of the ryanodine receptor." Biophysical journal **65**(6): 2418-2427.

O'Brien, J. J., W. Feng, et al. (2002). "Ca2+ activation of RyR1 is not necessary for the initiation of skeletal-type excitation-contraction coupling." Biophysical Journal **82**(5): 2428-2435.

O'Connell, K., J. Gannon, et al. (2007). "Proteomic profiling reveals a severely perturbed protein expression pattern in aged skeletal muscle." Int J Mol Med **20**(2): 145-153.

O'Connell, K., J. Gannon, et al. (2008). "Reduced expression of sarcalumenin and related Ca2+ -regulatory proteins in aged rat skeletal muscle." Exp Gerontol **43**(10): 958-961.

O'Connell, K. M., N. Yamaguchi, et al. (2002). "Calmodulin binding to the 3614-3643 region of RyR1 is not essential for excitation-contraction coupling in skeletal myotubes." J Gen Physiol **120**(3): 337-347.

Oba, T., T. Murayama, et al. (2002). "Redox states of type 1 ryanodine receptor alter Ca(2+) release channel response to modulators." American journal of physiology. Cell physiology **282**(4): C684-692.

Obermair, G. J., G. Kugler, et al. (2005). "The Ca2+ channel alpha2delta-1 subunit determines Ca2+ current kinetics in skeletal muscle but not targeting of alpha1S or excitation-contraction coupling." J Biol Chem **280**(3): 2229-2237.

Obermair, G. J., P. Tuluc, et al. (2008). "Auxiliary Ca(2+) channel subunits: lessons learned from muscle." Current opinion in pharmacology **8**(3): 311-318.

Oda, K. (1984). "Age changes of motor innervation and acetylcholine receptor distribution on human skeletal muscle fibres." Journal of the neurological sciences **66**(2-3): 327-338.

Ogata, T. and Y. Yamasaki (1985). "Scanning electron-microscopic studies on the three-dimensional structure of mitochondria in the mammalian red, white and intermediate muscle fibers." Cell Tissue Res **241**(2): 251-256.

Ohnishi, S. T. (1979). "Calcium-induced calcium release from fragmented sarcoplasmic reticulum." Journal of biochemistry **86**(4): 1147-1150.

Ohrtman, J., B. Ritter, et al. (2008). "Sequence differences in the IQ motifs of CaV1.1 and CaV1.2 strongly impact calmodulin binding and calcium-dependent inactivation." J Biol Chem **283**(43): 29301-29311.

Olivares, E. B., S. J. Tanksley, et al. (1991). "Nonmammalian vertebrate skeletal muscles express two triad junctional foot protein isoforms." Biophysical journal **59**(6): 1153-1163.

Opatowsky, Y., C. C. Chen, et al. (2004). "Structural analysis of the voltage-dependent calcium channel beta subunit functional core and its complex with the alpha 1 interaction domain." Neuron **42**(3): 387-399.

Orlova, E. V., Serysheva, II, et al. (1996). "Two structural configurations of the skeletal muscle calcium release channel." Nat Struct Biol **3**(6): 547-552.

Otsu, K., K. Nishida, et al. (1994). "The point mutation Arg615-->Cys in the Ca2+ release channel of skeletal sarcoplasmic reticulum is responsible for hypersensitivity to caffeine and halothane in malignant hyperthermia." The Journal of biological chemistry **269**(13): 9413-9415.

Otsu, K., H. F. Willard, et al. (1990). "Molecular cloning of cDNA encoding the Ca2+ release channel (ryanodine receptor) of rabbit cardiac muscle sarcoplasmic reticulum." The Journal of biological chemistry **265**(23): 13472-13483.

Ottini, L., G. Marziali, et al. (1996). "Alpha and beta isoforms of ryanodine receptor from chicken skeletal muscle are the homologues of mammalian RyR1 and RyR3." The Biochemical journal **315 (Pt 1)**: 207-216.

Overend, T. J., D. A. Cunningham, et al. (1992). "Thigh composition in young and elderly men determined by computed tomography." Clin Physiol **12**(6): 629-640.

Owen, V. J., N. L. Taske, et al. (1997). "Reduced Mg2+ inhibition of Ca2+ release in muscle fibers of pigs susceptible to malignant hyperthermia." The American journal of physiology **272**(1 Pt 1): C203-211.

Oyamada, H., T. Murayama, et al. (1994). "Primary structure and distribution of ryanodine-binding protein isoforms of the bullfrog skeletal muscle." The Journal of biological chemistry **269**(25): 17206-17214.

Paolini, C., J. D. Fessenden, et al. (2004). "Evidence for conformational coupling between two calcium channels." Proc Natl Acad Sci U S A **101**(34): 12748-12752.

Papadopoulos, S., V. Leuranguer, et al. (2004). "Mapping sites of potential proximity between the dihydropyridine receptor and RyR1 in muscle using a cyan fluorescent protein-yellow fluorescent protein tandem as a fluorescence resonance energy transfer probe." J Biol Chem **279**(42): 44046-44056.

Pape, P. C., D. S. Jong, et al. (1995). "Calcium release and its voltage dependence in frog cut muscle fibers equilibrated with 20 mM EGTA." The Journal of General Physiology **106**(2): 259-336.

Pate, P., J. Mochca-Morales, et al. (2000). "Determinants for calmodulin binding on voltage-dependent Ca2+ channels." J Biol Chem **275**(50): 39786-39792.

Patel, J. R., R. Coronado, et al. (1995). "Cardiac sarcoplasmic reticulum phosphorylation increases Ca2+ release induced by flash photolysis of nitr-5." Circulation research **77**(5): 943-949.

Paul-Pletzer, K., T. Yamamoto, et al. (2002). "Identification of a dantrolene-binding sequence on the skeletal muscle ryanodine receptor." The Journal of biological chemistry **277**(38): 34918-34923.

Payne, A. M. and O. Delbono (2004). "Neurogenesis of excitation-contraction uncoupling in aging skeletal muscle." Exerc Sport Sci Rev **32**(1): 36-40.

Payne, A. M., Z. Zheng, et al. (2004). "External Ca(2+)-dependent excitation--contraction coupling in a population of ageing mouse skeletal muscle fibres." J Physiol **560**(Pt 1): 137-155.

References

Pellegrino, M. A., M. Canepari, et al. (2003). "Orthologous myosin isoforms and scaling of shortening velocity with body size in mouse, rat, rabbit and human muscles." J Physiol **546**(Pt 3): 677-689.

Percival, A. L., A. J. Williams, et al. (1994). "Chicken skeletal muscle ryanodine receptor isoforms: ion channel properties." Biophysical Journal **67**(5): 1834-1850.

Pereon, Y., C. Dettbarn, et al. (1998). "Dihydropyridine receptor isoform expression in adult rat skeletal muscle." Pflugers Archiv : European journal of physiology **436**(3): 309-314.

Pereon, Y., J. Navarro, et al. (1997). "Regulation of dihydropyridine receptor and ryanodine receptor gene expression in regenerating skeletal muscle." Pflugers Arch **433**(3): 221-229.

Perez-Reyes, E., A. Castellano, et al. (1992). "Cloning and expression of a cardiac/brain beta subunit of the L-type calcium channel." The Journal of biological chemistry **267**(3): 1792-1797.

Perez, C. F. (2011). "On the footsteps of Triadin and its role in skeletal muscle." World journal of biological chemistry **2**(8): 177-183.

Perez, C. F., J. R. Lopez, et al. (2005). "Expression levels of RyR1 and RyR3 control resting free Ca2+ in skeletal muscle." Am J Physiol Cell Physiol **288**(3): C640-649.

Perez, C. F., S. Mukherjee, et al. (2003a). "Amino acids 1-1,680 of ryanodine receptor type 1 hold critical determinants of skeletal type for excitation-contraction coupling. Role of divergence domain D2." The Journal of biological chemistry **278**(41): 39644-39652.

Perez, C. F., A. Voss, et al. (2003b). "RyR1/RyR3 chimeras reveal that multiple domains of RyR1 are involved in skeletal-type E-C coupling." Biophys J **84**(4): 2655-2663.

Periasamy, M. and A. Kalyanasundaram (2007). "SERCA pump isoforms: their role in calcium transport and disease." Muscle Nerve **35**(4): 430-442.

Pessah, I. N., R. A. Stambuk, et al. (1987). "Ca2+-activated ryanodine binding: mechanisms of sensitivity and intensity modulation by Mg2+, caffeine, and adenine nucleotides." Molecular pharmacology **31**(3): 232-238.

Pessah, I. N., A. L. Waterhouse, et al. (1985). "The calcium-ryanodine receptor complex of skeletal and cardiac muscle." Biochemical and Biophysical Research Communications **128**(1): 449-456.

Pessah, I. N. and I. Zimanyi (1991). "Characterization of multiple [3H]ryanodine binding sites on the Ca2+ release channel of sarcoplasmic reticulum from skeletal and cardiac muscle: evidence for a sequential mechanism in ryanodine action." Molecular pharmacology **39**(5): 679-689.

Peter, J. B., R. J. Barnard, et al. (1972). "Metabolic profiles of three fiber types of skeletal muscle in guinea pigs and rabbits." Biochemistry **11**(14): 2627-2633.

Peterson, B. Z., C. D. DeMaria, et al. (1999). "Calmodulin is the Ca2+ sensor for Ca2+ -dependent inactivation of L-type calcium channels." Neuron **22**(3): 549-558.

Pette, D. and R. S. Staron (1990). "Cellular and molecular diversities of mammalian skeletal muscle fibers." Rev Physiol Biochem Pharmacol **116**: 1-76.

Pette, D. and R. S. Staron (1997). "Mammalian skeletal muscle fiber type transitions." Int Rev Cytol **170**: 143-223.

Pette, D. and G. Vrbova (1999). "What does chronic electrical stimulation teach us about muscle plasticity?" Muscle Nerve **22**(6): 666-677.

Piotrkiewicz, M. and J. Celichowski (2007). "Tetanic potentiation in motor units of rat medial gastrocnemius." Acta Neurobiol Exp (Wars) **67**(1): 35-42.

Porter, M. M., A. A. Vandervoort, et al. (1995). "Aging of human muscle: structure, function and adaptability." Scand J Med Sci Sports **5**(3): 129-142.

Porter Moore, C., G. Rodney, et al. (1999a). "Apocalmodulin and Ca2+ Calmodulin Bind to the Same Region on the Skeletal Muscle Ca2+ Release Channel†." Biochemistry **38**(26): 8532-8537.

Porter Moore, C., J. Z. Zhang, et al. (1999b). "A role for cysteine 3635 of RYR1 in redox modulation and calmodulin binding." J Biol Chem **274**(52): 36831-36834.

Prakash, Y. S. and G. C. Sieck (1998). "Age-related remodeling of neuromuscular junctions on type-identified diaphragm fibers." Muscle & nerve **21**(7): 887-895.

Proenza, C., J. O'Brien, et al. (2002). "Identification of a region of RyR1 that participates in allosteric coupling with the alpha(1S) (Ca(V)1.1) II-III loop." J Biol Chem **277**(8): 6530-6535.

Proenza, C., C. Wilkens, et al. (2000a). "A carboxyl-terminal region important for the expression and targeting of the skeletal muscle dihydropyridine receptor." J Biol Chem **275**(30): 23169-23174.

Proenza, C., C. M. Wilkens, et al. (2000b). "Excitation-contraction coupling is not affected by scrambled sequence in residues 681-690 of the dihydropyridine receptor II-III loop." J Biol Chem **275**(39): 29935-29937.

Protasi, F., C. Franzini-Armstrong, et al. (1998). "Role of ryanodine receptors in the assembly of calcium release units in skeletal muscle." J Cell Biol **140**(4): 831-842.

Protasi, F., C. Paolini, et al. (2002). "Multiple regions of RyR1 mediate functional and structural interactions with alpha(1S)-dihydropyridine receptors in skeletal muscle." Biophys J **83**(6): 3230-3244.

Protasi, F., X. H. Sun, et al. (1996). "Formation and maturation of the calcium release apparatus in developing and adult avian myocardium." Dev Biol **173**(1): 265-278.

Qi, Y., E. M. Ogunbunmi, et al. (1998). "FK-binding protein is associated with the ryanodine receptor of skeletal muscle in vertebrate animals." The Journal of biological chemistry **273**(52): 34813-34819.

Qin, J., G. Valle, et al. (2008). "Luminal Ca2+ regulation of single cardiac ryanodine receptors: insights provided by calsequestrin and its mutants." The Journal of General Physiology **131**(4): 325-334.

Qin, N., D. Platano, et al. (1997). "Direct interaction of gbetagamma with a C-terminal gbetagamma-binding domain of the Ca2+ channel alpha1 subunit is responsible for channel inhibition by G protein-coupled receptors." Proceedings of the National Academy of Sciences of the United States of America **94**(16): 8866-8871.

Quane, K. A., J. M. Healy, et al. (1993). "Mutations in the ryanodine receptor gene in central core disease and malignant hyperthermia." Nat Genet **5**(1): 51-55.

Querfurth, H. W., N. J. Haughey, et al. (1998). "Expression of ryanodine receptors in human embryonic kidney (HEK293) cells." The Biochemical journal **334 (Pt 1)**: 79-86.

Quinn, R. (2005). "Comparing rat's to human's age: how old is my rat in people years?" Nutrition **21**(6): 775-777.

Racay, P., P. Gregory, et al. (2006). "Parvalbumin deficiency in fast-twitch muscles leads to increased 'slow-twitch type' mitochondria, but does not affect the expression of fiber specific proteins." FEBS J **273**(1): 96-108.

Radermacher, M., V. Rao, et al. (1994). "Cryo-electron microscopy and three-dimensional reconstruction of the calcium release channel/ryanodine receptor from skeletal muscle." J Cell Biol **127**(2): 411-423.

Rando, T. A. (2001). "The dystrophin-glycoprotein complex, cellular signaling, and the regulation of cell survival in the muscular dystrophies." Muscle Nerve **24**(12): 1575-1594.

Rantanen, T., K. Masaki, et al. (1998). "Grip strength changes over 27 yr in Japanese-American men." Journal of applied physiology **85**(6): 2047-2053.

Rau, F., F. Freyermuth, et al. (2011). "Misregulation of miR-1 processing is associated with heart defects in myotonic dystrophy." Nat Struct Mol Biol **18**(7): 840-845.

Realini, C., S. W. Rogers, et al. (1994). "KEKE motifs. Proposed roles in protein-protein association and presentation of peptides by MHC class I receptors." FEBS letters **348**(2): 109-113.

Rebbeck, R. T., Y. Karunasekara, et al. (2011). "The beta(1a) subunit of the skeletal DHPR binds to skeletal RyR1 and activates the channel via its 35-residue C-terminal tail." Biophys J **100**(4): 922-930.

Reiken, S., A. Lacampagne, et al. (2003). "PKA phosphorylation activates the calcium release channel (ryanodine receptor) in skeletal muscle: defective regulation in heart failure." The Journal of cell biology **160**(6): 919-928.

Renganathan, M., M. L. Messi, et al. (1997). "Dihydropyridine receptor-ryanodine receptor uncoupling in aged skeletal muscle." J Membr Biol **157**(3): 247-253.

References

Renganathan, M., M. L. Messi, et al. (1998). "Overexpression of IGF-1 exclusively in skeletal muscle prevents age-related decline in the number of dihydropyridine receptors." J Biol Chem **273**(44): 28845-28851.

Reuter, H. (1979). "Properties of two inward membrane currents in the heart." Annual review of physiology **41**: 413-424.

Rhee, H. S., C. A. Lucas, et al. (2004). "Fiber types in rat laryngeal muscles and their transformations after denervation and reinnervation." J Histochem Cytochem **52**(5): 581-590.

Rice, C. L., D. A. Cunningham, et al. (1989). "Arm and leg composition determined by computed tomography in young and elderly men." Clin Physiol **9**(3): 207-220.

Richards, M. W., A. J. Butcher, et al. (2004). "Ca2+ channel beta-subunits: structural insights AID our understanding." Trends Pharmacol Sci **25**(12): 626-632.

Rios, E. and G. Brum (1987). "Involvement of dihydropyridine receptors in excitation-contraction coupling in skeletal muscle." Nature **325**(6106): 717-720.

Rios, E. and G. Pizarro (1991). "Voltage sensor of excitation-contraction coupling in skeletal muscle." Physiological reviews **71**(3): 849-908.

Rios, E., N. Shirokova, et al. (2001). "A preferred amplitude of calcium sparks in skeletal muscle." Biophysical Journal **80**(1): 169-183.

Rios, E. and M. D. Stern (1997). "Calcium in close quarters: microdomain feedback in excitation-contraction coupling and other cell biological phenomena." Annual review of biophysics and biomolecular structure **26**: 47-82.

Ritucci, N. A. and A. M. Corbett (1995). "Effect of Mg2+ and ATP on depolarization-induced Ca2+ release in isolated triads." The American journal of physiology **269**(1 Pt 1): C85-95.

Rivero, J. L., R. J. Talmadge, et al. (1998). "Fibre size and metabolic properties of myosin heavy chain-based fibre types in rat skeletal muscle." J Muscle Res Cell Motil **19**(7): 733-742.

Rizzuto, R. and T. Pozzan (2006). "Microdomains of intracellular Ca2+: molecular determinants and functional consequences." Physiol Rev **86**(1): 369-408.

Robbins, N. (1992). "Compensatory plasticity of aging at the neuromuscular junction." Experimental gerontology **27**(1): 75-81.

Robbins, N. and M. A. Fahim (1985). "Progression of age changes in mature mouse motor nerve terminals and its relation to locomotor activity." Journal of neurocytology **14**(6): 1019-1036.

Rodney, G. G., B. Y. Williams, et al. (2000). "Regulation of RYR1 Activity by Ca2+ and Calmodulin†." Biochemistry **39**(26): 7807-7812.

Rome, L. C., A. A. Sosnicki, et al. (1990). "Maximum velocity of shortening of three fibre types from horse soleus muscle: implications for scaling with body size." J Physiol **431**: 173-185.

Romero, N. B., N. Monnier, et al. (2003). "Dominant and recessive central core disease associated with RYR1 mutations and fetal akinesia." Brain : a journal of neurology **126**(Pt 11): 2341-2349.

Rosenblatt, J. D., D. J. Parry, et al. (1996). "Phenotype of adult mouse muscle myoblasts reflects their fiber type of origin." Differentiation **60**(1): 39-45.

Rosenheimer, J. L. and D. O. Smith (1985). "Differential changes in the end-plate architecture of functionally diverse muscles during aging." Journal of neurophysiology **53**(6): 1567-1581.

Rossi, A. C., C. Mammucari, et al. (2010). "Two novel/ancient myosins in mammalian skeletal muscles: MYH14/7b and MYH15 are expressed in extraocular muscles and muscle spindles." J Physiol **588**(Pt 2): 353-364.

Rossi, R., R. Bottinelli, et al. (2001). "Response to caffeine and ryanodine receptor isoforms in mouse skeletal muscles." Am J Physiol Cell Physiol **281**(2): C585-594.

Roubenoff, R. (2000). "Sarcopenic obesity: does muscle loss cause fat gain? Lessons from rheumatoid arthritis and osteoarthritis." Ann N Y Acad Sci **904**: 553-557.

Rousseau, E., J. Ladine, et al. (1988). "Activation of the Ca2+ release channel of skeletal muscle sarcoplasmic reticulum by caffeine and related compounds." Archives of biochemistry and biophysics **267**(1): 75-86.

Rousseau, E. and G. Meissner (1989). "Single cardiac sarcoplasmic reticulum Ca2+-release channel: activation by caffeine." The American journal of physiology **256**(2 Pt 2): H328-333.

Rousseau, E., J. S. Smith, et al. (1986). "Single channel and 45Ca2+ flux measurements of the cardiac sarcoplasmic reticulum calcium channel." Biophysical Journal **50**(5): 1009-1014.

Rousseau, E., J. S. Smith, et al. (1987). "Ryanodine modifies conductance and gating behavior of single Ca2+ release channel." The American journal of physiology **253**(3 Pt 1): C364-368.

Rudolf, R., M. Mongillo, et al. (2004). "In vivo monitoring of Ca(2+) uptake into mitochondria of mouse skeletal muscle during contraction." J Cell Biol **166**(4): 527-536.

Ruehr, M. L., M. A. Russell, et al. (2003). "Targeting of protein kinase A by muscle A kinase-anchoring protein (mAKAP) regulates phosphorylation and function of the skeletal muscle ryanodine receptor." J Biol Chem **278**(27): 24831-24836.

Ruth, P., A. Rohrkasten, et al. (1989). "Primary structure of the beta subunit of the DHP-sensitive calcium channel from skeletal muscle." Science **245**(4922): 1115-1118.

Ryan, M., G. Butler-Browne, et al. (2003). "Persistent expression of the α1s-dihydropyridine receptor in aged human skeletal muscle: Implications for the excitation-contraction uncoupling hypothesis of sarcopenia." International Journal of Molecular Medicine **11**: 425-434.

Ryan, M., B. M. Carlson, et al. (2000). "Oligomeric Status of the Dihydropyridine Receptor in Aged Skeletal Muscle." Molecular Cell Biology Research Communications **4**(4): 224-229.

Safdar, A., M. J. Hamadeh, et al. (2010). "Aberrant mitochondrial homeostasis in the skeletal muscle of sedentary older adults." PLoS One **5**(5): e10778.

Saiki, Y., R. El-Hayek, et al. (1999). "Involvement of the Glu724-Pro760 region of the dihydropyridine receptor II-III loop in skeletal muscle-type excitation-contraction coupling." J Biol Chem **274**(12): 7825-7832.

Saito, A., M. Inui, et al. (1988). "Ultrastructure of the calcium release channel of sarcoplasmic reticulum." The Journal of cell biology **107**(1): 211-219.

Salviati, G., R. Betto, et al. (1984). "Myofibrillar-protein isoforms and sarcoplasmic-reticulum Ca2+-transport activity of single human muscle fibres." Biochem J **224**(1): 215-225.

Salviati, G., M. M. Sorenson, et al. (1982). "Calcium accumulation by the sarcoplasmic reticulum in two populations of chemically skinned human muscle fibers. Effects of calcium and cyclic AMP." J Gen Physiol **79**(4): 603-632.

Salviati, G. and P. Volpe (1988). "Ca2+ release from sarcoplasmic reticulum of skinned fast- and slow-twitch muscle fibers." The American journal of physiology **254**(3 Pt 1): C459-465.

Sambrook, J. and D. W. Russell (2001). Molecular cloning : a laboratory manual. Cold Spring Harbor, N.Y., Cold Spring Harbor Laboratory Press.

Sambrook, P. (2001). The musculoskeletal system. Edinburgh, Churchill Livingstone.

Samso, M., W. Feng, et al. (2009). "Coordinated movement of cytoplasmic and transmembrane domains of RyR1 upon gating." PLoS Biol **7**(4): e85.

Samso, M., X. Shen, et al. (2006). "Structural characterization of the RyR1-FKBP12 interaction." Journal of Molecular Biology **356**(4): 917-927.

Samso, M. and T. Wagenknecht (2002). "Apocalmodulin and Ca2+-calmodulin bind to neighboring locations on the ryanodine receptor." J Biol Chem **277**(2): 1349-1353.

Samso, M., T. Wagenknecht, et al. (2005). "Internal structure and visualization of transmembrane domains of the RyR1 calcium release channel by cryo-EM." Nat Struct Mol Biol **12**(6): 539-544.

Sanchez, G., Z. Pedrozo, et al. (2005). "Tachycardia increases NADPH oxidase activity and RyR2 S-glutathionylation in ventricular muscle." Journal of molecular and cellular cardiology **39**(6): 982-991.

Sartore, S., L. Gorza, et al. (1982). "Fetal myosin heavy chains in regenerating muscle." Nature **298**(5871): 294-296.

Sathasivam, S. and B. Lecky (2008). "Statin induced myopathy." BMJ **337**: a2286.

Satrustegui, J., B. Pardo, et al. (2007). "Mitochondrial transporters as novel targets for intracellular calcium signaling." Physiol Rev **87**(1): 29-67.

Savolainen, J. and M. Vornanen (1995). "Fiber types and myosin heavy chain composition in muscles of common shrew (Sorex araneus)." J Exp Zool **271**(1): 27-35.

Schell, M. J., S. K. Danoff, et al. (1993). "Inositol (1,4,5)-trisphosphate receptor: characterization of neuron-specific alternative splicing in rat brain and peripheral tissues." Brain research. Molecular brain research **17**(3-4): 212-216.

Schiaffino, S., S. Ausoni, et al. (1988). "Myosin heavy chain isoforms and velocity of shortening of type 2 skeletal muscle fibres." Acta Physiol Scand **134**(4): 575-576.

Schiaffino, S., K. A. Dyar, et al. (2013). "Mechanisms regulating skeletal muscle growth and atrophy." The FEBS journal.

Schiaffino, S., L. Gorza, et al. (1986). "Fetal myosin immunoreactivity in human dystrophic muscle." Muscle Nerve **9**(1): 51-58.

Schiaffino, S., L. Gorza, et al. (1989). "Three myosin heavy chain isoforms in type 2 skeletal muscle fibres." Journal of muscle research and cell motility **10**(3): 197-205.

Schiaffino, S., V. Hanzlikova, et al. (1970). "Relations between structure and function in rat skeletal muscle fibers." J Cell Biol **47**(1): 107-119.

Schiaffino, S. and C. Reggiani (1996). "Molecular diversity of myofibrillar proteins: gene regulation and functional significance." Physiol Rev **76**(2): 371-423.

Schiaffino, S. and C. Reggiani (2011). "Fiber types in mammalian skeletal muscles." Physiol Rev **91**(4): 1447-1531.

Schneider, M. F. and W. K. Chandler (1973). "Voltage dependent charge movement of skeletal muscle: a possible step in excitation-contraction coupling." Nature **242**(5395): 244-246.

Schredelseker, J., A. Dayal, et al. (2009). "Proper restoration of excitation-contraction coupling in the dihydropyridine receptor beta1-null zebrafish relaxed is an exclusive function of the beta1a subunit." J Biol Chem **284**(2): 1242-1251.

Schredelseker, J., V. Di Biase, et al. (2005). "The beta 1a subunit is essential for the assembly of dihydropyridine-receptor arrays in skeletal muscle." Proc Natl Acad Sci U S A **102**(47): 17219-17224.

Schwaller, B., J. Dick, et al. (1999). "Prolonged contraction-relaxation cycle of fast-twitch muscles in parvalbumin knockout mice." Am J Physiol **276**(2 Pt 1): C395-403.

Sciandra, F., M. Bozzi, et al. (2003). "Dystroglycan and muscular dystrophies related to the dystrophin-glycoprotein complex." Ann Ist Super Sanita **39**(2): 173-181.

Scott, B. T., H. K. Simmerman, et al. (1988). "Complete amino acid sequence of canine cardiac calsequestrin deduced by cDNA cloning." The Journal of biological chemistry **263**(18): 8958-8964.

Sencer, S., R. V. Papineni, et al. (2001). "Coupling of RYR1 and L-type calcium channels via calmodulin binding domains." J Biol Chem **276**(41): 38237-38241.

Seo, A. Y., J. Xu, et al. (2008). "Mitochondrial iron accumulation with age and functional consequences." Aging Cell **7**(5): 706-716.

Seoh, S. A., D. Sigg, et al. (1996). "Voltage-sensing residues in the S2 and S4 segments of the Shaker K+ channel." Neuron **16**(6): 1159-1167.

Seow, C. Y. and L. E. Ford (1991). "Shortening velocity and power output of skinned muscle fibers from mammals having a 25,000-fold range of body mass." J Gen Physiol **97**(3): 541-560.

Serysheva, II (2004). "Structural insights into excitation-contraction coupling by electron cryomicroscopy." Biochemistry (Mosc) **69**(11): 1226-1232.

Serysheva, II, S. L. Hamilton, et al. (2005). "Structure of Ca2+ release channel at 14 A resolution." J Mol Biol **345**(3): 427-431.

Serysheva, II, S. J. Ludtke, et al. (2008). "Subnanometer-resolution electron cryomicroscopy-based domain models for the cytoplasmic region of skeletal muscle RyR channel." Proc Natl Acad Sci U S A **105**(28): 9610-9615.

Serysheva, II, S. J. Ludtke, et al. (2002). "Structure of the voltage-gated L-type Ca2+ channel by electron cryomicroscopy." Proc Natl Acad Sci U S A **99**(16): 10370-10375.

Serysheva, II, E. V. Orlova, et al. (1995). "Electron cryomicroscopy and angular reconstitution used to visualize the skeletal muscle calcium release channel." Nat Struct Biol **2**(1): 18-24.

Serysheva, II, M. Schatz, et al. (1999). "Structure of the skeletal muscle calcium release channel activated with Ca2+ and AMP-PCP." Biophys J **77**(4): 1936-1944.

Sewry, C. A., C. Muller, et al. (2002). "The spectrum of pathology in central core disease." Neuromuscular disorders : NMD **12**(10): 930-938.

Sham, J. S., L. Cleemann, et al. (1995). "Functional coupling of Ca2+ channels and ryanodine receptors in cardiac myocytes." Proc Natl Acad Sci U S A **92**(1): 121-125.

Sharma, M. R., L. H. Jeyakumar, et al. (2000). "Three-dimensional structure of ryanodine receptor isoform three in two conformational states as visualized by cryo-electron microscopy." J Biol Chem **275**(13): 9485-9491.

Sharma, M. R., L. H. Jeyakumar, et al. (2006). "Three-dimensional visualization of FKBP12.6 binding to an open conformation of cardiac ryanodine receptor." Biophys J **90**(1): 164-172.

Sharma, M. R., P. Penczek, et al. (1998). "Cryoelectron microscopy and image analysis of the cardiac ryanodine receptor." The Journal of biological chemistry **273**(29): 18429-18434.

Sharp, A. H., P. S. McPherson, et al. (1993). "Differential immunohistochemical localization of inositol 1,4,5-trisphosphate- and ryanodine-sensitive Ca2+ release channels in rat brain." The Journal of neuroscience : the official journal of the Society for Neuroscience **13**(7): 3051-3063.

Shen, X., C. Franzini-Armstrong, et al. (2007). "Triadins modulate intracellular Ca(2+) homeostasis but are not essential for excitation-contraction coupling in skeletal muscle." The Journal of biological chemistry **282**(52): 37864-37874.

Sheridan, D. C., H. Takekura, et al. (2006). "Bidirectional signaling between calcium channels of skeletal muscle requires multiple direct and indirect interactions." Proc Natl Acad Sci U S A **103**(52): 19760-19765.

Shigemoto, K., S. Kubo, et al. (2010). "Muscle weakness and neuromuscular junctions in aging and disease." Geriatr Gerontol Int **10 Suppl 1**: S137-147.

Shtifman, A., C. W. Ward, et al. (2002). "Interdomain interactions within ryanodine receptors regulate Ca2+ spark frequency in skeletal muscle." The Journal of General Physiology **119**(1): 15-32.

Shuaib, A., R. T. Paasuke, et al. (1987). "Central core disease. Clinical features in 13 patients." Medicine **66**(5): 389-396.

Silverthorn, D. U. (1998). Human physiology : an integrated approach. Upper Saddle River, N.J., Prentice Hall ; London : Prentice-Hall International.

Silverthorn, D. U. (2004). Human physiology : an integrated approach. San Francisco, Pearson/Benjamin Cummings.

Simoneau, J. A. and C. Bouchard (1989). "Human variation in skeletal muscle fiber-type proportion and enzyme activities." Am J Physiol **257**(4 Pt 1): E567-572.

Simoneau, J. A. and C. Bouchard (1995). "Genetic determinism of fiber type proportion in human skeletal muscle." FASEB J **9**(11): 1091-1095.

Sirvent, P., S. Bordenave, et al. (2005a). "Simvastatin induces impairment in skeletal muscle while heart is protected." Biochem Biophys Res Commun **338**(3): 1426-1434.

Sirvent, P., O. Fabre, et al. (2012). "Muscle mitochondrial metabolism and calcium signaling impairment in patients treated with statins." Toxicol Appl Pharmacol **259**(2): 263-268.

Sirvent, P., J. Mercier, et al. (2008). "New insights into mechanisms of statin-associated myotoxicity." Curr Opin Pharmacol **8**(3): 333-338.

Sirvent, P., J. Mercier, et al. (2005b). "Simvastatin triggers mitochondria-induced Ca2+ signaling alteration in skeletal muscle." Biochem Biophys Res Commun **329**(3): 1067-1075.

Sitsapesan, R. and A. J. Williams (1990). "Mechanisms of caffeine activation of single calcium-release channels of sheep cardiac sarcoplasmic reticulum." The Journal of physiology **423**: 425-439.

Sitsapesan, R. and A. J. Williams (1994a). "Gating of the native and purified cardiac SR Ca(2+)-release channel with monovalent cations as permeant species." Biophysical journal **67**(4): 1484-1494.

Sitsapesan, R. and A. J. Williams (1994b). "Regulation of the gating of the sheep cardiac sarcoplasmic reticulum Ca(2+)-release channel by luminal Ca2+." The Journal of membrane biology **137**(3): 215-226.

References

Sitsapesan, R. and A. J. Williams (1995). "The gating of the sheep skeletal sarcoplasmic reticulum Ca(2+)-release channel is regulated by luminal Ca2+." The Journal of membrane biology **146**(2): 133-144.

Siu, P. M. and S. E. Alway (2009). "Response and adaptation of skeletal muscle to denervation stress: the role of apoptosis in muscle loss." Frontiers in bioscience **14**: 432-452.

Slavik, K. J., J. P. Wang, et al. (1997). "A carboxy-terminal peptide of the alpha 1-subunit of the dihydropyridine receptor inhibits Ca(2+)-release channels." Am J Physiol **272**(5 Pt 1): C1475-1481.

Smerdu, V., I. Karsch-Mizrachi, et al. (1994). "Type IIx myosin heavy chain transcripts are expressed in type IIb fibers of human skeletal muscle." The American journal of physiology **267**(6 Pt 1): C1723-1728.

Smith, D. O. (1979). "Reduced capabilities of synaptic transmission in aged rats." Experimental neurology **66**(3): 650-666.

Smith, D. O. (1984). "Acetylcholine storage, release and leakage at the neuromuscular junction of mature adult and aged rats." The Journal of physiology **347**: 161-176.

Smith, J. S., R. Coronado, et al. (1986). "Single channel measurements of the calcium release channel from skeletal muscle sarcoplasmic reticulum. Activation by Ca2+ and ATP and modulation by Mg2+." The Journal of General Physiology **88**(5): 573-588.

Smith, J. S., T. Imagawa, et al. (1988). "Purified ryanodine receptor from rabbit skeletal muscle is the calcium-release channel of sarcoplasmic reticulum." J Gen Physiol **92**(1): 1-26.

Smith, J. S., E. Rousseau, et al. (1989). "Calmodulin modulation of single sarcoplasmic reticulum Ca2+-release channels from cardiac and skeletal muscle." Circ Res **64**(2): 352-359.

Smith, P. K., R. I. Krohn, et al. (1985). "Measurement of protein using bicinchoninic acid." Analytical biochemistry **150**(1): 76-85.

Snutch, T. P. and P. B. Reiner (1992). "Ca2+ channels: diversity of form and function." Current opinion in neurobiology **2**(3): 247-253.

Solomon, E. P. (2009). Introduction to human anatomy and physiology. St. Louis, Mo., Saunders/Elsevier.

Sorrentino, V. and C. Reggiani (1999). "Expression of the ryanodine receptor type 3 in skeletal muscle. A new partner in excitation-contraction coupling?" Trends Cardiovasc Med **9**(1-2): 54-61.

Sorrentino, V. and P. Volpe (1993). "Ryanodine receptors: how many, where and why?" Trends in pharmacological sciences **14**(3): 98-103.

Sreter, F. A. and J. Gergely (1964). "Comparative studies of the MG activated ATPase activity and Ca uptake of fractions of white and red muscle homogenates." Biochem Biophys Res Commun **16**(5): 438-443.

Sreter, F. A., J. R. Lopez, et al. (1987). "Changes in intracellular ionized Ca concentration associated with muscle fiber type transformation." Am J Physiol **253**(2 Pt 1): C296-300.

Stalberg, E. and P. R. Fawcett (1982). "Macro EMG in healthy subjects of different ages." Journal of neurology, neurosurgery, and psychiatry **45**(10): 870-878.

Stephens, G. J., K. M. Page, et al. (2000). "The alpha1B Ca2+ channel amino terminus contributes determinants for beta subunit-mediated voltage-dependent inactivation properties." The Journal of physiology **525 Pt 2**: 377-390.

Stephenson, D. G., G. D. Lamb, et al. (1998). "Events of the excitation-contraction-relaxation (E-C-R) cycle in fast- and slow-twitch mammalian muscle fibres relevant to muscle fatigue." Acta physiologica Scandinavica **162**(3): 229-245.

Stern, M. D., G. Pizarro, et al. (1997). "Local control model of excitation-contraction coupling in skeletal muscle." J Gen Physiol **110**(4): 415-440.

Stoyanovsky, D., T. Murphy, et al. (1997). "Nitric oxide activates skeletal and cardiac ryanodine receptors." Cell Calcium **21**(1): 19-29.

Striessnig, J., H. G. Knaus, et al. (1987). "Photoaffinity labelling of the phenylalkylamine receptor of the skeletal muscle transverse-tubule calcium channel." FEBS letters **212**(2): 247-253.

Strube, C., M. Beurg, et al. (1996). "Reduced Ca2+ current, charge movement, and absence of Ca2+ transients in skeletal muscle deficient in dihydropyridine receptor beta 1 subunit." Biophys J **71**(5): 2531-2543.

Sugiura, M. and K. Kanda (2004). "Progress of age-related changes in properties of motor units in the gastrocnemius muscle of rats." Journal of neurophysiology **92**(3): 1357-1365.

Suko, J., I. Maurer-Fogy, et al. (1993). "Phosphorylation of serine 2843 in ryanodine receptor-calcium release channel of skeletal muscle by cAMP-, cGMP- and CaM-dependent protein kinase." Biochimica et biophysica acta **1175**(2): 193-206.

Sun, J., L. Xu, et al. (2001). "Classes of thiols that influence the activity of the skeletal muscle calcium release channel." The Journal of biological chemistry **276**(19): 15625-15630.

Sun, J., N. Yamaguchi, et al. (2008). "Regulation of the cardiac muscle ryanodine receptor by O(2) tension and S-nitrosoglutathione." Biochemistry **47**(52): 13985-13990.

Sun, X. H., F. Protasi, et al. (1995). "Molecular architecture of membranes involved in excitation-contraction coupling of cardiac muscle." J Cell Biol **129**(3): 659-671.

Sutko, J. L., K. Ito, et al. (1985). "Ryanodine: a modifier of sarcoplasmic reticulum calcium release in striated muscle." Federation proceedings **44**(15): 2984-2988.

Szegedi, C., S. Sarkozi, et al. (1999). "Calsequestrin: more than 'only' a luminal Ca2+ buffer inside the sarcoplasmic reticulum." Biochem J **337 (Pt 1)**: 19-22.

Tada, M. and M. A. Kirchberger (1976). "Significance of the membrane protein phospholamban in cyclic AMP-mediated regulation of calcium transport by sarcoplasmic reticulum." Recent Adv Stud Cardiac Struct Metab **11**: 265-272.

Takahashi, M., M. J. Seagar, et al. (1987). "Subunit structure of dihydropyridine-sensitive calcium channels from skeletal muscle." Proc Natl Acad Sci U S A **84**(15): 5478-5482.

Takasago, T., T. Imagawa, et al. (1991). "Regulation of the cardiac ryanodine receptor by protein kinase-dependent phosphorylation." Journal of biochemistry **109**(1): 163-170.

Takasago, T., T. Imagawa, et al. (1989). "Phosphorylation of the cardiac ryanodine receptor by cAMP-dependent protein kinase." Journal of biochemistry **106**(5): 872-877.

Takekura, H., N. Kasuga, et al. (1994). "Differences in ultrastructural and metabolic profiles within the same type of fibres in various muscles of young and adult rats." Acta Physiol Scand **150**(3): 335-344.

Takekura, H., M. Nishi, et al. (1995a). "Abnormal junctions between surface membrane and sarcoplasmic reticulum in skeletal muscle with a mutation targeted to the ryanodine receptor." Proceedings of the National Academy of Sciences of the United States of America **92**(8): 3381-3385.

Takekura, H., H. Takeshima, et al. (1995b). "Co-expression in CHO cells of two muscle proteins involved in excitation-contraction coupling." Journal of muscle research and cell motility **16**(5): 465-480.

Takeshima, H., S. Komazaki, et al. (2000). "Junctophilins: a novel family of junctional membrane complex proteins." Molecular cell **6**(1): 11-22.

Takeshima, H., S. Nishimura, et al. (1989). "Primary structure and expression from complementary DNA of skeletal muscle ryanodine receptor." Nature **339**(6224): 439-445.

Takeshima, H., T. Yamazawa, et al. (1995). "Ca(2+)-induced Ca2+ release in myocytes from dyspedic mice lacking the type-1 ryanodine receptor." The EMBO journal **14**(13): 2999-3006.

Talmadge, R. J. and R. R. Roy (1993). "Electrophoretic separation of rat skeletal muscle myosin heavy-chain isoforms." J Appl Physiol **75**(5): 2337-2340.

Tanabe, T., K. G. Beam, et al. (1990a). "Regions of the skeletal muscle dihydropyridine receptor critical for excitation-contraction coupling." Nature **346**(6284): 567-569.

Tanabe, T., K. G. Beam, et al. (1988). "Restoration of excitation-contraction coupling and slow calcium current in dysgenic muscle by dihydropyridine receptor complementary DNA." Nature **336**(6195): 134-139.

Tanabe, T., A. Mikami, et al. (1990b). "Cardiac-type excitation-contraction coupling in dysgenic skeletal muscle injected with cardiac dihydropyridine receptor cDNA." Nature **344**(6265): 451-453.

Tanabe, T., H. Takeshima, et al. (1987). "Primary structure of the receptor for calcium channel blockers from skeletal muscle." Nature **328**(6128): 313-318.

Tang, W., C. P. Ingalls, et al. (2004). "Altered excitation-contraction coupling with skeletal muscle specific FKBP12 deficiency." FASEB J **18**(13): 1597-1599.

Tang, W., S. Sencer, et al. (2002). "Calmodulin modulation of proteins involved in excitation-contraction coupling." Front Biosci **7**: d1583-1589.

Tang, Z. Z., V. Yarotskyy, et al. (2012). "Muscle weakness in myotonic dystrophy associated with misregulated splicing and altered gating of Ca(V)1.1 calcium channel." Hum Mol Genet **21**(6): 1312-1324.

Taske, N. L., H. J. Eyre, et al. (1995). "Molecular cloning of the cDNA encoding human skeletal muscle triadin and its localisation to chromosome 6q22-6q23." European journal of biochemistry / FEBS **233**(1): 258-265.

Taylor, J. R., Z. Zheng, et al. (2009). "Increased CaVbeta1A expression with aging contributes to skeletal muscle weakness." Aging Cell **8**(5): 584-594.

Tempel, B. L., D. M. Papazian, et al. (1987). "Sequence of a probable potassium channel component encoded at Shaker locus of Drosophila." Science **237**(4816): 770-775.

Thevenon, D., S. Smida-Rezgui, et al. (2003). "Human skeletal muscle triadin: gene organization and cloning of the major isoform, Trisk 51." Biochemical and Biophysical Research Communications **303**(2): 669-675.

Thompson, W. J., L. A. Sutton, et al. (1984). "Fibre type composition of single motor units during synapse elimination in neonatal rat soleus muscle." Nature **309**(5970): 709-711.

Tilgen, N., F. Zorzato, et al. (2001). "Identification of four novel mutations in the C-terminal membrane spanning domain of the ryanodine receptor 1: association with central core disease and alteration of calcium homeostasis." Human molecular genetics **10**(25): 2879-2887.

Timerman, A. P., E. Ogunbumni, et al. (1993). "The calcium release channel of sarcoplasmic reticulum is modulated by FK-506-binding protein. Dissociation and reconstitution of FKBP-12 to the calcium release channel of skeletal muscle sarcoplasmic reticulum." The Journal of biological chemistry **268**(31): 22992-22999.

Timerman, A. P., H. Onoue, et al. (1996). "Selective binding of FKBP12.6 by the cardiac ryanodine receptor." The Journal of biological chemistry **271**(34): 20385-20391.

Timerman, A. P., G. Wiederrecht, et al. (1995). "Characterization of an exchange reaction between soluble FKBP-12 and the FKBP.ryanodine receptor complex. Modulation by FKBP mutants deficient in peptidyl-prolyl isomerase activity." The Journal of biological chemistry **270**(6): 2451-2459.

Tomlinson, B. E. and D. Irving (1977). "The numbers of limb motor neurons in the human lumbosacral cord throughout life." Journal of the neurological sciences **34**(2): 213-219.

Tong, J., T. V. McCarthy, et al. (1999). "Measurement of resting cytosolic Ca2+ concentrations and Ca2+ store size in HEK-293 cells transfected with malignant hyperthermia or central core disease mutant Ca2+ release channels." The Journal of biological chemistry **274**(2): 693-702.

Tong, J., H. Oyamada, et al. (1997). "Caffeine and halothane sensitivity of intracellular Ca2+ release is altered by 15 calcium release channel (ryanodine receptor) mutations associated with malignant hyperthermia and/or central core disease." The Journal of biological chemistry **272**(42): 26332-26339.

Toniolo, L., L. Maccatrozzo, et al. (2005). "Expression of eight distinct MHC isoforms in bovine striated muscles: evidence for MHC-2B presence only in extraocular muscles." J Exp Biol **208**(Pt 22): 4243-4253.

Treves, S., A. A. Anderson, et al. (2005). "Ryanodine receptor 1 mutations, dysregulation of calcium homeostasis and neuromuscular disorders." Neuromuscular disorders : NMD **15**(9-10): 577-587.

Treves, S., F. Larini, et al. (1994). "Alteration of intracellular Ca2+ transients in COS-7 cells transfected with the cDNA encoding skeletal-muscle ryanodine receptor carrying a mutation associated with malignant hyperthermia." The Biochemical journal **301 (Pt 3)**: 661-665.

Tripathy, A. and G. Meissner (1996). "Sarcoplasmic reticulum lumenal Ca2+ has access to cytosolic activation and inactivation sites of skeletal muscle Ca2+ release channel." Biophysical Journal **70**(6): 2600-2615.

Tripathy, A., L. Xu, et al. (1995). "Calmodulin activation and inhibition of skeletal muscle Ca2+ release channel (ryanodine receptor)." Biophysical Journal **69**(1): 106-119.

Tsien, R. W., D. Lipscombe, et al. (1988). "Multiple types of neuronal calcium channels and their selective modulation." Trends in neurosciences **11**(10): 431-438.

Tsugorka, A., E. Rios, et al. (1995). "Imaging elementary events of calcium release in skeletal muscle cells." Science **269**(5231): 1723-1726.

Tung, C. C., P. A. Lobo, et al. (2010). "The amino-terminal disease hotspot of ryanodine receptors forms a cytoplasmic vestibule." Nature.

Tunwell, R. E., C. Wickenden, et al. (1996). "The human cardiac muscle ryanodine receptor-calcium release channel: identification, primary structure and topological analysis." The Biochemical journal **318 (Pt 2)**: 477-487.

Uehara, A., M. Yasukochi, et al. (2002). "Gating kinetics and ligand sensitivity modified by phosphorylation of cardiac ryanodine receptors." Pflugers Archiv : European journal of physiology **444**(1-2): 202-212.

Ursu, D., R. P. Schuhmeier, et al. (2004). "Altered inactivation of Ca2+ current and Ca2+ release in mouse muscle fibers deficient in the DHP receptor gamma1 subunit." The Journal of General Physiology **124**(5): 605-618.

Vaillancourt, D. E., L. Larsson, et al. (2003). "Effects of aging on force variability, single motor unit discharge patterns, and the structure of 10, 20, and 40 Hz EMG activity." Neurobiology of aging **24**(1): 25-35.

Valdivia, H. H., J. H. Kaplan, et al. (1995). "Rapid adaptation of cardiac ryanodine receptors: modulation by Mg2+ and phosphorylation." Science **267**(5206): 1997-2000.

Van Duyne, G. D., R. F. Standaert, et al. (1991). "Atomic structure of the rapamycin human immunophilin FKBP-12 complex." Journal of the American Chemical Society **113**(19): 7433-7434.

Van Petegem, F., K. A. Clark, et al. (2004). "Structure of a complex between a voltage-gated calcium channel beta-subunit and an alpha-subunit domain." Nature **429**(6992): 671-675.

Vandervoort, A. A. (2002). "Aging of the human neuromuscular system." Muscle & nerve **25**(1): 17-25.

Vandervoort, A. A. and A. J. McComas (1986). "Contractile changes in opposing muscles of the human ankle joint with aging." Journal of applied physiology **61**(1): 361-367.

Vangheluwe, P., M. Schuermans, et al. (2005). "Sarcolipin and phospholamban mRNA and protein expression in cardiac and skeletal muscle of different species." Biochem J **389**(Pt 1): 151-159.

Vassilopoulos, S., D. Thevenon, et al. (2005). "Triadins are not triad-specific proteins: two new skeletal muscle triadins possibly involved in the architecture of sarcoplasmic reticulum." J Biol Chem **280**(31): 28601-28609.

Vendelin, M., N. Beraud, et al. (2005). "Mitochondrial regular arrangement in muscle cells: a "crystal-like" pattern." Am J Physiol Cell Physiol **288**(3): C757-767.

Venero, C. V. and P. D. Thompson (2009). "Managing statin myopathy." Endocrinol Metab Clin North Am **38**(1): 121-136.

Vukcevic, M., M. Broman, et al. (2010). "Functional properties of RYR1 mutations identified in Swedish patients with malignant hyperthermia and central core disease." Anesthesia and analgesia **111**(1): 185-190.

Wagenknecht, T., J. Berkowitz, et al. (1994). "Localization of calmodulin binding sites on the ryanodine receptor from skeletal muscle by electron microscopy." Biophys J **67**(6): 2286-2295.

Wagenknecht, T., R. Grassucci, et al. (1996). "Cryoelectron microscopy resolves FK506-binding protein sites on the skeletal muscle ryanodine receptor." Biophys J **70**(4): 1709-1715.

Wagenknecht, T., M. Radermacher, et al. (1997). "Locations of calmodulin and FK506-binding protein on the three-dimensional architecture of the skeletal muscle ryanodine receptor." J Biol Chem **272**(51): 32463-32471.

Wagenknecht, T. and M. Samso (2002). "Three-dimensional reconstruction of ryanodine receptors." Front Biosci **7**: d1464-1474.

Walker, D., D. Bichet, et al. (1999). "A new beta subtype-specific interaction in alpha1A subunit controls P/Q-type Ca2+ channel activation." The Journal of biological chemistry **274**(18): 12383-12390.

Wang, M. C., G. Velarde, et al. (2002). "3D structure of the skeletal muscle dihydropyridine receptor." J Mol Biol **323**(1): 85-98.

Wang, S., W. R. Trumble, et al. (1998). "Crystal structure of calsequestrin from rabbit skeletal muscle sarcoplasmic reticulum." Nature structural biology **5**(6): 476-483.

Wang, S. Q., L. S. Song, et al. (2001). "Ca2+ signalling between single L-type Ca2+ channels and ryanodine receptors in heart cells." Nature **410**(6828): 592-596.

Wang, Z. M., M. L. Messi, et al. (2000). "L-Type Ca(2+) channel charge movement and intracellular Ca(2+) in skeletal muscle fibers from aging mice." Biophys J **78**(4): 1947-1954.

Warf, M. B. and J. A. Berglund (2007). "MBNL binds similar RNA structures in the CUG repeats of myotonic dystrophy and its pre-mRNA substrate cardiac troponin T." RNA **13**(12): 2238-2251.

Weber, A. (1968). "The mechanism of the action of caffeine on sarcoplasmic reticulum." The Journal of General Physiology **52**(5): 760-772.

Weber, A. and R. Herz (1968). "The relationship between caffeine contracture of intact muscle and the effect of caffeine on reticulum." The Journal of General Physiology **52**(5): 750-759.

Wehner, M., H. Rueffert, et al. (2004). "Functional characterization of malignant hyperthermia-associated RyR1 mutations in exon 44, using the human myotube model." Neuromuscular disorders : NMD **14**(7): 429-437.

Wehrle, U., S. Dusterhoft, et al. (1994). "Effects of chronic electrical stimulation on myosin heavy chain expression in satellite cell cultures derived from rat muscles of different fiber-type composition." Differentiation **58**(1): 37-46.

Wei, L., E. M. Gallant, et al. (2009). "Junctin and triadin each activate skeletal ryanodine receptors but junctin alone mediates functional interactions with calsequestrin." Int J Biochem Cell Biol **41**(11): 2214-2224.

Wei, L., M. Varsanyi, et al. (2006). "The conformation of calsequestrin determines its ability to regulate skeletal ryanodine receptors." Biophys J **91**(4): 1288-1301.

Weiss, R. G., K. M. O'Connell, et al. (2004). "Functional analysis of the R1086H malignant hyperthermia mutation in the DHPR reveals an unexpected influence of the III-IV loop on skeletal muscle EC coupling." Am J Physiol Cell Physiol **287**(4): C1094-1102.

Welch, W., S. Rheault, et al. (2004). "A model of the putative pore region of the cardiac ryanodine receptor channel." Biophysical journal **87**(4): 2335-2351.

Welle, S., R. Tawil, et al. (2008). "Sex-related differences in gene expression in human skeletal muscle." PLoS One **3**(1): e1385.

Whalen, R. G., J. B. Harris, et al. (1990). "Expression of myosin isoforms during notexin-induced regeneration of rat soleus muscles." Dev Biol **141**(1): 24-40.

Whalen, R. G., D. Johnstone, et al. (1984). "A developmentally regulated disappearance of slow myosin in fast-type muscles of the mouse." FEBS Lett **177**(1): 51-56.

Wigston, D. (1990a). "Tug-of-war at the neuromuscular junction." Trends in neurosciences **13**(8): 309-312.

Wigston, D. J. (1990b). "Repeated in vivo visualization of neuromuscular junctions in adult mouse lateral gastrocnemius." The Journal of neuroscience : the official journal of the Society for Neuroscience **10**(6): 1753-1761.

Wilkens, C. M. and K. G. Beam (2003). "Insertion of alpha1S II-III loop and C terminal sequences into alpha1H fails to restore excitation-contraction coupling in dysgenic myotubes." J Muscle Res Cell Motil **24**(1): 99-109.

Wilkens, C. M., N. Kasielke, et al. (2001). "Excitation-contraction coupling is unaffected by drastic alteration of the sequence surrounding residues L720-L764 of the alpha 1S II-III loop." Proc Natl Acad Sci U S A **98**(10): 5892-5897.

Witcher, D. R., M. De Waard, et al. (1995). "Association of native Ca2+ channel beta subunits with the alpha 1 subunit interaction domain." J Biol Chem **270**(30): 18088-18093.

Witcher, D. R., R. J. Kovacs, et al. (1991). "Unique phosphorylation site on the cardiac ryanodine receptor regulates calcium channel activity." The Journal of biological chemistry **266**(17): 11144-11152.

Wolf, M., A. Eberhart, et al. (2003). "Visualization of the domain structure of an L-type Ca2+ channel using electron cryo-microscopy." J Mol Biol **332**(1): 171-182.

Wright, N. T., B. L. Prosser, et al. (2008). "S100A1 and calmodulin compete for the same binding site on ryanodine receptor." The Journal of biological chemistry **283**(39): 26676-26683.

Wu, K. D. and J. Lytton (1993). "Molecular cloning and quantification of sarcoplasmic reticulum Ca(2+)-ATPase isoforms in rat muscles." Am J Physiol **264**(2 Pt 1): C333-341.

Wu, Y., B. Aghdasi, et al. (1997). "Functional interactions between cytoplasmic domains of the skeletal muscle Ca2+ release channel." The Journal of biological chemistry **272**(40): 25051-25061.

Xia, R., T. Stangler, et al. (2000). "Skeletal muscle ryanodine receptor is a redox sensor with a well defined redox potential that is sensitive to channel modulators." The Journal of biological chemistry **275**(47): 36556-36561.

Xu, L., J. P. Eu, et al. (1998). "Activation of the cardiac calcium release channel (ryanodine receptor) by poly-S-nitrosylation." Science **279**(5348): 234-237.

Xu, L. and G. Meissner (1998). "Regulation of cardiac muscle Ca2+ release channel by sarcoplasmic reticulum lumenal Ca2+." Biophysical Journal **75**(5): 2302-2312.

Xu, L., Y. Wang, et al. (2008). "Single channel properties of heterotetrameric mutant RyR1 ion channels linked to core myopathies." J Biol Chem **283**(10): 6321-6329.

Yamaguchi, N., L. Xu, et al. (2005). "Calmodulin Regulation and Identification of Calmodulin Binding Region of Type-3 Ryanodine Receptor Calcium Release Channel†." Biochemistry **44**(45): 15074-15081.

Yamaguchi, N., L. Xu, et al. (2003). "Molecular basis of calmodulin binding to cardiac muscle Ca(2+) release channel (ryanodine receptor)." The Journal of biological chemistry **278**(26): 23480-23486.

Yamamoto, T., R. El-Hayek, et al. (2000). "Postulated role of interdomain interaction within the ryanodine receptor in Ca(2+) channel regulation." J Biol Chem **275**(16): 11618-11625.

Yamamoto, T. and N. Ikemoto (2002). "Spectroscopic monitoring of local conformational changes during the intramolecular domain-domain interaction of the ryanodine receptor." Biochemistry **41**(5): 1492-1501.

Yamashita, S., K. F. McGrath, et al. (2007). "Assembly of transverse tubule architecture in the middle and myotendinous junctional regions in developing rat skeletal muscle fibers." J Muscle Res Cell Motil **28**(2-3): 141-151.

Yamazawa, T., H. Takeshima, et al. (1997). "A region of the ryanodine receptor critical for excitation-contraction coupling in skeletal muscle." The Journal of biological chemistry **272**(13): 8161-8164.

Yang, H. C., M. M. Reedy, et al. (1994). "Calmodulin interaction with the skeletal muscle sarcoplasmic reticulum calcium channel protein." Biochemistry **33**(2): 518-525.

Yang, T., T. A. Ta, et al. (2003). "Functional defects in six ryanodine receptor isoform-1 (RyR1) mutations associated with malignant hyperthermia and their impact on skeletal excitation-contraction coupling." The Journal of biological chemistry **278**(28): 25722-25730.

Yin, C. C., L. M. Blayney, et al. (2005a). "Physical coupling between ryanodine receptor-calcium release channels." J Mol Biol **349**(3): 538-546.

Yin, C. C., L. G. D'Cruz, et al. (2008). "Ryanodine receptor arrays: not just a pretty pattern?" Trends Cell Biol **18**(4): 149-156.

Yin, C. C., H. Han, et al. (2005b). "Two-dimensional crystallization of the ryanodine receptor Ca2+ release channel on lipid membranes." Journal of structural biology **149**(2): 219-224.

Yoon, T., B. S. De-Lap, et al. (2008). "Age-related muscle fatigue after a low-force fatiguing contraction is explained by central fatigue." Muscle & nerve **37**(4): 457-466.

Young, A., M. Stokes, et al. (1984). "Size and strength of the quadriceps muscles of old and young women." European journal of clinical investigation **14**(4): 282-287.

Young, A., M. Stokes, et al. (1985). "The size and strength of the quadriceps muscles of old and young men." Clinical physiology **5**(2): 145-154.

Yu, F., M. Hedstrom, et al. (2007). "Effects of ageing and gender on contractile properties in human skeletal muscle and single fibres." Acta Physiol (Oxf) **190**(3): 229-241.

Yuan, Q., P. Han, et al. (2009). "Partial downregulation of junctin enhances cardiac calcium cycling without eliciting ventricular arrhythmias in mice." Am J Physiol Heart Circ Physiol **296**(5): H1484-1490.

Yuan, S. H., W. Arnold, et al. (1991). "Biogenesis of transverse tubules and triads: immunolocalization of the 1,4-dihydropyridine receptor, TS28, and the ryanodine receptor in rabbit skeletal muscle developing in situ." J Cell Biol **112**(2): 289-301.

Yuan, Y., S. A. Compton, et al. (2007). "Muscleblind-like 1 interacts with RNA hairpins in splicing target and pathogenic RNAs." Nucleic Acids Res **35**(16): 5474-5486.

Zable, A. C., T. G. Favero, et al. (1997). "Glutathione modulates ryanodine receptor from skeletal muscle sarcoplasmic reticulum. Evidence for redox regulation of the Ca2+ release mechanism." The Journal of biological chemistry **272**(11): 7069-7077.

Zarka, A. and V. Shoshan-Barmatz (1993). "Characterization and photoaffinity labeling of the ATP binding site of the ryanodine receptor from skeletal muscle." European journal of biochemistry / FEBS **213**(1): 147-154.

Zhang, J.-Z., Y. Wu, et al. (1999). "Oxidation of the skeletal muscle Ca2+ release channel alters calmodulin binding." American Journal of Physiology - Cell Physiolog **276**(1): C46-C53.

Zhang, J., Z. Liu, et al. (2003). "Three-dimensional localization of divergent region 3 of the ryanodine receptor to the clamp-shaped structures adjacent to the FKBP binding sites." J Biol Chem **278**(16): 14211-14218.

Zhang, L., J. Kelley, et al. (1997). "Complex formation between junctin, triadin, calsequestrin, and the ryanodine receptor. Proteins of the cardiac junctional sarcoplasmic reticulum membrane." J Biol Chem **272**(37): 23389-23397.

Zhang, Y., H. S. Chen, et al. (1993). "A mutation in the human ryanodine receptor gene associated with central core disease." Nat Genet **5**(1): 46-50.

Zhao, F., P. Li, et al. (2001). "Dantrolene inhibition of ryanodine receptor Ca2+ release channels. Molecular mechanism and isoform selectivity." The Journal of biological chemistry **276**(17): 13810-13816.

Zheng, Z., Z. M. Wang, et al. (2002). "Insulin-like growth factor-1 increases skeletal muscle dihydropyridine receptor alpha 1S transcriptional activity by acting on the cAMP-response element-binding protein element of the promoter region." J Biol Chem **277**(52): 50535-50542.

Zima, A. V., J. A. Copello, et al. (2004). "Effects of cytosolic NADH/NAD(+) levels on sarcoplasmic reticulum Ca(2+) release in permeabilized rat ventricular myocytes." The Journal of physiology **555**(Pt 3): 727-741.

Zimanyi, I., E. Buck, et al. (1992). "Ryanodine induces persistent inactivation of the Ca2+ release channel from skeletal muscle sarcoplasmic reticulum." Mol Pharmacol **42**(6): 1049-1057.

Zimanyi, I. and I. N. Pessah (1991). "Pharmacological characterization of the specific binding of [3H]ryanodine to rat brain microsomal membranes." Brain research **561**(2): 181-191.

Zissimopoulos, S. and F. A. Lai (2007). Ryanodine receptor structure, function and pathophysiology. New Comprehensive Biochemistry. K. Joachim and M. Marek, Elsevier. **Volume 41:** 287-342.

Zorzato, F., J. Fujii, et al. (1990). "Molecular cloning of cDNA encoding human and rabbit forms of the Ca2+ release channel (ryanodine receptor) of skeletal muscle sarcoplasmic reticulum." J Biol Chem **265**(4): 2244-2256.

Zorzato, F., R. Sacchetto, et al. (1994). "Identification of two ryanodine receptor transcripts in neonatal, slow-, and fast-twitch rabbit skeletal muscles." Biochem Biophys Res Commun **203**(3): 1725-1730.

Zorzato, F., N. Yamaguchi, et al. (2003). "Clinical and functional effects of a deletion in a COOH-terminal lumenal loop of the skeletal muscle ryanodine receptor." Human molecular genetics **12**(4): 379-388.

Zucchi, R. and S. Ronca-Testoni (1997). "The sarcoplasmic reticulum Ca2+ channel/ryanodine receptor: modulation by endogenous effectors, drugs and disease states." Pharmacological reviews **49**(1): 1-51.

Zuhlke, R. D., G. S. Pitt, et al. (1999). "Calmodulin supports both inactivation and facilitation of L-type calcium channels." Nature **399**(6732): 159-162.

Zuhlke, R. D., G. S. Pitt, et al. (2000). "Ca2+-sensitive inactivation and facilitation of L-type Ca2+ channels both depend on specific amino acid residues in a consensus calmodulin-binding motif in the(alpha)1C subunit." J Biol Chem **275**(28): 21121-21129.